THE INFRARED ELECTRONIC SPECTRUM OF FeO

by

ALAN WILLIAM TAYLOR

B.Sc. (Hon.), University of Victoria, 1978
M.Sc., University of Victoria, 1981

A THESIS SUBMITTED IN PARTIAL FULFILMENT OF

THE REQUIREMENTS FOR THE DEGREE OF

DOCTOR OF PHILOSOPHY

in

THE FACULTY OF GRADUATE STUDIES

Department of Chemistry

We accept this thesis as conforming

to the required standard

THE UNIVERSITY OF BRITISH COLUMBIA

February, 1986

In presenting this thesis in partial fulfilment of the requirements for an advanced degree at the University of British Columbia, I agree that the Library shall make it freely available for reference and study. I further agree that permission for extensive copying of this thesis for scholarly purposes may be granted by the head of my department or by his or her representatives. It is understood that copying or publication of this thesis for financial gain shall not be allowed without my written permission.

Department of Chemistry

The University of British Columbia
1956 Main Mall
Vancouver, Canada
V6T 1Y3

Date February 21, 1986

ABSTRACT

The near-infrared electronic system of FeO has been recorded in emission at high resolution with the 1-meter FT spectrometer at Kitt Peak National Observatory. The system has been found to consist of two overlapping band systems lying in the region 7 000 - 14 000 cm^{-1}. These share a common lower state and this is the same lower state as that of the orange system. This state, which has vibrational constants (in cm^{-1}) ω_e = 880.4148, $\omega_e x_e$ = 4.632 15, and $\omega_e y_e$ = 5.55 x 10^{-4} has been established as the ground state of the molecule by the matrix isolation experiments of Green, Reedy, and Kay (*J. Mol. Spectrosc.* **1979**, 78, 257-266) and has been identified as a $^5\Delta_i$ state in earlier studies done in this laboratory on the orange system. The present work has proven this identity, and least-squares data reduction has yielded the ground state constants: B_e = 0.518 721 cm^{-1} a_e = 0.003 825 cm^{-1} γ_e = -4.8×10^{-7} cm^{-1} D_e = 7.210×10^{-7} cm^{-1} β_e = 1.51×10^{-9} cm^{-1} r_e = 0.161 64 nm, and A = -94.9 cm^{-1}. These were based on combined data from the infrared and orange systems for the levels v = 0-3, together with six microwave frequencies obtained by Endo, Saito, and Hirota (*Ap. J.* **1984**, 278, L131-L132). Both the $^5\Delta_0$ and $^5\Delta_1$ substates are found to show small Λ-doublings, with that in $^5\Delta_0$ being the larger (~0.3 cm^{-1}). In contrast to all the known excited states of FeO, the ground state is well-behaved, but even this state possesses one small rotational perturbation. This is observed only in one parity component of the J = 15 level of the v = 2 level of the $X^5\Delta_2$ substate and is probably caused by the low-lying $^7\Sigma$ state predicted by Krauss and Stevens (J. Chem. Phys. **1985**, 82, 5584-5596).

The upper level of the infrared system consists of two overlapping states about 10 200 cm^{-1} above the ground state and separated by only about 213 cm^{-1} at their v = 0 levels. The upper of these, a $^5\Pi_i$ state, has the approximate values $\Delta G_{1/2} \simeq 627$ cm^{-1} and $A_0 \simeq -217$ cm^{-1} and for the lower $^5\Phi_i$ state $\Delta G_{1/2} \simeq 593$ cm^{-1} and $A_0 \simeq -47$ cm^{-1}. These are very rough estimates only, as a result of the

vast number of rotational perturbations present. Effective rotational constants for the individual substates have been determined rather than a global set of constants, again because of the perturbations. Amongst the perturbing states, at least one multiplet Σ state is present and there may be as many as three. Evidence is also presented for the existence of a $^3\Phi$ state.

TABLE OF CONTENTS

TABLE OF CONTENTS (cont.)

TABLE OF CONTENTS (cont.)

LIST OF TABLES

LIST OF FIGURES

LIST OF FIGURES (cont.)

ACKNOWLEDGEMENTS

First and foremost, I sincerely wish to thank Dr. Anthony J. Merer for suggesting this project, for many helpful comments and suggestions throughout my time here, for helping with the task of assigning the lines, for answering my many questions, for patience, and — by being such an expert in his field — for serving as a role model; ...I hope that someday I may know so much!

I wish to thank Dr. Walter J. Balfour for first introducing me to the subject of high resolution electronic molecular spectroscopy.

I shall always be indebted to Dr. Allan S-C. Cheung for all his assistance in integrating me into the FeO experiments that were already going on when I arrived here and for all his subsequent help. My thanks also go to Dr. Marjatta Lyyra for all her laser-induced-fluorescence work and to Mr. Nelson Lee for his assistance in assigning lines in the infrared system. I also thank Mr. Rob Hubbard of the Kitt Peak National Observatory staff for his very capable technical help in recording the infrared system. And, more recently, I thank Dr. Ulf Sassenberg for many useful and interesting discussions.

I wish to thank my parents for endless support and encouragement and, well, for just being my parents!

Financial assistance from the Natural Sciences and Engineering Research Council of Canada in the form of a Postgraduate Scholarship during much of my stay here is gratefully acknowledged.

AUTHOR'S PREFACE

The work reported in this thesis was part of an ongoing study into the electronic spectrum of FeO being conducted in this laboratory and begun prior to the author's arrival. Thus, while the present thesis deals with the electronic infrared system of FeO, this cannot be considered in isolation from the work on the orange system, which formed part of the subject matter of the thesis by Cheung (Ph.D., The University of British Columbia, 1981). Since the two projects were going on simultaneously for awhile, and in particular since the orange and infrared systems involve a common lower state, the two projects were interactive in nature, with information from one contributing to the analysis of the other and vice versa.

In light of this, although described in the section "Other Work Done in This Laboratory" (Section I.B), the author was partly involved with the work in which the spin-orbit intervals of the ground state were determined. On the other hand, tables of rotational lines of the orange system have been included in this thesis (Appendix I), although the author was only slightly involved in their determination. Justifications for this inclusion are (1) for completeness (since most of the line positions were not included in the thesis of Cheung) and (2) the fact that orange-system data were included in the ground state least-squares fit that forms part of this thesis.

CHAPTER I

INTRODUCTION

Iron monoxide, FeO. . . at first glance, a simple molecule: diatomic, consisting of two commonly occurring elements, relatively easy to obtain by several methods. Yet FeO possesses an electronic spectrum so complex it has repeatedly defied analysis, including attempts by a number of notable spectroscopists.

The present chapter summarizes these early investigations into the spectrum of FeO and culminates with a description of the recent cracking of the ground state problem in this lab by Cheung and Merer. The following chapters present a continuation of the investigation into the electronic spectrum of FeO, namely the analysis of the infrared system.

I.A. Historical Survey

Over the years, the spectrum of FeO has been observed in numerous laboratories, not always by design. Since the spectrum can be obtained simply by striking an iron arc in air, it had probably been observed on a number of occasions before it was actually identified. Early references to the spectrum of FeO have been summarized by Kayser (1) and by Eder and Valenta (2).

The most detailed of these early studies was that reported by Domek (3) in 1910. The emission spectrum obtained from an iron arc was found to exhibit a weak band in the green plus two bands in the yellow and red beginning respectively at 578.974 and 618.066 nm and both degrading towards the red. The latter two "bands" actually consisted of a large number of narrower bands and close-lying lines, the positions of which were tabulated. Comparison with the grating spectra obtained in this laboratory as part of the present study shows that individual rotational lines were resolved but that only the more intense lines were reported. This was considerably higher resolution work than that of many of the later studies (to be described shortly). No vibrational or rotational analysis was done, however, since this was prior to the development of modern quantum mechanical theory and its application to spectroscopy.

Howell and Rochester (4) made prism spectrographic observations of FeO in an arc flame during the early 1930s but gave no details of the spectrum or its analysis.

Richardson (5) also photographed the spectrum of an iron-arc flame and, in 1934, published the band-head positions of six red-degraded bands, together with the wavelengths of the fourteen strongest lines in the strongest band (head: 578.965 nm), but was unable to provide an analysis. Comparison with the present grating spectra shows that two of the fourteen lines (those with λ_{air} = 582.2182 nm and 582.8916 nm) are absent or very weak in our spectra.

Based upon absorption work with a prism spectrograph, Trivedi (6), in 1935, reported a continuous region of absorption, with a long wavelength limit of 250 nm. There is some doubt as to whether FeO was actually present, since the visible bands were not seen, though this may have been due to the experimental conditions, as explained by Trivedi.

The emission spectrum of FeO is also obtained, usually as an impurity, when CO is burned in air or oxygen if the carbon monoxide has been stored in steel cylinders. This is due to the formation of a small amount of iron pentacarbonyl. Not surprisingly, the spectrum is also obtained if iron pentacarbonyl is introduced deliberately into a flame, and this is one of the favorite sources that has been used over the years. This relationship between FeO, CO, and $Fe(CO)_5$ has been mentioned by Gaydon in several publications (7,8,9).

In fact, work on the spectrum of FeO formed part of Gaydon's PhD thesis in 1937 (10). He observed, at low resolution, a number of strong emission bands in the orange and near-infrared regions. This work was apparently not published, however (other than as the above-mentioned thesis), until the appearance of the (now well-known) book by Pearse and Gaydon, *The Identification of Molecular Spectra* (11).

Initially unaware of the work done by Gaydon, during the early 1940s Rosen also studied the spectrum of FeO, again at low resolution, this time by means of exploding wires as well as with an arc (12,13). During 1940 he studied the yellow region of the spectrum in collaboration with Delsemme (14) and later, with Malet (1942) (15), extended the investigation to the blue and photographic infrared. These investigators found that band systems observed in the orange and blue regions of the spectrum appeared to have the same lower state vibrational frequency (ω_0 = 875 cm^{-1} $\omega_0 x_0$ = 5 cm^{-1})[1] and thus probably possessed a common lower level, which they believed likely to be the ground state. They also observed bands in the near-infrared

---

[1]Standard spectroscopic notation is used throughout this thesis (16).

region, most of which they classified into a system having a lower state vibrational frequency of 955 cm^{-1} which does not agree with more recent work (this thesis), though they did recognize that some of the infrared bands belonged to a series having the 875 cm^{-1} frequency. They classified the orange bands into two systems, which they called A and B, with the A system being further subdivided into A_1 and A_2. The blue system was labelled C and that part of the infrared system having a lower state frequency of 955 cm^{-1} D. These designations, especially A and B, are still frequently referred to today, though another subdivision of the A system, introduced by Pearse and Gaydon (11), *viz.* A_i and A_{ii}, is sometimes used.

In 1952, Bass and Benedict (17), although not specifically looking for FeO, did in fact record its near-infrared spectrum while doing studies on the combustion of carbon monoxide containing a small quantity of iron pentacarbonyl. The spectrum was observed as an intense band system extending from 7 000 to 15 000 cm^{-1} Although the resolution was very low, Bass and Benedict were able to analyze the vibrational structure, and their analysis was basically correct. Their assignments of the bands as (2,0), (1,0), (0,0), (0,1), and (0,2) were correct for what is shown in the present work to be the $^5\Pi - X^5\Delta$ system. They did not, however, realize that there were two overlapping systems, so some of their sequence band labels were not correct.

In a compilation of metallic oxide spectra by Gatterer, Junkes, and Salpeter (18), Rosen revised much of the existing data on FeO but was still not satisfied with the proposed analysis of the band systems. He suggested that further work needed to be done.

During the course of flash photolysis experiments involving explosions of amyl nitrite, *n*-heptane, and oxygen mixtures containing ferrocene or iron pentacarbonyl additives, Callear and Norrish, in 1959-60 (19) observed not only the orange system (in emission and absorption) and the infrared system (in emission) but also a diffuse ultraviolet system (in absorption) between 241 and 243 nm. They reported the latter

system as a new feature of FeO, though we point out that there is a slight possibility that this was the continuous region mentioned previously as having been reported by Trivedi (6). This diffuse absorption band was seen again (at 241 nm) about 1966 by Callear and Oldman (20), who speculated that this may be a Rydberg type of transition and that it probably involves a low-lying state of FeO, but not the ground state. No further work has been done on this feature, and its true nature remains undetermined.

In 1962, Bass, Kuebler, and Nelson (21) recorded the FeO spectrum in absorption in selected parts of the visible and near UV regions using a flash heating technique. They observed some of the orange system bands and interpreted their presence in the *absorption* spectrum as indicating that their lower state was the ground state of the molecule, in agreement with Rosen's earlier interpretation. They did not, however, detect any absorption due to the blue system. This implied a different lower state for this system, a different conclusion to that arrived at by Rosen. They also obtained the diffuse absorption feature of Callear and Norrish at approximately 242 nm.

In 1966, Dhumwad and Narasimham (22) recorded the orange system at higher resolution than in any of the previous investigations, using an arc at low pressure. Their analysis showed that the system possessed simple R and P branches with no Λ-doubling. An attempt was made to analyze several of the bands in terms of a $^1\Sigma - {}^1\Sigma$ transition. However, this analysis was refuted by Barrow and Senior (23) three years later on the following grounds:

(a) The ground states of Fe and O are respectively ^{5}D and ^{3}P. These cannot give singlet molecular states.

(b) Comparison with other first-row transition metal oxides shows that the derived ground state internuclear distance is much too large:

VALUES OF r_e (nm) (from ref. (23))

ScO	TiO	VO	CrO	MnO	FeO
0.1668	0.1620	0.1589	0.1627	---	?0.197?

Barrow and Senior recorded the orange system using similar experimental conditions to those of Dhumwad and Narasimham. Their new analysis yielded the much more reasonable value of r_e = 0.1626 nm. They obtained the ground state constants (in cm^{-1}): ω_e = 880.53, $\omega_e x_e$ = 4.63, B_e = 0.512 71, a_e = 0.003 76. Their interpretation was that the lines analyzed probably belonged to the $\Omega' = 0 - \Omega'' = 0$ part of a multiplet $\Sigma - \Sigma$ transition, with the states most likely being $^5\Sigma$ or $^7\Sigma$.

West and Broida (24), in 1974, studied the visible and infrared systems at relatively low resolution in chemiluminescent flames. They observed some weak new bands in the orange region and a "new"[2] group of weak bands between 500 and 540 nm which they called the "Green System." Some of the new orange bands were found to be separated by the ground state vibrational spacing, $\omega''_e \simeq 880$ cm^{-1}, and the green system had upper and lower state vibrational constants the same as those given by Malet and Rosen for the blue system, although it did not *appear* to be connected to this system nor to the orange system when looking at the spectrum. They also did some laser-induced fluorescence and radiative lifetime studies on the orange system and obtained values of ω_e = 875.8 cm^{-1} and $\omega_e x_e$ = 4.6 cm^{-1} for the ground state. This ω_e value was in rather poor agreement with the value of Barrow and Senior (880.53 cm^{-1}), a point which we will return to shortly. Although they determined some additional spectroscopic constants, they were unable to settle the question of the natures of the states involved — in particular, was the ground state $^5\Sigma$, $^7\Sigma$, or what? Even $^3\Pi$ had once been proposed (by Lagerqvist and Huldt (25)).

---

[2]Possibly this was the weak green band mentioned previously as having been reported much earlier by Domek (3).

Shortly after this, Montano, Barrett, and Shanfield (26), while performing low-temperature Mössbauer studies on iron monomers and dimers in inert gas matrices, happened to obtain a six-line spectrum which they attributed to FeO. They found a large positive internal magnetic field at the Fe nucleus ($(3.52\pm0.06)\times10^{7}$ $A\cdot m^{-1}$ in an argon matrix). This was indicative of a high spin multiplicity for the ground state (27), but unfortunately did not remove the ambiguity as to what this state was since most of the candidates for ground state were of high multiplicity.

Engelking and Lineberger (27) studied FeO by means of photoelectron spectrometry of FeO^- in 1976, with mixed success. They obtained a ground state vibrational frequency of 970 ± 60 cm^{-1} which was in poor agreement with the previously accepted value of ω_e = 875–880 cm^{-1} They also observed another state lying 3990 ± 100 cm^{-1} higher. Their interpretation was as follows: The state with a vibrational frequency of 970 cm^{-1} was the true ground state (which they therefore labelled X), and the previously accepted ground state with a vibrational frequency of ~880 cm^{-1} was the excited state at 3990 cm^{-1} (which they labelled X'). Calling upon the theoretical predictions by Bagus and Preston (28) and Walch and Goddard (29), they assigned the X state as a $^5\Delta$ state and the X' state as a $^5\Sigma^+$ state.

Influenced by Engelking and Lineberger, DeVore and Gallaher (30), in 1978, attempted to obtain the infrared vibrational spectrum at ~970 cm^{-1} They claimed to have found this band at 943 cm^{-1} but this author finds the line assignments in their published spectrum unconvincing.

Weltner (31,32) attempted, unsuccessfully, to observe the ground state via ESR in a low-temperature matrix. As discussed by Weltner, this negative result was evidence that the ground state was an orbitally degenerate state, such as Engelking and Lineberger's $^5\Delta$ state.

Kay, Bartelt, and Byler (33) conducted flash heating-kinetic spectroscopy studies of gaseous FeO and obtained high-resolution electronic absorption spectra of the orange B system. Their measured rotational constants and band separations were in good agreement with the emission values of Barrow and Senior. The ease with which these bands were obtained in absorption in this and the previous absorption studies provided some supporting evidence for the lower state of these transitions being the ground state, as had been assumed prior to the work of Engelking and Lineberger.

So we see that as recently as 1978, despite the efforts of many people over the course of many years, not even the ground state, let alone any of the excited states, had yet been established. The questions still to be answered for the ground state were:

(i) Which of the observed states was the ground state?

and (ii) What was the identity of this state?

The choice of candidates had essentially been narrowed down to two: the state seen as the lower state in a number of studies having a vibrational frequency of ~880 cm^{-1} and labelled as either $^5\Sigma$ or $^7\Sigma$ by Barrow and Senior, versus the state with a vibrational frequency of ~970 cm^{-1} seen by Engelking and Lineberger and labelled by them as $^5\Delta$.

In an effort to clarify the situation, Green, Reedy, and Kay (34), in 1978, recorded the infrared vibrational spectrum of FeO in an Ar matrix at 14 K. They obtained values of ω_e = 880 cm^{-1} and $\omega_e x_e$ = 3.5 cm^{-1} That the species being studied was indeed FeO was established beyond a doubt by the identification of peaks due not only to $^{56}Fe^{16}O$ but also to the other three isotopomers $^{54}Fe^{16}O$, $^{54}Fe^{18}O$, and $^{56}Fe^{18}O$, with relative absorbances in agreement with the natural abundances of the isotopes of iron and the known oxygen isotopic composition of the reaction mixture. Any shift in vibrational frequency due to the matrix would not be expected to exceed about 1% of the observed value (34) and would probably be much less than this.

No state other than the ground state has ever been shown to be populated in matrix-isolated molecules near absolute zero (34). Hence this study definitively established the ground state of FeO as having a vibrational frequency of ~880 cm^{-1}. The conclusion was that the ground state was the lower state of the orange A and B systems and possibly of the blue, green, and infrared systems also.

(FeO had actually been seen previously (1977) in a low-temperature matrix by Abramowitz and Acquista (35) during the course of studies on FeO_2. They observed a frequency of 873 cm^{-1} in agreement with the $\Delta G_{1/2}$ value of Green, Reedy, and Kay. Of the two studies, that of the latter group is considered the definitive study on the subject due to the isotopic work performed.)

Since there cannot be a state lower than the ground state, the photodetachment spectrum of Engelking and Lineberger must now be reinterpreted. The discrepancy between 970 and 880 cm^{-1} leads to some uncertainty as to whether it was actually the $FeO^- \rightarrow FeO$ system that was seen at all. Assuming that it was, it may have been an excited electronic state of FeO that was produced by the laser photodetachment process, as suggested by Green, Reedy, and Kay (34). In this thesis we will assume that it was the ground state that was observed and attribute the discrepancy to experimental error or to interpretational error.

One possible cause for this could be that the vibrational peaks (v'_{FeO}, v''_{FeO^-}) assigned by Engelking and Lineberger as "(1,0)" and "(2,0)" may actually have contributions from transitions involving $v''_{FeO^-} = 1$ and 2. We point out that the energy difference between the peaks labelled as (0,1) and "(2,0)" corresponds very closely to three FeO vibrational intervals (using the correct ground state interval, rather than the value of Engelking and Lineberger) and the separation between (0,2) and "(2,0)" corresponds to four times this interval. Therefore, the peak labelled as "(2,0)" may actually be a superposition of the transitions (3,1) and (4,2). Similarly the peak labelled as "(1,0)" may actually be a superposition of (2,1), (3,2), and (1,0). While

the populations of the FeO^- v = 1 and 2 levels appear small from the intensities of the (0,1) and (0,2) bands, the Franck–Condon factors may favor the sequence bands, since the FeO^- vibration frequency is smaller than that of FeO.

Another anomaly visible in the spectrum published by Engelking and Lineberger, though not commented on by them, is that the peak labelled as "(2,0)" appears to have extra intensity relative to the other bands in the sequence "(0,0)", "(1,0)", "(2,0)", and (not labelled) "(3,0)." A Franck–Condon envelope for such a sequence cannot have any extra bumps in it. Here again, the reinterpretation given in the preceding paragraph could account for this. Yet another explanation will be presented later in this thesis (Section IV.D)

While the foregoing interpretation is admittedly pure speculation — it could be tested by redoing the experiment at higher resolution or at a different temperature — we have dwelt on this because, assuming that it was indeed the ground state of FeO that was seen, the work of Engelking and Lineberger is important in that it contains the only observation of the state at ~3990 cm^{-1} Although there is no experimental evidence as to the nature of this state, it is currently assumed to be a $^5\Sigma^+$ state on theoretical grounds (see Section IV.D). We point out, however, that in view of the uncertainty surrounding the ground state vibrational frequency, the value of 3990 cm^{-1} could easily be in error by an amount larger than the quoted ±100 cm^{-1}

We will have cause to return to the work of Engelking and Lineberger later in this thesis in connection with a new $^7\Sigma^+$ state found during the course of the present work.

Meanwhile, work on FeO continued in several laboratories around the world. McDonald (36), in 1979, photographed the orange systems in emission with a 3.4 meter Ebert spectrograph. He confirmed the analysis by Barrow and Senior of the orange A_{ii} bands and rotationally analyzed several other bands all having the same lower state as the A_{ii} bands but new upper state levels.

At about this same time, Harris and Barrow (37) also recorded the orange system on a 3.4 meter Ebert spectrograph (Jarrell-Ash). They extended the analysis of Barrow and Senior and determined that the bands involved in that earlier study belonged to a common, but highly perturbed, upper state level. They additionally analyzed bands belonging to three other, also highly perturbed, upper state levels. All the transitions analyzed were parallel ones, and no Q branches were found. The bands were shown to belong to a lower state vibrational progression having a frequency of 880 cm^{-1} thus leading to the conclusion, in view of the work of Green, Reedy, and Kay, that the orange system lower state is the ground state. They obtained the following values for the ground state (in cm^{-1}): $\omega_e = 880.61$, $\omega_e x_e = 4.643$, $B_e = 0.512\,72$, $a_e = 0.003\,760$.

Harris and Barrow were able to account for the poor agreement of the West and Broida vibration frequency value ($\omega_e = 875.8$ cm^{-1}). The latter investigators had neglected to allow for the effect of the rotational J-dependence on the vibrational intervals.

(In 1980, Trkula (38) also started work on FeO, as did Lindgren and Sassenberg (39) in 1981 or 2. Trkula obtained low-resolution spectra that showed the orange and blue systems, but did not show the green system, and he started some laser-induced fluorescence work on the orange system. This study by Trkula was terminated, however, upon his learning of the state of advancement of the corresponding studies being conducted in this lab. Lindgren and Sassenberg obtained spectra of the 550 - 620-nm region, but these were found to be similar to those already published by Harris and Barrow and by this lab, so no further analysis was done.)

Although the matrix-isolation study of Green, Reedy, and Kay had established which of the observed states was the ground state of FeO, neither this nor the more recent gas-phase studies were able to characterize the state involved (i.e. identify its

symmetry or multiplicity). For example, the orange-system bands observed by Harris and Barrow were all parallel-polarized, with simple R- and P-branch structure and no Q lines detected, but such structure would be consistent with any of the most commonly proposed transitions for these bands: $^5\Sigma - {}^5\Sigma$, $^5\Delta - {}^5\Delta$, $^7\Sigma - {}^7\Sigma$.

Several theoreticians have conducted *ab initio* investigations into the electronic structure of FeO. One study by Bagus and Preston (28) predicted three low-lying states: $^5\Sigma$, $^5\Pi$, and $^5\Delta$. The study concluded that the ground state is not $^5\Sigma^+$; thus leaving $^5\Pi$ and $^5\Delta$ as possibilities. Walch and Goddard (29) obtained similar results. Based on the work of these two groups, Engelking and Lineberger (27) gave a state ordering $^5\Delta$, $^5\Sigma^+$, $^5\Pi$, ... Michels (40), on the other hand, predicted that the ground state *is* $^5\Sigma^+$. His assignments for the upper states of the A and B orange systems were $^5\Sigma^+$ and $^5\Pi$, respectively, and for the infrared system, $^5\Pi$.

The theoreticians, being unable to come to agreement amongst themselves, were unable to help in characterizing the ground state. The lack of a low-temperature, matrix-isolated ESR spectrum would seem to eliminate Σ states, but more positive evidence was really needed to establish the identity.

Such was the state of affairs when work was begun in this laboratory. This work will be the subject of the next section and the following chapters; but first, brief mention will be made of a number of other FeO-related studies.

Various estimates of the dissociation energy of FeO have been made. Gaydon, in the first edition of his book, *Dissociation Energies and Spectra of Diatomic Molecules* (1947) (41a), gave a linear Birge-Sponer (42) extrapolation value of 480 $kJ \cdot mol^{-1}$ (5.0 eV) for the ground state:

$$FeO_{(g)} \rightleftharpoons Fe_{(g)} + O_{(g)} \qquad \Delta H_0^\circ = D_0^\circ = 480\ kJ \cdot mol^{-1} \qquad ...(I.A.1)$$

with the recommendation that this value be reduced by 20% to 390 $kJ \cdot mol^{-1}$ (4 ± 1 eV) to take into account the fact that deviations from linearity frequently occur.

By the third edition of this book (1968) (41(b)), the recommended value had been revised to 410 $kJ \cdot mol^{-1}$ (4.3±0.5 eV) on the basis of a number of other studies that had been done by this time.

More recently (1971), Balducci, de Maria, Guido, and Piacente (43) obtained a value of $D_0^\circ = 406 \pm 13$ $kJ \cdot mol^{-1}$ during mass spectrometric measurements of the vaporization of Apollo 12 lunar samples. The reaction studied was

$$FeO_{(g)} \rightleftharpoons Fe_{(g)} + \tfrac{1}{2}O_{2(g)} \qquad ...(I.A.2)$$

and the ΔH_0° obtained by second- and third-law calculations together with the accurately known dissociation energy of O_2 yielded the above value.

Jensen and Jones (1973) (44) obtained the value $D_0^\circ = 402 \pm 20$ $kJ \cdot mol^{-1}$ from spectrophotometric studies of iron-containing flames by second-law analysis only. The reaction studied was

$$Fe_{(g)} + OH_{(g)} \rightleftharpoons FeO_{(g)} + H_{(g)} \qquad ...(I.A.3)$$

By means of high temperature mass spectrometric measurements of the components of an effusion beam, Hildenbrand (1975) (45) determined, by third-law analysis, the value $D_0^\circ = 405 \pm 13$ $kJ \cdot mol^{-1}$. This time, the reaction looked at was

$$Fe_{(g)} + O_{2(g)} \rightleftharpoons FeO_{(g)} + O_{(g)} \qquad ...(I.A.4)$$

While these various recent values for $D_0^\circ(FeO)$ may appear to be in fairly good agreement with each other, as pointed out by Hildenbrand (45), caution must be exercised when interpreting the results obtained from equilibrium measurements. The values depend significantly on the particular molecular and spectroscopic constants used in the analysis. For example, Hildenbrand recalculated the results of Balducci *et al.* (see above) using the constants that he had employed in his analysis and obtained $D_0^\circ = 427$ $kJ \cdot mol^{-1}$, considerably different from the value of 406 $kJ \cdot mol^{-1}$ obtained

by Balducci *et al.* The spectroscopic constants of FeO used by Hildenbrand were those of Barrow and Senior (23).

Thus, although thermodynamic studies such as these hold the potential of yielding a much more accurate value for the dissociation energy than a simple Birge–Sponer type of extrapolation, they still require accurate spectroscopic values.

For completeness, we briefly mention several other specialized studies on FeO not directly related to the present work. Intensity measurements of the ground state vibrational band were made during the early 1970s by von Rosenberg and Wray (46), who additionally studied the kinetics of reaction (I.A.4), as did also Fontijn and Kurzius (47) around the same time. Also at about this time, absorption coefficients for the infrared vibration–rotation spectrum were calculated by Fissan and Sulzmann (48).

I.B. Other Work Done in This Laboratory (49,50,51,52)

I.B.1. Characterization of the ground state

Work was begun in this laboratory on the electronic spectrum of FeO in September, 1979. High resolution spectra of the region 550 - 630 nm were photographed, following which a laser-induced fluorescence study of a number of bands of the orange system was performed. This provided the breakthrough which finally allowed for the rotational analysis of the ground state and identified the ground state as being a $^5\Delta$ state.

At the time work was started, the lower level of the orange system had been established as the ground state of the molecule by the matrix isolation study of Green, Reedy, and Kay (34), but the classification of this state was still undecided upon. The possible candidates, supported by various theoretical studies, were $^5\Sigma^+$, $^7\Sigma^+$, or $^5\Delta$.

The unravelling of the problem proceeded as follows. The band first studied was the 582-nm band, since it occurred in a comparatively uncrowded region of the spectrum. This band, which was one of the bands also studied by Harris and Barrow (37), exhibits a number of small rotational perturbations in which the lines appear doubled, with two lines of *equal* intensity. Such a pair of lines could be produced either by an *exact* coincidence of perturbed and perturbing levels or by Λ-doubling. The existence of *several* exact coincidences would seem rather unlikely, so Λ-doubling was the more probable explanation. The Λ-doublet splitting had been too small to resolve in the spectra of Dhumwad and Narasimham (22) or those of Harris and Barrow or (at other J values) in the current grating spectra, but a sub-Doppler intermodulated fluorescence spectrum of the ***unperturbed*** line R(15) at a resolution of about 75 MHz showed that Λ-doubling was indeed present, there being two equally intense components having a separation of about 120 MHz (51). Lower J lines, however, such as R(10), did not show any resolvable Λ-doubling. Thus Λ-doubling

was present but was small and J-dependent.

Since Λ-doubling cannot occur in Σ states, which are non-degenerate, the existence of Λ-doubling indicated that the states involved were not Σ states.

Harris and Barrow showed that the 558-nm band, which was the (0,0) band of Delsemme and Rosen's (14) A_1 system, possessed a common lower level with the 582-nm band (which, incidentally belongs to Delsemme and Rosen's B system). The 558-nm band had been studied previously by Barrow and Senior (23), who had postulated that the states involved had $\Omega = 0$. Since, to first approximation, Λ-doublet splitting is given by $[J(J+1)]^{\Omega}$ for $\Omega = 0$ a constant, J-independent Λ-doublet splitting would be expected, with any J-dependence being small relative to this. This was not what was observed, a fact which would imply that either the constant Λ-doubling term in the lower state was being cancelled by an equal constant term in the upper state (not very likely) or that $\Omega \neq 0$.[3]

Q lines are forbidden for $\Omega' = 0 \leftrightarrow \Omega'' = 0$ transitions in Hund's coupling cases (a) and (c) and for $\Sigma - \Sigma$ transitions in case (b) but are allowed for other transitions (16(a)). Although Barrow and co-workers (23,37) had not found any Q lines, armed with the above new evidence that Ω may not have the value 0 and since the existence of Λ-doubling showed that the states were not Σ states, a search was made for Q lines in the grating spectra. A branch was indeed found and its numbering established by plotting the line positions against $n(n+1)$, where n was an arbitrary running number, and choosing the best straight line. The analysis of the Q-branch was confirmed with rotationally resolved laser-induced fluorescence experiments.

The lowest-J Q line observed in the grating spectrum was Q(4). This was confirmed as being the lowest-J line by the laser-induced fluorescence work: while excitation of higher-J Q lines gave R-, Q-, and P-branch emission, excitation of the

---

[3]Ref. (49) seems to imply that the very existence of Λ-doubling is the reason why $\Omega \neq 0$. This is not correct. The real reason is as presented here.

Q(4) line yielded only Q(4) and P(5) emission (no R(3) emission). This meant that $\Omega' = \Omega'' = 4$.

Several of the other bands studied by Harris and Barrow were also studied and all were shown to possess Q branches and to have J = 4 first Q lines. Some of these bands form a lower-state vibrational progression. As shown by Harris and Barrow and confirmed here, the vibrational constants are in close agreement with the matrix-isolated values of Green *et al.* (34):

Gas:	$\omega_e = 880.61\ cm^{-1}$	$\omega_e x_e = 4.64\ cm^{-1}$
Matrix:	$\omega_e = 880.02\ cm^{-1}$	$\omega_e x_e = 3.47\ cm^{-1}$

Therefore the ground state of FeO contains an $\Omega = 4$ spin-orbit component.

Of the three possible candidates for the ground state ($^5\Sigma^+$, $^7\Sigma^+$ or $^5\Delta$), only $^5\Delta$ is consistent with the presence of Λ-doubling and only $^5\Delta$ possesses an $\Omega = 4$ component. The Ω values for a $^5\Delta$ state run from 0 to 4, whereas the highest Ω values for $^7\Sigma^+$ and $^5\Sigma^+$ are 3 and 2, respectively. Thus the ground state of FeO was finally established as being a $^5\Delta_i$ state.

All subsequent work performed in this laboratory has yielded no information inconsistent with this assignment and in fact has firmly established it as being correct.

I.B.2. The orange system

All of the bands (actually subbands) studied in the work described in the previous section involved $\Omega' = \Omega'' = 4$ levels as did, it is now known, all subbands which had ever been rotationally analyzed by previous investigators (22,23,24,37). Subbands involving other spin components must also be present. Following submission of the foregoing work for publication (49), continuing laser-induced fluorescence experiments on the orange system did eventually find, not one, but several subbands involving each of the Ω values 0, 1, 2, and 3.

The prominence of the $\Omega = 4$ subbands results from the fact that at this high an Ω value the Λ-doubling is usually not resolved, at least not until high J values, so that the lines are effectively twice as strong as those of other subbands where the Λ-doubling causes resolved splittings often even at low J values. In the case of absorption experiments, the $\Omega = 4$ subbands are additionally enhanced, especially for $v'' = 0$, due to the Maxwell-Boltzmann distribution that governs the populations of the levels. Since the effective temperature of the molecules involved in the excitation spectra obtained in this lab was roughly 350 K, the $\Omega'' = 4$ substate — being the lowest in energy of the five inverted $^5\Delta$ substates, which have a spin-orbit separation of about 190 cm^{-1} (see next section) — is heavily favored over the other substates.

A total of 34 subbands (including two ^{54}FeO isotopic subbands), lying in the wavelength regions 558-564 and 579-623 nm were rotationally analyzed in this laboratory. These involve over 20 Ω' substates lying between 16 350 and 18 550 cm^{-1}. Every one of these substates is extensively perturbed, and the rotational analysis of most would not have been possible without the use of rotationally resolved laser-induced fluorescence.

The measured line positions of the orange system are presented in Appendix I. A detailed description of the individual subbands and corresponding upper state energy levels has been given in ref. (51) and will not be repeated here. Instead we describe only the overall pattern which emerged from this study.

The upper state of the orange system is a $^5\Delta_i$ state, together with a large number of extra Ω substates. The $^5\Delta$ state has a B value of about 0.475 cm^{-1} corresponding to a bond length of 0.169 nm. Some of the "extra" substates *may* form another $^5\Delta_i$ state, but this is much less certain.

When the upper energy levels are plotted against J(J+1), many of the substates show marked curvatures to their plots over and above that caused by centrifugal distortion. Such curvatures indicate interaction with fairly distant perturbing

states via large interaction matrix elements, and the matrix elements are rotation-dependent and/or the zero-order energy separations are rotation-dependent. In some cases, the curvature is probably due to spin-uncoupling, with the "fairly distant perturbing states" just being other Ω substates of the same vibrational level of the same case (a) state, acting via the $-2B\underset{\sim}{J} \cdot \underset{\sim}{S}$ operator,[4] although it is not always clear which of the observed (or unobserved) levels are the other Ω components.

Other instances of curvature are due to avoided crossings, with the interactions being either homogeneous or heterogeneous in nature. An example of the latter effect is shown in Fig. 1, in which the rotation-dependent nature of the interaction between the $\Omega = 2$ and $\Omega = 3$ upper levels of the 592- and 585-nm bands is clearly seen. The large difference between the B values of these substates (as determined at low J before the "onset" of the interaction) indicates that the substates belong to two different electronic states. In this case the interaction is via the $-2B\underset{\sim}{J} \cdot \underset{\sim}{L}$ operator. This type of perturbation has proved to be extremely useful in that the resultant mixing of the upper state levels of different Ω' values has allowed the determination of the spin-orbit coupling of the ground state, as will be discussed in the next section.

In addition to the perturbations causing large overall curvatures, *numerous* small perturbations are seen throughout the upper states of the orange system in the form of local avoided crossings.

From arguments based on the anomalous vibrational intensity patterns observed, the conclusion is reached in ref. (51) that many of the observed levels probably would not, in isolation, possess transition moments to the ground state. They obtain their oscillator strengths by various interaction mechanisms. In view of the large energy separations between these levels and the levels from which they borrow intensity, the interaction matrix elements in a case (a) basis must be very large (hundreds of cm^{-1}

---

[4]Vectors are denoted by a $\sim$ symbol in this thesis.

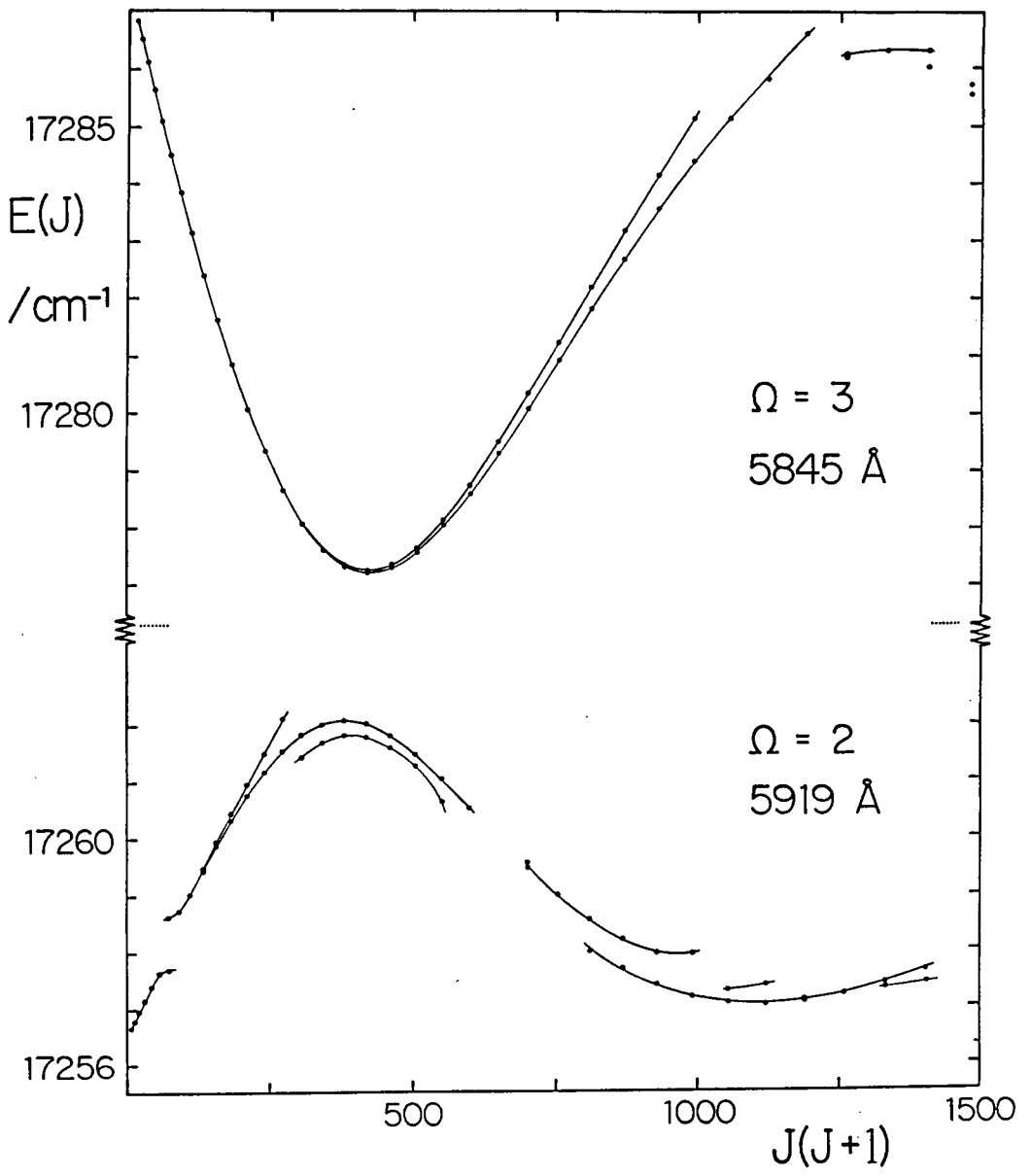

Fig. 1. Interaction between the $\Omega' = 2$ and $\Omega' = 3$ substates of the 585– and 592–nm bands. Upper state energy levels are plotted as a function of $J(J+1)$ after having been scaled by subtraction of the quantity $0.428J(J+1) - 10^{-6}J^2(J+1)^2$. The separation between the two components has been reduced by ~12 cm^{-1} A number of small local avoided crossings and splitting apart of the Λ–doublet components are apparent in addition to the large interaction between the two substates.

units). This suggests that electrostatic interactions are present, in addition to the more common spin–orbit interactions. Electrostatic interactions have similarly been proposed to explain some of the effects in the MnO spectrum (53).

Yet another feature is the presence of numerous branch fragments that can be followed for only a few J values and that have non–Boltzmann intensity distributions, yet which bear no simple relation to a pattern of avoided crossings. These also appear to result from levels which have no zero–order transition moments of their own, and which obtain small transition moments by spin–orbit or some other form of homogeneous mixing with comparatively distant states having the same Ω' value. In this case, the oscillator strengths picked up are small. The observed intensities vary erratically with J because of interactions with other such states that have also picked up small transition moments by similar means, but which have different B' values. Where the transition moments happen to reinforce for several J values, a "branch fragment" appears. Such effects commonly occur in perturbed polyatomic spectra (e.g. CS_2 (54,55)), but have apparently not been encountered before in diatomic molecules.

In short, the upper states of the orange system are extremely complex. The density and magnitude of the rotational perturbations are quite exceptional for a diatomic molecule and are more comparable with the notorious visible system of NO_2 (56,57,58). Although the FeO orange system upper states basically belong to Hund's coupling case (a), they show strong tendencies toward Hund's case (c) coupling.

I.B.3. Ground state spin–orbit intervals

As mentioned in the last section and shown in Fig. 1, the upper levels of the 592– and 585–nm bands, with $\Omega' = 2$ and 3 respectively, perturb each other. The spin–orbit components belong to different electronic states, and the rotational–electronic matrix element is

$$\langle v\,\Lambda\,\Omega=3\;J\,|-2B\underset{\sim}{J}\cdot\underset{\sim}{L}|\;v'\;\Lambda-1\;\Omega=2\;J\rangle$$

$$= -\langle v\,\Lambda\,|BL_{+}|\;v'\;\Lambda-1\rangle\,[J(J+1)\;-\;6]^{1/2} \qquad \text{...(I.A.1)}$$

where we find $\left|-\langle v\,\Lambda\,|BL_{+}|\;v'\;\Lambda-1\rangle\right| = 0.374\ \text{cm}^{-1}$

The result of this interaction is that the substates mix with each other. In the absence of such mixing, transitions to the ground state would be purely parallel transitions ($\Delta\Omega = 0$) and there would be no way of accurately determining the separations between the ground substate levels. As a result of the mixing, however, $\Delta\Omega = \pm 1$ transitions can occur. That is, because the upper state wavefunctions are really mixtures of $\Omega' = 2$ and $\Omega' = 3$ wavefunctions, transitions to both $\Omega'' = 2$ and $\Omega'' = 3$ levels of the ground state can occur from a single upper level. The difference gives directly the ground state spin-orbit separation between the $\Omega'' = 2$ and $\Omega'' = 3$ substates.

Figure 2 shows the resolved laser-induced fluorescence obtained upon excitation of the R(20) line of the 585-nm band. Four fluorescence lines result, arranged in two pairs separated by about 192 cm^{-1} One pair, the excited R(20) line together with P(22) has a separation (ground state rotational combination difference, Δ_2F'') showing that this pair has $\Omega'' = 3$. The other two, another R(20), P(22) pair, likewise has $\Omega'' = 2$. Laser excitation of either member of the latter pair gives the same resolved fluorescence pattern.

The intensity of the $P_3(22)$ line, where the subscript denotes $\Omega'' = 3$, is greater than that of the $P_2(22)$ line (Fig. 2). (The R(20) line intensities cannot be directly compared because of laser light scattering at the excitation frequency.) This indicates that the upper state wavefunction has more $\Omega' = 3$ character than $\Omega' = 2$ character. Beyond $J = 30$, the states become essentially completely mixed, so that four equally intense lines are obtained in the resolved fluorescence spectra.

The weak 587-nm band, which has an upper level that is primarily $\Omega' = 3$, also gives $\Omega'' = 2$ spin-orbit satellites. The interacting $\Omega' = 2$ level is again probably

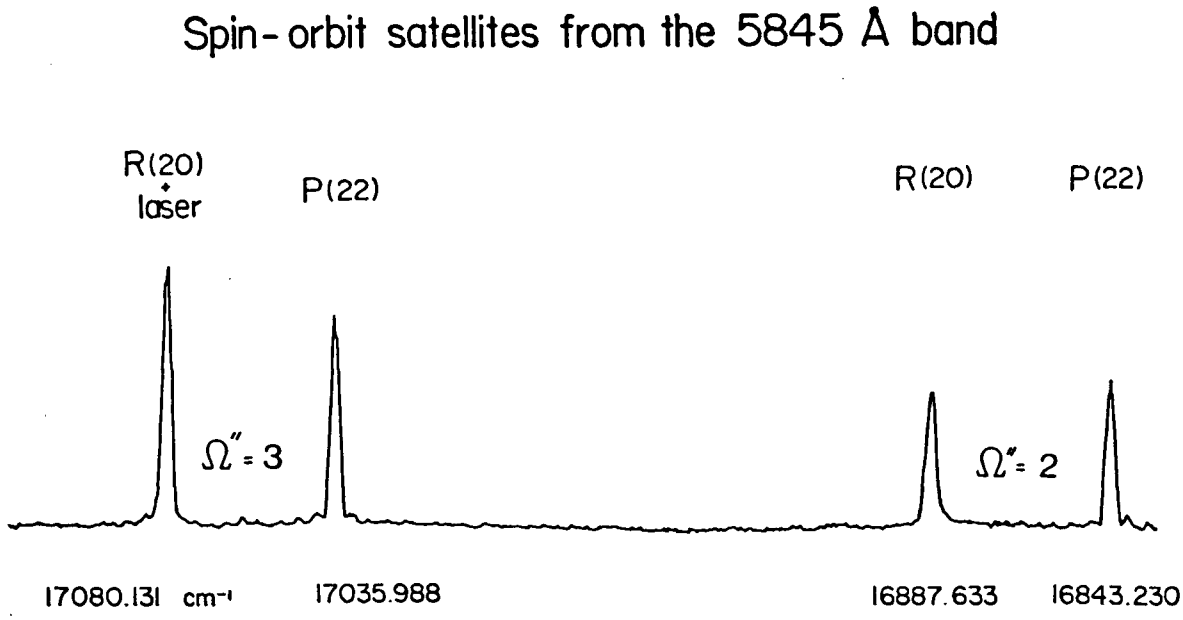

Fig. 2. Rotationally resolved fluorescence of FeO excited at 17 080.131 cm^{-1} Because of perturbations in the excited state the $\Omega' = 3$ level emits to both the $\Omega'' = 2$ and 3 components of the ground state, permitting determination of the $\Omega = 2-3$ spin–orbit interval.

the upper level of the 592-nm band.

Altogether, it has been possible to measure the spin-orbit separations between the $\Omega = 2$ and $\Omega = 3$ substates of the $v = 0$ level of the ground state for almost every J value between 11 and 34.

Likewise, the $\Omega'' = 1-2$ separation has been measured from spin-orbit satellites induced by an unseen $\Omega' = 1$ level in the $\Omega' = 2$ upper level of the 582-nm band. Unfortunately, this separation has only been measured for one J value ($J = 21$) and even for this one, the lines are weak and blended. The $\Omega'' = 1-2$ interval is therefore not as well determined as the 2-3 interval.

Weak spin-orbit satellites occur fairly commonly in the resolved fluorescence of many of the bands of the orange system. Since the upper state spin-orbit separations are very large and since the spin-orbit satellites are often seen at quite low J values, these must arise from rotational-electronic interactions between different electronic states, caused by the $-2B\underset{\sim}{J} \cdot \underset{\sim}{L}$ operator, rather than from spin-uncoupling effects within a single electronic state. The frequency of occurrence of these satellites indicates that such interactions are widespread.

Unfortunately, other than in those cases already mentioned, the extra lines resulting from these interactions are too weak to identify in the laser excitation spectra, so accurate measurements of the line positions have not been possible. Thus only the $\Omega'' = 2-3$ and (less accurately) 1-2 intervals of the $v = 0$ level have been measured. This does, however, provide enough information to determine the major spin-orbit parameters, not only for the ground state $v = 0$ level, but for the other observed vibrational levels ($v = 1-3$) as well (see Section IV.C).

I.C. Reasons for studying FeO

Prior to the work done in this lab, not even the symmetry classification of the ground state was known, let alone that of any of the excited states. Over and above the challenge of being the first group to establish such a seemingly fundamental property as the classification of the ground state, the information is itself very useful in diverse ways.

Comparison of the properties of FeO with those of other transition metal oxides yields information regarding trends across the periodic table and down the Fe, Ru, Os column — such trends as the change in ground-state bond length and the relative energy ordering of the $4s\sigma$ and $3d\delta$ molecular orbitals (Section III.K) as one progresses across the first-row transition metal oxides, and the effects of shielding as the d orbitals become progressively filled.

As described previously (Section I.A), theoreticians have been unable from purely *ab initio* arguments to correctly predict the energy ordering of the states of FeO. Experimental determination of the correct energy ordering should help the theoreticians refine their basis sets.

FeO possesses such esoteric states as $^5\Phi$, $^5\Delta$, $^5\Pi$, $^5\Sigma$, and $^7\Sigma$. Such states are comparatively rare and little has so far been published about them — e.g. the rotational matrix elements for $^5\Delta$ and $^5\Phi$ states are not available in the literature, and had to be worked out (Section III.H). Of the three types of states with which the present thesis is mainly concerned, only examples of $^5\Pi$ states have ever been reported and rotationally analyzed and these only in one molecule (CrO — also, incidentally, studied in this lab (59,60)); to the author's knowledge, $^5\Delta$ and $^5\Phi$ states have never been reported, although there is indirect evidence for the presence of a $^5\Delta$ state in CrO (60).

It has previously been indicated (Section I.A) that accurate moments of inertia and vibration frequencies are required for the most reliable third-law treatments of the

high temperature equilibria from which dissociation energies are derived. Moreover, the ground state and any nearby states must be well-characterized in order to establish the electronic partition function. The importance of this is illustrated by TiO (61). The ground state could be $^1\Sigma^+$, $^3\Sigma^-$, or $^3\Delta$ according to various qualitative arguments. The corresponding electronic degeneracy factors, if only one of these states contributes, would be 1, 3, or 6, respectively, with corresponding contributions to the free energy (at 2500 K) of 0, 23, or 38 $kJ \cdot mol^{-1}$, respectively. The difference between these values cannot be ignored when calculating an accurate value for the dissociation energy. In actual fact, the ground state is known to be $^3\Delta$ (62), but a $^1\Delta$ and a $^1\Sigma^+$ state lie very close to the ground state and contributions from all three states must be considered. In FeO, if the ground state were a $^5\Sigma^+$ state as once thought, the electronic partition function, q_e for this state in isolation would be 5, whereas for the actual $^5\Delta$ ground state it is 10 (ignoring the spin-orbit intervals; 7.8 taking them into account, at 2000 K). A $^5\Sigma$ state at 3990 cm^{-1} would have $q_e = 0.3$ at 2000 K (a typical temperature in the mass spectrometric methods used for FeO dissociation energy determinations). We show in this thesis that there is also another low-lying state, a $^7\Sigma$ state. For this, $q_e = 1.5$ at 2000 K, assuming this state to have its $v = 0$ level at 2100 cm^{-1}. This state therefore has a significant population relative to the ground state, and possibly even higher than indicated here if the level detected has $v > 0$. Thus, a thorough description of the low-lying states is of importance to the accurate determination of the dissociation energy.

An application where accurate thermochemical data (such as dissociation energies and ionization potentials) are required is upper atmospheric research. Chemiluminescence and resonance fluorescence of FeO were studied by Best and co-workers (63) upon release of iron pentacarbonyl from a rocket into the atomic oxygen-rich region of the upper atmosphere. The formation of FeO from $Fe(CO)_5$ plus atomic oxygen and its destruction to Fe and O_2 were studied.

An example of a more direct application of spectroscopic information to "atmospheric research" was provided by the detection of FeO, amongst other species, in a meteor as the meteor passed through the atmosphere. Ceplecha (64) was able to attribute 157 lines to the FeO molecule. Individual rotational lines or groups of lines were identified by comparison with the tables published by Domek (3). In fact, FeO turned out to be the third brightest molecular species visible in the whole meteor spectrum and the second brightest, behind only N_2, in the continuum part of the emission. The meteor was of cometary origin, and thus the information derived is of use not only in studying the composition of meteors but of comets also. The published line positions resulting from work in this laboratory should be of use in future studies of this sort.

Proceeding farther from the earth's surface, FeO is potentially of great astrophysical importance because of the high cosmic abundances of both Fe and O. Optical absorption spectra have shown the presence of the metal oxides TiO, VO, CrO, YO, ZrO, and others in the atmospheres of M stars (65). Since FeO is formed at relatively high temperatures in the laboratory it could be abundant in the atmospheres of late-type stars and/or circumstellar shells. Although TiO and CaO have not been found in molecular clouds despite radio-wavelength searches (66), gas-phase Fe is more abundant than Ti and Ca in interstellar clouds, so FeO is a potential species to be found there. Again, such searches are dependent on laboratory-obtained line positions by which to identify the astrophysically-observed frequencies.

Delsemme and Rosen (14) have pointed out the close agreement between the position of the R-head of the 579-nm band and one of the previously unidentified lines in the solar spectrum. This line is listed at 578.9767 nm in the *Revision of Rowland's Preliminary Table of Solar Spectrum Wave-lengths* (1928) (67) and also appears as a weak line at 578.976 nm in the more recent atlas of Delbouille, Roland,

and Neven (68). The first "line" of the yellow band measured by Domek (3) occurs at 578.974 nm, which is in very good agreement with the solar line. The higher resolution grating spectra obtained in this laboratory show that the R-head of the 579-nm band actually occurs at 578.963 nm. (Richardson (5) reported 578.965 nm, in good agreement with our value.) There are, however, several other intense lines to the long wavelength side of this so that Domek's "line" is really a blend. We therefore conclude that the R-head (actually several lines) of the 579-nm band is a *possible* assignment for this solar spectrum line.

Richardson (5) compared the wavelengths of fourteen of the strongest lines in the 579-nm band (not in the region of the head) with the line positions present in the spectrum of a sunspot. Although good matches were found for twelve of the fourteen lines, the other two were conspicuously absent in the sunspot spectra.[5] The conclusion was that FeO was either absent from the sunspot or not present in sufficient abundance to be detected.

Lest the reader be left with the impression that a study of the spectrum of FeO is of use only to theoreticians and star-gazers, the following examples illustrate "down-to-earth" applications.

Garger (69) studied the spectrum of the Bessemer flame and found that lines for FeO and atomic Fe predominate in the spectrum during the second half of the fusion operation and that the spectrum could be divided into 5 periods, with each period having characteristic lines. This research could lead to insight into mechanisms occurring in this industrially important process.

It is known that a number of transition metal compounds act as antiknock agents in spark ignition systems. Ferrocene and iron pentacarbonyl are two such compounds which have been studied in this regard by Callear and Norrish (70,19) and by Erhard (71,72). These investigators performed flash photolysis experiments in which

---

[5]These are *not* the same two lines reported in Section I.A as being absent in our grating spectra.

ferrocene or iron pentacarbonyl were used as additives to various fuel mixtures in the presence of oxygen. Spectroscopic observations of the resultant explosions detected, amongst other species, the presence of FeO. In fact, the FeO visible and infrared emission spectum occurs with extraordinary brilliance under these conditions, and it was even speculated (70,19) that this FeO emission could be responsible for the antiknock behavior of these compounds: the emission could affect the temperature of the burning gas by radiative cooling and/or propagating centers of preignition could be deactivated by electronic excitation of FeO. While this mechanism has been cast into doubt by the later work of Erhard, both groups of workers used the spectrum of FeO extensively to monitor the course of the explosions and thus helped advance mankind's knowledge of how to prevent knocking in spark ignition engines.

Finally, we point out that the infrared system, the analysis of which forms the basis of this thesis, has never been studied previously at high resolution. This alone is justification for the project!

I.D. Some Very Recent Studies Based on the Results of the Present Work

In Section I.A the history of research on FeO was traced prior to the beginning of work in this laboratory. In Section I.C an attempt was made to justify the present study. We now continue the historical review and present some very recent studies which have been done or are being done or will be done. All these studies are based in part on information obtained in this laboratory. The work has already proved useful; . . . what better justification than this?

While working out the matrix elements for a $^5\Delta$ state for the first time (Section III.H), the problem of how to handle the Λ-doubling in the $X^5\Delta$ state came up. This led to the question of Λ-doubling in Δ states in general. In the past, Λ-doubling in Δ states has often been considered too small to be of any significance, since it would be a fourth-order effect. It has been resolved on previous occasions, but only in a very few molecules. Those that the author is aware of are: in the $A^2\Delta_{5/2}$ state of PtH (73), in several $^2\Delta$ states of NiH (74), in the $X^6\Delta_{1/2}$ state of FeCl (75), in a $^4\Delta - {}^4\Delta$ transition of FeH (76), and, reported very recently, in the $A^2\Delta$ state of CH (77). At the time of the early stages of the current project, no detailed treatment of Λ-doubling in Δ states had yet been published. (Recently a partial treatment for the case of a $^6\Delta$ state has been performed by Delaval and Schamps (75), and more recently still Brazier and Brown (77) have dealt with the $^2\Delta$ case.) Early in the present work, Λ-doubling in the $\Omega = 0$ component of the $X^5\Delta$ state was handled in a phenomenological manner by means of the terms $\pm\frac{1}{2}[o + o_J J(J+1)]$ in the diagonal positon of the energy matrix. However, upon finding Λ-doubling in the $\Omega = 1$ substate as well, it was decided that such an approach was no longer adequate. Clearly the entire phenomenon of Λ-doubling in Δ states needed to be studied. This provided a theoretical project for Cheung and Merer, the results of which are to be published shortly (78); this paper will undoubtedly become the definitive work on the subject of Λ-doubling in Δ states.

As stated in previous sections, theoreticians have been unable to correctly predict the energy-ordering of the lower states of FeO. This statement still stands, although the situation is improving. Krauss and Stevens (79) have very recently performed multiconfiguration self-consistent-field (MC-SCF) calculations for FeO and RuO. In the case of FeO, five states are calculated to lie within 0.1 eV of each other, of which $^7\Sigma^+$ is the predicted ground state — the order, from lowest in energy to highest, is $^7\Sigma^+ < {}^5\Pi \lesssim {}^5\Phi < {}^5\Delta < {}^5\Sigma^+$. While unable to predict the correct ground state, the complete active space (CAS) MC-SCF wavefunctions provide a qualitatively correct description of the electronic structure as shown by comparison of the calculated spin-orbit coupling constants, A, with the experimental values determined in this laboratory (in cm^{-1}):

	$^5\Delta$	$^5\Pi$	$^5\Phi$
calculated:	-84	-203	-40
experimental:	-95	~-217	~-47.

Agreement is also fair for the ground state bond length:

calculated:	$r_e = 0.168$ nm
experimental:	$r_e = 0.162$ nm

but poor for the vibrational frequency:

calculated:	$\omega_e = 681$ cm^{-1}	$\omega_e x_e = 6.3$ cm^{-1}
experimental:	$\omega_e = 880$ cm^{-1}	$\omega_e x_e = 4.6$ cm^{-1}

The agreement is better for RuO. The calculated natural orbitals and their occupancies (i.e. electron configurations) for the various states are useful for understanding the bonding in FeO, and, given the experimental fact that the $^5\Delta$ state is the ground state, Krauss and Stevens were able to formulate an aufbau for the ground states of most of the first and second row transition metal oxides in terms of these orbitals.

In the last section, the importance of a correct experimental description of the lower states of a molecule for the accurate determination of such thermodynamic properties as the dissociation energy was discussed. Most of the previous determinations of the FeO dissociation energy have assumed a $^5\Sigma$ ground state. Armed with the information provided by this laboratory that the ground state is actually a $^5\Delta$ state, Smoes and Drowart (80) have recently made a new determination of the dissociation energy by the mass spectrometric Knudsen cell method:

$$D_0^0(FeO) = 403 \pm 8 \text{ kJ} \cdot \text{mol}^{-1}$$

This value should be more reliable than any of the previous determinations. The authors have critically compared this value with the literature data and have explained a number of discrepancies. We point out, however, that the low-lying state tentatively identified as a $^7\Sigma$ state, discovered during the course of the present work (Section IV.D), was not allowed for in the determination of the above D_0^0 value, since the existence of this state had not at that time been published. The foregoing value for D_0^0, while being an improvement over the previous values in the literature, may therefore not yet be the ultimate determination.

The potential astrophysical importance of FeO due to the high cosmic abundances of both Fe and O was indicated in the previous section. This prompted a search by Merer, Walmsley, and Churchwell (65) for FeO in a number of astrophysical environments based on line frequencies predicted by the work of this laboratory. The pure rotational lines searched for and their predicted rest frequencies are as follows[6]:

$^5\Delta_4$	v = 0	J = 5–4	153.141 GHz
$^5\Delta_4$	v = 1	J = 5–4	152.014 GHz
$^5\Delta_3$	v = 0	J = 5–4	154.058 GHz

---

[6]Later work (Endo, Saito, and Hirota (81) and this thesis) has refined the frequency values slightly to 153.135, 152.013, and 154.060 GHz, respectively. The conclusions of ref. (65) are not altered.

with 3σ errors of ± 0.005 GHz. Although a selection of molecular clouds, stars, supernova remnants, and planetary nebulae were searched, the results were negative in all cases. The search was not in vain, however, as the absence of FeO also carries information. In the Orion nebula, for example, at most 2×10^{-7} of the cosmic abundance of iron can be in the form of FeO, otherwise it would have been detected. One cause for the lack of FeO could be condensation of interstellar iron onto grain surfaces, thus depleting the amount available in the gas phase. The very low value for the upper limit on the abundance of FeO implies that such depletion must be very efficient. Other possible reasons for the low abundance of FeO are discussed in the paper by Merer, Walmsley, and Churchwell (65).

P. Feldman (82) has recently expressed interest in conducting further astronomical searches for FeO (and other metal oxides) at other frequencies and has requested predicted frequencies from this laboratory. The values obtained in this thesis have been forwarded to him.

Meanwhile back on earth, Endo, Saito, and Hirota (81) have detected and measured six pure rotational lines of FeO in the millimeter-wave region, observations made possible by the predictions of this work. The measured frequencies are listed in Table I and, because of their high accuracy, have been included in the latest least-squares fits presented in this thesis (Section IV.C).

Cheung and Radford (83) and Evenson (84) are currently looking at the far-infrared laser magnetic resonance (LMR) spectrum of FeO. Again, line-frequency predictions from the present work have been communicated to both groups. These will show where to look and will help in the interpretation of their spectra.

TABLE I. Millimeter-wave pure-rotational transitions of FeO[a]

J' ← J"	Ω	Frequency[b]
5 ← 4	4	153.135 259 (55)
6 ← 5	4	183.757 163 (23)
5 ← 4	3	154.059 726 (31)
6 ← 5	3	184.867 223 (14)
5 ← 4	2	154.948 453 (19)
6 ← 5	2	185.932 444 (20)

(a) Measurements by Endo, Saito, and Hirota (80).
(b) Values in GHz; numbers in parentheses are the standard deviations of the measurements in units of the last two figures.

CHAPTER II

EXPERIMENTAL DETAILS

II.A. Introduction

A variety of methods of obtaining FeO have been successfully employed in the past. In emission work, Rosen and co-workers (12,13,14,15) used arcs and the method of exploding wires to study the visible and near infrared regions. Arcs were also employed by Domek (3) (visible), by Dhumwad and Bass (85) (orange system), by Dhumwad and Narasimham (22) (orange), and by Barrow and Senior (23) (orange). Low-pressure chemiluminescent flames obtained by reacting Fe, evaporated from a furnace, with O_3, N_2O, NO_2, or discharged O_2, in a flowing inert gas allowed West and Broida (24) to study the infrared, orange, and blue systems at a relatively low temperature (700 K). They also produced FeO at atmospheric pressure by seeding an oxygen-acetylene flame with $Fe(CO)_5$. Bass and Benedict (17) obtained the near infrared spectrum during combustion studies of CO containing a small quantity of iron pentacarbonyl. McDonald (36) used an electrodeless discharge through a mixture of $Fe(CO)_5$, O_2, and Ar (orange system). Trkula (38) has recently looked at the orange and blue regions by sputtering an Fe cathode; a mixture of 5% O_3 in O_2 was used and a bright yellow "flame" was obtained.

In absorption work, Green, Reedy, and Kay (34) used a hollow-cathode sputtering technique to study the vibrational infrared spectrum of matrix-isolated FeO. Bass, Kuebler, and Nelson (21) studied the orange system and the diffuse feature at ~241 nm by flash heating metallic Fe in the presence of O_2. Callear and Norrish (70,19) conducted emission and absorption flash photolysis experiments (orange system and 241-nm feature) in which ferrocene or iron pentacarbonyl were used as additives to amyl nitrite and *n*-heptane fuel explosions in the presence of oxygen.

Similar experiments using pentyl nitrite plus hydrogen or isoamyl nitrite and hydrogen as fuel were performed by Erhard (71,72). Mixtures of $Fe(CO)_5$ in Ar were flash photolyzed by Callear and Oldman (20) to obtain the 241-nm feature in absorption. Lindgren and Sassenberg (39) conducted flash-photolysis experiments involving the reaction of $Fe(CO)_5$ with N_2O (whether in absorption or emission is not stated). Very recently, Endo *et al.* (81) have studied the millimeter-wave region by means of a DC glow discharge in a mixture of ferrocene and oxygen in a 1-meter long free-space absorption cell.

Some more exotic sources have been employed to obtain FeO for various specialized studies such as the shock tube experiments on $Fe(CO)_5 + O_2$ in Ar by von Rosenberg and Wray (46) and the tubular fast-flow reactor used by Fontijn and Kurzius (47) for a kinetic study of the reaction $Fe + O_2 \longrightarrow FeO + O$. Even vaporization of Apollo 12 lunar samples has been used as a source of FeO (by Balducci *et al.* (43) for a thermodynamic study).

None of the sources are completely ideal for spectroscopic work. Many produced strong atomic Fe lines. Dhumwad and co-workers (85,22) experimented with various sources, including a hollow cathode discharge and found that a low-pressure arc (~50 mm Hg) was best at suppressing atomic lines. Barrow and co-workers (23,37) also tried low-pressure arcs, but the lines obtained were weak and broad and occurred against a continuous background. A water-cooled composite-wall hollow cathode discharge of the type described by Bacis (86) was found to produce better spectra (orange system), but its behaviour was described by Harris and Barrow (37) as "capricious."

II.B. Description of the Source

Gaseous FeO molecules were produced in a flow system by passing a mixture of ferrocene, oxygen, and a noble gas through a 2450-MHz electrodeless discharge at low pressure. The experimental arrangement was as follows. Ferrocene (dicyclopentadienyliron, $Fe(C_5H_5)_2$) was heated to between 65 and 80°C in a wide-bore pyrex tube wrapped with heating tape, and the vapor was entrained in a stream of noble gas. Argon was used for the visible region; helium for the near-infrared. A small amount of O_2 was added, and the mixture (at a total pressure of a few mm Hg) was pumped rapidly through a microwave discharge cavity, with the discharge operated at a power of 120 W. A long orange-white "flame" resulted, the orange color being due to the orange emission system of FeO.

Solid rust-like products tended to accumulate on the walls of the apparatus, and if allowed to become excessive resulted in the discharge becoming unstable, presumably because of interference with the transmission of the microwave power. However, with experience it was found possible to run the discharge continuously for several hours, with only occasional "tweaking" of conditions.

II.C. Methods of Detection

II.C.1. Grating spectra[1]

"Survey" emission spectra covering the region 550–630 nm were obtained with a 7-meter Ebert-mounted plane grating spectrograph and photographed on Kodak IIa-D plates. Calibration spectra were provided by a neon-filled iron hollow cathode lamp, for which the wavelengths have been listed by Crosswhite (87). The spectra were measured on a Grant Instruments Co. oscilloscope-setting comparator, and reduced to vacuum wavenumbers using a four-term polynomial.

II.C.2. Laser-induced fluorescence[2]

The tail of the "flame" of the microwave discharge was pumped across a cube-shaped metal fluorescence cell fitted with Brewster-angle windows and light baffles. The laser beam was sent through this tail, and the resulting fluorescence was observed at right angles to the beam and to the stream of molecules.

The laser system consisted of a Coherent Inc. model CR 599-21 cw tunable dye laser, operating with rhodamine 560 or 590, and pumped by a model CR-10 argon ion laser. In some of the later experiments the blue-green lines from a model CR 3000K krypton ion laser were used to pump a model CR 699-21 ring dye laser. Laser powers of up to 450 mW were used.

Non-laser-induced FeO emission (from the microwave discharge) was present as a background, but this was weak in comparison with the laser-induced fluorescence and could be almost entirely suppressed by chopping the laser beam and using phase-sensitive detection.

Laser excitation spectra were obtained for large regions of the orange system (see Section I.B.2). Additionally, sub-Doppler intermodulated fluorescence spectra (88) were recorded for certain regions of the 582-nm band. With both types of spectra,

---

[1]Work done by R. M. Gordon and A. J. Merer.

[2]Work done by A. S-C. Cheung, A. M. Lyyra, A. J. Merer, and the author.

molecular iodine fluorescence lines were recorded simultaneously for calibration. Wavenumbers from the iodine spectrum atlas of Gerstenkorn and Luc (89a) were used, but with 0.0056 cm^{-1} subtracted from each listed value as a calibration correction (89b). Markers for interpolation between the iodine lines were provided by a Tropel 299-MHz free-spectral-range fixed length semiconfocal Fabry-Perot interferometer.

The FeO fluorescence was detected through a sharp-cut yellow filter with an RCA C31025C photomultiplier tube. For the sub-Doppler spectra, the sum of the chopper frequencies was selected with a narrow-band electrical filter, and a Princeton Applied Research model 128A lock-in-amplifier was used to extract the intermodulated signal. Fluorescence from the calibration I_2 cell was detected by an RCA 1P28 photomultiplier tube operated at -870 V DC.

Resolved fluorescence spectra were obtained using a Spex 0.75-meter scanning monochromator in first order.

II.C.3. Fourier transform spectroscopy

Fourier transform spectra covering the near-infrared region 4 000 - 14 000 cm^{-1} were recorded at Kitt Peak National Observatory near Tucson, Arizona, using the 1-meter FT spectrometer constructed by Dr. J. W. Brault for the McMath Solar Telescope. The bright center of the microwave discharge was focused directly into the aperture of the spectrometer. Suitable wavelength cutoff filters (CS5-56 and RG715) were used, and the emission was detected with a liquid nitrogen-cooled indium antimonide detector. The resolving power of the spectrometer was set to just over 800 000. A total of 46 interferograms, each of which took 6 minutes to record, were co-added for the final spectrum. A quintic window and apodization were applied to the transform.

II.D. The Spectra

The complexity of the orange system spectrum has already been described in Section I.B.2. In many regions, the spectrum as recorded on the grating photographs appears very dense, with numerous branch fragments overlapping each other. Very few bandheads stand out, and the only obvious progressions are the two corresponding to Delsemme and Rosen's A_1 and A_2 systems, which begin at 558 and 561 nm, respectively. The analysis of most regions was only made possible by extensive rotationally resolved fluorescence studies and the very accurate Δ_2F'' combination differences obtained from the laser excitation spectra, together with a simultaneous analysis of the infrared system, which involves the same lower state.

The infrared system, analysis of which is the main subject of this thesis, will be described more fully in Chapters IV and V. Suffice it to say for now that this region of the spectrum is also very complex, with numerous perturbations, and in many regions involves extensive overlap of branches belonging to various vibrational levels of various substates of two separate band systems. The analysis of this region was, in its initial stages, somewhat more tractable than that of the orange region, especially with the availability of accurate Δ_2F'' combination differences obtained from the orange system. However, the extensive perturbations and the pileup of branch structure in certain areas still made analysis of this system a challenging problem, as will become evident in later chapters.

As previously mentioned, reaction by-products tended to build up on the walls of the discharge cell and then made the discharge susceptible to unstable operation. Continued running under these conditions often gave mainly CO spectra. It was possible to obtain CO-free grating spectra with good FeO intensity if recording times were kept to under one hour.

Operating times much longer than one hour were used when doing the laser experiments and recording the Fourier transform spectra, due to experience gained in

maintaining optimal running conditions. It was usually possible to avoid CO emission by observing the color of the discharge with and without a hand-held spectroscope, although admittedly one band due to CO has been discovered in the FT spectra. This band, the (2,0) Asundi band, was identified from line positions calculated from the molecular constants and matrix elements published by Effantin *et al.* (90), and, once identified, caused only minor difficulties in the FeO analysis.

Atomic Fe lines were present in the grating spectra. These were often absent in the laser spectra, however, and therefore caused no great problem: where a portion of the grating spectrum was "blanked out" by an atomic emission line, the laser could often "see through" to excite the FeO spectrum. A notable example is provided by the strong Fe I emission line at 17 802.46 cm^{-1} which blanks out about 3 cm^{-1} of the grating spectrum but is entirely absent in the laser excitation spectrum because it does not involve the ^5D ground level of iron (Fig. 3).

Atomic lines present in the FT spectra were of greater consequence, particularly the very intense ones, not merely because of the areas blanked out by the lines themselves, but, more significantly, because of "ringing" and loss of signal-to-noise in the surrounding regions. One particularly bad region was caused by the extremely intense O I lines at 11 836.17 and 11 836.32 cm^{-1}: the effect extends to some 70 cm^{-1} to either side of these lines.

The FT spectra were obtained in the form of tables of intensity versus wavenumber, which were subsequently plotted out. Line positions were extracted with a third-degree polynomial fitting program. In cases where this method failed, due to blending, a simple three-point comparison was used to find the intensity maxima. The spacing between data points was 0.013 608 cm^{-1} corresponding to three or four data points within the Doppler profile of each molecular line. The Doppler-limited full-width-at-half-maximum for unblended lines is 0.03 cm^{-1} and the experimental accuracy

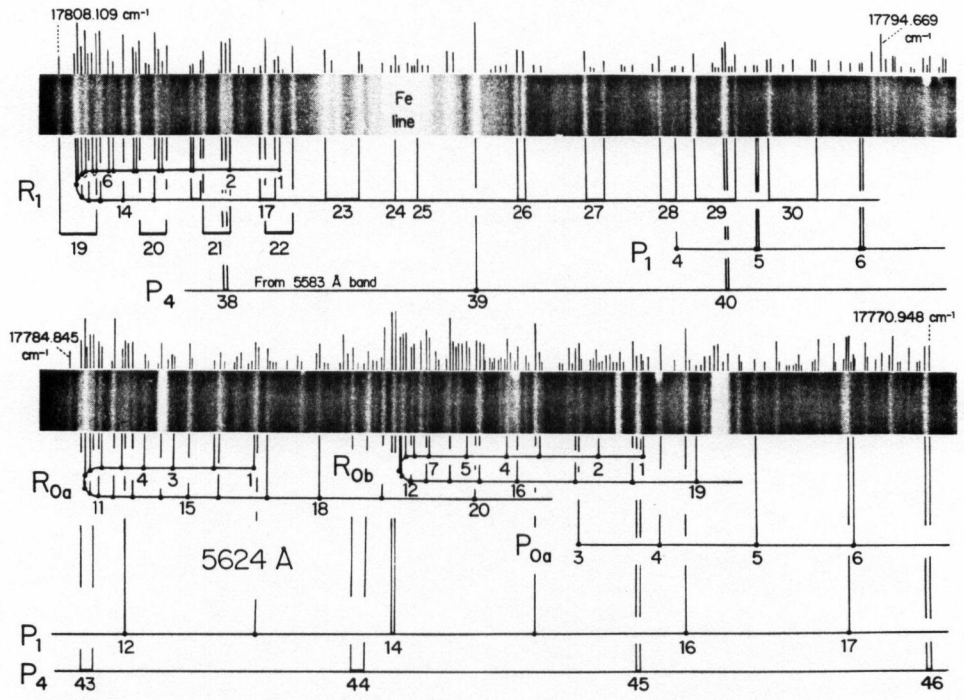

Fig. 3. Heads of the $\Omega' = 1$ band at 561.4 nm and of the $\Omega' = 0$ bands near 562.4 nm. The laser excitation spectra are shown as stick diagrams above the photographic prints of the discharge emission spectra, with stick height roughly proportional to intensity. Note the difference between the two types of spectra in the regions of the strong Fe lines.

of the positions of unblended lines should be better than 0.007 cm^{-1} [3] The accuracy of the laser excitation line positions is roughly 0.002 cm^{-1} for unblended lines of the orange system.

---

[3] 0.007 cm^{-1} = one-half the spacing between data points.

CHAPTER III

THEORY

III.A. Introduction

The energy levels of any atomic or molecular system are given by solution of the time-independent Schrödinger equation

$$H\psi = E\psi \qquad \text{...(III.A.1)}$$

where H is the hamiltonian operator, ψ is the wavefunction, and E the desired energy. Unfortunately, this equation can only be solved exactly for the hydrogen atom, so already in only the second sentence of this chapter we must start considering the use of approximate methods if we are to have any hope of understanding our experimental results!

The first approximation, due originally to Born and Oppenheimer (1), is to consider the motions of the electrons and nuclei as occurring independently of each other. The result is that the Schrödinger equation can be divided into separate electronic and nuclear parts, as will be shown in Section III.C. The next step (Section III.D), which again involves approximation, is to continue this division process and separate the nuclear motion into vibrational and rotational parts.

The hamiltonian used in Sections III.C and D neglects the spin of the electrons. Spin, which arises as a relativistic effect, is then introduced in Section E.

To improve upon the approximations made in the above separations, an effective hamiltonian can be constructed (Section H) that operates on the rotational wavefunctions within a given vibronic[1] level as does the hamiltonian derived from the

---

[1]The term "vibrational level" is used to refer to the vibrational levels of a specific electronic state, whereas the term "vibronic level" is used to refer to *any* vibrational level regardless of which electronic state it belongs to, the electronic state then being included within the vibronic state labelling information.

Born-Oppenheimer and rotation-vibration separation methods, but which, unlike the latter hamiltonian, takes into account interactions with energetically distant-lying states. This method does not take into account interactions with close-lying states, however; these effects are treated as perturbations — the topic of Section J.

Since $^5\Delta$ and $^5\Phi$ states have never previously been identified, their energy matrix elements have not been derived before. Also, there is only one known example of a molecule possessing a $^5\Pi$ state where a detailed rotational analysis has been attempted, namely CrO (2,3). Hence much of this chapter is devoted to the derivation of the effective hamiltonian and matrix elements for these high multiplicity states, together with sufficient background theory to carry out this derivation.

During the course of the foregoing procedures, the eigenfunction ψ is expanded in terms of a complete set of basis functions ϕ_i,

$$\psi = \sum_i c_i \phi_i \qquad \text{...(III.A.2)}$$

where the c_i's are constants. In Sections C and D, the basis functions are the Born-Oppenheimer basis functions (defined by eqn. (III.C.4)). In Section H, the effective hamiltonian is derived in terms of a different basis. In fact, a choice of several bases exists for this purpose and the form of the effective hamiltonian is dependent on the choice made. Each of these bases consists of the eigenfunctions of a certain set of commuting angular momentum operators corresponding to one of Hund's coupling cases, as will be discussed in Section F. Once a suitable basis is chosen, the energies of the rotational levels are obtained by writing the matrix $\underline{H}$ of the hamiltonian H and diagonalizing it.

Lambda-doubling is discussed in a general way in Section G, then for the specific case of a $^5\Delta$ state in Section H.2.a. This topic is of particular interest in that observations of Λ-doubling in states with $|\Lambda| > 1$ have been comparatively rare.

While a study of intensities in the spectrum of FeO was not a primary objective of this project, a derivation of the intensity formulas is still useful since it demonstrates the origin of the selection rules operating in the spectrum. Also, the intensity formulas are useful in a qualitative sense for understanding the relative branch intensities and the relative line intensities within a branch. Section I (for intensity!) thus covers this subject.

One cannot go far in studying any part of the spectrum of FeO before one encounters perturbations — lots and lots of them! Hence this chapter would not be complete without a section on this topic. Section J provides a general introduction to the subject of perturbations.

Finally, in Section K, single-configuration representations of electronic structures are used to view FeO in terms of the more general picture of the first-row transition metal oxides considered as a series.

III.B. The General Molecular Hamiltonian

The non-relativistic hamiltonian operator for a molecule consisting of N nuclei and n electrons is

$$H_0 = -\frac{\hbar^2}{2}\sum_{A}^{N}\frac{\nabla_A^2}{M_A} \quad \text{(kinetic energy of nuclei)}$$

$$-\frac{\hbar^2}{2m_e}\sum_{a}^{n}\nabla_a^2 \quad \text{(kinetic energy of electrons)}$$

$$+ V(q,Q) \quad \text{(potential energy)} \qquad \text{...(III.B.1)}$$

where M_A is the mass of nucleus A; m_e is the mass of an electron; $\hbar$ is Planck's constant divided by 2π; and ∇^2 ("del squared") is the Laplacian operator, which is, in Cartesian coordinates,

$$\nabla^2 = \frac{\partial^2}{\partial X^2} + \frac{\partial^2}{\partial Y^2} + \frac{\partial^2}{\partial Z^2} \qquad \text{...(III.B.2)}$$

and in spherical polar coordinates,

$$\nabla^2 = \frac{1}{R^2}\frac{\partial}{\partial R}\left(R^2\frac{\partial}{\partial R}\right) + \frac{1}{R^2\sin\theta}\frac{\partial}{\partial\theta}\left(\sin\theta\frac{\partial}{\partial\theta}\right) + \frac{1}{R^2\sin^2\theta}\frac{\partial^2}{\partial\phi^2}$$

...(III.B.3)

The potential $V(q,Q)$, which depends on the positions both of the electrons (q) and of the nuclei (Q), consists of three terms,

$$V(q,Q) = \sum_{A}^{N}\sum_{B>A}^{N}\frac{Z_A Z_B e^2}{r_{AB}} \quad \text{(nuclear-nuclear repulsion)}$$

$$-\sum_{A}^{N}\sum_{a}^{n}\frac{Z_A e^2}{r_{aA}} \quad \text{(electron-nuclear attraction)}$$

$$+\sum_{a}^{n}\sum_{b>a}^{n}\frac{e^2}{r_{ba}} \quad \text{(electron-electron repulsion)} \qquad \text{...(III.B.4)}$$

where e is the charge of an electron, $Z_A e$ is the charge on nucleus A, and r_{xy} is the distance from particle x to particle y.

A relativistic treatment (4) yields a hamiltonian in agreement with the above but with a number of additional terms. Most of these extra terms describe effects that are too small to be detected by the vast majority of spectroscopic methods, but two are of importance and must be added to the non-relativistic hamiltonian H_o:

$$H = H_o + H_s + H_{hfs} \qquad \text{...(III.B.5)}$$

These new terms involve electron spin (H_s) and nuclear hyperfine structure (H_{hfs}). In the case of iron oxide, both Fe and O have nuclear spins of zero, hence nothing further will be said about H_{hfs}. The electron spin hamiltonian H_s, however, will be considered in detail in Section III.E.

The hamiltonian H_o is written in a space-fixed (= laboratory-fixed) coordinate system. We are not interested in the kinetic energy due to translation of the molecules, because in free space this is not quantized. The translational motion can be separated off by shifting to a coordinate system parallel to the laboratory-fixed system, but with its origin at the center of mass of some particular molecule (5a,6). This is very nearly an exact separation for a low-pressure gas in the absence of externally applied electromagnetic fields, since intermolecular forces are too weak under these conditions to perturb the free translational motions to any significant extent.

III.C. Separation of Electronic and Nuclear Motions — The Born-Oppenheimer Approximation

The mass of a proton is about 1840 times that of an electron. As a result of their smaller masses, electrons move much faster than nuclei, and this fact provides the foundation for the Born-Oppenheimer separation of electronic and nuclear motions. The electrons are treated as if they move in a field of fixed nuclei and are able to adapt themselves instantaneously to successive nuclear configurations as the nuclei move.

The original derivation by Born and Oppenheimer (1) is rather long and complicated and will not be described here. Born later published a simpler, yet more general, derivation (7,8), and this is the treatment we follow. A more detailed derivation, including relativistic terms, has been given by Bunker (9).

The Schrödinger equation for the non-relativistic hamiltonian is

$$H_o\psi = \left\{ -\frac{\hbar^2}{2}\sum_A^N \frac{\nabla_A^2}{M_A} - \frac{\hbar^2}{2m_e}\sum_a^n \nabla_a^2 + V(q,Q) \right\} \psi = E\psi \qquad \text{...(III.C.1)}$$

In the limit of infinitely heavy nuclei, the hamiltonian, H_o, becomes

$$H_e = -\frac{\hbar^2}{2m_e}\sum_a^n \nabla_a^2 + V(q,Q) \qquad \text{...(III.C.2)}$$

which can equivalently be regarded as the electronic hamiltonian for the case of *fixed* nuclei. Born (7,8) assumes that the electronic problem has been solved for each fixed value of Q,

$$H_e\psi_e^k(q,Q) = E_e^k(Q)\psi_e^k(q,Q) \qquad \text{...(III.C.3)}$$

where $\psi_e^k(q,Q)$ is the electronic wavefunction for the k^{th} state and is a member of the complete set of normalized orthogonal electronic wavefunctions. He then tries an expansion of the total wavefunction $\psi(q,Q)$,

$$\psi(q,Q) = \sum_i \psi_e^i(q,Q)\psi_n^i(Q) \qquad \text{...(III.C.4)}$$

as a solution to the Schrödinger equation for the complete system, where $\psi_n^i(Q)$ depends only on the nuclear positions. Substitution of this into eqn. (III.C.1), left-multiplication with $\psi_e^{k*}(q,Q)$, and integration over the electronic coordinates q, selects out the k^{th} electronic state and yields as the final result[2]

$$\left\{H_n + U^k(Q)\right\}\psi_n^k(Q) + C = E^k\psi_n^k(Q) \qquad \text{...(III.C.5)}$$

where

$$H_n = -\frac{\hbar^2}{2}\sum_A^N \frac{\nabla_A^2}{M_A} \qquad \text{...(III.C.6)}$$

$$U^k(Q) = E_e^k(Q) + \frac{\hbar^2}{2}\sum_A^N \frac{1}{M_A}\int[\nabla_A\psi_e^k(q,Q)]^2 dq \qquad \text{...(III.C.7)}$$

and C stands for the cross-terms

$$C = \sum_{i\neq k}\left\{\int\psi_e^k(q,Q)H_n\psi_e^i(q,Q)dq - \hbar^2\sum_A^N \frac{1}{M_A}\int\psi_e^k(q,Q)\nabla_A\psi_e^i(q,Q)dq\nabla_A\right\}\psi_n^i(Q) \qquad \text{...(III.C.8)}$$

Neglect of the cross-terms constitutes the Born-Oppenheimer approximation. The energy E^k obtained by solution of the resulting equation is really the *total* energy of the k^{th} state, but because of the way the calculations are actually carried out, in practice this is regarded as only the *nuclear* energy, E_n^k. This comes about as follows. The electronic energy $E_e^k(Q)$ obtained from eqn. (III.C.3) varies with changing values of the nuclear coordinates represented by Q to form what is called a potential well. In practice, only that value corresponding to the bottom of the potential well is called the "electronic energy" of the k^{th} state. The variation in $E_e^k(Q)$ with Q is then incorporated into the "nuclear energy" (actually into the vibrational part of the "nuclear energy") via the $U^k(Q)$ operator. That is, the electronic energy function $E_e^k(Q)$ (actually $U^k(Q)$ — see next paragraph) plays the part of potential energy for

---

[2]The steps involved are given in more detail by Schutte (10).

the nuclei. The zero of the "nuclear energy" scale is then set to coincide with the bottom of the potential well for the k^{th} state.

To sum up, provided that the cross-terms can be omitted, the nuclear motion has been separated from the electronic motions. The nuclei are found to move against a potential $U^k(Q)$ which depends on the positions of the nuclei. This potential is almost equal to the energy determined from the electronic Schrödinger equation as a function of Q to which is added a small correction term (the second term on the right-hand side of eqn. (III.C.7)). This term, which contributes to the electronic isotope shift, was not actually derived in the original Born-Oppenheimer treatment.[3] It is therefore often overlooked in discussions about the electronic/nuclear separation. However, it should be included, especially for light molecules.

The cross-terms neglected in the Born-Oppenheimer approximation couple the electronic and vibrational motions in different electronic states. If, in specific cases, the electronic wavefunctions $\psi_e^i(q,Q)$ can be solved for, the magnitude of these terms can be determined. In general, it can be seen if these terms are treated by perturbation theory that, provided the energy separation between the k^{th} state and any other electronic state is large, the effect of these terms will be small. In the other extreme, if the symmetry is high enough to permit two electronic states to become degenerate, the Born-Oppenheimer approximation breaks down[4] and the phenomena known as the Renner-Teller effect (for linear molecules) or the Jahn-Teller effect (for symmetric top molecules) occur (11,12).

---

[3]Often the phrase "Born-Oppenheimer approximation" is used to refer to the approximation resulting from the neglect of the second term on the right-hand side of eqn. (III.C.7) in addition to the neglect of the cross-terms C, whereas "adiabatic approximation" is used to refer to the neglect of only the cross-terms.

[4]The term labelled $[c]_{i=k} \neq 0$ in this situation, since the stationary states are complex, rather than real.

III.D. Separation of the Vibrational and Rotational Motions

The separation of the nuclear motion into vibrational and rotational parts, for polyatomic molecules, is not a trivial process due to the presence of cross-terms between the two motions (13,14). For diatomic molecules, the process is considerably simpler since there are no such cross-terms to couple the vibrational and rotational motions.

The separation for diatomic molecules follows directly from the fact that the vibrational and rotational motions of the nuclei must be orthogonal. Vibrational motion can only occur in a direction along the internuclear axis — i.e. stretching or compression of the internuclear distance. Motions of either or both nuclei in any other direction(s) must automatically produce a translational or rotational motion of the molecule as a whole.

The derivation of the energy level expressions for the individual vibrational and rotational parts is well known (5b,15) and is not reproduced here. Experimentalists usually express the vibrational energies in the form (16a)

$$G(v) = \omega_e(v+\tfrac{1}{2}) - \omega_e x_e(v+\tfrac{1}{2})^2 + \omega_e y_e(v+\tfrac{1}{2})^3 + \ldots \qquad \text{...(III.D.1)}$$

where G(v) is the "energy" (in cm^{-1})[5] of the v^{th} vibrational level and v is the vibrational quantum number. If only the first term in the series is retained, the expression describes the energy levels of a harmonic oscillator; the additional terms are anharmonic terms. The vibrational frequency ω_e and the anharmonicity constants $\omega_e x_e$, $\omega_e y_e$, ... are treated as empirical constants, which are obtained by fitting the observed vibrational spacings (extrapolated if necessary to zero rotation) to eqn. (III.D.4).

If the internuclear distance R is assumed to be fixed (the "rigid rotor approximation"), the solution to the rotational Schrödinger equation is

---

[5]Obtained by dividing energies in joules by hc.

$$F(J) = \frac{h}{8\pi^2 c\mu R^2} J(J+1) \qquad \text{...(III.D.2)}$$

where F(J) is the rotational "energy" (in cm^{-1}) of the J^{th} rotational level, J is the total angular momentum quantum number, c is the velocity of light (in $cm \cdot s^{-1}$), and μ is the reduced mass of the molecule. In reality, the molecule is not a rigid rotator. To correct for this, eqn. (III.D.2) is modified in two ways. First, because the molecule is vibrating, it is necessary to average over the coordinate R, which we do by defining the rotational constant B_v such that

$$B_v = \frac{h}{8\pi^2 c\mu} \int \psi_v^* \frac{1}{R^2} \psi_v dR \qquad \text{...(III.D.3)}$$

Since the value of B varies with vibrational level, as denoted by the subscript v, it is usual to express this dependence on v as a power series,

$$B_v = B_e - \alpha_e(v+\tfrac{1}{2}) + \gamma_e(v+\tfrac{1}{2})^2 + \delta_e(v+\tfrac{1}{2})^3 + \ldots \qquad \text{...(III.D.4)}$$

where $B_e = \frac{h}{8\pi^2 c\mu R_e^2}$, the value of B at the bottom of the potential well (where $R = R_e$, the equilibrium bond length), and α_e, γ_e, δ_e, ... are vibration–rotation interaction constants.

Another type of vibration–rotation interaction arises from the centrifugal force that results when the molecule rotates. This occurs even for v = 0 and has the effect of stretching the bond. This is taken into account by means of additional terms,[6]

$$F_v(J) = B_v J(J+1) - D_v[J(J+1)]^2 + H_v[J(J+1)]^3 + L_v[J(J+1)]^4 + \ldots \qquad \text{...(III.D.5)}$$

Usually it is only necessary to use one centrifugal distortion term, the D_v term. Its power series expansion is

$$D_v = D_e + \beta_e(v+\tfrac{1}{2}) + \ldots \qquad \text{...(III.D.6)}$$

---

[6]Some authors use a "–" sign in front of the L_v term.

In summary, as a result of the separations described in this and the previous section, the total energy for a diatomic molecule (neglecting spin for now — see next section) can be written as the sum of electronic, vibrational, and rotational parts,

$$E^{kvJ} = E_e^k(R_e) + G^{(k)}(v) + F_v^{(k)}(J) \qquad \text{...(III.D.7)}$$

where the electronic energy (now in cm^{-1}) is defined as that value of $E_e^k(Q)$ occurring at the bottom of the potential well, the vibrational energy scale has its zero value at this same point, and the rotational energies are defined relative to the appropriate vibrational level.

III.E. Electron Spin

While not present in classical theory, the concept of spin arises when relativity theory is applied to the wave equation for the electron (or nucleus) (17). This explains a number of properties not accounted for with the non-relativistic hamiltonian. For a molecule such as FeO with no nuclear spin, the additional features of interest are:

(i) spin-orbit coupling;

(ii) spin-rotation coupling; and

(iii) spin-spin coupling.

i.e.

$$H_S = H_{SO} + H_{SR} + H_{SS} \qquad \text{...(III.E.1)}$$

An electron possesses a magnetic moment μ, which, according to the relativistic theory, is given by

$$\underset{\sim}{\mu} = -\frac{g\mu_B \underset{\sim}{S}}{\hbar} \qquad \text{...(III.E.2)}$$

where g is the gyromagnetic ratio (= magnetogyric ratio = 2.002 3); μ_B, the Bohr magneton, stands for the collection of constants $\frac{e\hbar}{2m_e} = 9.274 \times 10^{-24}\ J \cdot T^{-1}$ (where $-e$ is the charge on the electron,[7] -1.602×10^{-19} C, and m_e is the mass of the electron, 9.110×10^{-31} kg); and $\underset{\sim}{S}$ is the spin angular momentum[8] of the electron.

The interactions of this electron spin magnetic moment with

(i) the magnetic field generated by the orbital motions of the electrons;

(ii) the magnetic field generated by the rotation of the nuclei; and

(iii) the spin magnetic moments of the other electrons

give rise to the three coupling terms listed above.

---

[7]The convention $e = +|e|$ is used here.

[8]Angular momenta will be defined and discussed in Section III.F.

III.E.1. Spin-orbit interaction

We first consider a single atom possessing one electron with non-zero orbital angular momentum. The positive charge of the nucleus produces an electric field $\underset{\sim}{E}$. Thinking classically, an observer positioned on the electron would experience a magnetic field $\underset{\sim}{B}$ due to the apparent motion of the nuclear electric field,

$$\underset{\sim}{B} = -\frac{1}{c^2}\underset{\sim}{v}_{en} \times \underset{\sim}{E} = \frac{1}{c^2}\underset{\sim}{E} \times \underset{\sim}{v}_{en} \qquad \text{...(III.E.3)}$$

where $\underset{\sim}{v}_{en}$ is the velocity of the electron relative to the nucleus. Since the electric field is the gradient of the potential V, and since the spherically symmetrical field arising from the point charge of the nucleus corresponds to a central field potential $V = V(r_{en})$, we can write

$$\underset{\sim}{E} = -\text{grad } V = -\left(\frac{\underset{\sim}{r}_{en}}{r_{en}}\right)\frac{dV}{dr_{en}} \qquad \text{...(III.E.4)}$$

where $\underset{\sim}{r}_{en}$ is the position vector of the electron from the nucleus and r_{en} its corresponding magnitude. Then

$$\underset{\sim}{B} = -\frac{1}{c^2 r_{en}}\left(\frac{dV}{dr_{en}}\right)\underset{\sim}{r}_{en} \times \underset{\sim}{v}_{en} \qquad \text{...(III.E.5)}$$

Classically the hamiltonian for the interaction of a magnetic field and a magnetic moment is given by

$$H = -\underset{\sim}{\mu}\cdot\underset{\sim}{B} \qquad \text{...(III.E.6)}$$

Upon substitution of the relativistic expression for $\underset{\sim}{\mu}$ (eqn. (III.E.2)) and the expression for $\underset{\sim}{B}$ from (III.E.5), this becomes

$$H = -\frac{g\mu_B}{\hbar c^2 r_{en}}\left(\frac{dV}{dr_{en}}\right)\underset{\sim}{r}_{en} \times \underset{\sim}{v}_{en}\cdot\underset{\sim}{S} \qquad \text{...(III.E.7)}$$

We now decompose the vector $\underset{\sim}{v}_{en}$, the velocity of the electron relative to the nucleus, into components corresponding to the individual velocities of the electron and

nucleus in a laboratory-fixed coordinate system. Unlike in classical mechanics, however, $\underset{\sim}{v}_{en}$ is not simply the vector difference of the electron velocity $\underset{\sim}{v}_e$ and the nuclear velocity $\underset{\sim}{v}_n$. There is an additional relativistic correction (a factor of $\frac{1}{2}$) that arises from a phenomenon known as Thomas precession (18). As discussed by Jackson (19), this occurs because the electron rotates with respect to the laboratory frame of reference as a result of the acceleration experienced by the electron as it moves in the Coulombic field of the nuclei and other electrons. With this correction the vector $\underset{\sim}{v}_{en}$ becomes

$$\underset{\sim}{v}_{en} = \tfrac{1}{2}\underset{\sim}{v}_e - \underset{\sim}{v}_n \qquad \text{...(III.E.8)}$$

so that

$$H = -\frac{g\mu_B}{\hbar c^2 r_{en}}\left(\frac{dV}{dr_{en}}\right)\underset{\sim}{r}_{en} \times (\tfrac{1}{2}\underset{\sim}{v}_e - \underset{\sim}{v}_n)\cdot\underset{\sim}{s} \qquad \text{...(III.E.9)}$$

The coordinate system was specified above to be a laboratory-fixed frame, but it can actually be chosen to be a frame moving with the molecule, with origin at the center of mass for example, provided that it is regarded as instantaneously space fixed (20).

For an atom with more than one electron, the interaction energies are assumed to be additive.[9] Likewise, in a molecule, each electron is assumed to interact with every nucleus, and each such interaction contributes a term of the form of eqn. (III.E.9), i.e.

$$H_{so} = -\frac{g\mu_B}{\hbar c^2}\sum_e\sum_n \frac{1}{r_{en}}\left(\frac{dV_{en}}{dr_{en}}\right)\underset{\sim}{r}_{en} \times (\tfrac{1}{2}\underset{\sim}{v}_e - \underset{\sim}{v}_n)\cdot\underset{\sim}{s}_e \qquad \text{...(III.E.10)}$$

---

[9]These procedures are not strictly correct. For example, the interaction of $\underset{\sim}{\mu}$ with the magnetic fields resulting from the relative motion of the electric fields of the other electrons has not been taken into consideration. To account for this, Van Vleck (21) includes an additional term, itself similar to eqn. (III.E.10) but for the other electrons. Here, we allow for this in an approximate way when we introduce Z_{eff} (see eqn. (III.E.14)). (Note that eqn. (37) of Van Vleck's paper (21) contains several errors. A corrected version has been given by Kayama and Baird (20); this version also contains misprints (two of the subscript K's in their eqn. (28) should be k's).)

By the distributive principle, this breaks up into two terms,

$$H = -\frac{g\mu_B}{2\hbar m_e c^2} \sum_e \sum_n \frac{1}{r_{en}} \left(\frac{dV_{en}}{dr_{en}}\right) \underset{\sim}{r}_{en} \times m_e \underset{\sim}{v}_e \cdot \underset{\sim}{s}_e + \frac{g\mu_B}{\hbar c^2} \sum_e \sum_n \frac{1}{r_{en}} \left(\frac{dV_{en}}{dr_{en}}\right) \underset{\sim}{r}_{en} \times \underset{\sim}{v}_n \cdot \underset{\sim}{s}_e \quad \text{...(III.E.11)}$$

where the first term has been multiplied and divided by the mass of the electron.

It can now be recognized what the two terms represent. The second term, which contains $\underset{\sim}{v}_n$, involves the motion of the nuclei — specifically, for diatomic molecules, the rotation of the nuclei.[10] This is the spin-rotation interaction, which will be discussed later. The first term is the spin-orbit interaction, H_{so}, as becomes clear if this term is rewritten as

$$H_{so} = -\frac{g\mu_B}{2\hbar m_e c^2} \sum_e \sum_n \frac{1}{r_{en}} \left(\frac{dV_{en}}{dr_{en}}\right) \underset{\sim}{l}_{en} \cdot \underset{\sim}{s}_e \quad \text{...(III.E.12)}$$

where the substitution

$$\underset{\sim}{l}_{en} = \underset{\sim}{r}_{en} \times m_e \underset{\sim}{v}_{en} \quad \text{...(III.E.13)}$$

has been made. $\underset{\sim}{l}_{en}$ is the orbital angular momentum of electron e about nucleus n.

So far we have not allowed for the effect of the charges on the other electrons. This can be done satisfactorily by taking the potentials V_{en} as Coulomb potentials in which "effective" nuclear charges $Z_{eff,n}e$ describe the screening effect of the electrons:

$$V_{en} = \frac{Z_{eff,n}e}{4\pi\epsilon_o r_{en}} \quad \text{...(III.E.14)}$$

where ϵ_o is the permittivity of free space. Then

$$\frac{dV_{en}}{dr_{en}} = -\frac{Z_{eff,n}e}{4\pi\epsilon_o r_{en}^2} \quad \text{...(III.E.15)}$$

---

[10]Diatomic molecules possess no vibrational angular momentum, so there is no spin-vibration interaction.

giving

$$H_{so} = \frac{g\mu_B^2}{4\pi\epsilon_0 c^2\hbar^2} \sum_e \sum_n \frac{Z_{eff,n}}{r_{en}^3} \underset{\sim}{l}_{en} \cdot \underset{\sim}{s}_e \qquad \text{...(III.E.16)}$$

This can be rewritten as (22)[11]

$$H_{so} = \sum_e a_e(r) \underset{\sim}{l}_e \cdot \underset{\sim}{s}_e \qquad \text{...(III.E.17)}$$

by summing over the nuclei, where

$$a_e(r) \underset{\sim}{l}_e = \frac{g\mu_B^2}{4\pi\epsilon_0 c^2\hbar^2} \sum_n \frac{Z_{eff,n}}{r_{en}^3} \underset{\sim}{l}_{en} \qquad \text{...(III.E.18)}$$

The relation between $\underset{\sim}{l}_e$, the total orbital angular momentum of electron e, and the $\underset{\sim}{l}_{en}$'s, the orbital angular momenta of electron e with respect to each nucleus n, is deliberately left vague because of the lack of a common origin for the $\underset{\sim}{l}_{en}$'s, a point which has been addressed by Veseth (23) for diatomic molecules. The hamiltonian given by eqn. (III.E.17) is called the "microscopic spin-orbit hamiltonian." A simplification of this equation that is often used in practice, but which involves further approximations, will be presented in Section III.H.2.

III.E.2. Spin-rotation interaction

The second term in eqn. (III.E.11) gives the spin-rotation interaction. As with the spin-orbit interaction, the potentials V_{en} are approximated as Coulomb potentials for each nucleus, with the nuclear charges being partially shielded by the electrons,

$$H_{sr} = -\frac{g\mu_B e}{4\pi\epsilon_0 c^2\hbar} \sum_e \sum_n \frac{Z_{eff,n}}{r_{en}^3} \underset{\sim}{r}_{en} \times \underset{\sim}{v}_n \cdot \underset{\sim}{s}_e \qquad \text{...(III.E.19)}$$

Following Van Vleck (21), we write the nuclear velocities as

---

[11]Note that $\underset{\sim}{l}_e$, $\underset{\sim}{l}_{en}$, and $\underset{\sim}{s}$ each contain $\hbar$. The units of H_{so} are joules (or cm^{-1} if the expressions are divided by hc).

$$\underset{\sim}{v}_n = \underset{\sim}{\omega} \times \underset{\sim}{r}_n \qquad \text{...(III.E.20)}$$

where $\underset{\sim}{r}_n$ is the position vector of nucleus n relative to the center of mass and $\underset{\sim}{\omega}$ is the angular velocity of the nuclei, with the nuclei being regarded as forming a rigid rotator.[12] The rotational angular momentum $\underset{\sim}{R}$ is the moment of inertia multiplied by the angular velocity

$$\underset{\sim}{R} = I\underset{\sim}{\omega} \qquad \text{...(III.E.21)}$$

We therefore obtain

$$H_{sr} = -\frac{g\mu_B e}{4\pi\epsilon_0 c^2 I\hbar} \sum_e \sum_n \frac{Z_{eff,n}}{r_{en}^3} [\underset{\sim}{r}_{en} \times (\underset{\sim}{R} \times \underset{\sim}{r}_n)]\cdot\underset{\sim}{s}_e \qquad \text{...(III.E.22)}$$

which, upon use of the identity

$$\underset{\sim}{a} \times (\underset{\sim}{b} \times \underset{\sim}{c}) = (\underset{\sim}{c}\cdot\underset{\sim}{a})\underset{\sim}{b} - (\underset{\sim}{b}\cdot\underset{\sim}{a})\underset{\sim}{c} \qquad \text{...(III.E.23)}$$

becomes

$$H_{sr} = -\frac{g\mu_B e}{4\pi\epsilon_0 c^2 I\hbar} \sum_e \sum_n \frac{Z_{eff,n}}{r_{en}^3} [(\underset{\sim}{r}_n\cdot\underset{\sim}{r}_{en})\underset{\sim}{R}]\cdot\underset{\sim}{s}_e + \frac{g\mu_B e}{4\pi\epsilon_0 c^2 I\hbar} \sum_e \sum_n \frac{Z_{eff,n}}{r_{en}^3} [(\underset{\sim}{R}\cdot\underset{\sim}{r}_{en})\underset{\sim}{r}_{en}]\cdot\underset{\sim}{s}_e \qquad \text{...(III.E.24)}$$

In fact, at least for diatomic molecules, only the first term contributes to the spin-rotation interaction of a given state. (The second term, which is very small, connects different electronic states.) The "microscopic form" of the spin-rotation interaction hamiltonian is then (24,25,26)

$$H_{sr} = \underset{\sim}{R}\cdot \sum_e b_e(r)\underset{\sim}{s}_e \qquad \text{...(III.E.25)}$$

---

[12]The motion of the nuclei due to vibration can be ignored, since positive and negative contributions cancel in the mean. The variation of the bond lengths due to anharmonicity and centrifugal distortion will be discussed in Section III.H.2.

where

$$b_e = -\frac{g\mu_B e}{4\pi\epsilon_o c^2 I\hbar} \sum_n \frac{Z_{eff,n}}{r_{en}^3} \underset{\sim}{r}_n \cdot \underset{\sim}{r}_{en} \qquad \text{...(III.E.26)}$$

As with the spin-orbit interaction, a simplified version of this expression is usually used in practice (see Section III.H.2).

III.E.3. Spin-spin interaction

Each spinning electron behaves as a tiny bar magnet. According to classical electromagnetic field theory, the magnetic field at a point i that is a distance r_{ij} from an electron at point j is (27a)

$$\underset{\sim}{B}_i = \nabla \times \underset{\sim}{A}_i \qquad \text{...(III.E.27)}$$

where $\underset{\sim}{A}_i$ is the magnetic vector potential,[13] which is related to the magnetic dipole moment $\underset{\sim}{\mu}_j$ of the electron at j according to (27b)

$$\underset{\sim}{A}_i = \frac{\mu_o}{4\pi} \frac{\underset{\sim}{\mu}_j \times \underset{\sim}{r}_{ij}}{r_{ij}^3} \qquad \text{...(III.E.28)}$$

where μ_o is the permeability of free space. Eqn. (III.E.6) gives the hamiltonian for the interaction of the magnetic moment of an electron located at point i with the magnetic field due to the electron at j, namely

$$H_{ss,ij} = -\underset{\sim}{\mu}_i \cdot \underset{\sim}{B}_i$$

$$= -\frac{\mu_o g^2 \mu_B^2}{4\pi\hbar^2} \underset{\sim}{s}_i \cdot \left[\nabla \times \underset{\sim}{s}_j \times \frac{\underset{\sim}{r}_{ij}}{r_{ij}^3}\right] \qquad \text{...(III.E.29)}$$

where the magnetic moments have been written in terms of the spin angular momenta using eqn. (III.E.2). The relation

$$\nabla\left(\frac{1}{r_{ij}}\right) = -\frac{\underset{\sim}{r}_{ij}}{r_{ij}^3} \qquad \text{...(III.E.30)}$$

---

[13] In SI units, $\underset{\sim}{A}_i$ has units of $Wb \cdot m^{-1}$

then gives

$$H_{ss,ij} = +\frac{\mu_o g^2 \mu_B^2}{4\pi\hbar^2}\, \underset{\sim}{s}_i \cdot \left[\nabla \times \underset{\sim}{s}_j \times \nabla\right]\frac{1}{r_{ij}}$$

$$= -\frac{\mu_o g^2 \mu_B^2}{4\pi\hbar^2}\, \underset{\sim}{s}_i \cdot \left[\nabla \times \nabla \times \underset{\sim}{s}_j\right]\frac{1}{r_{ij}}$$

$$= -\frac{\mu_o g^2 \mu_B^2}{4\pi\hbar^2}\, \underset{\sim}{s}_i \cdot \left[\nabla(\nabla\cdot\underset{\sim}{s}_j) - \nabla^2\underset{\sim}{s}_j\right]\frac{1}{r_{ij}}$$

$$= +\frac{\mu_o g^2 \mu_B^2}{4\pi\hbar^2}\, \left[(\underset{\sim}{s}_i\cdot\underset{\sim}{s}_j)\nabla^2 - (\underset{\sim}{s}_i\cdot\nabla)(\underset{\sim}{s}_j\cdot\nabla)\right]\frac{1}{r_{ij}} \qquad \text{...(III.E.31)}$$

where the relationship

$$\nabla \times \nabla \times \underset{\sim}{a} = \nabla(\nabla\cdot\underset{\sim}{a}) - \nabla^2\underset{\sim}{a} \qquad \text{...(III.E.32)}$$

has also been used.[14] Now let

$$[a] = (\underset{\sim}{s}_i\cdot\underset{\sim}{s}_j)\nabla^2\frac{1}{r_{ij}} \qquad \text{...(III.E.33)}$$

and $$[b] = (\underset{\sim}{s}_i\cdot\nabla)(\underset{\sim}{s}_j\cdot\nabla)\frac{1}{r_{ij}} \qquad \text{...(III.E.34)}$$

Consider the [b] term. This will become undefined for $r_{ij} = 0$ because of the r_{ij} in the denominator. We can handle this problem by dividing [b] into two parts,

$$[b] = [b]_{r\neq 0} + [b]_{r=0} \qquad \text{...(III.E.35)}$$

The first part is easily treated, as follows:

$$[b]_{r\neq 0} = \underset{\sim}{s}_i \cdot \left[\nabla(\underset{\sim}{s}_j\cdot\nabla)\frac{1}{r_{ij}}\right]$$

---

[14]Note that eqn. (III.E.32) is not a general vector relation (28). It holds only in cartesian coordinates and then only for the individual cartesian components. If

$$\nabla \times \nabla \times \underset{\sim}{a} = \underset{\sim}{b}$$

then for the x-component, b_x is

$$\frac{\partial}{\partial x}(\nabla\cdot\underset{\sim}{a}) - \nabla^2 a_x = b_x$$

with similar equations for the y- and z-components. The right-hand side of eqn. (III.E.32) is a symbolic shorthand for these three equations.

$$= \underset{\sim}{s}_i \cdot \left[(\underset{\sim}{s}_j \cdot \nabla) \nabla \frac{1}{r_{ij}} \right]$$

$$= - \underset{\sim}{s}_i \cdot \left[(\underset{\sim}{s}_j \cdot \nabla) \left(\frac{1}{r_{ij}^3} \underset{\sim}{r}_{ij} \right) \right] \qquad \text{...(III.E.36)}$$

Then by the usual rule for differentiating a product,

$$[b]_{r \neq 0} = - \underset{\sim}{s}_i \cdot \left[\underset{\sim}{s}_j \cdot \frac{1}{r_{ij}^3} - 3 \underset{\sim}{r}_{ij} \frac{1}{r_{ij}^4} \frac{\underset{\sim}{r}_{ij}}{r_{ij}} \right]$$

$$= - \frac{\underset{\sim}{s}_i \cdot \underset{\sim}{s}_j}{r_{ij}^3} + 3 \frac{(\underset{\sim}{s}_i \cdot \underset{\sim}{r}_{ij})(\underset{\sim}{s}_j \cdot \underset{\sim}{r}_{ij})}{r_{ij}^5} \qquad \text{...(III.E.37)}$$

The second part of [b] is more difficult to treat — but, not impossible! Any use to which the hamiltonian will be put will involve multiplication by some function (e.g. the square of the electronic wavefunction $\psi_e^* \psi_e$) then integration over the spatial coordinates. For the $[b]_{r=0}$ part, this can be done by carrying out the integration over a small spherical volume of space of radius ϵ surrounding the origin, then letting ϵ go to zero — i.e. $\lim_{\epsilon \to 0} \left[\int_\epsilon [b] f(r) d\tau \right]$. Now $(\underset{\sim}{s}_i \cdot \nabla)(\underset{\sim}{s}_j \cdot \nabla)$ can be rewritten as

$$(\underset{\sim}{s}_i \cdot \nabla)(\underset{\sim}{s}_j \cdot \nabla) = s_{ix} s_{jx} \frac{\partial^2}{\partial x^2} + s_{ix} s_{jy} \frac{\partial}{\partial x} \frac{\partial}{\partial y} + \ldots \qquad \text{...(III.E.38)}$$

where only the first two of nine terms have been shown. After operating on $\frac{1}{r_{ij}}$ with this expression, multiplying by f(r), and then integrating over the region bounded by $r = \epsilon$, when the limit as $\epsilon \to 0$ is taken, the cross-terms (such as the second term on the right-hand side of eqn. (III.E.38)) will become infinite. These can be ignored, since we will only be interested in energy differences; the infinities, which are constant, will cancel. Thus we are left with

$$\lim_{\epsilon \to 0} \left[\int_\epsilon [b] f(r) d\tau \right] = \lim_{\epsilon \to 0} \left[\int \left(s_{ix} s_{jx} \frac{\partial^2}{\partial x^2} + s_{iy} s_{jy} \frac{\partial^2}{\partial y^2} + s_{iz} s_{jz} \frac{\partial^2}{\partial z^2} \right) \frac{1}{r_{ij}} f(r) d\tau \right] \qquad \text{...(III.E.39)}$$

By symmetry, the value of the integral does not depend on the absolute spatial orientation of the vectors $\underset{\sim}{s}_i$ and $\underset{\sim}{s}_j$, but only on their relative orientation. Therefore, $s_{ix}s_{jx}$, $s_{iy}s_{jy}$, and $s_{iz}s_{jz}$ can each be replaced by the average value $\frac{1}{3}\underset{\sim}{s}_i \cdot \underset{\sim}{s}_j$,

$$\lim_{\epsilon \to 0} \left[\int_\epsilon [b] f(r) d\tau\right] = \tfrac{1}{3}(\underset{\sim}{s}_i \cdot \underset{\sim}{s}_j) \lim_{\epsilon \to 0} \left[\int_\epsilon \nabla^2 \frac{1}{r_{ij}} f(r) d\tau\right] \qquad \text{...(III.E.40)}$$

where the definition of ∇^2 (eqn. (III.B.2)) has been employed. Since all uses to which the hamiltonian will be put involve integrals of this type, we can effectively set

$$[b]_{r=0} = \left[\tfrac{1}{3}(\underset{\sim}{s}_i \cdot \underset{\sim}{s}_j)\nabla^2 \frac{1}{r_{ij}}\right]_{\epsilon \to 0} \qquad \text{...(III.E.41)}$$

This is of the same form as the [a] term, which we now look at.

A consequence of Gauss's divergence theorem is that (29)

$$\nabla^2 \frac{1}{r_{ij}} = -4\pi\delta(r_{ij}) \qquad \text{...(III.E.42)}$$

where $\delta(r_{ij})$ is the Dirac delta function, which is defined to be zero everywhere except at $r_{ij} = 0$. This definition is consistent with the way in which the $[b]_{r=0}$ term is to be evaluated (i.e. $\lim_{\epsilon \to 0}$). Thus the [a] and $[b]_{r=0}$ terms have the same form and can be combined, giving

$$H_{ss,ij} = \frac{\mu_0 g^2 \mu_B^2}{4\pi\hbar^2} \left\{ -\frac{8\pi}{3}(\underset{\sim}{s}_i \cdot \underset{\sim}{s}_j)\delta(r_{ij}) + \left[(\underset{\sim}{s}_i \cdot \underset{\sim}{s}_j) r_{ij}^{-3} - 3(\underset{\sim}{s}_i \cdot \underset{\sim}{r}_{ij})(\underset{\sim}{s}_j \cdot \underset{\sim}{r}_{ij}) r_{ij}^{-5}\right]_{r \neq 0} \right\} \qquad \text{...(III.E.43)}$$

where the $[\ ]_{r \neq 0}$ indicates that any integrals involving this part of the hamiltonian are to be evaluated excluding the infinitesimally small region about $r_{ij} = 0$.

In summary, the hamiltonian as given in eqn. (III.E.31), when present in integrals evaluated over all spatial coordinates, will yield values of infinity — actually, infinity plus additional finite terms. The derivation following eqn. (III.E.31) has projected out these finite terms (by neglecting the infinite parts, a legitimate procedure

since they cancel upon taking differences ...spectral lines being energy differences).

The first term in eqn. (III.E.43) is a contact term — i.e. the two electrons are in contact with each other, since $r_{ij} = 0$. The contact interaction was first worked out quantitatively by Fermi (30), using the relativistic Dirac equation. It can, however, be treated using purely classical theory, as has been shown by Ferrell (31).[15] The derivation of the spin-spin interaction presented here is a "middle-ground" treatment in the sense that the spin was assumed to come from relativity theory, then classical theory was used to derive the hamiltonian (29). That part of the derivation dealing with the contact term is a modified version of that given by Bethe and Salpeter (33).

Eqn. (III.E.43) describes the interaction of two electrons. For more than two electrons, we sum over the electrons, being careful not to count twice,

$$H_{ss} = \frac{\mu_o g^2 \mu_B^2}{4\pi\hbar^2} \sum_{j>i} \left\{ -\frac{8\pi}{3}(\underset{\sim}{s}_i \cdot \underset{\sim}{s}_j)\delta(r_{ij}) + \left[(\underset{\sim}{s}_i \cdot \underset{\sim}{s}_j) r_{ij}^{-3} - 3(\underset{\sim}{s}_i \cdot \underset{\sim}{r}_{ij})(\underset{\sim}{s}_j \cdot \underset{\sim}{r}_{ij}) r_{ij}^{-5}\right]_{r\neq 0} \right\} \quad \text{...(III.E.44)}$$

This equation applies equally well to atoms and to molecules. The first term, the contact term, gives a constant contribution to the energy of a given electronic state, so in practice it is included with the potential energy functon $U^k(Q)$ obtained during the derivation of the Born-Oppenheimer approximation — i.e. this part of H_{ss} is to be included as an additional term in eqn. (III.C.7). Only the remaining part, the dipolar term, is conventionally regarded as giving rise to the electron spin-spin interaction.

---

[15]See also Levine (32) for a clearer explanation of Ferrell's work. The derivations by Fermi and by Ferrell were actually for the case of interacting electron and nuclear spins, rather than for electron and electron spins as here. The arguments and forms of the equations are the same, however. The contact interaction in the electron-nuclear case is called the Fermi contact interaction.

III.F. Angular Momenta and Hund's Coupling Cases

The last several sections have derived the various parts of the hamiltonian operator. In this section some basic properties of angular momenta will be presented, following which the types of angular momenta that occur in diatomic molecules and the ways in which they couple will be considered.

III.F.1. Angular momenta

A quantum mechanical operator $\underset{\sim}{A}$ is an **angular momentum** operator if its space-fixed cartesian components obey the commutation rules (34a,22)

$$[A_I, A_J] = i\hbar \sum_K \epsilon_{IJK} A_K \qquad \text{...(III.F.1)}$$

where

$$\epsilon_{IJK} = \begin{cases} +1 & \text{if IJK are a cyclic permutation of XYZ} \\ 0 & \text{if any two coordinates are repeated} \\ -1 & \text{if IJK are an anticyclic permutation of XYZ} \end{cases} \qquad \text{...(III.F.2)}$$

It is often convenient to refer to a molecule-fixed coordinate system (denoted by small x,y,z, as opposed to capital X,Y,Z for space-fixed components). When referred to molecule-fixed axes, some angular momenta ($\underset{\sim}{I}$, $\underset{\sim}{L}$, $\underset{\sim}{S}$, $\underset{\sim}{J}_a$)[16] obey commutation rules analogous to those in space-fixed coordinates, namely

$$[A_i, A_j] = i\hbar \sum_k \epsilon_{ijk} A_k \qquad \text{...(III.F.3)}$$

while others ($\underset{\sim}{R}$, $\underset{\sim}{F}$, $\underset{\sim}{J}$, $\underset{\sim}{N}$, $\underset{\sim}{O}$) obey anomalous rules (22)

$$[A_i, A_j] = -i\hbar \sum_k \epsilon_{ijk} A_k \qquad \text{...(III.F.4)}$$

---

[16]For definitions of the angular momentum symbols, see Table II.

TABLE II. Angular momenta present in a diatomic molecule possessing no nuclear spin.

	Total angular momentum		Projection on molecular axis	
	Vector	Quantum no.	Vector projection	Quantum no.
Orbital ang. mom. of the i^{th} electron	$\underset{\sim}{l}_i$	l_i	l_{iz}	λ_i [a]
Spin of the i^{th} electron	$\underset{\sim}{s}_i$	s_i	s_{iz}	σ_i
Total ang. mom. of the i^{th} electron	$\underset{\sim}{j}_i$	j_i	j_{iz}	$\omega_i = \lambda_i + \sigma_i$
Total electronic orbital ang. mom.	$\underset{\sim}{L} = \sum_i \underset{\sim}{l}_i$	L	L_z	Λ [b]
Total electron spin	$\underset{\sim}{S} = \sum_i \underset{\sim}{s}_i$	S	S_z	Σ
Rotation of the nuclear framework	$\underset{\sim}{R}$	-	-	-
Total ang. mom.	$\underset{\sim}{J} = \underset{\sim}{R} + \underset{\sim}{L} + \underset{\sim}{S}$	J	J_z	$\Omega = \Lambda + \Sigma$
Total ang. mom. excluding electron spin	$\underset{\sim}{N} = \underset{\sim}{R} + \underset{\sim}{L} = \underset{\sim}{J} - \underset{\sim}{S}$	N	N_z ($\equiv L_z$)	Λ
Total ang. mom. excluding electron orbital ang. mom.	$\underset{\sim}{O} = \underset{\sim}{R} + \underset{\sim}{S} = \underset{\sim}{J} - \underset{\sim}{L}$	-	-	-
Total electronic ang. mom.	$\underset{\sim}{J}_a = \underset{\sim}{L} + \underset{\sim}{S}$	J_a	J_{az} ($\equiv J_z$)	Ω
Total atomic electron orbital ang. mom. (e.g. for atom A)	$\underset{\sim}{L}_A = \sum_i \underset{\sim}{l}_{Ai}$	L_A	-	-
Total atomic electron spin (e.g. for atom A)	$\underset{\sim}{S}_A = \sum_i \underset{\sim}{s}_{Ai}$	S_A	-	-
Total atomic electronic ang. mom. (e.g. for atom A)	$\underset{\sim}{J}_A = \underset{\sim}{L}_A + \underset{\sim}{S}_A$	J_A	-	-

(a) $\lambda_i = 0,1,2,3,\ldots$ are signified by $\sigma,\pi,\delta,\phi,\ldots$

(b) $\Lambda = 0,1,2,3,\ldots$ are signified by $\Sigma,\Pi,\Delta,\Phi,\ldots$

An angular momentum basis function $|A\alpha M_A\rangle$ is simultaneously an eigenfunction of three operators:

(i) $\underset{\sim}{A}^2$...the square of $\underset{\sim}{A}$ itself

(ii) A_z...the projection of $\underset{\sim}{A}$ onto the molecular (z) axis

(iii) A_Z...the projection of $\underset{\sim}{A}$ onto the space-fixed Z axis.

The eigenvalues are $\hbar^2 A(A+1)$, $\hbar\alpha$, and $\hbar M_A$, respectively, where A, α, and M_A are quantum numbers and are also used as labels for the basis function, i.e. $|A\alpha M_A\rangle$.

All matrix elements of $\underset{\sim}{A}^2$, A_X, A_Y, and A_Z can be derived from the commutation rules (eqn. (III.F.1)) without ever specifying the explicit functional form of $|A\alpha M_A\rangle$ or the differential operator form of $\underset{\sim}{A}$ (35a)

$$\langle A'\alpha' M_A' | \underset{\sim}{A}^2 | A\alpha M_A\rangle = +\hbar^2 A(A+1)\delta_{A'A}\delta_{\alpha'\alpha}\delta_{M_A' M_A} \quad \text{...(III.F.5)}$$

$$\langle A'\alpha' M_A' | A_Z | A\alpha M_A\rangle = +\hbar M_A \delta_{A'A}\delta_{\alpha'\alpha}\delta_{M_A' M_A} \quad \text{...(III.F.6)}$$

$$\langle A'\alpha' M_A' | A_\pm | A\alpha M_A\rangle = +\hbar e^{i(\theta_{M_A} - \theta_{M_A\pm 1})}[A(A+1)-M_A(M_A\pm 1)]^{1/2} \cdot \delta_{A'A}\delta_{\alpha'\alpha}\delta_{M_A' M_A\pm 1} \quad \text{...(III.F.7)}$$

For the molecule-fixed components of angular momenta that obey the normal commutation rules (eqn. (III.F.3)), we have the analogous matrix elements

$$\langle A'\alpha' M_A' | A_z | A\alpha M_A\rangle = +\hbar\alpha \delta_{A'A}\delta_{\alpha'\alpha}\delta_{M_A' M_A} \quad \text{...(III.F.8)}$$

$$\langle A'\alpha' M_A' | A^\pm | A\alpha M_A\rangle = +\hbar e^{i(\phi_\alpha - \phi_{\alpha\pm 1})}[A(A+1)-\alpha(\alpha\pm 1)]^{1/2} \cdot \delta_{A'A}\delta_{\alpha'\alpha\pm 1}\delta_{M_A' M_A} \quad \text{...(III.F.9)}$$

For the molecule-fixed components of angular momenta that obey the anomalous commutation rules (eqn. (III.F.4)), eqn. (III.F.8) still holds, but

$$\langle A'\alpha'M'_A|A^{\pm}|A\alpha M_A\rangle = +\hbar e^{i(\phi_\alpha-\phi_{\alpha\mp1})}[A(A+1)-\alpha(\alpha\mp1)]^{1/2}$$
$$\cdot\delta_{A'A}\delta_{\alpha'\alpha\mp1}\delta_{M'_AM_A} \quad ...(III.F.10)$$

In the foregoing equations, ladder operators have been used; these are defined as

$$A_{\pm} = A_X \pm iA_Y \quad ...(III.F.11)$$

and $A^{\pm} = A_x \pm iA_y$ ...(III.F.12)

θ_{M_A}, $\theta_{M_A\pm1}$, ϕ_α and $\phi_{\alpha\pm1}$ are arbitrary phase factors of the basis functions. For space-fixed components, the convention of Condon and Shortley (35(a)) is generally adopted. By this convention, the $2A+1$ $|A\alpha M_A\rangle$ basis functions (with $M_A = -A, -A+1, \ldots, +A$) all have the same phase factor, obtained by requiring all matrix elements of $A_X = \frac{1}{2}(A_+ + A_-)$ to be real and positive. Unfortunately, for molecule-fixed components, a standard phase convention is not in universal use, though such a standard convention has been proposed by Brown and Howard (36) (see also Lefebvre-Brion and Field (22)). For this work we choose

$$e^{i(\phi_\alpha-\phi_{\alpha\pm1})} = e^{i(\phi_\alpha-\phi_{\alpha\mp1})} = +1 \quad ...(III.F.13)$$

III.F.2. Hund's coupling cases

Table II serves to define the various types of angular momenta present in diatomic molecules, though only certain ones will be relevant in any particular case.

The angular momenta present in a diatomic molecule are described as "coupled" according to the relative strengths of their various interactions. Hund (37) distinguished four such types of coupling, labeled (a) to (d). A fifth type, case (e), not discussed by Hund, was introduced by Mulliken (38). A number of sub-categories

have been described (36)[17]: cases (b') and (d') and the close-nuclei and far-nuclei forms of case (c). Yet further sub-categories arise when nuclear spin is present (42). All of these cases and sub-categories thereof are limiting situations. Any given state of any given molecule may be best described by one or another of these limits or may be somewhere in between. By "best described by" we mean the basis set is the one in which the hamiltonian matrix is the most nearly diagonal — see next section. Within a particular state, conditions may change from being closer to one limiting coupling case to being closer to another as rotation increases (i.e. as J or N increases).

Since the states of FeO studied in this thesis exhibit behavior typical of the case (a) situation, the present discussion is limited to Hund's case (a) coupling. For the other cases, the reader is referred to such general texts as Herzberg (16), Townes and Schawlow (43), or King (44a).

Case (a) coupling occurs when the energy separations between the components of a $^{2S+1}\Lambda_{\Omega}$ multiplet state resulting from the diagonal elements of H_{so} are much larger than the off-diagonal elements of the $\underset{\sim}{S}$-uncoupling operator $B\underset{\sim}{J}^{\pm}\underset{\sim}{S}^{\mp}$. The matrix elements involved will become clearer after Sections III.F.3 and III.H; for now they are just stated without explanation:

$$\left|\langle\eta\Lambda S\Sigma\Omega JM|H_{so}|\eta\Lambda S\Sigma\Omega JM\rangle-\langle\eta\Lambda S\Sigma'\Omega' JM|H_{so}|\eta\Lambda S\Sigma'\Omega' JM\rangle\right|=\left|A\Lambda\right| \qquad ...(III.F.14)$$

$$\left|\langle\eta\Lambda S\Sigma\Omega JM|B\underset{\sim}{J}^{-}\underset{\sim}{S}^{+}|\eta\Lambda S\Sigma'\Omega' JM\rangle\right| = BJ\sqrt{2S} \qquad ...(III.F.15)$$

where

$$\Sigma' = \Sigma - 1$$
$$\Omega' = \Omega - 1 \qquad ...(III.F.16)$$

---

[17]Kopp and Hougen (39) defined a case (a') for Σ states, but the prime is not really necessary (see, for example, Refs. (40) or (41)).

Thus case (a) occurs when

$$|A\Lambda| >> BJ\sqrt{2S} \qquad \text{...(III.F.17)}$$

In principle, the limit of *pure* case (a) is approached more and more closely as $|A| \rightarrow \infty$ or as $B \rightarrow 0$. However, in practice, if the spin-orbit interaction becomes too large, it becomes difficult to recognize the multiplet components as belonging to the same state and the case (c) model becomes more appropriate. Thus the best examples of case (a) occur when A is moderate in value and B is small. Note also the J-dependence in eqn. (III.F.17); as a consequence, as J increases case (a) becomes a less good description and eventually case (b) may become a better one.

In Fig. 4 the angular momenta present in case (a) are represented as vectors. Both the total electronic orbital angular momentum $\underset{\sim}{L}$ and the total electron spin $\underset{\sim}{S}$ are coupled to, and precess rapidly about, the molecular axis, with constant projections L_z and S_z and associated quantum numbers Λ and Σ, respectively. The total angular momentum, in the absence of nuclear spin, is $\underset{\sim}{J} = \underset{\sim}{R} + \underset{\sim}{L} + \underset{\sim}{S}$, and its component along the molecular axis is represented by the quantum number $\Omega = \Lambda + \Sigma$.

The quantum number Σ can take the $2S+1$ values

$$\Sigma = S, S-1, \ldots, -S \qquad \text{...(III.F.18)}$$

The total angular momentum $\underset{\sim}{J}$ cannot be smaller than its component and so, for a given Ω, J has values

$$J = |\Omega|, |\Omega+1|, |\Omega+2|, \ldots \qquad \text{...(III.F.19)}$$

Since $S = \sum_i s_i$, where $s_i = \pm\frac{1}{2}$, and since $\Omega = \Lambda + \Sigma$; S, Σ, Ω, and J will all be integral or half-integral depending on whether there are an even or an odd number of electrons present in the molecule, respectively, and this will hold for all states of the molecule. The multiplicities, $2S+1$, of the states must correspondingly be odd or even. With a total of 34 electrons, all states of FeO must have odd multiplicity and the values of S, Σ, Ω, and J will all be integral.

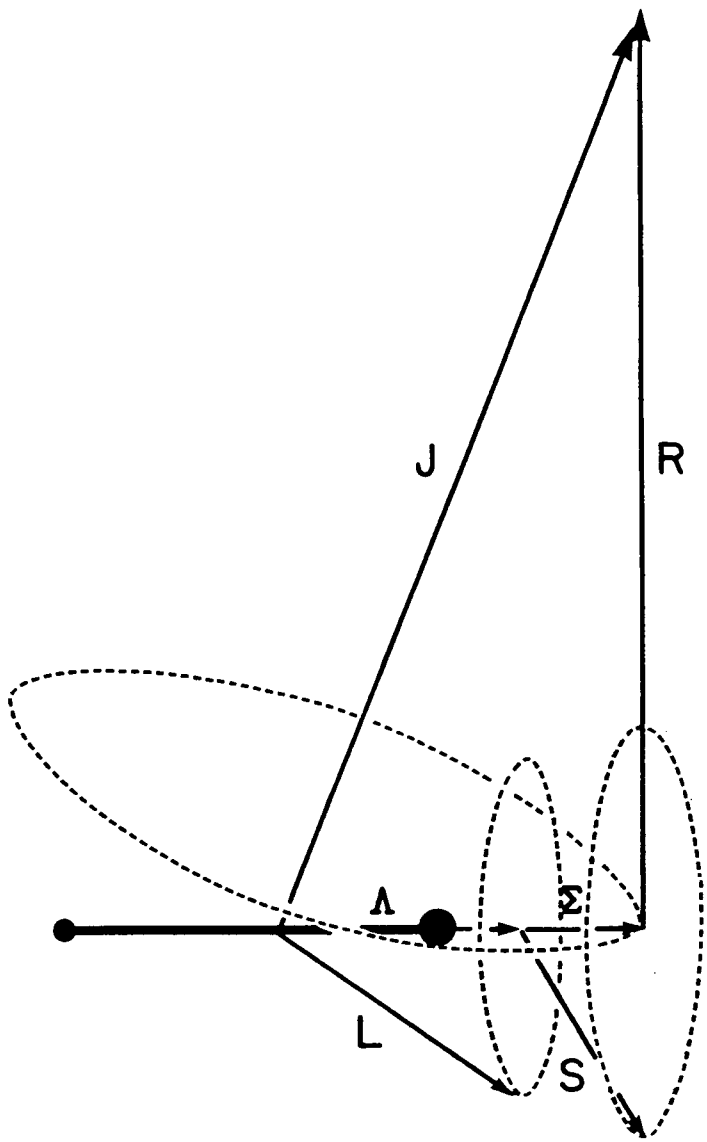

Fig. 4. Vector diagram for Hund's coupling case (a).

III.F.3. Angular momentum basis functions

If two (or more) operators commute, that is, if

$$AB\phi - BA\phi = 0 \qquad \text{...(III.F.20)}$$

for all functions ϕ, or symbolically, if

$$[A,B] = AB - BA = 0 \qquad \text{...(III.F.21)}$$

then a complete set of functions must exist that are eigenfunctions of the two (or more) operators simultaneously. While there are only a few operators that commute with the exact hamiltonian H (two examples being $\underset{\sim}{J}^2$ and $\underset{\sim}{J}_z$), there are many that commute with parts of H — notably, and of most importance here, a number of angular momentum operators.

In Section (III.H), H will be partitioned into two parts

$$H = H^0 + H' \qquad \text{...(III.F.22)}$$

Hund's coupling cases each correspond to a set of mutually commuting angular momentum operators. The partitioning indicated by eqn. (III.F.22) can be done in such a manner that H^0 commutes with the set of angular momentum operators of a given coupling case. Therefore, there must exist simultaneous eigenfunctions of H^0 and the angular momenta of that coupling case. Since the actual functional form of an angular momentum eigenfunction does not have to be specified (Section III.F.1), these eigenfunctions can be designated simply by listing the quantum numbers associated with the angular momenta of the particular coupling case. These are called **good quantum numbers** for H^0, since H^0 possesses only diagonal matrix elements in this basis set.

The choice of basis set is, in principle, completely arbitrary, provided the basis set forms a complete set of functions. However, usually one set will be more

appropriate or convenient than the others. In this thesis, a case (a) basis set will always be used, because the states of FeO being studied exhibit good case (a) behavior (although one could argue that they are tending towards case (c) as a result of the large number of perturbations present), and because the matrix elements of H_r and H_{so} can be evaluated in this basis using simple ladder operator techniques (see Section III.H) as a result of the presence of the maximum number of molecule-fixed z-components of the angular momenta (Λ, Σ, and Ω) and the absence of intermediate angular momenta (such as N in case (b), $\underset{\sim}{J}_a$ in case (c)).

The good quantum numbers in Hund's case (a) are Λ, S, Σ, Ω, J, and M. The basis states are therefore written as $|nv\Lambda S\Sigma\Omega JM\rangle$, where nv (sometimes written as η) designates some particular vibronic state — n is a label standing for the electronic state and v is the vibrational quantum number. M, the quantum number associated with the projection of $\underset{\sim}{J}$ on the space-fixed Z axis, has 2J+1 values: -J, -J+1, ..., +J. In the absence of external electric or magnetic fields, each J level has a degeneracy of 2J+1 and M does not need to be specified in the basis set labels. The basis states can be factorized as follows

$$\begin{aligned} |nv\Lambda S\Sigma\Omega JM\rangle &= |n\Lambda;\ v;\ S\Sigma;\ \Omega JM\rangle \\ &= |n\Lambda\rangle\,|v\rangle\,|S\Sigma\rangle\,|\Omega JM\rangle \end{aligned} \qquad \text{...(III.F.23)}$$

where the parts have the meanings

$|n\Lambda\rangle$ electronic
$|v\rangle$ vibrational (=radial)
$|S\Sigma\rangle$ spin
$|\Omega JM\rangle$ rotational (=angular)

} non-rotational basis

} rotational (total) basis

III.G. Symmetry, Parity, and Lambda-doubling

The concepts of symmetry and parity form an integral part of any discussion of Λ-doubling, so we begin with these. Parity refers to the behavior of the complete wavefunction (apart from translation) when the signs of the space-fixed Cartesian components of all particles are reversed. The parity operator or inversion operator E^* can be defined by its behavior on the space-fixed coordinates of the i^{th} particle as[18]

$$E^*(X_i, Y_i, Z_i) = (-X_i, -Y_i, -Z_i) \qquad \text{...(III.G.1)}$$

Another operator of importance here is the reflection operator in a plane containing the molecular axis, $\sigma_{v(xz)}$ (46b)

$$\sigma_{v(xz)}(x_i, y_i, z_i) = (x_i, -y_i, z_i) \qquad \text{...(III.G.2)}$$

$$\sigma_{v(xz)}(X_i, Y_i, Z_i) = (-X_i, -Y_i, -Z_i) \qquad \text{...(III.G.3)}$$

If the total molecular wavefunction ψ is represented by a case (a) basis function $|\eta\Lambda S\Sigma\Omega JM\rangle$ with signed values of Λ, Σ, and Ω, and if $|\eta\Lambda S\Sigma\rangle$ represents the corresponding nonrotating molecule basis function, and if $|\eta\Lambda\rangle$ represents the electronic orbital part of the wavefunction ψ_e, then it can be shown that the actions of these operators are as follows (45,22)

$$E^*|\eta\Lambda S\Sigma\Omega JM\rangle = (-1)^{J-S+s}|\eta, -\Lambda, S, -\Sigma, -\Omega, J, M\rangle \qquad \text{...(III.G.4)}$$

$$\sigma_{v(xz)}|\eta\Lambda S\Sigma\rangle = (-1)^{\Lambda+\Sigma-S+s}|\eta, -\Lambda, S, -\Sigma\rangle \qquad \text{...(III.G.5)}$$

$$\sigma_{v(xz)}|\eta\Lambda\rangle = (-1)^{\Lambda+s}|\eta, -\Lambda\rangle \qquad \text{...(III.G.6)}$$

---

[18]Some authors use a different symbol: E^* (Larsson (45)) ≡ I (Hougen (46a)) ≡ i (King (44b)) ≡ i_{sp} (Zare *et al.* (47)) ≡ P (Landau and Lifshitz (35b)). Note that the space-fixed inversion operator is different from the molecule-fixed inversion operator.

where (47)

$$s = \begin{cases} 1 \text{ for } \Sigma^- \text{ states} \\ 0 \text{ for } \Sigma^+ \text{ states and (by arbitrary choice) for all other states} \end{cases} \quad \text{...(III.G.7)}$$

See Larsson (45) and Lefebvre-Brion and Field (22) for discussions about the phase choices implicit in these equations. The two operators are related as follows (45):

$$E^* \,|\, \eta\Lambda S\Sigma\Omega JM\rangle = \sigma_{v(xz)} \,|\, \eta\Lambda S\Sigma\rangle C_{2(y)} \,|\, \Omega JM\rangle \quad \text{...(III.G.8)}$$

where $C_{2(y)}$ rotates the molecular frame around the y-axis by an angle of π.

The eigenvalues of these operators must be ± 1, as follows immediately from the fact that two successive operations must return the original eigenfunction

$$(E^*)^2 \,|\, \eta\Lambda S\Sigma\Omega JM\rangle = p^2 \,|\, \eta\Lambda S\Sigma\Omega JM\rangle = |\, \eta\Lambda S\Sigma\Omega JM\rangle \longrightarrow p = \pm 1 \quad \text{...(III.G.9)}$$

$$(\sigma_{v(xz)})^2 \,|\, \eta\Lambda\rangle = p_e^2 \,|\, \eta\Lambda\rangle = |\, \eta\Lambda\rangle \longrightarrow p_e = \pm 1 \quad \text{...(III.G.10)}$$

p (= + or −; or "even" or "odd") is called the parity of the total wavefunction, and p_e (= + or −) is called the symmetry of the electronic wavefunction, where we are considering only the spatial (molecule-fixed) coordinates of the electronic wavefunction (not spin). Corresponding to the two eigenvalues of E^* are two eigenfunctions, which can be distinguished by means of + and − signs denoting their parity,

$$\begin{aligned} E^* \psi^+ &= +\psi^+ \\ E^* \psi^- &= -\psi^- \end{aligned} \quad \text{...(III.G.11)}$$

and similarly for the $\sigma_{v(xz)}$ eigenfunctions,

$$\begin{aligned} \sigma_{v(xz)} \psi_e^+ &= +\psi_e^+ \\ \sigma_{v(xz)} \psi_e^- &= -\psi_e^- \end{aligned} \quad \text{...(III.G.12)}$$

States with $|\Lambda| \geq 1$, if completely isolated from all other states, are doubly degenerate because there are two values, $\pm|\Lambda|$. As can be seen from eqns. (III.G.4)–(G.6), for $|\Lambda| \geq 1$ the case (a) basis functions, or parts thereof, are not eigenfunctions of the inversion or reflection operators, since they are themselves changed by the actions of the operators. However, we are free to take linear combinations of the basis functions, since by the definition of a complete basis set, any linear combination of basis functions must also be a member of the set. Hence we can choose as our basis set those linear combinations that are eigenfunctions of E^* and of $\sigma_{v(xz)}$ so long as they are linearly independent. As can easily be checked by the use of eqns. (III.G.4) or (G.6), these are, for E^*,

$$|\eta\Lambda S\Sigma\Omega JMp\rangle = \frac{1}{\sqrt{2}}\left[|\eta\Lambda S\Sigma\Omega JM\rangle \pm |\eta,-\Lambda,S,-\Sigma,-\Omega,J,M\rangle\right] \quad ...(III.G.13)$$

and for $\sigma_{v(xz)}$,

$$|\eta\Lambda p_e\rangle = \frac{1}{\sqrt{2}}\left[|\eta\Lambda\rangle \pm |\eta,-\Lambda\rangle\right] \quad ...(III.G.14)$$

where

$$p = \pm (-1)^{J-S+s} \quad ...(III.G.15)$$

$$p_e = \pm (-1)^{\Lambda+s} \quad ...(III.G.16)$$

The basis set formed by taking the linear combinations of case (a) basis functions as in eqn. (III.G.13) is called a parity basis, since the resulting basis functions have a definite parity. These parity basis functions correspond to the eigenfunctions called ψ^+ and ψ^- in eqn. (III.G.11), i.e.

$$\begin{aligned} |\eta\Lambda S\Sigma\Omega JM+\rangle &\equiv \psi^+ \\ |\eta\Lambda S\Sigma\Omega JM-\rangle &\equiv \psi^- \end{aligned} \quad ...(III.G.17)$$

The corresponding electronic wavefunctions likewise have definite symmetries as seen

from eqn. (III.G.14), where

$$|\eta\Lambda+> \equiv \psi_e^+$$
$$|\eta\Lambda-> \equiv \psi_e^- \qquad \text{...(III.G.18)}$$

Note that a total wavefunction having positive (= even) parity, for example, does not necessarily belong with an electronic wavefunction having positive symmetry. In fact, each Ω substate of a given electronic state has two components corresponding to the symmetries + and −, and each of these has associated with it a set of rotational levels whose parities (even or odd) alternate with J. For a given value of J, the two symmetry components have opposite parities, where the parity of a rotational level is that of the corresponding total wavefunction. The symmetry components of an electronic state can be denoted in the state symbol by means of a superscript + or −, e.g. $^5\Delta^+$ or $^5\Delta^-$.[19]

For Σ states, $\Lambda = 0$, so there is no double degeneracy. Σ states normally belong to Hund's case (b), for which

$$E^*|\eta,\Lambda=0,SJN> = (-1)^{N+S}|\eta,\Lambda=0,SJN> \qquad \text{...(III.G.19)}$$

Thus the case (b) functions themselves form a parity basis without needing to take linear combinations. Since there is no degeneracy in Λ, a given Σ state will be *either* a Σ^+ state *or* a Σ^- state. If a Σ state is represented by a case (a) basis, eqn. (III.G.13) still applies, with $\Lambda = -\Lambda = 0$.

The hamiltonian is invariant under inversion (i.e. H commutes with E^*); hence, according to group theory, nonzero matrix elements can only occur between rotational levels having the same parity, i.e.

selection rule: $+ \longleftrightarrow +$ $\quad - \longleftrightarrow -$ ...(III.G.20)

---

[19]Herzberg gives a different definition of + and − on page 239 of his book (16). However, in two other places (pp. 217 and 237) he gives the same definition as used here. King (44c,b) also defines the + and − symmetry labels as used in this thesis. Some authors (e.g. Kovács (48a) and Merer (49)) define + and − as $p_e = \pm$ instead of as in eqn. (III.G.16); this definition is not based on σ_v.

Another selection rule is (see Section III.J)

$$\Delta J = 0 \qquad \text{...(III.G.21)}$$

Since + and - parity levels so not occur in pairs in Σ states as they do in non-Σ states, interaction of a non-Σ state with a Σ state or states results in a lifting of the degeneracy in the non-Σ state — i.e. Λ-doubling occurs. Specifically for odd-multiplicity states, as in FeO, it is the $\Omega = 0$ component of the Σ state(s) that causes Λ-doubling, since the other Ω components occur as parity pairs.

It is convenient to distinguish the two Λ-doubled members of each rotational level by means of a label other than the symmetry label $\pm$, since this is too easily confused with the parity symbol $\pm$ with which each level is also labelled. Various conventions have been used in the past; the modern labelling scheme uses the letters e and f, defined as follows (50):

$$\text{levels with parity } \pm(-1)^{J-\sigma} \text{ are } \begin{matrix} e \\ f \end{matrix} \text{ levels} \qquad \text{...(III.G.22)}$$

where

$$\sigma = \begin{cases} \frac{1}{2} & \text{for even-multiplicity states} \\ 0 & \text{for odd-multiplicity states} \end{cases} \qquad \text{...(III.G.23)}$$

The definitions of e and f are such that for a given non-Σ state all e levels have electronic wavefunctions with the same symmetry (+ or -) and all f levels have electronic wavefunctions with the same symmetry but opposite to that of the e levels (- or +).[20] When the hamiltonian matrix is written in a parity basis, it factorizes

---

[20]Whether the e levels correspond to an electronic wavefunction symmetry of + or of - depends on the values of Λ and S. This can be determined from the simultaneous use of eqns. (III.G.13), (G.14), (G.15), (G.16), and (G.22). For example, for a $^5\Delta$ state, these equations yield $^5\Delta^+ \sim e$; $^5\Delta^- \sim f$.

into two submatrices — one of symmetry e and one of symmetry f.[21] The selection rules for interactions between levels become, in this nomenclature,

$$e \leftrightarrow e \qquad f \leftrightarrow f \qquad \text{...(III.G.24)}$$

and, as before,

$$\Delta J = 0 \qquad \text{...(III.G.25)}$$

In situations where it is not known which level of a parity-doublet pair is e and which f, the labels a and b are used for the levels lying lower and upper in energy, respectively (50).

Since the $\Omega = 0$ components of Σ states are of particular interest (see above), the parities and e/f labels for these are given in Table III. For other Ω components and for even multiplicity Σ states, eqns. (III.G.13) and (G.15) are used to determine the total parities just as for non-Σ states.

The matrix elements responsible for the interactions that lead to Λ-doubling will be discussed in Section III.H.2.a, where the specific case of Λ-doubling in a $^5\Delta$ state will be treated in terms of an effective hamiltonian.

---

[21]Sometimes in the literature the word "parity" is used loosely to refer to the e/f labels, or even to the +/- symmetries, instead of just in its restrictive meaning used in this section — i.e. the behavior with respect to E^* of the total wavefunction.

TABLE III. Total parity and e/f labels in the $\Omega = 0$ components of odd-multiplicity Σ states.[a]

	+ total parity	- total parity	e levels	f levels
$^1\Sigma^+$, $^3\Sigma_0^-$, $^5\Sigma_0^+$, etc.	even J	odd J	all J	-
$^1\Sigma^-$, $^3\Sigma_0^+$, $^5\Sigma_0^-$, etc.	odd J	even J	-	all J

(a) Based on Lefebvre-Brion and Field (22).

III.H. Effective Hamiltonian and Matrix Elements

During the analysis of a spectrum, a process of data reduction must of necessity occur. Starting with often as many as thousands of measurements of line frequencies, the object is to mathematically reduce these to only a certain few parameters ("constants"), without loss of information, and in the process to enhance understanding by emphasizing physical interpretations. If enough terms are included, experimental data can always, in principle, be fitted to a mathematical formula of some sort, but such a process is only worthwhile if the terms can be interpreted to convey physically useful information.

Since the nuclei and electrons in a molecule can arrange themselves in essentially an infinite number of ways, a complete mathematical description of a molecule could, in principle, contain an infinite number of terms — obviously not a desirable nor physically enlightening approach to take. The key to making the situation more tractable is the separation into individual electronic, vibrational, and rotational sub-problems described in Sections III.C and D. While these sub-problems still involve infinite series (see eqns. (III.D.1) and (D.4)), in practice, since the terms in the series become successively smaller, only a few are actually needed.

The problem is that the separations do involve approximations. In reality, interactions between the various motions do exist, and for high resolution work cannot be completely neglected.

The solution is to manipulate the hamiltonian in such a way that the separation into individual electronic, vibrational, and rotational parts becomes an acceptable approximation. This can be accomplished by creating an effective hamiltonian that operates only within the rotational sub-space of a given vibronic state. A number of methods of doing this have been developed — see, for example, Miller (51), Soliverez (52), and Brown and co-workers (53,54). These usually start by dividing the exact hamiltonian into two parts

$$H = H^0 + H' \qquad \text{...(III.H.1)}$$

in such a manner that the matrix representation of H^0 is completely diagonal in the basis set being used and that any off-diagonal matrix elements will come from H'. Some form of perturbation theory treatment is then used to bring the effects of H' onto the diagonal positions or into diagonal blocks.

Ordinary nondegenerate perturbation theory is not appropriate for this purpose since it does not apply to close-lying energy levels such as the different spin-levels of a multiplet state. Degenerate perturbation theory can be used (51,52) but is very complicated in practice. An alternative method, derived initially by Van Vleck (55) and later described in more detail by several other authors (56,57,58,22), is simpler to use than degenerate perturbation theory. This method applies a form of nondegenerate perturbation theory to situations where there are close-lying levels (such as the spin levels of a multiplet state or several close-lying vibronic levels), and separates these levels from all distant-lying levels. Unlike ordinary nondegenerate perturbation theory, which only introduces energy correction terms into on-diagonal matrix positions, Van Vleck's method yields both on- and off-diagonal elements within the group of close-lying levels.[22]

III.H.1. The Van Vleck transformation

Following Löwdin (59), the infinite basis set is partitioned into two classes: **class 1** includes the one or more (but a finite number of) basis functions whose associated energies lie in the energy region of interest; **class 2** consists of the infinite number of remaining basis functions, which lie at remote energies to the class 1 functions.

---

[22]This will be seen in eqns. (III.H.18)-(H.22) below: there are matrix elements $\tilde{H}_{ab}$ for $a \neq b$ as well as for $a = b$.

The Van Vleck method consists of applying a specific unitary transformation, a type of contact transformation called a Van Vleck transformation, to the original exact hamiltonian matrix, $\underline{H}$, to produce a new, still exact, matrix, $\underline{\tilde{H}}$, in which class 1-class 2 elements are smaller by a factor of $[\underline{H}_{12}/(E_1^0 - E_2^0)]^2$ [23] than the corresponding elements in $\underline{H}$. That is,

$$\underline{T}^\dagger \underline{H} \underline{T} = \underline{\tilde{H}} \qquad \text{...(III.H.2)}$$

or, in terms of the submatrices,

$$\begin{bmatrix} \underline{H}_{22} & \underline{H}_{12} \\ \underline{H}_{21} & \underline{H}_{11} \end{bmatrix} \xrightarrow[\text{TRANSFORMATION}]{\text{VAN VLECK}} \begin{bmatrix} \underline{\tilde{H}}_{22} & \underline{\tilde{H}}_{12} \\ \underline{\tilde{H}}_{21} & \underline{\tilde{H}}_{11} \end{bmatrix} \qquad \text{...(III.H.3)}$$

Since the matrix elements in $\underline{\tilde{H}}_{12}$ $(=\underline{\tilde{H}}_{21})$ are smaller than the original $\underline{H}_{12}$ $(=\underline{H}_{21})$ elements, it is a better approximation to neglect these elements than to neglect the original off-diagonal elements (as would be done in the Born-Oppenheimer approximation). Thus, to a good approximation, an **effective hamiltonian matrix** can be defined as

$$\underline{H}^{eff} = \underline{\tilde{H}}_{11} \qquad \text{...(III.H.4)}$$

that is, only the class 1 part of $\underline{\tilde{H}}$ is retained.

Expressions will now be derived for the matrix elements of $\underline{\tilde{H}}_{11}$ following Kemble (57), Wollrab (58), and Lefebvre-Brion and Field (22). We start by writing the matrix representation of eqn. (III.H.1) with a perturbation parameter λ inserted,

$$\underline{H} = \underline{H}^0 + \lambda \underline{H}' \qquad \text{...(III.H.5)}$$

where λ can have values between 0 and 1, and the second term, $\lambda \underline{H}'$, is regarded as a perturbation. The situation for $\lambda = 0$ corresponds to the unperturbed problem (the

---

[23] The symbols will be defined shortly.

class 1 states in isolation), and when $\lambda = 1$, the corresponding hamiltonian is the exact hamiltonian for the complete system (class 1 + class 2). As used here, λ is an order-sorting parameter.

The matrix after transformation can be expanded as a power series in λ,

$$\underline{\tilde{H}} = \underline{\tilde{H}}^{(0)} + \lambda\underline{\tilde{H}}^{(1)} + \lambda^2\underline{\tilde{H}}^{(2)} + \ldots \qquad \text{...(III.H.6)}$$

It is the aim of the Van Vleck method to eliminate the first-order terms in λ that connect classes 1 and 2. This is accomplished as follows. Let $\underline{T}$ be a unitary matrix, which can always be written in terms of a hermitian matrix $\underline{S}$ as follows, then expanded,

$$\underline{T} = e^{i\lambda\underline{S}} = 1 + i\lambda\underline{S} - \frac{\lambda^2}{2}\underline{S}^2 - \frac{i\lambda^3}{6}\underline{S}^3 + \ldots \qquad \text{...(III.H.7)}$$

Performing the unitary transformation indicated by eqn. (III.H.2)

$$\begin{aligned}\underline{\tilde{H}} &= \underline{\tilde{H}}^{(0)} + \lambda\underline{\tilde{H}}^{(1)} + \lambda^2\underline{\tilde{H}}^{(2)} + \ldots \\ &= (1 - i\lambda\underline{S} - \frac{\lambda^2}{2}\underline{S}^2 + \ldots)(\underline{H}^0 + \lambda\underline{H}')(1 + i\lambda\underline{S} - \frac{\lambda^2}{2}\underline{S}^2 - \ldots)\end{aligned} \qquad \text{...(III.H.8)}$$

terms in equal powers of λ can be equated,

$$\lambda^0: \quad \underline{\tilde{H}}^{(0)} = \underline{H}^0 \qquad \text{...(III.H.9)}$$

$$\lambda^1: \quad \underline{\tilde{H}}^{(1)} = \underline{H}' + i(\underline{H}^0\underline{S} - \underline{S}\underline{H}^0) \qquad \text{...(III.H.10)}$$

$$\lambda^2: \quad \underline{\tilde{H}}^{(2)} = i(\underline{H}'\underline{S} - \underline{S}\underline{H}') + \underline{S}\underline{H}^0\underline{S} - \tfrac{1}{2}(\underline{H}^0\underline{S}^2 - \underline{S}^2\underline{H}^0) \qquad \text{...(III.H.11)}$$

The functional form of the elements in $\underline{S}$ has so far not been specified, other than that it be hermitian. We are free to construct $\underline{S}$ so that $\underline{T}$ will transform $\underline{H}$ into the desired approximately block-diagonal form. Denoting the individual elements within each class by Roman letters (a,b) for class 1 and by Greek letters (α,β) for

class 2, $\underline{S}$ is constrained so that no mixing can occur among the class 1 functions,

$$S_{ab} = 0 \qquad \text{...(III.H.12)}$$

or among the class 2 functions,

$$S_{\alpha\beta} = 0 \qquad \text{...(III.H.13)}$$

for all values of a and b ($a \neq b$) and of α and β ($\alpha \neq \beta$). In order to force the first order elements of $\underline{\tilde{H}}$ off-diagonal in class to vanish, it follows that, for any values of a and α,

$$S_{a\alpha} = \frac{iH'_{a\alpha}}{E^0_a - E^0_\alpha} \qquad \text{...(III.H.14)}$$

where

$$\begin{aligned} E^0_a &= \langle a|\underline{H}^0|a\rangle = H^0_{aa} \\ E^0_\alpha &= \langle \alpha|\underline{H}^0|\alpha\rangle = H^0_{\alpha\alpha} \end{aligned} \qquad \text{...(III.H.15)}$$

This can easily be checked by substituting eqn. (III.H.14) into the appropriate element of (III.H.10), which we look at first:

$$\begin{aligned} \tilde{H}^{(1)}_{a\alpha} &= H'_{a\alpha} + i[(\underline{H}^0\underline{S})_{a\alpha} - (\underline{S}\underline{H}^0)_{a\alpha}] \\ &= H'_{a\alpha} + i[H^0_{aa}S_{a\alpha} - S_{a\alpha}H^0_{\alpha\alpha}] \end{aligned} \qquad \text{...(III.H.16)}$$

where use has been made of eqns. (III.H.12) and (H.13), together with the diagonal nature of $\underline{H}^0$ (within the classes as well as between classes). Substitution of eqns. (III.H.14) and (H.15) gives

$$\begin{aligned} \tilde{H}^{(1)}_{a\alpha} &= H'_{a\alpha} - \left[\frac{E^0_a H'_{a\alpha}}{E^0_a - E^0_\alpha} - \frac{H'_{a\alpha}E^0_\alpha}{E^0_a - E^0_\alpha}\right] \\ &= H'_{a\alpha} - H'_{a\alpha} \end{aligned}$$

$$\tilde{H}^{(1)}_{aa} = 0 \qquad \text{...(III.H.17)}$$

which is the desired result. As a consequence, the lowest order class 1–class 2 interaction terms in $\underline{\tilde{H}}$ occur in the second-order term $\underline{\tilde{H}}^{(2)}$, and these do not contribute to the energies until the fourth order (56).

The Van Vleck transformation is completely defined by eqns. (III.H.9) – (H.14) and similar equations for higher orders. The class 1 block matrix elements $\underline{\tilde{H}}_{11}$ are

$$\tilde{H}_{ab} = \tilde{H}^{(0)}_{ab} + \tilde{H}^{(1)}_{ab} + \tilde{H}^{(2)}_{ab} + \tilde{H}^{(3)}_{ab} + \ldots \qquad \text{...(III.H.18)}$$

where

$$\tilde{H}^{(0)}_{ab} = \langle a|H^0|b\rangle = E^0_a \delta_{ab} \qquad \text{...(III.H.19)}$$

$$\tilde{H}^{(1)}_{ab} = \langle a|H'|b\rangle = H'_{ab} \qquad \text{...(III.H.20)}$$

$$\tilde{H}^{(2)}_{ab} = \tfrac{1}{2} \sum_{\alpha} \left[\frac{H'_{a\alpha}H'_{\alpha b}}{E^0_a - E^0_\alpha} + \frac{H'_{a\alpha}H'_{\alpha b}}{E^0_b - E^0_\alpha} \right] \qquad \text{...(III.H.21)}$$

$$\tilde{H}^{(3)}_{ab} = \sum_{\alpha,\beta} \left[\frac{H'_{a\alpha}H'_{\alpha\beta}H'_{\beta b}}{(E^0_a - E^0_\alpha)(E^0_\beta - E^0_b)} \right] - \tfrac{1}{2} \sum_{\alpha,c} \left[\frac{H'_{ac}H'_{c\alpha}H'_{\alpha b}}{(E^0_c - E^0_\alpha)(E^0_b - E^0_\alpha)} + \frac{H'_{a\alpha}H'_{\alpha c}H'_{cb}}{(E^0_a - E^0_\alpha)(E^0_c - E^0_\alpha)} \right] \qquad \text{...(III.H.22)}$$

where δ_{ab} is the Kronecker delta. Notice that the zeroth- and first-order terms for the (a,b) element are the same as the (a,b) element of the exact hamiltonian, i.e. H_{ab}. The higher-order terms fold into the class 1 submatrix the effects that were originally off-diagonal in class.

The second-order term is often rewritten in terms of an averaged energy denominator

$$\tilde{H}^{(2)}_{ab} = \sum_{\alpha} \frac{H'_{a\alpha}H'_{\alpha b}}{(E^0_a + E^0_b)/2 - E^0_\alpha} \qquad \text{...(III.H.23)}$$

which differs from the version given in eqn. (III.H.21) by a negligible amount if

$$|E_a^\circ - E_b^\circ| << \frac{E_a^\circ + E_b^\circ}{2} - E_a^\circ \qquad \text{...(III.H.24)}$$

Furthermore, when several of the class 2 levels are close in energy, it is sometimes convenient to similarly use an average energy value $\overline{E_a^\circ}$ for these levels. This will be done in writing eqn. (III.H.41) in the next section. In a similar manner to eqn. (III.H.24), this approximation will be good if the energy separation between the class 2 levels involved is much smaller than the class 1–class 2 separation.

The summations over the class 2 levels in the above equations are for *all* spin substates of *all* vibronic levels of class 2, regardless of how near or far in energy they lie and regardless of symmetry species, including ionization and dissociation continua (which are integrated over rather than summed over).

In summary, the Van Vleck transformation has eliminated the first-order off-diagonal terms connecting the class 1 levels with all distant states. The information has not been lost but has been "folded" into the class 1 block of $\underline{H}$. The remaining class 1–class 2 off-diagonal elements, which are very small, are then neglected; only that part of the transformed hamiltonian acting within the class 1 block is retained, and this is called an effective hamiltonian. Note that the effective hamiltonian is really defined in terms of its matrix representation (eqn. (III.H.4)); thus its form is specific to the particular basis set being used.

III.H.2. Construction of the effective hamiltonian and matrix elements in a case (a) basis

Brown *et al.* (54) and Brown and Merer (60) support the concept of an effective hamiltonian involving a minimum number of experimental fitting parameters. Certain (small) interactions are neglected in the construction of the effective hamiltonian; their effects are then incorporated into the other parameters when a fit to

the experimental data is performed. Thus the physical interpretation of the parameters differs somewhat from what it would be if the parameters were the exact parameters. This is a disadvantage but is done in the interests of practicality.

For the reasons stated at the end of Section III.F.3, a case (a) basis $|\eta\Lambda S\Sigma J\Omega>$ is chosen. We write the effective hamiltonian for the rotational levels of any given multiplet state as

$$H^{eff} = H^{eff}_{ev} + H^{eff}_{r} + H^{eff}_{so} + H^{eff}_{ss} + H^{eff}_{sr} + H^{eff}_{cd} + H^{eff}_{LD} \quad ...(III.H.25)$$

where the terms are the vibronic, rotational, spin-orbit, spin-spin, spin-rotation, centrifugal distortion, and lambda-doubling terms, respectively. Zare *et al.* (47) have given expressions for most of the terms in the effective hamiltonian, and these were derived in a manner similar to that used here. Some of their signs are different from ours, however, due to a different phase choice.[24]

The vibronic hamiltonian is of little interest here and will be handled in a phenomenological manner by including T_o terms in the diagonal positions of the energy matrix to represent the vibronic origins.

The rotational hamiltonian is given by[25]

$$H_r = B(r)\underset{\sim}{R}^2 = B(r)(\underset{\sim}{J} - \underset{\sim}{L} - \underset{\sim}{S})\cdot(\underset{\sim}{J} - \underset{\sim}{L} - \underset{\sim}{S}) \quad ...(III.H.26)$$

where

$$B(r) = \frac{h}{8\pi^2 c\mu r^2} \quad ...(III.H.27)$$

The constants have been defined previously (cf. eq. (III.D.2)) except that the

---

[24]They chose $e^{i(\phi_a - \phi_{a\pm1})} = -1$ in eqn. (III.F.9) for $S^{\pm}$, in contrast with our choice of +1 (eqn. (III.F.13)).

[25]Some authors (e.g. Hougen (46) write $H_r = B(r)(R_x^2+R_y^2)$ to explicitly show that $R_z^2 = 0$ in a diatomic molecule. However, if R_z^2 is included, as here, all contributions from it will cancel each other out anyway. Thus both versions of H_r are completely equivalent.

internuclear separation is now represented by small r to avoid confusion with $\underset{\sim}{R}$. Eqn. (III.H.26) can be expanded to give

$$H_r = B(r)[\underset{\sim}{J}^2 + \underset{\sim}{S}^2 + L_z^2 - 2J_zL_z - 2J_zS_z + 2L_zS_z]$$
$$+ B(r)[L_x^2 + L_y^2]$$
$$- B(r)[2(J_xS_x+J_yS_y) - 2(L_xS_x+L_yS_y) + 2(J_xL_x+J_yL_y)] \quad ...(III.H.28)$$

The term on the second line of eqn. (III.H.28) possesses non-zero matrix elements that are diagonal in all quantum numbers associated with the case (a) basis, including Λ, but they can be on- or off-diagonal in electronic state. It can be seen how this arises by rewriting this term in ladder operator form (cf. eqn. (III.F.12))

$$[L_x^2 + L_y^2] = \tfrac{1}{2}[L^+L^- + L^-L^+] \quad ...(III.H.29)$$

The ladder operators ladder up and down in Λ, but the final state, although having the same value of Λ as the initial state, may be different. Those matrix elements diagonal in electronic state are often represented by the symbol $B_v\langle L_\perp^2\rangle$ (46c)

$$B_v\langle \Lambda S\Sigma\Omega J | L_x^2 + L_y^2 | \Lambda S\Sigma\Omega J\rangle = B_v\langle \Lambda S\Sigma\Omega J | \underset{\sim}{L}^2 - L_z^2 | \Lambda S\Sigma\Omega J\rangle = B_v\langle L_\perp^2\rangle \quad ...(III.H.30)$$

where the vibrational level has been integrated over (eqn. (III.D.3)). It can be shown that, to a good approximation, this term is constant for a given electronic state (46c,22). We therefore neglect it entirely from H_r^{eff} which is equivalent to saying that we include it with the electronic energy (where it, incidentally, causes part of the electronic isotope shift (9)). Those elements off-diagonal in electronic state will presumably also contribute an approximately constant shift to a given electronic state; in any case, their effects will be small, so they are ignored also.

All the terms in the first line of eqn. (III.H.28) are diagonal in all quantum numbers within a given vibronic state, and furthermore, there are no off-diagonal

elements between different electronic states, — e.g. for $\underset{\sim}{J}^2$,

$$\langle n'v'\Lambda'S'\Sigma'\Omega'J'M'|B(r)\underset{\sim}{J}^2|nv\Lambda S\Sigma\Omega JM\rangle$$
$$= B_{v'v}J(J+1)\delta_{n'n}\delta_{\Lambda'\Lambda}\delta_{S'S}\delta_{\Sigma'\Sigma}\delta_{\Omega'\Omega}\delta_{J'J}\delta_{M'M} \quad ...(III.H.31)$$

where

$$B_{v'v} = \langle v'|B(r)|v\rangle = \frac{h}{8\pi^2 c\mu}\langle v'|\frac{1}{r^2}|v\rangle \quad ...(III.H.32)$$

These terms are therefore assigned to H^0 for the purpose of performing a Van Vleck transformation. (For the moment, the existence of non-zero matrix elements of these terms between different vibrational levels of the same electronic state (cf. eqn. (III.H.32)) will be ignored.) The terms from the third line, which are off-diagonal in at least one quantum number, then form H',

$$H_r^0 = B(r)[\underset{\sim}{J}^2 + \underset{\sim}{S}^2 + L_z^2 - 2J_zL_z - 2J_zS_z + 2L_zS_z] \quad ...(III.H.33)$$

$$H_r' = -2B(r)[(J_xS_x + J_yS_y) - (L_xS_x + L_yS_y) + (J_xL_x + J_yL_y)] \quad ...(III.H.34)$$

The matrix elements of H_r for a given vibronic state are, through first order,

$$\langle nv\Lambda S\Sigma J\Omega|H_r^0|nv\Lambda S\Sigma J\Omega\rangle = B_v[J(J+1) + S(S+1) - \Omega^2 - \Sigma^2] \quad ...(III.H.35)$$

$$\langle n,v,\Lambda,S,\Sigma\pm1,\Omega\pm1,J|H_r'|nv\Lambda S\Sigma J\Omega\rangle$$
$$= -B_v[J(J+1) - \Omega(\Omega\pm1)]^{1/2}[S(S+1) - \Sigma(\Sigma\pm1)]^{1/2} \quad ...(III.H.36)$$

where the vibrational level has again been integrated over (eqn. (III.D.3)). The diagonal elements (eqn. (III.H.35)) have come from the terms in (III.H.33) by means of eqns. (III.F.5) and (F.8), while the off-diagonal elements (III.H.36) have arisen from the $-2B(r)(J_xS_x + J_yS_y)$ operator with the aid of eqns. (III.F.9), (F.10), (F.12), and (F.13). The latter operator, which can be rewritten as

$$-2B(r)(J_xS_x + J_yS_y) = -B(r)(J^+\Sigma^- + J^-\Sigma^+) \quad ...(III.H.37)$$

mixes together the components within the multiplet state and is called the $\underset{\sim}{S}$-uncoupling operator; it is responsible for the transition from Hund's case (a) to case (b) as J increases. The remaining two terms in eqn. (III.H.34) only produce non-zero matrix elements that are off-diagonal in Λ and these therefore do not contribute in first order.

Second- and higher-order terms arising from matrix elements connecting the multiplet vibronic state of interest with other, distant vibronic states could be included in H_r^{eff}. However, we choose not to do so. Their effects will be included as, or absorbed into, other parts of the total effective hamiltonian. Second- and higher-order contributions from the terms in eqn. (III.H.33) and from the $\underset{\sim}{S}$-uncoupling operator in eqn. (III.H.34) provide a centrifugal distortion correction to H_r^{eff}. This will be included as part of H_{cd}^{eff}.

The operator $2B(r)(L_xS_x + L_yS_y) = B(r)(L^+\Sigma^- + L^-\Sigma^+)$ has the same form as part of the spin-orbit hamiltonian,[26] namely $A(r)(L_xS_x + L_yS_y)$ (see below), so that only their sum, $[A(r) + 2B(r)](L_xS_x + L_yS_y)$, will be determinable. Since for case (a) states A(r) is larger then B(r), the combined operators are included with H_{so}^{eff}, where they contribute in second and higher orders. They also contribute to H_{LD}^{eff}.

The operator $-2B(r)(J_xL_x + J_yL_y) = -B(r)(J^+L^- + J^-L^+)$ is known as the $\underset{\sim}{L}$-uncoupling operator, and it is responsible for a gradual transition from case (a) to case (d) as J increases. It possesses non-zero matrix elements between electronic states differing by one unit in Λ and will therefore be assigned to H_{LD}^{eff}.

In the foregoing discussion, it has actually been the effective rotational *matrix elements* that we have been deriving (cf. eqn. (III.H.4)). The effective rotational *hamiltonian* then follows: it is that hamiltonian which when operating solely within

---

[26]There is a slight difference if one considers the microscopic forms of the operators as is done in calculating the higher-order spin-orbit terms (22) but this is ignored here since $A(r) >> B(r)$ for FeO and since the difference will be absorbed by the effective nature of the parameters.

the vibronic state of interest produces matrix elements that are the same as the effective matrix elements. The effective rotational hamiltonian is

$$H_r^{eff} = B_v[\underset{\sim}{J}^2 + \underset{\sim}{S}^2 + L_z^2 - 2J_zL_z - 2J_zS_z + 2L_zS_z - (J^+S^- + J^-S^+)] \quad ...(III.H.38)$$

for a particular vibrational level of the multiplet state under consideration. Sometimes this is written as

$$H_r^{eff} = B_v\underset{\sim}{R}^2 = B_v(\underset{\sim}{J} - \underset{\sim}{L} - \underset{\sim}{S})^2 \quad ...(III.H.39)$$

but then one must remember that certain parts of this are to be thrown away, as discussed above.

We next consider that part of the centrifugal distortion hamiltonian H_{cd} arising from H_r, and use it to illustrate how second- and higher-order contributions to H^{eff} are handled. As a result of the r-dependence of B(r),

$$B_{v'v} \neq 0 \quad ...(III.H.40)$$

(cf. eqn. (III.H.32)). Thus all the terms in H_r, except those off-diagonal in Λ (i.e. except the last two terms in eqn. (III.H.34)), cause the vibrational levels within a given electronic state to couple together. If the vibrational spacings are large compared with the splittings between the multiplet components, then the matrix elements off-diagonal in v can be treated by the Van Vleck transformation method. They give rise to second- and higher-order contributions to the matrix elements acting within the vibrational level of interest. We must now repartition H_r such that all those terms that previously formed H_r^0 (eqn. (III.H.33)) are now included with H_r', leaving $H_r^0 = 0$.[27] From eqn. (III.H.23)

---

[27]Actually H_r^0 and H_r' could have been defined this way in the first place instead of as in eqns. (III.H.33) and (34), and the same results would have been obtained. It is conventionally done as here, however, to emphasize the usefulness of Hund's coupling cases.

$$\tilde{H}^{(2)}_{ab} = \sum_{\substack{v' \neq v \\ \Omega'\Sigma'}} \frac{\langle nv\Lambda S\Sigma_a\Omega_a J | H_r' | nv'\Lambda S\Sigma'\Omega' J\rangle\langle nv'\Lambda S\Sigma'\Omega' J | H_r' | nv\Lambda S\Sigma_b\Omega_b J\rangle}{E_{nv} - E_{nv'}} \quad ...(III.H.41)$$

where E_{nv} is the average value of the energies of all the multiplet components of vibrational level v, and $E_{nv'}$ has the corresponding meaning for level v'. Using these average energy values is a good approximation provided that $E_{nv} - E_{nv'}$ is large compared with the multiplet separations. As per Section III.D, eqn. (III.H.41) can be separated into a product of radial (i.e. vibrational) and angular (i.e. rotational) parts,

$$\tilde{H}^{(2)}_{ab} = \left[\sum_{v' \neq v} \frac{\langle nv|B(r)|nv'\rangle\langle nv'|B(r)|nv\rangle}{E_{nv} - E_{nv'}} \right] \cdot \left[\sum_{\Omega'\Sigma'} \langle \Lambda S\Sigma_a\Omega_a J | \underset{\sim}{R}^2 | \Lambda S\Sigma'\Omega' J\rangle\langle \Lambda S\Sigma'\Omega' J | \underset{\sim}{R}^2 | \Lambda S\Sigma_b\Omega_b J\rangle \right] \quad ...(III.H.42)$$

where we have written $\underset{\sim}{R}^2$ for convenience, but it must be remembered that certain parts are to be neglected. Following Zare *et al.* (47) (see also Albritton *et al.* (61)) we let the first factor in this equation define $-D_v$, the centrifugal distortion constant for the v^{th} vibrational level,[28]

$$D_v = - \sum_{v' \neq v} \frac{\langle nv|B(r)|nv'\rangle\langle nv'|B(r)|nv\rangle}{E_{nv} - E_{nv'}} \quad ...(III.H.43)$$

so that[29]

---

[28]D could alternatively be called B_D by analogy with A_D, λ_D, etc. D is more usual.

[29]When working out the matrix elements of $H^{eff}_{cd,r}$, the angular part of eqn. (III.H.42) or (H.44), i.e. $\sum_{\Omega'\Sigma'} \langle \Sigma_a\Omega_a | \underset{\sim}{R}^2 | \Sigma'\Omega'\rangle\langle \Sigma'\Omega' | \underset{\sim}{R}^2 | \Sigma_b\Omega_b\rangle$, is conveniently calculated by writing down the matrix of H_r for any vibrational level but with the common factor B_v omitted, then squaring it. This automatically carries out the summation $\sum_{\Omega'\Sigma'}$. It works because, as a result of the factorization into radial and angular parts, the angular parts are the same for all values of v', including v' = v.

The summation over v' in the foregoing equations, in principle, really includes integration over the vibrational continuum. However, as the $|v'\rangle$ states differ progressively in quantum number from the $|v\rangle$ state, the increasing difference in number of nodes in the two states results in a rapid decrease in magnitude of the nondiagonal matrix elements $\langle v|B(r)|v'\rangle$, so that, except for states near the dissociation limit, the contribution from the continuum is seldom needed (61).

$$\tilde{H}^{(2)}_{ab} = -D_v \langle \Lambda S \Sigma_a \Omega_a J | \underset{\sim}{R}^4 | \Lambda S \Sigma_b \Omega_b J \rangle \qquad \text{...(III.H.44)}$$

Higher-order centrifugal distortion terms can be included as needed, though they seldom are. These are worked out in a similar manner to the second-order term (61). The effective centifugal distortion hamiltonian for rotation is then

$$H^{eff}_{cd,r} = - D_v \underset{\sim}{R}^4 + H_v \underset{\sim}{R}^6 + \ldots \qquad \text{...(III.H.45)}$$

The microscopic forms of the spin-orbit, spin-rotation, and spin-spin hamiltonians have been given earlier in eqns. (III.E.17) and (E.18); (E.25) and (E.26); and (E.44); respectively. However, these forms are not practical for the purpose of data reduction. It is traditional to replace them by phenomenological expressions involving a limited number of adjustable parameters:

$$H_{so} = A(r) \underset{\sim}{L} \cdot \underset{\sim}{S} \qquad \text{...(III.H.46)}$$

$$H_{sr} = \gamma(r) \underset{\sim}{R} \cdot \underset{\sim}{S} \quad \text{or} \quad H_{sr} = \gamma(r) \underset{\sim}{N} \cdot \underset{\sim}{S} \qquad \text{...(III.H.47)}$$

$$H_{ss} = \tfrac{2}{3} \lambda(r) (3 S_z^2 - \underset{\sim}{S}^2) \qquad \text{...(III.H.48)}$$

where

$$\underset{\sim}{L} = \sum_e \underset{\sim}{l}_e \qquad \text{...(III.H.49)}$$

and $$\underset{\sim}{S} = \sum_e \underset{\sim}{s}_e \qquad \text{...(III.H.50)}$$

Two forms of the spin-rotation hamiltonian have been given in eqn. (III.H.47). Both forms are in common use in the literature. For case (b) states, the form in $\underset{\sim}{N}$ is perhaps more convenient (47,22), but for case (a) states the choice is arbitrary. Since $\underset{\sim}{N} = \underset{\sim}{R} + \underset{\sim}{L}$, the two forms differ by the amount $\gamma(r) \underset{\sim}{L} \cdot \underset{\sim}{S}$, which is of the same form as the spin-orbit hamiltonian, $A(r) \underset{\sim}{L} \cdot \underset{\sim}{S}$. Therefore the choice of form used for H_{sr} affects the value of A, but since usually $A >> \gamma$, this difference can

normally be ignored (except for very light molecules like H_2 (62)). The $\gamma(r)\underset{\sim}{R}\cdot\underset{\sim}{S}$ version has been used in this thesis.

By means of the Van Vleck transformation method, the effective spin-orbit hamiltonian is found to have the following diagonal contributions:

$$H_{so}^{eff(0)} = 0 \qquad \text{...(III.H.51a)}$$

$$H_{so}^{eff(1)} = A_v L_z S_z \qquad \text{...(III.H.51b)}$$

$$H_{so}^{eff(2)} = \tfrac{2}{3}\lambda_v(3S_z^2 - \underset{\sim}{S}^2) \qquad \text{...(III.H.51c)}$$

$$H_{so}^{eff(3)} = \eta_v L_z S_z[S_z^2 - \tfrac{1}{5}(3\underset{\sim}{S}^2 - 1)] \qquad \text{...(III.H.51d)}$$

$$H_{so}^{eff(4)} = \tfrac{1}{12}\theta_v[35S_z^4 - 30\underset{\sim}{S}^2S_z^2 + 25S_z^2 - 6\underset{\sim}{S}^2 + 3\underset{\sim}{S}^4] \qquad \text{...(III.H.51e)}$$

As discussed earlier, these terms contain small contributions from the $2B(r)(L_xS_x + L_yS_y)$ part of H_r. There are also even smaller contributions from $-\gamma(r)(L_xS_x + L_yS_y)$ if the $\underset{\sim}{R}\cdot\underset{\sim}{S}$ version of H_{SR} is used — see below.

It may seem excessive to include terms as high as fourth order in pertubation theory. However, for quintet states, with five substates and four spin-orbit intervals, it is necessary, in principle, to use five parameters to give their positions. These can be written either as five term origins T_Ω, as has been done by Cheung, Żyrnicki, and Merer (63), or as one vibronic term origin T_o plus four parameters characterizing the four spin-orbit intervals. The latter method has been used here; hence the necessity of going to fourth order.

The spin-rotation hamiltonian expands out as

$$\begin{aligned} H_{SR} &= \gamma(r)(\underset{\sim}{J} - \underset{\sim}{L} - \underset{\sim}{S})\cdot\underset{\sim}{S} \\ &= \gamma(r)[J_zS_z - L_zS_z - \underset{\sim}{S}^2 + (J_xS_x + J_yS_y) - (L_xS_x + L_yS_y)] \end{aligned} \qquad \text{...(III.H.52)}$$

from which we get

$$H_{sr}^{eff(0)} = 0 \qquad \text{...(III.H.53a)}$$

$$H_{sr}^{eff(1)} = \gamma_v[J_z S_z - L_z S_z - \underset{\sim}{S}^2 + \tfrac{1}{2}(J^+S^- + J^-S^+)] \qquad \text{...(III.H.53b)}$$

Higher-order contributions are usually not needed, since γ is usually small in comparison with A. In any case, higher-order contributions from $-\gamma(r)(L_x S_x + L_y S_y)$ can be assumed to be included in with the corresponding higher-order terms of H_{so}^{eff}.

Comparison of eqns. (III.H.48) and (H.51c) will show that the (first-order) spin-spin hamiltonian has exactly the same form as the second-order spin-orbit hamiltonian. The two are 100% correlated and are experimentally indistinguishable. The parameter λ_v therefore contains contributions from both interactions. Since the second-order spin-orbit contribution is usually the larger, we set

$$H_{ss}^{eff} = 0 \qquad \text{...(III.H.54)}$$

and let the spin-spin interaction be included with H_{so}^{eff}. In states of high multiplicity, the term in λ has the effect of making the spin-orbit intervals unequal — an effect which may be considered as the early stages of a transition to case (c) coupling.

Until now, when calculating second- and higher-order contributions to the effective hamiltonian, we have considered each part of the hamiltonian in isolation from all other parts — e.g. H_r by itself or H_{so} by itself. Really, the *total* hamiltonian must be employed when calculating higher-order terms, and if this is done, cross-terms between the various parts of the hamiltonian occur. We illustrate this by considering two parts of the hamiltonian together, namely

$$H = H_r + H_{so} \qquad \text{...(III.H.55)}$$

and writing, in shorthand form, the second-order correction,

$$\tilde{H}^{(2)} = \Sigma \frac{\langle H_r + H_{so}\rangle\langle H_r + H_{so}\rangle}{\Delta E}$$

$$= \Sigma \frac{\langle H_r\rangle^2 + \langle H_{so}\rangle\langle H_r\rangle + \langle H_r\rangle\langle H_{so}\rangle + \langle H_{so}\rangle^2}{\Delta E} \quad \text{...(III.H.56)}$$

The first and last terms in the final line are the second-order centrifugal distortion correction to H_r and the second-order spin-orbit correction, both of which have already been considered. The middle two cross-terms are new, however, and these together, by analogy with $\Sigma \frac{\langle H_r\rangle\langle H_r\rangle}{\Delta E}$, are called the centrifugal distortion correction to H_{so}. The two terms are not identical, because H_{so} and H_r do not commute; hence both terms have to be retained. The r-dependent part can be taken out as a common factor and is given the symbol $A_{D,v}$

$$A_{D,v} = 2 \sum_{v' \neq v} \frac{\langle nv|A(r)|nv'\rangle\langle nv'|B(r)|nv\rangle}{E_{nv} - E_{nv'}} \quad \text{...(III.H.57)}$$

The factor 2 has been inserted in order to write $H^{eff}_{cd,so}$ in the form of an average,

$$H^{eff}_{cd,so} = A_{D,v} \frac{(\underset{\sim}{L}\cdot\underset{\sim}{S})\underset{\sim}{R}^2 + \underset{\sim}{R}^2(\underset{\sim}{L}\cdot\underset{\sim}{S})}{2} \quad \text{...(III.H.58)}$$

where the parts off-diagonal in Λ are to be neglected. (From an alternative but equivalent point of view, the form of $H^{eff}_{cd,so}$ as an average is necessary to ensure that the energy matrix is hermitian (63).)

In the same manner we obtain

$$H^{eff}_{cd,sr} = \gamma_{D,v} \frac{(\underset{\sim}{R}\cdot\underset{\sim}{S})\underset{\sim}{R}^2 + \underset{\sim}{R}^2(\underset{\sim}{R}\cdot\underset{\sim}{S})}{2} \quad \text{...(III.H.59)}$$

$$H^{eff}_{cd,ss} = \tfrac{2}{3}\lambda_{D,v} \frac{(3S_z^2 - \underset{\sim}{S}^2)\underset{\sim}{R}^2 + \underset{\sim}{R}^2(3S_z^2 - \underset{\sim}{S}^2)}{2} \quad \text{...(III.H.60)}$$

There are also other cross-terms, such as that between H_{so} and H_{sr}, but these are ignored; their effects will be absorbed into the various effective parameters. One such cross-term that should be specifically mentioned is that arising from $(H_{so} + H_r)$. When calculating $H^{eff}_{cd,so}$, only those parts of H_{so} and H_r diagonal in Λ were used.

If the off-diagonal parts are now considered, we find that the second-order terms arising from the product of matrix elements involving the J^+L^- and L^+S^- operators are of the same form as those from γJ^+S^-. In fact, except for H_2, these second-order effects are larger than the first-order H_{SI} contribution (22). However, since they are experimentally indistinguishable from the true spin-rotation contribution, we retain the name "spin-rotation" coupling constant for γ_v.

In the same manner in which the vibrational dependences of B_v and D_v were expressed in the form of a power series (eqns. (III.D.4) and (D.6)), so also can this be done for the other parameters. For example, for A_v (25)

$$A_v = A_e - a_A(v+\tfrac{1}{2}) + \ldots \qquad \text{...(III.H.61)}$$

where a_A is a vibration-rotation interaction constant.

Tables will be presented summarizing the effective hamiltonian and giving the matrix elements for a number of states at the end of the following section dealing with H_{LD}.

III.H.2.a. Lambda-doubling in a $^5\Delta$ state

Lambda-doubling arises because of interactions with Σ states. There are only two types of interaction terms that have arisen in the previous section that can connect different electronic states, namely terms involving the operators

(i) $L^+S^- + L^-S^+$ and

(ii) $L^+J^- + L^-J^+$.

The first type arises primarily from H_{SO}, with a small contribution from H_r and smaller still contributions from elsewhere.[30] The second type arises primarily from H_r.

These both involve the ladder operators $L^{\pm}$, which ladder up or down in Λ by only one unit at a time. Therefore, in order for Λ-doubling to occur in a Δ state, the Δ state must interact with the Σ state(s) via an intermediate Π state(s). This

---

[30]Again, small differences at the microscopic level are being ignored.

means that the lowest order of perturbation theory in which the interaction between a Δ and a Σ state can occur is fourth order. That part of the expression for the fourth-order perturbation term of relevance has the form

$$\underline{\tilde{H}}^{(4)} = \Sigma \frac{\langle {}^5\Delta | H_{so}+H_r | {}^5\Pi \rangle \langle {}^5\Pi | H_{so}+H_r | {}^5\Sigma \rangle \langle {}^5\Sigma | H_{so}+H_r | {}^5\Pi \rangle \langle {}^5\Pi | H_{so}+H_r | {}^5\Delta \rangle}{\text{energy denominator}}$$

...(III.H.62)

where the operators are represented by their primary sources in this simplified equation and where the specific substates within the various states have not been shown. The effect of the $L^{\pm}$ ladder operators can be represented schematically as

$$\begin{array}{lll} L^+ & \Lambda = +2 & L^- \\ L^+ & \Lambda = +1 & L^- \\ L^+ & \Lambda = 0 & L^- \\ L^+ & \Lambda = -1 & L^- \\ L^+ & \Lambda = -2 & L^- \end{array}$$

We could go from $\Lambda = -2 \rightarrow -1 \rightarrow 0 \rightarrow -1 \rightarrow -2$, for example, but because of the symmetry of the energy matrix, this will produce a matrix element equal to that from $\Lambda = -2 \rightarrow -1 \rightarrow 0 \rightarrow +1 \rightarrow +2$, so we need only consider the latter type. The $L^{\pm}S^{\mp}$ and $L^{\pm}J^{\mp}$ operators can occur in various combinations within this scheme. For example, four applications of the $L^{\pm}S^{\mp}$ operator alone, i.e.

$$\Sigma \frac{\langle {}^5\Delta | H_{so} | {}^5\Pi \rangle \langle {}^5\Pi | H_{so} | {}^5\Sigma \rangle \langle {}^5\Sigma | H_{so} | {}^5\Pi \rangle \langle {}^5\Pi | H_{so} | {}^5\Delta \rangle}{\text{energy denominator}}$$

produces a term in the effective energy matrix for the $^5\Delta$ state that is J-independent. The four applications of the $S^{\pm}$ part of this operator produces a selection rule $\Delta\Sigma = \pm 4$ and this can only occur in a $^5\Delta$ state in the $\Omega = 0$ part of the matrix — e.g. the ($\Lambda=-2$, $\Sigma=2$, $\Omega=0$; $\Lambda=+2$, $\Sigma=-2$, $\Omega=0$) element. Other combinations of the $L^{\pm}S^{\mp}$ and $L^{\pm}J^{\mp}$ operators produce J-dependent terms in other locations in the matrix.

The effect of this treatment is to sum over the interactions involving all distant Σ states (Σ^+ states and Σ^- states) and thereby to produce effective matrix elements lying only within the rotational manifold of the $^5\Delta$ state. The resulting matrix is, however, for each value of J, a 10x10 matrix, because there are elements off-diagonal in Λ in the region connecting the $+|\Lambda|$ and $-|\Lambda|$ blocks. This is then subjected to a Wang transformation,

$$\underline{H}^{eff}_{sym} = \underline{U}^{-1}_{sym}\,\underline{H}^{eff}\,\underline{U}_{sym} \qquad \text{...(III.H.63)}$$

where, for a 10x10 matrix, the Wang symmetrizing matrix is

$$\underline{U}_{sym} = \underline{U}^{-1}_{sym} = \frac{1}{\sqrt{2}} \begin{bmatrix} -1 & & & & & & & & & 1 \\ & -1 & & & & & & & 1 & \\ & & -1 & & & & & 1 & & \\ & & & -1 & & & 1 & & & \\ & & & & -1 & 1 & & & & \\ & & & & 1 & 1 & & & & \\ & & & 1 & & & & 1 & & \\ & & 1 & & & & & & 1 & \\ & 1 & & & & & & & & 1 \\ 1 & & & & & & & & & \end{bmatrix} \qquad \text{...(III.H.64)}$$

with zeros in all other positions. The effect of applying a Wang transformation is to factorize the 10x10 matrix into two 5x5 blocks — one block having symmetry e, the other f. Thus the Wang transformation produces that matrix which would have resulted if the matrix had been written directly in a parity basis. The advantage of originally deriving the matrix in a non-parity basis (sometimes called a signed basis) is that interactions with all (distant) Σ states can easily be summed over, without regard to symmetry.

It can readily be shown that for all the effective matrix elements derived in the previous section (47)

$$\langle nv\Lambda S\Sigma' J\Omega' \pm | H^{eff} | nv\Lambda S\Sigma J\Omega \pm \rangle = \langle nv\Lambda S\Sigma' J\Omega' | H^{eff} | nv\Lambda S\Sigma J\Omega \rangle$$

...(III.H.65)

so the matrix elements derived previously still apply. The effect of the Wang transformation has been to fold into the two blocks effective terms dealing with the Λ-doubling. The two blocks differ only in the signs of the Λ-doubling parameters.

The number of parameters needed to adequately describe the Λ-doubling depends on the multiplicity of the state involved. For a $^1\Pi$ state, one parameter is needed. This has traditionally been called q. For a $^2\Pi$ state, two are needed: q and p (64). For triplet and higher-multiplicity Π states, three Λ-doubling parameters are needed (60): q, p, and o.[31] A subscript Π can be appended to each symbol to distinguish from the parameters for Δ states.

In Δ states, again one parameter is needed for singlet states, two for doublets, and so on. This time a maximum of five parameters are required, so a $^5\Delta$ state is the lowest-multiplicity state in which all five make their appearance.

Due to the scarcity of observations on Λ-doubling in Δ states, a standard nomenclature has not yet been established. Rather than break from the tradition established with Π states, we adopt the following names (65). The one parameter in a $^1\Delta$ state is called q_Δ, the two in a $^2\Delta$ state are called q_Δ and p_Δ, and so on. For quintet and higher-multiplicity Δ states, the five parameters are called q_Δ, p_Δ, o_Δ, n_Δ, and m_Δ.

The Λ-doubling parameters in Π states have historically been defined in a case (b) basis. Likewise we define the above Δ-state parameters in a case (b) basis. In case (a), only a single parameter is required for any given matrix element, but these parameters appear as linear combinations of the case (b) parameters. With a string of up to five parameters defining each single constant, the nomenclature becomes rather clumsy. We therefore introduce the following new symbols for use in Δ states in case (a) (65):

---

[31]Mulliken and Christy's (64) "o" has a different definition from that of o used here. Their o is not a Λ-doubling parameter. See Brown and Merer (60).

case (a) symbol		corresponding combinations of case (b) symbols
$\tilde{q}_\Delta$	$\equiv$	q_Δ
$\tilde{p}_\Delta$	$\equiv$	$p_\Delta + 4q_\Delta$
$\tilde{o}_\Delta$	$\equiv$	$o_\Delta + 3p_\Delta + 6q_\Delta$
$\tilde{n}_\Delta$	$\equiv$	$n_\Delta + 2o_\Delta + 3p_\Delta + 4q_\Delta$
$\tilde{m}_\Delta$	$\equiv$	$m_\Delta + n_\Delta + o_\Delta + p_\Delta + q_\Delta$

We then suggest a similar convention be adopted for Π states in case (a):

case (a) symbol		corresponding combinations of case (b) symbols
$\tilde{q}_\Pi$	$\equiv$	q_Π
$\tilde{p}_\Pi$	$\equiv$	$p_\Pi + 2q_\Pi$
$\tilde{o}_\Pi$	$\equiv$	$o_\Pi + p_\Pi + q_\Pi$

In terms of this nomenclature, the effective Λ-doubling hamiltonian for any Δ state can be written as

$$H_{LD}^{eff} = \tfrac{1}{2}\tilde{m}_\Delta(S^{+4}+S^{-4}) - \tfrac{1}{2}\tilde{n}_\Delta(S^{+3}J^{+}+S^{-3}J^{-}) + \tfrac{1}{2}\tilde{o}_\Delta(S^{+2}J^{+2}+S^{-2}J^{-2}) - \tfrac{1}{2}\tilde{p}_\Delta(S^{+}J^{+3}+S^{-}J^{-3}) + \tfrac{1}{2}\tilde{q}_\Delta(J^{+4}+J^{-4}) \quad \text{...(III.H.66)}$$

where it is understood implicitly that the operators link the $\Lambda = +2$ and $\Lambda = -2$ components of the Δ state only. A Wang transformation is to be applied subsequently to the evaluation of the matrix elements.

Centrifugal distortion effects on the Λ-doubling parameters can be handled in a similar manner to that used in the previous section for the other parameters (63):

$$H^{eff}_{cd,LD} = \tfrac{1}{4} D_{\tilde{m}_\Delta} \left[(S^{+4} + S^{-4}) \underset{\sim}{R}^2 + \underset{\sim}{R}^2 (S^{+4} + S^{-4}) \right] + \ldots \quad \text{...(III.H.67)}$$

Table IV summarizes the effective hamiltonian derived in this and the previous section. Tables V - VII then give the effective matrix elements for $^5\Pi$, $^5\Delta$, and $^5\Phi$ states, and Table VIII gives the effective matrix elements for a $^3\Phi$ state (for use in Chapter V).

TABLE IV. Effective rotational and spin hamiltonian for Δ states.

$$H = H_r + H_{so} + H_{sr} + H_{cd} + H_{LD}$$

where

$$H_r = B(\underset{\sim}{J}-\underset{\sim}{L}-\underset{\sim}{S})^2$$

$$H_{so} = AL_zS_z + \tfrac{2}{3}\lambda(3S_z^2-\underset{\sim}{S}^2) + \eta L_zS_z[S_z^2-(3\underset{\sim}{S}^2-1)/5] + \tfrac{1}{12}\theta[35S_z^4-30\underset{\sim}{S}^2S_z^2+25S_z^2-6\underset{\sim}{S}^2+3\underset{\sim}{S}^4]$$

$$H_{sr} = \gamma(\underset{\sim}{J}-\underset{\sim}{L}-\underset{\sim}{S})\cdot\underset{\sim}{S}$$

$$H_{cd} = -D(\underset{\sim}{J}-\underset{\sim}{L}-\underset{\sim}{S})^4 + \tfrac{1}{2}A_D[(\underset{\sim}{J}-\underset{\sim}{L}-\underset{\sim}{S})^2L_zS_z+L_zS_z(\underset{\sim}{J}-\underset{\sim}{L}-\underset{\sim}{S})^2] + \tfrac{1}{3}\lambda_D[(\underset{\sim}{J}-\underset{\sim}{L}-\underset{\sim}{S})^2(3S_z^2-\underset{\sim}{S}^2)+(3S_z^2-\underset{\sim}{S}^2)(\underset{\sim}{J}-\underset{\sim}{L}-\underset{\sim}{S})^2]$$

$$H_{LD} = \tfrac{1}{2}\tilde{m}_\Delta(S^{+4}+S^{-4}) - \tfrac{1}{2}\tilde{n}_\Delta(S^{+3}J^{+}+S^{-3}J^{-}) + \tfrac{1}{2}\tilde{o}_\Delta(S^{+2}J^{+2}+S^{-2}J^{-2}) - \tfrac{1}{2}\tilde{p}_\Delta(S^{+}J^{+3}+S^{-}J^{-3}) + \tfrac{1}{2}\tilde{q}_\Delta(J^{+4}+J^{-4})$$

TABLE V. Effective matrix elements for a $^5\Pi$ state in case (a) coupling.

Diagonal Elements

$$^5\Pi_{-1}: T_0 - 2A + (x+2)[B-2A_D+4\lambda_D] - 2\gamma + 4\lambda - 6\eta/5 - D(x^2+8x+4)$$

$$^5\Pi_0 : T_0 - A + (x+6)[B- A_D-2\lambda_D] - 5\gamma - 2\lambda + 12\eta/5 - D(x^2+22x+36) \pm 3\tilde{o}_\Pi$$

$$^5\Pi_1 : T_0 + (x+6)[B-4\lambda_D] - 6\gamma - 4\lambda - D(x^2+24x+24) \pm \tfrac{1}{2}\tilde{q}_\Pi x$$

$$^5\Pi_2 : T_0 + A + (x+2)[B+ A_D-2\lambda_D] - 5\gamma - 2\lambda - 12\eta/5 - D(x^2+14x-32)$$

$$^5\Pi_3 : T_0 + 2A + (x-6)[B+2A_D+4\lambda_D] - 2\gamma + 4\lambda + 6\eta/5 - D(x^2- 8x+12)$$

Off-diagonal Elements

$$\langle ^5\Pi_{-1}|H|^5\Pi_0\rangle = -2(x)^{1/2} \quad [B - \tfrac{1}{2}\gamma - \tfrac{3}{2}A_D + \lambda_D - 2D(x+4)]$$

$$\langle ^5\Pi_0 |H|^5\Pi_1\rangle = -(6x)^{1/2} \quad [B - \tfrac{1}{2}\gamma - \tfrac{1}{2}A_D - 3\lambda_D - 2D(x+6) \pm \tfrac{1}{2}\tilde{p}_\Pi]$$

$$\langle ^5\Pi_1 |H|^5\Pi_2\rangle = -[6(x-2)]^{1/2}[B - \tfrac{1}{2}\gamma + \tfrac{1}{2}A_D - 3\lambda_D - 2D(x+4)]$$

$$\langle ^5\Pi_2 |H|^5\Pi_3\rangle = -2(x-6)^{1/2} \quad [B - \tfrac{1}{2}\gamma + \tfrac{3}{2}A_D + \lambda_D - 2D(x-2)]$$

$$\langle ^5\Pi_{-1}|H|^5\Pi_1\rangle = -6^{1/2}[2Dx \mp \tilde{o}_\Pi]$$

$$\langle ^5\Pi_0 |H|^5\Pi_2\rangle = -[x(x-2)]^{1/2}[6D \mp \tfrac{1}{2}\tilde{q}_\Pi]$$

$$\langle ^5\Pi_1 |H|^5\Pi_3\rangle = -2D[6(x-2)(x-6)]^{1/2}$$

$$\langle ^5\Pi_{-1}|H|^5\Pi_2\rangle = \mp\tilde{p}_\Pi(x-2)^{1/2}$$

$$\langle ^5\Pi_0 |H|^5\Pi_3\rangle = 0$$

$$\langle ^5\Pi_{-1}|H|^5\Pi_3\rangle = \pm \tfrac{1}{2}\tilde{q}_\Pi[(x-2)(x-6)]^{1/2}$$

---

x=J(J+1). Upper and lower sign choices refer to e and f levels, respectively.

TABLE VI. Effective matrix elements for a $^5\Delta$ state in case (a) coupling.

Diagonal Elements

$$^5\Delta_0: \quad T_0 - 4A + (x+2)[B-4A_D+4\lambda_D] - 2\gamma + 4\lambda - 12\eta/5 + \theta - D(x^2+8x+4) \pm 12\tilde{m}_\Delta$$

$$^5\Delta_1: \quad T_0 - 2A + (x+4)[B-2A_D-2\lambda_D] - 5\gamma - 2\lambda + 24\eta/5 - 4\theta - D(x^2+18x+4) \pm 3\tilde{o}_\Delta$$

$$^5\Delta_2: \quad T_0 + (x+2)[B-4\lambda_D] - 6\gamma - 4\lambda + 6\theta - D(x^2+16x-44) \pm \tfrac{1}{2}\tilde{q}_\Delta x(x-2)$$

$$^5\Delta_3: \quad T_0 + 2A + (x-4)[B+2A_D-2\lambda_D] - 5\gamma - 2\lambda - 24\eta/5 - 4\theta - D(x^2+2x-68)$$

$$^5\Delta_4: \quad T_0 + 4A + (x-14)[B+4A_D+4\lambda_D] - 2\gamma + 4\lambda + 12\eta/5 + \theta - D(x^2-24x+148)$$

Off-diagonal Elements

$$\langle ^5\Delta_0|H|^5\Delta_1\rangle = -2(x)^{1/2} \quad [B - \tfrac{1}{2}\gamma - 3A_D + \lambda_D - 2D(x+3) \pm 3\tilde{n}_\Delta]$$

$$\langle ^5\Delta_1|H|^5\Delta_2\rangle = -[6(x-2)]^{1/2}[B - \tfrac{1}{2}\gamma - A_D - 3\lambda_D - 2D(x+3) \pm \tfrac{1}{2}\tilde{p}_\Delta x]$$

$$\langle ^5\Delta_2|H|^5\Delta_3\rangle = -[6(x-6)]^{1/2}[B - \tfrac{1}{2}\gamma + A_D - 3\lambda_D - 2D(x-1)]$$

$$\langle ^5\Delta_3|H|^5\Delta_4\rangle = -2(x-12)^{1/2}\ [B - \tfrac{1}{2}\gamma + 3A_D + \lambda_D - 2D(x-9)]$$

$$\langle ^5\Delta_0|H|^5\Delta_2\rangle = [6x(x-2)]^{1/2}[-2D \pm \tilde{o}_\Delta]$$

$$\langle ^5\Delta_1|H|^5\Delta_3\rangle = [(x-2)(x-6)]^{1/2}[-6D \pm \tfrac{1}{2}q_\Delta x]$$

$$\langle ^5\Delta_2|H|^5\Delta_4\rangle = -2D[6(x-6)(x-12)]^{1/2}$$

$$\langle ^5\Delta_0|H|^5\Delta_3\rangle = \mp\tilde{p}_\Delta[x(x-2)(x-6)]^{1/2}$$

$$\langle ^5\Delta_1|H|^5\Delta_4\rangle = 0$$

$$\langle ^5\Delta_0|H|^5\Delta_4\rangle = \pm\tfrac{1}{2}\tilde{q}_\Delta[x(x-2)(x-6)(x-12)]^{1/2}$$

x=J(J+1). Upper and lower sign choices refer to e and f levels, respectively.

TABLE VII. Effective matrix elements for a $^5\Phi$ state in case (a) coupling.

Diagonal Elements

$$^5\Phi_1: \quad T_0 - 6A + (x+1)[B-6A_D+4\lambda_D] - 2\gamma + 4\lambda - 18\eta/5 - D(x^2+6x-7)$$

$$^5\Phi_2: \quad T_0 - 3A + (x+1)[B-3A_D-2\lambda_D] - 5\gamma - 2\lambda + 36\eta/5 - D(x^2+12x-43)$$

$$^5\Phi_3: \quad T_0 + (x-3)[B-4\lambda_D] - 6\gamma - 4\lambda - D(x^2+6x-99)$$

$$^5\Phi_4: \quad T_0 + 3A + (x-11)[B+3A_D-2\lambda_D] - 5\gamma - 2\lambda - 36\eta/5 - D(x^2-12x-31)$$

$$^5\Phi_5: \quad T_0 + 6A + (x-23)[B+6A_D+4\lambda_D] - 2\gamma + 4\lambda + 18\eta/5 - D(x^2-42x+449)$$

Off-diagonal Elements

$$\langle ^5\Phi_1|H|^5\Phi_2\rangle = -2(x-2)^{1/2} \quad [B - \tfrac{1}{2}\gamma - \tfrac{9}{2}A_D + \lambda_D - 2D(x+1)]$$

$$\langle ^5\Phi_2|H|^5\Phi_3\rangle = -[6(x-6)]^{1/2} \quad [B - \tfrac{1}{2}\gamma - \tfrac{3}{2}A_D - 3\lambda_D - 2D(x-1)]$$

$$\langle ^5\Phi_3|H|^5\Phi_4\rangle = -[6(x-12)]^{1/2} [B - \tfrac{1}{2}\gamma + \tfrac{3}{2}A_D - 3\lambda_D - 2D(x-7)]$$

$$\langle ^5\Phi_4|H|^5\Phi_5\rangle = -2(x-20)^{1/2} \quad [B - \tfrac{1}{2}\gamma + \tfrac{9}{2}A_D + \lambda_D - 2D(x-17)]$$

$$\langle ^5\Phi_1|H|^5\Phi_3\rangle = -2D[6(x-2)(x-6)]^{1/2}$$

$$\langle ^5\Phi_2|H|^5\Phi_4\rangle = -6D[(x-6)(x-12)]^{1/2}$$

$$\langle ^5\Phi_3|H|^5\Phi_5\rangle = -2D[6(x-12)(x-20)]^{1/2}$$

$x=J(J+1)$.

TABLE VIII. Effective matrix elements for a $^3\Phi$ state in case (a) coupling.

Diagonal Elements

$$^3\Phi_2: \quad T_0 - 3A + (x-3)\left[B-3A_D+\frac{2}{3}\lambda_D\right] - \gamma + \frac{2}{3}\lambda - D(x^2-4x-3)$$

$$^3\Phi_3: \quad T_0 + (x-7)\left[B-\frac{4}{3}\lambda_D\right] - 2\gamma - \frac{4}{3}\lambda - D(x^2-10x+13)$$

$$^3\Phi_4: \quad T_0 + 3A + (x-15)\left[B+3A_D+\frac{2}{3}\lambda_D\right] - \gamma + \frac{2}{3}\lambda - D(x^2-28x+201)$$

Off-diagonal Elements

$$\langle ^3\Phi_2 | H | ^3\Phi_3 \rangle = -[2(x-6)]^{1/2}\left[B - \frac{1}{2}\gamma - \frac{3}{2}A_D - \frac{1}{3}\lambda_D - 2D(x-5)\right]$$

$$\langle ^3\Phi_3 | H | ^3\Phi_4 \rangle = -[2(x-12)]^{1/2}\left[B - \frac{1}{2}\gamma + \frac{3}{2}A_D - \frac{1}{3}\lambda_D - 2D(x-11)\right]$$

$x=J(J+1)$. There are no non-zero third-order spin-orbit terms.

III.I. Intensities

Paralleling the definitions of Condon and Shortley (35b) for atoms, for molecules a rotational **level** consists of (2J+1) Zeeman states corresponding to the (2J+1) possible values of M. This definition is used regardless of whether the (2J+1) states are degenerate or not. A spectral **line** corresponds to all possible transitions between two levels — again, regardless of whether the levels are degenerate or not. A Λ-doublet then consists of two rotational lines, even when the Λ-doublet levels are degenerate. The term **component of a line** is used to refer to a transition between a particular pair of Zeeman states.

The **intensity** of a line or line component is defined as the energy emitted or absorbed per second. The intensity for a line component in emission from upper Zeeman state a to lower Zeeman state b is equal to

$$I(a,b) = N(a)hc\overline{\nu}_{ab}[A(a,b) + B(a,b)\rho(\overline{\nu}_{ab})] \qquad \text{...(III.I.1)}$$

where N(a) is the number of molecules in state a, h is Planck's constant, c is the velocity of light, $\overline{\nu}_{ab}$ is the frequency corresponding to the transition in wavenumber units, and the intensity per unit volume of the radiation field in the wavenumber range $d\overline{\nu}$ at $\overline{\nu}_{ab}$ is $\rho(\overline{\nu}_{ab})d\overline{\nu}$. The transition probabilities for spontaneous and induced (=stimulated) emission from state a to state b are given by the Einstein coefficients A(a,b) and B(a,b), respectively. These coefficients are related to each other as follows (35c):

$$A(a,b) = 8\pi hc\overline{\nu}_{ab}^{3}B(a,b) \qquad \text{...(III.I.2)}$$

Under normal experimental conditions,[32] the spontaneous emission greatly exceeds the stimulated emission, so we need only consider the former,

$$I(a,b) = N(a)hc\overline{\nu}_{ab}A(a,b) \qquad \text{...(III.I.3)}$$

---

[32]The conditions inside a laser are not classified as "normal."

The Einstein A(a,b) coefficient is related to the matrix element of the electric dipole moment of the molecule according to (35d)

$$A(a,b) = \frac{16\pi^3\bar{\nu}_{ab}^3}{3h\epsilon_0}\left|\langle\psi_a|\underset{\sim}{\mu}|\psi_b\rangle\right|^2 \qquad \text{...(III.I.4)}$$

where ϵ_0 is the permittivity of a vacuum.[33] Defining the quantity

$$S(a,b) = \left|\langle\psi_a|\underset{\sim}{\mu}|\psi_b\rangle\right|^2 \qquad \text{...(III.I.5)}$$

eqn. (III.I.4) becomes

$$I(a,b) = N(a)\frac{64\pi^4 c\bar{\nu}_{ab}^4}{3}S(a,b) \qquad \text{...(III.I.6)}$$

S(a,b) is called the **strength** of the line component. ψ_a and ψ_b are the wavefunctions of the upper and lower Zeeman states and $\underset{\sim}{\mu}$ is the electric dipole moment operator in the space-fixed coordinate system.

We now focus on S(a,b). A vector, such as the electric dipole moment $\underset{\sim}{\mu}$, can be written as a first rank spherical tensor. Doing this, eqn. (III.I.5) becomes

$$S(a,b) = \sum_p\left|\langle\psi_a|T_p^1(\underset{\sim}{\mu})|\psi_b\rangle\right|^2 \qquad \text{...(III.I.7)}$$

where the summation is over the three components of the first rank tensor,

$$T_{p=1}^1(\underset{\sim}{\mu}) = -\frac{1}{\sqrt{2}}(\mu_X + i\mu_Y)$$

$$T_{p=0}^1(\underset{\sim}{\mu}) = \mu_Z \qquad \text{...(III.I.8)}$$

$$T_{p=-1}^1(\underset{\sim}{\mu}) = \frac{1}{\sqrt{2}}(\mu_X - i\mu_Y)$$

Except in some simple cases, the matrix elements $\langle\psi_a|T_p^1(\underset{\sim}{\mu})|\psi_b\rangle$ cannot be solved to yield simple expressions. Instead, the wavefunctions are expanded in terms of a complete set of basis functions ϕ. The matrix elements of the dipole moment operator are solved for in terms of these basis states and are then transformed back into matrix elements in terms of the wavefunctions. This transformation is performed

---

[33]The units of A are s^{-1}

as follows (66,46). Let $\underline{U}_{sym}$ be a unitary transformation matrix which symmetrizes the basis functions. This is the transformation matrix that would be used to transform the hamiltonian matrix $\underline{H}$ into a matrix expressed in a parity basis (cf. eqn. (III.H.64)) — for example, for the upper vibronic state u to which Zeeman state a belongs

$$\underline{H}_{sym,u} = \underline{U}^{-1}_{sym,u}\, \underline{H}_{u}\, \underline{U}_{sym,u} \qquad \text{...(III.I.9)}$$

with a similar equation for the lower state l to which b belongs. Let $\underline{U}_{diag}$ be a unitary transformation matrix which diagonalizes the hamiltonian matrix expressed in a parity basis, e.g.

$$\underline{H}_{diag,u} = \underline{U}^{-1}_{diag,u}\, \underline{H}_{sym,u}\, \underline{U}_{diag,u} \qquad \text{...(III.I.10)}$$

where $\underline{H}_{diag}$ is diagonal. The columns of $\underline{U}_{diag}$ contain the eigenvectors of $\underline{H}_{sym}$. The transformation for the matrix of the dipole moment operator $\underline{S}$ is then

$$\underline{S} = \underline{U}^{-1}\underline{S}^{s}\underline{U} \qquad \text{...(III.I.11)}$$

where

$$\underline{U} = \underline{U}_{sym}\,\underline{U}_{diag} \qquad \text{...(III.I.12)}$$

and where the superscript s indicates that simplified (i.e. not symmetrized, not diagonalized) basis functions are being used.

For the rest of the derivation, signed case (a) basis functions will be used, since the observed FeO electronic states exhibit good case (a) coupling behavior; states $|\phi_a\rangle$ and $|\phi_b\rangle$ are written as $|n'v'\Lambda'S'\Sigma'J'\Omega'M'\rangle$ and $|n''v''\Lambda''S''\Sigma''J''\Omega''M''\rangle$, respectively, and eqn. (III.I.7) is now

$$S^{s}(a,b) = \sum_{p} \left| \langle n'v'\Lambda'S'\Sigma'J'\Omega'M' | T^{1}_{p}(\underset{\sim}{\mu}) | n''v''\Lambda''S''\Sigma''J''\Omega''M'' \rangle \right|^{2} \qquad \text{...(III.I.13)}$$

Assuming the electronic and vibrational wavefunctions to be separable from the rotational wavefunctions, this factorizes into

$$S^S(a,b) = \left|\langle n'v'|n''v''\rangle\right|^2 \cdot \sum_p \left|\langle \Lambda'S'\Sigma'\Omega'J'M'|T^1_p(\underset{\sim}{\mu})|\Lambda''S''\Sigma''\Omega''J''M''\rangle\right|^2 \quad ...(III.I.14)$$

where $\left|\langle n'v'|n''v''\rangle\right|^2$ is the Franck-Condon factor — the square of the overlap integral for the vibrational wavefunctions of the two states involved. This is omitted from the following formulas, which are used for relative intensities within a given vibrational band.

The Wigner-Eckart theorem allows the M dependence to be factored out

$$\langle \Lambda'S'\Sigma'\Omega'J'M'|T^1_p(\underset{\sim}{\mu})|\Lambda''S''\Sigma''\Omega''J''M''\rangle = (-1)^{J'-M'}\begin{pmatrix} J' & 1 & J'' \\ -M' & p & M'' \end{pmatrix} \cdot \langle \Lambda'S'\Sigma'J'\Omega'\|T^1(\underset{\sim}{\mu})\|\Lambda''S''\Sigma''J''\Omega''\rangle \quad ...(III.I.15)$$

where the double bars $\langle \| \ldots \| \rangle$ denote a reduced matrix element (i.e. one with no M dependence (in this case)) and the large parentheses $\begin{pmatrix} \\ \end{pmatrix}$ denote a Wigner 3j-symbol (67).

$T^1(\underset{\sim}{\mu})$ is the space-fixed dipole moment operator. The basis functions, however, represent wavefunctions expressed in terms of molecule-fixed coordinates. The dipole moment operator must therefore be projected into the molecule-fixed axis system (46d) by means of the relation (68)

$$T^1(\underset{\sim}{\mu}) = \sum_q D^{(1)}_{\cdot q}(\omega)^*_A T^1_q(\underset{\sim}{\mu}) \quad ...(III.I.16)$$

where $D^{(1)}_{\cdot q}(\omega)^*_A$ is the complex conjugate of the $(\cdot,q)$ element of the first rank Wigner rotation matrix; ω stands for the three Euler angles (α,β,γ), which are here defined so as to give an "active" rotation (denoted by the subscript A);[34] the dot indicates that space-fixed subscript p has been omitted, since the equation is for the *total* space-fixed dipole moment operator, not just the p^{th} component; and the

---

[34]See Larsson (45) for a discussion about phase conventions. An active rotation corresponds to the phase convention of Brink and Satchler (69) and of Rose (70). This is opposite to the convention used by Edmonds (71), who uses a passive rotation.

molecule-fixed components of the dipole operator $T^1_q(\underset{\sim}{\mu})$ are

$$T^1_{q=1}(\underset{\sim}{\mu}) = -\frac{1}{\sqrt{2}}(\mu_x + i\mu_y)$$

$$T^1_{q=0}(\underset{\sim}{\mu}) = \mu_z \qquad \text{...(III.I.17)}$$

$$T^1_{q=-1}(\underset{\sim}{\mu}) = \frac{1}{\sqrt{2}}(\mu_x - i\mu_y)$$

Substitution into eqn. (III.I.13) gives

$$S^S(a,b) = \sum_p \begin{pmatrix} J' & 1 & J'' \\ -M' & p & M'' \end{pmatrix}^2 \cdot \left| \sum_q \langle \Lambda' S' \Sigma' J' \Omega' \| D^{(1)}_{\cdot q}(\omega)^* T^1_q(\underset{\sim}{\mu}) \| \Lambda'' S'' \Sigma'' J'' \Omega'' \rangle \right|^2 \qquad \text{...(III.I.18)}$$

The advantage of using the factorization in eqn. (III.I.15) is that since the basis functions can be written as products of a rotating molecule part and a non-rotating molecule part, i.e.

$$|\Lambda S \Sigma J \Omega\rangle = |\Lambda S \Sigma\rangle |J \Omega\rangle \qquad \text{...(III.I.19)}$$

then the calculation of the dipole matrix elements can similarly be factorized into two parts. This is accomplished as follows. We introduce the identity in the form of the closure relation for the projection operator

$$P = |\Lambda S \Sigma J \Omega\rangle\langle \Lambda S \Sigma J \Omega| \qquad \text{...(III.I.20)}$$

onto the space spanned by the complete set of basis functions $\{|\Lambda S \Sigma J \Omega\rangle\}$, i.e.

$$\sum_{\Lambda S \Sigma J \Omega} |\Lambda S \Sigma J \Omega\rangle\langle \Lambda S \Sigma J \Omega| = 1 \qquad \text{...(III.I.21)}$$

This gives

$$\langle \Lambda' S' \Sigma' J' \Omega' \| D^{(1)}_{\cdot q}(\omega)^* T^1_q(\underset{\sim}{\mu}) \| \Lambda'' S'' \Sigma'' J'' \Omega'' \rangle = \sum_{\Lambda S \Sigma J \Omega} \langle \Lambda' S' \Sigma' J' \Omega' \| D^{(1)}_{\cdot q}(\omega)^* \| \Lambda S \Sigma J \Omega \rangle \cdot \langle \Lambda S \Sigma J \Omega | T^1_q(\underset{\sim}{\mu}) | \Lambda'' S'' \Sigma'' J'' \Omega'' \rangle \qquad \text{...(III.I.22)}$$

The double bar notation has been dropped from the molecule-fixed matrix element of $T^1_q(\underset{\sim}{\mu})$, since M is not defined in a molecule-fixed basis. Since $D^{(1)}_{\cdot q}(\omega)^*$ does not depend on the non-rotating part of the eigenfunctions and the molecule-fixed electric dipole moment operator is independent of the rotating part, we can write, using eqn. (III.I.19),

$$\begin{aligned}
&\langle \Lambda' S' \Sigma' J' \Omega' \| D^{(1)}_{\cdot q}(\omega)^* \| \Lambda'' S'' \Sigma'' J'' \Omega'' \rangle \\
&\quad = \sum_{\Lambda S \Sigma J \Omega} \langle J' \Omega' \| D^{(1)}_{\cdot q}(\omega)^* \| J \Omega \rangle \delta_{\Lambda' \Lambda} \delta_{S' S} \delta_{\Sigma' \Sigma} \\
&\qquad\qquad \cdot \langle \Lambda S \Sigma | T^1_q(\underset{\sim}{\mu}) | \Lambda'' S'' \Sigma'' \rangle \ \delta_{J J''} \delta_{\Omega \Omega''} \\
&\quad = \langle J' \Omega' \| D^{(1)}_{\cdot q}(\omega)^* \| J'' \Omega'' \rangle \langle \Lambda' S' \Sigma' | T^1_q(\underset{\sim}{\mu}) | \Lambda'' S'' \Sigma'' \rangle \qquad \text{...(III.I.23)}
\end{aligned}$$

The reduced matrix elements of $D^{(1)}_{\cdot q}(\omega)^*$ are given by (72)

$$\begin{aligned}
&\langle J' \Omega' \| D^{(k)}_{\cdot q}(\omega)^* \| J'' \Omega'' \rangle \\
&\qquad = (-1)^{J' - \Omega'} [(2J'+1)(2J''+1)]^{1/2} \begin{pmatrix} J' & k & J'' \\ -\Omega' & q & \Omega'' \end{pmatrix}
\end{aligned} \qquad \text{...(III.I.24)}$$

The expression for the strength of the line component now becomes

$$\begin{aligned}
S^S(a,b) &= \sum_p \begin{pmatrix} J' & 1 & J'' \\ -M' & p & M'' \end{pmatrix}^2 (2J'+1)(2J''+1) \\
&\qquad \cdot \left| \sum_q \begin{pmatrix} J' & 1 & J'' \\ -\Omega' & q & \Omega'' \end{pmatrix} \langle \Lambda' S' \Sigma' | T^1_q(\underset{\sim}{\mu}) | \Lambda'' S'' \Sigma'' \rangle \right|^2
\end{aligned} \qquad \text{...(III.I.25)}$$

The foregoing derivation has been for the intensity of one component of a line. For the complete line we sum over the components:

$$\begin{aligned}
I(A,B) &= \sum_{ab} I(a,b) \\
&= \sum_{ab} N(a) \frac{64 \pi^4 c \bar{\nu}^4_{ab}}{3} S(a,b)
\end{aligned} \qquad \text{...(III.I.26)}$$

If the (2J' +1) M' components of the A level and the (2J" +1) M" components of the B level are sufficiently close to each other that all the $\bar{\nu}_{ab}$'s and all the N(a)'s can be considered to be equal, then

$$I(A,B) = N(a) \frac{64\pi^4 c \bar{\nu}_{ab}^4}{3} S(A,B) \qquad \text{...(III.I.27)}$$

where

$$S(A,B) = \sum_{ab} S(a,b) \qquad \text{...(III.I.28)}$$

Therefore

$$S^S(A,B) = \sum_{M'M''p} \begin{pmatrix} J' & 1 & J'' \\ -M' & p & M'' \end{pmatrix}^2 (2J'+1)(2J''+1)$$
$$\cdot \left| \sum_q \begin{pmatrix} J' & 1 & J'' \\ -\Omega' & q & \Omega'' \end{pmatrix} \langle \Lambda' S' \Sigma' | T_q^1(\underset{\sim}{\mu}) | \Lambda'' S'' \Sigma'' \rangle \right|^2$$
$$= \sum_{M'} (2J''+1)$$
$$\cdot \left| \sum_q \begin{pmatrix} J' & 1 & J'' \\ -\Omega' & q & \Omega'' \end{pmatrix} \langle \Lambda' S' \Sigma' | T_q^1(\underset{\sim}{\mu}) | \Lambda'' S'' \Sigma'' \rangle \right|^2 \qquad \text{...(III.I.29)}$$

where the 3j orthogonality property

$$\sum_{m_1 m_2} \begin{pmatrix} j_1 & j_2 & j_3 \\ m_1 & m_2 & m_3 \end{pmatrix} \begin{pmatrix} j_1 & j_2 & j_3' \\ m_1 & m_2 & m_3' \end{pmatrix} = (2j_3+1)^{-1} \delta_{j_3 j_3'} \delta_{m_3 m_3'} \delta(j_1 j_2 j_3)$$

...(III.I.30)

(Edmonds (71), eqn. (3.7.8)) has been used; $\delta(j_1 j_2 j_3) = 1$ or 0 depending on whether the following triangular condition holds or not:

Triangular condition: $j_3 = j_1+j_2,\ j_1+j_2-1,\ j_1+j_2-2,\ \ldots,\ |j_1-j_2|$

...(III.I.31)

Since there are (2J' +1) values of M', summation over M' gives

$$S^S(A,B) = (2J'+1)(2J''+1) \cdot \left| \sum_q \begin{pmatrix} J' & 1 & J'' \\ -\Omega' & q & \Omega'' \end{pmatrix} \langle \Lambda' S' \Sigma' | T^1_q(\underset{\sim}{\mu}) | \Lambda'' S'' \Sigma'' \rangle \right|^2 \quad \text{...(III.I.32)}$$

This equation not only gives line strengths for allowed transitions, but also tells which transitions are allowed (i.e. gives selection rules). If the functions $|\Lambda S\Sigma\rangle$ are considered to be products of orbital and spin parts (46e)

$$|\Lambda S\Sigma\rangle = |\Lambda\rangle|S\Sigma\rangle \quad \text{...(III.I.33)}$$

then, since the dipole moment operator does not depend on spin (46e),

$$\langle \Lambda' S' \Sigma' | T^1_q(\underset{\sim}{\mu}) | \Lambda'' S'' \Sigma'' \rangle = \langle \Lambda' | T^1_q(\underset{\sim}{\mu}) | \Lambda'' \rangle \delta_{S'S''} \delta_{\Sigma'\Sigma''} \quad \text{...(III.I.34)}$$

Therefore the spin selection rules are

$$\Delta S = 0 \qquad \Delta\Sigma = 0 \quad \text{...(III.I.35)}$$

The properties of 3j-symbols provide selection rules on J and Ω. The sum of the lower three elements of a 3j-symbol must equal zero. For each of the three values of q, where q designates the molecule-fixed components of the first rank tensor operator (eqn. (III.I.17)), there is only one possible value for $\Delta\Omega$ which satisfies this condition. The summation in eqn. (III.I.32) therefore reduces to a single term for each pair of Ω values. Furthermore, this condition also determines $\Delta\Lambda$, since $\Lambda = \Omega + \Sigma$ and $\Delta\Sigma = 0$: we have $\Delta\Lambda = \Delta\Omega = \Lambda' - \Lambda'' = \Omega' - \Omega'' = q$. The triangular condition, eqn. (III.I.31), restricts the values of J to those in accord with the selection rule

$$\Delta J = J' - J'' = 0, \pm 1 \quad \text{...(III.I.36)}$$

For each pair of Ω values there are thus three branches, labelled R, Q, and P in the usual manner and corresponding to $\Delta J = +1$, 0, and -1, respectively.

The matrix elements of the molecule-fixed dipole moment operator $\langle \ldots | T^1_q(\underset{\sim}{\mu}) | \ldots \rangle$ cannot be readily calculated. Since this quantity is J-independent and is constant for any particular value of q (and hence of $\Delta\Lambda$), it can simply be ignored; its square becomes a proportionality constant, which is usually not ever determined. The line strength factors in a case (a) basis, written in terms of the lower state Ω values, become

$$\Delta\Lambda = \Delta\Omega = +1 \quad S^S(A,B) \propto (2J'+1)(2J''+1) \begin{pmatrix} J' & 1 & J'' \\ -\Omega-1 & 1 & \Omega \end{pmatrix}^2$$

$$\Delta\Lambda = \Delta\Omega = 0 \quad S^S(A,B) \propto (2J'+1)(2J''+1) \begin{pmatrix} J' & 1 & J'' \\ -\Omega & 0 & \Omega \end{pmatrix}^2$$

$$\Delta\Lambda = \Delta\Omega = -1 \quad S^S(A,B) \propto (2J'+1)(2J''+1) \begin{pmatrix} J' & 1 & J'' \\ -\Omega+1 & -1 & \Omega \end{pmatrix}^2$$

...(III.I.37)

Evaluation of the 3j-symbols gives the explicit formulae in Table IX. These agree with those given by Kovács (48b).

For use in any given application, these formulae are to be symmetrized and diagonalized by means of eqn. (III.I.11). For non-Σ states, due to the symmetry between the $+\Lambda$ and $-\Lambda$ submatrices, symmetrizing (i.e. transforming to a parity basis) has no effect, so this step can be ignored. For states exhibiting good case (a) behavior, the diagonalization matrix $\underset{\sim}{U}_{diag}$ will itself be virtually diagonal, so the diagonalization step will also have negligible effect on the intensities. For these situations, the formulae in Table IX can be applied directly. When comparing intensities of lines having different starting-state J values, the line strength factors must be multiplied by a Boltzman factor to account for population differences.

TABLE IX. Line strength factors in a case (a) basis.[a]

Branch	$\Delta\Lambda = \Delta\Omega = -1$	$\Delta\Lambda = \Delta\Omega = 0$	$\Delta\Lambda = \Delta\Omega = +1$
R(J)	$\frac{(J+\Omega+1)(J+\Omega+2)}{2(J+1)}$	$\frac{(J+1)^2-\Omega^2}{J+1}$	$\frac{(J-\Omega+1)(J-\Omega+2)}{2(J+1)}$
Q(J)	$\frac{(J+\Omega+1)(J-\Omega)(2J+1)}{2J(J+1)}$	$\frac{\Omega^2(2J+1)}{J(J+1)}$	$\frac{(J-\Omega+1)(J+\Omega)(2J+1)}{2J(J+1)}$
P(J)	$\frac{(J-\Omega)(J-\Omega-1)}{2J}$	$\frac{J^2-\Omega^2}{J}$	$\frac{(J+\Omega)(J+\Omega-1)}{2J}$

(a) The formulas give S^S (A,B) expressed in terms of the lower state Ω value and lower state J value.

III.J. Perturbations

A complete treatment of all the types of perturbations exhibited by diatomic molecules in their spectra cannot possibly be given here. Rather a brief, general introduction is presented that will serve as background for the discussions in the following chapters. For a more detailed account, the reader is referred to the excellent new book by Lefebvre-Brion and Field (22).

A **perturbation** can be defined as any behaviour that is deviant from that predicted by the model currently being used to describe the system.

In the effective hamiltonian approach, provided sufficiently high order terms are included, the hamiltonian will completely describe those contributions to the energies of the levels within a given vibronic state arising from that state itself (i.e. terms diagonal in vibronic state) and those arising from interactions with distant states (cross-terms). But if there are vibronic states lying close in energy to the state of interest, there will be additional cross-terms, which may be non-negligible. Since these terms have not been allowed for, the effects they produce will appear, anomalous and are regarded as perturbations.

Since the cross-terms connecting different electronic states are terms that are neglected by the Born-Oppenheimer approximation, perturbations are often described as just that: effects resulting from terms neglected by the Born-Oppenheimer approximation — but more specifically, in the effective hamiltonian model used here, they are those terms neglected by the Born-Oppenheimer approximation which are not accounted for by the Van Vleck transformation or whose effects cannot be absorbed into the effective terms of the hamiltonian matrix. Perturbations can also result between different vibrational levels of the same electronic state if a near degeneracy occurs (e.g. between the $\Omega+1$ component of the v^{th} level and the Ω component of the $v+1^{th}$ level).

Perturbations can be classified as either homogeneous or heterogeneous (46f,73,22). **Homogeneous** perturbations are those for which the selection rule $\Delta\Omega = 0$ holds. These are characterized by interaction matrix elements H_{12} that do not depend on the rotational quantum number J. Perturbations obeying the selection rule $\Delta\Omega = \pm 1$ are called **heterogeneous** perturbations. For these, H_{12} does depend on J — specifically H_{12} is approximately proportional to $\sqrt{J(J+1)}$.

Table X lists the operators responsible for perturbations, together with their selection rules. The selection rule $\Delta J = 0$ always applies (in the absence of nuclear spin) because none of the perturbation operators contain the angular coordinates of the nuclei, so they cannot act on the rotational basis functions.

The final column in Table X lists the "number of different spin-orbitals." The term spin-orbital refers to a one-electron wavefunction when both the spatial and spin parts are to be considered (22). If the "number of different spin-orbitals" is one, for example, the operator can only connect states whose electron configurations differ by one spin-orbital.

Due to the very nature of perturbations, each one has to be studied on an individual basis. If the perturbing state is so far unknown, study of the perturbation may provide information about this state. The study of a perturbation involves determining the interaction matrix element H_{12} between the perturbed and perturbing states. The magnitude of H_{12}, together with the selection rules associated with it can give information about the identity of the perturbing state.

If several Ω substates of a given vibronic multiplet state are perturbed by several substates of a perturbing vibronic state, provided enough information is available, diagonalization of a large matrix containing complete submatrices for the perturbed and perturbing states together with interaction matrix elements between them will produce a complete deperturbation of both states and yield spectroscopic constants for both.

TABLE X. Operators responsible for perturbations and their selection rules.[a]

Classification	Nature of the perturbation	Operator	Selection rules[b] $\Delta\Lambda$	$\Delta\Sigma$	ΔS	$\Delta\Omega$	other	Number of different spin-orbitals[c]
Homogeneous	Electrostatic ($\equiv$ Diabatic)	H_e	0	0	0	0		1 or 2
	Vibrational ($\equiv$ Adiabatic)	H_n	0	0	0	0		1
	Spin-orbit	H_{so}	0	0	0[d] or 1	0	for Σ states: $\Sigma^+ \leftrightarrow \Sigma^-$	0 or 1
			or					
			± 1	∓ 1	0 or 1	0		1
	Spin-spin	H_{ss}	0	0	0[e], 1[f], or 2	0	$\Sigma^\pm \leftrightarrow \Sigma^\pm$	0
			± 1	∓ 1	0, 1, or 2	0		1
			± 2	∓ 2	0, 1, or 2	0		2
	Spin-electronic	$B(r)(L^+S^- + L^-S^+)$	± 1	∓ 1	0	0		1 or 2
Heterogeneous	$\underset{\sim}{L}$-uncoupling	$-B(r)(J^+L^- + J^-L^+)$	± 1	0	0	± 1		1
	$\underset{\sim}{S}$-uncoupling	$-B(r)(J^+S^- + J^-S^+)$	0	± 1	0	± 1		1

(a) Based on Lefebvre-Brion and Field (22). Non-symmetrized basis functions are assumed.

(b) Additionally, the selection rules $\Delta J = 0$, $e \leftrightarrow e$, $f \leftrightarrow f$, $e \not\leftrightarrow f$ always hold, as does $g \leftrightarrow g$, $u \leftrightarrow u$, $g \not\leftrightarrow u$ for homonuclear molecules.

(c) Each state must be well represented by a single configuration.

(d) The matrix element is zero if $\Omega' = \Omega'' = 0$.

(e) The matrix element is zero if $\Sigma' = \Sigma'' = 0$ and $S' = S'' = 0$.

(f) The matrix element is zero if $\Sigma' = \Sigma'' = 0$ (no restriction on S).

In many cases, however, such a complete deperturbation will not be possible. For example, if the various Ω substates of a multiplet state are perturbed by a number of other perturbing states that bear no obvious relation to each other, as often happens in FeO, it will at best only be possible to do an approximate deperturbation of one Ω substate (possibly of only one part of it) at a time, together with part of the perturbing state. This can be done by writing an approximate energy level expression for each Ω substate, e.g.

$$E_1 = T_{v,1}^{eff} + B_{v,1}^{eff} J(J+1) - D_{v,1}^{eff} [J(J+1)]^2 + \ldots \qquad \text{...(III.J.1)}$$

and setting up the secular determinant

$$\begin{vmatrix} E_1-\lambda & H_{12} \\ H_{12} & E_2-\lambda \end{vmatrix} = 0 \qquad \text{...(III.J.2)}$$

The solutions are

$$\lambda = \frac{E_1+E_2}{2} \pm \sqrt{\frac{(E_1-E_2)^2}{4} + H_{12}^2} \qquad \text{...(III.J.3)}$$

If the unperturbed substates actually cross each other, say at $J = J_c$, the solutions at this point are

$$\lambda(J=J_c) = E_1 \pm H_{12} = E_2 \pm H_{12} \qquad \text{...(III.J.4)}$$

Thus the separation of the two perturbed levels is $2H_{12}$ at the crossing point. This is shown in Fig. 5, where the energies of the two perturbed substates have been labelled E_1' and E_2'.

The effective rotational constant B_v^{eff} introduced in eqn. (III.J.1) is related to the value for the complete vibronic-state rotational level, B_v (itself an effective value), according to (38)

$$B_v^{eff} = B_v\left(1 + \frac{2B\Sigma}{A\Lambda} + \ldots\right) \qquad \text{...(III.J.5)}$$

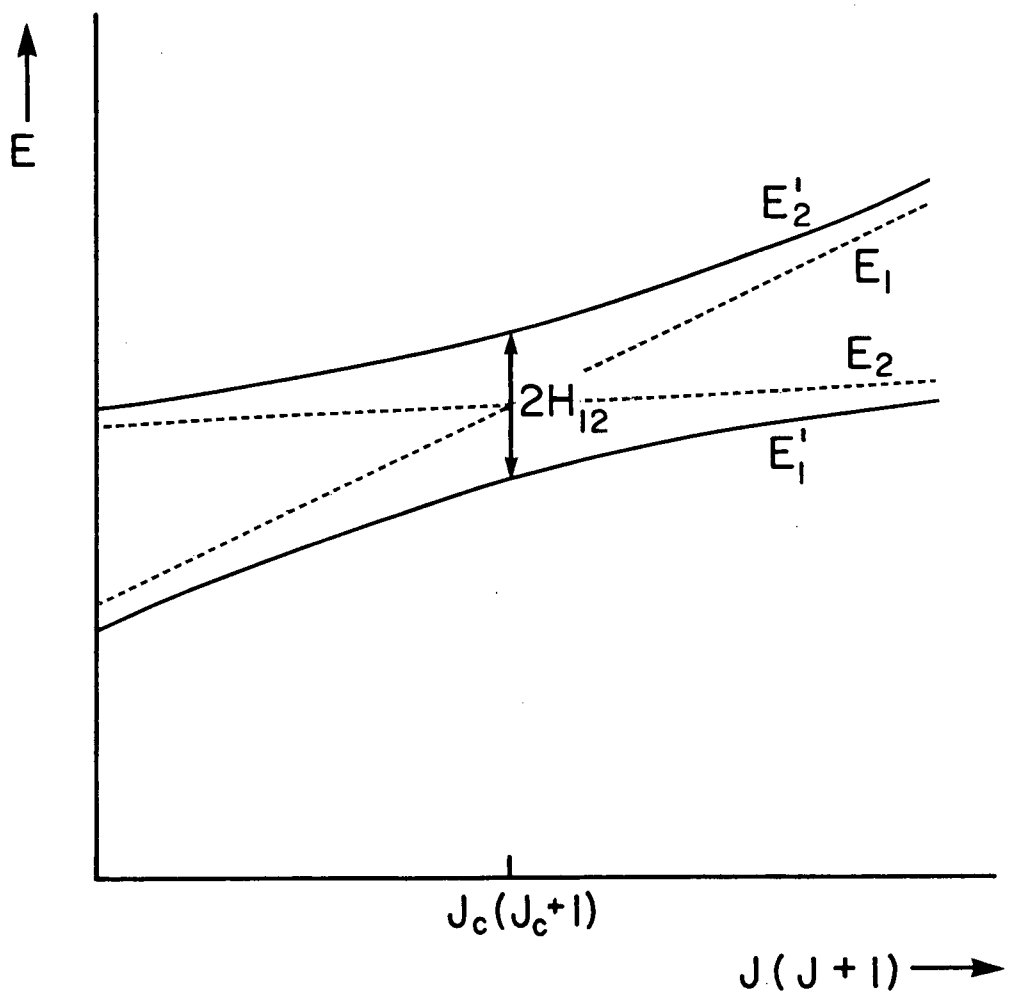

Fig. 5. Schematic representation of two perturbing states.

We now consider the two classifications of perturbations, homogeneous versus heterogeneous, and treat this same problem by second-order non-degenerate perturbation theory assuming H_{12} to be small relative to ΔT_0. For the homogeneous case, H_{12} is independent of J and

$$E_1' = \lambda_1 = E_1 + \frac{H_{12}^2}{E_1 - E_2} \qquad \text{...(III.J.6)}$$

$$\Delta E = E_1' - E_1 = \frac{H_{12}^2}{E_1 - E_2} \qquad \text{...(III.J.7)}$$

$$= \frac{H_{12}^2}{T_{v,1}^{eff} + B_{v,1}^{eff} J(J+1) - T_{v,2}^{eff} - B_{v,2}^{eff} J(J+1)}$$

$$= \frac{H_{12}^2}{\Delta T_v^{eff}\left[1 + \frac{\Delta B_v^{eff}}{\Delta T_v^{eff}} J(J+1)\right]} \qquad \text{...(III.J.8)}$$

Using the expansion

$$\frac{1}{1+x} = 1 - x + \ldots \qquad \text{...(III.J.9)}$$

this becomes

$$\Delta E \simeq \frac{H_{12}^2}{\Delta T_v^{eff}} - \frac{H_{12}^2}{(\Delta T_v^{eff})^2} \Delta B_v^{eff} J(J+1) \qquad \text{...(III.J.10)}$$

As a result of the first term on the right-hand-side of this equation, homogeneous perturbations produce non-zero energy shifts at J=0.

For heterogeneous perturbations, H_{12} depends on J,

$$H_{12} \simeq h_{12}[J(J+1)]^{1/2} \qquad \text{...(III.J.11)}$$

where the J-dependence has been written in the approximate form $[J(J+1)]^{1/2}$ [35] and h_{12} is a constant. Second-order perturbation theory gives

---

[35]The more detailed form is $H_{12} = h_{12}[J(J+1) - \Omega(\Omega \pm 1)]^{1/2}$

$$\Delta E = E_1' - E_1 = \frac{H_{12}'^2 J(J+1)}{\Delta T_v^{eff}\left[1 + \frac{\Delta B_v^{eff}}{\Delta T_v^{eff}} J(J+1)\right]} \qquad \text{...(III.J.12)}$$

which, in the same manner as for the homogeneous case, becomes

$$\Delta E \simeq \frac{H_{12}'^2}{\Delta T_v^{eff}} J(J+1) - \frac{H_{12}'^2}{(\Delta T_v^{eff})^2} \Delta B_v^{eff} J^2(J+1)^2 \qquad \text{...(III.J.13)}$$

from which it is seen that, in contrast to the homogeneous case, heterogeneous perturbations produce no energy shifts at J = 0. On the other hand, returning to eqn. (III.J.12), we see that at large values of J and far from the crossing point

$$\Delta E \simeq \frac{H_{12}'^2 J(J+1)}{\Delta B_v^{eff} J(J+1)} = \frac{H_{12}'^2}{\Delta B_v^{eff}} \qquad \text{...(III.J.14)}$$

Constant energy shifts are produced by heterogeneous perturbations at large J, in contrast to homogeneous perturbations, which become zero at very large J. These two situations are illustrated in Fig. 6.

Another effect of a perturbation is to mix the wavefunctions of the perturbed and perturbing states (or substates) (16b),

$$\begin{aligned} \psi_1' &= a\psi_1 - b\psi_2 \\ \psi_2' &= b\psi_1 + a\psi_2 \end{aligned} \qquad \text{...(III.J.15)}$$

where

$$a = \left[\frac{W + (E_1 - E_2)}{2W}\right]^{1/2} \qquad \text{...(III.J.16a)}$$

$$b = \left[\frac{W - (E_1 - E_2)}{2W}\right]^{1/2} \qquad \text{...(III.J.16b)}$$

with

$$W = [4H_{12}^2 + (E_1 - E_2)^2]^{1/2} \qquad \text{...(III.J.17)}$$

At the crossing point of the two unperturbed states (i.e. at $J = J_c$)

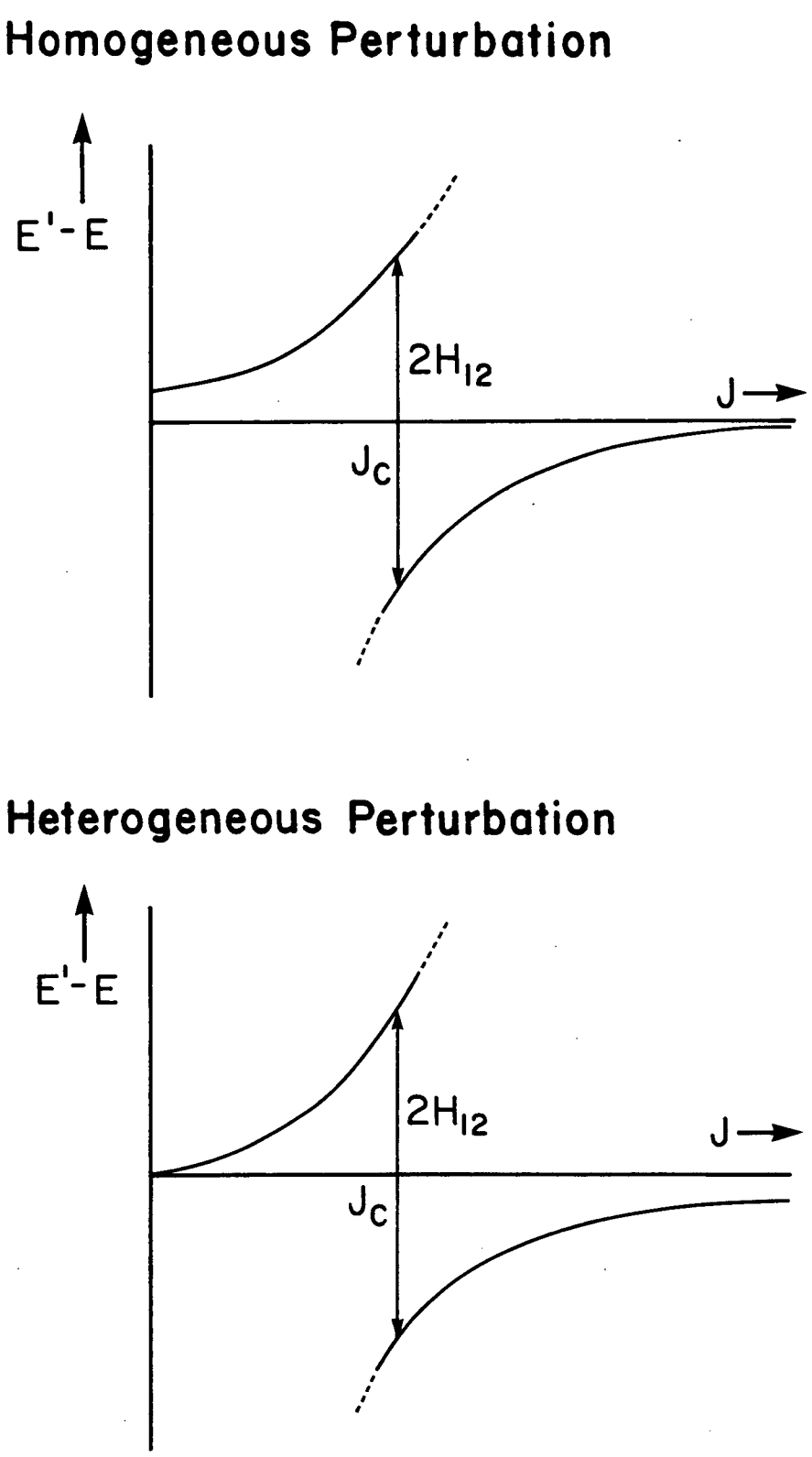

Fig. 6. Homogeneous and heterogeneous perturbations.

$$a = b = \frac{1}{\sqrt{2}} \qquad \text{...(III.J.18)}$$

so we have a fifty-fifty mixture.

If ψ_1 is involved in some transition having non-zero intensity to some other state ψ_3, and ψ_2 possesses no intensity with respect to a transition to that same other state, then as J increases towards the perturbation region, intensity will be progressively "borrowed" from the $\psi_1 - \psi_3$ transition (which becomes the perturbed $\psi_1' - \psi_3$ transition) by the $\psi_2 - \psi_3$ transition (which becomes $\psi_2' - \psi_3$), so for each J value there will be two lines. At the crossing point, since ψ_1' and ψ_2' are each fifty-fifty mixtures of the starting states, there will be two lines of equal intensity and this intensity will be one-half of what it would have been for an unperturbed $\psi_1 - \psi_3$ transition. Continuing to still higher J values, the $\psi_1' - \psi_3$ transition fades away entirely and the $\psi_2' - \psi_3$ transition eventually becomes the $\psi_1 - \psi_3$ transition and carries all the intensity.

Quantitatively, from eqns. (III.I.3) and (III.I.4),

$$I(1',3) \propto \left|\langle\psi_1'|\underset{\sim}{\mu}|\psi_3\rangle\right|^2$$

$$I(2',3) \propto \left|\langle\psi_2'|\underset{\sim}{\mu}|\psi_3\rangle\right|^2 \qquad \text{...(III.J.19)}$$

For the zeroth-order (crossing) states,

$$I(1,3) \propto \left|\langle\psi_1|\underset{\sim}{\mu}|\psi_3\rangle\right|^2$$

$$I(2,3) \propto \left|\langle\psi_2|\underset{\sim}{\mu}|\psi_3\rangle\right|^2 = 0 \qquad \text{...(III.J.20)}$$

From eqn. (III.J.15),

$$\langle\psi_1'|\underset{\sim}{\mu}|\psi_3\rangle = a\langle\psi_1|\underset{\sim}{\mu}|\psi_3\rangle - b\langle\psi_2|\underset{\sim}{\mu}|\psi_3\rangle$$

$$= a\langle\psi_1|\underset{\sim}{\mu}|\psi_3\rangle \qquad \text{...(III.J.21a)}$$

$$\langle\psi_2'|\underset{\sim}{\mu}|\psi_3\rangle = b\langle\psi_1|\underset{\sim}{\mu}|\psi_3\rangle + a\langle\psi_2|\underset{\sim}{\mu}|\psi_3\rangle$$

$$= b\langle\psi_1|\underset{\sim}{\mu}|\psi_3\rangle \qquad \text{...(III.J.21b)}$$

so that

$$I(1',3) \propto a^2\left|\langle\psi_1|\underset{\sim}{\mu}|\psi_3\rangle\right|^2$$

$$I(2',3) \propto b^2\left|\langle\psi_1|\underset{\sim}{\mu}|\psi_3\rangle\right|^2 \qquad \text{...(III.J.22)}$$

and the ratio of the intensities is

$$\frac{I(1',3)}{I(2',3)} = \frac{a^2}{b^2} \qquad \text{...(III.J.23)}$$

where a and b are given by eqn. (III.J.16).

In addition to the situation described so far involving one or more components of a multiplet state interacting with one or more components of a perturbing state, more complicated types of perturbations can occur, and these are, of course, even more difficult to treat. A perturbation may occur via an intermediate state, rather than directly. How this can occur can be seen from a second-order Van Vleck transformation matrix element

$$\tilde{H}_{12} = \frac{\langle\psi_1|H|\psi_3\rangle\langle\psi_3|H|\psi_2\rangle}{\frac{1}{2}[E_1+E_2] - E_3} \qquad \text{...(III.J.24)}$$

Another situation that can occur is that two or more states may simultaneously interact with a given state. Examples of this situation have been seen in FeO and will be presented in Chapter V.

III.K. Electron Configurations

In Chapter I it was seen that it was difficult to determine the symmetry classifications of the ground and excited states of FeO — in fact, the determination was finally done experimentally. *Ab initio* methods have so far proved incapable of establishing the correct energy ordering of the states. A qualitative explanation is given in this section, using single-configuration approximations to the electron configurations.

One of the more thoroughly studied molecules in spectroscopy is TiO, and its electronic states are fairly well understood. A crude molecular orbital (MO) scheme for TiO is shown in Fig. 7. This diagram is now frequently used not only with reference to TiO, but when describing the ground and excited states of any diatomic oxide (74). According to the calculations of Carlson and coworkers (75), the σ and δ orbitals shown near the center of the figure are largely Ti 4s and 3d, respectively, and are quite close together in energy. The ground state of TiO is known (76) to be a $^3\Delta_r$ state, arising from a $(4s\sigma)^1(3d\delta)^1$ configuration (74).[36] A similar MO diagram can be drawn for ScO (78), in which the $3d\sigma$ electron of TiO is not present. Proceeding across the first row of transition element oxides, the configurations and ground states can be obtained by adding electrons to the orbitals of the TiO MO diagram. Of course, the orbital energies will vary from molecule to molecule (especially the close-lying $4s\sigma$ and $3d\delta$ molecular orbitals), but a qualitative understanding of the states involved can still be gained. The ground state electron configurations of the first five first-row transition element oxides are (74)

---

[36]In this thesis we show only simple single-configuation approximations, and only the outermost orbitals are listed, the inner orbitals being completely filled. Such an approximation is useful because it provides a simple physical picture of the bonding in the molecule. We leave to the theoreticians the job of providing a more accurate representation. For FeO, the recent theoretical calculations by Krauss and Stevens (77), are in general agreement with our simple picture.

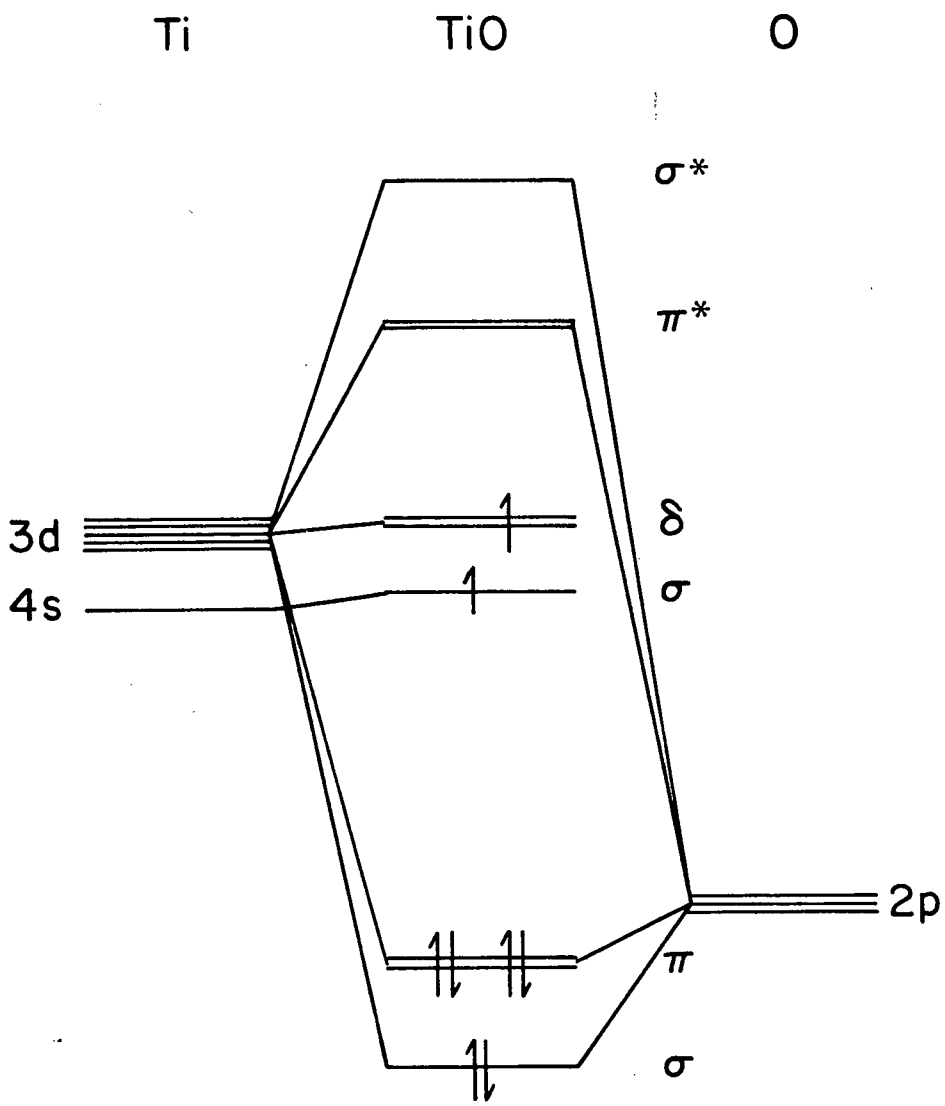

Fig. 7. Energy level diagram for TiO, showing the orbital occupancy for the ground state.

ScO	$(4s\sigma)^1$	$^2\Sigma^+$
TiO	$(4s\sigma)^1(3d\delta)^1$	$^3\Delta$
VO	$(4s\sigma)^1(3d\delta)^2$	$^4\Sigma^-$
CrO	$(4s\sigma)^1(3d\delta)^2(3d\pi)^1$	$^5\Pi$
MnO	$(4s\sigma)^1(3d\delta)^2(3d\pi)^2$	$^6\Sigma^+$

The states listed on the right hand side are now well-established experimentally as being the correct ground states of their respective molecules (76).

Proceeding on to FeO, the additional electron could go into the next unoccupied MO, $3d\sigma$, or into either the $4s\sigma$ or $3d\delta$ MOs, giving $^7\Sigma^+$, $^5\Sigma^+$, or $^5\Delta$, respectively, for the ground state. As described in Chapter I, theoretical computations were unable to establish which alternative was correct. Experimentally the ground state is now known to be $^5\Delta$, so the configuration of the ground state of FeO is

FeO ground state: $(4s\sigma)^1(3d\delta)^3(3d\pi)^2$ $^5\Delta$

The other two possibilities are then excited states:

FeO excited states: $(4s\sigma)^1(3d\delta)^2(3d\pi)^2(3d\sigma)^1$ $^7\Sigma^+$

$(4s\sigma)^2(3d\delta)^2(3d\pi)^2$ $^5\Sigma^+$

If the $4s\sigma$, $3d\delta$, $3d\pi$, and $3d\sigma$ MOs are considered to be primarily localized on the Fe atom and the $2p\sigma$ and $2p\pi$ MOs on the O atom, these three configurations correspond to a doubly-charged ionic model for the molecule, *viz.* $Fe^{2+}O^{2-}$.[37] Excitation of one of the oxygen $2p\pi$ electrons to the antibonding $3d\sigma$ orbital would be a charge transfer transition, yielding Fe^+O^- and an electron configuration

FeO excited state: $(2p\pi)^3(4s\sigma)^1(3d\delta)^3(3d\pi)^2(3d\sigma)^1$ $^5\Pi$, $^5\Phi$

---

[37]The recent *ab initio* calculations of Krauss and Stevens referred to in the previous footnote yield a description of the ground and low-lying states of FeO in terms of Fe^+O^- rather than the $Fe^{2+}O^{2-}$ model assumed here. As indicated in Section I.D, these calculations must be treated with some reservations since they are not completely adequate in their description of these states. Whether $Fe^{2+}O^{2-}$ or Fe^+O^- ultimately proves to be the better model is of little consequence to the present work; the $Fe^{2+}O^{2-}$ model is used here simply as a convenient book-keeping device.

As will be shown, these $^5\Pi$ and $^5\Phi$ states, both deriving from the same electron configuration, form the upper levels of the infrared electronic system. Excitation of the $4s\sigma$ electron from the ground state configuration to the $4p\sigma$ orbital may yield one of the states corresponding to the upper level of the orange system, though this assignment is less certain than the others:

FeO excited state: $(3d\delta)^3(3d\pi)^2(4p\sigma)^1$ $^5\Delta$

Other excited states can be derived by a similar process.

To complete the first-row transition metal oxide ground state series, Weltner (74) predicts the following single-configuration approximations and state assignments:

CoO	$(4s\sigma)^2(3d\delta)^3(3d\pi)^2$	$^4\Delta$
NiO	$(4s\sigma)^2(3d\delta)^3(3d\pi)^3$	$^3\Phi$
CuO	$(4s\sigma)^2(3d\delta)^4(3d\pi)^3$	$^2\Pi$
ZnO	$(4s\sigma)^2(3d\delta)^4(3d\pi)^4$	$^1\Sigma$

Krauss and Stevens (77) have also given predictions for the first-row transition metal oxide ground states given the experimental information that the ground state of FeO is a $^5\Delta$ state. These predictions agree with those given here and earlier in this section, except for CoO and NiO, for which they give

CoO	$(4s\sigma)^1(3d\delta)^4(3d\pi)^2$	$^4\Sigma^-$
NiO	$(4s\sigma)^2(3d\delta)^4(3d\pi)^2$	$^3\Sigma^-$

Of these post-FeO first-row transition metal oxide predictions, only CuO and NiO have been confirmed experimentally (76,79). In the case of NiO, $^3\Sigma^-$ has proven to be the correct assignment, as demonstrated by the recent work of Harris (79).

CHAPTER IV

THE GROUND STATE: $X\,^5\Delta_i$

IV.A. Introduction

The near-infrared spectrum of FeO was first seen in its entirety by Bass and Benedict (1) in the early 1950s, though parts of it had been seen by Gaydon (2) and by Malet and Rosen (3). Obtained in the present study for the first time at high resolution, it appears in emission as a highly complex system of bands in the region 7 000 - 14 000 cm^{-1}. Some areas contain obvious heads and regular branch structures, which are relatively easy to analyze. Other areas are extremely dense and featureless. Since much of the complexity arises from the upper states, a detailed description of the more complicated regions is reserved for the next chapter, though these regions were also used in the analysis of the ground state.

An example of a more regular region is shown in Fig. 8. Ignoring the "background" lines for now, two subbands are apparent, each consisting of red-degraded R, Q, and P branches. The subbands illustrated comprise two of the five that make up a single band of a type found frequently in the infrared region. In these bands the R branches are strong and often form heads. The Q-branch intensities are moderate at low J, increase with increasing J, eventually exceeding the corresponding R-branch intensities, and reach maximum strengths at J values in the low- to mid-20s. The P branches are relatively weak in comparison with the R and Q branches. All three types of branches can be followed to high values of J (except when they are lost because of perturbations). Such an intensity pattern (strong Q branch; R branch stronger than P branch) is characteristic of $\Delta\Lambda = \Lambda' - \Lambda'' = +1$ transitions (4), as can be seen from Table IX. Other bands, mostly falling in the "more complicated regions" to be described in the next chapter, also possess five

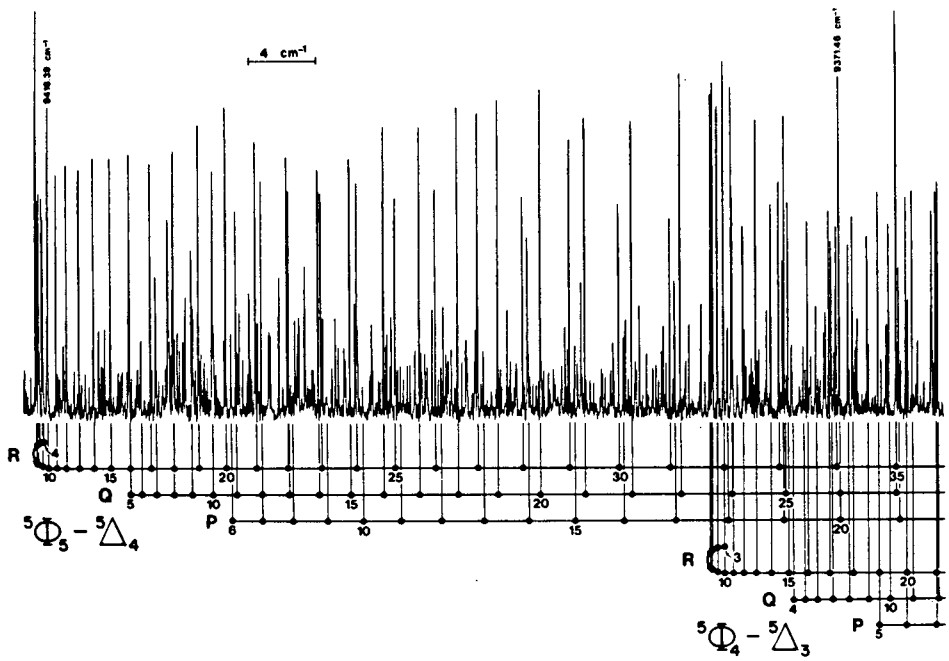

Fig. 8. Fourier transform ir spectrum of FeO in the region 9365 - 9420 cm^{-1} showing the heads of the Ω = 5–4 and 4–3 subbands of the $^5\Phi - {}^5\Delta$ (0,1) band.

subband components, each with three branches. These bands also have strong Q branches that can be followed to high J values (again, except where perturbed too badly), but have stronger P branches than R branches. The branches of these bands are also red-degraded, though the intensity in the R branches is often too weak for the branches to be followed to sufficiently low J values to see the R-heads. This intensity pattern is characteristic of $\Delta\Lambda = -1$ transitions (see Table IX).

The lower state rotational combination differences and vibrational differences are found to be the same for both band systems and also the same as those of the orange system lower state, which has already been established as being the ground state and as being a $^5\Delta_i$ state. The fact that this state is indeed a $^5\Delta$ state can also be shown from the infrared spectrum alone, in two different ways.

First, as was done with the orange system, the Q-branch line positions can be plotted against n(n+1), where n is an arbitrary running number. An example of such a plot is shown in Fig. 9. Use of a straight edge will convince the reader that the center one of the five possibilities shown yields the best straight line; hence the correct J numbering corresponds to the n numbering used in plotting these points. The numbering so established agrees with that found for the orange system. The smallest lower state J values present, using all branches (not just Q branches), establish the lower state Ω values, since J cannot be less than Ω. Although this method must be applied with care because many low-J perturbations occur, it is found that the lower state Ω values present are 0, 1, 2, 3, and 4, which corresponds to a $^5\Delta$ state.

Alternatively, assuming the transitions are spin-allowed, being very intense, the multiplicity of both upper and lower states must be five, since no more than five subbands can be found in any band. As mentioned above, the relative intensities of the branches indicate that for one band system $\Delta\Lambda = -1$. It will be shown in Chapter V that Λ-doubling is present in the upper state of this system. Since Λ-doubling is only possible for $\Lambda \geq 1$, the Λ value for the lower state must be

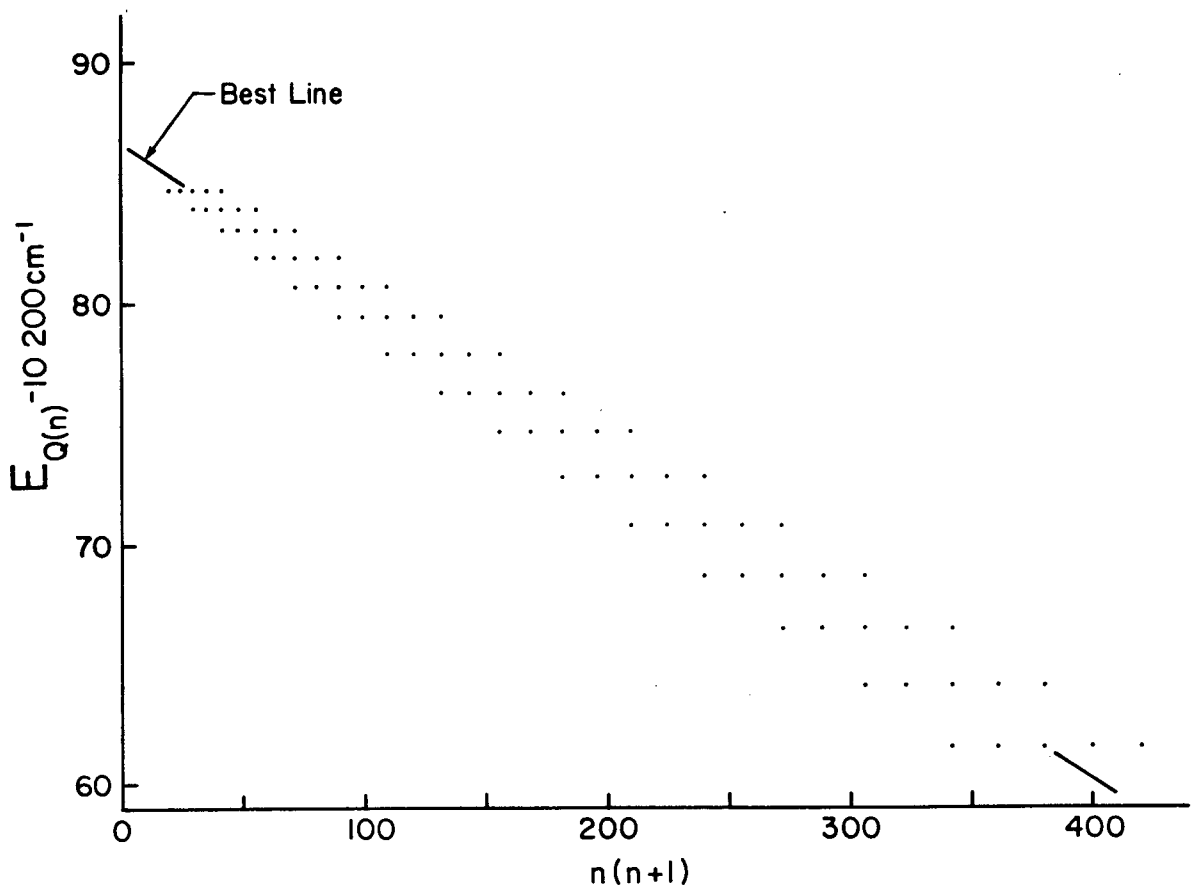

Fig. 9. J-number determination for the $^5\Phi_5 - X^5\Delta_4$ (0,0) subband. Various possibilities for the running number n are shown.

≥ 2. There is Λ-doubling also in the lower state, and in one subband of each band the Λ-doublet interval is almost constant, with only a small J-dependence. This indicates that for this subband the lower state must have $\Omega = 0$, since to a first approximation Λ-doublet splitting is proportional to $[J(J+1)]^{\Omega}$. For quintet states, $\Omega = 0$ can only occur for $\Lambda \leq 2$. We have established that $\Lambda \geq 2$ and $\Lambda \leq 2$. Therefore, Λ *equals* 2 and the lower state is a $^5\Delta$ state.

That the lower state is inverted (i.e. its spin-orbit coupling constant A is negative) follows from the B_{Ω}^{eff} values (cf. eqn. (III.J.5)) and also from the spin-orbit satellites observed in the orange system and described in Chapter I (Section I.B.3). The upper states of the infrared system are also inverted, as can be shown by simple addition of the observed transition frequencies to the lower state term values whose spin-orbit energies are known. The inverted natures of all these states are consistent with the electron configurations given in Section III.K (5,6).

We conclude that the near-infrared emission system consists of two electronic transitions, which both terminate on the same lower state; that this is the same lower state as that of the orange system; that this lower state is the ground state of the molecule and is a $^5\Delta_i$ state; and that the upper states of the infrared band systems are a $^5\Pi_i$ state and a $^5\Phi_i$ state.

Returning now to Fig. 8, while this figure was presented as an example of a relatively simple, regular region of the spectrum, even such a region as this is actually quite complicated. Although only one band has been labelled (for clarity), there are in fact parts of at least four bands present in this figure. In fact every line present, probably even the weakest line visible, is real — there is virtually no detectable noise. The other three bands, parts of which have been identified in this figure, are the $^5\Phi - X^5\Delta$ (0,1) and (3,3) bands and the $^5\Pi - X^5\Delta$ (0,1) band. The Π and Φ systems thus overlap each other, and this is typically the case, a point which will be returned to in Chapter V (Section V.A)

Such overlap, both of the Π and Φ systems with each other and of various bands and subbands within each system, can also be seen in Fig. 10, which is an overview of the infrared system. The spectrum has been expanded by plotting v', the upper state vibrational quantum number, on the vertical axis. This has been done not only for clarity but because it allows the figure to be easily used for band identification or prediction purposes (by extrapolation or interpolation from known band positions). Of course, projection of all the plotted lines onto the $v' = 0$ level reproduces the spectrum itself, except that only the Q(5) lines are shown. An idea of the relative intensities of the bands (and subbands) can also be gained from this figure, since the heights of the lines are proportional to the intensities of the strongest Q line in each subband.

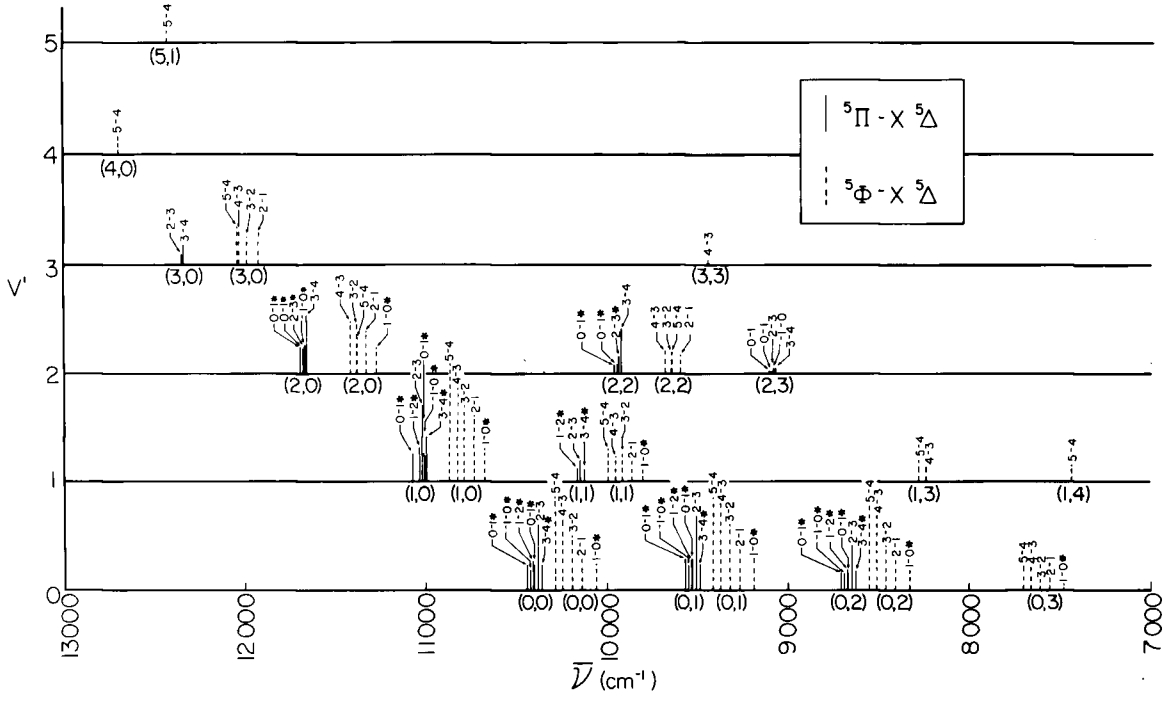

Fig. 10. Overview of the infrared spectrum of FeO. The positions of the Q(5) lines have been plotted, and the line heights have been drawn proportional to the intensity of the strongest Q line in each subband. When marked with an asterisk, the line height represents the intensity of only one Λ-doublet component.

IV.B. Lambda-doubling

Lambda-doubling in electronic Δ states is a phenomenon of relatively rare known occurrence (see Section I.D for references). In fact, the very existence of Λ-doubling in Δ states was long doubted by many. Since it is a fourth order effect, comments such as the following are found in the literature: "... the Λ-doubling effect is of importance only for Π terms ($\Lambda = 1$).... For $\Lambda > 1$, this quantity is so small that it is of no interest." (7a) Our spectra show otherwise!

Fig. 11 shows examples of Λ-doubling in both the $\Omega = 0$ and $\Omega = 1$ components of the $X^5\Delta$ state. The ground state Λ-doubling is most prominent in the $\Omega'' = 0$ subbands of the $^5\Pi - X^5\Delta$ and $^5\Phi - X^5\Delta$ systems. The $\Omega'' = 0$ substate exhibits a Λ-doubling of about 0.3 cm^{-1} which decreases slightly with increasing J. The Λ-doubling in the $X^5\Delta$ $\Omega'' = 1$ substate was not discovered until relatively late in the analysis, so in early least-squares fitting (see next section), the doubling in $\Omega'' = 0$ was handled in a phenomenological manner by adding the following terms to the $\Omega'' = 0$ diagonal element of the ground state effective hamiltonian matrix

$$\langle \Lambda S \Sigma J \Omega | H_{LD}^{eff} | \Lambda S \Sigma J \Omega \rangle = \pm\tfrac{1}{2}[o + o_J J(J+1)] \qquad \text{...(IV.B.1)}$$

where the term in o_J served to account for the slight J-dependence. With the discovery of Λ-doubling in the $\Omega'' = 1$ substate, however, the proper matrix elements of Table VI were used in the final fitting.

The Λ-doubling in the $X^5\Delta$ $\Omega'' = 1$ substate was first detected in bands of the $^5\Pi_0 - ^5\Delta_1$ system, where, because of the larger Λ-doubling in the upper state, it appears only in the form of combination defects. More recently, with some considerable effort, the perturbed J = 30 - 60 regions of the $^5\Phi_2 - ^5\Delta_1$ (0,0) and (0,1) bands have been analyzed, and here the Λ-doubling was seen directly, as shown in Fig. 11.

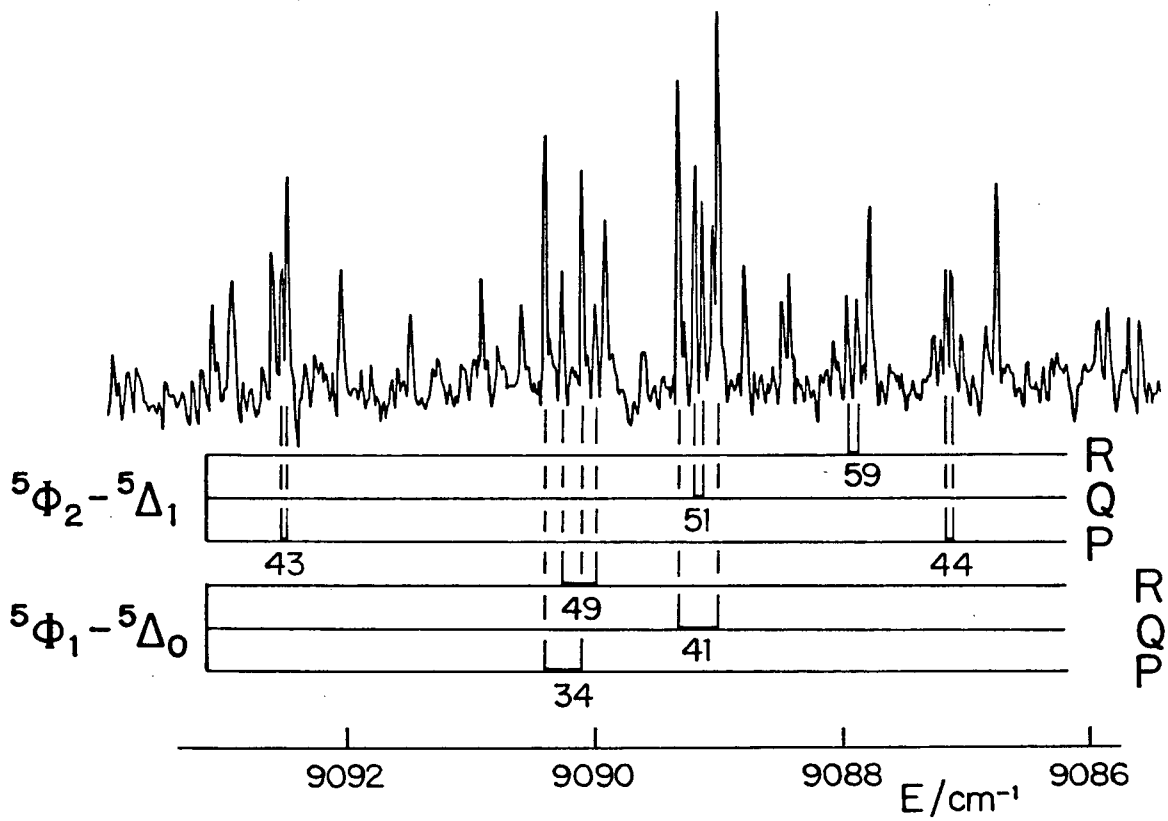

Fig. 11. A portion of the $^5\Phi - X^5\Delta$ (0,1) band near 9090 cm^{-1} showing Λ-doubling in both the $\Omega = 0$ and $\Omega = 1$ levels of the ground electronic state. (A few CO impurity lines have been removed for clarity.)

There is no direct evidence in the spectrum for the sense of the Λ-doubling because no transitions have been discovered that relate this Λ-doubling to a Σ state of known symmetry. The Σ state or states responsible for the Λ-doubling in the $^5\Delta$ state must lie above at least the v = 0 level of the $^5\Delta$ state in energy since this is the ground state.

None of the *ab initio* studies on FeO (see Sections I.A and I.D for references) have predicted any low-lying Σ^- states. Krauss and Stevens (8) have predicted a low-lying $^5\Sigma^+$ state and a low-lying $^7\Sigma^+$ state. The $^5\Sigma^+$ state is probably the state at 3990 cm^{-1} seen by Engelking and Lineberger (9) (see Sections I.A and IV.D) and we give evidence shortly (Section IV.D) that the $^7\Sigma^+$ state lies very close to the ground state. It is most likely one of these Σ states that is predominantly responsible for the Λ-doubling.

To determine which one, we consider the Λ-doubling term in the Ω = 0 diagonal element of the $^5\Delta$ energy matrix. This term arises from the H_{so} operator (used four times to connect $^5\Delta^+$ to $^5\Delta^-$ via intermediate $\Pi^{\pm}$ and Σ states). From Table X we see that either Σ state could cause the doubling according to the selection rules associated with H_{so} assuming a $^5\Pi$ intermediate state. However, H_{so} only connects states whose electron configurations differ by one spin-orbital. Reference to the electron configurations in Section III.K shows that in the single electronic configuration approximation only the $^7\Sigma^+$ state meets this latter criterion. The $^7\Sigma^+$ state differs by one spin-orbital from the $^5\Pi$ state lying at ~10 200 cm^{-1} above the ground state, which would be the most obvious candidate for the intermediate Π state, and this state in turn differs by one spin-orbital from the ground state.

Table III shows that the Ω = 0 component of a $^7\Sigma^+$ state has "parity" f. Since this lies above the $^5\Delta$ state, the f levels of the Ω = 0 component of the $^5\Delta$ state will be pushed downwards in energy relative to their unperturbed positions and relative to the e levels. Unfortunately, the assignment of e/f labels to other Ω

substates is not so straightforward to predict. However, it was found that for $\Omega = 1$ the least-squares fitting procedure itself determined these assignments. Having made the assignment in $^5\Delta_0$ (e levels above the f levels), it was found that one parity assignment for the doubling in $^5\Delta_1$ fitted better than the other: the e levels lie above the f levels in $^5\Delta_1$, also.

In an earlier publication from this laboratory (10), the Λ-doubling in $X^5\Delta_0$ was assigned as f levels above e. This was based on the assumption that it was the $^5\Sigma^+$ state that was responsible, since the $^7\Sigma^+$ state had not been discovered at that time. Although we now favor the e-over-f assignment, it is probably best at this stage simply to label the levels as a and b rather than e and f, where "a" designates the lower parity component and "b" the upper component, regardless of parity (11).

Since no Λ-doubling has been observed in the $X^5\Delta_2$ substate — the lines remain single and sharp to the highest J values observed (~60) — it has been possible to determine only three of the five Λ-doubling parameters potentially required for a $^5\Delta$ state, namely $\tilde{m}_\Delta$, which occurs in the $^5\Delta_0$ diagonal position of the energy matrix (see Table VI), $\tilde{o}_\Delta$, which occurs in the $^5\Delta_1$ diagonal position, and $\tilde{n}_\Delta$, which occurs in the off-diagonal position between these two substates. The J-dependences of the Λ-doubling in both $^5\Delta_0$ and $^5\Delta_1$ have been found to be essentially linear in $J(J+1)$, but they are not equal and opposite; hence the necessity of using three Λ-doubling parameters to describe the doubling in only two substates.

IV.C. Data Reduction

The spectroscopic constants were determined by the method of least-squares (12). Early in the analysis, although it was recognized that most of the upper levels of the $^5\Pi - X^5\Delta$ and $^5\Phi - X^5\Delta$ systems were perturbed, it was believed that the lowest vibrational level of the $^5\Phi$ state was relatively unperturbed. Hence only transitions involving this level were used in the early fitting work, which was done as follows. For the upper state, to allow for the presence of slight perturbations, the energies for each substate were calculated individually by means of equations of the form of (III.J.1), with a $\pm\frac{1}{2}qJ(J+1)$ Λ-doubling term added for $\Omega = 1$. The lower state energies were obtained by diagonalization of matrices of the type given in Table VI for each vibrational level. Differences between the resulting upper and lower state energies were taken corresponding to the allowed spectral transitions. These were then compared with the experimental values by least-squares, and, with the effective spectroscopic constants being allowed to vary freely, the process was repeated iteratively until convergence was reached. In addition to the spectral lines obtained from the FT spectra, the rotational combination differences and spin-orbit intervals for the $v = 0$ level of the ground state given by the laser-induced fluorescence work on the orange system (see Section (I.B)) were included in the fit.

However, it was later realized that even the $^5\Phi$, $v = 0$ level is highly perturbed. Because of concern that correlations between the upper and lower states (13) may have adversely influenced the ground state constants as a result of inadequacies in the model used to fit the perturbed upper level, it was felt that a better approach would be to fit ground state rotational combination differences rather than spectral lines. This approach also permitted all the lines of all the vibrational levels of the $^5\Phi - X^5\Delta$ and $^5\Pi - X^5\Delta$ systems to be used, instead of just those involving the $^5\Phi$, $v = 0$ upper state.

Pre-averaged Δ_1F values were used in the new least-squares fit, together with the above-mentioned laser-induced fluorescence values and the six microwave frequencies recently published by Endo, Saito, and Hirota (14). The latter values were weighted appropriately.[1] Due to lack of spin-orbit splitting information in the vibrational levels higher than v = 0, it was necessary to include vibrational differences (also pre-averaged) connecting these levels with the v = 0 level, where one of the spin-orbit intervals (Ω = 2-3) is very well determined and another (Ω = 1-2) fairly well determined, as described previously (Section I.B.3).

The use of vibrational differences has resulted in the least-squares fitting being done in a somewhat abnormal fashion. The v = 0 and 1 levels, for which the most information was available, were fitted simultaneously. The v = 0 constants were then fixed at the values so determined and used in individual fits of the v = 2 and v = 3 levels. If the four vibrational levels had been fitted simultaneously, lines involving the v = 0 level would have been counted more than once because of the use of the 1-0, 2-0, and 3-0 vibrational differences. Actually much of the data was counted more than once because the same line positions were used to calculate both the rotational combination differences and the vibrational differences. Also, the Q lines were used twice in calculating the RQ and QP Δ_1F'' values. It could be argued that the latter "sin" was justified on the grounds that the Q lines were, in general, more intense and precisely measured than the R and P lines.

The final values for the effective spectroscopic constants are given in Table XI. The derived vibrational constants ω_e, $\omega_e x_e$, and $\omega_e y_e$ were determined by fitting the term origins T_v to eqn. (III.D.1) in the usual manner (4a). The equilibrium B value B_e and the vibration-rotation interaction constants α_e and γ_e were obtained by fitting the B_v values to eqn. (III.D.4), as were D_e and β_e similarly derived from eqn. (III.D.6). The average bond length r_0 for the v = 0 level was calculated from

---

[1]A discussion of the weighting procedure is given in Appendix V.

TABLE XI. Effective spectroscopic constants for the $X^5\Delta_i$ ground state of ^{56}FeO (in cm^{-1}).

Effective rotational and spin constants[a]:

		v=0	v=1	v=2	v=3
	T_v	0	871.152 33 (33)	1 733.045 36 (36)	2 585.682 42 (55)
	B	0.516 808 64 (93)	0.512 982 58 (104)	0.509 155 98 (58)	0.505 328 00 (88)
10^7	D	7.219 0 (32)	7.231 4 (34)	7.248 3 (20)	7.263 5 (30)
	A	-94.946 2 (22)	-94.936 0 (22)	-94.925 49 (11)	-94.914 15 (15)
	λ	0.931 92 (82)	0.931 02 (82)	0.931 000 (96)	0.931 84 (14)
	η	0.030 75 (82)	0.030 32 (82)	0.029 964 (68)	0.029 59 (10)
10^5	A_D	-8.098 (38)	-8.114 (39)	-8.134 (10)	-8.144 (13)
10^2	$\tilde{m}_\Delta$	-1.326 1 (21)	-1.415 9 (26)	-1.482 4 (32)	-1.544 3 (49)
10^4	$\tilde{n}_\Delta$	0.780 (33)	1.063 (40)	0.872 (55)	1.028 (86)
10^6	$\tilde{o}_\Delta$	-0.81 (14)	-0.42 (13)	-1.19 (20)	-1.29 (47)
10^6	λ_D	-5.83 (22)	-5.57 (23)	-5.137 (94)	-4.76 (15)

Derived vibration-rotation parameters

$\omega_e = 880.414\ 8$ $\quad B_e = 0.518\ 721$ $\quad D_e = 7.210\times10^{-7}$

$\omega_e x_e = 4.632\ 15$ $\quad \alpha_e = 0.003\ 825$ $\quad \beta_e = 1.51\times10^{-9}$

$\omega_e y_e = 5.55\times10^{-4}$ $\quad \gamma_e = -4.8\times10^{-7}$

Bond lengths: $r_e = 0.161\ 64$ nm $\quad r_o = 0.161\ 94$ nm

(a) The numbers in parentheses represent the standard errors in the last significant digits.

B_0 using the equation

$$B_0 = \frac{h}{8\pi^2 c \mu r_0^2} \qquad \text{...(IV.C.1)}$$

and similarly the equilibrium bond length was determined from this same equation with B_0 and r_0 replaced by B_e and r_e. For the reasons given in the preceding paragraph, the standard errors quoted in the table should not be viewed in too rigorous a statistical sense. In particular, the standard errors for $v = 2$ and for $v = 3$ should not be compared with those for $v = 0$ and 1.

An alternative data reduction method that could have been used is the "new" term value approach of Åslund (15). By this method, the line positions could have been used directly as input to the computer program. The constants for the basically well-behaved ground state would still have been determined by fitting to a model for this state similar to the effective hamiltonian matrix used here, while the term values for the perturbed upper states would have been obtained at the same time. In the method that was used, combination differences had first to be calculated from the spectral lines, then averaged,[2] then inputted to the least-squares program which produced the spectroscopic constants and term values for the well-behaved state, then finally the term values for the other state had to be calculated as a separate step. However, as with this method, the term value approach may also produce error estimates that are less than statistically rigorous in meaning, as discussed by Albritton *et al.* (16) and by Åslund (15). Also, there would have been a risk in using the term value approach that any inadequacies in the lower-state model may not have become apparent in view of the free-floating nature of the upper-state term values (17).

Term values for the $X^5\Delta$ state calculated from the spectroscopic constants of Table XI are given in Appendix IV for vibrational levels 0 through 3. For $v = 4$,

---

[2]This step was optional and was done to cut down on computing costs.

only transitions involving the $\Omega = 4$ substate were identified, so for this vibrational level it was not possible to derive a complete set of spectroscopic constants. The term values for the one observed substate of $v = 4$ were calculated from the upper state term values using the line frequency measurements.

According to eqn. (III.F.17), good case (a) behavior is to be expected if

$$\frac{|A\Lambda|}{B\sqrt{2S}} >> J \qquad \text{...(IV.C.2)}$$

From the constants of Table XI we find, for example for $v = 0$,

$$\frac{|A_0\Lambda|}{B_0\sqrt{2S}} = 184 \qquad \text{...(IV.C.3)}$$

If partial transition towards case (b) coupling occurs as J increases, spin-orbit satellite branches would be expected to appear. For example, a Q-branch occurring between the substates $^5\Phi_3$ and $^5\Delta_3$ would be a satellite branch. No such satellite branches have been identified in the infrared spectrum even though the $\Omega = 2$-3 spin-orbit interval of the ground state is well-known (see Section I.B.3) so that accurate predictions for the locations of the satellites could be made. Unfortunately, this means that the only direct information available about the spin-orbit intervals is that obtained from the laser-induced fluorescence experiments on the orange system. This information was included in the least-squares fit, but since only two of the four intervals were determined it was not possible to determine all four of the spin-orbit parameters that would be necessary to completely specify the positions of the five substates (cf. eqn. (III.H.51) and discussion below it). Specifically, the fourth-order parameter θ was not determinable.

A consequence of the lack of direct measurement of the $\Omega = 0$-1 and 3-4 intervals is that the term values for the outermost substates (i.e. $\Omega = 0$ and 4) are less well determined relative to the other substate terms than is the case for $\Omega = 1$, 2, and 3. That is, the correct term values for the outermost substates may be shifted

by some small constant amount relative to those given in Appendix IV. Within any given substate, however, the rotational term values are well-determined relative to each other.

Brown and Watson (18) have shown that for $^2\Lambda$ electronic states with $\Lambda > 0$, the spin-rotation interaction and the centrifugal correction to the spin-orbit coupling make indistinguishable contributions to the energy levels, even though they arise by different physical mechanisms and are represented by distinct terms in the hamiltonian. That is, only a linear combination of A_D and γ can be determined. In triplet and higher multiplicity states the correlation is reduced by the presence of λ_D terms (17). However, in doing the least-squares fitting of the ground state of FeO it was found that A_D and γ were 100% correlated. In this case, this was probably yet another consequence of the lack of experimental information on the spin-orbit intervals. As a result, only one of the parameters A_D or γ could be used. The choice of which to use in doublet states is usually regarded as largely a matter of personal choice (18). Here it was tried both ways and it was found that the least-squares fit using A_D resulted in a slightly lower overall standard deviation than did the fit involving γ. Therefore A_D was kept in the final fitting procedure, whereas γ was not. Of course the physical interpretation of A_D has become altered by the inclusion of the spin-rotation effects.

IV.D. A Ground State Perturbation

While all the excited electronic states of FeO that have been studied so far suffer from extensive perturbations, until now the ground state has been thought to be unperturbed, at least up to v = 3, which is as far as the analysis could be taken.

A detailed examination of the emission transitions ending on the $X^5\Delta_2$, v = 2 level, however, shows evidence for a small, very local perturbation affecting only the J" = 15 level, as can be seen in Fig. 12. This figure is taken from the $^5\Phi_3 - {}^5\Delta_2$ (0,2) band and shows that both the R(15) and Q(15) lines are reduced to about 60% of their expected peak heights and are broadened asymmetrically, though the positions of the peak maxima are not shifted. Though blended, the $^5\Phi_3 - X^5\Delta_2$ (2,2) Q(15) line also is of reduced intensity. The remaining J" = 15 lines of these two bands are too badly blended to show the perturbation. The only other observed band that involves this level is the $^5\Pi_1 - X^5\Delta_2$ (0,2) band. Since the upper state of this band has a Λ-doubling of about 0.5 cm^{-1} observation of whether only one or both components are disturbed should, in principle, show whether the perturbing state is orbitally degenerate or non-degenerate. Unfortunately, of the six J" = 15 lines (the two R's, the two Q's, and the two P's) only two are unblended. The unblended lines are $R_b(15)$ and $P_b(15)$, where b represents the Λ-doubling component, whose absolute parity has not been established. These lines are quite weak, but their intensities and shapes are absolutely normal compared to neighboring lines in the branches. Furthermore the residuals that they give in the least-squares fit described in the previous section are both less than 0.002 cm^{-1} indicating that they are not shifted at all. Since these lines are unperturbed, the perturbation must occur in the *other* Λ-doubling component of $X^5\Delta_2$,v=2 — namely the a-parity component, whose lines unfortunately are completely blended for J" = 15 in the $^5\Pi_1 - X^5\Delta_2$ (0,2) band.

While the peak maxima of the $^5\Phi_3 - X^5\Delta_2$ (0,2) R(15) and Q(15) lines occur at the predicted frequencies for the unperturbed lines, due to their asymmetric

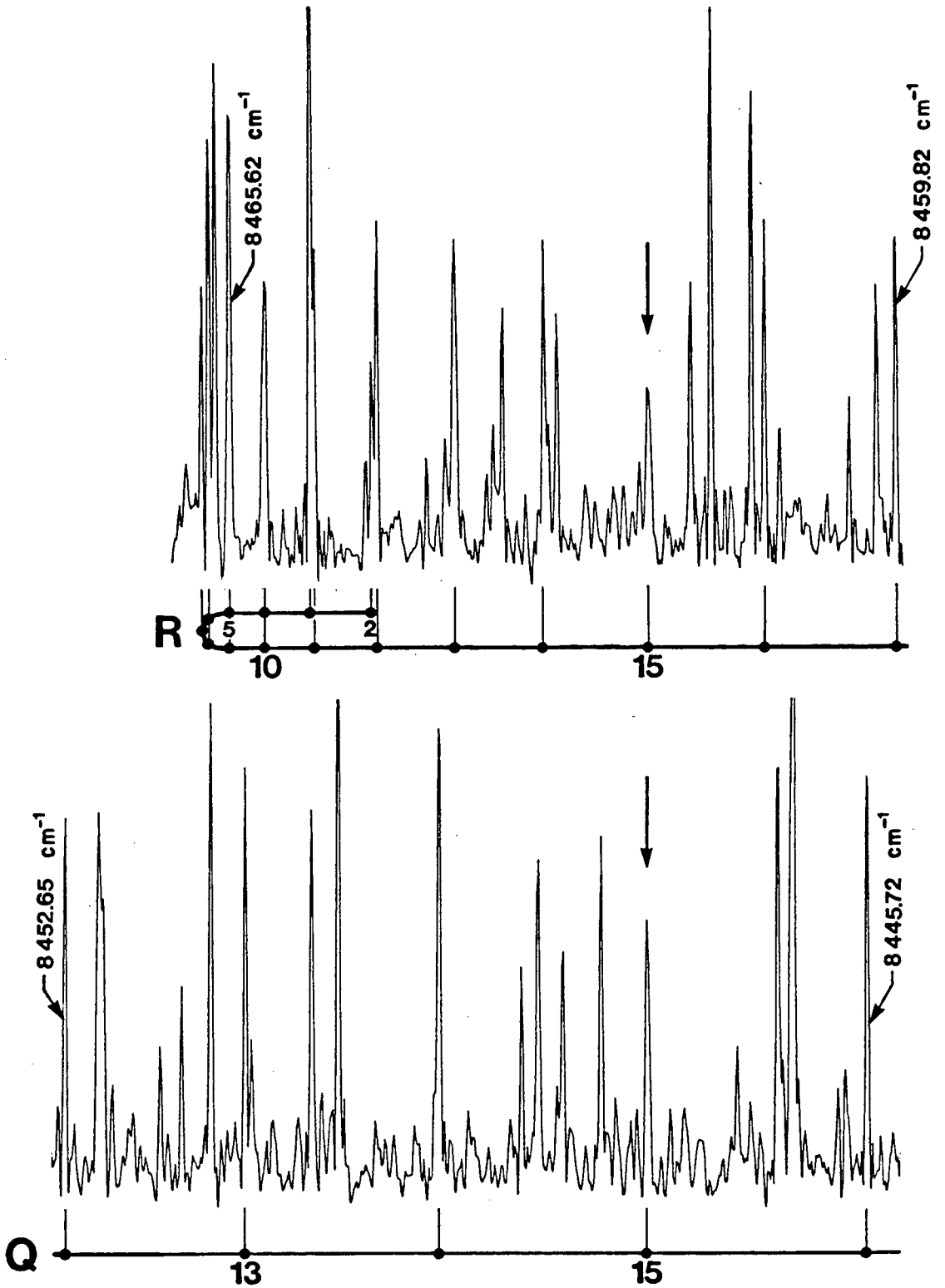

Fig. 12. Two portions of the $^5\Phi_3 - X^5\Delta_2$ (0,2) subband near 8450 cm^{-1} showing (arrows) a ground state perturbation at $J'' = 15$.

shapes, however, the positions determined by a third-degree polynomial fit to the line shapes are 0.009 and 0.006 cm^{-1} lower in frequency, respectively. This means that the a Λ-type component is pushed about 0.016 cm^{-1} to higher energy, and due to mixing of its wavefunction with that of the perturbing state, transitions involving this parity component are of reduced intensity. The observed asymmetric line shapes result from a combination of these lines with the unperturbed other Λ-doubling component. There must also be weak lines in the spectrum lying to the high-frequency side of the $J'' = 15$ lines, which have picked up their intensities by this same wavefunction mixing. Unfortunately it has not been possible to identify these lines in the spectrum due to the high density of lines present. It is quite possible in view of the very localized nature of the perturbation that these weak lines lie within the profiles of the identified $J'' = 15$ lines.

If only one parity component of an orbitally degenerate state is perturbed, the perturbing state must have a large Λ-doubling itself, or, alternatively, be orbitally non-degenerate. The *ab initio* calculations of Krauss and Stevens (8) predict that there are five states lying within 0.1 eV of the ground state: $^7\Sigma^+$, $^5\Pi$, $^5\Phi$, $^5\Delta$, and $^5\Sigma^+$. While the predicted energies and ordering of these states are not correct, three of them have been positively identified from the spectra of FeO — namely, the $^5\Delta$ ground state itself and the $^5\Pi$ and $^5\Phi$ upper states of the infrared system. This leaves the two multiplet Σ states

$$(4s\sigma)^1(3d\delta)^2(3d\pi)^2(3d\sigma)^1 \qquad ^7\Sigma^+$$

$$(4s\sigma)^2(3d\delta)^2(3d\pi)^2 \qquad ^5\Sigma^+$$

as the most likely candidates for the perturbing state.

As for the actual assignment, we consider now the laser photodetachment spectrum of FeO^- reported by Engelking and Lineberger (9). FeO^- is thought to

have a ground state

$$(4s\sigma)^2(3d\delta)^3(3d\pi)^2 \qquad {}^4\Delta_i$$

Two transitions are observed (9); one, which has some vibrational structure, goes to the ground state of FeO,

$$FeO\ (4s\sigma)^1(3d\delta)^3(3d\pi)^2\ {}^5\Delta_i \longleftarrow FeO^-\ (4s\sigma)^2(3d\delta)^3(3d\pi)^2\ {}^4\Delta_i$$

and the other, which is a single peak, goes to an excited state of FeO lying 3990 cm^{-1} above $X^5\Delta_i$. This is presumably the $^5\Sigma^+$ state mentioned above, since the photodetachment process

$$FeO\ (4s\sigma)^2(3d\delta)^2(3d\pi)^2\ {}^5\Sigma^+ \longleftarrow FeO^-\ (4s\sigma)^2(3d\delta)^3(3d\pi)^2\ {}^4\Delta_i$$

is fully allowed. A close inspection of Fig. 1 of ref. (9) shows an anomalous Franck-Condon pattern, with the (2,0) peak being quite a lot stronger than interpolation between the (1,0) and (3,0) peaks would predict. The Franck-Condon envelope for a set of vibrational transitions from $v'' = 0$ always follows a smooth curve with no extra bumps in it. Since this is not the case for the photodetachment spectrum, there must be something else contributing to the intensity of the (2,0) peak. A possible interpretation is that the additional intensity is caused by a very weak transition

$$FeO\ (4s\sigma)^1(3d\delta)^2(3d\pi)^2(3d\sigma)^1\ {}^7\Sigma^+ \longleftarrow FeO^-\ (4s\sigma)^2(3d\delta)^3(3d\pi)^2\ {}^4\Delta_i$$

lying under the transition to the $v = 2$ level of the FeO ground state. Now $v = 2$ is the very vibrational level where we observe the $^5\Delta_i$ ground state to be perturbed by an orbitally non-degenerate electronic state. The fact that the $^7\Sigma^+ - {}^4\Delta$ photodetachment does not correspond to an allowed one electron process has to be explained in terms of a complex spin-orbit mixing between the $^7\Sigma^+$ state and other

nearby states, which is the same mechanism that we have to invoke to account for the small rotational perturbation in Fig. 12.

The perturbation probably occurs via the spin-orbit operator and involves the $^5\Pi$ state which is one of the upper states of the infrared system as an intermediate, in the same manner as described in Section IV.B for the origin of the dominant contributor to the Λ-doubling in $X^5\Delta_0$. The weakness of the transition can be explained as being due to a combination of the necessity of having to act via the distant intermediate Π state and of non-favorable Franck-Condon factors.

Note that it is possible that the ordering of the two Σ states may actually be the reverse of that assumed here, since both the FeO $^5\Sigma^+ \leftarrow$ FeO$^-$ $^4\Delta_i$ and FeO $^7\Sigma^+ \leftarrow$ FeO$^-$ $^4\Delta_i$ transitions are observed in the photodetachment spectra if the foregoing interpretation is correct, even though only the former is an allowed process. We have assigned the lower of the two Σ states as $^7\Sigma^+$ and the upper one as $^5\Sigma^+$ on the following grounds:

(i) The upper state appears to produce a stronger peak in the photodetachment spectrum. Since only transition to the $^5\Sigma^+$ state is an allowed process, this is the more likely assignment. (This could be influenced by Franck-Condon factors, however.)

(ii) The theoretical calculations of Krauss and Stevens (8) predict the $^7\Sigma^+$ state to be lower than the $^5\Sigma^+$ state (though as indicated elsewhere (Section I.D) these predictions are not completely reliable).

To sum up, the perturbation in FeO $X^5\Delta_2$ $v = 2$ appears to be caused by the $^7\Sigma^+$ state predicted by Krauss and Stevens, and this state *may* also be responsible for the anomalous intensity distribution in the photodetachment spectrum of FeO$^-$. The perturbing vibrational level lies about 2100 cm^{-1} above the ground spin-orbit level of FeO, assuming that the B values of $X^5\Delta_i$ and $a^7\Sigma^+$ do not differ

unduly. Whether this is the v = 0 level or some other vibrational level of the $^7\Sigma^+$ state remains to be determined.[3]

---

[3]An alternative explanation, involving a reassignment of the photodetachment peaks was given in Section I.A. We do not have sufficient information to decide between these at this time. However, some very recent, higher-resolution photodetachment experiments by Lineberger (not yet published — private communication) seem to indicate the presence of another state. Assuming this state to be the one that we have detected, the vibrational level responsible for our perturbation appears to be v = 1, thus placing the v = 0 level very close to the ground state.

CHAPTER V

THE $^5\Pi/^5\Phi$ COMPLEX NEAR 10 000 cm^{-1}

V.A. Introduction

The upper states of the near infrared system are responsible for a number of features in the spectrum and these features can be be all described by one word: complex. Four phenomena are responsible for this complexity:

(i) overlap of the $^5\Pi$ and $^5\Phi$ states;

(ii) similarity in magnitude of the $^5\Pi$ and $X^5\Delta$ spin-orbit separations;

(iii) Λ-doubling; and

(iv) perturbations.

An example of the spectrum of the $^5\Phi_i - X^5\Delta_i$ system was presented earlier in Fig. 8. We now give an example of the $^5\Pi_i - X^5\Delta_i$ system in Fig. 13. Comparing these two figures, it is immediately obvious that the spectrum exhibited by the $^5\Pi - X^5\Delta$ system is considerably more complex than that of the $^5\Phi - X^5\Delta$ system. One of the causes of this is the fact that the spin-orbit intervals for the $^5\Pi$ and $X^5\Delta$ states are similar in magnitude, with the result that the subbands pile up on top of one another. There is even a reversal in the ordering of the subband heads, so that, for example, the $^5\Pi_{-1} - {}^5\Delta_0$ subband head occurs next to the $^5\Pi_3 - {}^5\Delta_4$ head. Lambda-doubling also adds to the complexity, especially since it is often *very* large. In the $^5\Pi_0 - {}^5\Delta_1$ spectrum in Fig. 13, the Λ-doubling is so large that the subband has been labelled as if it were two separate subbands, which is essentially how such cases have to be treated when assigning lines in the spectrum. The separation between the upper-state Λ-doublet components in this example is nearly 60 cm^{-1} at low J!

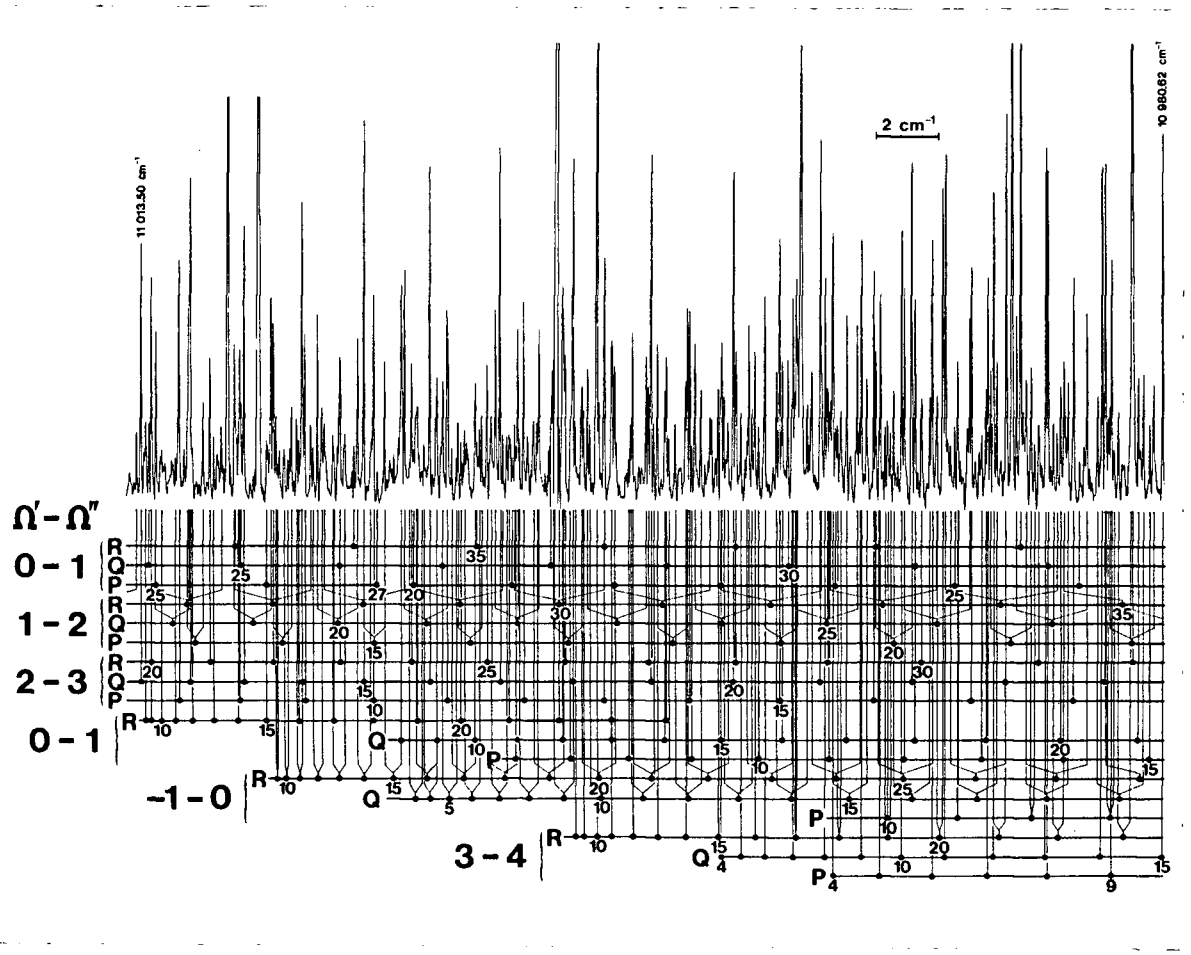

Fig. 13. Part of the $^5\Pi - X^5\Delta$ (1,0) band near 11 000 cm^{-1}.

Mention was made previously (Section IV.A with reference to Figs. 8 and 10) that the $^5\Pi$ - $X^5\Delta$ and $^5\Phi$ - $X^5\Delta$ systems overlap extensively. This occurs because the $^5\Pi$ and $^5\Phi$ states lie very close in energy, with the v = 0 level of the Π state being only about 213 cm^{-1} above that of the Φ state, and also because the spin-orbit structure of the two states is such that the two systems parallel each other, as can be seen in Fig. 14. This results in the extensive overlap in the spectrum. The two states are so similar because they both derive from the same electron configuration. In terms of the simple ionic description given in Section III.K, the Fe^+ and O^- ions have electron configurations

Fe^+	$(4s\sigma)^1(3d\delta)^3(3d\pi)^2(3d\sigma)^1$	$D\Delta$
O^-	$(2s\sigma)^2(2p\pi)^3$	$P\Pi$

The small differences between the $^5\Pi$ and $^5\Phi$ states result from the relatively small effect that the $O^-(P\Pi)$ state has on the $Fe^+(D\Delta)$ state, with the atomic orbital angular momentum of the former state adding or subtracting to that of the $D\Delta$ state, giving the $^5\Phi$ or $^5\Pi$ states, respectively (1).

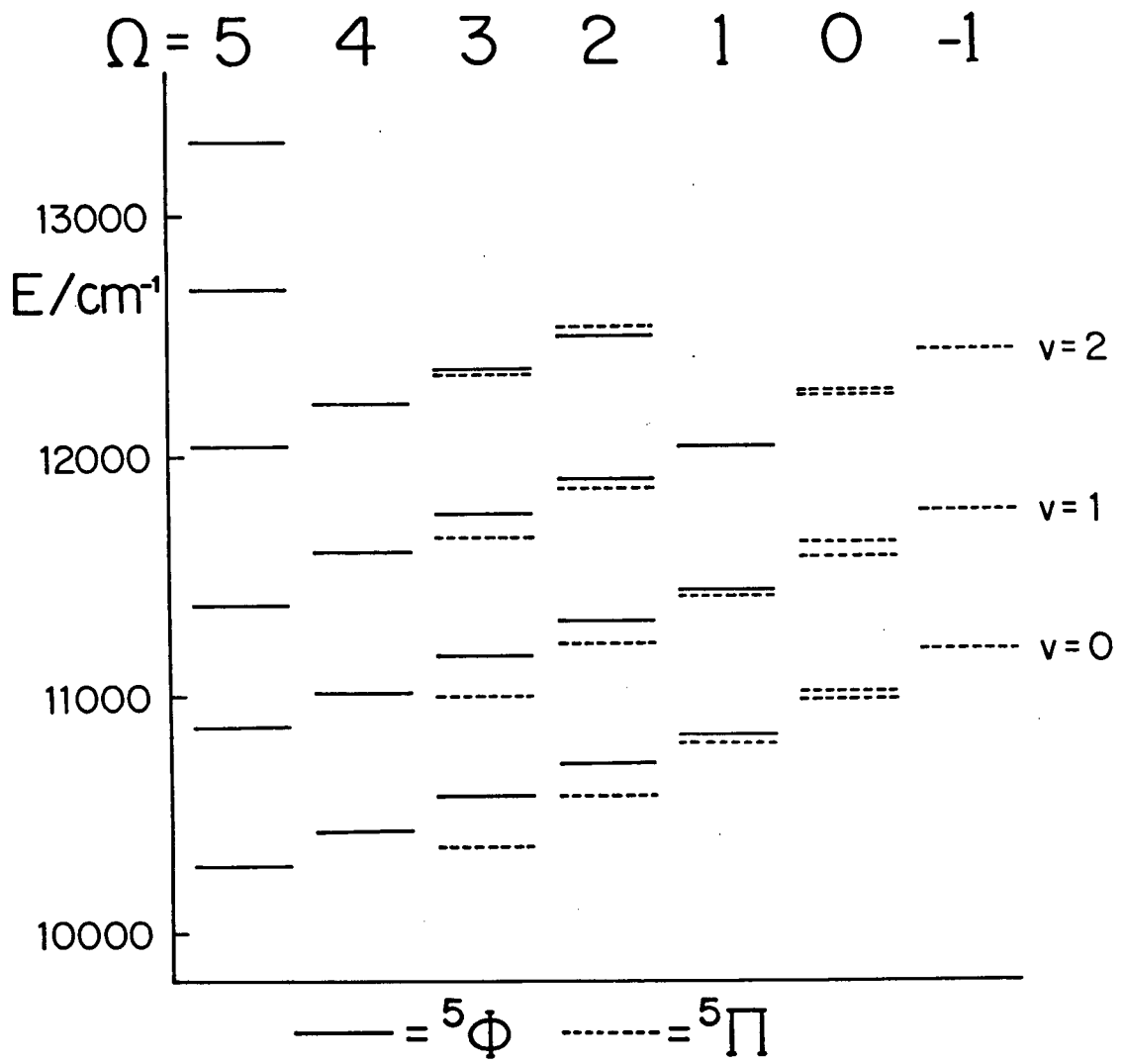

Fig. 14. The $^5\Pi/^5\Phi$ complex near 10 000 cm^{-1} (The J = 5 levels are shown, with the zero of the energy scale set to the $X^5\Delta_4$, v=0, J=4 level.)

V.B. Perturbations

Even on the small scale to which Fig. 14 is drawn, one can see evidence of massive perturbations. For example, the $^5\Phi_5$, v=2 level is pushed down by 80 cm^{-1} relative to the position expected for it based on interpolation between adjacent levels. Another example is the large but irregular Λ-doubling in $^5\Pi_0$:

v = 0	38 cm^{-1}
v = 1	58 cm^{-1}
v = 2	15 cm^{-1}

at J = 0. In fact, with the exception of only the $^5\Phi_5$, v = 0 level, every single vibrational level of every Ω substate has *at least* one perturbation!

Fig. 15 presents a grand overall picture of the level structure of the $^5\Pi$ and $^5\Phi$ states. This time the energies of all observed rotational levels have been plotted, not just one as in Fig. 14. The energies have been plotted against J(J+1) after scaling by subtracting off 0.4 J(J+1). This figure is admittedly rather complicated. It is, however, illuminating to see the level scheme in its entirety as in this figure, since relationships between the various perturbations become apparent. Some perturbing states cross (in zeroth order) and interact with more than one multiplet level. This figure is useful for detecting such cases; for example, a straight edge can be placed on the figure such that its orientation represents a perturbing state to one of the levels, then observed to see where it intersects other levels. Also, it may be possible to observe certain features repeating themselves at intervals corresponding to the vibrational spacings of the perturbing state.

No attempt has been made to analyze all the perturbations. Each perturbation has to be handled on an individual basis, and this is a laborious process. Deperturbation attempts have been confined to those cases where the possibility for success looked the most promising, such as where doubled lines were present.

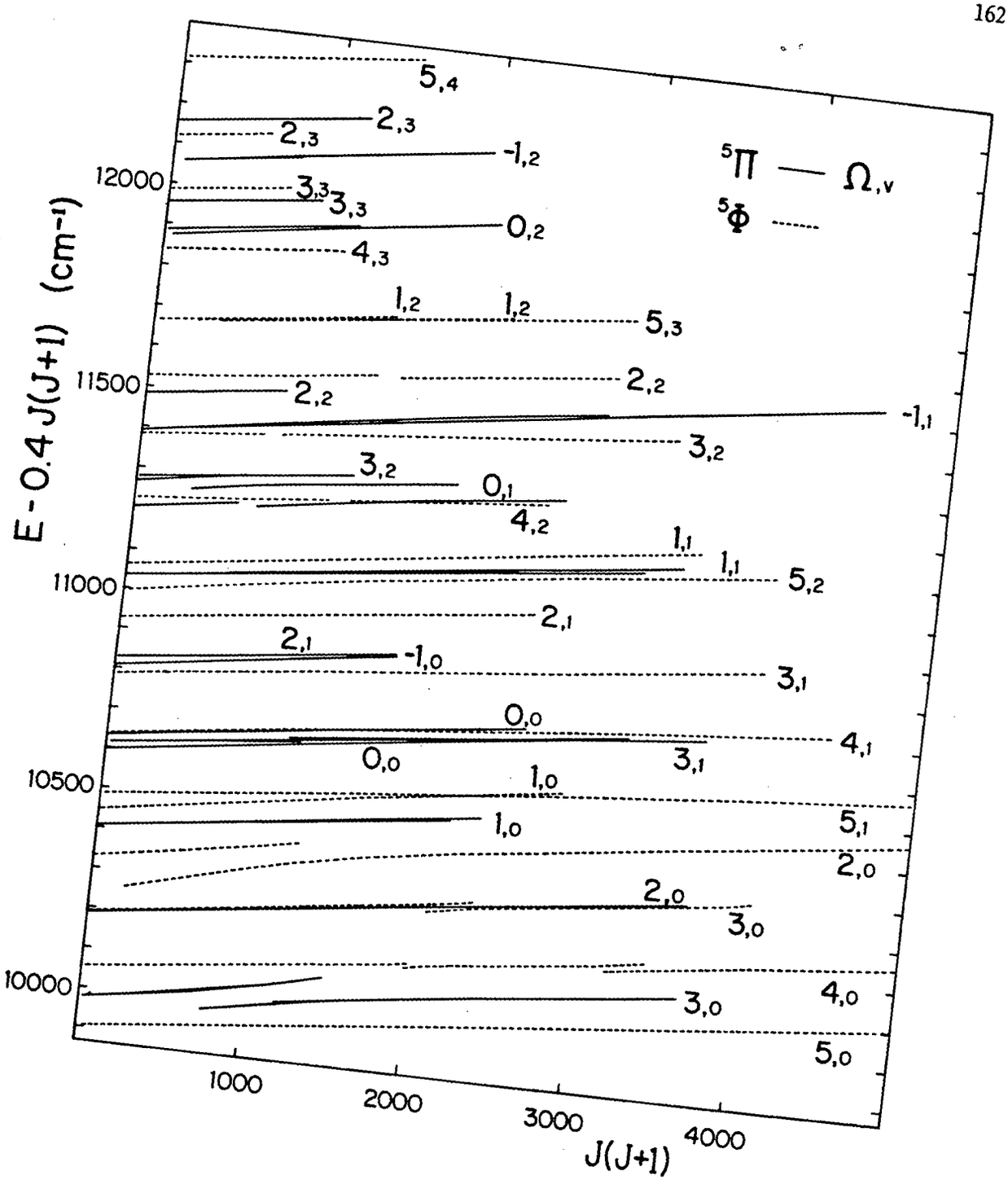

Fig. 15. The energies of the $^5\Pi$ and $^5\Phi$ states plotted against $J(J+1)$. The energies have been scaled by the subtraction of $0.4\,J(J+1)$.

V.B.1. Evidence for a $^3\Phi$ state

We start by considering some of the perturbations in the v = 0 level of the $^5\Phi$ state. Examination of Fig. 15 shows that the Ω = 3 and Ω = 4 components exhibit similar-appearing perturbations, centered at about J = 47 and 57, respectively. In both cases, it has been possible to identify three pairs of doubled lines in the spectrum, and the minimum separations between these doubled lines are similar in magnitude (~15.2 and ~14.2 cm^{-1}). The B values of the perturbing states also appear to be similar. This may indicate that the two perturbing states are related — in particular, that they are really two substates belonging to the same multiplet state.

By extrapolation, we might expect the $^5\Phi_2$ substate to exhibit a similar perturbation at around J = 30–35 due to yet another multiplet component. There is indeed a perturbation at this point; however, its appearance is totally different from that of the other two. It will be shown later (Section V.B.3) that this perturbation is a rather complicated one that must involve the simultaneous interaction of at least three states (i.e. the $^5\Phi_2$ substate and two other states), so the prediction that one of the states involved is a substate belonging to the same multiplet state that is postulated as being responsible for the $^5\Phi_3$ and $^5\Phi_4$ perturbations is a possibility.

Proceding on to the $^5\Phi_1$ substate, extrapolation from the positions of the perturbations in the other substates would predict that if yet another substate of the perturbing state were present it would interact with $^5\Phi_1$ at low J. Experimentally, we find that there is no local avoided crossing as in the other substates, but there is still some evidence for a perturbation. The effective term origin for this substate *may* be as much as 25 cm^{-1} lower than it should be based on prediction from the other substates of this vibrational level and also the v = 1 level. Also, the energy level diagram for this substate in Fig. 15 exhibits a greater curvature than that of the Ω = 5 substate, and at low J its slope is steeper than those of the Ω = 3, 4, and 5 substates — i.e. the effective B value for this substate is larger than those of the

other substates, *possibly* slightly larger than would be expected on the basis of the Mulliken formula (eqn. (III.J.5)). This evidence is far from being firm, however, because the term value prediction for the substate origin is not very certain, mainly due to the large perturbation in the $\Omega = 2$ substate, and because spin-uncoupling may be at least partially responsible for the curvature of the $\Omega = 1$ energy curve.

In summary, there appear to be two related perturbations affecting the $^5\Phi_4$ and $^5\Phi_3$ substates. There is likely a further related perturbation in $^5\Phi_2$ and there *may* be another in $^5\Phi_1$.

On the other hand, there are no perturbations in the $^5\Phi_5$ substate. In fact, this substate is the only known example of that rare phenomenon amongst the excited states of FeO: a substate possessing absolutely no detectable local perturbations anywhere!

To completely understand these perturbations, two interrelated questions must be answered:

(i) What is the perturbing state?

and (ii) By what mechanism does it interact with the $^5\Phi$ state – i.e. what operators are involved in the off-diagonal matrix elements connecting the perturbed and perturbing states?

We start the deperturbation analysis by considering whether the perturbation is homogeneous or heterogeneous. An effective hamiltonian can be constructed for the $^5\Phi_4$ substate alone having an effective matrix element (cf. eqn. (III.J.1))

$$H_{11} = T_1 + B_1^{eff} J(J+1) - D_1^{eff} [J(J+1)]^2 + H_1^{eff} [J(J+1)]^3 + \ldots \quad \ldots(V.B.1)$$

where as many terms are to be retained as needed. Similarly, for the perturbing substate,

$$H_{22} = T_2 + B_2^{eff} J(J+1) - D_2^{eff} [J(J+1)]^2 + H_2^{eff} [J(J+1)]^3 + \ldots \quad \ldots(V.B.2)$$

The off-diatonal matrix element connecting these two substates can then be taken as either

$$H_{12} = \text{constant} \qquad \text{for the homogeneous situation ...(V.B.3a)}$$

$$H_{12} = \text{constant} \times [J(J+1) - \Omega(\Omega \pm 1)]^{1/2} \qquad \text{for the heterogeneous situation}$$

$$\simeq \text{constant} \times [J(J+1)]^{1/2} \qquad \text{(except for small values of J) ...(V.B.3b)}$$

(cf. eqn. (III.J.11)). Least-squares fits were performed for both situations, and it was found that virtually identical fits were obtained — i.e. same standard deviations (cf. Parts A and B of Table XII) and same residuals (Table XII, Part C).

For now, we focus on the case of a homogeneous interaction, but the same comments and conclusions apply also to the heterogeneous case. A number of different fits were tried involving different regions of the total data set and different numbers of effective parameters. A better fit was obtained when only term values close to the region of the perturbation were employed than when low-J data points were included (compare the results in Table XII for DATA SET XII.2 (with B^{eff} and D^{eff}) with those for DATA SET XII.1), where the goodness of a fit is judged by the lowness of the overall standard deviation and the small magnitude of and lack of systematic errors in the residuals. The poorer fit that results when low-J data points are included is likely caused by interaction with the two additional states responsible for the two other avoided crossings observed in the $^5\Phi_4$ substate (at J = ~44 and ~47 — to be discussed later).

Comparison of the results for the three fits with DATA SET XII.2 shows that the more parameters included (cf. eqns. (V.B.1) and (B.2)) the better the fit. In particular, the fit with H^{eff} terms present was the best one as judged by the above criteria. However, the constants were less well determined (larger standard errors) than in the other fits and were also highly correlated. Even in the fits including terms through D^{eff} only (for both DATA SETS XII.1 and 2), the values of T^{eff}, B^{eff}, and

TABLE XII. Least-squares fitting: $^5\Phi_4$, v=0 and perturbing state, with crossing point at J ≃ 57.

(A) The results (in cm^{-1})[a] - homogeneous model

	Data Set XII.1		Data Set XII.2						Data Set XII.3	
Terms included[b]:	B^{eff}, D^{eff}		B^{eff}		B^{eff}, D^{eff}		B^{eff}, D^{eff}, H^{eff}		B^{eff}	
	$^5\Phi_4$	Perturbing State	$^5\Phi_4$	Perturbing State	$^5\Phi_4$	Perturbing State	$^5\Phi_4$	Perturbing State	$^5\Phi_4$	Perturbing State
T^{eff}	10 052.456 (48)	9 900 (20)	10 063.95 (51)	9 924.0 (45)	10 049.71 (19)	9 915.2 (53)	10 045.13 (93)	9 879 (99)	10 061.27 (54)	9 933.9 (14)
B^{eff}	0.445 887 (34)	0.499 (12)	0.439 50 (14)	0.481 8 (14)	0.447 37 (10)	0.490 1 (32)	0.451 26 (79)	0.527 (90)	0.440 36 (16)	0.478 74 (43)
10^6 D^{eff}	0.852 9 (87)	2.9 (19)	-	-	1.050 (14)	1.74 (48)	2.13 (22)	14 (27)	-	-
10^9 H^{eff}	-	-	-	-	-	-	0.096 (20)	1.4 (27)	-	-
H_{12}	7.064 (13)		6.984 (74)		7.085 2 (36)		7.083 4 (34)		7.086 (18)	
σ[c]	0.035 6		0.202		0.009 13		0.005 35		0.039 2	

(a) The numbers in parentheses are one standard error in units of the last two figures quoted.

(b) T^{eff} and H_{12} or h_{12} were included in all fits.

(c) Standard deviation based on 28, 19, or 10 data points for Data Sets XII.1, 2, or 3, respectively. All data points weighted equally (weight = 1).

(d) h_{12} is the "constant" in eqn. (V.B.3b).

(e) Observed-Calculated values of the term values.

(continued on next page)

TABLE XII (cont.)

(B) The results (in cm^{-1})[a] - heterogeneous model

	Data Set XII.1		Data Set XII.2						Data Set XII.3	
Terms included[b]:	B^{eff}, D^{eff}		B^{eff}		B^{eff}, D^{eff}		B^{eff}, D^{eff}, H^{eff}		B^{eff}	
	5_{ϕ_4}	Perturbing State	5_{ϕ_4}	Perturbing State	5_{ϕ_4}	Perturbing State	5_{ϕ_4}	Perturbing State	5_{ϕ_4}	Perturbing State
T^{eff}	10 052.782 (14)	9 899 (20)	10 064.29 (50)	9 923.7 (45)	10 050.08 (19)	9 914.8 (53)	10 045.4 (10)	9 876 (96)	10 061.67 (53)	9 933.5 (14)
B^{eff}	0.445 901 (30)	0.499 (12)	0.439 50 (14)	0.481 8 (14)	0.447 38 (10)	0.490 1 (32)	0.451 39 (88)	0.529 (87)	0.440 37 (16)	0.478 74 (43)
10^6 D^{eff}	0.851 8 (98)	3.0 (19)	-	-	1.050 (14)	1.74 (48)	2.15 (25)	15. (26)	-	-
10^9 H^{eff}	-	-	-	-	-	-	0.098 (21)	1.5 (27)	-	-
h_{12}[d]	0.122 35 (20)		0.121 2 (11)		0.122 684 (55)		0.122 652 (48)		0.122 80 (30)	
σ[c]	0.035 6		0.202		0.009 13		0.005 34		0.039 2	

(Footnotes on first page of Table)

(continued on next page)

TABLE XII (cont.)

(C) The data used in parts A and B and the residuals (same for homogeneous and heterogeneous models)

	J	Term Values	Residuals[e]				
			Data Set XII.1	Data Set XII.2			Data Set XII.3
			B^{eff}, D^{eff}	B^{eff}	B^{eff}, D^{eff}	B^{eff}, D^{eff}, H^{eff}	B^{eff}
Upper Component	7	10077.720	-0.035	-	-	-	-
	8	10084 858	-0.032	-	-	-	-
	9	10092.896	-0.019	-	-	-	-
	10	10101.814	-0.018	-	-	-	-
	11	10111.637	-0.003	-	-	-	-
	12	10122.350	0.012	-	-	-	-
	13	10133.951	0.024	-	-	-	-
	14	10146.440	0.034	-	-	-	-
	15	10159.828	0.053	-	-	-	-
	52	11276.770	-0.084	-0.377	-0.013	-0.002	-
	53	11323.968	-0.026	-0.139	0.004	0.001	-
	54	11372.172	0.017	0.060	0.012	0.003	-0.040
	55	11421.467	0.034	0.195	0.005	-0.001	0.015
	56	11472.007	0.032	0.235	-0.003	-0.002	0.035
	57	11523.973	0.009	0.116	-0.008	0.001	0.017
	58	11577.499	-0.017	-0.185	0.003	0.000	-0.028
Lower Component	56	11456.956	0.026	0.011	0.002	0.001	-0.023
	57	11509.783	-0.036	-0.105	-0.009	-0.004	0.009
	58	11562.855	-0.028	-0.075	0.004	0.005	0.035
	59	11616.165	-0.008	0.016	0.005	0.000	0.017
	60	11669.871	0.014	0.110	0.004	-0.002	-0.038
	61	11724.123	0.026	0.169	-0.001	-0.005	-
	62	11779.042	0.037	0.195	0.003	0.003	-
	63	11834.679	0.034	0.171	-0.001	0.004	-
	64	11891.066	0.007	0.089	-0.018	-0.010	-
	65	11948.275	0.007	-0.002	-0.001	0.006	-
	66	12006.273	-0.015	-0.148	0.002	0.004	-
	67	12065.084	-0.044	-0.336	0.008	-0.003	-

(Footnotes on first page of Table)

D^{eff} for the perturbing state were 100% correlated. For this reason fits including terms only through B^{eff} were tried. The resulting T^{eff} and B^{eff} values for the perturbing state were still found to be highly correlated (correlation coefficient, -0.999), and the goodness of the fit was considerably poorer (high standard deviation, large residuals) unless only a very small number of data points were used (DATA SET XII.3). However, in the latter case it is unlikely that the resulting constants have much physical meaning — e.g. it would not be expected that the B^{eff} value could be related to the "true" B value by means of eqn. (III.J.5). As for the fit with H^{eff} parameters included, it is doubtful that the H^{eff} constants have any meaning as centrifugal distortion parameters, especially since the fit was performed over only a limited range of J values.

We thus favor the two fits in which terms through D^{eff} only are included as being the best overall, since they give *reasonably* good fits by the above criteria and are probably the most physically meaningful. But which of these two is better depends on the use to which they are to be put. The DATA SET XII.2 fit has a lower standard deviation and smaller residuals, but the DATA SET XII.1 fit is applicable to a wider range of J values.

A similar least-squares fitting process was done for the $^5\Phi_3$ substate and its perturbing substate, the results of which are summarized in Table XIII. Again both homogeneous and heterogeneous interaction mechanisms were considered and the results of several different fits for each are summarized in the table. In this case, fits with H^{eff} terms included have not been given, since although such fits led to lower overall standard deviations (e.g. σ = 0.003 for DATA SET XIII.3), the D^{eff} and H^{eff} constants for the perturbing state came out negative and the standard deviations for some of the constants came out larger than the constants themselves.

Unlike the case with the $^5\Phi_4$ substate, $^5\Phi_3$ shows no local avoided crossings to the low-J side of the perturbation presently being considered. Therefore in doing

TABLE XIII. Least-squares fitting: $^5\Phi_3$, v=0 and perturbing state, with crossing point at J ≃ 47.

(A) The results (in cm^{-1})[a] - homogeneous model

	Data Set XIII.1		Data Set XIII.2		Data Set XIII.3				Data Set XIII.4	
Terms included[b]:	B^{eff}, D^{eff}		B^{eff}, D^{eff}		B^{eff}		B^{eff}, D^{eff}		B^{eff}	
	$^5\Phi_3$	Perturbing State	$^5\Phi_3$	Perturbing State	$^5\Phi_3$	Perturbing State	$^5\Phi_3$	Perturbing State	$^5\Phi_3$	Perturbing State
T^{eff}	10 191.731 (48)	10 089.8 (79)	10 191.670 (34)	10 104.2 (42)	10 195.89 (23)	10 108.7 (15)	10 192.24 (21)	10 098.6 (37)	10 196.16 (31)	10.108.86 (69)
B^{eff}	0.449 220 (29)	0.503 4 (73)	0.449 342 (27)	0.489 5 (32)	0.445 32 (11)	0.484 95 (70)	0.448 83 (19)	0.494 5 (34)	0.445 28 (14)	0.484 76 (32)
10^6 D^{eff}	0.835 (13)	4.5 (17)	0.898 (11)	1.20 (91)	-	-	0.784 (43)	2.33 (79)	-	-
H_{12}	7.577 (16)		7.579 2 (68)		7.603 (31)		7.576 8 (46)		7.582 1 (99)	
σ[c]	0.036 0		0.015 6		0.083 2		0.010 3		0.021 9	

(a) The numbers in parentheses are one standard error in units of the last two figures quoted.

(b) T^{eff} and H_{12} or h_{12} were included in all fits.

(c) Standard deviation based on 53, 26, 18, or 10 data points for Data Sets XIII.1,2,3, or 4, respectively. All data points weighted equally (weight = 1).

(d) h_{12} is the "constant" in eqn. (V.B.3b).

(e) Observed-Calculated values of the term values.

(f) Homogeneous model.

(g) Heterogeneous model.

(h) Homogeneous and heterogeneous models.

(continued on next page)

TABLE XIII (cont.)

(B) The results (in cm^{-1})[a] - heterogeneous model

	Data Set XIII.1		Data Set XIII.2		Data Set XIII.3				Data Set XIII.4	
Terms included[b]:	B^{eff}, D^{eff}		B^{eff}, D^{eff}		B^{eff}		B^{eff}, D^{eff}		B^{eff}	
	$^5\phi_3$	Perturbing State	$^5\phi_3$	Perturbing State	$^5\phi_3$	Perturbing State	$^5\phi_3$	Perturbing State	$^5\phi_3$	Perturbing State
T^{eff}	10 192.291 (12)	10 087.4 (76)	10 192.3210 (61)	10 103.4 (42)	10 196.54 (22)	10 108.0 (15)	10 192.85 (19)	10 098.0 (37)	10 196.81 (30)	10 108.21 (69)
B^{eff}	0.449 267 (31)	0.505 0 (70)	0.449 347 (22)	0.489 5 (39)	0.445 32 (11)	0.484 95 (70)	0.448 85 (18)	0.494 5 (34)	0.445 28 (14)	0.484 76 (32)
10^6 D^{eff}	0.828 (14)	4.9 (16)	0.898 (11)	1.21 (91)	-	-	0.783 (44)	2.33 (79)	-	-
h_{12}[d]	0.160 00 (38)		0.160 37 (16)		0.161 48 (61)		0.160 33 (11)		0.160 65 (20)	
σ[c]	0.035 9		0.015 6		0.083 2		0.010 3		0.021 9	

(Footnotes on first page of Table)

(continued on next page)

TABLE XIII (cont.)

(C) The data used in parts A and B and the residuals

	J	Term Values	Residuals[e]					
			Data Set XIII.1[f]	Data Set XIII.1[g]	Data Set XIII.2[h]	Data Set XIII.3[h]		Data Set XIII.4[h]
			B^{eff}, D^{eff}	B^{eff}, D^{eff}	B^{eff}, D^{eff}	B^{eff}	B^{eff}, D^{eff}	B^{eff}
Upper Component	4	10201.338	0.058	0.057	0.025	-	-	-
	5	10205.823	0.048	0.047	0.014	-	-	-
	6	10211.215	0.046	0.046	0.011	-	-	-
	7	10217.504	0.043	0.042	0.006	-	-	-
	8	10224.693	0.041	0.041	0.002	-	-	-
	9	10232.772	0.031	0.030	-0.010	-	-	-
	10	10241.750	0.021	0.021	-0.022	-	-	-
	11	10251.628	0.014	0.013	-0.032	-	-	-
	12	10262.398	0.000	-0.000	-	-	-	-
	13	10274.074	-0.005	-0.005	-	-	-	-
	14	10286.647	-0.011	-0.011	-	-	-	-
	15	10300.113	-0.021	-0.021	-	-	-	-
	16	10314.481	-0.027	-0.027	-	-	-	-
	17	10329.745	-0.033	-0.033	-	-	-	-
	18	10345.908	-0.037	-0.037	-	-	-	-
	19	10362.966	-0.042	-0.042	-	-	-	-
	20	10380.925	-0.043	-0.043	-	-	-	-
	21	10399.773	-0.051	-0.050	-	-	-	-
	22	10419.530	-0.045	-0.044	-	-	-	-
	23	10440.170	-0.052	-0.051	-	-	-	-
	24	10461.719	-0.045	-0.044	-	-	-	-
	25	10484.159	-0.042	-0.041	-	-	-	-
	26	10507.493	-0.040	-0.039	-	-	-	-
	27	10531.733	-0.027	-0.026	-	-	-	-
	28	10556.863	-0.019	-0.018	-	-	-	-
	29	10582.883	-0.016	-0.015	-	-	-	-
	30	10609.806	-0.005	-0.004	-	-	-	-
	31	10637.626	0.007	0.008	-	-	-	-
	32	10666.341	0.019	0.019	-	-	-	-
	33	10695.949	0.026	0.027	-	-	-	-
	34	10726.454	0.032	0.033	-	-	-	-
	35	10757.861	0.040	0.040	-	-	-	-
	36	10790.170	0.047	0.047	-	-	-	-
	37	10823.381	0.049	0.050	-	-	-	-
	38	10857.500	0.048	0.048	-	-	-	-
	39	10892.538	0.045	0.045	0.006	-0.148	-0.012	-
	40	10928.498	0.034	0.033	0.006	-0.064	-0.002	-
	41	10965.410	0.026	0.025	0.012	0.013	0.012	-
	42	11003.278	0.001	-0.000	0.003	0.059	0.008	-
	43	11042.161	-0.020	-0.021	-0.000	0.090	0.007	-0.022
	44	11082.106	-0.042	-0.044	-0.008	0.090	-0.001	0.009
	45	11123.199	-0.052	-0.054	-0.012	0.059	-0.009	0.021
	46	11165.537	-0.033	-0.033	-0.009	-0.005	-0.011	0.010
	47	11209.213	0.046	0.051	0.011	-0.092	0.008	-0.017
Lower Component	45	11107.011	-0.015	-0.012	-0.009	-0.065	-0.003	-0.015
	46	11150.251	0.002	0.000	0.009	-0.008	0.002	0.010
	47	11193.974	0.015	0.011	0.008	0.033	0.001	0.012
	48	11238.172	0.029	0.026	0.010	0.070	0.010	0.012
	49	11282.859	0.015	0.014	-0.007	0.068	-0.002	-0.019
	50	11328.139	0.000	0.000	-0.015	0.050	-0.006	-
	51	11374.085	-0.017	-0.016	-0.017	0.008	-0.011	-
	52	11420.767	-0.025	-0.024	-0.006	-0.047	-0.005	-
	53	11468.231	-0.020	-0.018	0.023	-0.112	0.013	-

the least-squares fitting it should be possible to include *all* data points from the region of the perturbation on down to the lowest-J values available. Table XIII shows, however, that the resulting residuals for DATA SET XIII.1 are larger than would be hoped for and show a definite systematic trend (a group of positive residuals, followed by a group of negative residuals, followed by a group of positives, etc. — behaviour which we refer to as "snaking"). This means that either the model used involving effective 1x1 submatrices for the individual substates (eqns. (V.B.1) and (B.2)) is inadequate due to its neglect of off-diagonal and higher-order terms that would be present in the complete matrices for the multiplet states (e.g. Table VII), or that the energy levels deviate from this simple model as a consequence of interactions with some other state or states which do not actually cross the $^5\Phi_3$ substate. Hence the necessity of considering the various other fits in Table XIII. As with $^5\Phi_4$, none are perfect; once again we have a compromise situation, where one must choose a fit depending on one's particular application.

Returning now to the question of whether the interactions are homogeneous or heterogeneous, in the case of $^5\Phi_3$, only DATA SET XIII.1 shows any significant difference in the least-squares fits, with the heterogeneous mechanism being *slightly* favored. However, in view of the fact that this difference is obtained only when the complete data set from the lowest J on up through the perturbation region is used, and not when only data points in the region of the perturbation are used (DATA SET XIII.3), it would not be realistic to try to interpret this as indicating that the interaction is heterogeneous in nature and not homogeneous. Rather, this probably reflects a greater flexibility in compensating for terms neglected in writing the hamiltonian in the simplified form of eqns. (V.B.1) and (B.2).

The inability to distinguish experimentally between the homogeneous and heterogeneous modes of interaction reflects a lack of data in the region of the zeroth-order crossover point. Unfortunately, the high density of weak lines present in

our spectra has resulted in our only being able to identify three pairs of doubled lines (for both the $\Omega = 3$ and $\Omega = 4$ substates) and this number does not carry enough information to show up any J-dependence, or lack of it, in the interaction matrix element.

Being unable to distinguish experimentally between the homogeneous and heterogeneous modes, we must turn to other arguments to try to deduce which mechanism is operating and, if possible, what the perturbing state is.

If the interactions are heterogeneous in nature, then the operator involved could be either the $\underset{\sim}{L}$-uncoupling operator, $-B(r)\, J^{\pm} L^{\mp}$, or the $\underset{\sim}{S}$-uncoupling operator, $-B(r)\, J^{\pm} S^{\mp}$ (Table X). Consider first the $\underset{\sim}{S}$-uncoupling operator: this has selection rules[1]

$$\Delta\Lambda = \Delta S = 0$$
$$\Delta\Sigma = \Delta\Omega = \pm 1 \qquad \text{...(V.B.4)}$$

Thus the only possible state that could interact with the $^5\Phi$ state via this operator would be another $^5\Phi$ state. But we can discard this possibility on the grounds that no other low-lying $^5\Phi$ state has been predicted in any of the theoretical studies discussed in Sections I.A and I.D; that a $^5\Phi$ state would be expected to produce large electrostatic perturbations of our $^5\Phi$ state, which we do not see; and that only one $^5\Phi - X^5\Delta$ transition is observed in the spectrum.

As for the $\underset{\sim}{L}$-uncoupling operator, the selection rules are

$$\Delta S = \Delta\Sigma = 0$$
$$\Delta\Lambda = \Delta\Omega = \pm 1 \qquad \text{...(V.B.5)}$$

and these limit the possibilities for perturbing state to $^5\Delta$ or $^5\Gamma$. If the perturbing

---

[1]In this thesis we need not concern ourselves with the more detailed $J \cdot \sum_i s_i$ version of the operator for which the selection rule on S is $\Delta S = 0, \pm 1$, since this is only of importance for exotic coupling cases such as case (d) Rydberg states, for which there is no evidence here.

state is a $^5\Delta$ state, it must be the $^5\Delta_2$ substate that interacts with the $^5\Phi_3$ substate and the $^5\Delta_3$ substate with $^5\Phi_4$. But the $^5\Delta_4$ substate should then interact with the $^5\Phi_5$ substate. Recalling that the $^5\Phi_5$, v=0 level is notable for its lack of any detectable perturbation allows us to eliminate $^5\Delta$ as the perturbing state. The very same argument also eliminates $^5\Gamma$, since if $^5\Gamma_4$ interacts with $^5\Phi_3$ and $^5\Gamma_5$ with $^5\Phi_4$, then $^5\Gamma_6$ should perturb $^5\Phi_5$.

The conclusion is that if the $^5\Phi_3$ and $^5\Phi_4$ perturbations are caused by different multiplet components of the same electronic state, then the interactions do not occur via a heterogeneous mechanism.

Of the homogeneous operators listed in Table X, the spin-orbit operator is the one most likely to be responsible for such perturbations in a relatively heavy molecule such as FeO, for the following reasons. If the interactions involved mechanisms that were electrostatic or vibrational in nature, the strengths of the interactions would be expected to probably be greater and extend over a larger J-range than those observed. Also, interactions of these types occur between states having identical symmetry (i.e. $\Delta\Lambda = \Delta S = \Delta\Sigma = 0$), which would mean that the perturbing state would be a $^5\Phi$ state. The arguments used previously to reject the possibility of a $^5\Phi$ state interacting heterogeneously also apply here, namely that the presence of another $^5\Phi$ state in this energy regime is not predicted by the theoreticians and that transitions from it to the ground state are not observed in the spectrum, although the latter absence could be due to an inappropriate electron configuration. Spin-spin or spin-electronic interactions are possibilities but would not be expected to produce perturbations as large as those observed and if present would probably be masked by larger spin-orbit-induced perturbations. We thus need consider only spin-orbit interactions.

The selection rules for spin-orbit perturbations are

$$\Delta\Lambda = 0, \pm 1$$
$$\Delta S = 0, \pm 1 \qquad \text{...(V.B.6)}$$

Therefore, the possible perturbing states are

$$^3\Delta,\ ^5\Delta,\ ^7\Delta,\ ^3\Phi,\ ^5\Phi,\ ^7\Phi,\ ^3\Gamma,\ ^5\Gamma, \text{ and } ^7\Gamma.$$

But almost all of these can be eliminated by the following arguments. A $^3\Delta$ state could not cause the perturbation in the $^5\Phi_4$ substate, because it does not possess an $\Omega = 4$ component. The reverse argument eliminates the $^7\Delta$, $^5\Phi$, $^7\Phi$, $^3\Gamma$, $^5\Gamma$, and $^7\Gamma$ states as candidates — namely, these states all possess $\Omega = 5$ components, but the lack of any observed perturbation in $^5\Phi_5$ precludes these states. This leaves only $^5\Delta$ and $^3\Phi$ as possibilities for the perturbing state.

The $^5\Pi_2$, v=0 substate lies very close to the perturbed $^5\Phi_3$ substate (see Fig. 15) but is itself completely regular in the region of the $^5\Phi_3$ perturbation, even though the perturbing state must cross it also. From the spin-orbit selection rules it might be expected that, if the perturbing state were a $^5\Delta$ state, the $^5\Pi_2$ substate should be perturbed also, at least slightly, with the interaction occurring via the heterogeneous $\underset{\sim}{L}$-uncoupling operator. The absence of such a perturbation could be taken as evidence against a $^5\Delta$ perturbing state. However, caution must be excercised in making such an interpretation, since one must also consider the number of different spin-orbitals existing between perturbed and perturbing states (final column in Table X). We thus turn to the theoreticians for help in assessing electron configurations for possible perturbing $^5\Delta$ states, but find that only one low-lying $^5\Delta$ state has been predicted, and this has already been "used up" — it is the ground state. Since the electron configuration of the hypothetical perturbing $^5\Delta$ state is not known, it cannot be stated for certain whether the $^5\Pi_2$ substate should show a perturbation. However, the lack of another theoretically predicted $^5\Delta$ state is itself evidence against such a state. Also, no $^5\Delta - X^5\Delta$ transition is observed in this

region of the spectrum, although again electron configurations have to be considered. Taken together, all these arguments make another $^5\Delta$ state an unlikely identity for the perturbing state.

It is possible that the perturbing state is an upper vibrational level of the *ground* state. With this in mind, G_v, B_v, and D_v values for the ground state were extrapolated to this energy region using eqns. (III.D.1), (D.4), and (D.6). Actually this was done for each substate individually using effective values in the sense of eqn. (III.J.1)[2] The results are plotted in Fig. 16. We find that it is the v = 12 and 13 levels of the $X^5\Delta$ state that lie at similar energies to the v = 0 levels of the $^5\Pi$ and $^5\Phi$ states, but that in no case does the right Ω substate of the $^5\Delta$ state fall in a place where it would cause perturbations in the v = 0 levels of the $^5\Pi$ or $^5\Phi$ states. However, once again we cannot make an absolutely definite statement that this state is not the one responsible for the perturbations, since the predictions involved extrapolation over some nine vibrational levels and over 7 000 cm^{-1} and the predictions were based on the data from only four vibrational levels (v = 0–3). We can merely state that it is not *likely* that this state is the one.

This leaves $^3\Phi$ as the most likely candidate for the perturbing state.

It is instructive to derive the matrix elements for the interaction between the perturbed and perturbing states. We use the microscopic form of the spin–orbit operator (eqn. (III.E.17)) and write it in spherical tensor notation using eqn. (5.2.4) of Edmonds (2),

$$H_{SO} = \sum_e a_e \underset{\sim}{l}_e \cdot \underset{\sim}{s}_e$$
$$= \sum_q \sum_e (-1)^q T^1_{-q}(a_e \underset{\sim}{l}_e) T^1_q(\underset{\sim}{s}_e) \qquad \text{...(V.B.7)}$$

The interaction matrix element is then

---

[2] G_v^{eff} and T_v^{eff} are equivalent.

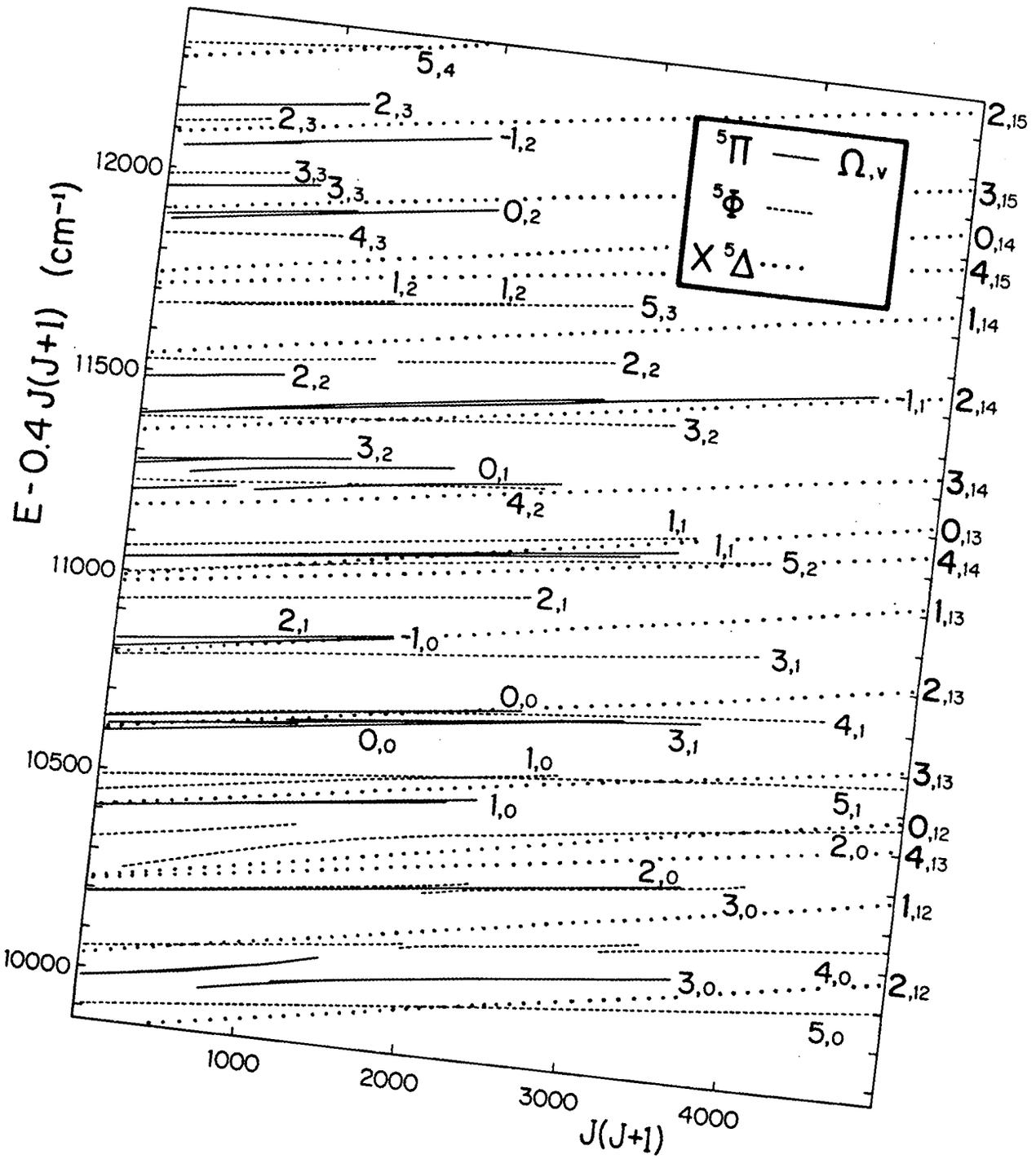

Fig. 16. Extrapolated high vibrational levels of the $X^5\Delta$ state superimposed on the energy level diagram of Fig. 15.

$$\begin{aligned}
&\langle \eta'\Lambda'S'\Sigma'J'\Omega' | H_{SO} | \eta\Lambda S\Sigma J\Omega\rangle \\
&\quad = \sum_q \sum_e (-1)^q \langle \eta'\Lambda' | T^1_{-q}(a_e \underset{\sim}{l}_e) | \eta\Lambda\rangle \\
&\qquad\qquad \cdot \langle S'\Sigma' | T^1_q(\underset{\sim}{s}_e) | S\Sigma\rangle \delta_{J'J}\delta_{\Omega'\Omega} \\
&\quad = \sum_q (-1)^q \sum_e \langle \eta'\Lambda' | T^1_{-q}(a_e \underset{\sim}{l}_e) | \eta\Lambda\rangle (-1)^{S'-\Sigma'} \begin{pmatrix} S' & 1 & S \\ -\Sigma' & q & \Sigma \end{pmatrix} \\
&\qquad\qquad \cdot \langle S' \| T^1(\underset{\sim}{s}_e) \| S\rangle \delta_{J'J}\delta_{\Omega'\Omega} \qquad \text{...(V.B.8)}
\end{aligned}$$

where the matrix element has been factored into spin and spatial parts, following which the Wigner-Eckart theorem has been applied (3,4,5,6); the resulting reduced matrix element is reduced with respect to Σ. Upon rearrangement, the non-zero matrix element is

$$\begin{aligned}
&\langle \eta'\Lambda'S'\Sigma'J\Omega | H_{SO} | \eta\Lambda S\Sigma J\Omega\rangle \\
&\quad = \sum_q (-1)^q (-1)^{S'-\Sigma'} \begin{pmatrix} S' & 1 & S \\ -\Sigma' & q & \Sigma \end{pmatrix} \sum_e \langle \eta'\Lambda' | T^1_{-q}(a_e \underset{\sim}{l}_e) | \eta\Lambda\rangle \\
&\qquad\qquad \cdot \langle S' \| T^1(\underset{\sim}{s}_e) \| S\rangle \qquad \text{...(V.B.9)}
\end{aligned}$$

The properties of a 3j symbol give rise to selection rules, as follows. The triangle rule (eqn. (III.I.31)) gives

$$S = S'+1,\ S',\ S'-1$$

or $$\Delta S = 0, \pm 1 \qquad \text{...(V.B.10)}$$

which is the selection rule on S found in Table X. The sum of the three elements on the bottom line of a 3j symbol must equal zero; thus

$$q = \Sigma' - \Sigma \qquad \text{...(V.B.11)}$$

For q = 0 (i.e. for both the diagonal ($\Delta\Lambda = \Delta\Sigma = \Delta S = 0$) and off-diagonal ($\Delta\Lambda = \Delta\Sigma = 0$, $\Delta S = \pm 1$) elements of the $l_z s_z$ part of H_{SO},

$$\Sigma' = \Sigma \qquad \text{...(V.B.12)}$$

This is the situation which applies in the case of a $^3\Phi/^5\Phi$ interaction. Eqn. (V.B.9)

becomes

$$\langle \eta' \Lambda' = 3, S' = 1, \Sigma J \Omega | H_{SO} | \eta \Lambda = 3, S = 2, \Sigma J \Omega \rangle$$

$$= (-1)^{1-\Sigma} \begin{pmatrix} 1 & 1 & 2 \\ -\Sigma & 0 & \Sigma \end{pmatrix} \xi_{^3\Phi, ^5\Phi} \qquad \text{...(V.B.13)}$$

where

$$\xi_{^3\Phi, ^5\Phi} = \sum_e \langle \eta' \Lambda' = 3 | T^1_{-q}(a_e \underset{\sim}{l}_e) | \eta \Lambda = 3 \rangle \langle S' = 1 \| T^1(\underset{\sim}{s}_e) \| S = 2 \rangle \qquad \text{...(V.B.14)}$$

The fact that $\xi_{^3\Phi, ^5\Phi}$ is a constant independent of Σ — a consequence of the Wigner-Eckart theorem — means that the interaction matrix elements for the various spin components of the multiplet states can be easily compared with one another; they are simply proportional to their respective 3j symbols, multiplied by $+1$ or -1 as appropriate;

$$\langle ^3\Phi_2 | H_{SO} | ^5\Phi_2 \rangle = \begin{pmatrix} 1 & 1 & 2 \\ 1 & 0 & -1 \end{pmatrix} \xi_{^3\Phi, ^5\Phi} = -0.3162\, \xi_{^3\Phi, ^5\Phi} \qquad \text{...(V.B.15a)}$$

$$\langle ^3\Phi_3 | H_{SO} | ^5\Phi_3 \rangle = -\begin{pmatrix} 1 & 1 & 2 \\ 0 & 0 & 0 \end{pmatrix} \xi_{^3\Phi, ^5\Phi} = -0.3651\, \xi_{^3\Phi, ^5\Phi} \qquad \text{...(V.B.15b)}$$

$$\langle ^3\Phi_4 | H_{SO} | ^5\Phi_4 \rangle = \begin{pmatrix} 1 & 1 & 2 \\ -1 & 0 & 1 \end{pmatrix} \xi_{^3\Phi, ^5\Phi} = -0.3162\, \xi_{^3\Phi, ^5\Phi} \qquad \text{...(V.B.15c)}$$

The ratio of the $\Omega = 3$ to $\Omega = 4$ interaction matrix elements is then

$$\frac{\langle ^3\Phi_3 | H_{SO} | ^5\Phi_3 \rangle}{\langle ^3\Phi_4 | H_{SO} | ^5\Phi_4 \rangle} = 1.15 \qquad \text{...(V.B.16)}$$

This number can be compared with the experimental value obtained from the least-squares fitting results of Tables XII and XIII,[3]

$$\frac{(H_{12})_{\Omega=3}}{(H_{12})_{\Omega=4}} = 1.07 \qquad \text{...(V.B.17)}$$

The numbers are close, but not in perfect agreement. The discrepancy means

---

[3]The values from the fits employing DATA SETS XII.2 (with terms through D^{eff}) and XIII.3 (with terms through D^{eff}) have been used. The other fits give similar results.

(i) that the perturbations in $^5\Phi_3$ and $^5\Phi_4$ are not related;

or (ii) that the perturbations *are* related but are not caused by a $^3\Phi$ state;

or (iii) that the perturbations *are* related and *are* caused by a $^3\Phi$ state but that the model being used is oversimplified.

Point (i) is always a possibility, but not one that can be tested for other than in the negative sense of all the other possibilities failing. As for point (ii), the only other state that we have given credence to as a viable (though unlikely) alternative for the perturbing state is a $^5\Delta$ state. For a $^5\Delta/^5\Phi$ interaction, q = 1, and

$$\Sigma' = \Sigma \pm 1 \qquad \text{...(V.B.18)}$$

and we obtain

$$\langle ^5\Delta_1 | H_{SO} | ^5\Phi_1 \rangle = \begin{pmatrix} 2 & 1 & 2 \\ 1 & 1 & -2 \end{pmatrix} \xi_{^5\Delta, ^5\Phi} = 0.2582\, \xi_{^5\Delta, ^5\Phi} \qquad \text{...(V.B.19a)}$$

$$\langle ^5\Delta_2 | H_{SO} | ^5\Phi_2 \rangle = -\begin{pmatrix} 2 & 1 & 2 \\ 0 & 1 & -1 \end{pmatrix} \xi_{^5\Delta, ^5\Phi} = 0.3162\, \xi_{^5\Delta, ^5\Phi} \qquad \text{...(V.B.19b)}$$

$$\langle ^5\Delta_3 | H_{SO} | ^5\Phi_3 \rangle = \begin{pmatrix} 2 & 1 & 2 \\ -1 & 1 & 0 \end{pmatrix} \xi_{^5\Delta, ^5\Phi} = 0.3162\, \xi_{^5\Delta, ^5\Phi} \qquad \text{...(V.B.19c)}$$

$$\langle ^5\Delta_4 | H_{SO} | ^5\Phi_4 \rangle = -\begin{pmatrix} 2 & 1 & 2 \\ -2 & 1 & 1 \end{pmatrix} \xi_{^5\Delta, ^5\Phi} = 0.2582\, \xi_{^5\Delta, ^5\Phi} \qquad \text{...(V.B.19d)}$$

and

$$\frac{\langle ^5\Delta_3 | H_{SO} | ^5\Phi_3 \rangle}{\langle ^5\Delta_4 | H_{SO} | ^5\Phi_4 \rangle} = 1.22 \qquad \text{...(V.B.20)}$$

This is in even poorer agreement with experiment so is yet further evidence that the perturbing state is not a $^5\Delta$ state.

We thus return to $^3\Phi$ as the most likely candidate for the perturbing state, and we must then look for other causes for the discrepancy.

The experimental value came from matrix elements that were obtained from fits to *effective* hamiltonians for the individual substates, whereas the theoretical value

involved the matrix elements of the full hamiltonians for the multiplet states. The effects of off-diagonal matrix elements neglected in the effective approach were absorbed into the various effective constants, including the H_{12}'s. In order to make the theoretical value more closely correspond to the experimental value, the effects of these other off-diagonal elements can be incorporated by means of perturbation theory. The most important of these elements are those involving the spin-uncoupling operator since the $\Omega = 3$ and $\Omega = 4$ perturbations occur at different J values. First-order corrections to the wavefunctions for the individual $^3\Phi_3$, $^3\Phi_4$, $^5\Phi_3$, $^5\Phi_4$ substates yielded a new theoretical value of 1.18. Clearly this is not the source of the discrepancy.

We must therefore assume that the discrepancy results from interactions with some (unidentified) other state or states which have caused the wavefunctions of either the $^5\Phi$ state or the $^3\Phi$ state or both to have become slightly mixed with those of the other state(s) so that they no longer "play true." This is a completely reasonable explanation in view of the high density of states known to be present, as evidenced by the large number of observed perturbations, and is in line with the failure to obtain really good least-squares fits for the individual substates. The same explanation has already been called upon to explain some of the complexities in the upper states of the orange system (see Section I.B.2).

Assuming that the perturbing state is a $^3\Phi$ state, it should be possible to do a single least-squares fit of the whole interacting system. This would involve an 8x8 matrix consisting of a 5x5 submatrix for the $^5\Phi$ state (Table VII), a 3x3 submatrix for the $^3\Phi$ state (Table VIII), and the off-diagonal elements of eqn. (V.B.15). Such a fit was attempted, with the Λ-doubling in the $^5\Phi_1$ substate handled by the phenomenological term

$$H_{LD} = \pm\tfrac{1}{2}qJ(J+1) \qquad \text{...(V.B.21)}$$

However, it was found impossible to obtain a good fit. The residuals typically had

values in the range $\pm(0.1-1.5)$ cm^{-1} which are very large, with severe "snaking" being present. The explanation is to be found amongst the three points listed on page 181. We favor point (iii) and attribute the poorness of the fit to the presence of other interacting states.

To verify this, it was tried fitting the $^5\Pi$ state (v = 0 level) alone using only those parts that were distant from the $^3\Phi$ avoided crossing and from any other known avoided crossings. The results are given in Table XIV. Due to the large perturbation in $^5\Phi_2$, data for this substate were not included. The resulting fit was better than the $^5\Phi/^3\Phi$ combined fit but was still not particularly good (see the results for DATA SET XIV.1). The Λ-doubling in $^5\Phi_1$ was again handled by means of eqn. (V.B.21). Another fit was tried with an additional Λ-doubling term in $J^2(J+1)^2$, i.e.

$$H_{LD} = \pm\tfrac{1}{2}\left\{qJ(J+1) + q_D[J(J+1)]^2\right\} \qquad \text{...(V.B.22)}$$

(cf. eqn. (III.H.67)), but this produced a worse fit, and both q and q_D were poorly determined. It was found that a considerably better fit was obtained if the $^5\Phi_1$ substate was also excluded (DATA SET XIV.2). This would imply that the $^5\Phi_1$ substate is perturbed. While no local avoided crossings have been observed in this substate (other than at its high-J end where an avoided crossing has prevented following the branch further), it has been previously mentioned that the low-J end of it may be "pushed" towards lower energy. The exclusion of this and the $\Omega = 2$ substate means that it is not possible to pin down all the spin-orbit paramaters. Only A, A_D, and λ have been included in the DATA SET XIV.2 fit. (Inclusion of a term in η was tried, but this resulted in λ being poorly determined.) Systematic errors ("snaking") are still present in the DATA SET XIV.2 fit, but the magnitudes of the residuals are considerably smaller than for the DATA SET XIV.1 fit. This appears to be the best that can be done. (A better fit in terms of a smaller

TABLE XIV. Least-squares fitting: $^5\Phi$, v=0 — "unperturbed" regions.

(A) The results (in cm^{-1})[a]

		Data Set XIV.1	Data Set XIV.2	Data Set XIV.3
	T	10 186.621 (25)	10 186.039 (17)	10 201.501 5 (45)
	B	0.452 034 (34)	0.450 185 (22)	0.448 743 (18)
10^6	D	1.069 8 (64)	1.053 9 (11)	1.036 85 (40)
	A	-44.317 8 (49)	-44.088 6 (47)	-47.794 69 (84)
10^4	A_D	-3.532 (50)	-0.353 (38)	2.059 (30)
	λ	-1.649 2 (54)	-1.919 9 (32)	-
10^2	η	-6.66 (59)	-	-
10^5	q	1.2 (72)	-	-
	σ[b]	0.179	0.023 5	0.005 5

(a) The numbers in parentheses are one standard error in units of the last two figures quoted.

(b) Standard deviation based on 191, 114, or 87 data points for Data Sets XIV.1,2, or 3, respectively. All data points weighted equally (weight = 1).

(c) The parity component is also given where appropriate.

(d) Observed-Calculated.

(continued on next page)

TABLE XIV (cont.)

(B) The data used in part (A) and the residuals

Ω	J	Term Values	Residuals[d] Data Set XIV.1	Ω	J	Term Values	Residuals Data Set XIV.1	Data Set XIV.2	Data Set XIV.3
1a	1	10447.297	-0.235	3	3	10197.748	0.518	0.034	-
1a	2	10449.149	-0.227	3	4	10201.338	0.497	0.028	-
1a	3	10451.921	-0.219	3	5	10205.823	0.469	0.018	-
1a	4	10455.622	-0.204	3	6	10211.215	0.444	0.016	-
1a	5	10460.240	-0.193	3	7	10217.504	0.415	0.013	-
1a	6	10465.783	-0.179	3	8	10224.693	0.383	0.011	-
1a	7	10472.256	-0.155	3	9	10232.772	0.339	0.002	-
1a	8	10479.652	-0.129	3	10	10241.750	0.293	-0.007	-
1a	9	10487.956	-0.116	3	11	10251.628	0.245	-0.014	-
1a	10	10497.202	-0.080	3	12	10262.398	0.188	-0.026	-
1a	11	10507.359	-0.054	3	13	10274.074	0.136	-0.029	-
1a	12	10518.443	-0.020	3	14	10286.647	0.080	-0.032	-
1a	13	10530.433	0.001	3	15	10300.113	0.018	-0.038	-
1a	14	10543.359	0.039	3	16	10314.481	-0.043	-0.039	-
1a	15	10557.183	0.056	3	17	10329.745	-0.107	-0.040	-
1a	16	10571.936	0.085	3	18	10345.908	-0.172	-0.036	-
1a	17	10587.603	0.111	3	19	10362.966	-0.240	-0.033	-
1a	18	10604.184	0.133	3	20	10380.925	-0.305	-0.023	-
1a	19	10621.676	0.150	3	21	10399.773	-0.379	-0.018	-
1a	20	10640.083	0.167	3	22	10419.530	-0.440	0.002	-
1a	21	10659.410	0.188	3	23	10440.170	-0.516	0.013	-
1a	22	10679.638	0.196	3	24	10461.719	-0.578	0.040	-
1a	23	10700.774	0.198	3	25	10484.159	-0.645	0.066	-
1a	24	10722.825	0.202	3	26	10507.493	-0.713	0.096	-
1a	25	10745.777	0.194	4	4	10061.646	0.212	0.052	0.007
1a	26	10769.640	0.186	4	5	10066.109	0.199	0.048	0.004
1a	27	10794.404	0.168	4	6	10071.464	0.183	0.042	0.001
1a	28	10820.076	0.148	4	7	10077.720	0.173	0.043	0.006
1a	29	10846.651	0.122	4	8	10084.858	0.150	0.034	0.001
1a	30	10874.123	0.084	4	9	10092.896	0.133	0.032	0.003
1a	31	10902.500	0.044	4	10	10101.814	0.102	0.018	-0.007
1a	32	10931.773	-0.006	4	11	10111.637	0.081	0.016	-0.003
1a	33	10961.949	-0.059	4	12	10122.350	0.057	0.012	-0.001
1a	34	10993.019	-0.122	4	13	10133.951	0.028	0.004	-0.003
1a	35	11024.992	-0.186	4	14	10146.440	-0.007	-0.007	-0.007
1a	36	11057.855	-0.263	4	15	10159.828	-0.036	-0.010	-0.004
1b	1	10447.305	-0.227	4	16	10174.104	-0.069	-0.017	-0.002
1b	2	10449.149	-0.227	4	17	10189.266	-0.109	-0.027	-0.005
1b	3	10451.921	-0.219	4	18	10205.317	-0.151	-0.039	-0.008
1b	4	10455.621	-0.205	4	19	10222.265	-0.188	-0.043	-0.003
1b	5	10460.243	-0.191	4	20	10240.104	-0.224	-0.046	0.005
1b	6	10465.787	-0.175	4	21	10258.823	-0.271	-0.057	0.004
1b	7	10472.255	-0.157	4	22	10278.438	-0.312	-0.060	0.012
1b	8	10479.652	-0.130	5	5	9916.917	-0.055	-0.006	0.001
1b	9	10487.967	-0.106	5	6	9922.254	-0.051	-0.003	0.004
1b	10	10497.205	-0.079	5	7	9928.472	-0.055	-0.008	-0.001
1b	11	10507.362	-0.052	5	8	9935.582	-0.055	-0.009	-0.003
1b	12	10518.442	-0.023	5	9	9943.581	-0.055	-0.010	-0.004
1b	13	10530.441	0.007	5	10	9952.465	-0.057	-0.014	-0.008
1b	14	10543.359	0.036	5	11	9962.241	-0.055	-0.013	-0.008
1b	15	10557.190	0.061	5	12	9972.910	-0.048	-0.008	-0.003
1b	16	10571.938	0.084	5	13	9984.459	-0.048	-0.009	-0.005
1b	17	10587.609	0.113	5	14	9996.897	-0.046	-0.009	-0.005
1b	18	10604.189	0.134	5	15	10010.222	-0.043	-0.009	-0.005
1b	19	10621.686	0.156	5	16	10024.433	-0.041	-0.009	-0.005
1b	20	10640.094	0.173	5	17	10039.535	-0.034	-0.004	-0.001
1b	21	10659.411	0.184	5	18	10055.515	-0.034	-0.007	-0.004
1b	22	10679.642	0.194	5	19	10072.385	-0.030	-0.004	-0.002
1b	23	10700.784	0.202	5	20	10090.144	-0.021	0.002	0.004
1b	24	10722.827	0.197	5	21	10108.777	-0.022	-0.002	-0.001
1b	25	10745.789	0.199	5	22	10128.297	-0.021	-0.003	-0.002
1b	26	10769.648	0.186	5	23	10148.706	-0.013	0.002	0.002
1b	27	10794.410	0.166	5	24	10169.992	-0.012	0.001	0.001
1b	28	10820.081	0.144	5	25	10192.163	-0.007	0.003	0.002
1b	29	10846.659	0.120	5	26	10215.214	-0.004	0.003	0.001
1b	30	10874.135	0.086	5	27	10239.147	-0.001	0.004	0.002
1b	31	10902.510	0.043	5	28	10263.959	0.001	0.003	0.001
1b	32	10931.783	-0.008	5	29	10289.652	0.005	0.004	0.001
1b	33	10961.963	-0.057	5	30	10316.227	0.011	0.007	0.004
1b	34	10993.032	-0.122	5	31	10343.677	0.014	0.007	0.004
1b	35	11025.003	-0.189	5	32	10372.002	0.014	0.005	0.001
1b	36	11057.870	-0.262	5	33	10401.214	0.024	0.012	0.008

(Footnotes on first page of Table)

(continued on next page)

TABLE XIV (cont.)

(B) The data used in part (A) and the residuals (cont.)

Ω	J	Term Values	Residuals		
			Data Set XIV.1	Data Set XIV.2	Data Set XIV.3
5	34	10431.290	0.021	0.007	0.003
5	35	10462.252	0.029	0.013	0.008
5	36	10494.080	0.029	0.010	0.005
5	37	10526.788	0.034	0.013	0.008
5	38	10560.363	0.034	0.011	0.005
5	39	10594.812	0.035	0.010	0.004
5	40	10630.134	0.038	0.011	0.005
5	41	10666.324	0.038	0.010	0.004
5	42	10703.386	0.042	0.011	0.006
5	43	10741.315	0.044	0.012	0.006
5	44	10780.108	0.042	0.009	0.003
5	45	10819.771	0.044	0.010	0.004
5	46	10860.299	0.045	0.010	0.005
5	47	10901.687	0.043	0.007	0.002
5	48	10943.939	0.040	0.004	-0.001
5	49	10987.056	0.041	0.004	-0.000
5	50	11031.031	0.039	0.002	-0.002
5	51	11075.866	0.037	0.000	-0.004
5	52	11121.561	0.037	-0.000	-0.004
5	53	11168.115	0.037	0.001	-0.001
5	54	11215.525	0.038	0.003	0.000
5	55	11263.785	0.034	-0.001	-0.002
5	56	11312.898	0.029	-0.004	-0.005
5	57	11362.865	0.026	-0.006	-0.006
5	58	11413.683	0.023	-0.007	-0.007
5	59	11465.349	0.018	-0.010	-0.009
5	60	11517.867	0.017	-0.009	-0.007
5	61	11571.228	0.012	-0.012	-0.009
5	62	11625.432	0.004	-0.016	-0.012
5	63	11680.494	0.011	-0.007	-0.002
5	64	11736.382	0.001	-0.013	-0.007
5	65	11793.122	0.003	-0.008	-0.002
5	66	11850.690	-0.008	-0.015	-0.007
5	67	11909.106	-0.008	-0.011	-0.002
5	68	11968.361	-0.005	-0.004	0.006
5	69	12028.434	-0.019	-0.013	-0.003
5	70	12089.358	-0.015	-0.004	0.007
5	71	12151.107	-0.017	-0.002	0.010
5	72	12213.689	-0.016	0.004	0.018
5	73	12277.109	-0.005	0.021	
5	74	12341.330	-0.020	0.013	
5	75	12406.394	-0.015	0.023	
5	76	12472.277	-0.015		
5	77	12538.984	-0.011		
5	78	12606.515	-0.002		
5	79	12674.860	0.003		
5	80	12744.024	0.013		

standard deviation and smaller residuals was obtained by fitting only the $^5\Phi_4$ and $^5\Phi_5$ substates, but with data for only one spin-orbit interval, only the A and A_D spin-orbit parameters could be determined. The results for this fit are included in Table XIV as DATA SET XIV.3. Systematic errors are still present.)

The conclusion from all this is that a $^3\Phi$ state is most likely responsible for the perturbation in the $^5\Phi_4$ substate at ~J = 57, for the perturbation in the $^5\Phi_3$ substate at ~J = 47, and for part of the complex perturbation in the $^5\Phi_2$ substate in the region J = 14-34. Due to the high density of states it has proven impossible to obtain a good fit of the $^5\Phi$ and $^3\Phi$ states simultaneously, so that the best that could be done was the individual $^5\Phi_3/^3\Phi_3$ and $^5\Phi_4/^3\Phi_4$ fits described earlier — an approach which would be used if the states belonged to Hund's case (c).

V.B.2. Perturbation in $^5\Phi_4$, v=0 at J=44

The $^5\Phi_4$, v=0 substate exhibits two other perturbations besides the one already studied, namely a very small perturbation involving only the J = 47 lines, which are weak and fat, and a larger perturbation centered at J = 44. The former perturbation will be discussed in Section V.B.4; we focus on the latter perturbation here. Doubled lines are observed at J = 44 with a separation of 9.693 cm^{-1} and the perturbed region extends over several J values to either side.

The results of least-squares fitting are given in Table XV. Since only one pair of doubled lines has been identified, T^{eff} and B^{eff} for the perturbing state are 100% correlated. Caution must therefore be exercised in using the results.

The state responsible for this perturbation will be discussed further in Section V.B.4.

TABLE XV. Least-squares fitting: $^5\Phi_4$, v=0 and perturbing state, with crossing point at J ≃ 44.

(A) The results (in cm^{-1})[a]

	Homogeneous Model		Heterogeneous Model	
	$^5\Phi_4$	Perturbing State	$^5\Phi_4$	Perturbing State
T^{eff}	10 053.058 (77)	9 930.5 (13)	10 053.247 (77)	9 930.3 (13)
B^{eff}	0.445 567 (97)	0.505 98 (65)	0.445 565 (97)	0.505 98 (65)
$10^6\ D^{eff}$	0.531 (28)	-	0.531 (28)	-
H_{12}	4.824 (13)		-	
h_{12}	-		0.107 96 (27)	
σ	0.019 2		0.019 2	

(B) The data[b] and residuals

	J	Term Values	Residuals[c]
Upper Component	31	10494.883	-0.027
	32	10523.372	-0.009
	33	10552.744	0.002
	34	10582.998	0.006
	35	10614.148	0.014
	36	10646.185	0.016
	37	10679.118	0.017
	38	10712.949	0.013
	39	10747.695	0.010
	40	10783.368	-0.000
	41	10820.019	-0.007
	42	10857.728	-0.022
	43	10896.752	-0.018
	44	10937.628	0.012
Lower Component	44	10927.935	0.005
	45	10970.112	0.000
	46	11012.005	-0.012
	48	11097.074	-0.028
	49	11140.712	-0.006
	50	11185.182	0.035

(a) The numbers in parentheses are one standard error in units of the last two figures quoted.

(b) All data points weighted equally (weight = 1).

(c) Observed-Calculated. Same residuals for homogeneous and heterogeneous fits.

V.B.3. Complex perturbation in $^5\Phi_2$, v=0

The appearance of the perturbation in the $^5\Phi_2$ substate is very different from those encountered in the previous sections. The separation between components is larger and the effects spread over a much wider range of J values. Doubled lines are present from J = 14 to 34.

It was shown in Section III.J (below eqn. (III.J.18)) that at J = J_c, the J value corresponding to the crossing point of two zeroth-order states (which for a homogeneous perturbation is also the point of minimum approach of the *actual* states[4]), the intensities of lines involving the two states ("doubled lines") will be equal to each other, since each of the two states will be a fifty-fifty mixture of a zeroth-order intensity-carrying state and a zeroth-order non-intensity-carrying state (with respect to transitions to some other common state). This is *not* the situation observed here. The upper component loses intensity much more rapidly than it "ought to," so that it has not even been possible to follow it to the point of minimum approach to the lower component. The last identifiable lines involve J' = 34, whereas by extrapolation the point of minimum approach would be at approximately J = 35 (homogeneous) or J = 38 (heterogeneous).

Lambda-doubling in the ground state happens to set in at about the same J value as where the upper-component lines can no longer be followed. This was considered as a possible explanation for the intensity anomaly, since the Λ-doubling would result in reduced intensities.

With this in mind, least-squares fitting was performed in the same manner as in the previous sections. The results are given in Table XVI. Equally good fits were obtained using a homogeneous or a heterogeneous model, even though twenty pairs of

---

[4]This is strictly true, in general, for homogeneous perturbations in which both states belong to case (a). For heterogeneneous perturbations, the point of minimum separation can occur to the low-J side of J_c, but this does not affect the argument given here.

TABLE XVI. Least-squares fitting: $^5\Phi_2$, v=0 and one perturbing state, with crossing point at J ≃ 35.

(A) The results (in cm^{-1})[a]

	Homogeneous Model		Heterogeneous Model	
	$^5\Phi_2$	Perturbing State	$^5\Phi_2$	Perturbing State
T^{eff}	10 324.687 (18)	10 242.347 (39)	10 331.681 (15)	10 235.358 (35)
B^{eff}	0.453 630 (32)	0.517 01 (11)	0.453 535 (39)	0.517 084 (98)
10^6 D^{eff}	1.132 5 (79)	0.307 (83)	1.130 3 (82)	0.292 (82)
H_{12}	24.995 (10)		-	
h_{12}	-		0.672 32 (34)	
σ	0.027 4		0.027 4	

(a) The numbers in parentheses are one standard error in units of the last two figures.

(b) All data points weighted equally (weight = 1).

(c) Observed-Calculated.

(continued on next page)

TABLE XVI (cont.)

(B) The data[b] and residuals

	J	Term Values	Residuals[c]	
			Homogeneous model	Heterogeneous model
Upper Component	13	10415.068	-0.079	-0.079
	14	10427.942	-0.060	-0.061
	15	10441.738	-0.044	-0.044
	16	10456.458	-0.028	-0.028
	17	10472.103	-0.015	-0.014
	18	10488.681	0.003	0.003
	19	10506.185	0.014	0.014
	20	10524.618	0.019	0.019
	21	10543.994	0.028	0.028
	22	10564.312	0.035	0.036
	23	10585.578	0.041	0.042
	24	10607.794	0.042	0.042
	25	10630.971	0.039	0.040
	26	10655.124	0.039	0.040
	27	10680.255	0.033	0.033
	28	10706.388	0.030	0.030
	29	10733.530	0.022	0.022
	30	10761.699	0.009	0.009
	31	10790.928	0.003	0.003
	32	10821.216	-0.020	-0.021
	33	10852.612	-0.037	-0.039
	34	10885.128	-0.060	-0.063
Lower Component	15	10358.161	0.039	0.037
	16	10374.464	0.009	0.008
	17	10391.806	0.009	0.008
	18	10410.148	0.002	0.002
	19	10429.500	0.002	0.002
	20	10449.841	-0.008	-0.008
	21	10471.180	-0.016	-0.015
	22	10493.516	-0.016	-0.015
	23	10516.834	-0.018	-0.017
	24	10541.132	-0.015	-0.014
	25	10566.398	-0.012	-0.011
	26	10592.617	-0.012	-0.011
	27	10619.781	-0.011	-0.011
	28	10647.880	-0.006	-0.005
	29	10676.884	-0.009	-0.009
	30	10706.790	-0.004	-0.004
	31	10737.561	-0.006	-0.006
	32	10769.190	0.002	0.002
	33	10801.638	0.007	0.007
	34	10834.880	0.011	0.011
	35	10868.892	0.016	0.016
	36	10903.646	0.018	0.017
	37	10939.144	0.036	0.035

(Footnotes on first page of Table)

(continued on next page)

TABLE XVI (cont.)

(B) The data and residuals (cont.)

	J	Term Values	Residuals	
			Homogeneous model	Heterogeneous model
Lower	38	10975.326	0.024	0.023
Component	39	11012.226	0.021	0.020
	40	11049.838	0.021	0.020
(cont.)	41	11088.156	0.012	0.011
	42	11127.202	0.005	0.005
	43	11166.996	0.009	0.009
	44	11207.533	0.004	0.004
	45	11248.830	-0.006	-0.006
	46	11290.912	-0.009	-0.009
	47	11333.782	-0.013	-0.013
	48	11377.443	-0.026	-0.025
	49	11421.932	-0.019	-0.018
	50	11467.226	-0.023	-0.022
	51	11513.340	-0.028	-0.027
	52	11560.286	-0.028	-0.027
	53	11608.066	-0.025	-0.025
	54	11656.681	-0.022	-0.021
	55	11706.136	-0.015	-0.015
	56	11756.426	-0.013	-0.013
	57	11807.570	0.003	0.003
	58	11859.554	0.018	0.017
	59	11912.374	0.026	0.025
	60	11966.056	0.054	0.052

doubled terms were included in the data. The fits themselves were only moderately good, with systematic errors being present in the residuals. Better fits (smaller residuals, smaller overall standard deviations) were obtained when H^{eff} terms were included, and in this case the heterogeneous model was slightly favored (σ_{het} = 0.007 84; σ_{hom} = 0.007 98), but these fits were discarded on the basis that both D^{eff} and H^{eff} for the perturbing state were negative and poorly determined.

The least-squares program also calculated the relative intensities of spectral lines involving the upper and lower components of the perturbed state by means of eqn. (III.J.23). The results are given in Table XVII in the form of a ratio along with the corresponding experimental values. This table clearly shows that something is wrong! Of the two fits, the homogeneous model gives results in far better agreement with experiment than the heterogeneous model, but even these results are out by a factor of two. This is so even at J values well below the point where Λ-doubling in the lower state is observable,[5] thus eliminating Λ-doubling as an explanation for the anomalous behavior.

Clearly the situation is more complicated than a simple two-state crossing system. The actual situation must involve at least three interacting states — i.e. the $^5\Phi_2$ substate plus *two* perturbing states.

In Section V.B.1, it was shown that one of these perturbing states is probably the Ω = 2 substate of a $^3\Phi$ state. This is consistent with the three-interacting-states scheme, since the magnitude of the perturbation caused by the $^3\Phi_2$ substate should be smaller than the observed perturbation, based on the magnitudes of the $^5\Phi_3/^3\Phi_3$ and $^5\Phi_4/^3\Phi_4$ interaction constants.

No attempt has been made to do a quantitative deperturbation analyis of the three interacting states. Of course the three-state model invalidates the previous least-squares fitting results (Tables XVI and XVII).

---

[5]The lines are sharp.

TABLE XVII. Relative intensities in the perturbed $^5\Phi_2$ substate. The ratios of intensities of doubled lines involving the upper and lower components of the $^5\Phi_2$ substate are given: $\frac{I_{\text{upper component}}}{I_{\text{lower component}}}$

J	Experimental[a]	Calculated[b]	
		Homogeneous model	Heterogeneous model
18	3.75	7.74	37.9
19	-	7.27	32.2
20	2.87	6.80	27.4
21	3.36[c]	6.32	23.3
22	3.36[c]	5.84	19.8
23	-	5.36	16.8
24	-	4.90	14.3
25	1.89	4.44	12.1
26	-	3.99	10.2
27	1.80	3.56	8.57
28	1.33	3.16	7.18
29	1.46	2.77	5.98
30	-	2.41	4.97
31	0.99	2.08	4.11

(a) Determined from the $^5\Phi_2$-x$^5\Delta_1$ (0,1) Q-branch.

(b) Based on the least-squares results of Table XVI.

(c) Blended lines involved.

V.B.4. Complex perturbation in $^5\Pi_3$, v=0

An even more complex perturbation is found in the $^5\Pi_3$, v=0 substate. This part of Fig. 15 is shown plotted to an enlarged energy scale in Fig. 17. With reference to the labels in the schematic inset, the following observations can be made:

(1) There is a large perturbation (P) of both parity components.

(2) In the upper component, Λ-doubling (LD1) increases to a maximum at about J = 20–22, then decreases to zero again as J increases.

(3) In the lower component, Λ-doubling (LD2) starts out large and gradually decreases as J increases.

(4) The magnitude of the Λ-doubling in the lower component is greater than that in the upper component.

(5) In the region U1, the energy of the upper parity component decreases with decreasing J less rapidly than expected based on the trend set in the immediately higher J region, with the result that the Λ-doublet splitting increases markedly.

(6) The same as (5) except for the other parity component in the region U2. However, the line assignments are not very certain here.

(7) At its high-J end, U1 starts at about the same J value as the Λ-doubling LD1 does.

Some thoughts:

(i) Clearly more than one perturbing state is present.

(ii) P must be caused by a degenerate state or states.

(iii) The Λ-doublings LD1 and LD2 must be caused by a nondegenerate (i.e. Σ) state or a degenerate state that is itself Λ-doubled.

(iv) The regions U1 and U2 indicate that either there are states below pushing upwards or states above that are moving farther away with decreasing J and, at least in the case of U2, that these states are non-degenerate or are

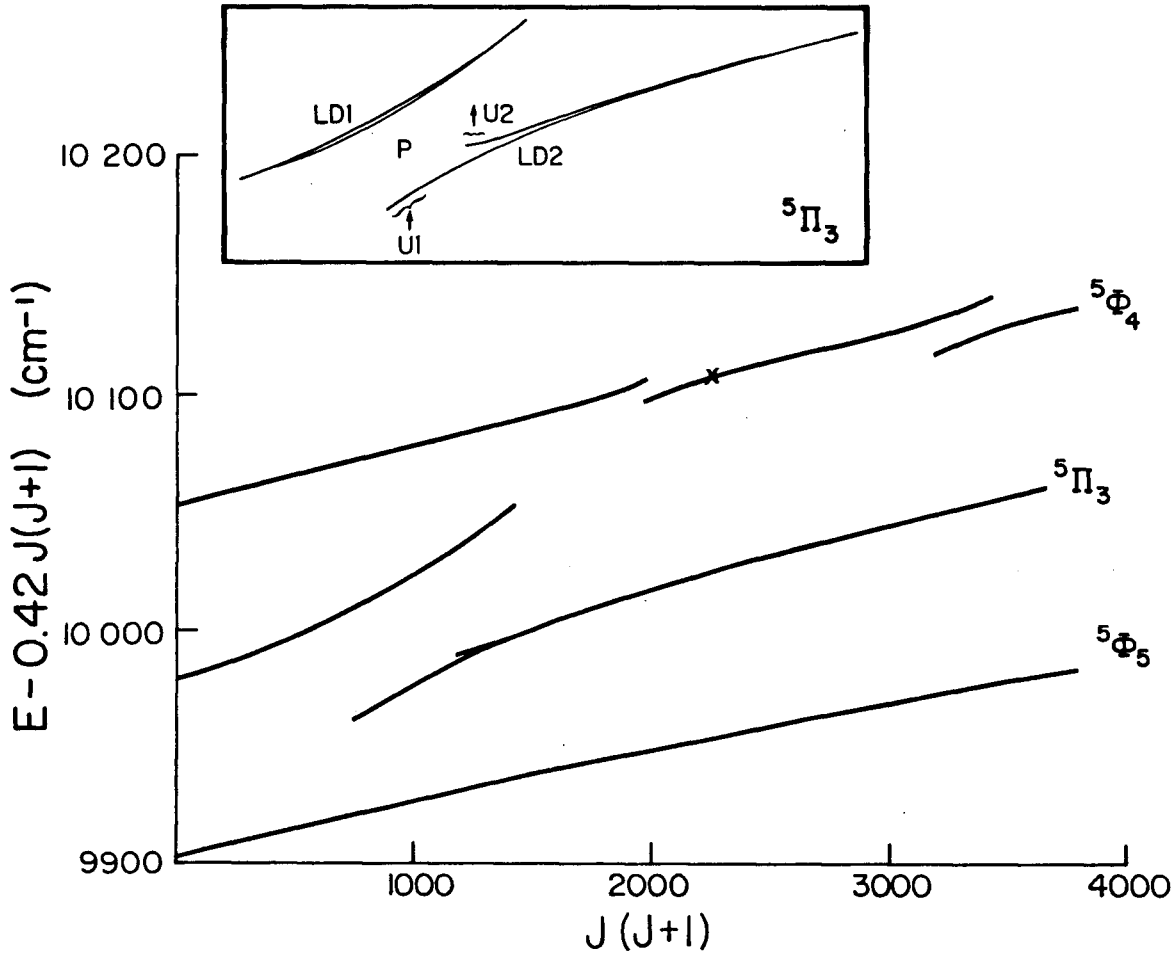

Fig. 17. The complex perturbation in $^5\Pi_3$, v=0. Perturbations in the nearby $^5\Phi_4$, v=0 substate are also shown, including a very small one, indicated by the "x," at J = 47. INSET: Schematic diagram pointing out various features. The labels cross-reference to the discussion in the text.

themselves Λ-doubled and so are probably the same state or states responsible for LD1 and LD2.

Based on the least-squares fitting results of Tables XII and XV, the two degenerate states that perturb the $^5\Phi_4$ substate (namely the $^3\Phi_4$ substate; and the unidentified substate that perturbs the $^5\Phi_4$ substate at J = 44, which will here be called "Y" for convenience), upon extrapolation are both in positions that make them obvious candidates for the states responsible for perturbation P. This is shown in Fig. 18(a). Ignoring the Λ-doubling effects for now, comparison with Fig. 5 shows that the upper component of the perturbed $^5\Pi_3$ substate appears to form a smooth transition from the $^5\Pi_3$ substate at low J to the Y substate at high J, just as state E_2' goes from E_2 to E_1 in Fig. 5. The crossing point of substates $^5\Pi_3$ and Y occurs at approximately $J_c = 25$. Similarly, the lower component forms a smooth transition from the $^5\Pi_3$ substate at high J to the $^3\Phi_4$ substate at low J, behaviour similar to that of E_1' in Fig. 5. For these two substates the crossing point occurs at approximately $J_c = 36$. The difference between this situation and that in Fig. 5 is that here there are *two* perturbing states. However, the two perturbing states are sufficiently far apart that the wavefunction of the upper component appears to be dominated by a mixture of $^5\Pi_3$ and Y, whereas the lower component appears to be predominantly a mixture of $^5\Pi_3$ and $^3\Phi_4$. Thus we can say that the interaction matrix element between the $^5\Pi_3$ and Y substates has the approximate value $|H_{12}| \simeq 17$ cm^{-1} obtained by subtracting the energy of Y from that of the perturbed $^5\Pi_3$ substate at $J = J_c$ (cf. eqn. (III.J.4)).[6] Similarly, for the $^5\Pi_3$ and $^3\Phi_4$ substates, $|H_{12}| \simeq 13$ cm^{-1} though this value is much less certain due to the much greater distance over which the $^3\Phi_4$ substate had to be extrapolated and due to the fact that the calculated energy position for the $^3\Phi_4$ substate varies by as much as

---

[6]The assumption is being made here that the crossing point of the zeroth-order states occurs at the same J value as the minimum separation of the perturbed states, as in a case (a)/case (a) homogeneous perturbation.

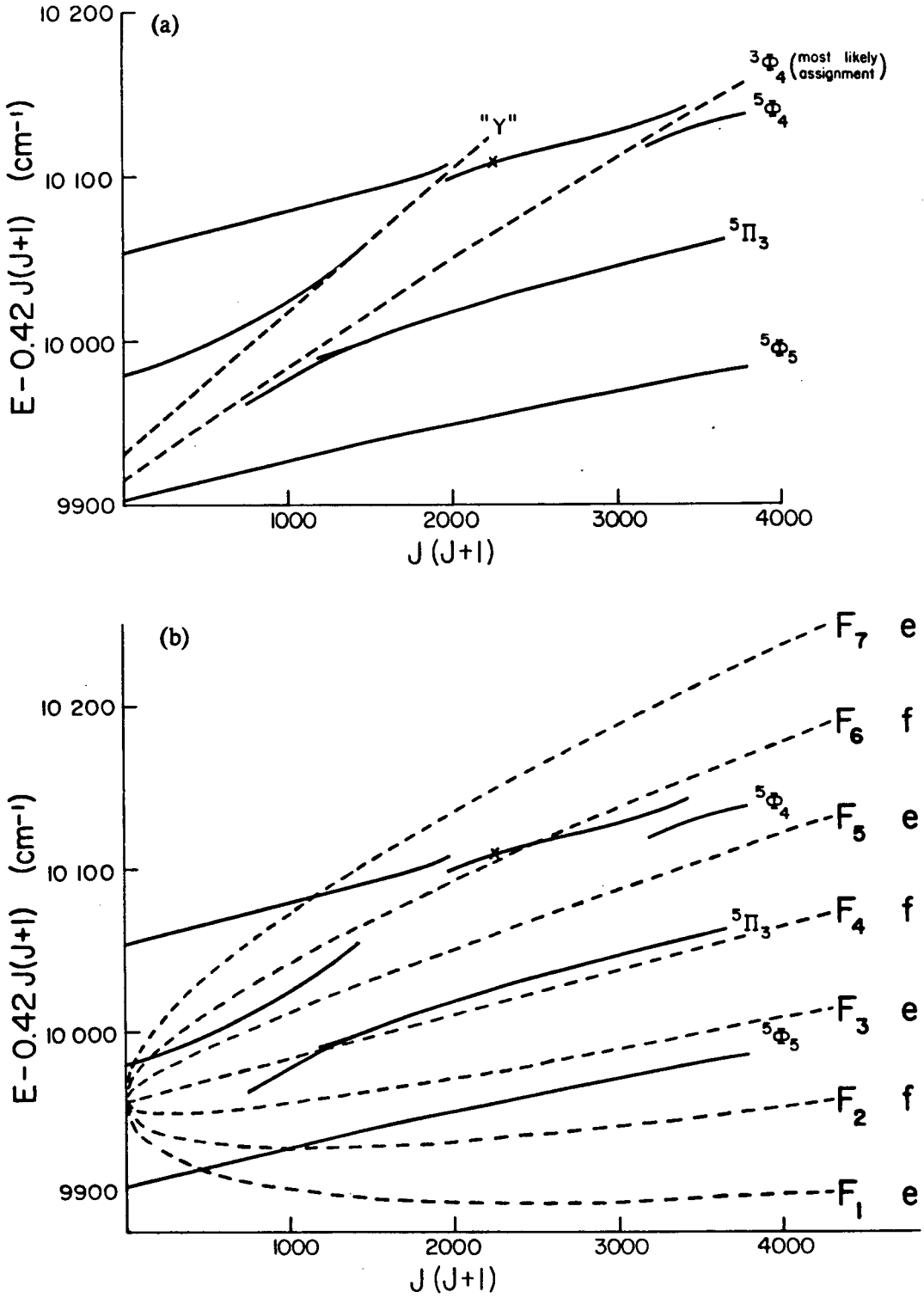

Fig. 18. Possible states responsible for the perturbation in $^5\Pi_3$, v=0.
(a) Substates $^3\Phi_4$ and "Y."
(b) A $^7\Sigma^+$ state.

several wavenumbers depending on which of the least-squares fits given in Table XII is used. Of course both these values of H_{12} are only very approximate and really represent limiting values, since each half of the perturbed set of levels cannot really be viewed in isolation. This is seen particularly in the $^5\Pi_3/^3\Phi_4$ interaction, which, assuming the identification $^3\Phi_4$ is correct, is not an allowed interaction by either homogeneous or heterogeneous mechanisms (cf. Table X). To make this interaction possible, state Y and/or the state responsible for the Λ-doubling must also be mixing in. The Λ-doubling effects appear to be smaller in magnitude than the other perturbations, so probably the contributions to the H_{12} values by the state responsible for the Λ-doublings is relatively small.

As for the state causing the Λ-doubling, the most obvious candidate would be a Σ state. As discussed in Section IV.B, the only low-lying Σ states predicted by the theoreticians are the $^5\Sigma^+$ and $^7\Sigma^+$ states that are now believed to lie close to the ground state (below 4 000 cm^{-1}). It is probably an upper vibrational level of one of these that makes its presence felt here.

Interactions involving $\Delta\Lambda = \pm 1$ can occur by means of the spin-orbit operator, the spin-electronic operator $H_{se} = B(r)L^{\pm}S^{\mp}$, or the $\underset{\sim}{L}$-uncoupling operator $-B(r)J^{\pm}L^{\mp}$ (Table X). Of these, only the spin-orbit operator is appropriate for a $^7\Sigma/^5\Pi$ interaction since it follows the selection rule $\Delta S = 0$ or 1, whereas the other two operators just have $\Delta S = 0$. All three operators must be considered for a $^5\Sigma/^5\Pi$ interaction, but if both H_{so} and H_{se} are acting, the effects of the latter would be small (since $B << A$) and difficult to distinguish from those of H_{so}. The matrix elements for a $^7\Sigma^+/^5\Pi$ interaction involving H_{so} are given in Table XVIII and those for a $^5\Sigma^+/^5\Pi$ interaction involving H_{so} and $-B(r)J^{\pm}L^{\mp}$ are given in Table XIX.

Considering the electron configurations of Section III.K and the number-of-different-spin-orbitals rules of Table X, the $^7\Sigma^+/^5\Pi_3$ interaction can occur via H_{so}, but no interaction between $^5\Sigma^+$ and $^5\Pi_3$ should occur with *any* of the three

TABLE XVIII. Spin-orbit matrix elements for a $^5\Pi_{(a)}/^7\Sigma^+_{(b)}$ interaction.[a,b,c]

$$\langle {}^5\Pi_{-1}^- | H_{so} | {}^7\Sigma_{F_1}^+ \rangle = -\frac{1}{2}\left[\frac{(J+1)(J-1)(J-2)}{7(2J+1)(2J-1)(2J-3)}\right]^{1/2} \xi_{^5\Pi,^7\Sigma}$$

$$\langle {}^5\Pi_{-1}^+ | H_{so} | {}^7\Sigma_{F_2}^+ \rangle = -\frac{1}{2}\left[\frac{(J-1)(J-2)}{21(2J+1)(2J-1)}\right]^{1/2} \xi_{^5\Pi,^7\Sigma}$$

$$\langle {}^5\Pi_{-1}^- | H_{so} | {}^7\Sigma_{F_3}^+ \rangle = +\frac{1}{2}(J+6)\cdot\frac{(J-1)}{105(2J+3)(2J+1)(2J-3)}\Bigg]^{1/2} \xi_{^5\Pi,^7\Sigma}$$

$$\langle {}^5\Pi_{-1}^+ | H_{so} | {}^7\Sigma_{F_4}^+ \rangle = +\left[\frac{(J+2)(J-1)}{70(2J+3)(2J-1)}\right]^{1/2} \xi_{^5\Pi,^7\Sigma}$$

$$\langle {}^5\Pi_{-1}^- | H_{so} | {}^7\Sigma_{F_5}^+ \rangle = +\frac{1}{2}(J-5)\left[\frac{(J+2)}{105(2J+5)(2J+1)(2J-1)}\right]^{1/2} \xi_{^5\Pi,^7\Sigma}$$

$$\langle {}^5\Pi_{-1}^+ | H_{so} | {}^7\Sigma_{F_6}^+ \rangle = -\frac{1}{2}\left[\frac{(J+3)(J+2)}{21(2J+3)(2J+1)}\right]^{1/2} \xi_{^5\Pi,^7\Sigma}$$

$$\langle {}^5\Pi_{-1}^- | H_{so} | {}^7\Sigma_{F_7}^+ \rangle = -\frac{1}{2}\left[\frac{(J+3)(J+2)(J)}{7(2J+5)(2J+3)(2J+1)}\right]^{1/2} \xi_{^5\Pi,^7\Sigma}$$

$$\langle {}^5\Pi_{0}^- | H_{so} | {}^7\Sigma_{F_1}^+ \rangle = -\left[\frac{J(J-1)(J-2)}{7(2J+1)(2J-1)(2J-3)}\right]^{1/2} \xi_{^5\Pi,^7\Sigma}$$

$$\langle {}^5\Pi_{0}^+ | H_{so} | {}^7\Sigma_{F_2}^+ \rangle = 0$$

$$\langle {}^5\Pi_{0}^- | H_{so} | {}^7\Sigma_{F_3}^+ \rangle = +\left[\frac{3(J+1)(J)(J-1)}{35(2J+3)(2J+1)(2J-3)}\right]^{1/2} \xi_{^5\Pi,^7\Sigma}$$

$$\langle {}^5\Pi_{0}^+ | H_{so} | {}^7\Sigma_{F_4}^+ \rangle = 0$$

$$\langle {}^5\Pi_{0}^- | H_{so} | {}^7\Sigma_{F_5}^+ \rangle = -\left[\frac{3(J+2)(J+1)J}{35(2J+5)(2J+1)(2J-1)}\right]^{1/2} \xi_{^5\Pi,^7\Sigma}$$

$$\langle {}^5\Pi_{0}^+ | H_{so} | {}^7\Sigma_{F_6}^+ \rangle = 0$$

$$\langle {}^5\Pi_{0}^- | H_{so} | {}^7\Sigma_{F_7}^+ \rangle = +\left[\frac{(J+3)(J+2)(J+1)}{7(2J+5)(2J+3)(2J+1)}\right]^{1/2} \xi_{^5\Pi,^7\Sigma}$$

(continued on next page)

TABLE XVIII (cont.)

$$\langle {}^5\Pi_1^- | H_{so} | {}^7\Sigma_{F_1}^+ \rangle = - \left[\frac{3(J+1)(J-1)(J-2)}{14(2J+1)(2J-1)(2J-3)} \right]^{1/2} \xi_{{}^5\Pi, {}^7\Sigma}$$

$$\langle {}^5\Pi_1^+ | H_{so} | {}^7\Sigma_{F_2}^+ \rangle = + \left[\frac{(J-1)(J-2)}{14(2J+1)(2J-1)} \right]^{1/2} \xi_{{}^5\Pi, {}^7\Sigma}$$

$$\langle {}^5\Pi_1^- | H_{so} | {}^7\Sigma_{F_3}^+ \rangle = + (J+6) \left[\frac{(J-1)}{70(2J+3)(2J+1)(2J-3)} \right]^{1/2} \xi_{{}^5\Pi, {}^7\Sigma}$$

$$\langle {}^5\Pi_1^+ | H_{so} | {}^7\Sigma_{F_4}^+ \rangle = - \left[\frac{3(J+2)(J-1)}{35(2J+3)(2J-1)} \right]^{1/2} \xi_{{}^5\Pi, {}^7\Sigma}$$

$$\langle {}^5\Pi_1^- | H_{so} | {}^7\Sigma_{F_5}^+ \rangle = + (J-5) \left[\frac{(J+2)}{70(2J+5)(2J+1)(2J-1)} \right]^{1/2} \xi_{{}^5\Pi, {}^7\Sigma}$$

$$\langle {}^5\Pi_1^+ | H_{so} | {}^7\Sigma_{F_6}^+ \rangle = + \left[\frac{(J+3)(J+2)}{14(2J+3)(2J+1)} \right]^{1/2} \xi_{{}^5\Pi, {}^7\Sigma}$$

$$\langle {}^5\Pi_1^- | H_{so} | {}^7\Sigma_{F_7}^+ \rangle = - \left[\frac{3(J+3)(J+2)(J)}{14(2J+5)(2J+3)(2J+1)} \right]^{1/2} \xi_{{}^5\Pi, {}^7\Sigma}$$

$$\langle {}^5\Pi_2^- | H_{so} | {}^7\Sigma_{F_1}^+ \rangle = - \left[\frac{(J+2)(J+1)(J-2)}{7(2J+1)(2J-1)(2J-3)} \right]^{1/2} \xi_{{}^5\Pi, {}^7\Sigma}$$

$$\langle {}^5\Pi_2^+ | H_{so} | {}^7\Sigma_{F_2}^+ \rangle = - 2 \left[\frac{(J+2)(J-2)}{21(2J+1)(2J-1)} \right]^{1/2} \xi_{{}^5\Pi, {}^7\Sigma}$$

$$\langle {}^5\Pi_2^- | H_{so} | {}^7\Sigma_{F_3}^+ \rangle = - (J-3) \left[\frac{5(J+2)}{21(2J+3)(2J+1)(2J-3)} \right]^{1/2} \xi_{{}^5\Pi, {}^7\Sigma}$$

$$\langle {}^5\Pi_2^+ | H_{so} | {}^7\Sigma_{F_4}^+ \rangle = - \left[\frac{10}{7(2J+3)(2J-1)} \right]^{1/2} \xi_{{}^5\Pi, {}^7\Sigma}$$

$$\langle {}^5\Pi_2^- | H_{so} | {}^7\Sigma_{F_5}^+ \rangle = + (J+4) \left[\frac{5(J-1)}{21(2J+5)(2J+1)(2J-1)} \right]^{1/2} \xi_{{}^5\Pi, {}^7\Sigma}$$

$$\langle {}^5\Pi_2^+ | H_{so} | {}^7\Sigma_{F_6}^+ \rangle = - 2 \left[\frac{(J+3)(J-1)}{21(2J+3)(2J+1)} \right]^{1/2} \xi_{{}^5\Pi, {}^7\Sigma}$$

$$\langle {}^5\Pi_2^- | H_{so} | {}^7\Sigma_{F_7}^+ \rangle = + \left[\frac{(J+3)(J)(J-1)}{7(2J+5)(2J+3)(2J+1)} \right]^{1/2} \xi_{{}^5\Pi, {}^7\Sigma}$$

(continued on next page)

TABLE XVIII (cont.)

$$\langle {}^5\Pi_3^- | H_{so} | {}^7\Sigma^+_{F_1} \rangle = -\frac{1}{2}\left[\frac{(J+3)(J+2)(J+1)}{7(2J+1)(2J-1)(2J-3)}\right]^{1/2} \xi_{{}^5\Pi,{}^7\Sigma}$$

$$\langle {}^5\Pi_3^+ | H_{so} | {}^7\Sigma^+_{F_2} \rangle = +\frac{1}{2}\left[\frac{(J+3)(J+2)}{7(2J+1)(2J-1)}\right]^{1/2} \xi_{{}^5\Pi,{}^7\Sigma}$$

$$\langle {}^5\Pi_3^- | H_{so} | {}^7\Sigma^+_{F_3} \rangle = -\frac{1}{2}\left[\frac{15(J+3)(J+2)(J-2)}{7(2J+3)(2J+1)(2J-3)}\right]^{1/2} \xi_{{}^5\Pi,{}^7\Sigma}$$

$$\langle {}^5\Pi_3^+ | H_{so} | {}^7\Sigma^+_{F_4} \rangle = +\left[\frac{5(J+3)(J-2)}{14(2J+3)(2J-1)}\right]^{1/2} \xi_{{}^5\Pi,{}^7\Sigma}$$

$$\langle {}^5\Pi_3^- | H_{so} | {}^7\Sigma^+_{F_5} \rangle = -\frac{1}{2}\left[\frac{15(J+3)(J-1)(J-2)}{7(2J+5)(2J+1)(2J-1)}\right]^{1/2} \xi_{{}^5\Pi,{}^7\Sigma}$$

$$\langle {}^5\Pi_3^+ | H_{so} | {}^7\Sigma^+_{F_6} \rangle = +\frac{1}{2}\left[\frac{3(J-1)(J-2)}{7(2J+3)(2J+1)}\right]^{1/2} \xi_{{}^5\Pi,{}^7\Sigma}$$

$$\langle {}^5\Pi_3^- | H_{so} | {}^7\Sigma^+_{F_7} \rangle = -\frac{1}{2}\left[\frac{J(J-1)(J-2)}{7(2J+5)(2J+3)(2J+1)}\right]^{1/2} \xi_{{}^5\Pi,{}^7\Sigma}$$

(a) Π^+ and Π^- are defined as in eqns. (III.G.14) and (III.G.16). For a ${}^5\Pi/{}^7\Sigma^-$ interaction, replace ${}^7\Sigma^+$ with ${}^7\Sigma^-$, ${}^5\Pi^-$ with ${}^5\Pi^+$, and ${}^5\Pi^+$ with ${}^5\Pi^-$, and change the signs of all the matrix elements.

(b) $$\xi_{{}^5\Pi,{}^7\Sigma} = \sum_e \langle \eta' \Lambda'=+1 | T'_{-q}(a_e \underset{\sim}{1}_e) | \eta\Lambda=0 \rangle \langle S'=2 \| T'(\underset{\sim}{s}_e) \| S=3 \rangle$$

(c) The subscripts (a) and (b) on ${}^5\Pi_{(a)}$ and ${}^7\Sigma^+_{(b)}$ denote Hund's coupling cases.

TABLE XIX. Spin-orbit and $\underset{\sim}{L}$-uncoupling matrix elements for a $^5\Pi_{(a)}/^5\Sigma^+_{(b)}$ interaction.[a,b,c]

$$\langle {}^5\Pi_{-1}^- | H | {}^5\Sigma_{F_1}^+ \rangle = -\left[\frac{(J+1)(J-1)}{(2J+1)(2J-1)}\right]^{1/2}\left\{\sqrt{\frac{2}{15}}\,\xi_{{}^5\Pi,{}^5\Sigma} + B_{v'v}(J+2)\,\eta_{\Pi,\Sigma}\right\}$$

$$\langle {}^5\Pi_{-1}^+ | H | {}^5\Sigma_{F_2}^+ \rangle = -\left[\frac{J-1}{2J+1}\right]^{1/2}\left\{\frac{1}{\sqrt{15}}\,\xi_{{}^5\Pi,{}^5\Sigma} + \sqrt{2}\,B_{v'v}(J+2)\,\eta_{\Pi,\Sigma}\right\}$$

$$\langle {}^5\Pi_{-1}^- | H | {}^5\Sigma_{F_3}^+ \rangle = +\left[\frac{1}{(2J+3)(2J-1)}\right]^{1/2}\left\{\frac{1}{\sqrt{5}}\,\xi_{{}^5\Pi,{}^5\Sigma} - \sqrt{6}\,B_{v'v}(J+2)(J-1)\,\eta_{\Pi,\Sigma}\right\}$$

$$\langle {}^5\Pi_{-1}^+ | H | {}^5\Sigma_{F_4}^+ \rangle = +\left[\frac{J+2}{2J+1}\right]^{1/2}\left\{\frac{1}{\sqrt{15}}\,\xi_{{}^5\Pi,{}^5\Sigma} - \sqrt{2}\,B_{v'v}(J-1)\,\eta_{\Pi,\Sigma}\right\}$$

$$\langle {}^5\Pi_{-1}^- | H | {}^5\Sigma_{F_5}^+ \rangle = +\left[\frac{(J+2)(J)}{(2J+3)(2J+1)}\right]^{1/2}\left\{\sqrt{\frac{2}{15}}\,\xi_{{}^5\Pi,{}^5\Sigma} - B_{v'v}(J-1)\,\eta_{\Pi,\Sigma}\right\}$$

$$\langle {}^5\Pi_{0}^- | H | {}^5\Sigma_{F_1}^+ \rangle = -\left[\frac{J(J-1)}{(2J+1)(2J-1)}\right]^{1/2}\left\{\sqrt{\frac{3}{10}}\,\xi_{{}^5\Pi,{}^5\Sigma} + 2(J+1)\,B_{v'v}\,\eta_{\Pi,\Sigma}\right\}$$

$$\langle {}^5\Pi_{0}^+ | H | {}^5\Sigma_{F_2}^+ \rangle = -B_{v'v}\left[\frac{2(J+1)(J)(J-1)}{2J+1}\right]^{1/2}\eta_{\Pi,\Sigma}$$

$$\langle {}^5\Pi_{0}^- | H | {}^5\Sigma_{F_3}^+ \rangle = +\left[\frac{J(J+1)}{(2J+3)(2J-1)}\right]^{1/2}\left\{\frac{1}{\sqrt{5}}\,\xi_{{}^5\Pi,{}^5\Sigma} - \sqrt{6}\,B_{v'v}\,\eta_{\Pi,\Sigma}\right\}$$

$$\langle {}^5\Pi_{0}^+ | H | {}^5\Sigma_{F_4}^- \rangle = +B_{v'v}\left[\frac{2(J+2)(J+1)J}{2J+1}\right]^{1/2}\eta_{\Pi,\Sigma}$$

$$\langle {}^5\Pi_{0}^- | H | {}^5\Sigma_{F_5}^+ \rangle = -\left[\frac{(J+2)(J+1)}{(2J+3)(2J+1)}\right]^{1/2}\left\{\sqrt{\frac{3}{10}}\,\xi_{{}^5\Pi,{}^5\Sigma} - 2\,B_{v'v}J\eta_{\Pi,\Sigma}\right\}$$

$$\langle {}^5\Pi_{1}^- | H | {}^5\Sigma_{F_1}^+ \rangle = -\left[\frac{(J+1)(J-1)}{(2J+1)(2J-1)}\right]^{1/2}\left\{\frac{1}{\sqrt{5}}\,\xi_{{}^5\Pi,{}^5\Sigma} + \sqrt{6}\,B_{v'v}\,\eta_{\Pi,\Sigma}\right\}$$

$$\langle {}^5\Pi_{1}^+ | H | {}^5\Sigma_{F_2}^+ \rangle = +\left[\frac{J-1}{10(2J+1)}\right]^{1/2}\xi_{{}^5\Pi,{}^5\Sigma}$$

$$\langle {}^5\Pi_{1}^- | H | {}^5\Sigma_{F_3}^+ \rangle = +\left[\frac{1}{(2J+3)(2J-1)}\right]^{1/2}\left\{\sqrt{\frac{3}{10}}\,\xi_{{}^5\Pi,{}^5\Sigma} + 2\,B_{v'v}J(J+1)\,\eta_{\Pi,\Sigma}\right\}$$

$$\langle {}^5\Pi_{1}^+ | H | {}^5\Sigma_{F_4}^+ \rangle = -\left[\frac{J+2}{10(2J+1)}\right]^{1/2}\xi_{{}^5\Pi,{}^5\Sigma}$$

$$\langle {}^5\Pi_{1}^- | H | {}^5\Sigma_{F_5}^+ \rangle = +\left[\frac{(J+2)J}{(2J+3)(2J+1)}\right]^{1/2}\left\{\frac{1}{\sqrt{5}}\,\xi_{{}^5\Pi,{}^5\Sigma} - \sqrt{6}\,B_{v'v}(J+1)\,\eta_{\Pi,\Sigma}\right\}$$

(continued on next page)

TABLE XIX (cont.)

$$\langle {}^5\Pi_2^- | H | {}^5\Sigma_{F_1}^+ \rangle = - \left[\frac{(J+2)(J+1)}{(2J+1)(2J-1)}\right]^{1/2} \left\{ \frac{1}{\sqrt{30}} \xi_{{}^5\Pi,{}^5\Sigma} + 2 B_{v'v} (J-1) \eta_{\Pi,\Sigma} \right\}$$

$$\langle {}^5\Pi_2^+ | H | {}^5\Sigma_{F_2}^+ \rangle = + \left[\frac{J+2}{2J+1}\right]^{1/2} \left\{ \frac{1}{\sqrt{15}} \xi_{{}^5\Pi,{}^5\Sigma} + \sqrt{2}\, B_{v'v} (J-1) \eta_{\Pi,\Sigma} \right\}$$

$$\langle {}^5\Pi_2^- | H | {}^5\Sigma_{F_3}^+ \rangle = - \left[\frac{(J+2)(J-1)}{(2J+3)(2J-1)}\right]^{1/2} \left\{ \frac{1}{\sqrt{5}} \xi_{{}^5\Pi,{}^5\Sigma} - \sqrt{6}\, B_{v'v} \eta_{\Pi,\Sigma} \right\}$$

$$\langle {}^5\Pi_2^+ | H | {}^5\Sigma_{F_4}^+ \rangle = + \left[\frac{J-1}{2J+1}\right]^{1/2} \left\{ \frac{1}{\sqrt{15}} \xi_{{}^5\Pi,{}^5\Sigma} - \sqrt{2}\, B_{v'v} (J+2) \eta_{\Pi,\Sigma} \right\}$$

$$\langle {}^5\Pi_2^- | H | {}^5\Sigma_{F_5}^+ \rangle = - \left[\frac{J(J-1)}{(2J+3)(2J+1)}\right]^{1/2} \left\{ \frac{1}{\sqrt{30}} \xi_{{}^5\Pi,{}^5\Sigma} - 2 B_{v'v} (J+2) \eta_{\Pi,\Sigma} \right\}$$

$$\langle {}^5\Pi_3^- | H | {}^5\Sigma_{F_1}^+ \rangle = -B_{v'v} \left[\frac{(J+3)(J+2)(J+1)(J-2)}{(2J+1)(2J-1)}\right]^{1/2} \eta_{\Pi,\Sigma}$$

$$\langle {}^5\Pi_3^+ | H | {}^5\Sigma_{F_2}^+ \rangle = +B_{v'v} \left[\frac{2(J+3)(J+2)(J-2)}{2J+1}\right]^{1/2} \eta_{\Pi,\Sigma}$$

$$\langle {}^5\Pi_3^- | H | {}^5\Sigma_{F_3}^+ \rangle = -B_{v'v} \left[\frac{6(J+3)(J+2)(J-1)(J-2)}{(2J+3)(2J-1)}\right]^{1/2} \eta_{\Pi,\Sigma}$$

$$\langle {}^5\Pi_3^+ | H | {}^5\Sigma_{F_4}^+ \rangle = +B_{v'v} \left[\frac{2(J+3)(J-1)(J-2)}{2J+1}\right]^{1/2} \eta_{\Pi,\Sigma}$$

$$\langle {}^5\Pi_3^- | H | {}^5\Sigma_{F_5}^+ \rangle = -B_{v'v} \left[\frac{(J+3)(J)(J-1)(J-2)}{(2J+3)(2J+1)}\right]^{1/2} \eta_{\Pi,\Sigma}$$

(a) Π^+ and Π^- are defined as in eqns. (III.G.14) and (III G.16). For a ${}^5\Pi/{}^5\Sigma^-$ interaction, replace ${}^5\Sigma^+$ with ${}^5\Sigma^-$, ${}^5\Pi^-$ with ${}^5\Pi^+$, and ${}^5\Pi^+$ with ${}^5\Pi^-$, and change the signs of all the matrix elements.

(b) $$\xi_{{}^5\Pi,{}^5\Sigma} = \sum_e \langle \eta'\Lambda'=+1 | T'_{-q}(a_e 1_e) | \eta\Lambda=0 \rangle \langle S'=2 \| T'(s_e) \| S=2 \rangle$$

$$\eta_{\Pi,\Sigma} = \sum_e \langle \eta'\Lambda'=+1 | T'_{-q}(1_e) | \eta\Lambda=0 \rangle$$

$$B_{v'v} = \frac{h}{8\pi^2 c\mu} \left\langle v' \left| \frac{1}{r^2} \right| v \right\rangle$$

(c) The subscripts (a) and (b) in ${}^5\Pi_{(a)}$ and ${}^5\Sigma^+_{(b)}$ denote Hund's coupling cases.

operators. Thus, based on the single electronic configuration picture, the $^7\Sigma^+$ state is the more likely perturbing state.

The rotational energy levels of Σ states are given approximately by the case (b) expression

$$F(N) = BN(N+1) \qquad \text{...(V.B.23)}$$

Each N-level is (2S+1)-fold degenerate in J,[7] with the possible values of J being

$$J = N+S,\ N+S-1,\ N+S-2,\ \ldots,\ |N-S| \qquad \text{...(V.B.24)}$$

The (2S+1) components are designated F_1, F_2, ..., F_{2S+1}, where the correspondence between these labels and the J and N quantum numbers is[7]

F_1	$J = N+S$	$N = J-S$	
F_2	$J = N+S-1$	$N = J-S+1$	
F_3	$J = N+S-2$	$N = J-S+2$	
⋮	⋮	⋮	
F_{2S+1}	$J = N-S$	$N = J+S$	...(V.B.25)

To the level of approximation of eqn. (V.B.23), the (2S+1) levels with the same N are degenerate,

$$F_1(N) = F_2(N) = \ldots = F_{2S+1}(N) \qquad \text{...(V.B.26)}$$

but the (2S+1) levels having the same J are not degenerate; rather

$$F_1(J) < F_2(N) < \ldots < F_{2S+1}(J) \qquad \text{...(V.B.27)}$$

Thus in a plot of energy versus J(J+1) the components of a multiplet Σ state will splay apart with increasing J into (2S+1) "arms".

---

[7]Except when N<S. Eqn. (V.B.24) still holds in this case.

Such a plot has been made for a $^7\Sigma$ state having term origin T_v = 9 956 cm^{-1} and a B value of 0.447 cm^{-1} in Fig. 18(b). From this figure the Λ-doubling effects are then readily explained. LD1 is caused by interaction with the F_5 arm of the $^7\Sigma^+$ state. This Λ-doubling reaches a maximum then decreases again due to the curvatures of both the perturbed $^5\Pi_3$ substate and the F_5 component of the $^7\Sigma^+$ state; these curvatures are such that the two states reach a minimum separation in the J = low-20s then depart from each other again. The Λ-doubling in the lower component of the perturbed $^5\Pi_3$ substate, i.e. LD2, is caused by the close-lying F_4 component, and in particular, U2 is caused by an avoided crossing between F_4 and one parity component of the $^5\Pi_3$ substate (the f component).

This model also explains yet another perturbation observed in the spectrum, namely a very small perturbation present in the $^5\Phi_4$ substate. It was mentioned briefly in Section V.B.2 that lines involving the J = 47 level of the $^5\Phi_4$ substate are fat and weak in intensity. In fact, this perturbation appears very similar to the ground state perturbation described in Section IV.D and shown in Fig. 12. In Fig. 18(b), the F_6 component is shown crossing the $^5\Phi_4$ substate in the neighborhood of J = 47, so it is tempting, and quite reasonable, to assign this $^7\Sigma^+$ component as the cause of this perturbation.

Quite a number of features in the spectrum are thus explained by this energy-level picture. Of course, when higher order effects, particularly the spin-spin interaction terms, are included in the $^7\Sigma^+$ model, the actual energies of the various components will shift around relative to each other, but the basic features will remain the same.

There is only one problem with this model. Both the F_6 and F_7 components of the $^7\Sigma^+$ state must cross the $^5\Pi_3$ substate somewhere in the low-J region. When they cross, they should cause Λ-doubling, and an avoided crossing of one Λ-doublet component or the other should be observed, just as the avoided crossing

with the F_4 component causes the U2 feature described previously. Such is not the case.

The interaction between the $^7\Sigma^+$ state and the $^5\Pi$ state must occur via the spin-orbit operator. The interaction matrix elements given in Table XVIII were derived using eqn. (V.B.8), with both the $^5\Pi$ and $^7\Sigma$ states initially written in case (a) bases. The Σ state was then converted to a case (b) basis by means of the following relation given by Brown and Howard (7):

$$|\eta N\Lambda SJ\rangle = \sum_{\Sigma\Omega} (-1)^{N-S+\Omega}(2N+1)^{1/2} \begin{pmatrix} J & S & N \\ \Omega & -\Sigma & -\Lambda \end{pmatrix} |\eta\Lambda S\Sigma J\Omega\rangle \quad ...(V.B.28)$$

The $^5\Pi$ state was then converted to a parity basis by performing a Wang transformation (eqn. (III.H.63)) or, equivalently, by means of eqn. (III.G.13).

The matrix element for the $^5\Pi_3/^7\Sigma^+_{F_6}$ and $^5\Pi_3/^7\Sigma^+_{F_7}$ interactions are non-zero. To take a specific example,

$$\langle ^5\Pi^+_3 | H_{SO} | ^7\Sigma^+_{F_6}\rangle = 0.14\,\xi_{^5\Pi,^7\Sigma} \qquad \text{at } J = 14 \qquad ...(V.B.29)$$

whereas near the $^5\Pi_3/^7\Sigma^+_{F_4}$ crossing point,

$$\langle ^5\Pi^+_3 | H_{SO} | ^7\Sigma^+_{F_4}\rangle = 0.30\,\xi_{^5\Pi,^7\Sigma} \qquad \text{at } J = 34 \qquad ...(V.B.30)$$

Although the strength of the $^5\Pi_3/^7\Sigma^+_{F_6}$ interaction is less than that of the $^5\Pi_3/^7\Sigma^+_{F_4}$ interaction and becomes even smaller at lower J values, when one considers that the Λ-doublet splitting at J = 34 is 2.18 cm^{-1} the Λ-doubling due to the $^5\Pi_3/^7\Sigma^+_{F_6}$ interaction should certainly by observable and if the crossing point occurs in the region LD1 where a small Λ-doubling is already present, it should be observable as a much larger splitting than in the rest of the LD1 region and the pattern should be recognizable as that of a local avoided crossing (cf. Fig. 5) for one of the Λ-doublet components (the f component).

There is no such evidence in the spectrum for an avoided crossing between the $^5\Pi_3$ (f) and $^7\Sigma^+_{F_6}$ components. It cannot be stated with absolute certainty that the perturbing state is not a $^7\Sigma^+$ state, since the model being used has omitted a number of small terms that may alter the picture. But the absence of evidence for a $^5\Pi_3/^7\Sigma^+_{F_6}$ perturbation does mean that we must at least consider other possibilities.

We therefore reconsider $^5\Sigma^+$ as a possibility for the perturbing state, even though this state has previously been rejected on electron configuration grounds. Fig. 18(b) also applies for a $^5\Sigma^+$ state, the only changes being that the top and bottom arms of the $^7\Sigma^+$ state are not present in the $^5\Sigma^+$ state; the remaining components must then be renumbered, with the old F_2 component being the new F_1 component, etc.; and all the e and f parity-doublet labels must be interchanged. All the observed spectral features explained by the $^7\Sigma^+$ model are still explained by the $^5\Sigma^+$ model.

The matrix elements for a $^5\Pi/^5\Sigma^+$ interacton have been given in Table XIX. The terms involving H_{SO} were derived in the same manner as described previously for the $^5\Pi/^7\Sigma^+$ interaction. In this case there are also terms arising from the $\underset{\sim}{L}$-uncloupling operator (which is part of the $-2B(r)\underset{\sim}{J}\cdot\underset{\sim}{L}$ operator — that part off-diagonal in Λ). These terms were derived using the same methods as those used for H_{SO} (although it was, of course, not necessary to use spherical tensor methods to set up the case (a) matrices for such a trivial situation as this — eqns. (III.F.9) and (F.10) could have been used instead).

Although the $\underset{\sim}{L}$-uncoupling terms will be much smaller than the spin-orbit terms (since $B<<A$), it is still necessary to consider the former, especially where spin-orbit interactions cannot occur while $\underset{\sim}{L}$-uncoupling interactions can. This is the situation for a $^5\Pi_3/^5\Sigma$ interaction — i.e.

$$\langle ^5\Pi_3 | H_{SO} | ^5\Sigma \rangle = 0 \qquad \text{...(V.B.31)}$$

for all components of the $^5\Sigma$ state. This arises because a $^5\Sigma$ state, when described in case (a) terms, does not contain $\Omega = 3$. Making a similar comparison to that performed in eqns. (V.B.29) and (30) for the $^5\Pi_3/^7\Sigma^+$ interaction,

$$<^5\Pi_3^- | -2B(r)J^-L^+ | ^5\Sigma^+_{F_5}> = -6.43\, B_{vv}, \eta_{\Pi,\Sigma} \text{ at } J = 14 \quad ...(V.B.32)$$

$$<^5\Pi_3^- | -2B(r)J^-L^+ | ^5\Sigma^+_{F_3}> = -42.1\, B_{vv}, \eta_{\Pi,\Sigma} \text{ at } J = 34 \quad ...(V.B.33)$$

The ratio of these is smaller than in the $^5\Pi_3/^7\Sigma^+$ case, but if an avoided crossing between the $^5\Pi_3^-$ and $^5\Sigma^+_{F_5}$ components occurs (where $^5\Sigma^+_{F_5}$ corresponds to $^7\Sigma^+_{F_6}$ in Fig. 18(b)), it still should be observable. Thus, the $^5\Sigma^+$ state is not really any more likely to be the perturbing state than the $^7\Sigma^+$ state and we must leave the question of which of these states is involved open.

In summary, the massive and very complex perturbation present in the $^5\Pi_3$, v=0 substate is probably primarily caused by the two substates that also perturb the $^5\Phi_4$ substate, namely the substate that has arbitrarily been labelled Y and the substate that is believed to be a $^3\Phi_4$ substate. Irregular Λ-doubling effects are also present and indicate the additional presence of a Σ state. Of the two theoretically predicted low-lying Σ states, the $^7\Sigma^+$ state is the only one that can interact with the $^5\Pi_3$ substate within the single electronic configuration picture, but this model is only an approximation and predictions based upon it need to be backed up with experimental evidence. Unfortunately, we are unable to distinguish experimentally between the $^7\Sigma^+$ and $^5\Sigma^+$ states, with both being equally consistent with observations. The apparent lack of certain expected perturbations for either state is probably the result of the crudeness of the model used for the Σ states, with spin-spin, spin-rotation, and higher-order terms omitted. The Σ state, whatever its identity, is probably also responsible for the small perturbation at J = 47 of the $^5\Phi_4$ substate.

This picture is consistent with and explains all seven observed features described at the beginning of this section, with point (7) being merely the result of an indirect relationship (i.e. essentially just a coincidence).

Effective spectroscopic constants for the $^3\Phi_4$ and Y substates have been given previously in Tables XIII and XVI, respectively, and with four interacting states present here no attempt has been made to improve upon these values by a deperturbation of this complex region. Based on the very crude model used here, the effective term origin and B value for the Σ state appear to be, very approximately, $T_v \simeq 9\,952$ cm^{-1} and $B_v \simeq 0.450$ cm^{-1}.

V.B.5. Complex perturbations in $^5\Pi_0$, v=0 and nearby substates

The $^5\Pi_0$, v=0, $^5\Pi_3$, v=1, and $^5\Phi_4$, v=1 substates lie in the same energy region, crossing one another, and so must be considered together as a group. Fortunately there is little interaction between these states themselves, though one such interaction has been observed and will be discussed below (in Section V.B.5.a). There is at least one other state lying in this same region, however, and it interacts with all of them. The pattern of interactions is very complex and it has not been possible to unscramble the levels of this state completely, but it can be said with certainty that this state must be a Σ state, and it is possible that there may be more than one Σ state.

The observed energy levels are shown in Fig. 19. The most obvious features are very large Λ-doubling in $^5\Pi_0$ (which will be discussed in Section V.C.1) and an avoided crossing in $^5\Pi_3$. The latter affects only one parity component of the $^5\Pi_3$ substate, with the other component passing through the perturbation region unscathed. The perturbing state clearly must be non-degenerate in nature. Least-squares fitting of the perturbed component was attempted using the standard homogeneous and heterogeneous fitting methods described in Section V.B.1, but neither model would

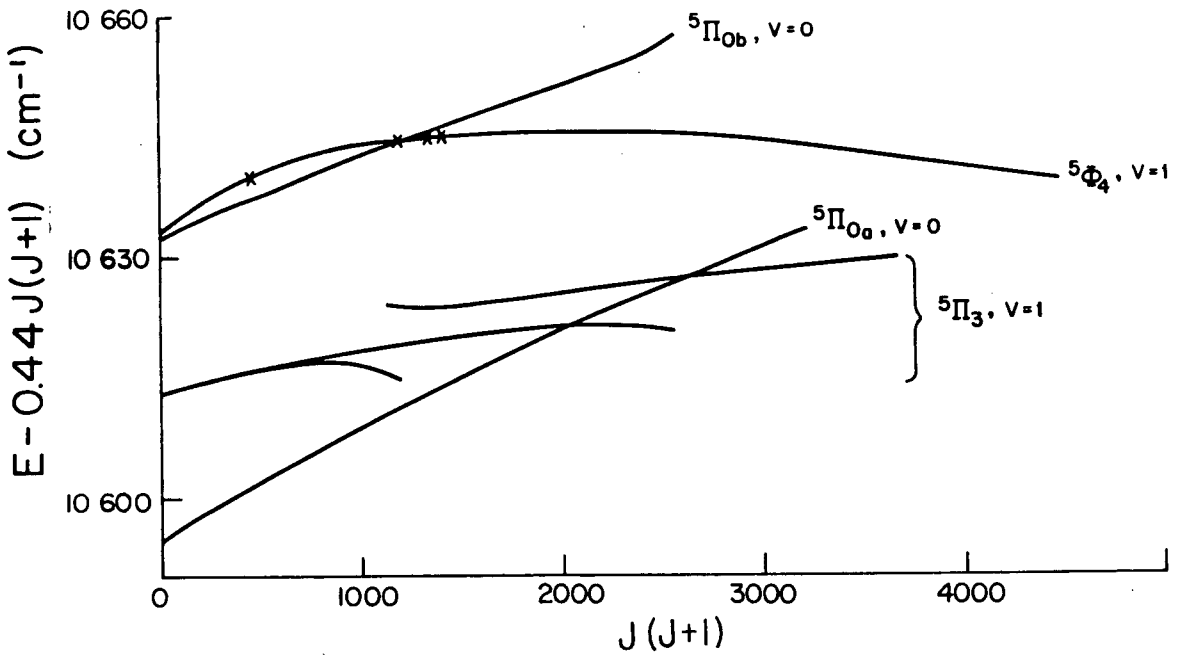

Fig. 19. The $^5\Pi_0$, v=0, $^5\Pi_3$, v=1, and $^5\Phi_4$, v=1 substates.

converge. This is readily explained if the perturbing state is a Σ state. The statement made earlier (Section III.J) that the interaction matrix element for a homogeneous perturbation is J-independent and that for a heterogeneous perturbation has an approximately $\sqrt{J(J+1)}$ J-dependence applies to a situation where both states exhibit case (a) coupling behavior. As seen for example from the matrix elements in Table XIX, however, when one of the states is in case (b), both homogeneous and heterogeneous interactions are J-dependent and this J-dependence can be quite complex. Also, the energy levels of a case (b) state when plotted against $J(J+1)$ appear curved (see e.g. Fig. 18(a)) and thus the case (a) model $T_v + B_v J(J+1) - \ldots$ is not appropriate. Thus if the perturbing state is a Σ state in case (b) it is not surprising that the least-squares fits, which were based on case (a) models, would not converge.

To the high-J side of this perturbation, the Λ-doublet separation does not return to zero again, but rather goes through a minimum, then starts to increase again. In this case, it is the other parity component that is perturbed — pushed down in energy, thus causing the increase in Λ-doublet splitting. The two perturbing states are probably adjacent components of a multiplet Σ state.

The energy levels of the upper parity component of the $^5\Pi_0$, $v=0$ substate, when plotted against $J(J+1)$ exhibit a dip in the region $J = 19$–26. This is just barely detectable in Fig. 19 and is shown enlarged in Fig. 20. This is not a pattern that would be produced by a simple avoided crossing of two levels. However, it could be caused by a state approaching the $^5\Pi_0$ substate from above then moving away again with increasing J — i.e. by a state that appears curved on an energy versus $J(J+1)$ plot, the most likely candidate being one of the components of a multiplet Σ state.

The $^5\Phi_4$, $v=1$ substate also exhibits a small perturbation in this same region. Lines involving the $^5\Phi_4$ $J = 21$ level are broadened and weak in intensity. This

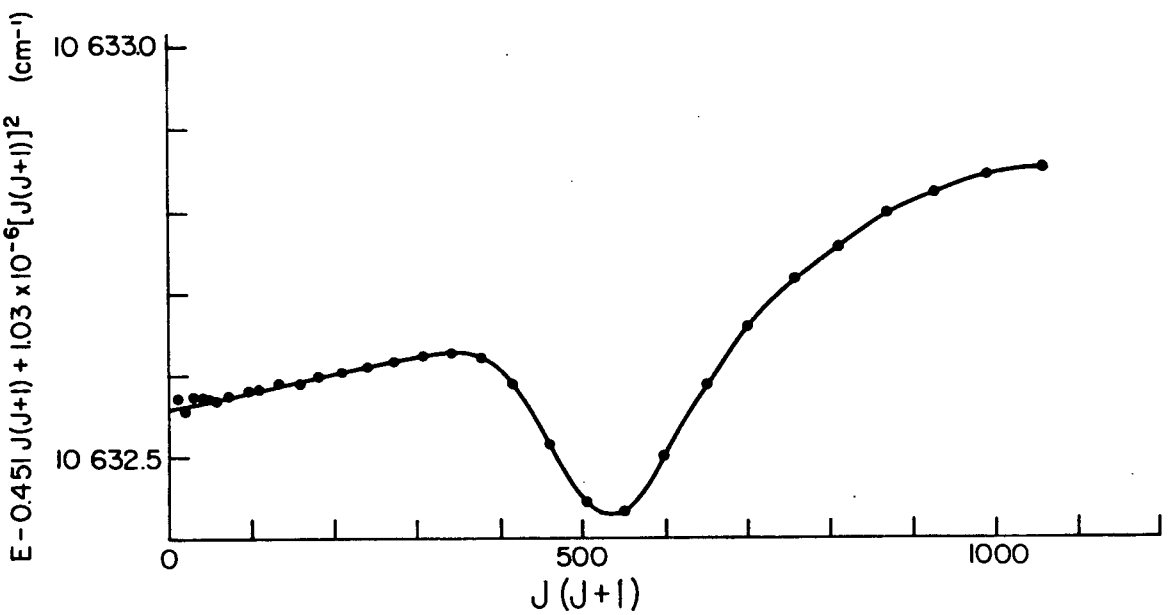

Fig. 20. Detail of one perturbation in the upper parity component of $^5\Pi_0$, v=0.

almost certainly ties in with the $^5\Pi_0$, v=0 perturbation, as shown schematically in Fig. 21.

There are several other small perturbations in the $^5\Phi_4$, v=1 substate. Lines involving the $^5\Phi_4$ levels having J = 34, 36, and 37 are doubled (those involving J = 35 are single and sharp, however). Also, Λ-doubling becomes detectable at J = 42 and gradually increases with J beyond this point. Discussion about the J = 34 perturbation will be reserved for Section V.B.5.a. Little can be said about the Λ-doubling from J = 42 on. It of course implies the presence of a Σ state or states somewhere, but in the absence of an avoided crossing it cannot be said how near or far away it lies, although it is *probably* fairly close-lying since interaction between a Σ state and a Φ state must be a very high-order effect so will probably be very small unless the levels are close together. As for the perturbation at J = 36–37, lines involving both J levels are doubled, with components of approximately equal intensities. One component of each pair appears to be in its unperturbed position, while the other is perturbed. At J = 36, the perturbed component is pushed to higher energy by ~0.047 cm^{-1} while at J = 37, the perturbed component is pushed ~0.043 cm^{-1} to lower energy. This is clearly an avoided crossing by a non-degenerate state (which therefore leaves one parity component unperturbed), probably one component of a multiplet Σ state.

Yet another component of the Σ state may be responsible for pushing the $^5\Pi_0$, v=0, upper parity component upwards in energy at its high-J end, though in this case there is no direct evidence as to whether the perturbing state is degenerate or non-degenerate. The assumption is being made that it is part of the Σ state or states that have already been shown to be present, rather than a new state. Also, when drawn as in Fig. 22, another component of a multiplet Σ state *appears* to fit. (However, an alternative explanation for this perturbation will be given in Section V.C.1)

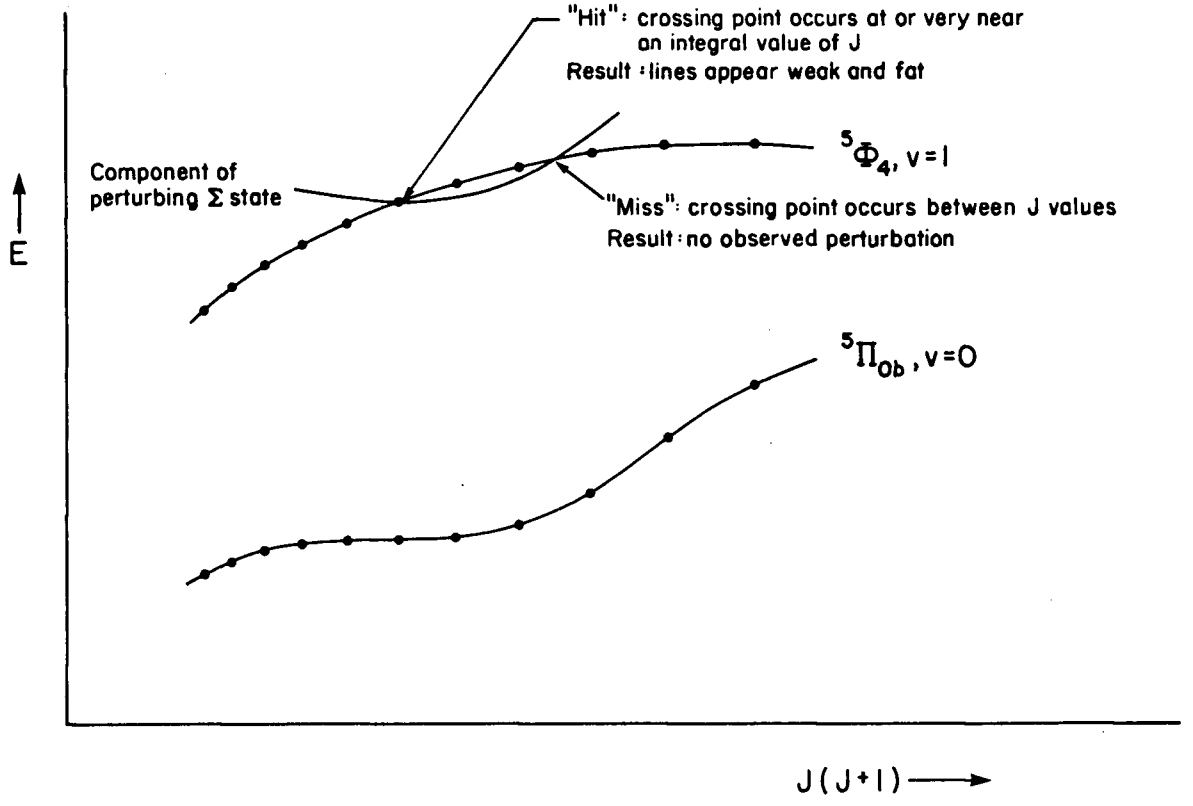

Fig. 21. Probable explanation for the perturbations in $^5\Pi_0$, v=0 and $^5\Phi_4$, v=1 (schematic).

Fig. 22 shows schematically the various components of a multiplet Σ state or states that have been demonstrated in this section to be present. Just how these various parts connect up and whether they all belong to one Σ state or to two remains to be determined, and, unfortunately, there is insufficient evidence to do so. The *appearance* is that the top three components belong to one multiplet Σ state and that the bottom two (or three if the component represented by the dotted curve is shown roughly correctly), which seem to have rather different B values even allowing for curvature due to the state being in case (b), belong to another. Also, the topmost component has been shown to curve upwards. Comparison with Fig. 18(b) shows that it is unlikely that an upward curving component would have at least four other components below it. However, this evidence is not very substantial.

The fact that neither of the two lowest components interacts with the lower parity component of the $^5\Pi_0$ substate (even though they must both cross it and even though one of these must have parity e and the other f) while two of the upper three components do interact with the upper $^5\Pi_0$ parity component might, at first thought, be regarded as evidence that the upper and lower sets of components belong to two different Σ states. However, examination of the matrix elements in Tables XVIII and XIX shows that only the e parity component of a $^5\Pi_0$ substate (i.e. $^5\Pi_0^-$) can interact with a $^7\Sigma^+$ state and only the e parity component can interact via the spin–orbit operator with a $^5\Sigma^+$ state, though a small interaction between the f comonent (i.e. $^5\Pi_0^+$) can occur with a $^5\Sigma^+$ state via the $\underset{\sim}{L}$–uncoupling operator. Thus if the lower parity component of the $^5\Pi_0$ substate has parity f, it cannot interact with a $^7\Sigma^+$ state and can do so only weakly with a $^5\Sigma^+$ state.

The conclusion from these considerations is that we are unable to decide whether the various components of a Σ state that have clearly been demonstrated to be present belong to one multiplet Σ state or to two. This result is unfortunate, because if it could be shown that all the components do belong to the same state,

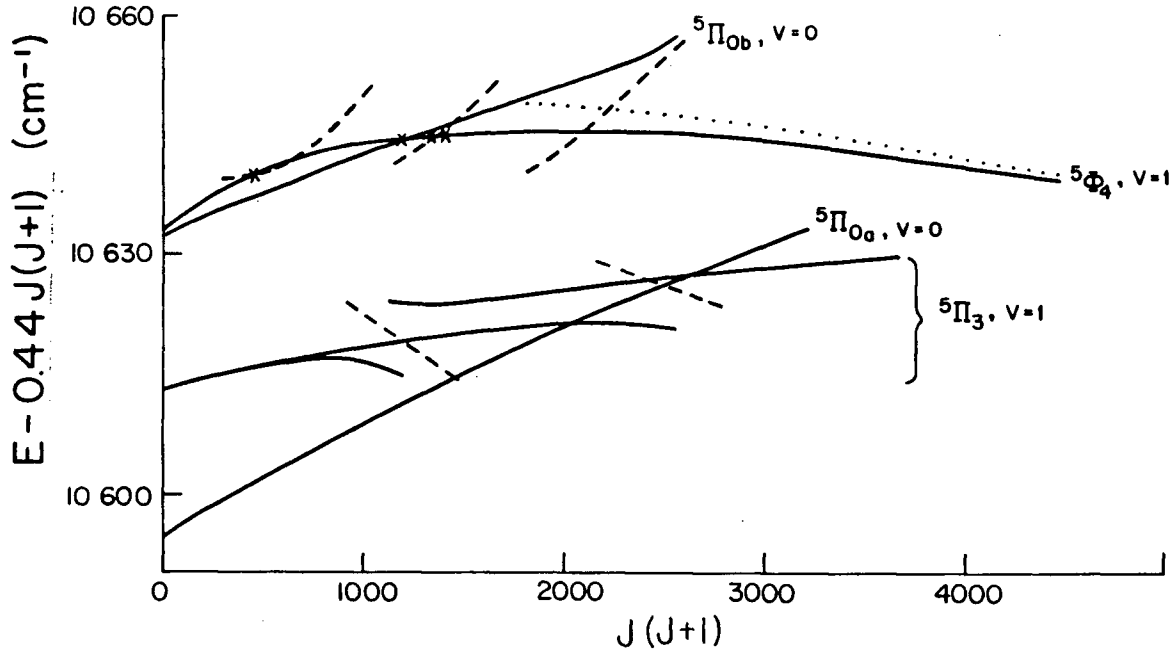

Fig. 22. Pieces of a Σ state or states superimosed on the energy level diagram of Fig. 19 (schematic). The existence and position of the component represented by the dotted curve are uncertain. This is the component responsible for the Λ-doubling in $^5\Phi_4$ from J = 42 on.

then the lack of perturbations in the lower $^5\Pi_0$ parity component would immediately assign the parity of this component as f, regardless of whether the Σ state is a $^5\Sigma^+$ state or a $^7\Sigma^+$. This, in turn, would assign the e/f parities in the ground state, one of the major remaining unanswered ground-state questions.

The perturbing Σ state, or one of the Σ states if there are two, may be the next higher vibrational level of the same Σ state that was shown in Section V.B.4 to perturb the v = 0 level of the $^5\Pi_3$ substate.

V.B.5.a. Avoided crossing between $^5\Phi_4$, v=1 and $^5\Pi_0$, v=0: a test of the ground state spin-orbit intervals

Fig. 19 shows that the $^5\Phi_4$, v=1 substate and the upper parity component of the $^5\Pi_0$, v=0 substate cross each other. The term values for the $^5\Pi$ and $^5\Phi$ systems (Appendices VII and VIII) — which were calculated from the ground state term values — predict the crossing point to occur between J = 33 and 34 (closer to 34).

Experimentally, we find that lines involving the J = 34 level of the $^5\Phi_4$, v=1 substate are weak in intensity and broadened, with two peaks of near equal intensity just being detectable in some cases, the best example being the R(33) line of the $^5\Phi_4 - X^5\Delta_3$ (0,0) band. Where this occurs, the position of one of the peaks shows no detectable shift from its expected position, while the other is displaced approximately 0.03 cm^{-1} to lower energy. This indicates that one Λ-doublet component of the $^5\Phi_4$ substate is pushed downwards in energy by this amount, while the other component remains untouched. The wavefunction of the perturbed parity component is still predominantly $^5\Phi_4$ as evidenced by the only slight loss in intensity. As for lines involving the upper parity component of the $^5\Pi_0$, v=0, J = 34 level, unfortunately most are spoiled by blending, but the relatively unblended $^5\Pi_0 - X^5\Delta_1$ (0,1) P(35) and (0,2) R(33) lines are pushed some 0.02-0.03 cm^{-1} to higher energy, with at most only a slight loss of intensity.

These observations are consistent with an avoided crossing between the upper parity component of the $^5\Pi_0$, v=0 substate and one of the parity components of the $^5\Phi_4$, v=1 substate. The interaction matrix element is very small (hardly surprising in view of the fact that $\Delta\Omega = 4$), with the result that the perturbation is detectable in each state only at the J level closest to the crossing point. The position of the predicted crossing point is dependent on the ground state spin-orbit intervals. It is expected to occur slightly to the low-J side of J = 34 so that at J = 34 the $^5\Pi_0$ level should be above the $^5\Phi_4$ level, and this is precisely what is observed. The $^5\Pi_0$ level is perturbed upwards, indicating that it must be above the state perturbing it, and the $^5\Phi_4$ level is pushed downwards, indicating it to be below its perturbing state. This good agreement between expectation and observation is evidence for the accuracy with which the ground state spin-orbit separation between the $\Omega = 1$ and $\Omega = 3$ substates at J = 34 has been determined.

V.B.6. Perturbations in $^5\Pi_0$, v=1

Moving up to the next higher vibrational level of the $^5\Pi_0$ substate, the v = 1 level is also perturbed, but in this case there is no evidence that the perturbing state is a Σ state. Like the v = 0 level, v = 1 exhibits a large Λ-doublet splitting. Both components are perturbed, but the appearances of the two perturbations are quite different (Fig. 23). The perturbation in the lower parity component is centered at J = 26 and is smaller in magnitude than that in the upper component. For the latter component it has been possible to detect doubled lines for each J value between 18 and 26, whereas no doubled lines have been found for the lower comonent. The conclusion is that the two perturbations are unrelated; two different perturbing states must be present.

With data available from doubled lines at nine J values, it has been possible to do a fairly accurate deperturbation of the upper parity component and its

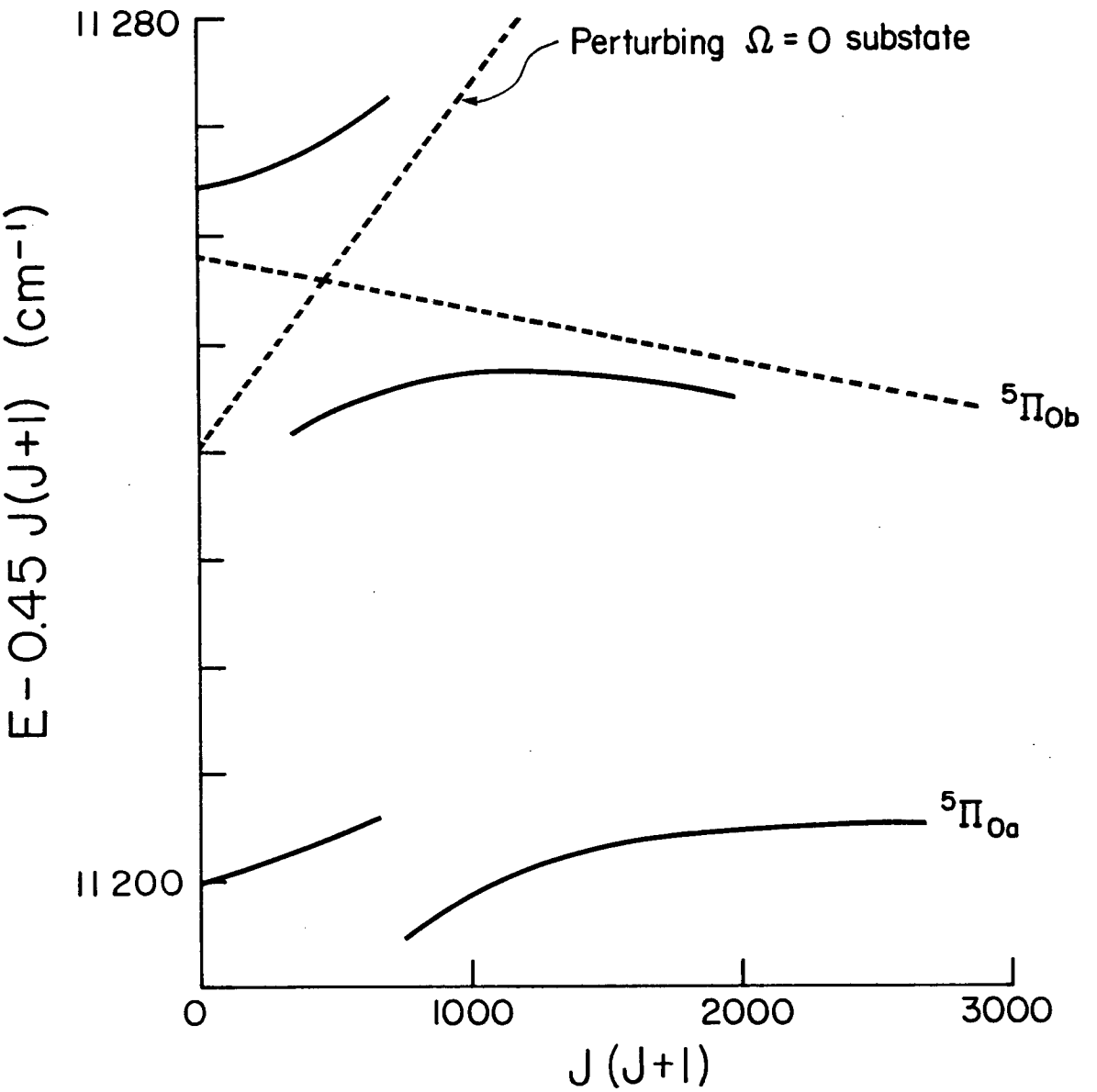

Fig. 23. Perturbations in $^5\Pi_0$, v=1. The deperturbed levels, based on the constants in Table XXI for the upper $^5\Pi_0$ parity component, are shown as broken lines.

perturbing state. Using the methods described in Section V.B.1, both homogeneous and heterogeneous models were tried and both were found to give equally good least-squares fits. However, the heterogeneous model predicted the crossing point between the zeroth-order perturbed and perturbing states to occur at $J \simeq 28$, whereas the homogeneous model predicted this to occur at $J \simeq 21$. Due to blending of many of the lines, it has not been possible to determine from the spectrum the exact J value at which the intensities of the two members of a doubled pair are equal, but this definitely occurs at a J value considerably less than 28. Therefore, the homogeneous fit must be the correct one, and the Ω value of the perturbing state is 0. The least-squares results are given in Table XX.

Assuming a spin-orbit interaction, the most likely candidates for the identity of the perturbing state are $^3\Pi_0$, $^7\Pi_0$, and $^7\Delta_0$. There are no theoretical predictions for a low-lying $^7\Delta$ state, but of the remaining two possibilities we cannot say which is correct.

V.B.7. Perturbation in $^5\Phi_3$, v=1 at $J \simeq 18.5$

The only remaining perturbation where doubled lines have been observed is that occurring in the $^5\Phi_3$, v=1 substate centred between J = 18 and 19. There is little to be said about this perturbation. It is caused by a degenerate state, but there is insufficient data to determine whether the interaction occurs homogeneously or heterogeneously. Least-squares results are given in Table XXI.

V.B.8. And the rest

There are *many* more perturbations present in the spectrum than those few selected for analysis in the foregoing sections. It has not been possible to identify doubled lines for any of the remaining perturbations, so little quantitative information is obtainable from them.

TABLE XX. Least-squares fitting: $^5\Pi_0$, v=1 and perturbing Ω = 0 state, with crossing point at J ≃ 21.

(A) The results (in cm^{-1})[a] - homogeneous model

	$^5\Pi_0$	Perturbing Ω=0 substate
T^{eff}	11 257 916 (58)	11 240.32 (12)
B^{eff}	0.445 49 (20)	0.484 91 (43)
$10^6\ D^{eff}$	0.14 (16)	1.65 (38)
H_{12}	12.561 8 (24)	
σ	0.008 04	

(B) The data[b] and residuals

	J	Term Values	Residuals[c]
Upper Component	13	11347.362	-0.002
	14	11360.182	0.001
	15	11373.932	-0.000
	16	11388.628	0.003
	17	11404.265	0.001
	18	11420.856	0.000
	19	11438.408	0.001
	20	11456.921	-0.002
	21	11476.406	-0.007
	22	11496.881	0.000
	23	11518.335	0.001
	24	11540.783	0.006
	25	11564.214	-0.000
	26	11588.647	-0.002
Lower Component	18	11395.361	-0.008
	19	11413.135	0.011
	20	11431.763	-0.003
	21	11451.282	-0.005
	22	11471.698	0.018
	23	11492.938	-0.000
	24	11515.048	-0.007
	25	11538.023	-0.002
	26	11561.827	-0.019
	27	11586.519	0.005
	28	11612.030	0.002
	29	11638.401	0.013
	30	11665.598	0.003
	31	11693.641	-0.009

(a) The numbers in parentheses are one standard error in units of the last two figures quoted.

(b) All data points weighted equally (weight = 1).

(c) Observed-Calculated.

TABLE XXI. Least-squares fitting: $^5\Phi_3$, v=1 and perturbing state, with crossing point at J ≃ 18.5.

(A) The results (in cm^{-1})[a]

	Homogeneous Model		Heterogeneous Model	
	$^5\Phi_3$	Perturbing State	$^5\Phi_3$	Perturbing State
T^{eff}	10 785.638 (28)	10 764.37 (17)	10 785.861 (27)	10 764.15 (16)
B^{eff}	0.447 94 (16)	0.506 76 (46)	0.447 93 (16)	0.506 77 (46)
$10^6\ D^{eff}$	1.95 (19)	-	1.95 (19)	-
H_{12}	2.191 4 (52)		-	
h_{12}	-		0.115 34 (20)	
σ	0.011 5		0.011 5	

(B) The data[b] and residuals

	J	Term Values	Residuals[c]
Upper Component	12	10855.854	-0.001
	13	10867.538	0.001
	14	10880.138	0.005
	15	10893.659	0.002
	16	10908.143	0.001
	17	10923.654	-0.008
	18	10940.374	-0.009
	19	10958.559	0.008
Lower Component	18	10935.917	0.013
	19	10953.933	-0.028
	20	10972.427	0.002
	21	10991.493	0.009
	22	11011.298	0.008
	23	11031.915	0.003
	24	11053.380	-0.000
	25	11075.704	-0.005

(a) The numbers in parentheses are one standard error in units of the last two figures quoted.

(b) All data points weighted equally (weight = 1).

(c) Observed-Calculated. Same residuals for homogeneous and heterogeneous fits.

Only one other perturbation will be specifically mentioned here. The $^5\Pi_1$ substate at the v = 2 level is so greatly perturbed that it has not been possible to identify it at all in the spectrum, even though the other four $^5\Pi$ substates at this vibrational level have been found and are involved in transitions having reasonable intensities.

V.C. Lambda-doubling

Lambda-doubling has been described previously in conjunction with various perturbations. We are interested here in the Λ-doubling in its own right, though this may still be the result of interactions with fairly nearby states.

V.C.1. Lambda-doubling in the $^5\Pi$ state

Lambda-doubling in a Π state can result from direct interaction of the Π state with a Σ state or states. Not surprisingly, therefore, it is observed in every substate of the $^5\Pi$ state and is often quite large. Plots of the Λ-doublet separations $\Delta\nu$ against J(J+1) are given in Figs. 24, 25, and 26 for the $\Omega = -1$, 0, and 1 substates, respectively. (No plot has been given for the v = 1 level of the $^5\Pi_0$ substate due to the large perturbations present in it that were discussed in Section V.B.6.) Λ-doubling is also present in the $\Omega = 2$ and 3 substates but is small and only becomes resolvable at moderate to high J values.

Comparing the three plots in Fig. 24, the v = 0 plot is completely linear and that for v = 2 may be also (though with local perturbations in it). The plot for v = 1, however, has a definite curvature. Thus the shapes of the plots appear not to be solely an intrinsic property of the Ω substate to which they belong. This may indicate that the shapes are influenced by the degree of closeness of the respective vibrational levels of the Σ state responsible for the Λ-doubling.

The magnitude of the Λ-doublet separations varies markedly with vibrational level in all three substates, with that in v = 1 being the largest, v = 0 next, and v = 2 the smallest. For example, the values of $\Delta\nu$ in $^5\Pi_0$ at J = 0 are 38, 58, and 15 cm^{-1} for v = 0, 1, and 2, respectively.[8] There are various possible explanations for this v-dependence. It is very likely that this also is caused by the

---

[8]The deperturbed position of the upper parity component (Section V.B.6) was used in obtaining 58 cm^{-1} for v = 1.

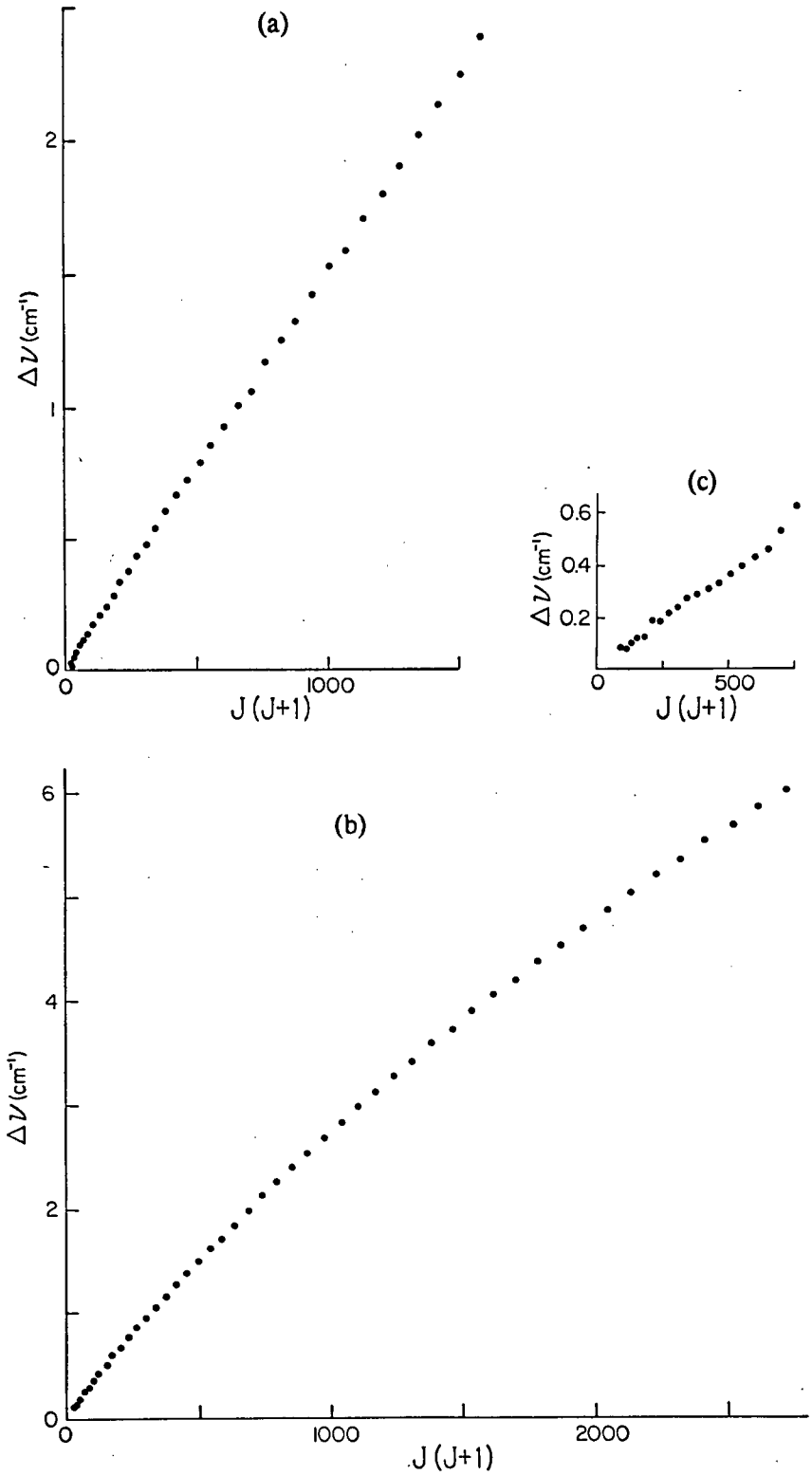

Fig. 24. Λ-doubling in $^5\Pi_{-1}$. (a) v = 0. (b) v = 1. (c) v = 2.

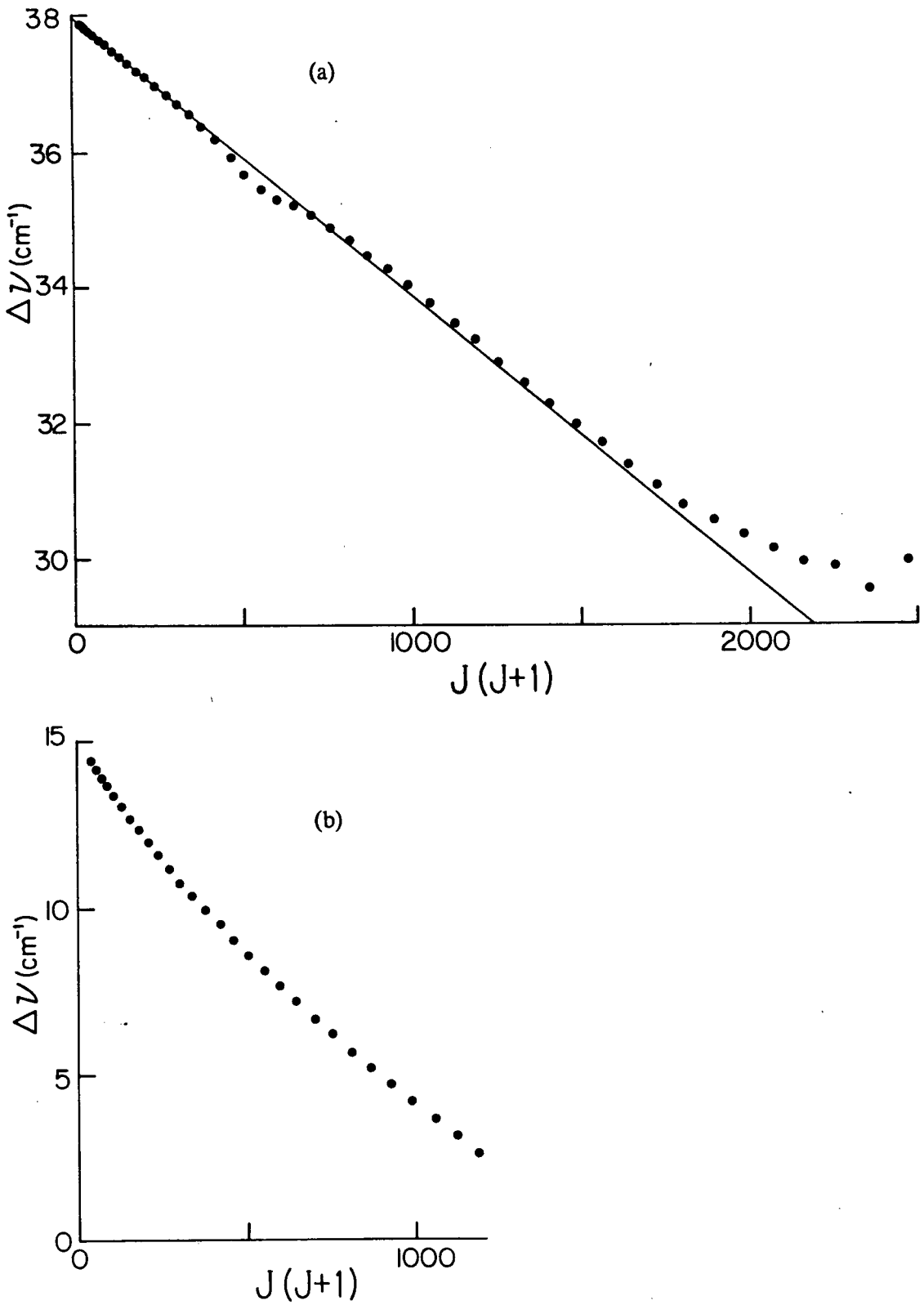

Fig. 25. Λ-doubling in $^5\Pi_0$. (a) v = 0. (b) v = 2.

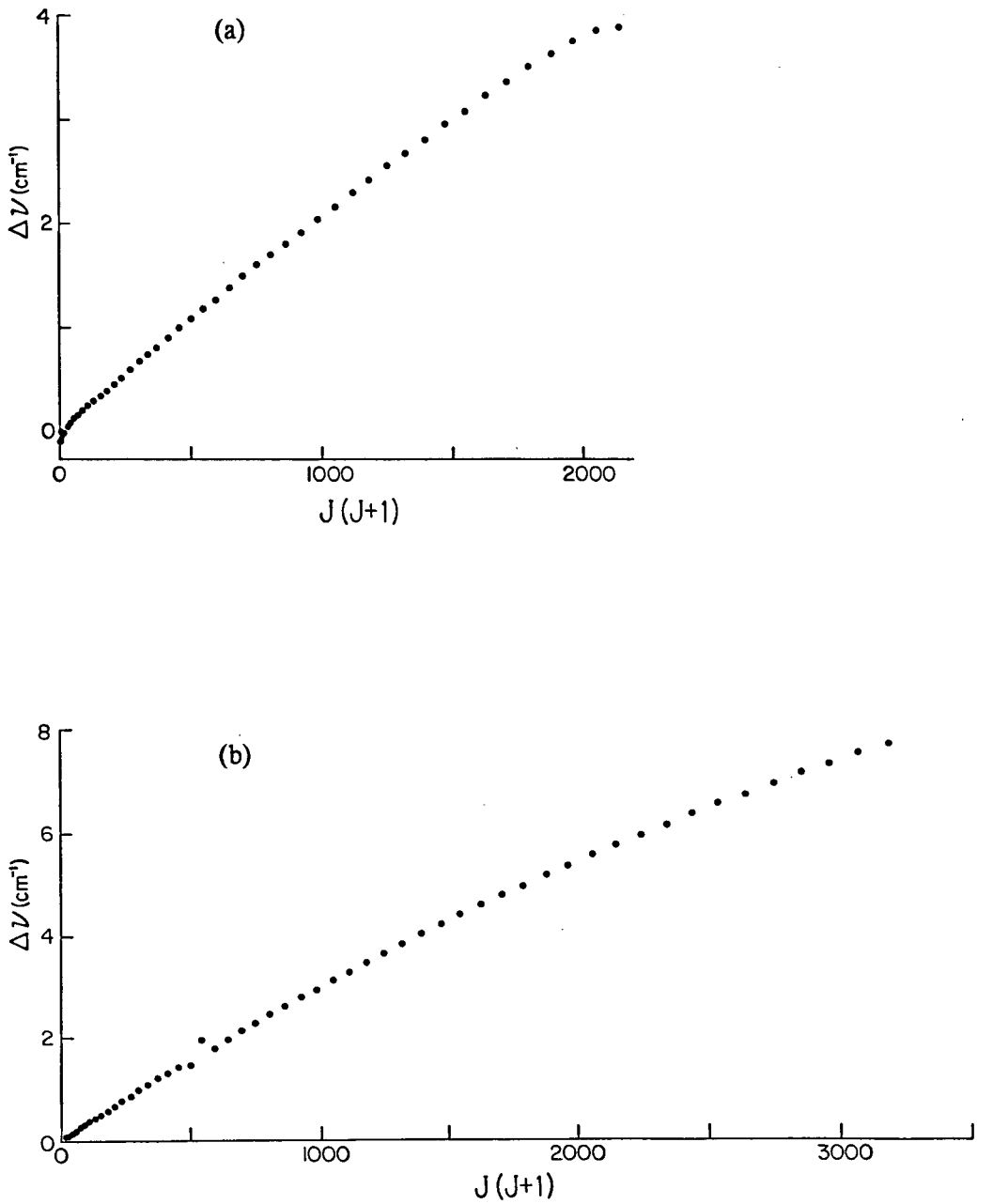

Fig. 26. Λ-doubling in $^5\Pi_1$. (a) v = 0. (b) v = 1.

relative closeness of the vibrational levels of the Σ state to those of the $^5\Pi$ state, with the level responsible for the v = 1 Λ-doubling being the closest. This would mean that the state responsible for the Λ-doubling would have a vibrational interval larger or smaller than that of the $^5\Pi$ state, but which we unfortunately cannot say. Franck-Condon factors, on the other hand, offer another explanation, and, in the case of the v = 1 level of the $^5\Pi_0$ substate, it is possible that the other parity component of the Ω = 0 substate that perturbs the upper $^5\Pi_0$ component may be contributing by pushing the lower $^5\Pi_0$ component down in energy.

In Section V.B.5., at least one multiplet Σ state was shown to lie at the same energy as the v = 0 level of the $^5\Pi_0$ substate, which we have seen exhibits a large Λ-doubling (38 cm^{-1} at J = 0), but we have still to address the question of whether the Σ state or states responsible for the local perturbations described in that section are also responsible for the Λ-doubling.

The plot of $\Delta\nu$ versus J(J+1) in Fig. 25(a) appears to be basically linear, but there are a number of slight "ripples" in it. The line drawn in the figure is based solely on the low-J data and is drawn mainly to show up these curvatures, rather than to represent the true course of the unperturbed values. Explanations for two of the curvatures, that occurring between J = 19 and 26 and the upturning at the high-J end, have already been given in Section V.B.5 in terms of local interactions with the various components of a multiplet Σ state. An alternative explanation for the upturning at high J is provided by comparison with the plot for v = 2 (Fig. 25(b)), which is found to be curved. It may be that the upturning in v = 0 is an intrinsic part of the Λ-doubling, rather than being just a local perturbation. The remaining irregularities are more difficult to explain; they are likely to be due to complex interactions with two or more components of the Σ state or states, simultaneously.

The important point here is that these "ripples" are all small relative to the Λ-doubling interval. This indicates that the interactions responsible for these are weak

in comparison with that responsible for the main Λ-doubling. This probably means that the Σ state causing the Λ-doubling is a different one from the state or states causing the local perturbations, and the basic regularity of the Λ-doublet separations (ignoring the small local perturbations) may indicate that the state responsible lies at some distance from the $^5\Pi_0$ substate. In particular, the Λ-doubling behavior is typical of that to be expected in an Ω = 0 substate acted upon by a "distant" Σ state, namely a large almost constant separation, with a relatively small J-dependence.

Also, examination of the pattern of Σ-state components in Fig. 22 suggests no conceivable way in which these could have caused the Λ-doublet components to be situated at the energy locations that they are, regardless of whether the components all belong to the same Σ state or to two states.

Furthermore, no local perturbations (e.g. avoided crossings) caused by a Σ state have been found in the $^5\Pi_0$, v=1 level, even though the magnitude of the Λ-doubling is larger. If the relative sizes of the Λ-doublet separations are caused by the degree of closeness of the Σ state responsible (and not by one of the other explanations offered above) then this means that the state causing the Λ-doubling must be a different one from that or those causing the local perturbations in v = 0. If this is indeed the case, then we have evidence for at least two Σ states and quite possibly for three, even though only two have been predicted by the theoreticians.

V.C.2. Lambda-doubling in the $^5\Phi$ state

Lambda-doubling in a Φ state can only occur indirectly through intermediate Π and Δ states and must be an even higher-order effect than Λ-doubling in a Δ state. Not surprisingly, therfore, Λ-doubling is considerably less frequent in occurrence in the $^5\Phi$ state than in the $^5\Pi$ state and is *usually* small in magnitude.

Lambda-doubling figures most prominantly in the Ω = 1 substate, where it is seen in all three detected vibrational levels. As for the $^5\Pi$ state, plots of $\Delta\nu$ versus

J(J+1) have been made and are given in Fig. 27. The Λ-doubling appears well-behaved in v = 0 and 1, though the splitting is an order of magnitude larger in v = 1 than in v = 0, probably for similar reasons to the vibrational-dependence in the $^5\Pi$ state. The doubling in v = 2, on the other hand, is very different in nature. Besides being yet another order of magnitude larger than that in v = 1, the $\Delta\nu$ versus J(J+1) plot goes through a minimum. In this case, the curvature is due to a combination of two perturbations, one in each parity component but at different J values (see Fig. 28). Unlike the situation for $^5\Pi_0$, v=0, where the "ripple" between J = 19 and 26 was due to a perturbation of only one parity component, here it is not necessary to invoke a case (b) Σ state as the cause. The perturbations may be caused by *either* an orbitally degenerate state, which lies between the two parity components but has a slightly larger B value and interacts with both components but at different J values, *or* by two adjacent "arms" of a multiplet Σ state, one of which lies above and "pushes" downward on the lower parity component at low J and the other of which lies below and pushes upward on the upper parity component at higher J.

The only other examples of Λ-doubling in the $^5\Phi$ state found anywhere in the spectrum are those in the v = 1 level of the $^5\Phi_4$ substate already described in Section V.B.5 as resulting from local interactions with a perturbing Σ state or states.

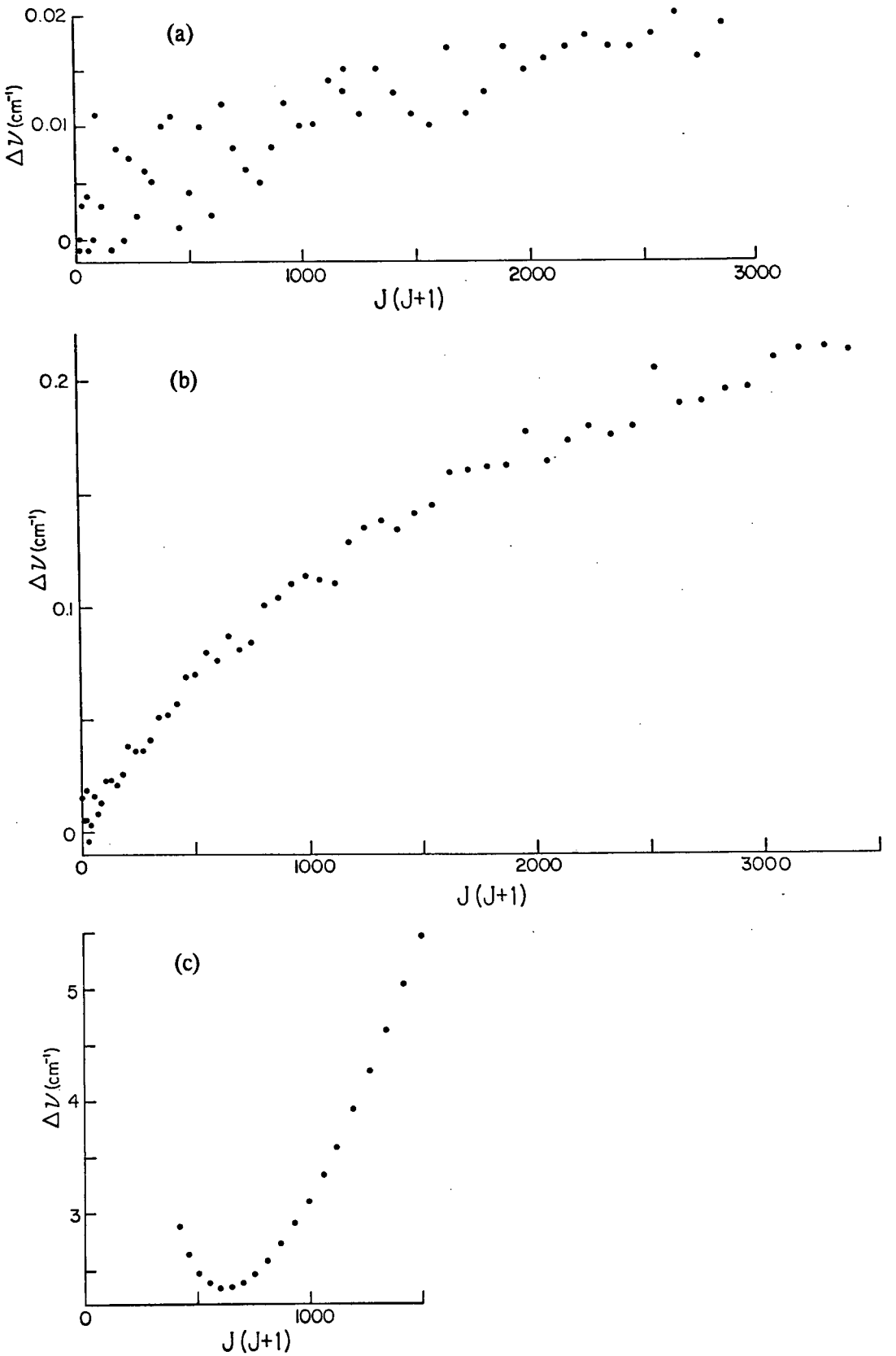

Fig. 27. Λ-doubling in $^5\Phi_1$. (a) v = 0. (b) v = 1. (c) v = 2.

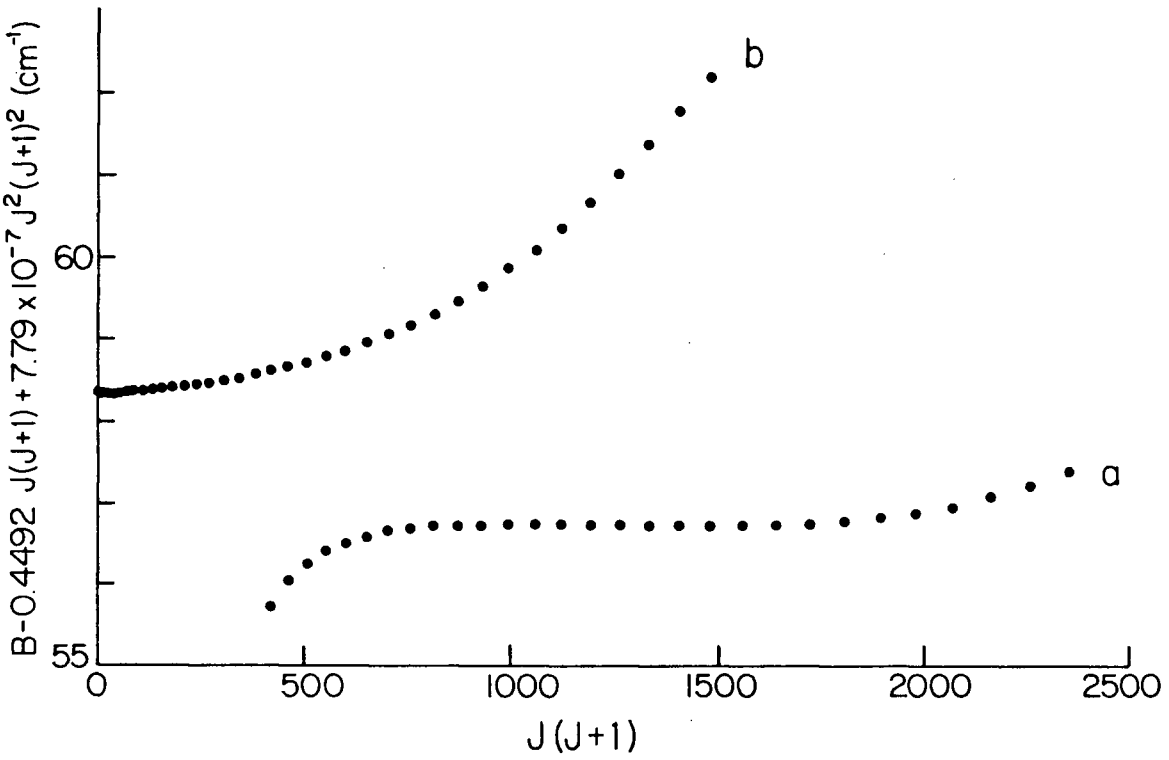

Fig. 28. Large scale plot of the energy levels of the $^5\Phi_1$, v=2 level, showing irregularities in both parity components. The D^{eff} value for the "b" component is negative (see Table XXIII).

V.D. Data Reduction

The large number of perturbations present in the $^5\Pi$ and $^5\Phi$ states make a global least-squares fit of all the substates of a given vibrational level of either state impractical. Even when an attempt is made to select only those parts that appear to be relatively unperturbed, as was tried for the $^5\Phi$ state in Section V.B.1 (Table XIV), the results are not very successful.

The best that can be done, therefore, is to fit the term values of each individual substate to an equation in effective constants as in eqn. (III.J.1). This has been done and the results are summarized in Tables XXII and XXIII. Sufficiently narrow J-ranges of data were selected such that reasonably good fits were obtained (in terms of low standard deviations and small residuals with minimal systematic errors) without using terms of higher order than D^{eff}. In many cases it was only possible to fit a narrow range of J values, and in such cases preference was given to the low-J end of the data.

One notable exception is the v = 0 level of the $^5\Phi_5$ substate. Here it was possible to obtain a good fit using every data point from J = 5 to J = 80 — hence our claim that this level is completely unperturbed (although a constant shift of the entire level would, of course, be possible, but undetectable; also unlikely). For the other vibrational levels of this substate it was only possible to fit a much narrower J-range of data, unless higher-order terms were included, so we conclude that these other levels are at least slightly perturbed, although in the case of v = 1, no obvious perturbation is apparent.

Only very rough estimates of the spin-orbit coupling constants and vibrational frequencies can be given. In the $^5\Pi$ state, the separation between the $\Omega = 1$ and $\Omega = 2$ substates is $-217.0\ cm^{-1}$ for the v = 0 level. Hence, $A_0 \simeq -217\ cm^{-1}$. Similarly, for the $^5\Phi$ state, using the $\Omega = 3$–4 interval, $3A_0 \simeq -139.64$. Hence, $A_0 \simeq -47\ cm^{-1}$ The value of $\Delta G_{1/2}$ for the $^5\Pi$ state, as determined from the

TABLE XXII. Effective rotational constants for the $^5\Pi$ state.

v	Ω	Parity component	T^{eff}	B^{eff}	$10^6\ D^{eff}$	J-range covered	σ	Notes[a]
0	-1	a	10.808.464 6 (15)	0.456 291 6 (84)	1.405 7 (89)	3-31	0.003 69	
		b	10 808.466 0 (35)	0.457.890 (22)	1.491 (27)	3-29	0.008 23	
	0	a	10 594.619 4 (14)	0.455 271 6 (41)	1.066 9 (21)	3-45	0.004 59	
		b	10 632.559 7 (31)	0.451 236 (43)	1.17 (11)	3-19	0.005 24	
	1	a	10 405.649 0 (17)	0.449 852 6 (64)	0.789 6 (43)	3-39	0.005 05	
		b	10 405.646 0 (16)	0.452 085 2 (60)	0.953 2 (44)	5-37	0.003 84	
	2	a	10 188.671 3 (30)	0.453 027 (36)	3.321 (83)	4-20	0.004 60	
		b	10 188.670 1 (30)	0.452 997 (34)	3.186 (69)	2-22	0.006 50	
	3							b
1	-1	a	11 389.880 0 (41)	0.459 898 (32)	2.051 (49)	5-25	0.007 09	
		b	11 389.892 8 (48)	0.463 220 (46)	2.877 (88)	5-22	0.007 06	
	0	a						b
		b						c
	1	a	11 033.093 7 (16)	0.447 071 1 (28)	0.659 29 (97)	3-14, 34-56	0.005 15	
		b	11 033.096 0 (26)	0.450 225 3 (81)	0.902 9 (34)	4-13, 40-51	0.007 45	
	2		10 828.271 5 (19)	0.447 552 (13)	0.610 (15)	2-29	0.004 89	
	3	a	10 612.938 7 (17)	0.446 586 (24)	1.401 (69)	4-18	0.002 34	
		b	10 612.945 3 (53)	0.446 430 (76)	0.81 (21)	4-18	0.007 25	
2	-1	a	12 053.707 0 (52)	0.455 659 (32)	1.344 (43)	10-25	0.004 20	
		b	12 053.708 0 (82)	0.456 491 (56)	1.539 (79)	8-25	0.009 26	
	0	a	11 871.382 1 (84)	0.465 142 (86)	7.97 (18)	7-20	0.007 61	
		b	11 886.387 6 (20)	0.448 985 (13)	1.043 (17)	4-28	0.004 24	
	1							d
	2		11 480.764 6 (37)	0.446 96 (11)	-3.70 (57)	2-13	0.005 36	
	3	a	11 276.912 5 (15)	0.446 059 (10)	0.970 (13)	3-28	0.003 39	
		b	11 276.910 5 (17)	0.446 077 7 (77)	0.991 2 (65)	3-35	0.004 63	
3	2		12 154.700 0 (26)	0.445 623 (22)	-0.642 (36)	2-25	0.005 96	
	3		11 955.311 9 (21)	0.444 491 (14)	0.156 (18)	3-28	0.004 88	

(Footnotes on next page)

TABLE XXII (cont.)

Notes:

(a) All term values weighted equally. Numbers in parentheses denote one standard error in units of the last two figures.

(b) Too perturbed to derive meaningful constants.

(c) See Table XX.

(d) Must be very perturbed; level not identified in spectrum.

TABLE XXIII. Effective rotational constants for the $^5\Phi$ state.

v	Ω	Parity component	T^{eff}	B^{eff}	$10^6\ D^{eff}$	J-range covered	σ	Notes[a]
0	1	a	10 446.373 8 (18)	0.462 354 (17)	2.682 (30)	2-24	0.004 12	
		b	10 446.374 1 (10)	0.462 382 6 (97)	2.718 (17)	2-24	0.002 34	
	2							b
	3		10 192.358 9 (19)	0.449 024 9 (79)	0.164 7 (59)	3-37	0.005 42	
	4		10 052.721 0 (21)	0.446 427 3 (99)	0.694 8 (86)	4-34	0.005 25	
	5		9 903.579 2 (17)	0.444 602 6 (15)	0.967 00 (25)	5-80	0.007 17	
1	1	a	11 062.165 8 (19)	0.452 152 9 (38)	0.951 6 (14)	2-54	0.006 96	
		b	11 062.169 0 (15)	0.452 290 6 (44)	0.978 6 (23)	2-45	0.005 09	
	2		10.925.735 1 (19)	0.448 906 2 (69)	0.944 3 (45)	2-40	0.006 00	
	3							c
	4		10 633.091 9 (40)	0.461 067 (53)	12.74 (13)	4-19	0.005 90	
	5		10 485.009 0 (14)	0.443 395 0 (41)	1.227 3 (23)	5-43	0.003 91	
2	1	a	11 656.744 (70)	0.449 20 (11)	0.780 (46)	29-40	0.008 20	d
		b	11 658.342 1 (35)	0.449 441 (39)	-0.198 (39)	2-22	0.007 56	
	2		11 522.393 5 (39)	0.443 632 (62)	-1.25 (18)	2-18	0.007 22	
	3		11 381.157 5 (33)	0.440 279 (26)	-	3-15	0.006 84	e
	4		11 222.269 (16)	0.431 20 (21)	-12.39 (58)	7-17	0.010 60	
	5		10 995.794 4 (25)	0.465 273 (13)	4.540 (14)	5-31	0.005 32	
3	1	a						
		b						
	2		12 117.243 0 (54)	0.443 652 (71)	-2.93 (18)	4-19	0.007 92	
	3		11 986.487 0 (66)	0.441 390 (51)	-3.64 (83)	8-23	0.006 44	
	4		11 839.526 0 (96)	0.434 09 (14)	-3.45 (43)	5-17	0.010 11	
	5		11 660.810 6 (24)	0.449 814 (15)	3.304 (19)	5-28	0.004 58	
4	5		12 312.539 8 (24)	0.434 859 4 (91)	-	5-22	0.005 70	e
5	5		12 917.552 3 (47)	0.425 926 (54)	-2.32 (13)	6-19	0.004 74	

(Footnotes on next page)

TABLE XXIII (cont.)

Notes:

(a) All term values weighted equally. Numbers in parentheses denote one standard error in units of the last two figures.

(b) Too perturbed to derive meaningful constants.

(c) See Table XXI.

(d) This component is perturbed; values not very meaningful.

(e) D^{eff} is not determinable.

center Ω component ($\Omega = 1$) is approximately 627 cm^{-1} Similarly for the $^5\Phi$ state, from the $\Omega = 3$ substate, $\Delta G_{1/2} \simeq 593$ cm^{-1} where the deperturbed value of T_0^{eff} from Table XXI was used for the $v = 1$ level.

CHAPTER VI

CONCLUDING REMARKS

VI.A. Energy Levels of FeO: The Current Picture

The energy level diagram of the low-lying states of FeO, as it is presently known, is given in Fig. 29. In summary, the ground state has now been conclusively established as being a $^5\Delta_i$ state. This state is basically well-behaved as far as it has been observed (up to v = 3 and part of v = 4), except for the presence of one very small, local rotational perturbation. This is probably caused by a $^7\Sigma^+$ state. This state is the one predicted by Krauss and Stevens (1) to be the ground state of the molecule, and although it has not been possible to determine its exact placement in the energy level diagram due to the fact that the vibrational quantum number of the perturbing level is not known, it does indeed lie very close to the true ground state.

Proceding to higher energy, the next state encountered, which has been tentatively identified as a $^5\Sigma^+$ state, lies approximately 3990 cm^{-1} above the ground state. This state has been observed directly only in the photodetachment experiments of Engelking and Lineberger (2). Highly excited vibrational levels of this and/or the $^7\Sigma^+$ state are probably responsible for some of the perturbations present in the upper states of the infrared system, and the Λ-doublings observed in these states and in the ground state are probably also caused by these states.

The upper levels of the infrared system comprise two states, a $^5\Pi_i$ state and a $^5\Phi_i$ state, with the former lying only about 200 cm^{-1} above the latter. Several other states also are present in this energy region, and, although possessing no oscillator strengths of their own for transition to the ground state and thus being not directly observable, do make their presence felt in the form of numerous perturbations. Definite evidence exists for the presence of at least one multiplet Σ state, and,

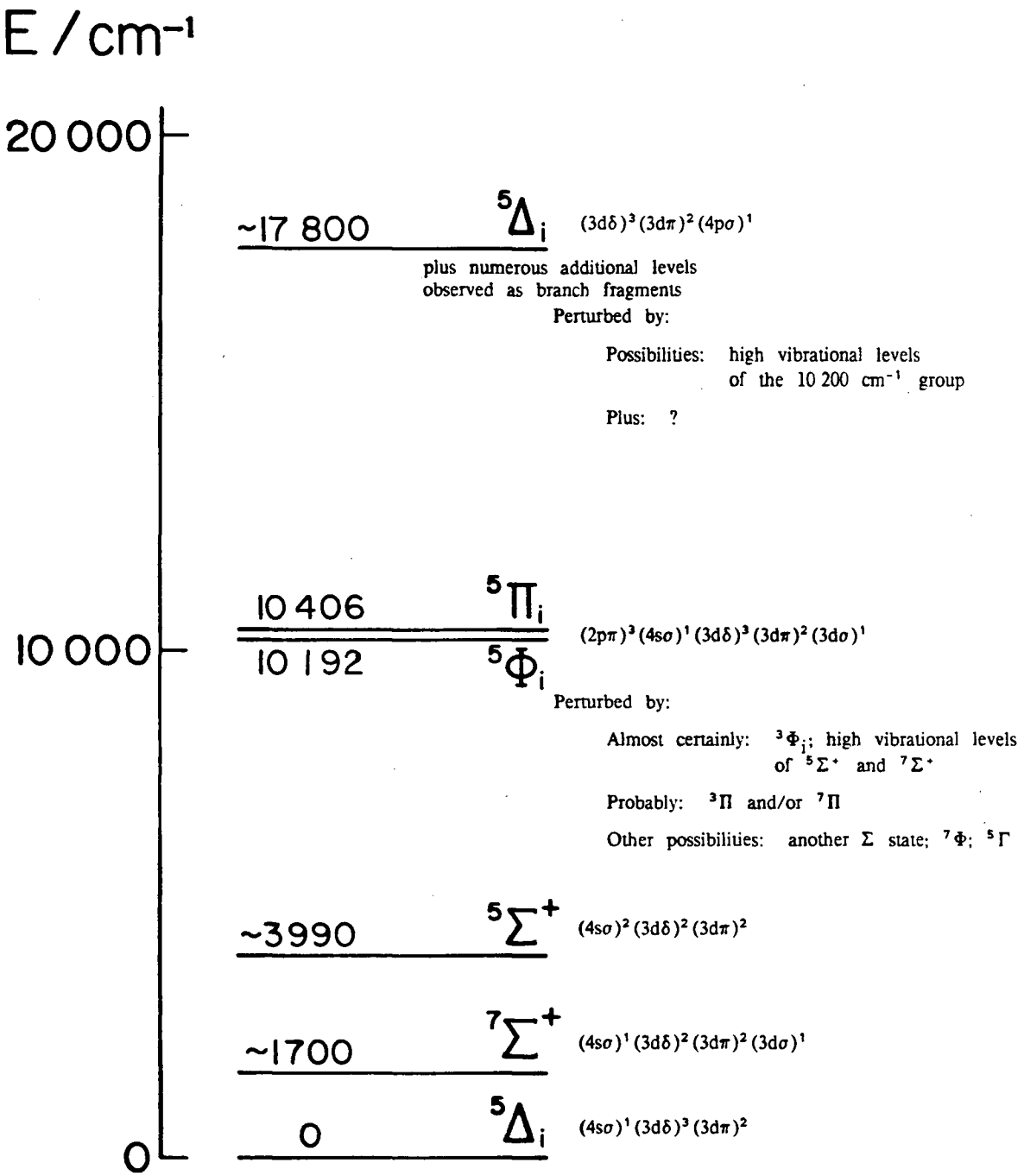

Fig. 29. The low-lying electronic states of FeO. Approximate values of T_0 are given; that for the $^7\Sigma^+$ state may not be for the v = 0 level.

including the state responsible for the Λ-doublings, there may be as many as three Σ states present. As stated above, likely candidates for at least one of these are the upper vibrational levels of the $^5\Sigma^+$ and/or $^7\Sigma^+$ states that have their v = 0 levels near the ground state. There is also fairly clear evidence for the presence of a $^3\Phi$ state, and a perturbation in the $^5\Pi_0$, v=1 substate was interpreted in the previous chapter as probably being caused by either a $^3\Pi$ state or a $^7\Pi$ state. It is quite possible that both the latter states are present, and $^7\Phi$ and $^5\Gamma$ are other possibilities, since these have all been predicted to lie at low energies (1) and there are still many perturbations to be accounted for.

The upper states of the orange system are even more perturbed. At least one $^5\Delta_i$ state is present, but there are a host of other states also in this region as evidenced by the many local perturbations and the existence of numerous branch fragments.

VI.B. For the Future

The picture of the low-lying energy states of FeO is now becoming clear, as indicated in the foregoing paragraphs, but a number of details still need further study before the spectrum can be laid to its final rest. Also, the higher-lying states still need to be studied at high resolution.

A large number of lines remain unassigned in the near-infrared region, particularly above 11 500 cm^{-1}. These do not form obvious branches, and conventional methods of line assigning are extremely difficult and tedious and often do not work at all. Tunable infrared lasers will be the key to any further analysis of this region. Rotationally resolved fluorescence studies will be particularly invaluable in helping to pin down the perturbing states by aiding with the assignment of some of the weaker lines in the vicinities of avoided crossings.

One tantalizing problem that remains is the assignment of e/f labels to the parity components. Several potential ways of determining these have come to light during the course of the present study. These are:

(i) by considering the electron configurations of the possible states responsible for the Λ-doubling in the $X^5\Delta$ state;

(ii) by determining which state or states are responsible for the Λ-doubling in the $^5\Pi$ and $^5\Phi$ states, whether by electron configuration considerations again or by linking these states with local perturbations that they may also cause;

(iii) by determining which non-degenerate state or states cause perturbations in the $^5\Pi$ or $^5\Phi$ states; and

(iv) by the absence or small size of perturbations in one parity component of the $^5\Pi_0$ substate and comparison with the tabulated $^5\Sigma/^5\Pi$ and $^7\Sigma/^5\Pi$ matrix elements.

Unfortunately, in no case has there been sufficient information available to carry out the assignment unambiguously. Based on single electronic configuration arguments, the

most likely state causing the ground-state Λ-doubling is the $^7\Sigma^+$ state, and this would put the e levels above the f levels. However, the single electronic configuration picture is only an approximation and cannot be relied on. The fact that the $^7\Sigma^+$ state appears to have showed up in the photodetachment spectrum of Engelking and Lineberger (2) may indicate that a single-configuration description is inadequate.

Nothing has been said about the vibrational numbering of the degenerate perturbing states, such as the $^3\Phi$ state. The reason is that this is so far unknown and therefore so also are the positions of the electronic term origins. One possible method for determining this information would be to observe the isotopic shifts in the positions of the perturbations upon substitution of oxygen-18 for oxygen-16. The same thing applies to the non-degenerate perturbing states, and for these it may then be possible to count down to the v = 0 level to determine to which of the two low-lying Σ states ($^5\Sigma^+$ or $^7\Sigma^+$) they belong.

The isotopic experiment may also simplify some of the very complex perturbations observed in the present work, since the isotopic shifts for different perturbing levels will most likely be different. What appears as a complex perturbation resulting from two or more perturbing states in the $Fe^{16}O$ spectrum may then be split apart into two or more separate perturbations occurring at different J values in the $Fe^{18}O$ spectrum. This experiment will, however, require a different experimental setup than the flow-through system used in the present work, since the latter would consume too much of the relatively expensive ^{18}O isotope.

Only the infrared and orange systems have so far been rotationally analyzed. The green and blue systems have never been studied at high resolution. The ground state information provided by this laboratory should greatly aid in the analysis of these systems, though it has yet to be established whether the bands in the green region involve the ground state.

The diffuse feature at ~242 nm has yet to be identified and it too could be studied at higher resolution to see whether it really is diffuse or whether it possesses fine structure that has just not been resolved so far.

REFERENCES

Chapters I and II

1. H. G. J. Kayser and H. Konen. *Handbuch der Spectroscopie*, vol. VII, pp. 497–498. (Verlag Von S. Hirzel in Leipzig). **1924.**

2. Eder and Valenta. *Atlas typ. Spektra*, Wien. **1928.** Cited by Ref. (14).

3. E. Domek. *Sitzb. Akad. Wiss. Wien IIa* **1910**, 119, 437–453.

4. H. G. Howell and G. D. Rochester. *Proc. Univ. Durham Phil. Soc.* **1934**, 9, 126–134.

5. R. S. Richardson. *Astron. Soc. Pacific* **1934**, 46, 154–155.

6. H. Trivedi. *Bull. Acad. Sc.* **1935**, 5, 27–33.

7. A. G. Gaydon. *Spectroscopy and Combustion Theory*, pp. 53 and 161–162. (Chapman & Hall: London). **1942.**

8. A. G. Gaydon and H. G. Wolfhard. *Proc. Roy. Soc. London* **1948**, 194, 169–184.

9. A. G. Gaydon. *The Spectroscopy of Flames*, pp. 92, 223, and 240. (Chapman & Hall: London). **1957.**

10. A. G. Gaydon. *Thesis.* (London). **1937.**

11. R. W. B. Pearse and A. G. Gaydon. *The Identification of Molecular Spectra.* (Chapman and Hall: London). 1st ed. **1941**; 4th ed. **1976.**

12. B. Rosen. *Nature* **1945**, 156, 570.

13. B. Rosen. *J. Phys. Radium* **1948**, 9, 155–158.

14. A. Delsemme and B. Rosen. *Bull. Soc. Roy. Sci., Liège* **1945**, 14, 70–80.

15. L. Malet and B. Rosen. *Bull. Soc. Roy. Sci., Liège* **1945**, 14, 377–381.

16. G. Herzberg. *Molecular Spectra and Molecular Structure: I. Spectra of Diatomic Molecules*, 2nd ed. (Van Nostrand Reinhold: New York). **1950.** (a) pp. 241–244.

17. A. M. Bass and W. S. Benedict. *Ap. J.* **1953**, 116, 652–653.

18. A. Gatterer, J. Junkes, and E. W. Salpeter. *Molecular Spectrum of Metallic Oxides.* (Specola Vaticana, Città del Vaticano). **1957.** Cited by Ref. (22).

19. A. B. Callear and R. G. W. Norrish. *Proc. Roy. Soc.* (London) **1960**, A259, 304–324.

REFERENCES: Chapters I and II (cont.)

20. A. B. Callear and R. J. Oldman. *Trans. Faraday Soc.* **1967**, 63, 2888–2897.

21. A. M. Bass, N. A. Kuebler, and L. S. Nelson. *J. Chem. Phys.* **1964**, 40, 3121–3122.

22. R. K. Dhumwad and N. A. Narasimham. *Proc. Ind. Acad. Sci., A* **1966**, 64, 283–290.

23. R. F. Barrow and M. Senior. *Nature* **1969**, 223, 1359.

24. J. B. West and H. P. Broida. *J. Chem. Phys.* **1975**, 62, 2566–2574.

25. A. Lagerqvist and L. Huldt. *Z. Naturfosch* **1953**, 8A, 493–498.

26. P. A. Montano, P. H. Barrett, and Z. Shanfield. *J. Chem. Phys.* **1976**, 64, 2896–2900.

27. P. C. Engelking and W. C. Lineberger. *J. Chem. Phys.* **1977**, 66, 5054–5058.

28. P. S. Bagus and K. J. T. Preston. *J. Chem. Phys.* **1973**, 59, 2986–3002.

29. S. P. Walch and W. A. Goddard III. Unpublished results quoted as Ref. (4) of Ref. (27).

30. T. C. DeVore and T. W. Gallaher. *J. Chem. Phys.* **1979**, 70, 4429–4431.

31. W. Weltner, Jr. *Ber. Bunsenges. Phys. Chem.* **1978**, 82, 80–89.

32. R. J. Van Zee, C. M. Brown, K. J. Zeringue, and W. Weltner, Jr. *Accts. Chem. Res.* **1980**, 13, 237–242.

33. J. G. Kay, K. E. Bartelt, and D. M. Byler. Unpublished results quoted as Ref. (9) of Ref. (34).

34. D. W. Green, G. T. Reedy, and J. G. Kay. *J. Mol. Spectrosc.* **1979**, 78, 257–266.

35. S. Abramowitz, N. Acquista, and I. W. Levin. *Chem. Phys. Lett.* **1977**, 50, 423–426.

36. J. K. McDonald. "Rotational Analysis of the Orange System of FeO." In *Thirty-fourth Symposium on Molecular Spectroscopy.* (Ohio State University: Columbus, Ohio). **1979.**

37. S. M. Harris and R. F. Barrow. *J. Mol. Spectrosc.* **1980**, 84, 334–341.

38. M. Trkula. Private communication. **1980.**

39. B. Lindgren and U. Sassenberg. *Annual Report 1981/82.* (Molecular Physics, Institute of Physics, University of Stockholm).

40. H. H. Michels. Unpublished results quoted as Ref. (17) of Ref. (24).

REFERENCES: Chapters I and II (cont.)

41. A. G. Gaydon. *Dissociation Energies and Spectra of Diatomic Molecules.* (Chapman and Hall: London). (a) 1st ed., p. 208. **1947**; (b) 3rd ed., p. 270. **1968.**

42. R. T. Birge and H. Sponer. *Phys. Rev.* **1926**, 28, 259–283.

43. G. Balducci, G. De Maria, M. Guido, and V. Piacente. *J. Chem. Phys.* **1971**, 55, 2596–2598.

44. D. E. Jensen and G. A. Jones. *J. Chem. Soc. Faraday Trans. I* **1973**, 69, 1448–1454.

45. D. L. Hildenbrand. *Chem. Phys. Lett.* **1975**, 34, 352–354.

46. C. W. von Rosenburg, Jr. and K. L. Wray. *J. Quant. Spectrosc. Radiat. Transfer* **1972**, 12, 531–547.

47. A. Fontijn and S. C. Kurzius. *Chem. Phys. Lett.* **1972**, 13, 507–510.

48. H. Fissan and K. G. P. Sulzmann. *J. Quant. Spectrosc. Radiat. Transfer* **1972**, 12, 979–984.

49. A. S–C. Cheung, R. M. Gordon, and A. J. Merer. *J. Mol. Spectrosc.* **1981**, 87, 289–296.

50. A. S–C. Cheung, N. Lee, A. M. Lyyra, A. J. Merer, and A. W. Taylor. *J. Mol. Spectrosc.* **1982**, 95, 213–225.

51. A. S–C. Cheung, A. M. Lyyra, A. J. Merer, and A. W. Taylor. *J. Mol. Spectrosc.* **1983**, 102, 224–257.

52. A. S–C. Cheung. *PhD. Thesis.* (U. of British Columbia). **1981.**

53. R. M. Gordon and A. J. Merer. *Can. J. Phys.* **1980**, 58, 642–656.

54. Ch. Jungen, D. N. Malm, and A. J. Merer. *Chem. Phys. Lett.* **1972**, 16, 302–304.

55. Ch. Jungen, D. N. Malm, and A. J. Merer. *Can. J. Phys.* **1973**, 51, 1471–1490.

56. R. E. Smalley, L. Wharton, and D. H. Levy. *J. Chem. Phys.* **1975**, 63, 4977–4989.

57. D. K. Hsu, D. L. Monts, and R. N. Zare. *Spectral Atlas of Nitrogen Dioxide, 5530 to 6480 Å.* (Academic Press: New York). **1978.**

58. K. Uehara and H. Sasada. *High Resolution Spectral Atlas of Nitrogen Dioxide 559–597 nm.* (Springer–Verlag: Berlin). **1985.**

59. W. H. Hocking, A. J. Merer, D. J. Milton, W. E. Jones, and G. Krishnamurty. *Can. J. Phys.* **1980**, 58, 516–533.

REFERENCES: Chapters I and II (cont.)

60. A. S-C. Cheung, W. Żyrnicki, and A. J. Merer. *J. Mol. Spectrosc.* **1984**, 104, 315-336.

61. C. J. Cheetham and R. F. Barrow. *Advan. High Temp. Chem.* **1967**, 1, 7-41.

62. K. P. Huber and G. Herzberg. *Molecular Spectra and Molecular Structure: IV. Constants of Diatomic Molecules.* (Van Nostrand Reinhold: New York). **1979.**

63. G. T. Best, C. A. Forsberg, D. Golomb, N. W. Rosenberg, and W. K. Vickery. *J. Geophys. Res.* **1972**, 77, 1677-1680.

64. Z. Ceplecha. *Bull. Astron. Inst. Czech.* **1971**, 22, 219-305. (Errata: **1972**, 23, 146.)

65. A. J. Merer, C. M. Walmsley, and E. Churchwell. *Ap. J.* **1982**, 256, 151-155.

66. W. H. Hocking, G. Winnewisser, E. Churchwell, and J. Percival. *Astr. Ap.* **1979**, 75, 268-272.

67. C. E. St. John, C. E. Moore, L. M. Ware, E. F. Adams, H. D. Babcock. *Revision of Rowland's Preliminary Table of Solar Spectrum Wave-lengths.* (Carnegie Institution of Washington, publication no. 396). **1928.**

68. L. Delbouille, G. Roland, and L. Neven. *Atlas Photométrique du Spectre Solaire de λ3000 a λ10000.* (Institut d'Astrophysique de l'Université de Liège, Observatoire Royal de Bellllgique). **1973.**

69. K. S. Garger. *Zhur. Tekh. Fiz.* **1952**, 22, 606-615; *Chem. Abs.* **1955**, 49, 11 410 b.

70. A. B. Callear and R. G. W. Norrish. *Nature* **1959**, 184, 1794-1795.

71. K. Erhard. *Chimia* **1961**, 15, 400-401.

72. K. Erhard. *Z. Physik. Chem.* (Frankfurt) **1963**, 36, 126-132.

73. R. Scullman. *Arkiv Fysik* **1965**, 28, 255-265.

74. R. Scullman. S. Löfgren, and S. A. Kadavathu. *Physica Scripta* **1982**, 25, 295-301.

75. J. M. Delaval and J. Schamps. *J. Phys. B: At. Mol. Phys.* **1982**, 15, 4137-4149.

76. W. J. Balfour, B. Lindgren, and S. O'Connor. *Physica Scripta* **1983**, 28, 551-560.

77. C. R. Brazier and J. M. Brown. *Can. J. Phys.* **1984**, 62, 1563-1578.

78. A. S-C. Cheung and A. J. Merer (and possibly J. M. Brown). To be published.

REFERENCES: Chapters I and II (cont.)

79. M. Krauss and W. J. Stevens. *J. Chem. Phys.* **1985**, 82, 5584–5596.

80. S. Smoes and J. Drowart. *High Temp. Sci.* **1984**, 17, 31–52.

81. Y. Endo, S. Saito, and E. Hirota. *Ap. J.* **1984**, 278, L131–L132.

82. P. Feldman. *Private communication.* **1984.**

83. A. S–C. Cheung and H. E. Radford. *Private communication.* **1985.**

84. K. Evenson. U.S. National Bureau of Standards. Private communication. **1985.**

85. R. K. Dhumwad and A. M. Bass. *Applied Optics* **1963**, 2, 1335.

86. R. Bacis. *J. Phys. E.* **1976**, 9, 1081–1086.

87. H. M. Crosswhite. *J. Res. Natl. Bur. Stand.*, Sect. A **1975**, 79, 17–69.

88. M. S. Sorem and A. L. Schawlow. *Optics Comm.* **1972**, 5, 148–151.

89. (a) S. Gerstenkorn and P. Luc. *Atlas du spectre d'Absorption de la Molécule d'Iode.* (Editions du CNRS: Paris). **1978.**
(b) S. Gerstenkorn and P. Luc. *Rev. Phys. Appl.* **1979**, 14, 791–794.

90. C. Effantin, F. Michaud, F. Roux, J. d'Incan, and J. Verges. *J. Mol. Spectrosc.* **1982**, 92, 349–362.

Chapter III

1. M. Born and J. R. Oppenheimer. *Ann. Physik.* **1927**, 84, 457–484.

2. W. H. Hocking, A. J. Merer, D. J. Milton, W. E. Jones, and G. Krishnamurty. *Can. J. Phys.* **1980**, 58, 516–533.

3. A. S–C. Cheung, W. Żyrnicki, and A. J. Merer. *J. Mol. Spectrosc.* **1984**, 104, 315–336.

4. B. J. Howard and R. E. Moss. *Mol. Phys.* **1970**, 19, 433–450; **1971**, 20, 147–159.

5. L. Pauling and E. B. Wilson. *Introduction to Quantum Mechanics.* (McGraw-Hill: New York). **1935.** (a) pp. 113–117; (b) pp. 263–274.

6. H. Margenau and G. M. Murphy. *The Mathematics of Physics and Chemistry,* 2nd ed., pp. 411–414. (D. Van Nostrand: Princeton, N.J.). **1956.**

REFERENCES: Chapter III (cont.)

7. M. Born. *Festschrift Gott. Nachr. Mat. Phys.* **1951**, Kl, 1. Cited by Refs. (8) and (9).

8. M. Born and K. Huang. *Dynamical Theory of Crystal Lattices*, pp. 406–407. (Clarendon Press: Oxford). **1954.**

9. P. R. Bunker. *J. Mol. Spectrosc.* **1968**, 28, 422–443.

10. C. J. H. Schutte. *The Theory of Molecular Spectroscopy*, vol. 1, pp. 239–247. (North-Holland: Amsterdam). **1976.**

11. H. C. Longuet-Higgins. *Adv. Spectrosc.* **1961**, 2, 429–472.

12. Ch. Jungen and A. J. Merer. "The Renner-Teller Effect." In K. N. Rao, ed., *Molecular Spectroscopy: Modern Research*, vol. II, pp. 127–164. (Academic Press: New York). **1976.**

13. E. B. Wilson, Jr., J. C. Decius, and P. C. Cross. *Molecular Vibrations*, chap. 11. (McGraw-Hill: New York). **1955.** (Corrected ed.: (Dover: New York). **1980.**)

14. H. C. Allen, Jr. and P. C. Cross. *Molecular Vib-Rotors*, chap. 1. (John Wiley & Sons: New York). **1963.**

15. M. Karplus and R. N. Porter. *Atoms and Molecules*, pp. 454–482. (W. A. Benjamin: New York). **1970.**

16. G. Herzberg. *Molecular Spectra and Molecular Structure: I. Spectra of Diatomic Molecules*, 2nd ed. (Van Nostrand Reinhold: New York). **1950.** (a) p. 92; (b) p. 283.

17. P. A. M. Dirac. *The Principles of Quantum Mechanics*, 1st ed. (Clarendon Press: Oxford). **1930**; 4th ed. **1958.**

18. L. H. Thomas. *Nature* **1926**, 117, 514.

19. J. D. Jackson. *Classical Electrodynamics*, pp. 364–369. (John Wiley & Sons: New York). **1962.**

20. K. Kayama and J. C. Baird. *J. Chem. Phys.* **1967**, 46, 2604–2618.

21. J. H. Van Vleck. *Rev. Mod. Phys.* **1951**, 23, 213–227.

22. H. Lefebvre-Brion and R. W. Field. *Perturbations in the Spectra of Diatomic Molecules.* Preprint. (Planned publisher: Academic Press).

23. L. Veseth. *Theoret. Chim. Acta* **1970**, 18, 368–384.

24. L. Veseth. *J. Phys. B* **1971**, 4, 20–27. (Corrected by Ref. (25).)

25. J. M. Brown and J. K. G. Watson. *J. Mol. Spectrosc.* **1977**, 65, 65–74.

REFERENCES: Chapter III (cont.)

26. S. Green and R. N. Zare. *J. Mol. Spectrosc.* **1977**, 64, 217–222.

27. D. K. Cheng. *Field and Wave Electromagnetics.* (Addison–Wesley: Reading, Mass.) **1983**. (a) p. 202; (b) p. 211.

28. L. Eyges. *The Classical Electromagnetic Field*, pp. 385–387. (Addison–Wesley: Reading, Mass.). **1972**.

29. M. Bersohn and J. C. Baird. *An Introduction to Electron Paramagnetic Resonance*, pp. 208–217. (W. A. Benjamin: New York) **1966**.

30. E. Fermi. *Z. Physik* **1930**, 60, 320–333.

31. R. A. Ferrell. *Am. J. Phys.* **1960**, 28, 484–486.

32. I. N. Levine. *Molecular Spectroscopy*, pp. 369–371. (Wiley–Interscience: New York). **1975**.

33. H. A. Bethe and E. E. Salpeter. *Quantum Mechanics of One- and Two-Electron Systems*, pp. 179–181. (Springer–Verlag: Berlin). **1957**.

34. L. D. Landau and E. M. Lifshitz. *Quantum Mechanics: Non-relativistic Theory*, 3rd ed., p. 97. (Pergamon Press: Oxford). **1977**. (a) p. 84; (b) p. 97.

35. E. U. Condon and G. H. Shortley. *The Theory of Atomic Spectra.* (University Press: Cambridge). **1935**. (Corrected ed.: **1951**). (a) pp. 45–50; (b) pp. 97–98; (c) p. 81; (d) p. 91.

36. J. M. Brown and B. J. Howard. *Mol. Phys.* **1976**, 31, 1517–1525. (Erratum: *Mol. Phys.* **1976**, 32, 1197.)

37. F. Hund. *Z. Physik* **1926**, 36, 657–674.

38. R. S. Mulliken. *Rev. Mod. Phys.* **1930**, 2, 60–115; **1931**, 3, 89–155.

39. I. Kopp and J. T. Hougen. *Can. J. Phys.* **1967**, 45, 2581–2596.

40. J. B. Tatum and J. K. G. Watson. *Can. J. Phys.* **1971**, 49, 2693–2703.

41. R. W. Martin and A. J. Merer. *Can. J. Phys.* **1973**, 51, 125–143.

42. A. S–C. Cheung. *PhD. Thesis* (U. of British Columbia). **1981**.

43. C. H. Townes and A. L. Schawlow. *Microwave Spectroscopy*, pp. 174–185. (Dover: New York). **1975**. (McGraw–Hill: **1955**).

44. G. W. King. *Spectroscopy and Molecular Structure.* (Holt, Rinehart and Winston: New York). **1964**. (a) pp. 201–211; (b) p. 177; (c) p. 118.

45. M. Larsson. *Physica Scripta* **1981**, 23, 835–836.

REFERENCES: Chapter III (cont.)

46. J. T. Hougen. *The Calulation of Rotational Energy Levels and Rotational Line Intensities in Diatomic Molecules.* U.S. National Bureau of Standards Monograph **115**. (Washington, D.C.). **1970**. (a) p. 17; (b) p. 19; (c) pp. 11 and 25; (d) p. 29; (e) p. 30; (f) p. 42.

47. R. N. Zare, A. L. Schmeltekopf, W. J. Harrop, and D. L. Albritton. *J. Mol. Spectrosc.* **1973**, 46, 37–66.

48. I. Kovács. *Rotational Structure in the Spectra of Diatomic Molecules.* (American Elsevier: New York). **1969**. (a) p. 24; (b) p. 121.

49. A. J. Merer. Private communication.

50. J. M. Brown, J. T. Hougen, K.-P. Huber, J. W. C. Johns, I. Kopp, H. Lefebvre-Brion, A. J. Merer, D. A. Ramsay, J. Rostas, and R. N. Zare. *J. Mol. Spectrosc.* **1975**, 55, 500–503.

51. T. A. Miller. *Mol. Phys.* **1969**, 16, 105–120.

52. C. E. Soliverez. *J. Phys. C* **1969**, 2161–2174.

53. J. M. Brown, M. Kaise, C. M. L. Kerr, and D. J. Milton. *Mol. Phys.* **1978**, 36, 553–582.

54. J. M. Brown, E. A. Colbourn, J. K. G. Watson, and F. G. Wayne. *J. Mol. Spectrosc.* **1979**, 74, 294–318.

55. J. H. Van Vleck. *Phys. Rev.* **1929**, 33, 467–506 (especially pp. 484–485).

56. O. M. Jordahl. *Phys. Rev.* **1934**, 45, 87–97.

57. E. C. Kemble. *The Fundamental Principles of Quantum Mechanics With Elementary Applications*, pp. 394–396. (Dover: New York). **1958**.

58. J. E. Wollrab. *Rotational Spectra and Molecular Structure*, Appendix 7, pp. 411–413. (Academic Press: New York). **1967**.

59. P-O. Löwdin. *J. Chem. Phys.* **1951**, 19, 1396–1401.

60. J. M. Brown and A. J. Merer. *J. Mol. Spectrosc.* **1979**, 74, 488–494.

61. D. L. Albritton, W. J. Harrop, A. L. Schmeltekopf, and R. N. Zare. *J. Mol. Spectrosc.* **1973**, 46, 25–36.

62. A. N. Jette and T. A. Miller. *Chem. Phys. Lett.* **1974**, 29, 547–550.

63. A. S-C. Cheung, W. Żyrnicki, and A. J. Merer. *J. Mol. Spectrosc.* **1984**, 104, 315–336.

64. R. S. Mulliken and A. Christy. *Phys. Rev.* **1931**, 38, 87–119.

65. A. S-C. Cheung and A. J. Merer (and possibly J. M. Brown). To be published.

REFERENCES: Chapter III (cont.)

66. E. E. Whiting. *Computer Program for Determining Rotational Line Intensity Factors for Diatomic Molecules. (NASA Report no. TN D-7268).* **1973.**

67. E. P. Wigner. "On the Matrices Which Reduce the Kronecker Products of Representations of S.R. Groups. (Unpublished, **1940**). Revised version later published by L. C. Biedenharn and H. van Dam, eds. *Quantum Theory of Angular Momentum,* pp. 87–133. (Academic Press: New York). **1965.**

68. J. M. Brown, B. J. Howard, and C. M. L. Kerr. *J. Mol. Spectrosc.* **1976**, 60, 433–436.

69. D. M. Brink and G. R. Satchler. *Angular Momentum.* (University Press: Oxford). **1971.**

70. M. E. Rose. *Elementary Theory of Angular Momenta.* (John Wiley & Sons: New York). **1957.**

71. A. R. Edmonds. *Angular Momentum in Quantum Mechanics,* 2nd ed. (Princeton University Press: Princeton, New Jersey). **1960.** (Corrected ed.: **1974.**)

72. I. C. Bowater, J. M. Brown, and A. Carrington. *Proc. Roy. Soc. London, A* **1973**, 265–288.

73. H. Lefebvre–Brion. Unpublished notes. "Perturbations in the Spectra of Diatomic Molecules. (Winter College on Atoms, Molecules and Lasers, International Centre for Theoretical Physics, International Atomic Energy Agency -- Paper SMR 12/42). **1973.**

74. W. Weltner, Jr. *Ber. Bunsenges. Phys. Chem.* **1978**, 82, 80–89.

75. K. D. Carlson and C. Moser. *J. Phys. Chem.* **1963**, 67, 2644–2647; K. D. Carlson and R. K. Nesbet. *J. Chem. Phys.* **1964**, 41, 1051–1062; K. D. Carlson and C. R. Claydon. *Adv. High Temp. Chem.* **1967**, 1, 43–94.

76. K. P. Huber and G. Herzberg. *Molecular Spectra and Molecular Structure: IV. Constants of Diatomic Molecules.* (Van Nostrand Reinhold: New York). **1979.**

77. M. Krauss and W. J. Stevens. *J. Chem. Phys.* **1985**, 82, 5584–5596.

78. T. M. Dunn. In H. Eyring, ed. *Physical Chemistry: An Advanced Treatise,* vol. V, chap. 5. (Academic Press: New York/London). **1970.**

79. V. I. Srdanov and D. O. Harris. *Thirty-ninth Symposium on Molecular Spectroscopy,* paper TC7. (Ohio State University: Columbus, Ohio). **1984.** Also D. O. Harris. Private communication. February, **1986.**

REFERENCES (cont.)

Chapter IV

1. A. M. Bass and W. S. Benedict. *Ap. J.* **1953**, 116, 652–653.

2. R. W. B. Pearse and A. G. Gaydon. *The Identification of Molecular Spectra.* (Chapman and Hall: London). 1st ed. **1941**; 4th ed. **1976.**

3. L. Malet and B. Rosen. *Bull. Soc. Roy. Sci., Liège* **1945**, 14, 377–381.

4. G. Herzberg. *Molecular Spectra and Molecular Structure: I. Spectra of Diatomic Molecules*, 2nd ed., pp. 95–96. (Van Nostrand Reidhold: New York). **1950.**

5. T. M. Dunn. In H. Eyring, ed. *Physical Chemistry: An Advanced Treatise*, vol. V, chap. 5. (Academic Press: New York/London). **1970.**

6. L. Veseth. *Theoret. Chim. Acta* **1970**, 18, 368–384.

7. L. D. Landau and E. M. Lifshitz. *Quantum Mechanics: Non-relativistic Theory*, 3rd ed., p. 337. (Pergamon Press: Oxford). **1977.**

8. M. Krauss and W. J. Stevens. *J. Chem. Phys.* **1985**, 82, 5584–5596.

9. P. C. Engelking and W. C. Lineberger. *J. Chem. Phys.* **1977**, 66, 5054–5058.

10. A. S–C. Cheung, N. Lee, A. M. Lyyra, A. J. Merer, and A. W. Taylor. *J. Mol. Spectrosc.* **1982**, 95, 213–225.

11. J. M. Brown, J. T. Hougen, K.–P. Huber, J. W. C. Johns, I. Kopp, H. Lefebvre–Brion, A. J. Merer, D. A. Ramsay, J. Rostas, and R. N. Zare. *J. Mol. Spectrosc.* **1975**, 55, 500–503.

12. L. Albritton, A. L. Schmeltekopf, and R. N. Zare. *Mol. Spectrosc. Mod. Res.* **1976**, II, 1–67.

13. D. A. Ramsay. "Critical Evaluation of Molecular Constants from Optical Spectra." In D. R. Lide, ed. *Crit. Eval. Chem. Phys. Struct. Inf., Proc. Conf.* 1973 (Pub. **1974**), 116–129. (NAS: Washington, D.C.).

14. Y. Endo, S. Saito, and E. Hirota. *Ap. J.* **1984**, 278, L131–L132.

15. N. Åslund. *J. Mol. Spectrosc.* **1974**, 50, 424–434.

16. D. L. Albritton, W. J. Harrop, A. L. Schmeltekopf, R. N. Zare, and E. L. Crow. *J. Mol. Spectrosc.* **1973**, 46, 67–88.

17. A. J. Merer. Private communication.

18. J. M. Brown and J. K. G. Watson. *J. Mol. Spectrosc.* **1977**, 65, 65–74.

REFERENCES (cont.)

Chapter V

1. M. Krauss and W. J. Stevens. *J. Chem. Phys.* **1985**, 82, 5584–5596.

2. A. R. Edmonds. *Angular Momentum in Quantum Mechanics*, 2nd ed. (Princeton University Press: Princeton, New Jersey). **1960**. (Corrected ed.: **1974**.)

3. S. R. Langhoff and C. W. Kern. In H. F. Schaefer, III, ed. *Modern Theoretical Chemistry. II. Electronic Structure. Ab initio Methods.* (Plenum Press: New York). **1975**.

4. R. McWeeny. *J. Chem. Phys.* **1965**, 42, 1717–1725.

5. I. L. Cooper and J. I. Musher. *J. Chem. Phys.* **1972**, 57, 1333–1342.

6. H. Lefebvre–Brion and R. W. Field. *Perturbations in the Spectra of Diatomic Molecules.* Preprint. (Planned publisher: Academic Press).

7. J. M. Brown and B. J. Howard. *Mol. Phys.* **1976**, 31, 1517–1525. (Erratum: *Mol. Phys.* **1976**, 32, 1197.)

Appendix V

1. D. L. Albritton, A. L. Schmeltekopf, and R. N. Zare. *Mol. Spectrosc. Mod. Res.* **1976**, II, 1–67.

2. P. R. Bevington. *Data Reduction and Error Analysis for the Physical Sciences*, p. 73. (McGraw–Hill: New York). **1969**.

3. Y. Endo, S. Saito, and E. Hirota. *Ap. J.* **1984**, 278, L131–L132.

APPENDIX I

Line Frequencies for the Orange System (cm^{-1})

$\Omega' = \Omega'' = 4$, $v'' = 0$ — except where noted

6110 Å

J	R	Q	P
4	16360.021*	16354.993	
5	60.689*	54.777*	16349.858
6	61.517*	54.590	48.663
7	62.124*	54.327	47.441
8	62.807	53.995	46.124
9	63.386	53.609	44.793
10	63.912*	53.179	43.395
11	64.322	52.684	41.960
12	64.640*	52.041	40.412
13	64.640* 69.629		38.778
14	64.451 68.821		37.027
15	63.710 68.783		35.072 39.985
16	67.925		32.781 37.166
17	67.783		30.014* 34.610
18	67.591		32.169
19	67.188*		30.014*
20	66.654		27.812
21	65.701		25.333*
22	64.074 74.626		22.763
23	61.517* 72.335		19.791
24	58.052 70.774		16.110 26.665
25	69.239		11.528 22.338
26	68.034		06.030 18.741
27	66.771		15.166
28	65.444		11.937
29	63.912*		08.648
30	62.124*		05.286
31	60.021*		01.735
32	57.630		16297.922
33	54.777		93.797
34	51.425		89.372
35	47.506*		84.477
36	42.772		79.126
37			73.201
38			66.447

5911 Å

J	R	Q	P
4	16912.044	16907.560	
5	12.318	06.933	16902.450
6	12.474*	06.195	00.805
7	12.474*	05.312	16899.033
8	12.390	04.302	97.137
9	12.166	03.194	95.121
10	11.818	01.946	92.980
11	11.338	00.578	90.718
12	10.729	16899.076	88.318
13	09.978 10.009	97.453	85.805
14	09.049	95.682 95.713	83.155
15	07.767*	93.735	80.360 80.390
16	07.767*	91.456	77.398
17	06.231	90.556	74.090
18	04.785	87.857	72.029
19	03.253	85.367?	68.462
20	01.596	82.849	64.976
21	16899.813	80.205*?	61.412
22	97.880	77.398*?	57.718
23	95.802	74.379*?	53.894
24	93.561		49.931
25	91.100 91.168		45.811
26	88.576 88.726		41.539
27	85.708 85.952		37.046 37.116*
28	82.846 83.053		32.497* 32.643
29	80.052 80.205*		27.588* 27.836
30	76.710 76.800		22.696 22.903
31	73.280		17.873 18.027
32	69.569 69.873		12.508 12.598
33	65.631 65.923		07.072
34	61.485 61.773		01.336 01.632
35			16795.364* 95.649

5836 Å

J	R	Q	P
4	17133.122	17129.312	
5	32.584	28.014	17124.202
6	31.786	26.455	21.883
7	30.725	24.630*	19.305
8	29.399	22.551	16.479*
9	27.810	20.198*	13.359
10	25.957	17.594	09.989
11	23.845	14.721	06.362
12	21.510		02.461*
13			17098.316
14			93.933

Ω = 4 cont.

5820 Å

J	R	Q	P
4	17180.200	17176.120	
5	79.990	75.091	17171.011
6	79.582	73.859	68.962
7	78.982	72.435	66.710
8	78.184	70.808	64.261
9	77.201	68.994	61.618
10	76.035	66.989	58.781
11	74.686	64.798	55.756
12	73.163	62.432	52.545
13	71.472	59.888	49.156
14	69.598	57.161	45.593
15	67.579	54.284	41.848
16	65.402	51.243	37.949
17	63.074	48.045	33.889
18	60.591	44.701	29.670
19	57.979	41.196	25.307
20	55.227	37.565	20.783
21	52.373	33.800	16.135
22	49.350	29.926	11.347
23	46.215	25.881	06.456
24	42.957	21.731	01.397
25	39.560	17.446	17096.228
26	35.998 36.161	13.045	90.936
	35.872		
27	32.401 32.458	---	85.311
28	28.647		79.912 80.077
			79.791
29	33.530 34.158		74.287 74.342
	24.630		
30	26.551 27.118*		68.503
	20.198 20.309		
	18.424 18.924		
31	20.604 21.284		71.356 71.985
	13.915 14.160		62.454
32	15.763 16.479		62.349 62.915
	07.427		55.996 56.106
			54.219 54.719
33	11.271 12.542		54.373 55.051
	10.355		47.685 47.928
34	06.897 09.723		47.503 48.223
	04.860 06.504		39.161
35	03.175 06.067		40.983 42.261
	00.992 02.461		40.072
36	17098.114 17098.961		34.588 37.411
	96.782?		32.548 34.197
37	93.698 94.656		28.842 31.747*
	92.564		26.653 28.131*
38	89.206 90.083*		21.759 22.603
	88.219		20.436*?
39	84.516 85.148		15.331 16.272
	83.566		14.187
40	81.173 82.393		08.809 09.690
	79.536		07.824
41	76.289 77.289		02.105 02.737*
	74.416		01.158
42	71.674 72.432		16996.744 16997.965
	68.655		95.111
43	66.931 67.514		89.846 90.842
			87.970
44	62.051 62.540		83.216* 83.971
			80.198*
45	57.325 57.903		76.455 77.041
	56.565		
46	55.590 55.652		70.053 69.567
	50.810 51.684		
47	49.724* 50.634		62.833 63.410
			62.067
48	46.329 46.507		59.087 59.145
	36.626* 37.676*		54.303 55.182
49	35.104 35.629*		51.232 52.124
50	31.747 31.793?		45.809 45.991
	39.341		36.118 37.248
51	27.344 27.394*		32.581 33.114
	35.204*?		
52	22.603* 22.659		27.225 27.283*
	33.325?		34.476 34.827?
53	18.156*		20.819 20.866
			28.680? 29.021?
54	12.436?		14.078 14.136
			24.777?
55	07.706		07.635*
56	02.356		
57	16996.915 16997.337?		16893.206*
58	91.272 91.482		85.872*
59	85.224		

6131 Å — v″ = 1

J	R	Q	P
4		16304.946	
5		03.946	
6		02.750	
7		01.409*	
8	16307.210	16299.768	
9	06.289		
10	05.286*		16287.980
11	03.870*		85.016
12	02.528		81.907
13	00.903		78.618
14	16299.138		75.118
15	97.230		71.496
16	95.165		67.724*
17	92.982		63.790*
18	90.612		59.711
19	88.245*		55.474
20	85.553		51.125
21	82.861		46.608
22	80.001		42.013*
23	77.042		37.284
24			32.407
25	70.750		27.431
26	67.371 67.572		22.335
	67.285		
27	64.028		17.090
28	60.436		11.703 11.879
29	65.590 66.168		06.338
	56.666		
30	58.809 59.342		00.739
	52.436 52.551		
	50.125* 50.650*		
31	53.101 53.759		
	46.109 46.405		
32	48.478 49.193		
	40.122*		
33	44.235 45.481		
	43.314		
34	40.122 42.938		
	38.091 39.753		
35	36.662 39.498		
	34.516 35.947		
36	31.862 32.728		
	30.531		
37	27.735 28.685		
	26.594		
38	23.530 24.388		
	22.538		
39	19.141 19.754		
	18.183*		
40	16.097 17.306		
	14.441		
41	11.494 12.496		
	09.612		
42	07.192 07.960		
	04.150		
43	02.778 03.380		
44	16198.224 16198.699		

Ω = 4 cont.

5790 Å

J	R	Q	P
4		17250.884	
5		50.650*	
6	17257.411	50.525	
7	58.130	50.200*	17243.369
8	58.856	49.961	42.058*
9	59.575*	49.676	40.814*
10	60.195	49.324*	39.489
11	60.888*		38.120
12	61.357		36.712
13	62.030		35.277
14	62.534		33.790
15	63.036		32.411
16	63.494		30.867
17	63.973		29.333
18	64.411*		27.773
19	64.777		26.199
20	65.131		24.577
21	65.485*		22.920
22	65.764*		21.265
23	66.105		19.589
24	66.367		17.834
25	66.625		16.121
26	66.795*		14.356*
27	67.026		12.561
28			10.741
29			08.897
30			07.028
31			05.131
32			03.203
33			01.245
34			17199.248
35			97.232
36			95.146
37			92.974
38			90.994
39			88.489 89.131*
40			86.447 87.665
41			85.001 85.384

5808 Å v″ = 1

J	R	Q	P
4	17219.727	17214.894	
5	20.443	14.659	17209.820
6	21.091	14.355*	08.570
7	21.663	13.996	07.261
8	22.138	13.550	05.879
9	22.280*	13.009	04.428
10	22.895*		02.869
11	22.985		00.988
12	22.829		17199.587
13	22.895*		97.638
14	22.280*		95.454
15			93.483
16			90.853

6105 Å — v″ = 1

J	P
4	
5	
6	
7	
8	
9	
10	
11	
12	16366.037
13	
14	
15	
16	60.581*
17	59.220
18	57.792
19	56.363
20	
21	53.426
22	51.916
23	50.390*
24	48.825
25	47.300
26	45.738
27	44.155
28	42.522
29	40.913
30	39.280
31	37.585
32	35.905
33	34.182
34	32.411*
35	30.705
36	28.880

5583 Å

J	P	
38	17805.389	17805.455
39	01.287	
40	17797.195	17797.241
41	92.998	93.055
42	88.670	88.779
43	84.452	84.680?
44	80.010	80.277
45	75.606	75.637
46	70.948	70.996
47	67.314	67.563
48	61.557	61.688
49	56.975	57.106
50	50.752?	

5868 Å — v″ = 1

J	R	Q	P
4	17034.890*	17030.227	
5	35.419	29.820	17025.156
6	35.866	29.336	23.735
7	36.232	28.769	22.237
8	36.522	28.131*	20.654
9	36.732	27.394*	18.995
10	36.865	26.592	17.264*
11	36.910*	25.715*	15.442
12	36.910*	24.753	13.543*
13	36.797		11.570
14	36.626		09.524
15	36.371		07.403
16	36.049		05.199
17	35.629		02.928
18	35.168		00.579
19	34.882*		16998.147
20	34.141		95.653
21	33.453		93.342
22	32.630		90.581
23	31.882		87.866
24	31.001		85.060*
25	30.021		82.262
26	29.093		79.364
27	28.025		76.360
28	26.900		73.419
29	25.715		70.334
30	24.470		67.195
31	23.165		63.993
32	21.810		60.742
33	20.332 20.375		57.418
34	18.848*? 18.901		54.049
35	17.222*		50.561 50.605
36	15.502 15.555*		47.072? 47.110
37	13.689		43.439
38	11.899*		39.705 39.769*
39	10.009 10.076		35.894
40	08.025 08.111*		32.153 32.109*
41	06.228		28.213* 28.272
42	04.273* 04.004		24.226* 24.314
43	01.927 01.957*		20.299 20.409*?
44	16999.665 16999.613		16.461 16.196
45			12.166*
46			07.846?

$\Omega' = \Omega'' = 3$, $v'' = 0$ — except where noted

6005 Å

J	R	Q	P
3	16644.311	16640.918	
4	44.440	40.190	16636.808
5	44.382	39.301	35.062
6	44.138	38.215	33.134
7	43.701	36.943	31.022
8	43.067	35.479	28.721
9	42.227	33.812	26.232
10	41.164* 41.198*	31.953	23.542
11	39.891 39.942		20.649
12	38.384? 38.497?		17.533* 17.562*
13	36.539 36.645		14.206 14.259
14	34.641 34.675		10.638 10.753
15	32.447 32.494		06.748 06.855
16	30.009 30.173		02.801 02.834
17	27.334 27.846		16598.555 16598.600
18	24.433		94.064 94.225
19	21.331?		89.336 89.849
20	18.034?		84.388

5874 Å

J	R	Q	P
3	17025.855	17022.783*	
4	25.588	21.759*	17018.691*
5	25.087*	20.436*	16.605
6	24.300 24.351*		14.279
7	23.329 23.407?		11.707*
8	22.127? 22.237		08.938
9	20.713? 20.879		05.850 05.932?
10	19.098? 19.326*		02.598? 02.737*
11	17.266* 17.515		16999.126? 99.299
12	15.237		95.462? 95.688*
13	13.009* 13.356*		91.788 91.829
14	10.576? 10.968		87.502
15	07.924? 08.348		83.216* 83.563
16	05.072 05.516		78.724? 79.122
17			74.033? 74.459
18			69.126 69.567*
19			
20			58.648??

5941 Å — $\Omega' = 3$, $\Omega'' = 2$

J	R	Q	P
3			
4			
5			
6			
7	16831.898 16831.979		
8	30.653 30.767		
9			16814.324 16814.413
10			
11	25.619 25.876*		
12			
13	21.210 21.560		

5975 Å

J	R	Q	P
3	16729.942	16726.084	
4	30.653	25.829	16721.977
5	31.289	25.505	20.695
6	31.859*	25.117	19.344
7	32.371	24.659?	17.928
8	32.798	24.145	16.438
9	33.156	23.547	14.901
10	33.444	22.878	13.272
11	33.615*	22.144	11.580
12	33.802*		09.815
13	33.866*		07.940*
14	33.866*		06.070
15	33.775*		04.082
16	33.615*		02.020
17	33.366		16699.881
18	33.033		97.670
19	32.600		95.371
20	31.901* 32.055		92.988
21	31.250 31.901*		90.504
22	31.039 31.593		87.763 87.914
23	30.035 30.407*		85.058 85.709
24	30.319 30.593		82.801 83.359
25	28.852 29.264		79.753 80.117
26	28.181 28.387		77.990 78.263
27	27.059 27.094		74.479 74.893
28	25.945 26.005		71.768 71.974
29	24.659 24.883		68.597 68.634
30	23.264 23.416		65.447 65.508
31	21.635 21.906		62.116 62.342
32	20.272 20.409		58.683 58.837
33	18.461 18.508		55.014 55.285
34	16.384		51.611 51.749
35	13.628 13.675		47.767 47.815
36	10.697		43.653
37			38.866 38.912
38			33.899

5907 Å

J	R	Q	P
3	16929.497*	16926.298*	
4	29.428*	25.381	16922.179
5	29.186		20.249
6	28.050		18.116*
7	27.847?		15.829
8	26.298*		12.615*
9	24.978		10.342*?
10	23.407		06.777
11	21.556*		03.397
12	19.521		16899.765
13			95.882
14			91.756?

Ω = 3 cont.

5845 Å

J	R	Q	P
3	17109.907	17106.805	
4	09.676	05.797	17102.696
5	09.206	04.539	00.661
6	08.493	03.040	17098.378
7	07.546	01.300	95.846
8	06.362*	17099.323	93.075
9	04.971	97.120	90.083*
10	03.361	94.656*	86.845
11	01.555	92.057	83.393
12	17099.569		79.732
13	97.419		75.871
14	95.126		71.831
15	92.726		67.627*
16	90.246		63.284
17	87.720		58.829
18	85.148* 85.198		54.301
19	82.640 82.684		49.724
20	80.131 80.191		45.122 45.163
21	77.635 77.722		40.545 40.587
22	75.168 75.269		35.988 36.049
23	72.599 72.753		31.442 31.528
24	70.007 70.205		26.935 27.033
25	67.321 67.574		22.314 22.462
26	64.523 64.837		17.678 17.878
27	61.579 61.969		12.949 13.198
28	58.467 58.946		08.111* 08.420
29	55.165 55.759		03.123* 03.512
30	51.643 52.399*		16997.965 16998.447
31	47.881*		92.626 93.215
32	43.854		87.060 87.809
33	39.770		81.252
34	34.308 34.345		75.209*
35	29.202*		69.075
36	23.508 23.790		61.572 61.619
37	17.477 17.628		54.441
38	10.788 10.868		46.708 46.985
39	03.456		38.648 38.804
40	16999.688*		29.942* 30.007
41	88.175?		20.573

5915 Å — Ω′ = 3, Ω″ = 2

J	R	Q	P
3			
4			
5			
6			
7			
8			
9			
10			
11			
12			
13			
14			
15	16900.760*		
16	16898.182		
17	95.569		
18			
19	90.240* 90.304		
20	87.633 87.695		
21	85.009 85.099		16847.921 16847.969
22	82.420 82.517		43.230 43.298
23	79.707 79.866		38.555 38.642
24	76.979 77.177		33.901 34.005
25			29.142 29.296
26	71.207 71.514		24.353 24.551
27	68.100 68.462		19.467 19.724
28	64.822 65.301		14.464 14.776
29	61.358* 61.949		
30	57.656 58.408		
31			
32	49.498		
33	45.227		
34	39.575 39.609		

5866 Å

J	R	Q	P
3	17047.800*	17044.434*	
4	47.881	43.694	17040.321
5	47.800*	---	38.554
6	47.503*	41.551?	36.586
7	46.965		34.435*
8	46.229		32.071
9	45.266		29.490
10	43.906?		26.707
11	42.522		23.683
12	40.752		20.288?
13	38.688*		16.851*
14	36.308*		13.009
15			08.897*
16			04.501
17	41.173 41.965		
18	39.894		
19	36.865* 37.676		03.179 03.972
20	34.465 35.302		16998.996 16999.848
21			94.782* 95.581
22			90.322 91.182*

$\Omega' = \Omega'' = 2$, $v'' = 0$ — except where noted

5919 Å

J	R	Q	P
2	16888.576*	16885.708 16885.872	
3	89.062	85.467	16882.609 16882.774
4	89.410	84.927	81.332
5	~89.62 *		79.756
6	89.620*		78.043
7	89.295 90.240*		76.178
8	89.781		74.131
9	89.336		71.717 72.668
10	88.827 88.869		70.137
11	88.152 88.226		67.664*
12	87.324 87.433		65.058 65.101
13	86.299 86.479		62.325 62.389
14	85.077 85.389		59.426 59.531
15	83.631 84.214?		56.336 56.517
16	81.523 81.928		53.050 53.365
17	79.629 79.943		49.537 50.121
18	77.398* 77.657		45.373 45.785*
19	74.828 75.053		41.416 41.726
20	71.927 72.128		37.116* 37.384
21	68.711 68.893		32.497* 32.716
22	64.976* 65.387		27.533 27.732
23	61.632		22.258 22.438
24			16.464 16.870
25	53.529 53.598		
26	49.242		
27	44.261 44.837		
28	39.810 40.333		
29	35.195 35.760		
30	30.480 31.214		
31	25.652 25.876		
32	20.751 ---		
33	15.738 15.776		

5821 Å

J	R	Q	P
2	17178.621	17175.791	
3	79.148	75.523?	17172.692
4	79.582	75.021	71.388
5	79.846	74.414	69.855
6	80.200*	73.639	68.209
7	79.753 79.792		66.407
8	79.235 79.286		64.696
9	80.368		62.185 62.217
10			59.598 59.648
11	78.621 78.683		58.670
12	77.472 77.616		
13	76.346 76.401		52.791 52.850
14	75.091*		49.585 49.719
15	72.999*? 73.280?		46.387 46.437
16			43.067
17	61.082		38.929 39.196
18			
19			22.870
20	61.380		
21	57.979* 58.968*		
22			16.987
23			11.532 12.542*
24			
25			
26	54.935		
27	51.167		
28	47.389		17098.205
29	43.621		92.377
30	39.783		86.550
31			80.724
32			74.841

5865 Å — $\Omega' = 2$, $\Omega'' = 3$

J	R	Q	P
20	17064.425 17064.628		
21	61.355? 61.513		
22	58.137 ---		17020.283 ---
23	54.519 ---		15.139 17015.331*
24			09.524* 09.868*
25	46.699 46.759		04.235 ---
26	42.559		
27	37.735 38.315		16992.330 16992.383
28	33.453* 33.973		86.144
29	29.014 29.571		79.278 79.852
30	24.470* 25.209		72.949 73.474
31	19.821* 20.046		66.471 67.030
32	15.104* 15.442		59.878 60.629
33	10.281 10.320		53.206 53.443*
34	05.352		46.439 46.787
35	00.234 00.313		39.582 39.623
36	16995.111*		32.626
37	89.828*		25.461 25.549
38	84.255?		18.116*? 18.334

5888 Å fragment — $\Omega' = 2$, $\Omega'' = 1$

J	R	Q	P
21	16963.705* 64.682*		
22			
23			16916.971* 17.948*

Ω = 2 cont.

5619 Å

J	R	Q	P
2	17789.268*?	17786.895	
3	89.711	86.192	17783.791
4	89.966	85.580	82.059
5			80.410
6	89.606 90.295		78.596
7			
8	89.768		74.106? 74.797
9	97.241* 97.414		
10	96.077 96.382		70.134
11	95.167		75.506 75.716
12	91.821 93.749*		72.305 72.613
13	94.669* 96.200		69.330
14	93.587 94.669		63.929 65.844
15	92.423 93.238		64.698 66.248
16	90.948 91.816		61.557 62.649
17	90.333		58.327* 59.142
18	88.317 88.670		54.669 54.800
19	85.832 86.895?		52.122
20	82.857		48.045 48.386
21	80.410		43.503 44.564?
	85.423 86.512		
22			38.460
23			33.953
			38.979 40.065*

5908 Å — v″ = 1

J	R	Q	P
2	16918.189		
3	18.557		
4	18.892		
5			
6	18.611 19.316		
7			
8	18.892*		
9	26.608 26.405		
10	25.339 25.650		
11	24.527*		
12	21.260 23.191*		
13	24.226 25.750		
14	23.239 24.314*		
15	22.179* 22.998*		
16	20.841 21.709		
17	20.352		
18	18.472 28.825		
19	16.139		
20	13.356		
21	11.043		
	16.040 17.117*		

Ω′ = Ω″ = 1, v″ = 0 — except where noted

5876 Å

J	R	Q	P
1			
2	17019.177*		
3	19.177* 19.277*		
4	19.326* 19.488		17011.899*
5	19.277* 19.536*		09.877 09.925
6	19.419		07.886* 08.054
7	18.594* 19.146*		05.761 06.018
8	18.691		03.830
9	18.083		00.931 01.473
10	17.266*		16998.949
11	16.181		96.258
12	13.774 16.061		93.372
	26.764		
13	13.356 14.630		90.206
	24.352		
14	09.297 13.148		85.722 88.009
	21.866		98.719
15	07.013 11.524		83.216* 84.503
	18.901 19.337*		94.225
16	09.605?		77.097 80.948
	16.762		89.669
17	10.448 14.132		72.727 77.245
			84.629 85.060
18	11.311		73.250?
			80.410
19	08.387 08.859		72.025 75.710
20	05.045 05.654		70.814
21	02.231		65.824 66.296
22	00.021		60.402 61.018
23			55.520
24	16990.413		51.232*
25	88.378		
26	85.615 95.776		37.493
27	82.472 92.383		33.395
28	78.836 88.627		28.567 38.729
29	74.714		23.358 33.274
30			17.660 27.450
31			11.472

Ω = 1 cont.

5614 Å

J	R		Q	P	
1	17804.525		17802.729		
2	05.306		02.478?		
3	05.911	05.948		17799.331*	
4	06.431?	06.484		98.029	
5	06.867?	06.919		96.556	96.588
6	07.207	07.276		95.000	95.045
7	07.483	07.547		93.350?	93.406
8	07.677	07.744		91.627	91.686
9	07.826*			89.830*	89.875
10	07.878			87.936	87.993
11	07.774			86.033	
12	07.643			83.979	
13	07.408	07.483?		81.803	
14	07.043			79.589	
15	06.526			77.281	
16	05.737	05.817		74.841	
17	04.525	04.749		72.253	
18	02.658			69.380	69.472
	08.938	09.754			
19				66.097	66.328
	07.483	08.109			
20				62.175	
	06.328	06.829*		68.442	69.254
21	05.306	05.737*		64.912	65.539
22	04.294	04.749*		61.688	62.175
23	03.181	03.753		58.599	59.036
24	01.287	02.701		55.521	55.916
25	02.412?			52.343?	52.907
26	00.514	00.627		48.386*	49.791
27	17799.185	17799.480		47.439?	
28	97.699	98.268		43.471*	43.580
29	95.517?	97.015		40.065	40.368*
30	95.734	96.466		36.534	37.089
31	94.567	94.781		32.282	33.773
32	92.998*	93.238*		30.436	31.166
33	91.513	91.627		27.205	27.432
34	89.606	90.187		23.599	23.830

5904 Å — v″ = 1

J	R		Q	P	
1	16933.395*		16931.620		
2	34.206*		31.399?	---	
3	34.827	34.875*		16928.272*	
4	35.393	35.441		26.996	
5	35.894*			25.549	25.591
6	36.266*	36.326*		24.047	24.089
7	36.589	36.655		22.452?	22.507
8	36.841	36.896		20.819*	20.866*
9	37.085*			19.060*	19.112
10	37.191*			17.242	17.300
11	37.191*			15.419	
12	37.144			13.459	
13	37.005	37.085?		11.385	
14	36.739			09.275*	
15	36.326*			07.086	
16	35.663	35.759*		04.772*	
17	34.589	34.827		02.314	
18	32.865			16899.579	16899.676
	39.148	39.954			
19				96.447	96.673
	37.837	38.466			
20	36.841	37.335		98.963	99.765
21	35.977	36.413			
22	35.137	35.582			
23	34.206*	34.761			
24	32.485	33.906			
25	30.535?				
26	32.109*	32.222			
27	30.994	31.282*			
28	29.726	30.285			
29	27.767	29.259			
30	28.213	28.944			
31	27.283	27.508			
32	25.972*	26.214			
33	24.722*	24.866*			
34	23.101*	23.669			
35	21.907*	22.359*			
36	20.655				
37	18.998	19.159			

Ω′ = Ω″ = 0, v″ = 0

5884 Å

J	R	P
0		
1	16993.995	
2	94.448	
3	94.712	16988.768*
4	94.782*	87.060*
5		85.308
6		83.290
7		
8		
9		
10		
11		
12		
13		
14		
15		
16	94.400	
17	92.913*	
18	91.272	57.857
19	89.466	54.267
20	87.471	50.561*
21	85.352	46.656
22	83.109	42.593
23	80.198?	38.398
24	78.072	34.066*
25	75.209*	
26	72.328*	24.866*
27	69.416	19.941
28	64.682*?	14.973*
29	63.093*	09.978*
30	58.762	03.194*
31	54.507	16899.513

5625 Å

J	R	P	
0			
1			
2			
3	17777.193		
4	77.756	17768.857*?	
5	77.778*?	78.257	67.787
6	78.698*		66.248*
7	79.026	64.205?	64.667
8	79.278		63.011
9	79.419		61.264
10	79.496		59.421
11	79.455		57.485
12	79.314		55.463
13	79.065		53.339
14	78.698*		51.111
15	78.214		48.777
16	77.572		46.327
17	76.687		43.750
18	75.716		41.020
19	74.634		38.054
20			35.003
21			31.834

Ω = 0 cont.

5895 Å

J	R	P
0		
1		
2	16965.177	
3		
4	64.895	16957.857*
5	64.462	
6	63.705*	53.408
7	62.714	50.876
8	61.470	48.040
9	59.999	44.952
10	58.286	41.619
11	56.339	38.057
12	54.199*	34.257
13	51.764	30.224
14	49.154	25.972*
15	46.327	21.474
16	43.696	16.774
17		11.864
18		07.151
19		
20		
21		
22		
23		
24		
25		
26		
27	16994.171	
28	89.466*	
29	84.577	16934.761
30	79.485	27.972
31		21.004
32		13.841

5623 Å

J	R	P
0		
1	17781.844	
2	82.544	
3	83.138*	17776.611
4	83.635	75.221*
5	84.023*	73.734
6	84.307*	72.139
7	84.507*	70.440
8	84.591*	68.633*
9	84.591*	66.735
10	84.507*	64.739*
11	84.357*	62.649*
12	84.118	60.486
13	83.791	58.234
14	83.392	55.906
15	82.902	53.503
16	82.419	51.014
17	81.652*	48.442
18	80.824*	45.868
19	79.769*	43.024
20	78.257	40.106
21		36.972
22		33.369

^{54}FeO isotopic bands

Ω′ = Ω″ = 4, v″ = 0

5911 Å

J	R	Q	P
4	---	16909.912	
5	16914.703	09.275	16904.772*
6	14.854*	08.530	03.102
7	14.887*	07.635*	01.313
8	14.778	06.647	16899.413
9	14.585	05.528	97.383
10	14.236	04.254*	95.228
11	13.761	---	92.980*
12	13.174	01.426	90.556*
13	12.387*		88.034
14	11.615		85.389*
15	10.629?		82.517
16			79.707
17			76.641

5820 Å

J	R	Q	P
4	17189.131*	17185.091	
5	88.838	83.985	17179.938
6	88.329	82.661	77.805
7	87.610	81.122	75.453
8	86.687	79.373	72.886
9	85.558	77.416	70.102
10	84.232	75.260	67.128?
11	82.709*		63.933
12	81.009		60.552
13	79.123		56.972
14	77.067		53.210
15	74.834		49.271
16	72.435*		45.160
17	69.916		40.870
18	67.245?		36.429
19	64.422		31.843
20	61.618*		27.118?
21	58.968		22.239
22	54.935* 54.994		17.446
23	51.797		12.673
24	48.205		06.585 06.652
25	43.947 44.581		01.397*
26			17095.762
27			89.436 90.083*

APPENDIX II

Line Frequencies for the $^5\Pi - X\,^5\Delta$ System (cm^{-1})

The parities are labelled where appropriate, with the first letter being the parity of the upper level and the second letter that of the lower level.

Appendix II -- $^5\Pi_{-1}$ - $X^5\Delta_0$ (0,0)

J	R				Q				P			
	aa		bb		ab		ba		aa		bb	
0					-		-		-		-	
1									-		-	
2												
3												
4												
5					10421.844	*						
6					10421.044		10421.422	*				
7					10420.108		10420.517		10414.021	*	10413.798	
8					10419.054	*	10419.484	*	10412.071	*	10411.845	*
9					10417.861	*	10418.326	*	10409.964	*	10409.756	*
10					10416.526		10417.028	*	10407.732	*	10407.556	*
11			10426.258	*	10415.073	*	10415.609		10405.367	*	10405.216	*
12	10425.632	*	10425.632	*	10413.482	*	10414.021		10402.851	*	10402.748	*
13	10424.827	*	10424.827	*	10411.751	*	10412.352	*	10400.207	*	10400.158	*
14	10423.867	*	10423.932		10409.835	*	10410.526		10397.439	*	10397.439	*
15	10422.782	*	10422.892	*	10407.896	*	10408.586	*	10394.529	*	10394.529	*
16	10421.554	*	10421.750	*	10405.752		10406.501		10391.487	*	10391.544	*
17	10420.191		10420.438	*	10403.487	*	10404.283		10388.306	*	10388.427	*
18	10418.710	*	10418.986		10401.085		10401.935	*	10384.993	*		
19	10417.068	*	10417.419	*	10398.547	*	10399.459	*	10381.564		10381.786	*
20	10415.297	*	10415.712		10395.870	*	10396.853		10377.984		10378.262	*
21	10413.393	*	10413.878		10393.074		10394.097	*	10374.272		10374.624	*
22	10411.347	*	10411.896		10390.133	*	10391.218		10370.417	*	10370.832	
23	10409.174	*	10409.835	*	10387.039		10388.206	*	10366.436	*	10366.886	*
24	10406.859		10407.556	*	10383.825		10385.062	*	10362.329	*	10362.857	
25	10404.408	*	10405.161	*	10380.484	*	10381.786		10358.041	*	10358.667	
26	10401.818		10402.684		10376.982		10378.338	*	10353.655		10354.352	*
27	10399.070	*	10400.036	*	10373.352	*	10374.826		10349.110		10349.910	*
28	10396.220	*	10397.254	*	10369.581		10371.150		10344.455	*	10345.339	*
29	10393.181	*	10394.311	*	10365.657	*	10367.320		10339.651	*	10340.604	*
30	10390.069		10391.303	*	10361.643		10363.360	*	10334.718	*	10335.751	*
31	10386.776	*	10388.103	*	10357.464	*	10359.256	*	10329.644	*	10330.760	*
32	10383.360	*	10384.793	*	10353.145		10355.019		10324.410		10325.687	*
33	10379.839	*	10381.306	*	10348.687		10350.702	*	10319.050	*	10320.341	*
34	10376.158	*	10377.716		10344.095	*	10346.192		10313.569	*		
35	10372.270	*	10373.994		10339.365	*	10341.574			*		
36	10368.306		10370.100	*	10334.502	*	10336.808		10302.186	*		
37	10364.204		10366.158	*	10329.493		10331.929		10296.275			
38	10359.957	*	10362.091	*	10324.361		10326.923		10290.228			
39					10319.117	*	10321.811	*	10284.081	*		
40					10313.770				10277.793	*		
41					10308.544				10271.434	*		
42									10265.174	*		

Appendix II (cont.) -- $^5\Pi_0 - X^5\Delta_1$ (0,0)

J	R				Q				P			
	aa		bb		ab		ba		aa		bb	
1												
2												
3												
4					10403.148	*	10440.951					
5					10402.459	*	10440.281	*				
6			10445.770	*	10401.673		10439.446	*				
7	10408.054		10445.706	*	10400.765	*	10438.493				10432.161	*
8	10407.926	*	10445.499	*	10399.735		10437.408		10392.467	*	10430.173	*
9	10407.691	*	10445.174	*	10398.547	*	10436.160		10390.396	*	10428.031	*
10	10407.343	*	10444.710		10397.295	*	10434.784		10388.206	*	10425.764	
11	10406.788	*	10444.099	*	10395.870	*	10433.278		10385.874	*	10423.350	
12	10406.169	*	10443.351	*	10394.311	*	10431.629		10383.401	*	10420.800	
13	10405.367	*	10442.466	*	10392.637		10429.843		10380.821	*	10418.123	
14	10404.454	*	10441.440	*	10390.834	*	10427.934	*	10378.117	*	10415.297	*
15	10403.451	*	10440.281	*	10388.873		10425.863	*	10375.256	*	10412.352	*
16	10402.280	*	10438.985	*	10386.805	*	10423.675		10372.270	*	10409.244	*
17	10401.005	*	10437.548	*	10384.631		10421.331		10369.174		10406.004	*
18	10399.581	*	10435.948	*	10382.299	*	10418.854	*	10365.942	*	10402.604	*
19	10398.023	*	10434.187		10379.839	*	10416.229		10362.572	*		
20	10396.340		10432.264	*	10377.241		10413.434	*	10359.075		10395.450	
21	10394.529	*	10430.173	*	10374.523		10410.464		10355.446	*	10391.627	
22	10392.566	*	10428.031	*	10371.679		10407.343	*	10351.700		10387.614	
23	10390.494	*		*	10368.701		10404.174	*	10347.824	*	10383.465	*
24	10388.306	*	10423.476	*	10365.580		10400.919		10343.792	*	10379.244	*
25	10385.960	*	10420.983		10362.329	*	10397.547		10339.651	*	10374.968	
26	10383.465			*	10358.951	*	10394.031	*	10335.369	*	10370.553	*
27	10380.858	*	10415.539		10355.446	*	10390.344	*	10330.939	*	10366.010	*
28	10378.117	*	10412.595		10351.807	*	10386.520	*	10326.424	*		*
29	10375.256	*	10409.478	*	10347.987	*	10382.549	*	10321.762	*	10356.430	*
30	10372.270	*	10406.253		10344.128	*		*	10316.954			*
31	10369.113		10402.851	*	10340.100	*	10374.142		10312.020	*	10346.265	*
32	10365.830	*		*	10335.893	*	10369.712	*	10306.949		10340.952	*
33	10362.421	*	10395.659	*	10331.620		10365.132		10301.759	*	10335.487	*
34	10358.893	*	10391.791	*	10327.183			*	10296.422	*	10329.874	
35	10355.234		10387.801	*	10322.612		10355.559	*	10290.940	*	10324.103	*
36	10351.463	*		*	10317.922		10350.548		10285.342		10318.240	*
37	10347.491	*		*	10313.077	*	10345.405		10279.647		10312.209	
38			10375.056		10308.102	*	10340.127	*			10306.036	*
39			10370.553	*	10303.014	*	10334.718	*			10299.731	*
40			10365.898	*	10297.758	*	10329.188				10293.302	
41			10361.148				10323.532	*			10286.721	*
42			10356.269				10317.746	*			10280.050	
43			10351.276	*				*				
44			10346.192	*			10305.822					
45							10299.731	*				

Appendix II -- $^5\Pi_0$ - $X^5\Delta_1$ (0,0) (cont.)

J	R		Q		P	
	aa	bb	ab	ba	aa	bb
46				10293.514 *		
47				10287.227		

$^5\Pi_1$ - $X^5\Delta_2$ (0,0)

J	R		Q		P	
	aa	bb	ab	ba	aa	bb
2						
3						
4						
5			10406.372 *	10406.433 *		
6			10405.561 *	10405.650		
7			10404.604	10404.748 *		
8			10403.547	10403.711	10396.340 *	10396.477
9			10402.335 *	10402.533 *	10394.256 *	10394.403
10	10410.879 *		10401.005 *	10401.248	10392.002 *	10392.208
11	10410.300 *	10410.664	10399.528	10399.821	10389.634 *	10389.873
12	10409.605 *	10410.009	10397.895 *	10398.253 *	10387.122 *	10387.418
13	10408.741	10409.244 *	10396.179 *	10396.581 *	10384.493 *	10384.793 *
14	10407.777	10408.304 *	10394.311 *	10394.757	10381.721 *	10382.102
15	10406.670 *	10407.262 *	10392.290	10392.807 *	10378.802 *	10379.244 *
16	10405.419 *	10406.076 *	10390.133 *	10390.713 *	10375.758	10376.282 *
17	10403.994 *	10404.748 *	10387.858	10388.522	10372.575 *	10373.169 *
18	10402.533 *	10403.337 *	10385.442 *	10386.190 *	10369.271 *	10369.938 *
19	10400.867 *	10401.772 *	10382.896	10383.717	10365.830 *	10366.561
20	10399.070 *	10400.071 *	10380.217	10381.121	10362.246 *	10363.070 *
21	10397.154	10398.253 *	10377.374	10378.396 *	10358.535	10359.437
22	10395.112 *	10396.274 *	10374.447	10375.532 *	10354.674 *	10355.673 *
23	10392.907	10394.179	10371.356	10372.529	10350.702 *	10351.807 *
24	10390.565	10391.957	10368.136	10369.403 *	10346.582 *	10347.766
25	10388.103 *	10389.593 *	10364.785	10366.158	10342.345 *	10343.614
26	10385.517 *	10387.122 *	10361.290 *	10362.768	10337.957 *	10339.312 *
27	10382.763	10384.493 *	10357.659	10359.256 *	10333.439	10334.915 *
28	10379.905 *	10381.721 *	10353.904 *	10355.587	10328.777	10330.365 *
29		10378.843 *	10350.007 *	10351.807 *	10323.994	10325.689 *
30	10373.783 *	10375.826 *	10345.977 *	10347.907 *	10319.050 *	10320.884
31	10370.498 *	10372.669 *	10341.813	10343.844	10314.034 *	10315.947
32	10367.073 *	10369.403 *	10337.509	10339.692 *	10308.822 *	10310.870 *
33	10363.533 *	10366.010 *	10333.077	10335.378 *	10303.499 *	10305.675
34	10359.878 *	10362.431 *	10328.512	10330.939 *	10298.025	10300.345
35	10356.053	10358.729	10323.800	10326.364	10292.409 *	10294.873 *
36	10352.097 *	10354.919 *	10318.967	10321.649	10286.721 *	10289.279 *
37	10347.987 *	10350.973 *	10314.000 *	10316.814	10280.898 *	10283.541
38	10343.792 *	10346.876 *	10308.888 *	10311.895 *	10274.870	10277.667 *

Appendix II -- $^5\Pi_1$ - $X^5\Delta_2$ (0,0) (cont.)

J	R		Q		P	
	aa	bb	ab	ba	aa	bb
39	10339.440 *	10342.663	10303.648	10306.697 *	10268.746	10271.659 *
40	10334.956 *	10338.310 *	10298.256	10301.514 *		
41	10330.365 *	10333.846	10292.771	10296.120	10256.055 *	10259.306 *
42		10329.248	10287.120 *	10290.641 *	10249.558 *	10252.956 *
43	10320.759	10324.520	10281.381	10285.002 *	10242.924 *	10246.412
44	10315.832	10319.684 *	10275.513	10279.266 *	*	10239.786
45	10310.870 *?		10269.575 *	10273.439	10229.256	
46			10263.610 ?	10267.508 *	10222.312 *	
47					10215.356 *?	

$^5\Pi_2$ - $X^5\Delta_3$ (0,0)

J	R	Q	P
3	10385.517 *		10379.184 *
4	10385.960 *	10381.432	10377.814
5		10380.821 *	10376.272 *
6		10380.101	10374.655
7	10386.520 *	10379.244 *	10372.900
8	10386.413 *	10378.262 *	10371.006
9	10386.190 *	10377.159 *	10369.012
10	10385.874	10375.937	10366.886
11	10385.438 *	10374.577	10364.630
12	10384.844 *	10373.101	10362.246 *
13	10384.140	10371.490	10359.741
14	10383.302	10369.740 *	10357.107
15	10382.340 *	10367.895	10354.352 *
16	10381.242 *	10365.898	10351.463 *
17	10380.007	10363.775	10348.435
18	10378.653 *	10361.526	10345.285 *
19	10377.159 *	10359.143	10342.009
20	10375.532 *	10356.627 *	10338.605 *
21	10373.783 *	10353.979	10335.067
22	10371.896	10351.195	10331.391 *
23	10369.863 *	10348.288	10327.597
24	10367.730	10345.252	10323.653 *
25	10365.441	10342.072	10319.598
26	10363.017 *	10338.762	10315.393
27	10360.466	10335.325	10311.048
28	10357.785	10331.753	10306.601
29	10354.968	10328.046	10302.008
30	10352.015	10324.202	10297.281
31	10348.934 *	10320.228	10292.409 *
32	10345.704	10316.126	10287.427 *

Appendix II -- $^5\Pi_2$ - $X^5\Delta_3$ (0,0) (cont.)

J	R		Q		P	
	aa	bb	ab	ba	aa	bb
33	10342.345 *		10311.895		10282.308	
34	10338.835 *		10307.515 *		10277.058 *	
35	10335.277 *		10303.014 *		10271.659 *	
36	10331.486 *	10331.526 *	10298.364 *	10298.391 *	10266.126 *	10266.154 *
37	10327.597 *	10327.637 *	10293.601 *	10293.642 *	10260.466 *	10260.506 *
38	10323.602 *	10323.653 *	10288.702 *	10288.743 *	10254.695 *	10254.736 *
39	10319.457 *	10319.498	10283.677 *	10283.708 *	10248.774 *	
40	10315.174	10315.246 *	10278.515 *	10278.575 *	10242.732 *	10242.775 *
41	10310.774 *	10310.842 *	10273.224	10273.291	10236.563	10236.616
42	10306.250	10306.316	10267.814 *	10267.876	10230.259 *	10230.310 *
43	10301.600 *	10301.673 *	10262.269 *	10262.346 *	10223.825 *	10223.887 *
44	10296.807	10296.897	10256.604	10256.677	10217.243 *	10217.328 *
45	10291.880 *	10291.991	10250.807	10250.889	10210.598	10210.661
46	10286.873 *	10286.947 *	10244.882	10244.980	10203.775	10203.877
47	10281.663	10281.795 *	10238.835		10196.858	10196.956 *
48	10276.380 *	10276.515	10232.654		10189.779 *	10189.896 *
49	10270.930 *	10271.053 *	10226.336	10226.457		
50			10219.895	10220.041 *	10175.292 *	*
51			10213.304	10213.438 *	10167.840 *	10167.963
52			10206.577 *		*	10160.365 *
53			10199.721 ?	10199.876 ?	10152.508	10152.663 *
54			10192.698 ?	10192.879 ?	10144.647 *	10144.815
55					10136.596 *	10136.796 *
56					10128.514 *	10128.674
57					10120.227	10120.438 *

$^5\Pi_3$ - $X^5\Delta_4$ (0,0)

J	R		Q		P	
	aa	bb	ab	ba	aa	bb
4					10355.903 *	
5			10359.002 *		10354.432 *	
6			10358.328		10352.873	
7			10357.567		10351.195 *	
8			10356.627 *		10349.388	
9			10355.673 *		10347.491 *	
10			10354.579 *	10354.633 *	10345.462 *	10345.489 *
11			10353.395 *	10353.436 *	10343.352 *	10343.393 *
12			10352.097 *		10341.148 *	10341.175 *
13	10363.533 *	10363.574 *	10350.702 *	10350.769 *	10338.835 *	10338.875 *
14			10349.231	10349.285 *	10336.400	10336.479 *
15	10362.329 *	10362.376 *	10347.644	10347.706	10333.915	10333.968
16	10361.574	10361.643 *	10345.977 *	10346.039	10331.318	10331.391 *
17	10360.777 *	10360.831 *	10344.227	10344.297	10328.619	10328.690

Appendix II -- $^3\Pi_3$ - $X^3\Delta_4$ (0,0) (cont.)

J	R		Q		P	
	aa	bb	ab	ba	aa	bb
18	10359.878 *	10359.957	10342.388	10342.464	10325.850	10325.926 *
19			10340.469	10340.561	10323.000	10323.071
20	10357.916	10358.008	10338.512	10338.605 *	10320.057	10320.156
21	10356.862	10356.954	10336.479	10336.573	10317.085	10317.165
22	10355.767	10355.858 *	10334.417	10334.502 *	10314.034 *	10314.127
23	10354.674 *	10354.752	10332.311	10332.388	10310.942	10311.048 *
24	10353.533	10353.655 *	10330.179	10330.266	10307.824	10307.910 *
25	10352.445 *	10352.520	10328.046 *	10328.126	10304.679	10304.764
26			10325.926 *	10326.000	10301.514 *	10301.600 *
27			10323.844	10323.907	10298.391 *	10298.463
28		10349.467 *	10321.811 *	10321.865	10295.295	10295.363 *
29	10348.596 *		10319.865	10319.906	10292.254 *	10292.312 *
30			10318.014 *	10318.041 *	10289.287 *	10289.328 *
31	10347.288 *		10316.287		10286.439 *	
32	10346.836 *		10314.686 *		10283.677 *	
33	10346.539 *		10313.216		10281.052 *	
34	10346.368 *		10311.895 *		10278.575 *	
35	10346.368 *		10310.723		10276.252 *	
36	10346.465		10309.692 *		10274.075 *	
37			10308.822 *		10272.032 *	
38			10308.066 *?		10270.107 *	
39					10268.317 *?	
27	10303.155 *		10275.928			
28	10302.718 *		10274.655 *		10247.367	
29	10302.052 *		10273.151		10245.050 *	
30	10301.171		10271.462		10242.568	
31	10300.046		10269.575 *		10239.864 *	
32	10298.657		10267.437 *		10236.959 *	
33	10296.983	10299.180 *	10265.031		10233.812	
34	10295.057 *	10296.612	10262.346 *	10264.540	10230.391 *	
35	10292.858 *	10294.042	10259.408	10260.960	10226.702	10228.867 *
36	10290.396	10291.354	10256.197	10257.377	10222.757	10224.299
37	10287.669	10288.503	10252.729	10253.687	10218.527	10219.702
38	10284.742 *	10285.444 *	10249.034 *	10249.815 *	10214.048 *	10215.002
39	10281.555	10282.217	10245.050	10245.743	10209.317	10210.124
40	10278.161	10278.757	10240.855	10241.504	10204.342	10205.059
41	10274.554	10275.112	10236.465 *	10237.046	10199.154 *	10199.792
42	10270.753 *	10271.276	10231.839	10232.393	10193.705 *	10194.328 *
43	10266.761	10267.260	10227.026	10227.535	10188.085 *	10188.667
44	10262.542 *	10263.099 *	10222.020	10222.531	10182.292	10182.791 *
45	10258.220 *	10258.671 *	10216.835	10217.328	10176.276 *	10176.782
46			10211.476 *	10211.948	10170.086	10170.580
47			10205.942	10206.388	10163.733	10164.198

Appendix II -- $^5\Pi_3$ - $X^5\Delta_4$ (0,0) (cont.)

J	R		Q		P	
	aa	bb	ab	ba	aa	bb
48			10200.247	10200.693	10157.214 *	10157.649
49			10194.392	10194.829	10150.490	10150.939
50			10188.379	10188.788 *	10143.639	10144.109 *
51			10182.208	10182.624 *		10137.039
52			10175.888	10176.276 *		10129.877
53			10169.382 *	10169.828		10122.532 *
54			10162.789	10163.199		10115.076 *
55			10156.015 *	10156.433		10107.445 *
56			10149.076	10149.539		*
57						10091.790 *
58						10083.754 *
59						10075.620 *

$^5\Pi_{-1}$ - $X^5\Delta_0$ (0,1)

J	R		Q		P	
	aa	bb	ab	ba	aa	bb
0			-	-	-	-
1					-	-
2						
3			9551.965	9552.339 *		
4			9551.482 *	9551.838		
5			9550.846	9551.243		9546.311
6			9550.099	9550.507		9544.664
7			9549.216	9549.643 *	9543.175	9542.936 *
8	9556.775		9548.222	9548.678	9541.262	9541.020 *
9	*	9556.389 *	9547.101	9547.584	9539.228	9539.007
10	9556.219	*	9545.853 *	9546.362	*	9536.872
11	9555.757	9555.678 *	9544.476	9545.006 *	9534.793 *	9534.621
12	9555.156	9555.115 *	9542.979	9543.560	9532.366 *	9532.226 *
13	9554.439	9554.439 *	9541.350	9541.957	9529.861 *	9529.764 *
14	9553.600 *	9553.645 *	9539.602 *	9540.258 *	9527.169 *	9527.123 *
15	9552.633	9552.735 *	9537.724 *	9538.430	*	*
16	9551.510 *	9551.660	9535.706	9536.473	9521.475 *	9521.508 *
17	9550.295	9550.507 *	9533.579 *	9534.391	9518.427 *	9518.543 *
18	9548.950 *	9549.216 *	9531.311	9532.180	9515.251 *	9515.401 *
19	9547.460	9547.782	9528.931 *	9529.861 *	9511.950 *	9512.161
20	9545.853 *	9546.238	9526.410	9527.387 *	9508.534 *	9508.794
21	9544.114 *	9544.566	9523.764	9524.797	9504.981	9505.315 *
22	9542.239	9542.768	9520.994	9522.101	9501.295	9501.695
23	9540.258 *	9540.841	9518.090	9519.274	9497.490 *	9497.968 *
24	9538.093	9538.777 *	9515.058 *	9516.318	9493.565 *	9494.091
25	9535.853	9536.609 *	9511.890 *	9513.210 *	9489.501	9490.099
26	9533.465 *	9534.315	9508.606	9509.981 *	9485.308	9485.984

Appendix II -- $^5\Pi_{-1}$ - $X^5\Delta_0$ (0,1) (cont.)

J	R		Q		P	
	aa	bb	ab	ba	aa	bb
27	9530.940	9531.879	*	9506.689	9480.985	9481.726 *
28	9528.298	9529.308	9501.643	9503.216 *	9476.542 *	9477.365 *
29	9525.517 *	9526.599 *	9497.968	9499.609	9471.962	9472.893
30	9522.618 *	9523.802 *	9494.157	9495.911	9467.258	9468.273 *
31	9519.558	9520.826	9490.222	*	9462.408	9463.532 *
32	9516.398	9517.781	9486.137	9488.050	*	9458.647 *
33	9513.094	9514.564 *	*	9483.999 *	9452.350	9453.614 *
34	9509.658 *	9511.257	9477.634	9479.745 *	*	9448.514
35	9506.101	9507.799 *	9473.171	9475.395 *	9441.774	9443.260
36	9502.409	9504.237	9468.585	9470.921	9436.290	*
37	9498.596	9500.554 *	9463.880	9466.324	9430.669 *	9432.387
38	9494.672 *	9496.781 *	9459.041 *	9461.609	9424.940 *	9426.769
39	9490.676 *		9454.093	9456.801	9419.086 *	*
40	9486.772		9449.083		9413.112 *	9415.203
41			9444.168		9407.066	
42					9401.129	

$^5\Pi_0$ - $X^5\Delta_1$ (0,1)

J	R		Q		P	
	aa	bb	ab	ba	aa	bb
1			9533.167			
2			9532.919		9531.110 *	
3			9532.551		*	
4			9532.067	9569.922 *	9528.429 *	9566.325
5			9531.459	9569.281	9526.900	9564.753 *
6			9530.723	9568.500	9525.265 *	9563.095
7	9537.159	9574.793	9529.861 *	9567.593 *	9523.503 *	9561.278
8	9537.102 *	9574.682	9528.881	9566.559	9521.628	9559.310 *
9	9536.920	9574.444 *	9527.817 *	9565.396	9519.611 *	9557.291 *
10	9536.609 *	9574.019 *	9526.599	9564.092	9517.505	9555.074 *
11	9536.178 *	9573.460 *	9525.265	9562.676	9515.251	9552.735 *
12	9535.642	9572.843 *	9523.802	9561.116	9512.901	9550.295 *
13	9534.961 *	9572.047	9522.231	9559.430 *	9510.407	9547.703
14	9534.175	9571.134	9520.531	9557.620	9507.799 *	9545.006 *
15	9533.267	9570.091	9518.706	9555.678 *	9505.071	9542.145
16	9532.226 *	9568.908 *	9516.762	9553.600 *	9502.215	9539.170
17	9531.064	9567.593 *	9514.673	9551.397	9499.240	9536.051
18	9529.764	9566.155	9512.501	9549.065	9496.116 *	9532.847 *
19	9528.377	9564.544	9510.183	9546.576	9492.931	9529.470
20	9526.840	9562.769	9507.749 *	9543.944	9489.582	9525.952 *
21	9525.190	9560.847	9505.202	9541.135	9486.137	9522.288
22	9523.404 *	9558.864	9502.502 *	9538.192	9482.536	9518.454 *
23	9521.508 *	9556.827	9499.690	9535.185	9478.829	9514.485

Appendix II -- $^5\Pi_0 - X^5\Delta_1$ (0,1) (cont.)

J	R		Q		P	
	aa	bb	ab	ba	aa	bb
24	9519.489 *	9554.682	9496.781 *	9532.124	9474.990	9510.450
25	9517.347	9552.388	9493.740 *	*	9471.044	9506.357
26	9515.058 *	9549.934	9490.550	9525.618 *	*	9502.166
27	9512.676	9547.332	9487.254	9522.153	9462.758	9497.807
28	9510.154 *	9544.615	9483.823 *	9518.543 *	9458.430	9493.323 *
29	9507.504	9541.755	9480.284 *	9514.791	9454.006	9488.676
30	9504.728	9538.738	9476.584 *	9510.897	9449.434	9483.897
31	9501.830	9535.577	9472.813	9506.860	9444.739 *	9478.980
32	9498.811	9532.226 *	9468.894 *	9502.673	9439.915	9473.923
33	9495.653	*	9464.845	9498.351	9434.976	9468.713
34	9492.394 *	9525.265 *	9460.666	9493.937	9429.907 *	9463.366
35	9488.952 *	9521.557 *	9456.366	9489.324	9424.714	9457.925 *
36		9517.714	9451.933 *	9484.584 *	9419.394	*
37		9513.753	9447.401 *	9479.745 *	9413.967	9446.530
38		9509.658 *	9442.732 *	9474.745	9408.395 *	9440.650
39		9505.468	9437.918 *	9469.637	9402.704 *	9434.642 *
40		9501.129	9432.989	9464.414	9396.881	*
41		9496.702 *	9427.936	9459.069 *	9390.935 *	9422.275 *
42		9492.138 *	9422.747	9453.614 *		9415.927
43		9487.483	9417.441 *	9448.052		*
44		9482.750 *	9411.972 *	9442.389 *		9402.875
45		*	9406.424	*		9396.183 *
46		9472.977	9400.730 *	9430.773		9389.413 *
47		9467.993	9394.920	9424.847		*
48		9463.058	9388.964			9375.610
49		9458.179	9382.890			*
50			9376.689			9361.636
51			9370.374 *			9354.749
52			9363.926 *			
53			9357.320 *			
54			9350.618			
55			9343.797			
56			9336.850			

$^5\Pi_1 - X^5\Delta_2$ (0,1)

J	R		Q		P	
	aa	bb	ab	ba	aa	bb
2					9535.047	
3			9536.473 *		*	
4			9535.977 *		9532.366 *	
5			9535.325 *	9535.396	9530.838	*
6			9534.576	9534.650	9529.172 *	9529.240
7			9533.685	9533.793 *	9527.387 *	9527.464

Appendix II -- $^3\Pi_1$ - $X^3\Delta_2$ (0,1) (cont.)

J	R			Q			P	
	aa	bb	ab	ba	aa	bb		
8		9540.982 *	9532.681 *	9532.847 *	9525.477 *	9525.618*		
9	9540.564 *	9540.775	9531.520	9531.739	*	9523.586		
10	9540.187 *	9540.454	9530.270	9530.518 *	9521.279	9521.475 *		
11	9539.653 *	9540.014	9528.881 *	9529.172 *	9518.995	9519.230 *		
12	9539.086 *	9539.459	*	9527.717	9516.577 *	9516.870		
13	9538.320 *	9538.777	9525.727	9526.124	9514.024 *	9514.377		
14	9537.445	9537.943	9523.953	9524.411 *	9511.366	9511.767		
15	9536.473 *	9537.034	9522.051	9522.578 *	9508.575 *	9509.016 *		
16	9535.325	9535.977	9520.033	9520.622	9505.656	9506.184		
17	9534.058	9534.793	9517.888	9518.543	9502.617 *	9503.216 *		
18	9532.681 *	9533.492	9515.604	9516.345 *	9499.432	9500.101 *		
19	9531.168	9532.067 *	9513.210	9514.024	9496.116 *	9496.869		
20	9529.519	9530.518 *	9510.676	9511.574	9492.700	9493.523		
21	9527.776 *	9528.881 *	9508.017 *	9509.016 *	9489.147	9490.053		
22	9525.886	9527.061 *	*	9506.309 *	9485.471 *	9486.465 *		
23	9523.866	9525.150 *	9502.321	9503.499	9481.664	9482.750		
24	9521.728	9523.100	9499.289	9500.554 *	9477.734	9478.915		
25	9519.448 *	9520.938	9496.116	9497.490 *	9473.658	9474.949 *		
26	9517.061	9518.645	9492.824	9494.306	9469.487	9470.868		
27	9514.535	9516.225	9489.395 *	9491.002	9465.162	9466.659		
28	9511.890 *	9513.688	9485.867	9487.562	9460.738	9462.330		
29	9509.059 *	9511.027	9482.189	9483.999	9456.174	9457.875		
30	9506.184 *	9508.259 *	9478.403	9480.325 *	9451.485	9453.300		
31	9503.155 *	9505.315	9474.465	9476.515 *	9446.668	9448.578		
32	9499.986	9502.274 *	9470.407	9472.585	9441.727	9443.772		
33	9496.702 *	9499.119	9466.226	9468.522	*	9438.808		
34	9493.258 *	9495.831	9461.921	9464.340	9431.454	9433.732 *		
35	9489.728	9492.394	9457.471	9460.042	9426.128	9428.534 *		
36	9486.050	9488.872	9452.918	9455.603	9420.655	9423.235		
37	9482.252	9485.199	9448.211	9451.047	9415.096	9417.783		
38	9478.352 *	9481.413 *	9443.411	9446.365	9409.399 *	9412.217		
39	9474.263	9477.496	9438.486 *	9441.563	9403.575 *	9406.518		
40	9470.073	9473.460	9433.412	9436.603 *	9397.617	9400.703 *		
41	9465.787	9469.296	9428.211	9431.587 *	9391.540	9394.751 *		
42	9461.374	9465.010	9422.903	9426.415	9385.334	9388.706		
43	9456.850 *	9460.620	9417.474	9421.104	9379.012 *	9382.516		
44	9452.275	9456.129 *	9411.972 *	?	9372.580	9376.201 *		
45		9451.562	9406.347	9410.210 *	9366.036	9369.782 *		
46		9446.957			9359.432	9363.288		
47		9442.324				9356.714		

Appendix II (cont.) -- $^5\Pi_i$ - $X^5\Delta_i$ (0,1)

J	R		Q		P	
	aa	bb	ab	ba	aa	bb
3		*	9510.775		9508.054	
4	9514.843		9510.322		9506.689	
5	9515.179		9509.752		9505.202 *	
6	9515.401		9509.059		9503.627	
7	9515.544 *		9508.259		9501.925	
8	9515.495		9507.342		9500.101	
9	9515.345		9506.309		9498.164	
10	9515.107		9505.159 *		9496.116	
11	9514.745		9503.884		9493.937	
12	9514.245		9502.502		9491.633 *	
13	9513.630		9500.986		9489.243	
14	9512.901		9499.358		9486.712	
15	9512.033		9497.612		9484.063	
16	9511.071		9495.736		9481.279	
17	9509.981		9493.740		9478.403	
18	9508.756		9491.633 *		9475.395 *	
19	9507.412		9489.395		9472.242	
20	9505.940		9487.028		9469.006	
21	9504.340		9484.535		9465.622	
22	9502.617		9481.925		9462.124	
23	9500.780		9479.187		9458.492	
24	9498.811		9476.312		9454.741	
25	9496.702		9473.343		9450.870	
26	9494.489		9470.237		9446.868	
27	9492.138		9466.990		9442.732	
28	9489.667		9463.634		9438.486	
29	9487.074		9460.149		9434.116	
30	9484.327		9456.532		9429.617	
31	9481.496		9452.798		9424.986	
32	9478.518 *		9448.936		9420.241	
33	9475.395 *		9444.948		9415.366	
34	9472.173 *	9472.200 *	9440.834 *		9410.364 *	
35	9468.853 *	9468.894 *	9436.603 *		9405.243 *	
36	9465.342 *	9465.383 *	9432.220 *	9432.261 *	9399.996 *	
37	9461.743	9461.782	9427.729 *	9427.770 *	9394.607 *	9394.648 *
38	9458.021	9458.062	9423.104 *	9423.164	9389.123 *	9389.181 *
39	9454.157	9454.230	9418.386 *	9418.435	9383.503	9383.538
40	9450.210 *	9450.263	9413.559 *	9413.604 *	9377.753	9377.820 *
41	9446.116	9446.176	9408.555 *	9408.650 *	9371.902	9371.944 *
42	9441.906	9441.974	9403.463	9403.531	*	*
43	9437.568	9437.655	9398.248	9398.329	9359.811	9359.877
44	9433.136 *	9433.208	9392.880 *	9392.994	9353.596	9353.667
45		9428.641 *	9387.457	9387.553	9347.238	9347.336
46	9423.862	9423.948	9381.889	9381.988	*	*
47	*	9419.142 *	9376.201	9376.278	9334.229	*

Appendix II -- $^3\Pi_2$ - $X^3\Delta_3$ (0,1) (cont.)

J	R		Q		P	
	aa	bb	ab	ba	aa	bb
48	9414.103	9414.216	9370.374	9370.484	*	9327.626
49	9409.037	9409.161	*	*	9320.712	*
50	9403.833 *	9403.973	9358.364	9358.499	9313.765	9313.886
51	9398.512	9398.636	9352.151	9352.288 *	9306.693	9306.808 *
52	9393.042	9393.203 *	9345.839	9345.985	9299.487	9299.629 *
53	*	9387.618	9339.359	9339.529 *	9292.193 *	9292.317
54	9381.708 *		9332.778 *	9332.951	*	9284.876
55	9375.851 *	9376.055	9326.066	9326.260 *	9277.132	*
56	9369.855	9370.078	9319.211	9319.407	*	*
57	*	9364.016	9312.244 *	9312.443	9261.548 *	9261.769
58	9357.567 *	9357.768	9305.135	9305.369	9253.601 *	9253.771 *
59			9297.940 *	9298.139 *	9245.526 *	9245.716 *
60				9290.838		9237.521

$^3\Pi_3$ - $X^3\Delta_4$ (0,1)

J	R		Q		P	
	aa	bb	ab	ba	aa	bb
4				9488.381 *	9484.742 *	
5				9487.868	9483.308 *	
6				9487.254 *	9481.797 *	
7				9486.504 *	*	
8				9485.682 *	9478.403 *	
9			9484.742 *	9484.802 *	9476.584 *	
10			9483.762 *	9483.795 *	9474.622 *	9474.663 *
11			9482.652	9482.693 *	9472.585 *	9472.637 *
12	9493.323	9493.378	9481.454 *	9481.496 *	9470.486 *	9470.525 *
13	*	9493.018	9480.136 *	9480.212	9468.273 *	9468.311
14	9492.513 *	9492.562 *	9478.773	9478.829 *	9465.968	9465.996
15	*	*	9477.309	9477.365 *	9463.565	9463.634 *
16	9491.357	9491.422	9475.761	9475.819	9461.089	9461.137 *
17	9490.676	9490.744	9474.126	9474.197	*	9458.591
18	9489.928	9490.006	9472.433	9472.504	9455.891	9455.955
19	9489.090	9489.197 *	9470.650	9470.750	9453.184	9453.258
20	9488.247	9488.334	9468.853 *	9468.928	9450.388	9450.489
21	9487.349	9487.442	*	9467.061	9447.558	9447.656
22	9486.465 *	9486.504 *	9465.068	9465.162 *	9444.698 *	9444.780 *
23	9485.471 *	9485.577	9463.132	9463.223	9441.774 *	9441.842
24	9484.535 *	9484.625	9461.181	9461.266	9438.808 *	9438.915
25	9483.638	9483.713 *	9459.237	9459.320	9435.855	9435.936
26	9482.750 *	9482.829	9457.301	9457.384	9432.922	9432.989 *
27	9481.925 *	9482.003	9455.441	9455.495	9429.988 *	9430.059
28	9481.250 *	9481.279 *	9453.614 *	9453.666	9427.095	9427.159 *
29	9480.611 *	9480.638 *	9451.884 *	9451.933 *	9424.269	9424.318

Appendix II -- $^5\Pi_3$ - $X^5\Delta_4$ (0,1) (cont.)

J	R				Q				P			
	aa		bb		ab		ba		aa		bb	
30	9480.136	*			9450.263	*			9421.535	*	9421.565	*
31	9479.745	*			9448.763				9418.897			
32	9479.548				9447.401	*			9416.389			
33	9479.495				9446.176	*			9414.020			
34	9479.590				9445.111				9411.799			
35	9479.839				9444.211				9409.725	*		
36		*			9443.411	*			9407.816	*		
37	9480.728	?			9442.827	*			9406.066	*		
38					9442.324	*?			9404.432			
39									9402.962	*?		
27	9434.766				9407.521	*						
28	9434.521				9406.424	*			9379.182			
29		*			9405.154				9377.077			
30	9433.412	*			9403.720				9374.817	*		
31	9432.525				9402.038				9372.354			
32	9431.371				9400.148	*			9369.688			
33	9429.947	*	9432.133		9397.986				9366.776			
34	9428.276		9429.825		9395.569		9397.765	*	9363.609			
35	9426.340		9427.520		9392.880	*	9394.444		9360.166	*	9362.372	
36	9424.148		9425.104		9389.943		9391.133		9356.497		9358.035	*
37	9421.723		9422.527		9386.761		9387.714		9352.554	*	9353.716	*
38		*	9419.767		9383.315		9384.137		9348.347	*	9349.313	
39	9416.150		9416.812		9379.653		9380.365		9343.921		9344.732	
40	9413.047	*	9413.662		9375.765		9376.420		9339.254		9339.966	
41	9409.774			*	9371.633	*	9372.267		9334.368		9335.010	
42	9406.278		9406.805		9367.362		9367.918	*	9329.261		9329.859	
43	9402.608		9403.120	*	9362.878		9363.409		9323.981	*	9324.520	
44	9398.763		9399.244		9358.198	*	9358.714		9318.474		9318.988	
45	9394.751		9395.217		9353.352		9353.839		9312.799		9313.307	
46	9390.565	*	9391.002		9348.347	*	9348.814		9306.939	*	9307.444	
47			9386.665		9343.160		9343.621		9300.942	*	9301.422	
48			9382.176	*	9337.826		9338.272		9294.772	*	9295.227	*
49			9377.517		9332.342		9332.778	*		*	9288.888	
50			9372.717		9326.694		9327.154	*	9281.949		9282.396	
51			9367.779		9320.915		9321.333			*	9275.755	
52			9362.682		9314.960		9315.400		9268.530	?	9268.959	*
53			9357.458		9308.905		9309.317				9262.037	
54			9352.083		9302.691		9303.080					*
55			9346.619		9296.337			*			9247.761	*
56					9289.820	?	9290.276				9240.405	
57					9283.213	?					9232.956	
58											9225.349	
59												*

Appendix II -- $^5\Pi_3$ - $X^5\Delta_4$ (0,1) (cont.)

J	R		Q		P	
	aa	bb	ab	ba	aa	bb
60						9209.787 ?
61						9201.818 *?

$^5\Pi_{-1}$ - $X^5\Delta_0$ (0,2)

J	R		Q		P	
	aa	bb	ab	ba	aa	bb
0			-	-	-	-
1					-	-
2	8693.597 *	8693.271 *				
3	8694.186 *	*	8690.184 *	8690.533 *		
4	*	8694.323 *	8689.692 *	8690.078		8686.096 *
5	8694.944 *	8694.665 *	8689.109 *	8689.522 *	8684.908 *	8684.566
6	8695.144	8694.898 *	8688.417 *	8688.828	8683.274 *	8683.006 *
7	8695.225 *	8695.006 *	8687.570	8688.034	8681.557 *	8681.268
8	8695.225 *	8695.006 *	8686.653	8687.112 *	8679.710 *	8679.410 *
9	8695.082	8694.898 *	8685.600 *	8686.096 *	8677.764 *	8677.540 *
10	8694.818	8694.665 *	8684.432	8684.987 *	8675.662 *	8675.445 *
11	8694.430	8694.323 *	8683.120	8683.692	8673.461 *	8673.289 *
12	8693.936	8693.876 *	8681.734 *	8682.318 *	8671.144	8671.008
13	8693.311 *	8693.311 *	8680.203	8680.853	8668.701 *	8668.599 *
14	*	8692.612 *	8678.571 *	8679.250 *	8666.150 *	8666.082 *
15	8691.726	8691.808	8676.797	8677.540 *	8663.460 *	8663.460 *
16	8690.733 *	8690.884 *	8674.901	8675.697	8660.693 *	8660.720 *
17	8689.660 *	8689.844	8672.921 *	8673.731	8657.776 *	8657.846 *
18	8688.417 *	8688.690 *	8670.778	8671.680	8654.757 *	8654.882 *
19	8687.112 *	8687.426	8668.553	8669.504	8651.626 *	8651.772 *
20	8685.650 *	8686.038 *	8666.178	8667.203	8648.333	8648.587
21	8684.059 *	8684.521	8663.717	8664.781	8644.949 *	8645.281 *
22	8682.371 *	8682.896	8661.082 *	8662.246	8641.438 *	8641.849 *
23	8680.563	8681.139 *	8658.393 *	8659.596	8637.813	8638.267 *
24	8678.618 *	8679.250 *	8655.545 *	8656.820	8634.062 *	8634.596 *
25	8676.552 *	8677.255	8652.589	8653.926	8630.190 *	8630.809 *
26	8674.373	8675.190 *	8649.496	8650.903 *	8626.215	8626.871
27	8672.069 *	8672.967 *	8646.290	8647.810	8622.104 *	8622.820 *
28	8669.617 *	8670.634	8642.969	8644.561	8617.861 *	8618.706
29	8667.063 *	8668.171	8639.519 *	8641.157 *	8613.524	8614.439 *
30	8664.401	8665.592	8635.935 *	8637.700	8609.080 *	8610.048 *
31	8661.595 *	8662.872 *	8632.246 *	8634.102 *	8604.456	8605.558 *
32	8658.691	8660.055 *	8628.432 *	*	8599.742 *	8600.937
33	8655.631 *	8657.113	8624.469	8626.516 *	8594.895	8596.138 *
34	8652.474 *	8654.016 *	8620.395 *	8622.564	*	8591.305 *
35	8649.198 *	8650.903 *	*	8618.474 *	8584.885 *	8586.338 *
36	8645.780	8647.584 *	8611.936	8614.281 *	8579.635 *	8581.236 *

Appendix II -- $^5\Pi_{-1}$ - $X^5\Delta_0$ (0,2) (cont.)

J	R		Q		P	
	aa	bb	ab	ba	aa	bb
37	8642.262	8644.154 *	8607.500	8609.984	8574.332 *	8576.035 *
38	8638.630	8640.696	8602.973 *	8605.558	8568.887 *	8570.702
39	8634.937		8598.337	8601.060	8563.334 *	8565.274 *
40			8593.642 *		*	8559.719 *
41			8589.026		*	
42					8546.358 *	

$^5\Pi_0$ - $X^5\Delta_1$ (0,2)

J	R		Q		P	
	aa	bb	ab	ba	aa	bb
1	8673.131 *					
2	8673.815 *		8671.061 *		8669.259 *	
3	8674.373 *		8670.724 *	8708.633	8668.005 *	
4	8674.820 *	8712.665	8670.287 *	8708.117 *	8666.653 *	8704.540 *
5	8675.190 *	8712.948 *	8669.708 *	8707.539	8665.173 *	8703.039 *
6	8675.406 *	8713.103 *	8669.057 *	8706.811	8663.564 *	8701.388
7	8675.520 *	8713.199 *	8668.237	8705.942 *	8661.885 *	8699.644
8	8675.520 *	8713.103 *	8667.327	8704.962 *	8660.055 *	8697.771 *
9	8675.406 *	8712.899	8666.304	8703.888	8658.121	8695.749 *
10	8675.190 *	8712.586 *	8665.173 *	8702.665 *	8656.073 *	8693.657 *
11	8674.820 *	8712.148	8663.921	8701.333	8653.926 *	8691.402
12	8674.373 *	8711.588 *	8662.553	8699.863	8651.626 *	8689.048 *
13	8673.815 *	8710.903	8661.082 *	8698.284	8649.249 *	8686.536
14	8673.131 *	8710.095	8659.487	8696.578	8646.752	8683.946
15	8672.305 *	8709.172	8657.776 *	8694.747	8644.154 *	8681.215 *
16	8671.404	8708.117 *	8655.952 *	8692.798	8641.411 *	8678.362 *
17	8670.390	8706.934 *	8654.016 *	8690.733	8638.570	8675.406 *
18	8669.259 *	8705.616	8651.968	8688.526	8635.610	8672.305 *
19	8668.005 *	8704.158 *	8649.801 *	8686.193	8632.506 *	8669.057 *
20	8666.619 *	8702.531 *	8647.526	8683.692 *	8629.342 *	8665.720 *
21	8665.129 *	8700.779 *	8645.127	8681.052	8626.055	8662.246 *
22	8663.510 *	8698.967 *	8642.615 *	8678.292 *	8622.639	8658.561
23	8661.795	8697.117 *	8639.969	8675.445 *	8619.112	8654.757 *
24	8659.965	8695.144 *	8637.246	8672.574 *	8615.465	8650.903 *
25	8657.986	8693.043	8634.386	8669.617 *	8611.716 *	8647.027
26	8655.952 *	8690.794	8631.396	8666.482 *	8607.831	8643.019
27	8653.753 *	8688.417 *	8628.325	8663.231	8603.851 *	*
28	8651.436	8685.902	8625.113	8659.826	*	8634.596 *
29	8649.026	8683.274 *	8621.794	8656.303	8595.521	8630.190 *
30	8646.473	8680.474	8618.357 *	8652.625	8591.176 *	8625.645 *
31	8643.816	8677.540 *	8614.793 *	8648.849	8586.707	8620.945
32	8641.038	8674.486 *	8611.114 *	8644.916 *	8582.147 *	8616.158 *
33	8638.144 *	8671.363	8607.331	8640.840	8577.471 *	8611.200 *

Appendix II -- $^3\Pi_0 - X^3\Delta_1$ (0,2) (cont.)

J	R		Q		P	
	aa	bb	ab	ba	aa	bb
34	8635.114 *	8668.005 *	8603.419	8636.717 *	8572.659	8606.109
35	8632.011 *	8664.571 *	8599.380 *	8632.338	8567.741	8600.937 *
36	8628.787 *	8661.018 *	8595.260 *	8627.884 *	8562.682 *	8595.581 *
37	8625.395 *	8657.341	8590.996 *	8623.318 *	8557.568 *	*
38	8621.908 *	8653.549 *	8586.604	8618.615	8552.277 *	8584.533
39	8618.285	8649.637 *	8582.092	8613.827 *	8546.881 *	8578.814 *
40	8614.574 *	8645.600 *	8577.471 *	8608.888	8541.363	8573.007
41	8610.708	8641.492 *	8572.734	8603.883 *	8535.731	8567.092
42	8606.726 *	8637.246 *	8567.876	8598.763 *	8530.001 *	8561.047 *
43	8602.645	8632.970 *	8562.895 *	8593.515 *	8524.131	8554.913
44	8598.440	8628.540 *	8557.824 *	8588.195	8518.141 *	8548.667
45	8594.122 *	8623.999 *	8552.589 *	8582.783 *	*	8542.342
46	8589.659 *	8619.487 *	8547.230	8577.263	*	8535.920
47	8585.091		8541.773	8571.726 *	*	8529.409
48	8580.398		8536.215 *	8566.129	*	8522.825 *
49	8575.586 *		8530.525 *	8560.544	8486.448 *	
50	8570.661 *		8524.698 *	8555.041 *	*	
51	8565.592 *		8518.769 *		8472.930 *	
52	*		8512.714 *		8466.004 *	
53	8555.140		8506.540		8458.962 *	
54			8500.253 *		8451.778	
55			8493.859 *		8444.514 *	
56			8487.360		8437.120 *	
57					8429.620	

$^3\Pi_1 - X^3\Delta_2$ (0,2)

J	R		Q		P	
	aa	bb	ab	ba	aa	bb
2			8674.988		8673.187 *	8673.090 *
3			8674.625 *		8671.940	8671.884
4			8674.157 *		8670.562 *	8670.562 *
5	8678.985 *		8673.562	8673.608	8669.057 *	8669.057 *
6	8679.150 *	8679.250 *	8672.850	8672.921 *	8667.430 *	8667.503 *
7	8679.250 *	8679.374 *	8672.018	8672.137 *	8665.720 *	8665.807 *
8	8679.150 *	8679.374 *	8671.061 *	8671.223	8663.877	8664.000 *
9	8678.985 *	8679.250 *	8669.993 *	8670.179	8661.885 *	8662.058 *
10	8678.684	8678.985 *	8668.813	8669.057 *	8659.787 *	8660.013 *
11	8678.292 *	8678.618 *	8667.503	8667.794	8657.612	8657.846 *
12	8677.764 *	8678.171	8666.082	8666.419	8655.277 *	8655.545 *
13	8677.121 *	8677.540 *	8664.535	8664.928 *	8652.845	8653.188
14	8676.355	8676.876	8662.872	8663.326	8650.277	8650.684
15	8675.445 *	8676.063	8661.082 *	8661.595 *	8647.584 *	8648.061
16	8674.486 *	8675.134 *	8659.170	8659.787 *	8644.830 *	8645.331

Appendix II -- $^5\Pi_1$ - $X^5\Delta_2$ (0,2) (cont.)

J	R		Q		P	
	aa	bb	ab	ba	aa	bb
17	8673.342	8674.093	8657.171	8657.846 *	8641.900 *	8642.461 *
18	8672.097 *	8672.921 *	8655.027	8655.755	*	8639.519 *
19	8670.724 *	8671.648 *	8652.766	8653.594 *	8635.701	8636.439
20	8669.259 *	8670.249 *	8650.396	8651.298	8632.422	8633.244
21	8667.659 *	8668.701 *	8647.876	8648.889 *	8629.033 *	8629.937 *
22	8665.942	8667.116 *	8645.281	8646.372 *	8625.529 *	8626.516 *
23	8664.083 *	8665.363 *	8642.545	8643.712 *	8621.908 *	8622.971 *
24	8662.141	8663.510 *	8639.695	8640.963 *	8618.146	8619.347 *
25	8660.055 *	8661.537	8636.717 *	8638.094	8614.281 *	8615.552 *
26	8657.846 *	8659.441 *	8633.625	8635.114 *	8610.293 *	8611.670 *
27	8655.545 *	8657.227 *	8630.402	8632.011 *	8606.187	8607.655 *
28	8653.103	8654.923 *	8627.100	8628.787 *	8601.967	8603.570
29	8650.543	8652.474 *	8623.645	8625.451 *	8597.622 *	8599.330 *
30	8647.876 *	8649.913	8620.069 *	8621.979	8593.164 *	8594.979
31	8645.067	8647.237 *	8616.378	8618.430 *	8588.576	8590.512 *
32	8642.139 *	8644.444 *	8612.548 *	8614.752 *	8583.884 *	8585.923
33	8639.110 *	8641.533 *	8608.657 *	8610.961 *	8579.073 *	8581.236
34	8635.935	8638.494	8604.595	8607.009	8574.131 *	8576.414 *
35	8632.660	8635.352 *	8600.413	8602.973	8569.072 *	8571.492 *
36	8629.277 *	8632.082 *	8596.138	8598.810 *	8563.872 *	8566.443 *
37	8625.751	8628.701	8591.738 *	8594.532 *	8558.597	8561.280
38	8622.104 *	8625.203	8587.209 *	8590.162 *	*	8556.000
39	8618.357	8621.608 *	8582.559 *	8585.653	8547.656 *	8550.613
40	8614.495	8617.861 *	8577.806 *	8581.039	8542.008 *	8545.096 *
41	8610.499 *	8614.008	8572.908	8576.310 *	8536.247 *	8539.479 *
42	8606.407 *	8610.048 *	8567.937	8571.451	8530.375	8533.703 *
43	8602.219 *	8605.983 *	8562.845	8566.484 *	8524.381 *	8527.877 *
44	8597.966 *	8601.827 *	8557.659 *	8561.416	8518.269 *	8521.918 *
45		8597.622 *	8552.394	8556.249 *	8512.051 *	8515.838 *
46		8593.360 *	8547.189 ?	8551.040 *	*	8509.688 *
47				8545.806 *	*	8503.471
48				8540.520 *		

$^5\Pi_2$ - $X^5\Delta_3$ (0,2)

J	R	Q	P
3		8648.889	8646.167
4	8653.005	8648.465	8644.830
5	8653.373	8647.930 *	8643.404
6	*	8647.295	8641.849
7	8653.780 *	8646.546	8640.187
8	8653.825	8645.690	8638.445
9	8653.753 *	8644.723	8636.586

Appendix II -- $^5\Pi_2$ - $X^5\Delta_3$ (0,2) (cont.)

J	R		Q		P	
	aa	bb	ab	ba	aa	bb
10	8653.594		8643.648		8634.596	
11	8653.309		8642.461		8632.506	
12	8652.904		8641.157		8630.313	
13	8652.396		8639.745		8627.995	
14	8651.772		8638.223		8625.558	
15	8651.025		8636.586		8623.053 *	
16	8650.177		8634.836		8620.395	
17	8649.198		8632.970		8617.630	
18	8648.125 *		8630.974		8614.752 *	
19	8646.912		8628.878		8611.774	
20	8645.600		8626.683		8608.657	
21	8644.154		8624.355		8605.445	
22	8642.615		8621.908		8602.105	
23	8640.934 *		8619.347		8598.655	
24	8639.150		8616.676		8595.083	
25	8637.246		8613.870		8591.395	
26	8635.218		8610.961		8587.597	
27	8633.076		8607.927		8583.676	
28	8630.809		8604.776		8579.635	
29	8628.432		8601.517		8575.484	
30	8625.935		8598.132		8571.206 *	
31	8623.318		8594.630		8566.817 *	
32	8620.587		8590.996		8562.313	
33	8617.718		8587.265		8557.659 *	
34	8614.752 *		8583.411 *		8552.944	
35	8611.670 *	8611.716 *	8579.425 *	8579.452 *	8548.079	
36	8608.435 *	8608.511	8575.343 *	8575.371 *	8543.124 *	
37	8605.145 *	8605.179 *	8571.112	8571.179 *	8538.002	8538.031
38	8601.690	8601.756 *	8566.817 *	8566.896 *	8532.804	8532.837
39	8598.132 *	8598.213	8562.374	8562.422	8527.482	8527.525
40	8594.495	8594.532	8557.824	8557.870	8522.044	8522.088
41	8590.711	8590.780	8553.166	8553.204	8516.493	8516.542
42	8586.802	8586.890	8548.381	8548.452	8510.821 *	8510.903
43	8582.813 *	8582.879	8543.493	8543.571	8505.064	8505.118
44	8578.697	8578.785 *	8538.499	8538.570	8499.164 *	*
45	8574.469	8574.575	8533.369 *	8533.469	8493.177 *	8493.259 *
46	8570.105 *	8570.248 *	8528.154	8528.252	8487.067	8487.149 *
47	8565.655	8565.792 *	8522.825	8522.923	8480.847	8480.935
48	8561.095	8561.215	8517.371 *	8517.475	8474.518	8474.588 *
49	8556.396 *	8556.527	8511.787	8511.918	8468.064	8468.159
50	8551.595 *	8551.692	8506.096	8506.215 *	8461.497	8461.628 *
51	8546.635	8546.779	8500.301	8500.435	8454.829	8454.961
52	8541.555	8541.729	8494.365	8494.509	8448.030	8448.160
53	8536.383	8536.537	8488.312	8488.469 *	8441.099 *	8441.226 *
54	8531.076	8531.239	8482.130	8482.295	8434.054	8434.213

Appendix II -- $^5\Pi_2$ - $X^5\Delta_3$ (0,2) (cont.)

J	R		Q		P	
	aa	bb	ab	ba	aa	bb
55			8475.831	8476.009	8426.881	8427.082 *
56			8469.395	8469.580 *	8419.598	8419.761
57			8462.858 *	8463.054		
58			8456.194	8456.427 *		

$^5\Pi_3$ - $X^5\Delta_4$ (0,2)

J	R		Q		P	
	aa	bb	ab	ba	aa	bb
4	8631.041 *		8626.468 *		8622.820 *	
5	8631.463 *		8625.999 *		8621.439	
6	8631.803 *			*	8619.958	
7	8632.011 *		8624.755		8618.357 *	
8	*		8623.965 *		8616.676 *	
9	8632.246 *			*	8614.902 *	8614.942 *
10	8632.246 *		8622.181 *	8622.216 *	8613.051 *	8613.092 *
11	8632.129 *	8632.167 *	8621.161 *	8621.197 *	8611.114 *	8611.159 *
12	8631.936 *	*	8620.069 *		8609.080 *	8609.118 *
13	8631.653	8631.721 *	8618.855 *	8618.898 *	8606.968 *	8607.009 *
14	8631.313 *	8631.359 *	8617.574	8617.630 *	8604.776 *	
15	8630.887 *	8630.945 *	8616.228 *	8616.277 *	8602.465	8602.539
16	8630.402 *	8630.456 *	8614.793 *	8614.853	8600.123	8600.175
17	8629.838	8629.937 *	8613.286	8613.357	8597.692	8597.747
18	8629.212 *	8629.277 *	8611.716 *	8611.774 *	8595.184	8595.260 *
19	8628.540 *	8628.628	8610.106	8610.167	8592.599	8592.678 *
20	8627.843 *	8627.924 *	8608.435 *	8608.511 *	*	*
21	8627.100 *	8627.164	8606.726	8606.808	8587.318 *	8587.404 *
22	8626.340	8626.418 *	8604.976	8605.067	8584.584	8584.682
23	8625.558 *	8625.645 *	8603.219	8603.298	8581.850	8581.941 *
24	8624.815 *	8624.894 *	8601.451	8601.517 *	8579.073 *	8579.171 *
25	8624.087 *	8624.155 *	8599.689 *	8599.769 *	8576.310 *	8576.414 *
26	8623.416 *	8623.473 *	8597.966 *	8598.015	8573.560	8573.642
27	8622.820 *	8622.862 *	8596.284	8596.348	8570.834	8570.898
28	8622.287 *	8622.332 *	8594.680 *	8594.721 *	8568.151 *	8568.216
29	8621.908 *		8593.164 *	8593.197 *	8565.548	8565.592 *
30	8621.608 *		8591.738 *	8591.782 *	8563.016 *	8563.068 *
31	8621.512 *		8590.512 *		8560.631 *	8560.666 *
32	8621.512 *		8589.363		8558.365 *	
33	8621.719 *		8588.400 *		8556.249 *	
34	8622.073 *		8587.597 *		8554.265 *	
35			8586.940 *		8552.468 *	
36			8586.453 *		8550.829 *	
37			8586.113		8549.325	
38			8585.923 *?			

Appendix II -- $^5\Pi_3$ - $X^5\Delta_4$ (0,2) (cont.)

J	R		Q		P	
	aa	bb	ab	ba	aa	bb
24						
25						
26	8575.484 *					
27	8575.586 *		8548.381 *			
28	8575.586 *		8547.477		8520.230 *	
29	8575.343 *		8546.446		8518.353	
30	8574.923 *		8545.202 *		8516.305 *	
31	8574.228 *		8543.791		8514.102 *	
32	8573.329 *		8542.125 *		8511.651 *	
33	8572.164 *	8574.332	8540.216 *		8508.989	
34	8570.750	8572.290 *	8538.031 *	*	8506.096 *	
35	8569.072 *	8570.248 *	8535.628	8537.186 *	8502.923 *	8505.118 *
36	8567.170 *	8568.117 *	8532.963 *	8534.128	8499.502 *	8501.056 *
37	8565.006 *	8565.792 *	8530.043	8530.998	8495.859 *	8497.002 *
38	8562.631 *	8563.334	8526.889	8527.703	8491.933 *	8492.865 *
39	8560.024 *	8560.666 *	8523.513	8524.230	8487.811 *	8488.601
40	8557.256 *	8557.824 *	8519.928	8520.575	8483.413 *	*
41	8554.237 *	8554.804	8516.136 *	8516.728	8478.826 *	8479.482
42	8551.040 *	8551.595 *	8512.146 *	8512.714 *	8474.044 *	8474.633 *
43	8547.713 *	8548.210 *	8507.991 *	8508.523	8469.073	8469.621 *
44	8544.207 *	*	8503.644	8504.164 *	8463.910	8464.436 *
45	8540.520 *	8540.989 *	8499.137 *	8499.619	8458.589 *	8459.082
46	8536.682	8537.145 *	8494.470 *	8494.917 *	8453.070 *	8453.570
47	8532.687 *	8533.144 *	8489.636 *	8490.096	8447.421	8447.894
48	8528.564	8529.017 *	8484.672 *	8485.117 *	8441.609 *	8442.073 *
49	8524.286	8524.698 *	8479.550	8479.965 *	8435.628 *	8436.085 *
50	8519.876		8474.282	8474.695 *	8429.536	8429.977
51	8515.304 *		8468.878 *	8469.298	8423.271 *	8423.716 *
52	8510.651 *		8463.322 *	8463.752 *	8416.904 *	8417.320 *
53	8505.792 *		8457.659	8458.072	8410.371 *	8410.781 *
54	8500.844 *		8451.842	8452.263	8403.710	8404.118 *
55	8495.709 *		8445.890 *	8446.310 *	8396.917	*
56	8490.533 *		8439.810	8440.270	8389.961 *	8390.408 *
57			8433.633 *	8434.090 *	8382.927 *	8383.354 *
58				8427.819 *		

$^5\Pi_{-1}$ - $X^5\Delta_0$ (1,0)

J	R		Q		P	
	aa	bb	ab	ba	aa	bb
0			-	-	-	-
1					-	-
2						
3				11004.858 *		

Appendix II -- $^5\Pi_{-1}$ - $X^5\Delta_0$ (1,0) (cont.)

J	R		Q		P	
	aa	bb	ab	ba	aa	bb
4				11004.388		
5			11003.357	11003.788 *		
6			11002.615	11003.093		
7			11001.733	11002.235 *		
8			11000.721 *	11001.296		
9		11009.158 *	*	11000.204 *		
10	11008.777	11008.890 *	*	10999.027	10989.453 *	
11	*	11008.487	10996.959	10997.700 *	10987.167 *	10987.204 *
12	11007.684	11007.960	10995.448	10996.267	10984.726	10984.846 *
13	11006.940 *	11007.325	10993.782	10994.702	10982.183	10982.351
14	11006.109 *	*	10992.035	10993.009	10979.498 *	10979.752 *
15	*	11005.669 *	10990.126	10991.216	10976.679	10977.035
16	*	11004.640 *	10988.099	10989.263	10973.734	10974.204 *
17	11002.754 *	11003.506	10985.947	10987.204	10970.660 *	10971.243 *
18	11001.392 *	11002.235 *	10983.660	10985.008	10967.454 *	10968.110 *
19	10999.891 *	11000.839	10981.241	10982.706	10964.128 *	10964.863 *
20	10998.232	10999.286	10978.687	10980.266	*	10961.513
21	10996.468	10997.649 *	10976.008	10977.690 *	10957.066 *	10958.037
22	10994.564	10995.879 *	10973.179	10974.993	10953.341 *	10954.424
23	10992.529 *	10993.949	10970.256	10972.171 *	10949.500 *	10950.692
24	10990.339	10991.890 *	10967.182	10969.222	10945.515	10946.824
25	10988.027 *	10989.739 *	10963.972	10966.137	10941.411 *	10942.840 *
26	*	10987.427	10960.635 *	10962.918	10937.157	10938.683 *
27	10983.048 *	10985.008 *	10957.121 *	10959.575	10932.775 *	10934.453
28	10980.322 *	*	10953.536	10956.098	10928.256	10930.078
29	10977.475 *	10979.723 *	10949.789	10952.478 *	10923.617 *	10925.567
30	10974.493	10976.848 *	10945.917	10948.746	*	10920.921
31	10971.387 *	10973.899	10941.895	10944.876	10913.916 *	10916.138
32	10968.110 *	10970.803	10937.742 *	10940.864	10908.874 *	10911.225
33	10964.732	10967.547	10933.449	10936.715	10903.662	10906.179
34	10961.193	10964.160	10929.009 *	10932.432	10898.343 *	10901.008
35	*	10960.635 *	10924.456	10928.019	10892.871	10895.688
36	10953.711	10956.985	10919.747	10923.453 *	10887.263	10890.232 *
37	10949.745 *	10953.187 *	10914.897	10918.780 *	10881.523	10884.639
38	10945.654	10949.241 *	10909.882 *	10913.916 *	10875.640	10878.946 *
39	10941.411 *	10945.172	10904.787	10908.949	10869.627	10873.071
40	10937.029	10940.944	10899.510	10903.858	10863.455 *	10867.069
41	*	10936.599 *	10894.109	10898.605	10857.171	10860.930 *
42	10927.849 *	*	10888.557	10893.223	*	10854.655
43	10923.026	10927.429	10882.866	10887.682	10844.133	10848.241
44	10918.078 *	10922.656	10877.028	10882.003 *	10837.424	10841.678 *
45	10912.968	10917.724	10871.042	10876.185 *	*	10834.980
46	10907.729	10912.643	10864.925 *	10870.232	10823.559	10828.145
47	10902.336		10858.643	10864.126	10816.396	*
48	10896.793		10852.235 *	10857.884	*	10814.064 *

Appendix II -- $^5\Pi_{-1}$ - $X^5\Delta_0$ (1,0) (cont.)

J	R		Q		P	
	aa	bb	ab	ba	aa	bb
49	10891.113		10845.649 *	10851.492	10801.704 *	
50	10885.269 *		10838.966	10844.948	10794.054 *	
51	*		10832.112 *	10838.257 *	10786.361	
52	*		10825.108 *	10831.408 *		
53	10866.878		*	10824.407		
54	10860.452		10810.666			
55	10853.863 *		10803.200			
56	10847.147 *		10795.627 *			
57	10840.264 *		10787.876 *			
58	10833.249 *		10779.976 *		10728.144	
59	10826.077 *		10771.954 *		10719.234 *	
60			10763.762		10710.182	
61			10755.415		10700.967 *	
62			10746.912 *		10691.625 *	
63			10738.245 *		10682.102 *	
64			10729.486			
65			10720.536 *			
66			10711.445			
67			10702.195			

$^5\Pi_0$ - $X^5\Delta_1$ (1,0)

J	R		Q		P	
	aa	bb	ab	ba	aa	bb
1						
2						
3						
4				11072.872 *		
5				11072.237		
6		11077.826 *		11071.449 *	11001.442 *	11065.995
7		11077.826 *		11070.551 *	*	11064.184 *
8	11013.342	11077.702 *	11005.122 *	11069.497	10997.754 *	11062.228
9	11013.171 *	11077.472 *	11003.985 *	11068.363	10995.732	11060.162 *
10	11012.828 *	11077.117 *	11002.754 *	11067.062 *	10993.582	11057.973
11	11012.371	11076.663 *	11001.392 *	11065.694	10991.318 *	11055.650
12	11011.838 *	11076.067	10999.918 *	11064.184 *	10988.921 *	11053.217 *
13	11011.151	11075.377	10998.312 *	11062.563	10986.423	11050.676 *
14	11010.369 *	11074.584	10996.603	11060.835	10983.786 *	11048.001 *
15	11009.449 *	11073.696	10994.777 *	11059.002 *	10981.034	11045.256
16	11008.419	11072.714	10992.823	11057.080 *	10978.150 *	11042.379
17	11007.280 *	11071.646 *	10990.762 *	11055.062	10975.178 *	11039.417
18	11006.014 *	11070.503 *	10988.576 *	11052.958	10972.075 *	11036.357
19	*	11069.281 *	10986.288	11050.776	10968.858 *	11033.227 *
20	11003.211	11068.003	10983.894	11048.537 *	10965.548 *	11030.011

Appendix II -- $^5\Pi_0$ - $X^5\Delta_1$ (1,0) (cont.)

J	R				Q				P	
	aa		bb		ab		ba		aa		bb	
21	11001.651	*	11066.683	*	10981.385		11046.201	*	10962.109	*	11026.711	*
22	10999.999	*	11065.298	*	10978.810		11043.849		10958.576		11023.375	*
23	10998.312	*			10976.133		11041.430		10954.973	*	11019.957	*
24	10996.550	*			10973.378		11038.965	*	10951.243	*	11016.517	*
25					10970.618	*	11036.464		10947.450	*	11013.024	*
26	10979.845	*					11033.919		10943.636		11009.457	*
27											11005.900	
17			11046.172	?				*				
18			11045.256	*			11027.462	*				
19			11044.127				11025.497	*				
20			11042.872	*			11023.375	*			11004.717	*
21							11021.089				11001.558	
22			11039.893				11018.671	*			10998.232	*
23			11038.117				11016.034				10994.777	*
24			11036.205				11013.246				10991.116	*
25			11034.064	*			11010.233	*			10987.288	
26	10979.845	*	11031.776	*			11007.099	*	10943.636		10983.279	
27	10978.272	*	11029.299	*	10951.863		11003.788	*				*
28	10976.418		11026.606	*	10949.200	*	11000.272	*	10922.841	*	10974.729	*
29	10974.375	*	11023.732	*	10946.333		10996.550	*	10919.193	*	10970.131	*
30	10972.075	*	11020.650	*	10943.254	*	10992.647		10915.255	*	10965.441	*
31	10969.551	*	11017.476	*	10939.926		10988.576	*	10911.129		10960.525	*
32	10966.808	*	11014.020		10936.369		10984.307	*	10906.788		10955.369	
33	10963.851		11010.450	*	10932.594		10979.845	*	10902.191	*	10950.078	*
34	10960.635	*	11006.628		10928.606	*	10975.223		10897.393	*	10944.599	
35	10957.331		11002.682		10924.410	*	10970.419	*	10892.360	*	10938.966	*
36	10953.804	*	10998.558	*	10920.015	*	10965.442	*	10887.154	*	10933.106	
37	10950.078		10994.315	*	10915.457	*	10960.284	*	10881.743	*	10927.101	*
38	10946.231	*	10989.836	*	10910.714	*	10954.973	*	10876.123	*	10920.921	*
39	10942.157	*	10985.189	*	10905.817		10949.500	*	10870.386		10914.601	*
40	10937.973	*	10980.399	*	10900.744		10943.825	*	10864.444	*	10908.074	*
41	10933.625	*	10975.382	*	10895.537	*	10938.014	*	10858.360	*	10901.396	
42	10929.137		10970.131	*	10890.155	*	10931.993		10852.136		10894.540	
43	10924.456	*			10884.639	*	10925.722	*	10845.753	*	10887.490	*
44	10919.662				10878.946	*	10919.193	*	10839.184		10880.185	*
45	10914.714	*			10873.105	*			10832.490		10872.647	*
46	10909.610	*			10867.147				10825.633	*		
47	10904.363				10861.029				10818.649			
48	10898.947	*			10854.758	*			10811.506	*		
49	10893.419	*			10848.334				10804.224			
50	10887.732	*			10841.803	*			10796.775	*		
51					10835.061					*		
52									10781.494	*		

Appendix II (cont.) -- $^5\Pi_1$ - $X^5\Delta_2$ (1,0)

J	R				Q				P			
	aa		bb		ab		ba		aa		bb	
2					11035.408				11033.611			
3					11034.984				11032.308			
4					11034.429		11034.489		11030.849	*		
5					11033.728		11033.803			*	11029.299	
6			11039.327	*	11032.889		11033.019		11027.519		11027.616	
7	11039.075		11039.300	*	11031.912		11032.091		11025.652	*	11025.787	
8	11038.830	*	11039.111		11030.793		11031.023		11023.650	*	11023.819	
9	11038.477		11038.830	*	11029.533		11029.824		11021.484	*	11021.740	*
10	11037.966	*	11038.376		11028.141		11028.489		11019.200		11019.477	*
11	11037.335		11037.837		11026.606		11027.029		11016.770		11017.122	
12	11036.544		11037.131		11024.931		11025.428		11014.213		11014.625	
13	11035.625		11036.292		11023.115		11023.698		11011.497			*
14	11034.569	*	11035.319		11021.164		11021.829	*	11008.651		11009.245	*
15	11033.370		11034.222		11019.072		11019.829		11005.669		11006.333	*
16	11032.023		11032.985	*	11016.839		11017.695		11002.541		11003.302	
17	11030.552		11031.618	*	11014.468		11015.426		10999.286			*
18	11028.937		11030.110		11011.947	*	11013.024		10995.879		10996.844	
19	11027.180		11028.489	*	11009.295		11010.487		10992.338		10993.393	*
20	11025.285		11026.711	*	11006.535		11007.821		10988.679	*	10989.836	
21	11023.375	*	11024.812	*	11003.648	*	11005.029		10984.846		10986.138	
22	11020.938	*			11000.670		11002.101		10980.916		10982.309	*
23	11018.671	*	11020.416	*	10997.200		10999.110		10976.925		10978.361	
24	11016.234	*	11018.173		10993.906		10995.639	*	10972.435		10974.338	*
25	11013.643		11015.755	*	10990.434		10992.367		10968.110		10969.818	*
26	11010.905		11013.171		10986.815		10988.921		10963.622	*	10965.548	
27	11008.032		11010.450		10983.048		10985.312		10958.959		10961.058	
28	11005.029	*	11007.581		10979.150	*	10981.606	*	10954.175		10956.436	
29	11001.871		11004.613	*	10975.114		10977.690	*	10949.241	*	10951.665	
30	10998.558		11001.474		10970.928		10973.676		10944.178		10946.751	*
31	10995.147		10998.232	*	10966.610		10969.524		10938.966		10941.750	*
32	10991.612	*	10994.777	*	10962.156		10965.229		10933.625	*	10936.537	
33	10987.871	*	10991.285		10957.558	*	10960.804		10928.147		10931.215	
34	10984.006		10987.597	*	10952.825		10956.241		10922.525		10925.767	*
35		*	10983.786	*	10947.950		10951.545		10916.765		10920.181	
36	10975.891		10979.845	*	10942.935		10946.710	*	10910.871		10914.465	*
37		*	10975.760		10937.786		10941.750	*	10904.829		10908.599	*
38		*	10971.550	*	10932.477		10936.633		10898.661		10902.613	
39	10962.669	*	10967.182	*	10927.071		10931.391		10892.360	*	10896.489	
40	10957.986	*	10962.669	*	10921.499		10926.016		10885.895		10890.232	
41	10953.147	*	10958.037	*	10915.792		10920.496		10879.312		10883.831	
42	10948.184		10953.283	*	10909.941		10914.846		10872.595		10877.295	
43	10943.071		10948.370		10903.961		10909.059		10865.726		10870.622	
44	10937.825		10943.297	*	10897.838		10903.116		10858.737	*	10863.809	
45	10932.477	*	10938.132		10891.588		10897.065		10851.589		10856.876	
46	10926.940		10932.808	*	10885.190		10890.865			*	10849.774	*

Appendix II -- $^3\Pi_1$ - $X^3\Delta_2$ (1,0) (cont.)

J	R				Q				P			
	aa		bb		ab		ba		aa		bb	
47	10921.275		10927.342		10878.630	*	10884.528		10836.900	*	10842.567	*
48	10915.457	*	10921.748		10871.985	*	10878.033		10829.349		10835.220	
49	10909.539		10916.013	*	10865.160		10871.457	*		*	10827.726	
50	10903.463	*	10910.105		10858.212		10864.679		10813.815	*	10820.106	
51	10897.248		10904.110		10851.117		10857.768		10805.867		10812.336	*
52		*	10897.951		10843.894		10850.763		10797.784		10804.429	*
53	10884.401		10891.658		10836.536		10843.597				10796.405	
54	10877.775			*	10829.041	*	10836.284				10788.223	
55					10821.386	*	10828.850	*			10779.899	
56					10813.623	*	10821.269	*			10771.469	
57							10813.548				10762.877	*
58											10754.148	
59											10745.293	

$^3\Pi_2$ - $X^3\Delta_3$ (1,0)

J	R		Q		P	
3			11021.484	*	11018.779	
4			11020.938		11017.337	
5			11020.266		11015.755	*
6	11025.732	*	11019.477		11014.099	
7	11025.705	*	11018.534	*	11012.279	*
8	11025.528	*	11017.476		11010.302	
9	11025.240		11016.283		11008.232	
10	11024.812		11014.952	*	11006.014	
11	11024.243		11013.504		11003.648	*
12	11023.540		11011.916	*	11001.171	
13	11022.713	*	11010.188		10998.558	
14	11021.740	*	11008.325		10995.779	
15	11020.650		11006.333		10992.918	
16	11019.424		11004.213		10989.904	
17	11018.057		11001.962		10986.753	
18	11016.563		10999.571		10983.473	
19	11014.952	*	10997.055		10980.071	
20	11013.171		10994.381	*	10976.520	
21	11011.279		10991.612		10972.840	
22	11009.245		10988.679		10969.034	
23	11007.099		10985.647		10965.089	
24	11004.798		10982.467		10961.017	
25	11002.377		10979.150		10956.811	
26	10999.823		10975.699		10952.478	*
27	10997.136		10972.120		10948.005	
28	10994.315		10968.415		10943.406	

Appendix II -- $^5\Pi_2$ - $X^5\Delta_3$ (1,0) (cont.)

J	R		Q		P	
	aa	bb	ab	ba	aa	bb
29	10991.382		10964.581		10938.683 *	
30	10988.370		10960.635 *		10933.818	
31	10984.599 *		10956.584		10928.844	
32	*		10951.794		10923.788	
33	10978.104 *	10978.150 *	10947.703 *	10947.758 *	10917.969	
34	10974.493 *	10974.538 *	10943.254 *	10943.297 *	10912.880 *	10912.921 *
35	10970.758 *	10970.803 *	*	10938.683 *	10907.410 *	10907.437 *
36	10966.895	10966.953	10933.891	10933.946	10901.766	10901.811
37	10962.918 *	10962.976	10929.009 *	10929.060	10895.995	10896.052
38	10958.783	10958.881	10923.991	10924.073	10890.092	10890.155 *
39	10954.563 *	10954.698 *	10918.867 *	10918.949 *	10884.057 *	10884.152
40	10950.304 *	10950.496	10913.642 *	10913.770	10877.943 *	10878.033 *
41			10908.357		10871.697	10871.811
42					10865.390	10865.582

$^5\Pi_3$ - $X^5\Delta_4$ (1,0)

J	R		Q		P	
	aa	bb	ab	ba	aa	bb
4			10994.777 *		10991.216	
5			10994.152		10989.693	
6			10993.393 *		10988.027	
7			10992.484		10986.236	
8	10999.492		10991.455		10984.307	
9	10999.229		10990.296		10982.259	
10	10998.810 *		10989.012		10980.071 *	
11	10998.312 *		10987.597		10977.772	
12	10997.649		10986.043		10975.332	
13	10996.844 *		10984.372		10972.768	
14	10995.931 *		10982.558		10970.068	
15	10994.887		10980.622		10967.240	
16	10993.714 *		10978.553		10964.282	
17	10992.367 *	10992.433 *	10976.358		10961.193	
18	10990.942	10991.051	10974.021 *	10974.062 *	10957.986	
19	10989.362	10989.540	10971.550	10971.656	10954.630	10954.671
20	10987.682 *	10987.871 *	10968.954	10969.131	10951.141	10951.243 *
21	10985.647 *	10986.043 *	10966.216	10966.413 *	10947.501 *	10947.709 *
22	10983.786 *	10984.128	10963.249 *	10963.622	10943.771	10943.999
23	*	10982.044	10960.284	10960.635 *	10939.733	10940.156
24	10979.304	10979.845	10957.121	10957.558 *	10935.795	10936.158 *
25	10976.848 *	10977.475 *	10953.804	10954.325	10931.615	10932.060
26	10974.204	10974.993 *	10950.304	10950.953	10927.286	10927.800
27	10971.387 *	10972.367	10946.683 *	10947.450 *	10922.791	10923.426
28	10968.415 *	10969.600	10942.840	10943.825	10918.123	10918.896

Appendix II -- $^5\Pi_3$ - $X^5\Delta_4$ (1,0) (cont.)

J	R		Q		P	
	aa	bb	ab	ba	aa	bb
29	10965.089 *	10966.731	10938.811	10940.052	10913.281	10914.257
30	10961.592	10963.712	10934.539	10936.158 *	10908.227	10909.475
31	10957.765	10960.525 *	10929.997	10932.113	10902.941	10904.540
32	10953.613	10957.264	10925.162	10927.951	10897.393	10899.510
33	10949.136 *	10953.804 *	10920.015 *	10923.617 *	10891.543	10894.306
34		10950.270 *	10914.465 *	10919.193 *	10885.362	10889.007
35		10946.521		10914.601	10878.850	10883.547
36		10942.679		10909.882		10877.943
37		10938.683 *		10905.008		10872.214
38		10934.539 *		10899.990		10866.328
39		10930.205		10894.830		10860.308
40		10925.767 *		10889.522		10854.092 *
41		10921.145		10884.057		10847.791 *
42		10916.374		10878.431		10841.316
43		10911.416		10872.647		10834.708
44		10906.299		10866.690		10827.904
45		10901.018		10860.568		10820.944 *
46		10895.537		10854.270		10813.815
47		10889.891		10847.791 *		10806.524
48				10841.137		10799.033
49				10834.288		10791.373
50				10827.237 *		10783.521
51						10775.480

32	10962.231			
33	10958.240	10928.606		
34	10954.276 *	10923.617	10893.973	
35	10950.270	10918.617	10887.962	
36	10946.231	10913.615 *	10881.957	
37	10942.157	*	10875.940	
38	10937.973 *	10903.463	10869.880 *	
39	10933.691	10898.269	10863.770	
40	10929.307	10892.995	10857.577 *	
41	10924.842	10887.617	10851.281 *	
42	10920.246	10882.126	10844.899	
43	10915.538	10876.529	10838.393	
44	10910.714	10870.807	10831.799	
45	10905.758	10864.970	10825.068	
46	10900.668	10859.009	10818.222	
47	10895.470	10852.925	10811.269	
48	10890.155	10846.716	10804.152	
49	10884.688	10840.372 *	10796.958	
50	10879.101	10833.889 *	10789.652 *	
51	10873.388	10827.335	10782.160 *	

Appendix II -- $^5\Pi_3$ - $X^5\Delta_4$ (1,0) (cont.)

J	R		Q		P	
	aa	bb	ab	ba	aa	bb
52	10867.538 *		10820.619		10774.573	
53	10861.557		10813.778		10766.847	
54	10855.458		10806.799 *		10759.020	
55	10849.223		10799.694		10751.038	
56	10842.849		10792.463		10742.933	
57	10836.353		10785.097		10734.707	
58	10829.711 *		10777.599 *		10726.355	
59	10822.951 *		10769.973 *		*	
60			10762.215		10709.244 *	
61					10700.484 *	

$^5\Pi_1$ - $X^5\Delta_2$ (1,1)

J	R		Q		P	
	aa	bb	ab	ba	aa	bb
2			10164.298		10162.495 *	
3				*	10161.198 *	
4				*	10159.741 *	
5			10162.702 *	10162.789 *	10158.187 *	10158.217 *
6			10161.915	10162.034 *	10156.527 *	10156.630
7			10160.986	10161.198 *	10154.699 *	10154.875
8			10159.929 *	10160.146 *	10152.775	
9			10158.731 *	10159.018	10150.689 *	
10			10157.403	10157.799 *	10148.471 *	
11			10155.969 *	10156.390 *	10146.131	
12			10154.376 *	10154.875 *	10143.694 *	
13			10152.663 *	10153.233	10141.055	
14			10150.819	10151.486	10138.287 *	
15			10148.843	10149.593	10135.440 *	
16			10146.729	10147.570 *	10132.458 *	
17			10144.483 *	10145.440 *	10129.306	
18			10142.118	10143.183	10126.047 *	
19			10139.617	10140.818 *	10122.638	
20			10136.992 *	10138.287 *	10119.105	
21			10134.224	10135.669 *	10115.465	
22			10131.452	10132.897	10111.689	
23			10128.161	10130.068	10107.892	
24			10125.038	10126.807 *	10103.577	
25			10121.748 *	10123.710	10099.462 *	
26			10118.356 *	*	10095.165	
27			10114.794 *	10117.053		
28			10111.108	10113.542 *		
29			10107.292 *	10109.868		
30			10103.336	10106.085		

Appendix II -- $^5\Pi_1$ - $X^5\Delta_2$ (1,1) (cont.)

J	R			Q				P		
	aa		bb	ab		ba		aa		bb
31				10099.272	*	10102.150	*			
32				10095.033		10098.105	*			
33				10090.686	*	10093.950				
34				10086.235		10089.630	*			
35				10081.622		10085.217				
36				10076.882		10080.666				
37				10072.040	*	10075.974				
38				10067.000		10071.157				
39					*	10066.221				
40				10056.615	*	10061.147	*			
41				10051.244	*	10055.946				
42				10045.724		10050.621				
43					*	10045.171				
44				10034.290	*	10039.567				
45				10028.363		10033.826				
46				10022.317		10027.992				
47				10016.138		10022.023	*			
48				10009.844	*	10015.919				
49				10003.398		10009.676				
50				9996.849	*	10003.303				
51					*	9996.753	*			
52				9983.309	*		*			
53				9976.334	*		*			
54				9969.265	*	9976.527				
55						9969.506	*			

$^5\Pi_2$ - $X^5\Delta_3$ (1,1)

J	R		Q		P	
3					10147.660	
4					10146.244	
5			10149.192	*	10144.692	
6		*	10148.439		10143.064	*
7	10154.699	*	10147.570		10141.286	*
8		*	10146.565	*	10139.389	*
9		*	10145.440	*		*
10	10154.019	*	10144.193	*	10135.246	
11		*	10142.809	*	10132.958	
12	10152.938		10141.286		10130.539	*
13	10152.216	*	10139.678		10128.050	
14	10151.354	*	10137.912		10125.396	*
15	10150.370		10136.053		10122.638	
16		*	10134.048		10119.737	

Appendix II -- $^5\Pi_2$ - $X^5\Delta_3$ (1,1) (cont.)

J	R				Q				P			
	aa		bb		ab		ba		aa		bb	
17	10148.027				10131.927				10116.742			
18	10146.668				10129.672						*	
19	10145.182	*			10127.301				10110.286	*		
20	10143.577	*			10124.807	*			10106.898	*		
21	10141.835				10122.170				10103.394			
22	10139.966	*			10119.417				10099.755	*		
23	10137.996				10116.550				10095.972			
24	10135.880				10113.542	*			10092.099			
25	10133.647				10110.437	*			10088.100	*		
26	10131.289				10107.162				10083.942			
27	10128.792	*			10103.800				10079.692	*		
28	10126.196	*			10100.303				10075.294			
29	10123.494				10096.696						*	
30	10120.711				10092.951				10066.151			
31			*		10089.149				10061.422	*		
32	10114.348	*	10114.396	*	10084.603	*					*	
33	10111.157	*	10111.198		10080.783	*	10080.810	*	10051.036	*		
34	10107.823	*	10107.892	*	10076.591			*	10046.192	*	10046.239	*
35		*	10104.388		10072.216	*	10072.265	*	10040.985		10041.022	
36	10100.760	*	10100.797	*	10067.747	*	10067.775		10035.612		10035.665	
37		*	10097.100	*	10063.150	*	10063.202	*	10030.094	*	10030.162	
38	10093.216		10093.292		10058.419	*	10058.497		10024.506		10024.579	
39	10089.296		10089.424		10053.585		10053.668		10018.787		10018.850	
40	10085.334		10085.519	*	10048.663	*	10048.791			*		*
41					10043.696	*	10043.878	*		*	10007.146	
42									10001.053		10001.209	*

$^5\Pi_3$ - $X^5\Delta_4$ (1,1)

J	R		Q		P	
4			10123.638	*		*
5			10123.029		10118.552	*
6			10122.302	*	10116.946	
7			10121.447	*	10115.223	*
8	10128.514	*	10120.481	*	10113.341	
9	10128.310	*	10119.417	*	10111.353	
10	10128.004	*	10118.184	*	10109.252	
11	10127.555	*	10116.842		10107.031	
12	10126.993		10115.385		10104.671	
13	10126.294		10113.802	*	10102.208	
14	10125.486	*	10112.101		10099.625	*
15	10124.547	*	10110.286	*	10096.909	*
16	10123.494	*	10108.333		10094.056	

Appendix II -- $^5\Pi_3$ - $X^5\Delta_4$ (1,1) (cont.)

J	R		Q		P	
	aa	bb	ab	ba	aa	bb
17	10122.302 *	10122.335 *	10106.246		10091.103 *	
18	10120.982 *	10121.091 *	10104.064 *	10104.094 *	10088.027	
19	10119.527	10119.737 *	10101.750 *	10101.837	10084.819 *	
20		10118.184 *	10099.272	10099.462	10081.469	10081.579
21		10116.550 *	10096.696 *	10096.937 *	10078.009	10078.187 *
22		10114.794	10093.853 *	10094.279 *	10074.426 *	10074.649 *
23		10112.888	10091.103	10091.468 *	10070.557	10070.991
24		10110.822	10088.100 *	10088.567 *	10066.787 *	10067.179 *
25		10108.664 *	10084.976	10085.519 *	10062.806	10063.243
26		10106.374	10081.715	10082.339	10058.676 *	10059.202 *
27		10103.962	10078.260	10079.051 *	10054.377	10055.012
28		10101.416	10074.649 *	10075.620 *	*	10050.697 *
29		10098.749	10070.822 *	10072.040 *	10045.283	*
30			10066.787	10068.400 *	10040.474 *	10041.719
31			10062.468 *	10064.601 *	10035.435 *	10037.034 *
32			10057.880	10060.665 *	10030.094 *	10032.216 *
33			10052.962	10056.615 *	10024.506 *	10027.284
34			10047.721	10052.417		10022.219
35				10048.130 *		10017.029 *
36				10043.609 *		10011.695 *
37				10039.045 *		10006.244
38				10034.290		10000.644
39				10029.434		9994.914
40				10024.406		9989.046
41				10019.271		9983.007 *
42				10013.951		9976.831 *
43				10008.498		9970.557 *
44				10002.880 *		9964.091
45				9997.092 ?		9957.467 *
46				9991.139 *?		9950.683
47				*		9943.755
48				9978.709 *?		
49				9972.237 ?		

33	10061.584 *		
34	10056.824	10027.189 *	
35	10052.126 *	10021.438 *	
36	10047.350	10015.704	
37	10042.594	10009.967 *	
38	10037.770	10004.160 *	
39	10032.869 *	9998.367	
40	10027.906 *	9992.480 *	
41	10022.826	9986.481	
42	10017.655		

Appendix II -- $^5\Pi_3$ - $X^5\Delta_4$ (1,1) (cont.)

J	R		Q		P	
	aa	bb	ab	ba	aa	bb
43			10012.375			
44			10006.991			
45			10001.489			
46			9995.872			
47			9990.149 *			
48			9984.302 *			
49			9978.328 *			
50			9972.237 *			
51			9966.014 *			
52			9959.717			
53			9953.255			
54			9946.705			
55			*			
56			9933.163 *			
57			9926.265			

$^5\Pi_{-1}$ - $X^5\Delta_0$ (2,0)

J	R		Q		P	
	aa	bb	ab	ba	aa	bb
0			-	-	-	-
1					-	-
2						
3						
4						
5						
6						
7		11672.685				
8	11672.752 *	11672.537		11664.629		
9	11672.463 *	11672.241	11663.042	11663.420 *		11654.910
10	11672.044 *	11671.824	11661.703	11662.103	11652.925 *	11652.677
11	11671.466	11671.267 *	11660.239 *	11660.647	11650.536	11650.298
12	11670.772	11670.577	11658.614	11659.029 *	11648.009	11647.787
13	11669.952 *	11669.837 *	11656.870	11657.326 *	11645.351	11645.155
14	11668.958	11668.846	11654.995	11655.494	11642.563	11642.371 *
15	11667.842	11667.747 *	11652.986	11653.481	11639.636	11639.515
16	11666.602 *	11666.535	11650.830	11651.363	11636.584	11636.461
17	11665.219	11665.179	11648.536	11649.089	11633.380	11633.286
18	11663.694 *	11663.694 *	11646.111	11646.693	11630.056	11629.987 *
19	11662.049 *	11662.049 *	11643.561	11644.158	11626.586	11626.545 *
20	11660.279 *	11660.279 *	11640.865	11641.495	11622.993 *	11622.993 *
21	11658.338	11658.392	11638.036	11638.682	11619.257 *	11619.257 *
22	11656.251 *	11656.354	11635.065	11635.740	11615.411 *	11615.411 *
23	11654.047 *	11654.230 *	11631.935 *	11632.663	11611.365 *	11611.427
24	11651.722	11651.870	11628.714	11629.452	11607.241 *	11607.299 *

Appendix II -- $^5\Pi_{-1}$ - $X^5\Delta_0$ (2,0) (cont.)

J	R		Q		P	
	aa	bb	ab	ba	aa	bb
25	11649.190	11649.429 *	11625.324	11626.101	11602.942	11603.057
26	11646.518	11646.837	11621.782 *	11622.619	11598.517	11598.676
27		11644.120 *	11618.054	11618.987	11593.931	11594.158
28		11641.257		11615.231	11589.180	11589.489
29		11638.263 *		11611.340 *		11584.694 *
30		11635.117 *		11607.299 *		11579.749
31		11631.844		11603.116		11574.678 *
32		11628.413		11598.798		11569.466
33		11624.859		11594.339		11564.145 *
34		11621.158 *		11589.743		11558.634
35		11617.315		11585.005		11553.011
36		11613.332		11580.132		11547.233
37		11609.208 *		11575.127 *		*
38		11604.933 *		11569.979 *		11535.293 *
39		11600.544		11564.673 *		11529.093 *
40		11596.007 *		11559.235 *		11522.776 *
41		11591.294 *		11553.663		11516.299 *
42		11586.489		11547.957 *		11509.707 *
43		11581.518 *		11542.088		11502.964
44				11536.075		11496.073
45						11489.041

$^5\Pi_0$ - $X^5\Delta_1$ (2,0)

J	R		Q		P	
	aa	bb	ab	ba	aa	bb
1						
2						
3				11695.297 *		
4				11694.733 *		
5				11694.039		
6	11685.347 *			11693.184		
7	11685.509 *		11678.072	11692.199 *	11671.561 *	
8	11685.547 *		11677.188	11691.061	11669.765 *	
9	11685.468 *		11676.167 *	11689.786	11667.842 *	
10	11685.244 *		11675.068 *	11688.375	11665.753 *	
11	11684.939 *		11673.820 *	11686.813 *	11663.627 *	
12	11684.489		11672.463 *	11685.110 *	11661.363 *	
13	11683.875 *		11670.976 *	11683.272 *	11658.975 *	11671.606 *
14	11683.219		11669.363	11681.287	11656.434 *	11668.717 *
15	11682.374	11693.508	11667.621	11679.162	11653.789 *	11665.703 *
16	11681.420 *	11692.129	11665.753 *	11676.846 *	11651.013 *	11662.529
17	11680.331 *	11690.605 *	11663.754 *	11674.461	11648.106 *	11659.243 *
18	11679.086 *	11688.942 *	11661.630	11671.936 *	11645.061 *	11655.774 *

Appendix II -- $^5\Pi_0$ - $X^5\Delta_1$ (2,0) (cont.)

J	R				Q				P			
	aa		bb		ab		ba		aa		bb	
19	11677.717	*	11687.141		11659.352	*	11669.224		11641.930	*	11652.189	
20	11676.167	*	11685.192	*	11656.934		11666.380		11638.618	*	11648.442	*
21	11674.576	*	11683.105	*	11654.416		11663.412	*	11635.154	*	11644.576	*
22	11672.802	*	11680.862	*	11651.730	*	11660.273	*	11631.596	*	11640.548	
23	11670.882	*	11678.481		11648.930		11657.013	*	11627.876		11636.388	*
24	11668.846	*	11675.956	*	11645.988	*	11653.590		11624.055	*	11632.082	
25	11666.669	*	11673.277	*	11642.895		11650.037		11620.084	*	11627.639	
26	11664.358	*	11670.479		11639.677	*	11646.335		11615.946		11623.038	*
27	11661.898		11667.526		11636.321	*	11642.491		11611.691	*	11618.305	*
28	11659.314	*	11664.415	*	11632.846	*	11638.473	*	11607.299	*	11613.433	*
29	11656.587	*	11661.197		11629.219		11634.375		11602.752	*	11608.414	*
30	11653.721	*	11657.818		11625.456	*	11630.110	*	11598.132	*	11603.259	*
31	11650.752	*	11654.306	*	11621.571		11625.693		11593.329		11597.972	*
32	11647.624	*	11650.613	*	11617.546		11621.158	*	11588.430		11592.520	
33	11644.358	*	11646.919	*	11613.394	*	11616.449		11583.372	*	11586.952	*
34	11640.949	*			11609.106		11611.691	*	11578.193		11581.204	*
35	11637.463				11604.678				11572.876	*		
36	11633.825				11600.152				11567.437			
37	11630.065	*			11595.488	*			11561.841	*		
38					11590.682	*			11556.186	*		
39					11585.765				11550.362	*		
40					11580.722				11544.420	*		
41					11575.564				11538.348			
42					11570.270				11532.136	*		
43					11564.868				11525.843	*		
44					11559.343				11519.403	*		
45					11553.694	*				*		

$^5\Pi_2$ - $X^5\Delta_3$ (2,0)

J	R		Q		P	
3			11673.930		11671.267	
4			11673.399		11669.837	
5			11672.752		11668.280	
6			11671.950	*	11666.602	
7	11678.174		11671.017		11664.764	
8	11678.006		11669.952		11662.800	*
9	11677.717	*	11668.767		11660.689	
10	11677.290		11667.439		11658.493	
11	11676.739		11665.987		11656.138	
12	11676.076		11664.415		11653.657	*
13	11675.273	*	11662.725		11651.054	
14			11660.914		11648.334	

Appendix II -- $^5\Pi_2$ - $X^5\Delta_3$ (2,0) (cont.)

J	R		Q		P	
	aa	bb	ab	ba	aa	bb
15			11659.029 *		11645.500	
16					11642.563	
17						
18			11650.613 *			
19	11666.459 *	11666.535 *	11648.406			
20	11664.764 *	11664.844	11645.916	11645.988 *	11627.876 *	
21	11662.954 *	11662.954 *	11643.223	11643.321 *	11624.354 *	11624.440
22	11660.914 *	11660.996	11640.349	11640.416	11620.647	11620.695
23	11658.764 *		11637.314	11637.391	11616.734 *	11616.810 *
24	11656.434 *	11656.587 *	11634.136	*	11612.692	11612.747 *
25	11654.047 *	11654.230 *	11630.811	11630.938	11608.461	11608.573
26	11651.499 *	11651.722 *	11627.370	11627.515	11604.146 *	11604.262
27	*	11649.134 *	11623.777	11624.014 *	11599.664	11599.824
28	11646.111		11620.084	11620.416	11595.060	11595.275 *
29			11616.355	11616.734 *?	11590.339	11590.682 *
30					11585.597	11585.986 ?

$^5\Pi_3$ - $X^5\Delta_4$ (2,0)

J	R	Q	P
4		11658.764 *	11655.207
5		11658.124	11653.657
6		11657.326	11651.989
7		11656.434	11650.192
8	11663.412 *	11655.397	11648.257 *
9	11663.138	11654.230	11646.199
10	11662.725 *	11652.925	11644.011
11	11662.197 *	11651.499	11641.698
12	11661.539	11649.943	11639.229
13	11660.740 *	11648.257 *	11636.667
14	11659.791	11646.441	11633.963
15	11658.764 *	11644.490	11631.124
16	11657.562 *	11642.419	11628.156
17	11656.251	11640.205	11625.054
18	11654.792	11637.874	11621.826
19	11653.211 *	11635.397	11618.471
20	11651.499 *	11632.801	11614.985
21	11649.647	11630.065	11611.365 *
22	11647.670	11627.201	11607.615
23	11645.560	11624.205	11603.730
24	11643.321 *	11621.081	11599.718
25	11640.949	11617.814	11595.588
26	11638.473 *	11614.424	11591.294

Appendix II -- $^5\Pi_3$ - $X^5\Delta_4$ (2,0) (cont.)

J	R		Q		P	
	aa	bb	ab	ba	aa	bb
27	11635.785		11610.905		11586.892	
28	11632.963 *	11633.023 *	11607.241		11582.350	
29	11630.065 *	11630.110 *	11603.437 *	11603.495 *	11577.671	
30	11627.000	11627.070	11599.492 *	11599.521	11572.847 *	11572.876 *
31	11623.777 *	11623.900 *	11595.406	11595.488 *	11567.904 *	11567.904 *
32	11620.416 *	11620.575	11591.166	11591.294 *	11562.791 *	11562.871
33	11616.810 *	11617.128 *	11586.766	11586.952 *	11557.538 *	11557.670
34	11612.972	11613.533 *	11582.157 *	11582.502	11552.131	11552.318
35	*	11609.879 *	11577.322	11577.904	11546.525 *	11546.843 *
36			11572.144 *	11573.208	11540.639 *	11541.203 *
37					11534.505 *	11535.539

$^5\Pi_{-1}$ - $X^5\Delta_0$ (2,2)

J	R		Q		P	
	aa	bb	ab	ba	aa	bb
0			-	-	-	-
1					-	-
2						
3						
4						
5						
6						
7						
8						
9				9931.210 *		
10				9930.033 *		
11				9928.760		
12				*		
13				9925.837 *		
14				9924.211		
15				9922.440 *		
16				9920.527 *		
17				9918.546		
18				9916.469 *		
19				9914.199 *		
20				9911.826		
21				9909.362 *		
22				9906.772		
23				9904.065 *		
24				9901.232 *		
25				9898.258 *		
26				9895.156		

Appendix II (cont.) -- $^5\Pi_0$ - $X^5\Delta_1$ (2,2)

J	R		Q		P	
	aa	bb	ab	ba	aa	bb
1						
2						
3						
4						
5						9956.800 *
6			9946.191 *	9960.549 *		9955.140 *
7			*	9959.649		9953.379 *
8			9944.762 *	9958.698 *		9951.475 *
9		9966.486 *	9943.876 *	9957.507 *		*
10		9966.121 *	9942.943 *	9956.261 *		9947.271
11		9965.631 *	9941.859	9954.877 *		9944.997 *
12		9965.000 *	9940.701 *	9953.379 *		9942.579 *
13		9964.262 *	9939.409 *	9951.706 *		9940.021 *
14		9963.382	9938.021 *	9949.941 *		9937.380 *
15	9951.261 *	*	9936.492 *	9948.050		9934.586 *
16	9950.565 *	9961.260 *	9934.902 *	9946.030 *		9931.673 *
17	9949.717 *	9960.011 *	9933.163 *	9943.876 *		*
18	*	*	9931.290 *	9941.600 *		9925.447
19	9947.696 *	9957.113 *	9929.325 *	9939.181 *	9911.881 *	9922.167 *
20	9946.507	9955.480 *	9927.238 *	9936.645 *	9908.847 *	9918.731 *
21	9945.178 *	9953.688 *	9925.020 *	9934.008 *	9905.766 *	9915.172 *
22	9943.755 *	9951.791 *	9922.686 *	9931.210 *	9902.537	9911.501 *
23	9942.182 *	9949.764 *	9920.226 *	9928.292 *	9899.183 *	9907.718 *
24	9940.538 *	9947.633 *	9917.649 *	9925.289 *	9895.701	9903.754 *
25	9938.716 *	9945.330 *	9914.957	9922.114 *	9892.116 *	9899.697 *
26	9936.810 *	9942.943 *	9912.125 *	9918.791	9888.412 *	9895.483 *
27	9934.789 *	9940.402 *	9909.196 *	9915.371 *	9884.561 *	9891.168 *
28			9906.160 *	9911.826 *	9880.622	*
29			9902.980 *	9908.146 *	9876.575 *	9882.180
30			9899.697 *	9904.335	9872.353 *	9877.484 *
31			9896.267	9900.414 *		9872.635 *
32			9892.752	9896.352 *		9867.712 *
33			9889.127 *	9892.183 *		9862.645 *
34			9885.330	9887.951		9857.434
35			9881.453 *			9852.193 *
36			9877.484 *			
37			9873.394 *			
38			9869.192 *			
39			9864.866 *			
40			9860.436 *			
41			9855.916 *			
42			9851.305 *			
43			*			
44			9841.669 *			
45			9836.739			

Appendix II (cont.) -- $^5\Pi_2$ - $X^5\Delta_3$ (2,2)

J	R		Q		P	
	aa	bb	ab	ba	aa	bb
3			9940.906		9938.233	
4			9940.443 *		9936.867	
5	9945.213 *		9939.844 *		9935.389	
6	9945.429 *		9939.150 *		9933.782	
7	9945.478		9938.321		9932.051	
8	9945.429 *		9937.380 *		9930.216	
9	9945.283 *		9936.321		9928.264 *	
10	9944.997 *		9935.147		9926.203	
11	9944.621 *		9933.861		9923.992	
12	9944.118		9932.463		9921.718	
13	9943.541		9930.966		9919.283 *	
14	9942.881 *		9929.382		9916.798	
15			9927.666 *		9914.199	
16					9911.501	

19		9918.163		9900.930		
20		9915.983	9916.064 *	9897.924		
21		9913.602	9913.651 *	9894.729 *	9894.813	
22		9911.044 *	9911.121	9891.351	9891.410 *	
23		9908.372	9908.447	9887.798	9887.864 *	
24		9905.562	9905.651 *	9884.105	9884.175 *	
25		9902.618	9902.720 *	9880.269	9880.374	
26		9899.563	9899.697 *	9876.326 *	9876.453	
27		9896.393 *	9896.611 *	9872.270	9872.431	
28		9893.101	9893.461 *	9868.090	9868.313	
29		9889.826		9863.815 *	9864.155 *	

$^5\Pi_3$ - $X^5\Delta_4$ (2,2)

J	R	Q	P
4		9925.693	9922.114
5		9925.100 *	9920.651
6		9924.422	9919.089 *
7		9923.625	9917.384
8		9922.686	9915.572
9	9930.614 *	9921.667	9913.651
10	9930.339	9920.527	9911.617 *
11	9929.965 *	9919.283 *	9909.461
12	9929.456 *	9917.868	9907.195 *
13	9928.869	9916.390	9904.795 *
14	9928.160 *	9914.782	9902.303
15	*	9913.064	9899.697 *
16	9926.368	9911.225 *	9896.972

Appendix II -- $^5\Pi_3$ - $X^5\Delta_4$ (2,2) (cont.)

J	R		Q		P	
	aa	bb	ab	ba	aa	bb
17	9925.289 *		9909.275		9894.125	
18	9924.130		9907.195 *		9891.168	
19	9922.829		9905.011		9888.095	
20	9921.409 *		9902.720		9884.901 *	
21	9919.886		9900.299		9881.599	
22	9918.245 *		9897.759		9878.160	
23	9916.469		9895.111		9874.622	
24	9914.589		9892.345		9870.990	
25	9912.595		9889.459		9867.223 *	
26	9910.465 *		9886.459 *		9863.344 *	
27	9908.235 *		9883.317 *		9859.333	
28	9905.851 *	9905.892 *	9880.121 *		9855.189	
29	9903.354	9903.408	9876.716 *	9876.746 *	9850.966	
30	9900.738 *	9900.840 *	9873.232 *	9873.261	9846.583	9846.628 *
31	9897.985 *	9898.102 *	9869.625 *	9869.693	9842.110 *	9842.151 *
32	9895.111 *	9895.273	9865.849	9865.974	9837.459 *	9837.559
33	9891.984 *	9892.345 *	9861.936	9862.141	9832.725	9832.831 *
34	9888.653 *	9889.263 *	9857.849 *	9858.186	9827.815	9828.022 *
35	9885.014 *	9886.078 *	9853.536	9854.126	9822.738	9823.078 *
36			9848.916	9849.966 *	9817.424	9818.001
37					9811.792 *	9812.864

$^5\Pi_{-1}$ - $X^5\Delta_0$ (2,3)

J	R		Q		P	
	aa	bb	ab	ba	aa	bb
0			-	-	-	-
1					-	-
2						
3						
4						
5						
6						
7						
8				9079.940 *		
9			9078.544 *	9078.956 *		9070.393 *
10			9077.415 *	9077.887 *	9068.706 *	*
11			9076.217 *	9076.685 *	9066.569 *	9066.297 *
12			9074.888	9075.379 *	9064.335 *	9064.065 *
13			9073.438 *	9073.935 *	9062.013 *	9061.711 *
14			9071.883 *	9072.464 *	9059.512 *	9059.282 *
15			9070.235 *	9070.803 *	9056.883 *	9056.778 *
16			9068.459 *	*	9054.284 *	9054.080 *
17			9066.569 *	9067.171	9051.471 *	9051.298 *

Appendix II -- $^5\Pi_{-1}$ - $X^5\Delta_0$ (2,3) (cont.)

J	R		Q		P	
	aa	bb	ab	ba	aa	bb
18			9064.565 *	9065.197 *	9048.544 *	9048.454 *
19			9062.468 *	9063.103 *	9045.543 *	9045.436 *
20			9060.229 *	9060.908 *	9042.405 *	9042.340 *
21			9057.853 *	9058.589 *	9039.159 *	9039.122 *
22			*	9056.184 *	9035.815 *	9035.717 *
23			9052.839 *	9053.622 *	9032.342 *	9032.342 *
24			9050.176	*	9028.748 *	*
25			9047.379 *	9048.212 *	9025.040 *	9025.134 *
26			9044.429 *	9045.320 *	9021.200 *	9021.332
27			9041.287 *	9042.340 *	9017.275 *	9017.455 *
28				9039.237	9013.157 *	9013.423 *
29				9036.018 *		
30				9032.685 *		
31				9029.239 *		
32				9025.660 *		
33				9022.005 *		
34				9018.173		
35				9014.264		
36				9010.212 *		
37				9006.078 *		
38				9001.818		
39				8997.426 *		
40				8992.923 *		
41				8988.323 *		
42				8983.583		
43				8978.737 *		
44				8973.748 *		

$^5\Pi_0$ - $X^5\Delta_1$ (2,3)

J	R		Q		P	
	aa	bb	ab	ba	aa	bb
1						
2						
3						
4						
5						
6						
7						
8					9085.000 *	
9					9083.312 *	
10					9081.493 *	
11					9079.616 *	
12					9077.607 *	

Appendix II -- $^5\Pi_0$ - $X^5\Delta_1$ (2,3) (cont.)

J	R		Q		P	
	aa	bb	ab	ba	aa	bb
13					9075.586 *	
14					9073.305 *	
15			9084.837 *		9071.023 *	9082.903 *
16			9083.348 *		9068.601 *	9080.116 *
17			9081.742 *		9066.098 *	9077.211 *
18			9080.027 *		9063.480 *	*
19			9078.159 *		9060.735 *	9071.023 *
20			9076.247 *		9057.853 *	9067.760 *
21			9074.240 *	9083.193	9054.921 *	9064.335 *
22			9072.064 *	9080.576	9051.898 *	9060.854
23			9069.763 *	9077.805 *	9048.717 *	9057.227 *
24			9067.386 *	9074.995 *	9045.436 *	9053.467
25			9064.842 *	9072.022 *	9042.011 *	9049.608 *
26			9062.268 *	9068.930 *	9038.492 *	*
27	9085.091 *		9059.512 *	9065.730 *	9034.903 *	9041.532 *
28	9083.193 *		9056.697 *	9062.371	9031.194	9037.278 *
29	9081.090 *		9053.748 *	9058.943 *	9027.297 *	9032.959 *
30	9078.956 *		9050.679 *	9055.329 *	9023.367 *	9028.480 *
31	9076.685 *		9047.530 *	9051.641 *	9019.294 *	9023.886 *
32	9074.339 *		9044.253	9047.859 *	9015.122	9019.215 *
33	9071.823 *		9040.843 *	9043.919 *	9010.830 *	9014.394 *
34	9069.221 *		9037.341		9006.440 *	9009.503 *
35	9066.542 *		9033.740 *		9001.937	9004.483 *
36	9063.728 *		9030.040 *		8997.317 *	
37	9060.735 *		9026.244 *		8992.617 *	
38	*		9022.356 *		8987.835 *	
39	9054.668 *		9018.311 *		8982.898	
40	9051.471 *		9014.205 *		8977.874 *	
41	9048.166		9009.961 *		8972.788	
42	9044.757		9005.673 *		8967.556 *	
43	9041.287 *		9001.281 *		8962.249 *	
44	9037.685 *		8996.780 *		8956.849 *	
45			8992.167 *		8951.368 *	
46					8945.753	

$^5\Pi_2$ - $X^5\Delta_3$ (2,3)

J	R	Q	P
3			
4			9084.246 *
5			*
6			9081.266 *
7			9079.616 *

Appendix II -- $^5\Pi_2$ - $X^5\Delta_3$ (2,3) (cont.)

J	R		Q		P	
	aa	bb	ab	ba	aa	bb
8			9085.000 *		9077.805 *	
9			9083.975 *		9075.931 *	
10			9082.903 *		9073.935 *	
11			9081.694		9071.823 *	
12			9080.385		9069.636 *	
13			9078.956 *		9067.318 *	
14			9077.503 *		9064.936 *	
15			9075.931 *		9062.447 *	
16					9059.860 *	
17						
18			9068.760 *			
19			9066.946 *			
20			9064.842 *	9064.963 *		
21			9062.676	9062.748 *		
22			9060.294	9060.365 *		
23			*	*		
24						
25			9052.403	9052.513 *		

$^5\Pi_3$ - $X^5\Delta_4$ (2,3)

J	R	Q	P
4		9073.006 *	9069.442 *
5		9072.464 *	9068.025 *
6		9071.823 *	9066.501 *
7	9078.258 *	9071.101 *	9064.842 *
8	9078.258 *	9070.235 *	9063.103
9	9078.159 *	9069.273 *	9061.220 *
10	9078.033 *	9068.190 *	9059.282 *
11	9077.698 *	9067.006 *	9057.227 *
12	9077.305 *	9065.730 *	9055.034 *
13	9076.877 *	9064.335	9052.757 *
14	9076.217 *	9062.832	9050.348 *
15	9075.473	9061.220 *	9047.859 *
16	9074.618 *	9059.512 *	9045.240 *
17	9073.727 *	9057.672	9042.546 *
18	9072.666 *	9055.745 *	*
19	9071.514 *	9053.710 *	9036.792
20	9070.235 *	9051.553	9033.740 *
21	9068.882 *	9049.294 *	9030.594
22	9067.386 *	9046.927 *	9027.297 *
23	9065.795 *	9044.429 *	9023.984 *
24	9064.105 *	9041.845 *	9020.480 *

Appendix II -- $^5\Pi_3$ - $X^5\Delta_4$ (2,3) (cont.)

J	R		Q		P	
	aa	bb	ab	ba	aa	bb
25	9062.268 *		9039.159		9016.927 *	
26	9060.365 *		9036.354		9013.212	
27	9058.324 *		9033.443 *		9009.415 *	
28			9030.407		9005.519 *	
29			9027.241 *	9027.297 *	9001.509 *	
30			9023.984 *	9024.030 *	8997.317 *	8997.371 *
31			9020.651 *	9020.651 *	8993.092 *	8993.140
32			9017.076 *	9017.185 *		
33			9013.423 *	9013.597 *		
34			9009.610 *	9009.925 *		
35			9005.519 *	9006.078 *		
36			9001.160 *	9002.249		

$^5\Pi_2$ - $X^5\Delta_3$ (3,0)

J	R	Q	P
3		12347.873	12345.193
4		12347.316 *	12343.767 *
5		12346.621	12342.178
6		12345.821	12340.471
7		12344.868	12338.626
8		12343.767	12336.659
9		12342.551	12334.532
10		12341.190	12332.282
11		12339.701	12329.895
12		12338.071	12327.368
13		12336.305	12324.728
14		12334.406	12321.910
15		12332.377	12319.002 *
16		12330.204	12315.946
17		12327.909	12312.742
18		12325.474	12309.427
19		12322.914	12305.988 *
20		12320.242	12302.392
21	12337.049	12317.416	12298.643 *
22	12335.007	12314.465	12294.835
23	12332.824	12311.395	12290.859
24	12330.500	12308.195	12286.759
25	12328.072 *	12304.844	12282.543
26	12325.535	12301.409	12278.186
27	12322.874 *	12297.848	12273.703
28	12320.095	12294.153	12269.121
29	12317.190	12290.351	12264.417 *

Appendix II -- $^5\Pi_2$ - $X^5\Delta_3$ (3,0) (cont.)

J	R	Q	P
30	12314.205 *	12286.431	12259.586
31	12311.108	12282.422	*
32	12307.903 *	12278.300	12249.629 *
33	12304.630	12274.094	12244.481 *
34		12269.803	12239.266 *
35			12233.955 *

$^5\Pi_3$ - $X^5\Delta_4$ (3,0)

J	R	Q	P
4		12337.132	12333.564 *
5		12336.471 *	12332.028 *
6		12335.679 *	12330.331 *
7		12334.745	12328.526
8		12333.684 *	12326.570 *
9		12332.486	12324.486
10		12331.168	12322.284
11		12329.708	12319.927
12		12328.122	12317.458
13		12326.404	12314.836 *
14		12324.558	12312.105
15		12322.566	12309.235
16		12320.457	12306.233
17	12334.191 *	12318.208	12303.095
18	12332.686 *	12315.830	12299.828
19	12331.090	12313.318	12296.427
20	12329.340 *	12310.678 *	12292.900
21	12327.455	12307.903 *	12289.245
22	12325.474 *	12305.011	12285.462
23	12323.300	12301.981	12281.537
24	12321.052 *	12298.822	12277.494
25	12318.637 *	12295.535	12273.320
26	12316.115	12292.120	12269.013 *
27	12313.501 *	12288.588	12264.586
28	12310.678 *	12284.914	12260.025
29	12307.783	12281.132	12255.351
30		12277.205	12250.556 *
31			12245.612 *

APPENDIX III

Line Frequencies for the $^5\Phi - X^5\Delta$ System (cm^{-1})

The parities are labelled where appropriate, with the first letter being the parity of the upper level and the second letter that of the lower level.

Appendix III -- $^5\Phi_1 - X^5\Delta_0$ (0.0)

J	R		Q		P	
	aa	bb	ab	ba	aa	bb
0			-	-	-	-
1					-	-
2	10064.458 *				10059.857 *	
3	10065.044		10061.011 *		10058.572	
4	10065.477	10065.155 *	10060.535 *	10060.882 *	10057.154	
5	10065.789	10065.477 *	10059.929	10060.256	10055.644 *	10055.319 *
6	10065.991 *	10065.678	10059.202	10059.525	10053.973	10053.668
7	10066.072	10065.760	10058.371	10058.676	10052.215 *	
8	10066.019 *	10065.719 *	10057.399	10057.704	10050.320 *	
9	10065.859	10065.555	10056.313 *	10056.615 *	10048.313	10047.989 *
10	10065.555	10065.250	10055.100	10055.421	10046.192 *	10045.868 *
11	10065.155	10064.844	10053.754	10054.072 *	*	10043.609 *
12	10064.601 *	10064.299	10052.303	10052.624	10041.543	10041.213 *
13	10063.950 *	10063.639	10050.697	10051.036	10039.045	10038.735
14	10063.150	10062.848	10049.015	10049.326	10036.416 *	10036.101 *
15	10062.238 *	10061.927 *	10047.159	10047.494	10033.668	10033.334
16	10061.193	10060.882 *	10045.200	10045.533	10030.777 *	10030.477
17	10060.026	10059.711	10043.134	10043.446	10027.776	10027.472
18	10058.725	10058.419	10040.917	10041.213 *	10024.642	10024.337
19	10057.297	10056.992	10038.559	10038.888	10021.391	10021.087 *
20	10055.736	10055.421 *	10036.101 *	10036.416 *	10017.997	10017.696
21	10054.072 *	10053.754 *	10033.501	10033.826	10014.479	10014.173
22	10052.215 *	10051.921	10030.777 *	10031.089	10010.859	10010.545
23	10050.267	10049.949	10027.906	10028.225	10007.086	10006.773
24	10048.179	10047.882	10024.923	10025.231	10003.183	10002.880
25	10045.958	10045.668	10021.798	10022.112	9999.135 *	9998.842
26	10043.609	10043.281 *	10018.536	10018.850	9994.984	9994.686
27	10041.116	10040.804	10015.145	10015.439	9990.687	9990.388
28	10038.498	10038.197	10011.621	10011.934	9986.255	9985.936 *
29	10035.733	10035.435	10007.961	10008.274	9981.687	9981.395
30	10032.842	10032.555 *	10004.160	10004.465	9976.994	9976.696
31	10029.817	10029.512	10000.227	10000.540	9972.154	9971.868
32	10026.635	10026.349	9996.163	9996.473	9967.170 *	9966.904
33	10023.337	10023.041	9991.965	9992.268	9962.067	9961.792
34	10019.887	10019.604	9987.612	9987.929	9956.841	9956.548
35	10016.297	10016.024	9983.148	9983.450	9951.475	9951.167
36	10012.588	10012.302	9978.527	9978.840	9945.942	9945.675
37	10008.723	10008.447	9973.774	9974.074	9940.315	9940.021
38	10004.714	10004.465 *	9968.890	9969.188	9934.533	9934.243
39	10000.591	10000.313 *	9963.854	9964.156	9928.596	9928.292 *
40	9996.310	9996.048 *	9958.698	9958.989	9922.543	9922.250
41	9991.887	9991.612	9953.379	9953.688	9916.343	9916.064
42	9987.338	9987.062	9947.938	9948.235	9910.008	9909.729
43	9982.638	9982.372	9942.352	9942.657	9903.532	9903.239 *
44	9977.804	9977.521 *	9936.645 *	9936.940	*	9896.638

Appendix III -- $^5\Phi_1 - X^5\Delta_0$ (0,0) (cont.)

J	R		Q		P	
	aa	bb	ab	ba	aa	bb
45	9972.853	9972.585	9930.788	9931.082	9890.180	9889.909
46	9967.724 *	*	9924.792	9925.100	*	9883.034
47	9962.519 ?		9918.676	9918.957 *	9876.281	9876.015
48			9912.425 *	9912.734 *	9869.136	9868.881
49			9906.071 *	*		
50			*	9899.938		
51			9893.174 *	9893.461 *		
52			9886.787 *	9887.069		

$^5\Phi_2 - X^5\Delta_1$ (0,0)

J	R	Q	P
1	10142.907	-	-
2	10143.577 *	10140.818 *	-
3	10144.109 *	10140.466	10137.733 *?
4	10144.583	10139.966	10136.318 *
5	10144.901	10139.389	10134.778 *
6	10145.119 *	10138.664	10133.135 *
7	10145.182 *	10137.822 *	10131.387
8	10145.119 *	10136.860	10129.518 *
9	10144.983 *	10135.779	10127.507 *
10	10144.692 *	10134.584	10125.396 *
11	10144.294	10133.263	10123.151
12	10143.773	10131.819	10120.783 *
13	10143.138	10130.250	10118.317 *
14	10142.387 *	10128.594	10115.743 *
15	10141.533	10126.807	10112.980 *
16	10140.560	10124.905	10110.191
17	10139.470	10122.892	10107.253 *
18	10138.287 *	10120.783	10104.183 *
19	10136.992 *	10118.552	10101.052
20	10135.596	10116.225	10097.791
21	10134.111	10113.802 *	10094.422 *
22	10132.541	10111.271	10090.957
23	10130.875 *	10108.664 *	10087.402
24	10129.166 *	10105.980	10083.754
25	10127.364	10103.218 *	10080.029
26	10125.516 *	10100.386	10076.240
27	10123.638 *	10097.516 *	10072.383 *
28	10121.748 *	10094.614 *	10068.482 *
29	10119.873 *	10091.676	10064.544 *
30	10117.969	10088.736	10060.575 *
31	10116.127 *	10085.841 *	10056.615 *

Appendix III -- $^5\Phi_2$ - $X\,^5\Delta_1$ (0,0) (cont.)

J	R		Q		P	
	aa	bb	ab	ba	aa	bb
32	10114.348 *		10082.955		10052.662 *	
33	10112.674 *		10080.157 *		10048.764 *	
34			10077.444 *		10044.926 *	
35					10041.184 *	
14			10043.497 *			
15			10043.225 *			
16			10042.931 *			
17			10042.594 *			
18			10042.252 *			
19			10041.874			
20			10041.447 *			
21			10040.985 *			
22			10040.474 *			
23			10039.927 *			
24			10039.317			
25			10038.626 *			
26			10037.881 *			
27			10037.034 *			
28			10036.101 *			
29			10035.033 *			
30			10033.826 *			
31			10032.454 *			
32			10030.927 *			
33			10029.183 *			
34			10027.189 *			
35			10024.923 *			
36			10022.404 *			
37			10019.662 *			
38			10016.448 *	10016.485 *		
39			10013.019 *			
40			10009.205 *	10009.246 *		
41			10005.103 *	10005.149 *		
42			10000.727 *	10000.768 *		
43			9996.048 *	9996.092 *		
44			9991.139 *			
45			9985.908 *	9985.949 *		
46			9980.465 *	9980.505 *		
47			9974.783 *	9974.830 *		
48			9968.890 *	9968.930 *		
49			9962.795 *	9962.838 *		
50			9956.491 *	9956.548 *		
51			9949.982 *	9950.050 *		
52			9943.306 *	9943.369 *		

Appendix III -- $^5\Phi_2$ - $X^5\Delta_1$ (0,0) (cont.)

J	R		Q		P	
	aa	bb	ab	ba	aa	bb
53			9936.442 *	9936.492 *		
54			9929.382 *	9929.456 *		
55			9922.167 *	9922.250 *		
56			9914.782 *	9914.858		
57			9907.195 *	9907.301		
58			9899.523 *	9899.563 *		
59			9891.626 *	9891.696 *		
60			9883.581 *	9883.666 *		
61			9875.392 *	9875.423 *		
62			9867.022 *	9867.091 *		
63			9858.496 *	9858.576 *		
64			9849.821 *	9849.902 *		
65			9840.966 *	9841.079 *		
66			9832.006 *	9832.095 *		
67			9822.847 *	9822.941 *		
68			9813.547 *	9813.640 *		
69			9804.149 *	9804.235 *		

$^5\Phi_1$ - $X^5\Delta_2$ (0,0)

J	R	Q	P
2	10197.380	-	-
3	10197.872	10194.275	-
4	10198.226	10193.705 *	
5	10198.439	10193.038	
6	10198.521	10192.239	
7	10198.480	10191.287	10185.008 *
8	10198.264 *	10190.204	10183.017
9	10197.945 *	10188.991 *	10180.898
10	*	10187.625	10178.645
11	10196.911	10186.139	10176.276 *
12	10196.168	10184.510	10173.732
13	10195.326	10182.756	10171.080
14	10194.328	10180.863	10168.291
15	10193.199	10178.834	10165.365
16	10191.935	10176.673	10162.284
17	10190.538	10174.371	10159.105
18	10188.991 *	10171.954	10155.784
19	10187.343	10169.382	10152.327
20	10185.544	10166.684	10148.737
21	10183.613	10163.854	10144.983 *
22	10181.549 *	10160.897	10141.141
23	10179.347	10157.799	10137.152

Appendix III -- $^5\Phi_3$ - $X^5\Delta_2$ (0,0) (cont.)

J	R		Q		P	
24	10177.015		10154.572		10133.013	
25	10174.550		10151.217		10128.792	*
26	10171.954	*	10147.732		10124.372	
27	10169.235		10144.109		10119.873	
28	10166.387	*	10140.334	*	10115.223	*
29	10163.392		10136.469		10110.437	*
30	10160.267	*	10132.458		10105.529	
31	10157.025		10128.310		10100.495	
32	10153.651		10124.037		10095.324	
33	10150.151		10119.644		10090.032	
34	10146.515		10115.109		10084.603	
35	10142.768		10110.437	*	10079.051	
36	10138.893		10105.689		10073.379	
37	10134.916		10100.797		10067.584	
38		*	10095.792		10061.675	
39	10126.648		10090.686		10055.644	
40	10122.384	*	10085.485		10049.518	*
41	10118.071		10080.201		10043.281	*
42	10113.756	*	10074.852		10036.993	*
43		*	10069.529		10030.650	
44	10105.323		10064.240		10024.296	*
45	10101.416		10059.073		10017.997	*
46	10097.791	*	10054.124	*	10011.798	
47	10094.229		10049.518	*	10005.848	
48			10044.899	*	10000.227	*
49					9994.602	*?
44	10089.149	*				
45	10086.127	*	10042.885	*		
46	10082.573		10038.856	*	9995.606	*
47	10078.473	*	10034.290	*	9990.567	*
48	10073.883	*	10029.183	*	9984.984	*
49	10068.833	*	10023.554		9978.87	*
50	10063.454		10017.510		9972.237	*
51	10057.795		10011.117		9965.171	
52	10051.921	*	10004.465	*	9957.771	
53	10045.868	*	9997.560	*	9950.091	*
54	10039.623		9990.488		9942.189	*
55	10033.255		9983.258	*	9934.126	*
56	10026.762		9975.878	*	9925.837	*
57	10020.192		9968.384	*	9917.486	*
58	10013.600	*	9960.787	*	9908.947	*
59	10006.991	*	9953.196	*	9900.414	*
60	10000.437	*?	9945.600	*	9891.742	*

$^5\Phi_3$ - $X^5\Delta_2$ (0,0) (cont.)

J	R		Q		P	
61		*	9938.075	*?	9883.162	*
62			9930.788	*?		?
63					9866.385	*?

$^5\Phi_4$ - $X^5\Delta_2$ (0,0)

J	R		Q		P	
3	10249.463		-		-	
4	10249.815		10245.353		-	
5	10250.062	*	10244.680			
6	10250.113		10243.873			
7	10250.062	*	10242.924		10236.675	
8	10249.882		10241.845		10234.712	
9	10249.558		10240.629		10232.603	
10	10249.108		10239.265		10230.350	*
11	10248.508		10237.782		10227.985	
12	10247.786		10236.180	*	10225.471	
13	10246.916		10234.423	*	10222.824	
14	10245.926		10232.536		10220.041	*
15	10244.790		10230.515		10217.111	
16	10243.527	*	10228.357		10214.075	
17	10242.102	*	10226.054		10210.901	
18	10240.558		10223.632		10207.558	
19	10238.903		10221.063		10204.102	
20	10237.091		10218.367		10200.529	
21	10235.143		10215.529		10196.797	*
22	10233.060		10212.557		10192.970	*
23	10230.843		10209.455		10188.991	*
24	10228.489		10206.213		10184.819	
25	10226.001		10202.834		10180.562	
26	10223.376		10199.320		10176.155	
27	10220.595		10195.673		10171.606	
28	10217.713	*	10191.892		10166.956	
29	10214.688		10187.979		10162.134	
30	10211.522		10183.924		10157.214	
31	10208.227		10179.745		10152.143	
32	10204.796		10175.420		10146.921	*
33	10201.235		10170.973		10141.628	*
34	10197.529	*	10166.387	*	10136.132	
35	10193.705	*	10161.685		10130.539	
36	10189.779		10156.845		10124.807	
37	10185.721		10151.892		10118.956	

Appendix III -- $^5\Phi_4$ - $X^5\Delta_3$ (0,0) (cont.)

J	R		Q		P	
38	10181.549	*	10146.816		10112.980	*
39	10177.313		10141.628	*	10106.898	
40	10173.024		10136.371		10100.696	
41	10168.781		10131.070		10094.422	*
42	10164.833		10125.821		10088.100	*
43	10161.738	*	10120.853		10081.835	
44			10116.742	*	10075.861	
45					10070.751	*
43	10152.041					
44	10149.226	*	10107.031	*		
45	10145.119		10103.218	*	10061.018	*
46		*	10098.105		10056.215	
47	10135.157		10092.291	*	10050.078	
48	10129.758		10086.127	*	10043.281	*
49	10124.188		10079.692	*	10036.101	*
50	10118.489	*	10073.144		10028.668	
51	10112.674	*	10066.431		10021.087	*
52	10106.809	*	10059.607	*	10013.369	*
53	10100.951	*	10052.725	*	10005.544	*
54	10095.165	*	10045.868	*		*
55			10039.091	*	9989.805	*
56					9982.028	*

$^5\Phi_5$ - $X^5\Delta_4$ (0,0)

J	R	Q	P
4	10289.849	-	-
5	10290.072	10284.742	-
6	10290.171	10283.946	
7	10290.117	10283.013	
8	10289.954	10281.942 *	
9	10289.629	10280.762	10272.754
10	10289.215	10279.431	10270.538
11	10288.642	10277.972	10268.180
12	10287.929	10276.380 *	*
13	10287.094	10274.655	10263.099 *
14	10286.121	10272.803	10260.365
15	10285.002	10270.808	10257.479
16	10283.784	10268.682	10254.469
17	10282.406	10266.429	10251.323

$^5\Phi_5$ - $X^5\Delta_4$ (0,0) (cont.)

J	R		Q		P	
18	10280.898		10264.027	*	10248.048	
19	10279.266		10261.504		10244.638	
20	10277.482		10258.852		10241.093	
21	10275.575		10256.055		10237.420	
22	10273.536		10253.126		10233.604	
23	10271.353		10250.062	*	10229.644	
24	10269.040		10246.868		10225.580	
25	10266.592		10243.527		10221.364	
26	10264.027	*	10240.073		10217.023	
27	10261.285		10236.465		10212.557	*
28	10258.428		10232.737		10207.915	
29	10255.435		10228.858		10203.170	
30	10252.307		10224.854		10198.264	*
31	10249.032		10220.707		10193.261	
32	10245.631		10216.425		10188.085	
33	10242.102	*	10212.015		10182.791	
34	10238.411		10207.454		10177.373	
35	10234.599		10202.766		10171.810	
36	10230.644		10197.945	*	10166.107	
37	10226.546		10192.970		10160.267	*
38	10222.312		10187.867		10154.295	
39	10217.975	*	10182.624		10148.179	
40	10213.438		10177.242		10141.931	*
41	10208.783		10171.724		10135.517	
42	10203.999		10166.067		10129.002	
43	10199.058		10160.267		10122.335	
44	10193.996		10154.325		10115.532	
45	10188.788		10148.252		10108.593	
46	10183.404		10142.035		10101.503	
47	10177.925		10135.669		10094.279	
48	10172.291		10129.166		10086.918	
49	10166.504		10122.532		10079.397	
50	10160.576		10115.743		10071.768	
51	10154.518		10108.823		10063.977	*
52	10148.302		10101.750		10056.055	
53	10141.931	*	10094.542		10047.989	
54	10135.440		10087.189		10039.774	
55	10128.792		10079.692		10031.427	
56	10122.007		10072.040		10022.927	
57	10115.076		10064.240		10014.289	
58	10107.989		10056.313		10005.507	*
59	10100.760		10048.241		9996.572	
60	10093.386		10040.022		9987.505	*
61	10085.841		10031.647		9978.287	*
62	10078.187		10023.113			*

Appendix III -- $^5\Phi_5$ - $X^5\Delta_4$ (0,0) (cont.)

J	R	Q	P
63	10070.357	10014.479	9959.414 *
64	10062.408	10005.641	9949.764
65	10054.263	9996.704	9939.968 *
66	10046.004	9987.612 *	9930.033 *
67	10037.581 *	9978.328	9919.921
68	10029.012	9968.890 *	9909.688 *
69	10020.295 *	9959.372	9899.301
70	10011.417	9949.676 *	9888.733 *
71	10002.337 *	9939.817 *	9878.070 *
72	9993.208 *	9929.801	9867.223 *
73	9983.886	9919.651	9856.238
74	9974.392	9909.321 *	9845.119
75	9964.762 ?	9898.869 *	
76		9838.261 ?	
77		9877.484 ?	
78		9866.551 ?	
79		9855.465 *?	
80		9844.221 ?	
81		9832.831 ?	
82		9821.297 *?	

$^5\Phi_1$ - $X^5\Delta_0$ (0,1)

J	R		Q		P	
	aa	bb	ab	ba	aa	bb
0		9191.561	-	-	-	-
1	9192.703	9192.363 *		9190.845 *	-	-
2	9193.397 *	9193.048 *		9190.621		
3	9193.991 *	9193.646 *		9190.285 *	*	
4	9194.466 *	9194.128 *		9189.838 *	9186.138	
5	9194.825 *	9194.466 *	9188.933 *	9189.278 *	9184.652 *	9184.307
6	9195.071	9194.718 *	9188.257	9188.601	9183.097 *	9182.729 *
7	9195.207 *	9194.875 *	9187.476 *	9187.804	9181.314 *	9181.004 *
8	9195.207 *	9194.875 *	9186.571	9186.900	9179.491	9179.171
9	9195.125 *	9194.781	9185.541	9185.885	9177.564	9177.240
10	9194.875 *	9194.573 *	9184.430 *	9184.753 *	9175.490 *	9175.169 *
11	9194.573	9194.245	9183.168 *	9183.502	9173.345	9172.978 *
12	9194.128	9193.797 *	9181.797	9182.135	9171.061	9170.722
13	9193.564	9193.219 *	9180.318	9180.653	9168.662	9168.305
14	9192.886	9192.541	9178.729	9179.063	9166.143	9165.804
15	9192.089	9191.754	9176.987	9177.345	9163.508	9163.209 *
16	9191.153	9190.845	9175.169 *	9175.490 *	9160.751 *	9160.423
17	9190.130	9189.838 *	9173.213	9173.548 *	9157.883	9157.547

Appendix III -- $^5\Phi_1 - X^5\Delta_0$ (0,1) (cont.)

J	R		Q		P	
	aa	bb	ab	ba	aa	bb
18	9188.966 *	9188.639	9171.141	9171.462	9154.892	9154.564
19	9187.687	9187.360	9168.931	9169.288	9151.790	9151.461
20	9186.288	9185.950	9166.618	9166.967	9148.561	9148.229
21	9184.753 *	9184.430 *	9164.204	9164.532	9145.216	9144.882
22	9183.097 *	9182.783 *	9161.644	9161.973	9141.734	9141.414
23	9181.314 *	9181.004 *	9158.959	9159.290	9138.141	9137.827
24	9179.431	9179.108 *	9156.141	9156.466	9134.425	9134.112
25	9177.406	9177.086	9153.218	9153.557	9130.595	9130.277
26	9175.259	9174.914 *	9150.164 *	9150.496	9126.627	9126.317
27	9172.978 *	9172.664	9146.968	9147.315	9122.537	9122.226
28	9170.572	9170.258	9143.681	9144.008	9118.325	9118.013
29	9168.038	9167.725	9140.246	9140.558	9113.994	9113.679
30	9165.381	9165.074	9136.678 *	9137.009	9109.530	9109.220
31	9162.594	9162.274	9132.990 *	9133.305	9104.939	9104.629
32	9159.667	9159.366	9129.177	9129.507 *	9100.224	9099.913
33	9156.602	9156.318	9125.232	9125.563	9095.372	9095.053
34	9153.438	9153.138	9121.155	9121.482	9090.404	9090.099
35	9150.123	9149.828	9116.952	9117.277	9085.281	9085.000
36	9146.691	9146.392	9112.622	9112.961	9080.068	9079.769
37	9143.103	9142.821	9108.157	9108.481	9074.712	9074.413
38	9139.413	9139.117	9103.563	9103.890	9069.221	9068.930
39	9135.564	9135.289	9098.841	9099.162	9063.597	9063.291
40	9131.615	9131.326	9093.964	9094.304	9057.853	9057.559
41	9127.525	9127.230	9088.996	9089.315	9051.976	9051.683
42	9123.276	9123.008	9083.889	9084.198	9045.972	9045.675
43	9118.936	9118.635	9078.630	9078.956	9039.824	9039.538
44	9114.447	9114.170	9073.255	9073.577	9033.567 *	9033.273
45	9109.809 *	9109.530 *	9067.760	9068.069	9027.161	9026.881
46	9105.102	9104.827	9062.125	9062.447	9020.651	9020.360
47	9100.224 *	9099.979	9056.381	9056.697	9013.991	9013.718
48	9095.288 *	9095.024 *	9050.514	9050.830	9007.230	9006.959
49	9090.261	9089.992	9044.546	9044.855	9000.343	9000.054
50	9085.185 *	9084.918	9038.492	9038.802	8993.367	8993.092
51	9080.222	9079.940 *	9032.412	9032.721	8986.300 *	8986.032 *
52	9075.661 *?	9075.379 *?	9026.430	9026.737 *	8979.200 *	8978.926 *
53			9020.880 *?	9021.200 *?	8972.206	8971.926 *
54					8965.651 *?	8965.387 *?

Appendix III (cont.) -- $^5\Phi_2$ - $X\,^5\Delta_1$ (0,1)

J	R			Q			P		
	aa		bb	ab		ba	aa		bb
1	9271.798			-			-		
2	9272.511	*		9269.744	*		-		
3	9273.080			9269.412	*		9266.651	*	
4	9273.545			9268.959			9265.275	*	
5	9273.906			9268.383			9263.736	*	
6	9274.144			9267.714			9262.200		
7	9274.289	*		9266.927			9260.477	*	
8	9274.289	*		9266.024			9258.671	*	
9	9274.208			9265.010			9256.738		
10	9274.005	*		9263.891			9254.676	*	
11	9273.688			9262.637			9252.547		
12	9273.263			9261.307			9250.279	*	
13	9272.722			9259.854	*		9247.885		
14	9272.086			9258.289			9245.426	*	
15	9271.331	*		9256.622			9242.812	*	
16	9270.493			9254.842			9240.124		
17	9269.540	*		9252.970	*		9237.316		
18	9268.490			9250.993	*		9234.409		
19	9267.338			9248.906			9231.398	*	
20	9266.103			9246.733			9228.295		
21	9264.780			9244.467			9225.093	*	
22	9263.380			9242.114			9221.803		
23	9261.899			9239.678	*		9218.418		
24	9260.357			9237.184			9214.957		
25	9258.763			9234.608			9211.433		
26	9257.116				*		9207.840	*	
27	9255.456	*		9229.324			9204.193		
28	9253.771	*		9226.627			9200.498		
29	9252.097	*		9223.924	*		9196.785	*	
30	9250.445	*		9221.216	*		9193.048	*	
31	9248.849	*		9218.550	*		9189.324	*	
32	9247.333	*		9215.927	*		9185.648	*	
33	9245.900			9213.375	*		9181.976	*	
34				9210.922	*		9178.417	*	
35							9174.914	*	
14	9188.512								
15	9189.324	*		9173.049	*		9157.707	*	
16	9190.192			9172.861	*		9156.533	*	
17	9191.006			9172.664	*		9155.323		
18	9191.805	*		9172.455			9154.111	*	
19	9192.541	*					9152.867		
20	9193.295	*		9171.952			9151.605		
21	9193.991	*		9171.648			9150.314	*	

Appendix III -- $^5\Phi_7$ - $X^5\Delta_1$ (0,1) (cont.)

J	R				Q				P			
	aa		bb		ab		ba		aa		bb	
22	9194.635	*			9171.318				9148.987	*		
23	9195.207	*			9170.938				9147.619	*		
24	9195.778	*			9170.518	*			9146.223			
25	9196.253	*			9170.040				9144.767	*		
26	9196.642	*			9169.482				9143.255	*		
27	9196.949	*			9168.847				9141.686	*		
28	9197.100	*			9168.124				9140.023			
29	9197.176	*			9167.279				9138.269			
30	9197.100	*			9166.317	*			9136.413	*		
31	9196.812	*			9165.193	*			9134.425	*		
32	9196.344				9163.903	*			9132.256	*		
33	9195.648	*			9162.396	*			9129.956	*		
34	9194.718	*				*			9127.459	*		
35	9193.502	*			9158.696	*	9158.740	*	9124.703			
36	9191.935	*			9156.437	*	9156.466	*	9121.739	*	9121.696	*
37	9190.130	*			9153.906	*	9153.994	*	9118.445	*		
38	9187.994	*	9187.948	*	9151.049	*	9151.090	*	9114.892	*	9114.851	*
39	9185.541	*			9147.897	*	9147.932	*	9111.027	*	9111.000	*
40	9182.783	*	9182.729	*	9144.430	*	9144.462	*	9106.851	*	9106.822	*
41	9179.748	*	9179.677	*	9140.661		9140.695		9102.372	*	9102.332	*
42	9176.430	*	9176.387	*	9136.596	*	9136.637	*	9097.582	*	9097.541	*
43	9172.861	*	9172.771	*	9132.256	*	9132.296	*	9092.507	*	9092.460	*
44	9168.998	*	9168.931	*	9127.630	*	9127.693		9087.160		9087.118	*
45	9164.915	*	9164.874	*	9122.790		9122.844		9081.538	*	9081.493	*
46	9160.629	*	9160.566	*	9117.702		9117.755		9075.661	*	9075.632	*
47	9156.141	*	9156.070		9112.401	*	9112.442	*	9069.581		9069.528	*
48	9151.407		9151.356	*	9106.851		9106.924		9063.262	*	9063.203	
49	9146.490		9146.449	*	9101.127	*	9101.210		9056.697	*		
50	9141.360	*	9141.414	*	9095.235		9095.288	*	9049.995	*	9049.935	
51	9136.134		9136.073	*	9089.124		9089.190		9043.075		9043.004	*
52	9130.704	*	9130.595	*	9082.846		9082.903		9035.951	*	9035.902	
53	9125.070	*	9125.000	*	9076.387		9076.455		9028.677		9028.606	
54	9119.283		9119.222		9069.763		9069.827		9021.200	*	9021.159	*
55	9113.331		9113.272	*	9062.970		9063.036		9013.597	*	9013.518	
56	9107.225		9107.158		9056.023	*	9056.076	*	9005.793		9005.723	
57	9100.971	*	9100.923	*	9048.902		9048.981	*	8997.822		8997.758	
58	9094.522	*	9094.432	*	9041.627	*	9041.703		8989.728		8989.630	*
59	9087.957		9087.881		9034.201	*	9034.281		8981.453	*	8981.377	*
60	9081.236	*	9081.090	*	9026.622		9026.737	*	8973.014		8972.949	
61	9074.339	*	9074.240	*	9018.892		9018.968		8964.451		8964.364	*
62	9067.318	*	9067.221		9011.021	*	9011.077	*	8955.727		8955.638	
63	9060.126	*	9060.037		9002.973	*	9003.070		8946.850	*	8946.758	
64		*	9052.703		8994.800		8994.888		8937.830		8937.730	
65	9045.320	*	9045.240	*	8986.464		8986.541		8928.651	*	8928.558	*
66	9037.685		9037.594	*	8978.001		8978.091		8919.338		8919.242	*

Appendix III -- $^5\Phi_2$ - $X^5\Delta_1$ (0,1) (cont.)

J	R		Q		P	
	aa	bb	ab	ba	aa	bb
67	9029.913 *	9029.828 *	8969.373 *	8969.465		
68	9022.005 *	9021.921 *	8960.583 *	8960.706		
69	9013.919 *	9013.878 *	8951.674 *	8951.785 *		
70			8942.677 *	8942.787 *		
71			8933.495 *	8933.610		

$^5\Phi_3$ - $X^5\Delta_2$ (0,1)

J	R	Q	P
2		-	-
3	9326.775 *	9323.152 *	-
4	9327.154 *	9322.672 *	
5	9327.410 *	9322.020	
6	9327.539 *	9321.233	
7	9327.539 *	9320.352	9314.073
8	9327.410 *	9319.335	9312.146 *
9	9327.154 *	9318.177	9310.098
10	9326.775 *	9316.898	9307.920
11	9326.260	9315.494	9305.615
12	9325.631	9313.959	9303.183
13	9324.871	9312.312 *	9300.626
14	9323.981	9310.497	9297.940
15	9322.964	9308.601	9295.134
16	9321.824	9306.565	9292.193
17	9320.556	9304.394	9289.137
18	9319.166	9302.101	9285.939
19	9317.627	9299.700	9282.631
20	9315.994 *	9297.145 *	9279.170
21	9314.232	9294.478	9275.622
22	9312.312 *	9291.682	9271.917
23	9310.310	9288.771	9268.118
24	9308.164	9285.723	9264.180
25	9305.894	9282.558	9260.118
26	9303.499 *	9279.270	9255.931
27	9300.980 *	9275.854	9251.615
28	9298.333 *	9272.316	9247.180
29	9295.555	9268.653	9242.623
30	9292.689	9264.868	9237.943
31	9289.676	9260.962	9233.142
32	9286.545	9256.938	9228.212
33	9283.296	9252.790	9223.180
34	9279.926	9248.517	9218.014
35	9276.443	9244.133	9212.734 *

Appendix III -- $^5\Phi_3$ - $X^5\Delta_2$ (0.1) (cont.)

J	R	Q	P
36	9272.855 *	9239.644 *	9207.333
37	9269.152 *	9235.028	9201.818
38	9265.354	9230.321	9196.195
39	9261.453	9225.507	9190.474
40	9257.519	9220.612	9184.652 *
41	9253.526	9215.652	9178.729 *
42	9249.519	9210.639	9172.771
43	9245.526 *	9205.623	9166.744
44	9241.755 *	9200.671	9160.713 *
45	9238.185	9195.854	9154.753
46	9234.951	9191.271	9148.934
47	*	9187.05 *	9143.344
48		9182.783 *	9138.081
49			9132.831
44	9225.571		
45	9222.898 *	9179.677 *	
46	9219.711 *	9175.985	9132.743
47	9215.965 *	9171.787 *	9128.055
48	9211.733	9167.045	9122.844 *
49	9207.075	9161.792	9117.141 *
50	9202.079	9156.141 *	9110.854
51	9196.812 *	9150.123 *	9104.184
52	9191.328 *	9143.864	9097.182 *
53	9185.648 *	9137.378	9089.910
54	9179.853 *	9130.704	9082.410
55	9173.894	9123.888 *	9074.764
56	9167.860 *	9116.952 *	9066.946 *
57	9161.706	9109.876 *	9059.000 *
58	9155.553	9102.762	9050.906 *
59	9149.401 *	9095.597 *	9042.816
60	9143.344 *?	9088.479 *	9034.682
61	9137.537 ?	9081.403 ?	9026.560 *
62		9074.618 *?	9018.485 *?
63		9068.459 ?	9010.681 *?
64			9003.536 ?

$^5\Phi_4$ - $X^5\Delta_3$ (0.1)

J	R	Q	P
3	9378.330 *	-	-
4	9378.687 *	9374.244	-
5	9378.964 *	9373.603	9369.149 *
6	9379.084 *	9372.842	9367.489 *
7	9379.084 *	9371.944	9365.697 *
8	9378.964 *	9370.926	9363.779 *
9	9378.687	9369.782	9361.739 *
10	9378.330 *	9368.512	9359.573 *
11	9377.820 *	9367.108	9357.273 *
12	9377.179	9365.580	9354.840 *
13	9376.420	9363.926	9352.288 *
14	9375.524	9362.144	9349.646 *
15	9374.504	9360.230	9346.830
16	9373.355	9358.198	9343.921
17	9372.080	9356.030	9340.862
18	9370.677	9353.716	9337.675
19	9369.149 *	9351.310	9334.368
20	9367.489 *	9348.766	9330.926
21	9365.697 *	9346.068	9327.349 *
22	9363.779 *	9343.265	9323.668 *
23	9361.739 *	9340.353	9319.851 *
24	9359.573 *	9337.294	9315.906
25	9357.273 *	9334.104	9311.829
26	9354.840 *	9330.793	9307.628
27	9352.288 *	9327.349 *	9303.297
28	9349.599 *	9323.779	9298.838 *
29	9346.796	9320.063	9294.260 *
30	9343.836	9316.256	9289.544
31	9340.789	9312.312 *	9284.710
32	9337.605	9308.232	9279.747
33	9334.292	9304.036	9274.662
34	9330.860	9299.700	9269.452 *
35	9327.309 *	9295.266	9264.123 *
36	9323.640 *	9290.699	9258.671
37	9319.851 *	9286.022	9253.084 *
38	9315.994	9281.239	9247.402
39	9312.034	9276.358	9241.612
40	9308.048	9271.394	9235.725
41	9304.100	9266.403	9229.752
42	9300.485	9261.453 *	9223.754
43	9297.714	9256.837	9217.818 *
44		9253.084 *	9212.194
45			9207.392

Appendix III -- $^5\Phi_4$ - $X^5\Delta_3$ (0,1) (cont.)

J	R		Q		P	
43	9288.022					
44	9285.547		9243.365			
45	9281.772		9239.878		9197.706	*
46	9277.312	*	9235.109		9193.219	*
47	9272.511	*	9229.667	*	9187.436	*
48	9267.484		9223.848		9181.004	*
49	9262.288		9217.818	*	9174.156	
50	9256.938	*	9211.614		9167.140	
51	9251.527	*	9205.296		9159.948	
52	9246.068		9198.864		9152.626	
53	9240.608		9192.407		9145.216	*
54	9235.250		9185.950	*	9137.727	
55	9230.129		9179.589		9130.277	*
56	9225.446		9173.483	*	9122.912	*
57	9221.322		9167.802		9115.835	
58			9162.686		9109.167	
59					9103.062	
55	9215.075					
56	9211.239		9158.426			
57	9206.677		9153.615		9100.779	
58	9201.354		9148.037		9094.983	
59	9195.412		9141.734	*	9088.420	*
60	9189.065		9134.814		9081.090	*
61	9182.374		9127.459	*	9073.210	*
62	9175.414	*	9119.774		9064.842	
63	9168.215		9111.827		9056.184	
64	9160.848	*	9103.638		9047.254	
65	9153.287		9095.288	*	9038.090	*
66	9145.539		9086.744		9028.748	
67	9137.661		9078.033	*	9019.215	
68	9129.618		9069.163		9009.503	*
69	9121.400		9060.126	*	8999.670	*
70		*	9050.906	*	8989.630	*
71	9104.525		9041.593		8979.484	
72	9095.845		9032.096		8969.163	
73	9087.025		9022.443		8958.695	
74	9078.033	*	9012.644		8948.059	
75	9068.930	*	9002.708		8937.280	
76	9059.663		8992.617		8926.381	
77	9050.240	*	8982.350			
78	9040.673		8971.926			
79	9030.952		8961.437			
80	9021.076		8950.754			

$^5\Phi_4$ - $X^5\Delta_3$ (0,1) (cont.)

J	R		Q		P	
81	9011.077	*	8939.893	*		
82	9000.866	*	8928.933	*		
83		*	8917.783			
84	8979.988	?	8906.506			

$^5\Phi_5$ - $X^5\Delta_4$ (0,1)

J	R		Q		P	
4	9418.681		-		-	
5	9418.946	*	9413.604	*	-	
6	9419.086	*	9412.863		9407.521	
7	9419.086	*	9411.972	*	9405.726	*
8	9418.979	*	9410.977	*	9403.874	*
9	9418.741		9409.853		9401.863	
10	9418.386	*	9408.608	*	9399.698	
11	9417.892		9407.209		9397.454	*
12	9417.276		9405.726		9395.044	
13	9416.517		9404.079		9392.544	
14	9415.667	*	9402.340		9389.943	*
15	9414.675		9400.462		9387.143	
16	9413.559	*	9398.463		9384.248	
17	9412.315		9396.327		9381.234	
18	9410.945	*	9394.071		9378.092	
19	9409.446		9391.687		9374.817	
20	9407.816		9389.181		9371.462	*
21	9406.066		9386.541		9367.918	
22	9404.186		9383.779		9364.258	*
23	9402.177		9380.894		9360.484	*
24	9400.042	*	9377.857		9356.596	*
25	9397.765		9374.713		9352.554	
26	9395.391		9371.462	*	9348.409	
27	9392.880	*	9368.064	*	9344.108	
28	9390.231		9364.537	*	9339.716	
29	9387.457		9360.876		9335.188	
30	9384.554		9357.093		9330.521	
31	9381.511		9353.185		9325.731	
32	9378.330	*	9349.145		9320.798	
33	9375.055		9344.971		9315.749	
34	9371.633	*	9340.672		9310.599	
35	9368.064	*	9336.251		9305.271	
36	9364.393	*	9331.671		9299.859	
37	9360.560	*	9326.996		9294.289	*

Appendix III -- $^5\Phi_5$ - $X^5\Delta_4$ (0,1) (cont.)

J	R	Q	P
38	9356.626 *	9322.179	9288.606
39	9352.554	9317.233	9282.778
40	9348.347	9312.146	9276.835 *
41	9344.000	9306.939	9270.746 *
42	9339.529	9301.595	9264.515
43	9334.912	9296.115	9258.194
44	9330.174	9290.509	9251.712
45	9325.295	9284.767 *	9245.112
46	9320.286	9278.901	9238.369 *
47	9315.144	9272.888 *	9231.502 *
48	9309.868 *	9266.749	9224.496
49	9304.462 *	9260.477	9217.360
50	9298.905 *	9254.066	9210.093
51	9293.217	9247.525	9202.689
52	9287.411 *	9240.850	9195.166 *
53	9281.448	9234.038	9187.476
54	9275.345	9227.083 *	9179.677 *
55	9269.113 *	9220.000	9171.721 *
56	9262.754	9212.763 *	9163.661
57	9256.224 *	9205.417	9155.447
58	9249.593	9197.921	9147.108
59	9242.812 *	9190.285	9138.621
60	9235.879	9182.514	9129.990 *
61	9228.815	9174.607	9121.240
62	9221.612	9166.552	9112.347
63	9214.262	9158.366	9103.319
64	9206.771	9150.035	9094.139 *
65	9199.129	9141.571	9084.837
66	9191.369 *	9132.990 *	9075.379
67	9183.459	9124.187 *	9065.795
68	9175.414 *	9115.315	9056.076 *
69	9167.192	9106.276	9046.201
70	9158.852	9097.101	9036.176
71	9150.360	9087.759	9026.017 *
72	9141.734	9078.311	9015.737
73	9132.959 *	9068.706	9005.293
74	9124.016	9058.943	8994.721
75	9114.892 *	9049.049	8983.969 *
76	9105.714	9039.003	8973.116
77	9096.333 *	9028.812	8962.118
78	9086.833	9018.485	8950.949 *
79	9077.162	9008.001	8939.654 *
80	9067.386 ?	8997.371	8928.213 *
81		8986.594 *	8916.624 *

Appendix III (cont.) -- $^5\Phi_1$ - $X^5\Delta_0$ (0,2)

J	R		Q		P	
	aa	bb	ab	ba	aa	bb
0			-	-	-	-
1					-	-
2	8331.582 *					
3	8332.186 *		8328.178 *			
4	8332.703	8332.352	8327.722	8328.083		
5	8333.103	8332.751 *	8327.186	8327.550		
6	8333.397 *	8333.042	8326.567	8326.930		
7	*	8333.227	8325.832	8326.191	8319.707	8319.366
8	*	8333.308 *	8324.993	8325.352 *	8317.957	8317.594
9	*	8333.268 *	8324.044	8324.388 *	8316.086	8315.735
10	8333.499	8333.151	8322.987	8323.354	8314.082	8313.761
11	8333.268 *	8332.906	8321.827	8322.165	8312.019	8311.670
12	8332.906	8332.561	8320.561	8320.914	8309.832	8309.486
13	8332.444	8332.097	8319.178	8319.532	8307.538	8307.177
14	8331.873	8331.534	8317.695	8318.050	8305.129	8304.777
15	8331.173	8330.839	8316.086	8316.440	8302.615	8302.261
16	8330.403	8330.047	8314.384	8314.736	8299.978	8299.617
17	8329.472	8329.149	8312.563	8312.898	8297.243	8296.881
18	8328.452	8328.131	8310.631	8310.986	8294.369 *	8294.053
19	8327.311	8327.001	8308.587	8308.932	8291.403 *	8291.096 *
20	8326.089	8325.744	8306.407	8306.778	8288.370	8288.021
21	8324.710	8324.388	8304.153	8304.503	8285.186	8284.840
22	8323.249	8322.908	8301.756	8302.110	8281.883 *	8281.538
23	8321.655	8321.314	8299.261	8299.617	8278.461	8278.115
24	8319.935	8319.605	8296.640	8296.995	8274.936	8274.600
25	8318.110	8317.791	8293.903	8294.258	8271.292	8270.964
26	8316.169	8315.826	8291.058	8291.403	8267.517	8267.196 *
27	8314.082	8313.761 *	8288.084	8288.417	8263.662	8263.310
28	8311.910	8311.564	8284.995	8285.327	8259.649	8259.327
29	8309.603 *	8309.292	8281.779 *	8282.138	8255.556	8255.218
30	8307.177	8306.849	8278.461 *	8278.813	8251.331	8251.000
31	8304.610	8304.301	8274.999	8275.365	8246.973	8246.639
32	8301.961	8301.631	8271.434	8271.789	8242.501	8242.188 *
33	8299.170	8298.843	8267.755	8268.104	8237.928	8237.598
34	8296.257	8295.934	8263.952	8264.302 *	8233.195	8232.907 *
35	8293.227	8292.898	8260.030	8260.370 *	8228.382	8228.058
36	8290.062	8289.741	8255.967	8256.315	8223.432	8223.119
37	8286.777	8286.461	8251.797	8252.138	8218.361	8218.038
38	8283.364	8283.041	8247.498	8247.844	8213.168	8212.862
39	8279.842 *	8279.532	8243.060	8243.401	8207.866	8207.546
40	8276.187	8275.882	8238.515	8238.873	8202.417	8202.111
41	8272.408 *	8272.106	8233.867	8234.188	8196.863	8196.551
42	8268.512	8268.206	8229.089	8229.418	8191.177	8190.860
43	8264.490	8264.208 *	8224.173	8224.503	8185.377	8185.069 *
44	8260.370 *	8260.030	8219.149	8219.479 *	8179.459	8179.146 *

Appendix III -- $^5\Phi_1 - X^5\Delta_0$ (0,2) (cont.)

J	R		Q		P	
	aa	bb	ab	ba	aa	bb
45	8256.103	8255.793	8213.986	8214.323	8173.413 *	8173.123
46	8251.714	8251.415	8208.722	8209.051	8167.246	8166.959
47	8247.223 *	8246.937 *	8203.347	8203.671 *	8160.967	8160.706 *
48			8197.848	8198.179	8154.575	8154.287
49			8192.263	8192.593	8148.082	8147.781
50			8186.606	8186.930	8141.497	8141.216 *

$^5\Phi_2 - X^5\Delta_1$ (0,2)

J	R	Q	P
1		-	-
2			-
3			
4		8407.187 *	
5		8406.652	
6		8406.021	8400.503
7		8405.270	8398.857
8		8404.426	8397.094
9		8403.492 *	8395.239 *
10		8402.459	8393.282
11		8401.315	8391.189
12	8412.004 *	8400.060	8389.024
13	8411.573	8398.702	8386.757
14	8411.039	8397.246	8384.395 *
15	8410.417	8395.692	8381.902
16	8409.687 *	8394.044	8379.326
17	8408.866	8392.292	8376.646
18	8407.956 *	8390.459	8373.862
19	8406.943	8388.522	8371.030 *
20	8405.876	8386.495	8368.061
21	8404.707	8384.395	8365.012
22	8403.492 *	8382.219	8361.887
23		8379.945 *	
24		8377.649	

Appendix III (cont.) -- $^5\Phi_3$ - $X^5\Delta_2$ (0,2)

J	R		Q		P	
2	8464.385		-		-	
3	8464.922		8461.323		-	
4	8465.315		8460.832		8457.265	*
5	8465.624		8460.250		8455.768	*
6	8465.803		8459.527		8454.120	
7	8465.871		8458.684		8452.378	*
8	8465.803		8457.722		8450.533	
9	8465.624		8456.636		8448.576	
10	8465.315		8455.432		8446.475	
11	8464.885	*	8454.120		8444.235	
12	8464.349		8452.653		8441.893	
13	8463.676		8451.109		8439.437	
14	8462.901		8449.431		8436.868	
15	8461.991		8447.626		8434.154	
16	8460.985		8445.716		8431.361	
17	8459.825		8443.680		8428.404	
18	8458.589		8441.526		8425.361	
19	8457.216		8439.255		8422.196	
20	8455.719		8436.868		8418.892	
21	8454.120		8434.360		8415.510	
22	8452.378	*	8431.736		8412.004	*
23	8450.533		8428.990		8408.349	
24	8448.576		8426.118		8404.595	
25	8446.475		8423.156		8400.731	
26	8444.301		8420.065		8396.725	
27	8441.987		8416.853		8392.618	
28	8439.569		8413.542		8388.406	
29	8437.004		8410.100		8384.076	
30	8434.360		8406.545		8379.605	
31	8431.592		8402.879		8375.064	
32	8428.703		8399.100		8370.383	
33	8425.702		8395.197		8365.591	
34	8422.596		8391.189		8360.685	
35	8419.375		8387.082		8355.671	
36	8416.069		8382.860		8350.547	
37	8412.657	*	8378.537		8345.320	
38	8409.148		8374.094		8339.995	
39			8369.593		8334.570	
40					8329.044	

$^5\Phi_4$ - $X^5\Delta_3$ (0,2)

J	R		Q		P	
3	8516.434		-		-	
4	8516.855	*	8512.383		-	
5	8517.126		8511.787		8507.321	
6	8517.304	*	8511.046	*	8505.675	*
7	8517.371		8510.224		8503.976	
8	8517.304	*	8509.266		8502.150	
9	8517.126		8508.193		8500.158	*
10	8516.814	*	8506.977		8498.068	
11	8516.392		8505.675		8495.859	*
12	8515.838		8504.240		8493.524	
13	8515.176		8502.679		8491.111	*
14	8514.388		8501.008		8488.509	*
15	8513.490		8499.213		8485.829	
16	8512.455		8497.274		8483.019	
17	8511.306		8495.252		8480.093	
18	8510.025		8493.101		8477.046	
19	8508.653		8490.820		8473.875	
20	8507.144		8488.421		8470.593	
21	8505.519		8485.905		8467.181	
22	8503.767		8483.270		8463.676	*
23	8501.914		8480.516		8460.007	
24	8499.912		8477.633		8456.248	
25	8497.797		8474.633		8452.339	*
26	8495.568		8471.500		8448.339	
27	8493.223		8468.278		8444.235	
28	8490.729		8464.922		8439.990	
29	8488.158		8461.451		8435.628	
30	8485.453		8457.854		8431.136	
31	8482.625		8454.120		8426.542	
32	8479.674		8450.303		8421.804	
33	8476.613		8446.363		8416.985	
34	8473.436		8442.288		8412.004	*
35	8470.145		8438.109		8406.943	*
36	8466.756		8433.825		8401.783	
37	8463.262		8429.427		8396.501	
38	8459.667		8424.906		8391.102	*
39	8456.016		8420.337		8385.591	
40	8452.339	*	8415.666		8380.004	
41	8448.714		8411.003		8374.353	
42	8445.403		8406.392		8368.671	
43	8442.937	*	8402.081		8363.044	
44			8398.634		8357.759	
45					8353.312	*

Appendix III -- $^5\Phi_4 - X^5\Delta_3$ (0,2) (cont.)

J	R		Q		P	
43	8433.267					
44	8431.136	*	8388.936			
45	8427.699		8385.783		8343.611	*
46	8423.597	*	8381.381	*	8339.495	
47	8419.141		8376.312	*	8334.077	*
48	8414.475		8370.833		8327.978	*
49	8409.650	*	8365.172		8321.525	*
50	8404.707	*	8359.356		8314.897	*
51	8399.671		8353.416		8308.074	
52	8394.593		8347.390		8301.148	
53	8389.535	*	8341.330		8294.128	
54	8384.581	*	8335.284		8287.079	
55	8379.889	*	8329.343		8280.046	
56	8375.630	*	8323.663		8273.114	
57	8371.939		8318.412		8266.433	
58			8313.761	*	8260.229	*
59					8254.572	*
55	8364.839	*				
56	8361.434		8308.587	*		
57	8357.302	*	8304.215		8251.415	*
58	8352.410	*	8299.091		8246.026	*
59	8346.937		8293.227	*	8239.909	*
60	8341.032		8286.777	*	8233.057	*
61	8334.794	*	8279.883		8225.612	*
62	8328.306		8272.673		8217.755	
63	8321.580	*	8265.204		8209.570	*
64	8314.736	*	8257.505		8201.126	*
65	8307.663	*	8249.651		8192.461	*
66	8300.426		8241.609		8183.604	
67	8293.035		8233.404		8174.597	*
68	8285.498	*	8225.048		8165.409	
69	8277.810	*	8216.537	*	8156.075	
70	8269.982	*	8207.866	*	8146.619	*
71	8262.013	*	8199.071	*	8136.961	*
72	8253.883		8190.132		8127.164	*
73	8245.611	*	8181.032		8117.238	*
74	8237.216		8171.807	*	8107.223	
75	8228.659		8162.423	*	8097.040	
76	8219.980	*	8152.919	*	8086.688	*
77	8211.121	*	8143.263	*	8076.193	
78	8202.177	*	8133.443	*	8065.582	*
79	8193.015	*	8123.523			
80	8183.769	*	8113.454	*		
81	8174.349	*	8103.230			
82			8092.864			

$^5\Phi_5 - X^5\Delta_4$ (0,2)

J	R		Q		P	
4			-		-	
5			8551.733	*	-	
6			8551.040		8545.690	*
7			8550.233	*	8543.958	*
8	8557.256		8549.260		8542.125	
9	8557.085		8548.210		8540.216	
10	8556.804	*	8547.012		8538.138	
11	8556.396		8545.740		8535.969	
12	8555.878		8544.320		8533.633	
13	8555.233		8542.794		8531.239	*
14	8554.473		8541.140		8528.727	*
15	8553.571		8539.379		8526.043	*
16	8552.589		8537.489		8523.225	*
17	8551.471		8535.493		8520.390	
18	8550.233		8533.369		8517.371	
19	8548.883		8531.123		8514.257	
20	8547.405		8528.762	*	8511.017	*
21	8545.806		8526.292		8507.648	
22	8544.095		8523.694		8504.164	
23	8542.262		8520.970		8500.572	
24	8540.310		8518.141		8496.847	
25	8538.234		8515.176	*	8493.012	
26	8536.035		8512.100		8489.050	
27	8533.703		8508.908		8484.978	
28	8531.268		8505.594		8480.771	
29	8528.727	*	8502.150		8476.457	
30	8526.043	*	8498.598		8472.004	
31	8523.225	*	8494.917		8467.445	
32	8520.315		8491.111		8462.783	
33	8517.277	*	8487.196		8457.987	
34	8514.102		8483.151		8453.070	
35	8510.821		8478.987		8448.030	
36	8507.403		8474.695		8442.859	
37	8503.867		8470.281		8437.562	
38	8500.207		8465.747		8432.170	
39	8496.413		8461.076		8426.644	
40	8492.502		8456.314		8420.990	
41	8488.469	*	8451.407		8415.224	
42	8484.291	*	8446.363		8409.318	
43	8480.021	*	8441.226	*	8403.302	
44	8475.616		8435.951		8397.158	
45	8471.074		8430.544		8390.890	
46	8466.415		8425.018		8384.476	
47	8461.628		8419.375		8377.979	
48	8456.703		8413.583	*	8371.334	

Appendix III -- $^5\Phi_5 - X^5\Delta_4$ (0,2) (cont.)

J	R	Q	P
49	8451.662	8407.686	8364.563
50	8446.475	8401.652	8357.655
51	8441.190	8395.489	8350.653
52	8435.751	8389.201	8343.516
53	8430.203	8382.790	8336.222
54	8424.509	8376.255 *	8328.838
55	8418.690	8369.593	8321.314
56	8412.739 *	8362.777	8313.664
57	8406.652	8355.851	8305.884
58	8400.447	8348.788	8297.963
59	8394.110	8341.603	8289.926
60	8387.638	8334.280	8281.779 *
61	8381.027	8326.805	8273.450
62	8374.290	8319.241	8265.027
63	8367.423	8311.530	8256.472
64	8360.402	8303.675	*
65	8353.277	8295.701	8238.963 *
66	8345.998	8287.581	8230.012
67	8338.579	8279.333	8220.928 *
68	8331.024	8270.964	8211.714
69	8323.354	8262.425	8202.332 *
70	8315.530	8253.787	8192.860
71	8307.583	8245.013 *	
72	8299.504	8236.082	
73	8291.246	8227.033 *	
74	8282.890	8217.834	
75	8274.378	8208.502	
76	8265.736	8199.024 *	
77	8256.953	8189.423	
78	8248.017	8179.681	
79	8238.963 *		

$^5\Phi_1 - X^5\Delta_0$ (0,3)

J	R		Q		P	
	aa	bb	ab	ba	aa	bb
0			-	-	-	-
1		7477.929			-	-
2		7478.661			7474.401 *	7474.069 *
3	7479.693 *	7479.304		7475.996 *	7473.164 *	7472.846
4	7480.215 *	7479.868 *	7475.212 *	7475.583	7471.889	7471.533 *
5	*	7480.243 *	7474.735	7475.089 *	7470.473 *	7470.124 *
6	7480.989 *	*	7474.140	7474.507	7468.943 *	7468.553 *

Appendix III -- $^5\Phi_1$ - $X^5\Delta_0$ (0,3) (cont.)

J	R				Q				P			
	aa		bb		ab		ba		aa		bb	
7	7481.235	*		*	7473.454	*	7473.820		7467.356			*
8	7481.352	*	7480.989	*	7472.676	*	7473.060	*	7465.667	*		*
9	7481.416	*	7481.031	*	7471.778	*	7472.160		7463.849		7463.464	*
10	7481.352	*	7480.989	*	7470.828	*	7471.193	*	7461.943	*	7461.593	
11	7481.169	*	7480.822		7469.742		7470.124		7459.946		7459.575	
12	7480.925		7480.578	*	7468.553	*	7468.943		7457.843	*	7457.516	*
13	7480.578	*	7480.215		7467.274		7467.662		7455.669		7455.298	*
14	7480.138	*	7479.766	*	7465.916		7466.307	*	7453.359	*		*
15	7479.545		7479.168		7464.430		7464.783	*	7450.964	*	7450.603	*
16	7478.870		7478.522		7462.845		7463.218		7448.463		7448.072	*
17	7478.111		7477.728		7461.159		7461.528		7445.857		7445.512	*
18	7477.209		7476.864		7459.361		7459.738		7443.138	*	7442.792	*
19	7476.229		7475.879		7457.467		7457.843		7440.317		7439.978	
20	7475.166	*	7474.789		7455.464		7455.831		7437.417		7437.065	
21	7473.950	*	7473.594		7453.359		7453.707		7434.399		7434.048	
22	7472.648	*	7472.278		7451.154		7451.507		7431.270			*
23	7471.233		7470.873		7448.816		7449.195		7428.044		7427.661	*
24	7469.709	*	7469.347		7446.396		7446.740		7424.681		7424.353	*
25	7468.065		7467.712		7443.848		7444.213	*	7421.248		7420.881	*
26	7466.307	*	7465.980		7441.196		7441.567	*	7417.695		7417.351	
27	7464.470	*	7464.098	*	7438.425		7438.798	*	7414.029		7413.685	*
28	7462.491	*	7462.171		7435.573		7435.921		7410.267		7409.916	
29	7460.421		7460.062	*	7432.586	*	7432.967	*	7406.367		7406.036	
30	7458.237		7457.897	*	7429.501		7429.863		7402.368		7402.036	
31	7455.931	*	7455.574		7426.298		7426.656		7398.259		7397.934	
32	7453.498		7453.163		7422.975		7423.338		7394.052		7393.706	
33	7450.964	*	7450.633		7419.554		7419.923		7389.718		7389.416	*
34	7448.325		7447.990	*	7416.007		7416.371		7385.275		7384.949	
35	7445.555	*	7445.255	*	7412.355		7412.696		7380.723		7380.383	
36	7442.676		7442.357	*	7408.574		7408.939		7376.085	*		*
37	7439.681		7439.337		7404.716	*	7405.057	*	7371.268		7370.945	
38	7436.583		7436.249		7400.693		7401.030			*	7366.056	
39	7433.351		7433.017	*	7396.579		7396.924		7361.368		7361.042	*
40	7429.988	*	7429.734	*	7392.347	*	7392.687		7356.255		7355.924	*
41	7426.547		7426.234		7387.992	*	7388.349		7351.006		7350.706	*
42	7422.975		7422.656		7383.560	*	7383.883		7345.665			*
43	7419.298		7419.007	*	7378.961		7379.324	*	7340.200	*	7339.881	
44	7415.527	?	7415.198	*	7374.277	*	7374.622		7334.594	*	7334.294	
45					7369.472			*	7328.919		7328.595	
46					7364.573		7364.901		7323.120		7322.831	*
47					7359.530	*	7359.892		7317.203		7316.893	
48					7354.407	*	7354.792	*	7311.189		7310.879	
49									7305.067	*		

Appendix III (cont.) -- $^5\Phi_1$ - $X^5\Delta_1$ (0,3)

J	R		Q		P	
1	7557.383	*	-		-	
2	7558.094	*			-	
3						
4	7559.259	*				
5	7559.689	*	7554.157		7549.575	*
6	7560.021	*	7553.587		7548.076	*
7	7560.260	*	7552.911		7546.463	*
8	7560.402	*	7552.142		7544.785	*
9	7560.448	*	7551.263		7542.989	*
10	7560.402	*	7550.290		7541.085	
11	7560.260		7549.227		7539.124	*
12	7560.021		7548.076		7537.042	
13	7559.689		7546.820		7534.862	
14	7559.259		7545.466	*	7532.595	
15	7558.765	*	7544.031		7530.242	
16	7558.143		7542.495		7527.775	
17	7557.456	*	7540.884		7525.244	*
18	7556.687		7539.180			*
19	7555.831		7537.395		7519.886	
20	7554.903		7535.530		7517.088	
21	7553.908		7533.587	*	7514.210	
22	7552.840		7531.572		7511.255	
23	7551.721		7529.509		7508.246	
24	7550.541	*	7527.370		7505.168	
25	7549.340		7525.184	*	7502.023	*
26			7522.956	*	7498.815	
27					7495.593	

$^5\Phi_2$ - $X^5\Delta_2$ (0,3)

J	R		Q		P	
3	7612.348	*	-		-	
4	7612.773	*			-	
5	7613.125	*				
6	7613.347	*	7607.056	*		
7	7613.465	*	7606.283			
8	7613.465	*	7605.373			
9	7613.347	*	7604.357		7596.278	*
10	7613.125	*	7603.244			*
11	7612.773	*	7602.003		7592.103	*
12	7612.348	*	7600.649		7589.870	
13	7611.764		7599.180		7587.504	

$^5\Phi_3$ - $X^5\Delta_2$ (0,3) (cont.)

J	R		Q		P	
14	7611.070	*	7597.619		7585.052	*
15	7610.322	*	7595.923		7582.466	*
16	7609.399	*		*	7579.756	*
17	7608.395		7592.223	*	7576.963	
18	7607.294	*	7590.212	*	7574.048	
19	7606.039		7588.088		7571.028	
20	7604.698		7585.856		7567.890	
21	7603.244	*	7583.488		7564.671	
22	7601.701		7581.047		7561.292	*
23	7600.017	*	7578.462		7557.838	
24	7598.249		7575.805		7554.244	
25	7596.348		7573.033			*
26		*	7570.133		7546.772	*
27	7592.264	*	7567.143		7542.881	
28	7590.034		7564.021		7538.901	*
29	7587.723		7560.802		7534.787	
30	7585.297	*	7557.456	*	7530.557	
31	7582.766		7554.060		7526.243	
32	7580.128		7550.514	*	7521.798	
33	7577.383		7546.862		7517.260	
34	7574.532		7543.129			*
35			7539.274		7507.854	
36			7535.341		7503.024	*
37	7565.415		7531.279			
38			7527.145			

$^5\Phi_4$ - $X^5\Delta_3$ (0,3)

J	R		Q		P	
3	7663.802		-		-	
4	7664.251	*	7659.792	*	-	
5	7664.565	*	7659.224			
6	7664.791	*	7658.545			
7	7664.896	*	7657.774			
8	7664.896	*	7656.869		7649.738	
9	7664.791	*	7655.866		7647.812	*
10	7664.565	*	7654.735		7645.831	
11	7664.221	*	7653.509		7643.682	
12	7663.758		7652.162		7641.451	
13	7663.196		7650.701		7639.095	
14	7662.516		7649.127		7636.638	
15	7661.720		7647.448		7634.042	

Appendix III -- $^5\Phi_4$ - $X^5\Delta_3$ (0,3) (cont.)

J	R	Q	P
16	7660.814	7645.653	7631.361
17	7659.792 *	7643.738	7628.578
18	7658.662	7641.704	7625.666
19	7657.427	7639.585	7622.625
20	7656.064	7637.340	7619.507
21	7654.593	7634.967	7616.260
22	7653.015	7632.511	7612.897
23	7651.317	7629.932	7609.458 *
24	7649.519	7627.237	7605.845 *
25	7647.588	7624.424	7602.150
26	7645.541	7621.509	7598.340
27	7643.406	7618.474	*
28	7641.151	7615.328	7590.390
29	7638.765	7612.069	7586.249 *
30	7636.304	7608.709	7581.993
31	7633.705	7605.226	7577.624
32	7631.006 *	7601.635	7573.132
33	7628.177	7597.939	7568.564
34	7625.277	7594.134 *	7563.870
35	7622.249	7590.212	7559.068
36	7619.130	7586.203	7554.157
37	7615.917	7582.083	7549.144
38	7612.612	7577.870	7544.031
39	7609.258	7573.584	7538.826
40	7605.886 *	7569.213	7533.559 *
41	7602.579	7564.865	7528.217
42	7599.593	7560.564 *	7522.844
43	7597.460	7556.590	7517.535 *
44		7553.473	7512.583 *
45			7508.495

43	7587.776		
44	7585.951	7543.769 *	
45	7582.862 *	7540.983	7498.815 *
46	7579.124 *	7536.909 *	7495.017 *
47	7575.018	7532.180 *	7489.942 *
48	7570.722	7527.084	7484.215 *
49	7566.260	7521.798	7478.167
50	7561.711	7516.358 *	7471.889
51	7557.061	7510.811	7465.463
52	7552.384	7505.168 *	7458.937
53	7547.703 *	7499.524	7452.326 *
54	7543.186 *	7493.883	7445.682
55	7538.901 *	7488.356	7439.073

$^5\Phi_4$ - $X^5\Delta_3$ (0,3) (cont.)

J	R	Q	P
56	7535.049	7483.105	7432.558 *
57	7531.798 *	7478.299	*
58		7474.069 *	*
59			7415.337 *
55	7523.836 *		
56	7520.908 *	7468.065 *	
57	7517.189	7464.098 *	7411.275 *
58	7512.736 *	7459.421	7406.367 *
59	7507.706	7453.998 *	7400.693 *
60	7502.242 *	7447.990 *	7394.289
61	7496.521 *	7441.567 *	7387.327
62	7490.464 *	7434.829 *	7379.919 *
63	7484.215 *	7427.833 *	7372.207 *
64	7477.833 *	7420.597 *	7364.246 *
65	7471.274 *	7413.275 *	
66	*	7405.726	
67	*	7398.043	
68	7450.644 *	7390.202	
69	7443.486 *	7382.221 *	
70	7436.249 *	7374.092 *	
71	7428.753 *	7365.823	
72	*	7357.455 *	
73	7413.474 *	7348.900	
74		7340.232 *	
75		7331.437 *	
76		7322.537 *	
77		7313.420 *	

$^5\Phi_5$ - $X^5\Delta_4$ (0,3)

J	R	Q	P
4	7704.104	-	-
5	7704.450 *	7699.115 *	-
6	7704.685	7698.454	
7	7704.797	7697.682	
8	7704.797	7696.794	
9	7704.685	7695.804	7687.794
10	7704.477 *	7694.710	7685.820
11	7704.154	7693.494	7683.694 *
12	7703.720	7692.168	7681.506

Appendix III -- $^5\Phi_4$ - $X^5\Delta_4$ (0,3) (cont.)

J	R	Q	P
13	7703.158	7690.720	7679.186
14	7702.524	7689.194	7676.757 *
15	7701.748	7687.522	7674.223
16	7700.879	7685.775	7671.552
17	7699.865	7683.901	7668.796
18	7698.763 *	7681.911	7665.932
19	7697.572	7679.812	7662.942
20	7696.243	7677.609	7659.856
21	7694.789	7675.280	7656.644 *
22	7693.254	7672.853	7653.332
23	7691.598	7670.308	7649.903
24	7689.818	7667.646	7646.366
25	7687.937	7664.896	7642.715
26	7685.937	7661.996	7638.945
27	7683.817	7659.002	7635.086
28	7681.596	7655.896	7631.088
29	7679.255	7652.675	7626.962
30	7676.798	7649.343	7622.773
31	7674.223	7645.902	7618.474 *
32	7671.552	7642.335	7614.007
33	7668.729	7638.661	7609.458
34	7665.838	7634.858	7604.798
35	7662.799	7630.953 *	7600.017
36	7659.657	7626.962	7595.129
37	7656.399	7622.818	7590.128 *
38	7653.015	7618.556	7584.996
39	7649.519	7614.207	7579.756 *
40	7645.902 *	7609.726	7574.403
41	7642.196	7605.140	7568.948
42	7638.348	7600.419	7563.348
43	7634.384	7595.588	7557.686 *
44	7630.303	7590.642	7551.855 *
45	7626.109	7585.585	7545.902
46	7621.789	7580.391	7539.875
47	7617.352 *	7575.101	7533.716
48	7612.773 *	7569.674	7527.421
49	7608.124	7564.141	7521.032
50	7603.337 *	7558.483	7514.512
51	7598.389	7552.708	7507.854
52	7593.364	7546.820	7501.104
53	7588.186 *	7540.805	7494.245
54	7582.920	7534.669	
55	7577.517	7528.409	
56	7571.993	7522.032	
57	7566.354	7515.521	

Appendix III -- $^5\Phi_5$ - $X^5\Delta_4$ (0,3) (cont.)

J	R		Q		P	
58	7560.564		7508.888	*		
59	7554.678		7502.139			
60	7548.655		7495.284			
61	7542.495		7488.296			
62	7536.245		7481.169			
63	7529.823	*	7473.950			
64	7523.324	*	7466.593	*		
65	7516.645					
66	7509.907	*				

$^5\Phi_1$ - $X^5\Delta_0$ (1,0)

J	R				Q				P			
	aa		bb		ab		ba		aa		bb	
0			10678.457	*	-		-		-		-	
1	10679.545		10679.223	*	10677.385	*	10677.718		-		-	
2	10680.154		10679.841		10677.119		10677.439					
3		*	10680.324		10676.705		10677.023			*		*
4	10680.970			*	10676.141	*	10676.458			*		*
5		*	10680.848	*	10675.430		10675.737			*		*
6	10681.223	*	10680.920		10674.580		10674.905			*		*
7	10681.147	*	10680.848	*	10673.589		10673.920		10667.583		10667.255	
8	10680.920	*	10680.622	*	10672.469		10672.796		10665.548		10665.246	
9	10680.548		10680.256		10671.190		10671.530		10663.379		10663.073	*
10	10680.038		10679.747		10669.782		10670.121		10661.064		10660.760	
11	10679.398	*	10679.100		10668.229		10668.565		10658.604		10658.313	*
12	10678.596		10678.314		10666.533	*	10666.886		10656.006			*
13	10677.668		10677.385		10664.702		10665.031	*	10653.275		10652.966	
14	10676.594		10676.333	*	10662.710		10663.073	*		*	10650.106	
15	10675.380		10675.108		10660.610		10660.958		10647.368		10647.094	
16	10674.004		10673.710	*	10658.355		10658.706		10644.219		10643.933	
17	10672.522		10672.257		10655.953		10656.323	*	10640.915		10640.623	
18	10670.889		10670.625		10653.419		10653.775		10637.474		10637.204	
19	10669.104		10668.854		10650.736		10651.098		10633.874		10633.626	
20	10667.179		10666.931		10647.933	*	10648.280		10630.189	*	10629.910	
21	10665.110		10664.872	*	10644.944		10645.321	*	10626.293	*	10626.055	
22	10662.918	*	10662.670		10641.841		10642.225		10622.299		10622.051	
23	10660.554		10660.319		10638.596		10638.978		10618.147		10617.910	
24	10658.063		10657.837		10635.207		10635.595		10613.843		10613.630	
25	10655.431		10655.206		10631.672		10632.065		10609.435		10609.205	
26	10652.653		10652.441		10628.007		10628.392		10604.864		10604.638	
27	10649.736		10649.521	*	10624.189		10624.566		10600.150		10599.933	
28	10646.669		10646.466		10620.232	*	10620.630		10595.292		10595.081	

Appendix III -- $^5\Phi_1$ - $X^5\Delta_0$ (1,0) (cont.)

J	R				Q				P			
	aa		bb		ab		ba		aa		bb	
29	10643.459		10643.266		10616.132		10616.532		10590.289		10590.092	
30	10640.105		10639.918		10611.890		10612.297		10585.143		10584.955	
31	10636.614		10636.428		10607.501		10607.916		10579.879		10579.692	
32	10632.973		10632.801		10602.956	*	10603.384			*	10574.272	
33	10629.195	*	10629.002	*	10598.302		10598.713	*	10568.891		10568.707	
34	10625.267	*	10625.101		10593.488		10593.911		10563.189		10563.005	
35	10621.198		10621.044		10588.530		10588.956		10557.340		10557.166	
36	10616.988	*	10616.831		10583.426		10583.837	*	10551.346		10551.183	
37	10612.629		10612.477		10578.181		10578.617		10545.209		10545.048	
38	10608.126		10607.982		10572.794		10573.209		10538.933		10538.768	
39	10603.460		10603.343	*	10567.257		10567.697		10532.509		10532.365	
40		*	10598.554		10561.577		10562.023		10525.939		10525.784	
41	10593.749		10593.612		10555.755		10556.203		10519.231		10519.108	
42	10588.662	*	10588.530	*	10549.776		10550.244		10512.382		10512.251	
43	10583.426	*	10583.313		10543.686		10544.135		10505.372		10505.259	
44	10578.057		10577.944			*	10537.880		10498.228	*	10498.123	
45	10572.531		10572.429		10531.030		10531.478		10490.966			*
46	10566.863		10566.763		10524.481		10524.932		10483.538		10483.427	
47	10561.053	*	10560.956		10517.794		10518.252		10475.961		10475.859	
48	10555.095		10554.994		10510.956		10511.418		10468.253		10468.155	
49	10548.969	*	10548.920	*	10503.973		10504.425			*	10460.275	
50	10542.731	*	10542.671	*	10496.847		10497.331		10452.369		10452.281	
51	10536.354	*	10536.279		10489.591		10490.056		10444.258	*	10444.166	
52	10529.812			*	10482.177		10482.637		10435.948	*	10435.870	
53	10523.124	*	10523.059	*	10474.620		10475.086		10427.526	*	10427.439	*
54	10516.293	*	10516.238	*	10466.906		10467.365		10418.945	*	10418.854	*
55	10509.324	*	10509.260	*	10459.062		10459.552	*	10410.170	*	10410.170	*
56	10502.187	*	10502.146	*	10451.065		10451.547		10401.397	*	10401.288	*
57	10494.939		10494.887		10442.941		10443.420		10392.365	*	10392.290	*
58			10487.463	*	10434.670		10435.152	*		*	10383.154	*
59			10479.969	*	10426.258		10426.722				10373.910	?
60					10417.688		10418.171					
61					10408.972		10409.478	*				

$^5\Phi_2$ - $X^5\Delta_1$ (1,0)

J	R				Q				P			
	aa		bb		ab		ba		aa		bb	
1	10737.157				-		-		-			
2	10737.773				10735.084	*			-			
3	10738.245	*			10734.650				10731.961	*?		
4	10738.578				10734.077	*			10730.479			
5	10738.769				10733.382				10728.927	*		
6	10738.809				10732.525				10727.150			

Appendix III -- $^5\Phi_7 - X^5\Delta_1$ (1,0) (cont.)

J	R				Q				P			
	aa		bb		ab		ba		aa		bb	
7	10738.723				10731.534	*			10725.258			
8	10738.486	*			10730.398				10723.222			
9	10738.104	*			10729.125				10721.050			
10	10737.583				10727.707				10718.737	*		
11	10736.920				10726.152				10716.277			
12	10736.119				10724.452				10713.679			
13	10735.162				10722.603				10710.929	*		
14	10734.077	*			10720.618				10708.057			
15	10732.853	*			10718.496				10705.041			
16	10731.465				10716.220						*	
17	10729.951				10713.812				10698.564			
18	10728.286				10711.258	*			10695.097			
19	10726.464	*			10708.560				10691.522			
20	10724.538				10705.720				10687.793			
21	10722.443				10702.735				10683.916			
22	10720.211				10699.595	*			10679.899	*		
23	10717.833				10696.340	*			10675.737	*		
24	10715.308				10692.922				10671.431			
25	10712.642				10689.373	*			10666.987			
26	10709.836				10685.673	*			10662.397			
27	10706.884				10681.829				10657.662			
28	10703.783				10677.844				10652.788			
29	10700.547				10673.710				10647.775	*		
30	10697.158	*			10669.440	*			10642.607			
31	10693.631				10665.031	*			10637.310	*		
32	10689.950	*			10660.456	*			10631.858	*		
33	10686.132				10655.761	*			10626.266	*		
34	10682.166				10650.910	*			10620.530	*		
35	10678.058	*			10645.913				10614.647	*		
36	10673.814	*			10640.777	*			10608.645	*		
37	10669.440	*			10635.508	*			10602.477	*		
38	10664.872	*			10630.062	*	10630.083	*	10596.159	*		
39	10660.204	*	10660.177	*	10624.496	*	10624.537	*	10589.713	*		
40	10655.387	*	10655.346	*	10618.795	*	10618.822	*	10583.141	*	10583.114	*
41	10650.390	*			10612.943	*	10612.970	*	10576.405	*	10576.378	*
42	10645.321	*	10645.276	*	10606.941	*	10606.983	*	10569.553	*	10569.506	*
43	10640.059	*			10600.819	*	10600.848	*	10562.525	*	10562.488	*
44	10634.662	*		*	10594.551	*	10594.586	*	10555.370	*	10555.336	*
45	10629.195	*	10629.150	*	10588.145	*	10588.190	*	10548.087	*	10548.037	*
46	10623.572	*	10623.530	*	10581.605	*	10581.665	*	10540.671		10540.630	
47	10617.861	*	10617.815	*	10574.985	*	10575.035		10533.120	*	10533.082	*
48	10612.100	*	10612.059	*	10568.254	*	10568.295	*	10525.465	*	10525.417	*
49	10606.501	*	10606.465	*	10561.472	*	10561.506	*	10517.715	*	10517.673	*
50					10554.864	*	10554.910	*	10509.924		10509.874	

Appendix III (cont.) -- $^5\Phi_3$ - $X^5\Delta_2$ (1,0)

J	R		Q		P	
2	10790.826		-		-	
3	10791.294	*	10787.723		-	
4	10791.672		10787.183		10783.603	*
5		*	10786.501		10782.024	*
6	10792.002		10785.673		10780.304	
7	10791.915		10784.735		10778.458	
8	10791.750	*	10783.649		10776.476	
9	10791.410		10782.422		10774.351	
10	10790.957		10781.081		10772.078	
11	10790.367		10779.590		10769.712	
12	10789.652		10777.965		10767.185	
13	10788.813		10776.201	*	10764.533	
14	10787.876		10774.351		10761.751	
15	10786.859		10772.379		10758.854	
16	10785.837		10770.330		10755.847	
17	10784.998		10768.284		10752.772	
18	10784.595	*	10766.409		10749.691	
19			10764.979		10746.793	
20					10744.324	
17	10780.581	*				
18	10779.976		10761.957	*		
19	10778.848		10760.355		10742.297	*
20	10777.264	*	10758.189		10739.677	
21	10775.375		10755.578		10736.505	
22	10773.285		10752.665		10732.853	*
23	10770.990		10749.547		10728.927	*
24	10768.561		10746.240		10724.769	
25	10765.956		10742.762		10720.442	
26	10763.196		10739.125		10715.917	
27	10760.277		10735.340		10711.258	*
28	10757.212		10731.376		10706.454	
29	10753.984		10727.296		10701.483	
30	10750.622		10723.051		10696.340	*
31	10747.096		10718.639		10691.092	*
32	10743.427		10714.113	*	10685.673	*
33	10739.614	*	10709.417		10680.105	
34	10735.622		10704.571		10674.381	
35	10731.534	*	10699.595	*	10668.515	
36	10727.245	*	10694.444		10662.500	
37	10722.834		10689.149		10656.323	*
38	10718.259	*	10683.711		10650.022	
39	10713.550		10678.137	*	10643.553	*
40	10708.681		10672.379		10636.957	

$^5\Phi_1$ - $X^5\Delta_2$ (1,0) (cont.)

J	R		Q		P	
41	10703.665	*	10666.497		10630.189	
42	10698.492		10660.456		10623.292	
43	10693.181		10654.274		10616.239	
44	10687.710		10647.933		10609.036	
45	10682.102		10641.413	*	10601.680	
46	10676.333		10634.832	*	10594.187	
47	10670.431		10628.036		10586.540	
48	10664.407		10621.133		10578.755	
49	10658.258		10614.086		10570.818	
50	10651.810		10606.941	*	10562.761	
51	10645.079		10599.474		10554.601	
52	10638.411		10591.731		10546.102	*
53	10631.627		10584.047			*
54	10624.667		10576.250		10528.684	
55	10617.569	*	10568.295	*	10519.870	
56	10610.307		10560.180		10510.909	*
57	10602.914		10551.923		10501.791	
58	10595.381		10543.520		10492.528	
59	10587.709		10534.977		10483.119	
60	10579.976		10526.323		10473.579	
61			10517.572		10463.920	*
62			10508.678	*?	10454.157	
63					10444.258	*?

$^5\Phi_4$ - $X^5\Delta_3$ (1,0)

J	R		Q		P	
3	10830.120		-		-	
4	10830.615		10826.022		-	
5	10831.007		10825.475		10820.944	*
6	10831.278		10824.837		10819.315	
7	10831.436	*	10824.080	*	10817.655	
8	10831.476		10823.220		10815.835	
9	10831.408	*	10822.227		10813.944	*
10	10831.197		10821.127		10811.948	*
11	10830.880		10819.903	*		*
12	10830.423		10818.543		10807.587	*
13	10829.835		10817.065		10805.178	*
14	10829.102	*	10815.453			*
15	10828.242		10813.687	*	10800.036	*
16	10827.237		10811.805			*
17	10826.077		10809.774		10794.327	*

Appendix III -- $^5\Phi_4$ - $X^5\Delta_3$ (1,0) (cont.)

J	R				Q				P			
	aa		bb		ab		ba		aa		bb	
18	10824.772	*			10807.587				10791.284	*		
19	10823.305				10805.261				10788.081			
20	10821.702	*			10802.770				10784.735	*		
21	10819.903	*			10800.120	*			10781.196			
22	10817.996					*			10777.520	*		
23	10815.925				10794.391				10773.717			
24	10813.687	*			10791.294	*			10769.762			
25	10811.269				10788.023				10765.635			
26	10808.700				10784.595				10761.347			
27	10805.973				10781.005				10756.878			
28	10803.083				10777.264	*			10752.283			
29	10800.036				10773.340				10747.517			
30	10796.824				10769.278				10742.581			
31	10793.465				10765.050				10737.489			
32	10789.935				10760.660				10732.243			
33	10786.243	*			10756.114				10726.834			
34	10782.422	*			10751.414	*			10721.278			
35	10778.405				10746.545				10715.556	*		
36	10774.200	*	10774.241	*	10741.526				10709.673			
37	10769.921				10736.312	*	10736.355	*	10703.665	*		
38	10765.457				10731.018				10697.409	*	10697.450	*
39	10760.843				10725.533				10691.092			
40	10756.067	*			10719.898				10684.595			
41	10751.124	*			10714.113	*			10677.941			
42	10746.017	*	10746.044	*	10708.146	*			10671.133			
43	10740.800	*			10702.048	*			10664.177	*		
44		*			10695.776	*	10695.817	*	10657.058	*		
45	10729.821		10729.864	*	10689.373	*	10689.373	*	10649.785	*	10649.785	*
46	10724.122	*	10724.160	*	10682.807	*	10682.848	*	10642.346	*		
47	10718.259	*	10718.311	*	10676.099	*	10676.141	*		*	10634.784	*
48	10712.256		10712.302		10669.231		10669.270		10527.068	*	10627.104	*
49	10706.083		10706.132		10662.193		10662.256		10619.189	*	10619.230	*
50		*	10699.872	*	10655.042		10655.076		10611.162	*	10611.204	*
51	10693.302		10693.370		10647.722		10647.775	*	10602.956	*	10603.035	
52	10686.660		10686.750		10640.235		10640.299		10594.657		10594.696	
53	10679.899	*	10679.988		10632.607		10632.683		10586.176		10586.244	*
54	10672.978	*	10673.038	*	10624.829		10624.912		10577.588	*		
55	10665.906		10665.974	*	10616.898		10616.988		10568.758		10568.813	*
56	10658.667	*	10658.769		10608.819		10608.911		10559.817	*	10559.912	
57	10651.278		10651.399	*	10600.583		10600.688		10550.742	*	10550.832	
58	10643.745		10643.876		10592.199		10592.322		10541.502	*	10541.620	*
59	10636.063	*	10636.172	*	10583.668		10583.808		10532.127		10532.241	
60	10628.258	*	10628.392	*	10574.985	*	10575.133		10522.592	*	10522.721	*
61	10620.232	*	10620.415	*	10566.149		10566.318		10512.910	*	10513.047	
62	10612.165		10612.344	*	10557.166	*	10557.340	*	10503.113	*	10503.240	*

Appendix III -- $^5\Phi_4$ - $X^5\Delta_3$ (1,0) (cont.)

J	R		Q		P	
	aa	bb	ab	ba	aa	bb
63			10548.087 *	10548.272		10493.297 *
64			10538.865	10539.028		
65			10529.465	10529.675 *		
66			10519.974	10520.175		

$^5\Phi_5$ - $X^5\Delta_4$ (1,0)

J	R	Q	P
4	10871.239 *	-	-
5	10871.457 *	10866.110 *	-
6	10871.525	10865.318	10859.985
7	10871.457 *	10864.371	
8	10871.267 *	10863.296	10856.187
9	10870.947	10862.079	10854.105 *
10	10870.482	10860.727	
11	10869.880	10859.241	*
12	10869.138	10857.625	10846.983
13	10868.263	10855.865	*
14	10867.246 *	10853.969	10841.563 *
15	10866.110	10851.950 *	10838.648 *
16	10864.821	10849.774	10835.587
17	10863.403	10847.471	10832.415
18	10861.824	10845.024	10829.102 *
19	10860.143	10842.451	10825.633
20	10858.306	10839.730	10822.036
21	10856.331	10836.879	10818.300
22	10854.218	10833.889	10814.431
23	10851.950 *	10830.755	10810.417
24	10849.578	10827.481	10806.270
25	10847.048	10824.080	10801.980
26	10844.369	10820.531	10797.555
27	10841.563	10816.842	*
28	10838.606	10813.003	10788.291
29	10835.492	10809.044	10783.446
30	10832.270	10804.933	10778.458
31	10828.899	10800.675	10773.340 *
32	10825.375	10796.284	10768.068
33	10821.702 *	10791.750 *	10762.653
34	10817.901	10787.069	10757.116
35	10813.944 *	10782.245	10751.414 *
36	10809.843	10777.264 *	10745.569
37	10805.606	10772.180	10739.614 *
38	10801.216	10766.928	10733.492

Appendix III -- $^5\Phi_5 - X^5\Delta_4$ (1,0) (cont.)

J	R	Q	P
39	10796.690	10761.525	10727.245
40	10792.002	10755.966	10720.823
41	10787.183	10750.294	10714.278
42	10782.215 *	10744.462	10707.581
43	10777.072 *	10738.486 *	10700.734
44	10771.826	10732.359	10693.752
45	10766.409	10726.085	10686.615
46	10760.843	10719.665	10679.335
47	10755.125	10713.090	10671.915
48	10749.261	10706.371	10664.334
49	10743.249	10699.508	10656.621
50	10737.082	10692.470 *	10648.767 *
51	10730.767	10685.323	10640.731 *
52	10724.305	10678.010	10632.555
53	10717.681	10670.541	10624.226
54	10710.929 *	10662.918	10615.778
55	10703.982	10655.146	10607.157
56	10696.907	10647.221	10598.390
57	10689.670	10639.148	10589.458
58	10682.283	10630.926	10580.396
59	10674.746	10622.544	10571.173
60	10667.044	10614.005	10561.798
61	10659.193	10605.319	10552.274
62	10651.188	10596.471	10542.588
63	10643.021	10587.471	10532.750
64	10634.692 *	10578.314	10522.763
65	10626.211 *	10568.998	10512.617
66	10617.569	10559.531	10502.312
67	10608.779 *	10549.909	10491.862
68	10599.820	10540.121	10481.244
69	10590.709	10530.185	10470.467 *
70	10581.432	10520.081	10459.552 *
71	10571.992	10509.823	10448.470
72	10562.394	10499.405	10437.201 *
73	10552.639	10488.832	10425.863 *
74	10542.731	10478.092	10414.278
75	10532.633	10467.174 *	
76	10522.396	10456.138	
77	10511.978	10444.918	
78	10501.411	10433.532 *	
79	10490.680	10421.992 ?	
80	10479.793	10410.300 *?	
81	10468.788	10398.475 *?	

Appendix III (cont.) -- $^5\Phi_1 - X^5\Delta_0$ (1,1)

J	R				Q				P			
	aa		bb		ab		ba		aa		bb	
0					-		-		-		-	
1									-		-	
2												
3					9805.630							
4					9805.087		9805.450					
5					9804.427		9804.774					
6					9803.633		9803.994	*	9798.553		9798.204	
7	9810.296	*				*	9803.051		9796.701		9796.401	*
8	9810.118				9801.634		9801.981		9794.731		9794.408	
9		*	9809.500		9800.427		9800.770		9792.656	*	9792.309	
10	9809.377		9809.064		9799.104		9799.473	*	9790.371	*	9790.082	
11	9808.817		9808.501		9797.644		9797.998		9788.022		9787.704	
12	9808.121	*	9807.797		9796.043		9796.401			*	9785.215	
13	9807.286		9806.990		9794.306		9794.666		9782.897		9782.584	
14		*	9806.021		9792.434		9792.804		9780.120		9779.826	*
15	9805.219		9804.931		9790.431		9790.812		9777.227		9776.923	
16	9803.994	*	9803.722	*	9788.309		9788.677		9774.192	*	9773.916	*
17	9802.634		9802.339		9786.041		9786.426	*	9771.028		9770.730	
18	9801.123		9800.849		9783.636		9784.024		9767.719		9767.417	
19	9799.503	*	9799.219		9781.117	*	9781.500		9764.276		9764.005	
20	9797.738	*	9797.457		9778.445		9778.829		9760.720		9760.435	*
21	9795.829		9795.564		9775.623		9776.029	*	9757.011		9756.739	
22	9793.795		9793.529	*	9772.713		9773.108		9753.191	*	9752.924	
23	9791.616		9791.381		9769.621		9770.032		9749.214	*	9748.956	
24	9789.299		9789.073		9766.444		9766.836		9745.088	*	9744.835	*
25	9786.882		9786.618		9763.107		9763.520		9740.888		9740.628	
26	9784.294		9784.059		9759.638		9760.045		9736.506		9736.270	
27	9781.581			*	9756.032		9756.441		9732.010		9731.778	
28	9778.748		9778.533		9752.311	*	9752.713		9727.371		9727.123	
29	9775.768		9775.560		9748.413		9748.836		9722.594		9722.375	
30	9772.652		9772.429		9744.408		9744.835		9717.694		9717.474	*
31	9769.397		9769.190		9740.262		9740.696		9712.645		9712.444	
32	9766.021		9765.815		9735.987		9736.416		9707.480		9707.287	
33	9762.485		9762.303		9731.569		9732.010		9702.185		9701.977	
34	9758.818		9758.648		9727.018		9727.462		9696.744		9696.549	
35	9755.024		9754.872	*	9722.319		9722.783		9691.162		9690.981	*
36	9751.103		9750.922		9717.519		9717.970		9685.487	*	9685.263	
37	9747.019		9746.860		9712.571		9713.010		9679.588	*	9679.429	
38	9742.820		9742.655		9707.480		9707.917		9673.621		9673.428	*
39	9738.479		9738.316		9702.246		9702.705		9667.492		9667.362	*
40	9733.984		9733.851		9696.879		9697.336		9661.258	*	9661.094	*
41	9729.362		9729.221		9691.378		9691.841		9654.861		9654.722	
42	9724.619		9724.486		9685.739		9686.191		9648.346		9648.200	
43	9719.707		9719.602		9679.964		9680.406	*	9641.679		9641.533	
44	9714.706		9714.563		9674.047		9674.513		9634.894		9634.756	

Appendix III -- $^5\Phi_1 - X^5\Delta_0$ (1,1) (cont.)

J	R		Q		P	
	aa	bb	ab	ba	aa	bb
45	9709.532	9709.397	9667.981 *	9668.460	9627.950 *	9627.830
46			*	9662.279	9620.884	9620.754
47			9655.498	9655.969	9613.684 *	9613.562
48					9606.331	9606.218

$^5\Phi_2 - X^5\Delta_1$ (1,1)

J	R	Q	P
1	9866.051	-	-
2	9866.680	9863.999 *	-
3	9867.177 *	9863.577	9860.872 *
4	9867.536	9863.045	9859.474 *
5	9867.750	9862.380	9857.849 *
6	9867.857	9861.578	*
7	9867.814	9860.636	9854.348
8	9867.646	9859.563	9852.387
9	9867.335	9858.357	*
10	9866.894	9857.025	9848.049
11	9866.294	9855.529	9845.668
12	9865.603	9853.937	9843.204 *
13	9864.751	9852.193	9840.530
14	9863.774	9850.309	9837.765
15	9862.645	9848.303	9834.857
16	9861.404	9846.159	9831.815
17	9860.010	9843.873	9828.630
18	9858.496	9841.453	9825.322
19	9856.840	9838.907	9821.874 *
20	9855.042	9836.228	9818.296
21	9853.108	9833.407	9814.587
22	9851.044	9830.444	9810.737
23	9848.850	9827.353	9806.760
24	9846.513	9824.134	9802.634
25	9844.048	9820.765	9798.376 *
26	9841.453	9817.268	9793.988
27	9838.689	9813.640	9789.469
28	9835.804	9809.866	9784.817
29	9832.794	9805.944 *	9779.992 *
30	9829.637	9801.927	9775.082
31	9826.350	9797.738 *	9770.032
32	9822.941	9793.430	9764.835
33	9819.348	9788.977 *	*
34	9815.655 *	9784.377 *	9754.004 *
35	9811.833 *	9779.684	9748.413

Appendix III -- $^5\Phi_2$ - $X^5\Delta_1$ (1,1) (cont.)

J	R		Q		P	
	aa	bb	ab	ba	aa	bb
36	9807.860		9774.832 *		9742.655 *	
37	9803.752 *	9803.722 *	9769.828 *		9736.779	
38	9799.503 *	9799.473 *	9764.680 *	9764.708 *	9730.801 *	9730.769 *
39	9795.121 *	9795.094 *	9759.411 *			* 9724.619
40	9790.571 *		9754.004 *	9754.044 *	9718.372 *	9718.331
41	9785.936	9785.895	9748.477	9748.520	9711.962	9711.915
42	9781.160	9781.117	9742.820 *	9742.853 *	9705.444 *	9705.376 *
43	*	9776.228	9737.015 *	9737.058 *	9698.725 *	9698.690 *
44	9771.228	9771.181	9731.095	9731.133		
45	9766.082	9766.021	9725.027	9725.085		
46	9760.776 *	9760.720 *	9718.875	9718.916		
47			9712.571 *	9712.645		
48			9706.225	9706.278		

$^5\Phi_3$ - $X^5\Delta_2$ (1,1)

J	R	Q	P
2	9919.705 *	-	-
3	9920.226 *	9916.624	-
4	9920.609 *	9916.111 *	9912.546 *
5	9920.862 *	9915.464	9910.974
6	9920.992 *	9914.696	9909.321
7	9920.992 *	9913.806	9907.503 *
8	9920.862 *	9912.777	9905.606
9	9920.609 *	9911.617	9903.532
10	9920.226 *	9910.350	9901.371
11	9919.705 *	9908.947	9899.070
12	9919.089	9907.410	9896.638
13	9918.361	9905.766	*
14	9917.529	9904.008	9891.410
15	9916.624	9902.147	9888.653 *
16	9915.729 *	9900.225	9885.726
17	9915.016	9898.302	9882.793
18	9914.782 *	9896.570	9879.853
19		9895.273 *	9877.105
20			9874.769
18	9910.129	9892.116	
19	9909.141	9890.656	9872.635
20	9907.718	9888.653	9870.175 *
21	9905.999	9886.187	9867.091 *
22	9904.065	9883.455	9863.645

Appendix III -- $^5\Phi_1$ - $X^5\Delta_2$ (1,1) (cont.)

J	R		Q		P	
23	9901.973		9880.503		9859.888	
24	9899.697	*	9877.388		9855.916	
25	9897.295		9874.103		9851.775	
26	9894.729		9870.648		9847.479	
27	9892.011		9867.091		9842.996	
28	9889.176		9863.344		9838.378	*
29	9886.187		9859.474	*	9833.667	
30	9883.034		9855.465		9828.780	
31	9879.752		9851.305		9823.745	
32	9876.326		9847.009		9818.566	
33	9872.752		9842.564		9813.252	
34	9869.044		9837.987		9807.797	*
35	9865.211		9833.258		9802.198	
36	9861.209		9828.396		9796.429	
37	9857.071		9823.383		9790.571	
38	9852.789		9818.216		9784.547	
39	9848.366		9812.946		9778.397	
40	9843.810		9807.510		9772.087	
41	9839.110		9801.927		9765.655	*
42	9834.242	*	9796.229		9759.052	
43	9829.278		9790.371		9752.311	*
44	9824.134		9784.377		9745.475	
45	9818.873		9778.243		9738.479	
46	9813.474	*	9771.962		9731.327	*
47	9807.914		9765.543		9724.035	
48	9802.226	*	9758.991		9716.620	
49	9796.496	*	9752.311	*	9709.056	
50	9790.431		9745.596	*	9701.378	*
51	9784.059	*	9738.479		9693.599	
52	9777.812	*	9731.133		9685.487	*
53	9771.437	*	9723.871		9677.184	
54	9764.905		9716.484		9668.894	
55	9758.218		9708.951		9660.495	*
56	9751.390		9701.272		9651.998	
57	9744.408	*	9693.440		9643.297	
58	9737.330		9685.487		9634.469	*
59	9730.144		9677.391		9625.544	
60	9722.849	*	9669.180			
61			9660.892			
62			9652.464			

Appendix III (cont.) -- $^5\Phi_4$ - $X^5\Delta_3$ (1,1)

J	R			Q			P		
	aa	bb		ab	ba		aa	bb	
3	9958.989			-			-		
4	9959.510			9954.937	*?				
5	9959.920			9954.420	*				
6	9960.240			9953.807			9948.235	*	
7	9960.433	*		9953.102			9946.648		
8	9960.549	*		9952.308			9944.925		
9	9960.549	*		9951.370	*		9943.105		
10	9960.433	*		9950.344			9941.152	*	
11	9960.183			9949.206			9939.150		
12	9959.813			9947.938			9936.940	*	
13	9959.325			9946.558			9934.688	*	
14	9958.698			9945.053			9932.275		
15	9957.962			9943.419			9929.761		
16	9957.069			9941.647			9927.098		
17	9956.046			9939.738			9924.320		
18	9954.877			9937.695			9921.409		
19	9953.551			9935.522			9918.303	*	
20	9952.076	*		9933.163			9915.122		
21	9950.462			9930.679	*				
22	9948.723			9928.039			9908.235	*	
23	9946.817			9925.289			9904.612		
24	9944.762			9922.378	*		9900.840		
25	9942.543			9919.283			9896.898	*	
26	9940.167			9916.064			9892.820		
27	9937.648			9912.673			9888.573		
28	9934.963			9909.141			9884.175		
29	9932.142			9905.430			9879.602		
30	9929.161			9901.608			9874.913		
31	9926.032			9897.611			9870.062		
32	9922.755			9893.461			9865.055		
33	9919.283			9889.176			9859.888		
34	9915.729			9884.723			9854.601		
35	9911.988			9880.121			9849.132		
36	9908.091	*		9875.392			9843.519		
37	9904.065			9870.431	9870.503	*	9837.765		
38	9899.881			9865.445			9831.815	9831.874	*
39				9860.254			9825.812		

Appendix III (cont.) -- $^5\Phi_5$ - $X^5\Delta_4$ (1,1)

J	R		Q		P	
4			-		-	
5			9994.984	*	-	
6	10000.437	*	9994.232			
7	10000.437	*	9993.351	*	9987.177	*
8	10000.313		9992.331	*		*
9	10000.042	*	9991.139	*	9983.200	*
10	9999.660		9989.883		9981.036	
11	9999.135		9988.500		9978.750	
12	9998.486		9986.961		9976.334	
13	9997.707		9985.300		9973.774	
14	9996.797		9983.515		9971.104	
15	9995.748		9981.602		9968.308	
16	9994.602		9979.549		9965.380	
17	9993.304		9977.367		9962.322	
18	9991.887		9975.049		9959.132	
19	9990.322		9972.634		9955.809	
20	9988.640		9970.068		9952.368	
21	9986.807		9967.366		9948.791	
22	9984.879		9964.529		9945.053	*
23	9982.800		9961.586		9941.248	
24	9980.583		9958.495		9937.279	
25	9978.221		9955.267		9933.163	
26	9975.760		9951.916		9928.952	
27	9973.131		9948.429		9924.590	
28	9970.408		9944.812		9920.086	
29	9967.527		9941.062		9915.464	
30	9964.529		9937.172		9910.702	
31	9961.371		9933.163		9905.810	*
32	9958.084		9929.003		9900.789	
33	9954.667		9924.712		9895.627	
34	9951.120		9920.289		9890.335	
35	9947.425		9915.729		9884.901	
36	9943.601		9911.044		9879.336	
37	9939.635		9906.206		9873.646	
38	9935.522		9901.232		9867.814	
39	9931.290		9896.132		9861.835	
40	9926.908		9890.889		9855.737	
41	9922.378		9885.514		9849.486	*
42	9917.741		9879.996		9843.106	
43	9912.938		9874.335		9836.595	
44	9908.008		9868.543		9829.924	
45	9902.935		9862.603		9823.142	
46	9897.713		9856.521		9816.208	
47	9892.345		9850.309		9809.112	
48	9886.843		9843.952		9801.927	

$^5\Phi_5$ - $X^5\Delta_4$ (1,1) (cont.)

J	R		Q		P	
49	9881.181		9837.459	*	9794.555	
50	9875.423	*	9830.817		9787.070	
51	9869.475		9824.034		9779.431	*
52	9863.393	*	9817.104		9771.656	
53	9857.180				9763.736	
54	9850.814		9802.822		9755.681	
55	9844.293		9795.466		9747.486	
56	9837.621		9787.954		9739.143	
57	9830.817	*	9780.327	*	9730.635	
58	9823.882	*	9772.527		9721.991	
59	9816.795		9764.592		9713.229	
60	9809.536		9756.496		9704.275	
61	9802.151		9748.264		9695.232	
62	9794.604		9739.897		9686.014	
63	9786.916		9731.363		9676.645	*
64	9779.052		9722.673		9667.151	*
65	9771.084		9713.866			
66	9762.944		9704.894			
67	9754.646		9695.774			
68	9746.227	*	9686.489			
69			9677.078			
70			9667.492			
71			9657.783			
72			9647.909	*		

$^5\Phi_4$ - $X^5\Delta_3$ (1,3)

J	R		Q		P	
3	8244.462		-		-	
4	8245.046		8240.436		-	
5	8245.524	*	8240.011	*		
6	8245.948		8239.544	*		
7	8246.276		8238.922	*		
8	8246.498		8238.232			
9	8246.639	*	8237.462			
10	8246.639	*	8236.574			
11		*	8235.609			
12	8246.399		8234.521			
13	8246.086		8233.329			
14	8245.695		8232.039			
15	8245.156		8230.609			
16	8244.519		8229.089			

Appendix III -- $^5\Phi_4 - X^5\Delta_3$ (1,3) (cont.)

J	R		Q		P	
17	8243.759		8227.453			
18	8242.863		8225.676			
19	8241.826		8223.781			
20		*	8221.752			
21	8239.370		8219.585	*		
22	8237.928	*	8217.279			
23	8236.397		8214.869			
24	8234.705		8212.313			
25	8232.841		8209.619			
26	8230.885		8206.787			
27	8228.771		8203.810			
28	8226.516		8200.691			
29	8224.090	*	8197.438			
30	8221.602		8194.053			
31	8218.944					
32	8216.147					
33						
34	8210.139					

$^5\Phi_5 - X^5\Delta_4$ (1,3)

J	R		Q		P	
4	8285.498		-		-	
5	8285.820		8280.483	*	-	
6	8286.035		8279.842			
7	8286.121	*	8279.042			
8	8286.121	*	8278.115	*		
9	8285.993		8277.108			
10	8285.755		8276.001			
11	8285.382		8274.758		8265.027	
12	8284.926		8273.393		8262.770	
13	8284.346		8271.939		8260.423	
14	8283.651		8270.345		8257.963	
15	8282.824		8268.673		8255.380	
16	8281.911	*	8266.868		8252.698	
17	8280.880		8264.948		8249.888	
18	8279.725		8262.888		8246.973	
19	8278.461		8260.738		8243.933	
20	8277.067		8258.487		8240.793	
21	8275.560		8256.103		8237.532	
22	8273.943		8253.613		8234.146	
23	8272.215		8251.000		8230.662	*

$^5\Phi_5 - X^5\Delta_4$ (1,3) (cont.)

J	R		Q		P	
24	8270.345		8248.261		8227.033	
25	8268.372		8245.401		8223.323	
26	8266.297		8242.435		8219.479	
27	8264.092		8239.370		8215.525	
28	8261.775		8236.173		8211.461	*
29	8259.327		8232.841		8207.263	
30	8256.764		8229.418		8202.947	
31	8254.085		8225.864		8198.524	
32	8251.279		8222.191		8193.986	
33	8248.362		8218.410		8189.312	
34	8245.313		8214.470		8184.535	
35	8242.147		8210.454		8179.628	
36	8238.873		8206.297		8174.597	
37	8235.460		8202.024		8169.467	
38	8231.921		8197.626		8164.200	
39	8228.273		8193.112		8158.825	
40	8224.503	*	8188.451		8153.306	
41	8220.581		8183.688		8147.668	
42	8216.564	*	8178.821		8141.928	
43	8212.417		8173.806		8136.046	
44	8208.134		8168.672		8130.048	
45	8203.720		8163.414		8123.942	
46	8199.198		8158.010		8117.707	
47	8194.534		8152.518		8111.346	
48	8189.775	*	8146.877		8104.832	
49		*	8141.114		8098.248	*
50	8179.836		8135.235		8091.487	
51	8174.654		8129.220		8084.639	*
52	8169.358		8123.068		8077.630	
53	8163.944		8116.799		8070.503	
54		*	8110.392		8063.256	*
55	8152.701		8103.869		8055.870	
56	8146.877		8097.217		8048.368	*
57	8140.952		8090.431		8040.749	
58	8134.865		8083.504		8032.977	
59	8128.658		8076.456		8025.087	
60	8122.307		8069.270			
61		*	8061.957			
62	8109.242		8054.515			
63	8102.493		8046.927	*		

Appendix III (cont.) -- $^5\Phi_5 - X^5\Delta_4$ (1,4)

J	R		Q		P	
4	7442.059	*	-		-	
5	7442.438		7437.133		-	
6	7442.676	*	7436.485		7431.176	
7	7442.838	*	7435.755		7429.552	*
8	7442.887		7434.921		7427.833	*
9	7442.838	*	7433.969		7425.994	
10	7442.676	*	7432.920	*	7424.048	*
11	7442.397		7431.761		7422.007	
12	7442.025		7430.499		7419.863	*
13	7441.540	*	7429.124		7417.604	*
14	7440.948		7427.661		7415.258	
15	7440.250		7426.080		7412.795	
16	7439.440		7424.391	*	7410.228	*
17	7438.530		7422.596		7407.545	
18	7437.509		7420.701		7404.759	*
19	7436.380	*	7418.683		7401.875	
20	7435.153		7416.572		7398.879	*
21	7433.785		7414.343	*	7395.766	*
22	7432.348		7411.998		7292.539	
23	7430.784		7409.570		7389.237	
24	7429.124	*	7407.030		7385.807	
25	7427.336		7404.365		7382.271	*
26	7425.439		7401.593		7378.622	*
27	7423.435		7398.717		7374.867	
28	7421.323		7395.709		7371.009	
29	7419.102		7392.630		7367.010	*
30	7416.765		7389.416	*	7362.958	
31	7414.311	*	7386.097		7358.750	*
32	7411.750		7382.662		7354.442	
33	7409.076		7379.121		7350.038	
34	7406.287		7375.463		7345.497	*
35	7403.381	*	7371.697		7340.863	*
36	7400.369		7367.805		7336.108	
37	7397.235	*	7363.798	*	7331.246	*
38	7393.997		7359.697		7326.271	*
39	7390.632	*	7355.456	*	7321.183	*
40	7387.153		7351.115		7315.969	
41	7383.560	*	7346.683		7310.676	*
42	7379.859	*	7342.101		7305.218	
43	7376.024		7337.415		7299.672	
44	7372.084		7332.611		7294.011	
45	7368.018		7327.700		7288.225	
46	7363.798	*	7322.650		7282.332	*
47	7359.530	*	7317.493		7276.324	*
48	7355.107		7312.226		7270.19	*

$^5\Phi_5 - X^5\Delta_4$ (1,4) (cont.)

J	R		Q		P	
49	7350.589	*	7306.827		7263.928	*
50	7345.890	*	7301.314		7259.580	
51	7341.124	*	7295.684	*	7251.095	
52	7336.231	*	7289.933		7244.491	*
53	7331.199	*	7284.080	*	7237.762	*
54	7326.058		7278.071		7230.901	*
55	7320.784	*	7271.946		7223.954	*
56	7315.358	*	7265.711			
57	7309.878	*	7259.360	*		
58	7304.234	*	7252.851	*		
59	7298.464	*	7246.266			
60	7292.583	*	7239.542			
61	7286.545	*	7232.692			
62	7280.443	*	7225.699			
63	7274.153		7218.608			
64		*	7211.390			
65	7261.229	*	7204.013			
66	7254.593	*	7196.555			
67			7188.942	*		

$^5\Phi_1 - X^5\Delta_0$ (2,0)

J	R bb		Q ba		P bb	
0			-		-	
1					-	
2			11273.606	*		
3			11273.142	*		
4			11272.570	*		
5			11271.823	*		
6			11270.939			
7	11276.808	*	11269.935		11263.309	*
8	11276.551	*	11268.767		11261.249	*
9	11276.122	*	11267.450		11259.054	*
10	11275.564	*	11265.994		11256.688	
11	11274.884	*	11264.387		11254.195	*
12	11274.003	*	11262.645		11251.543	*
13	11273.015		11260.736	*	11248.750	
14	11271.876	*	11258.710	*	11245.833	*
15	11270.610	*	11256.525			*
16	11269.175	*	11254.195	*	11239.496	
17	11267.604		11251.729	*	11236.122	
18	11265.905	*	11249.115		11232.602	*

Appendix III -- $^5\Phi_1 - X^5\Delta_0$ (2,0) (cont.)

J	R		Q		P	
	aa	bb	ab	ba	aa	bb
19		11264.037		11246.368		11228.963
20		11262.026	11240.258	11243.468		11225.172 *
21	11257.743 *	11259.903	11237.490	11240.432		11221.235
22	11255.567	11257.643	11234.487	11237.261	11214.839	11217.166
23	11253.200	11255.236	11231.264	11233.953	11210.783	11212.957
24	11250.639 *	11252.710 *	11227.846	11230.504	11206.504	11208.607
25	11247.938	11250.020 *	11224.257	11226.919	11202.073	11204.116
26	11245.045	11247.217	11220.499	11223.208	11197.444	11199.499
27	11241.993 *	11244.280 *	11216.580 *	11219.367	11192.652	11194.743
28	11238.802	11241.205 *	11212.496 *	11215.396	11187.691	11189.860 *
29	11235.434 *	11238.042	11208.261	11211.301	11182.566 *	11184.858
30	11231.931	11234.744	11203.867	11207.077	11177.274	11179.722
31	11228.236 *	11231.316	11199.327 *	11202.739	11171.844	11174.473
32	11224.472 *	11227.725 *	11194.630	11198.275	11166.284	11169.120 *
33	11220.499 *	11224.169 *	11189.789	11193.685	11160.565 *	11163.577 *
34	11216.392	11220.360	11184.772	11189.019	11154.663	11158.001 ?
35	11212.144	11216.483	11179.644	11184.217	11148.637	11152.265
36	*		11174.366	11179.302	11142.471	11146.443
37	11203.193		11168.935	11174.269 *	11136.157	
38	11198.508 *		11163.357	11169.120	11129.679 *	
39	11193.685 *		11157.646		11123.082 *	
40	11188.711		11151.781		11116.327	
41	11183.607		11145.784		11109.435	
42	11178.365		11139.650		11102.397 *	
43	11172.991		11133.381		11095.246	
44	11167.476 *		11126.995		11087.949	
45	11161.881 *		11120.468		11080.523	
46	11156.147		11113.819		11072.973 *	
47			11107.067		11065.298 *	
48			11100.203 ?		11057.526 *	

$^5\Phi_2 - X^5\Delta_1$ (2,0)

J	R	Q	P
1		-	-
2		11331.705 *	-
3	11334.795	11331.245	
4	11335.073 *	11330.666 *	11327.128 *?
5	11335.220 *	11329.881 *	11325.467 *
6	11335.220 *	11328.990 *	11323.703 *
7	11335.013	11327.909	11321.711 *
8	11334.673 *	11326.698 *	11319.593 *
9	*	11325.333 *	11317.354

Appendix III -- $^5\Phi_2$ - $X^5\Delta_1$ (2,0) (cont.)

J	R				Q				P			
	aa		bb		ab		ba		aa		bb	
10	11333.585				11323.820				11314.935	*		
11	11332.810				11322.133	*			11312.392	*		
12	11331.880				11320.339				11309.684			
13	11330.808				11318.373	*			11306.837			
14		*			11316.262				11303.835			
15	11328.216	*			11313.999	*			11300.681			
16	11326.698				11311.594				11297.393	*		
17	11325.065				11309.047	*			11293.955	*		
18	11323.445				11306.378				11290.349	*		
19	11320.884	*			11303.744	*			11286.655	*		
20	11318.883				11300.123	*			11282.975	*		
21	11316.632	*			11297.083				11278.325			
22	11314.223				11293.806				11274.248			
23	11311.643	*			11290.349	*			11269.935	*		
24	11308.915	*			11286.743	*			11265.447			
25	11306.041	*			11282.975				11260.810	*		
26	11303.002	*			11279.064	*			11256.005			
27	11299.845				11275.012	*			11251.060			
28	11296.512	*			11270.811	*			11245.972			
29	11293.015	*			11266.447				11240.727			
30	11289.461	*			11261.949				11235.348	*		
31	11285.713	*			11257.296	*			11229.819			
32	11281.855				11252.546	*			11224.169	*		
33	11277.884	*			11247.660	*			11218.333	*		
34	11273.870				11242.654	*			11212.439	*		
35	11269.869	*			11237.618	*			11206.404	*		
36	11266.073	*			11232.602	*			11200.348	*		
37					11227.800	*			11194.277	*		
38	11251.060	*							11188.464	*		
39	11247.074	*			11210.640	*	11210.681	*				
40	11242.405	*			11205.646	*	11205.687	*	11169.278	*		
41	11237.331	*			11199.957	*	11200.012	*	11163.270	*	11163.243	*
42	11232.014	*			11193.888	*	11193.929	*	11156.534	*		
43	11226.466	*			11187.547	*	11187.587	*	11149.444	*		
44	11220.778	*	11220.737	*	11180.974	*	11181.028		11142.095	*	11142.068	*
45	11214.839	*			11174.231	*	11174.269	*	11134.516	*	11134.488	*
46	11208.746	*			11167.298		11167.352	*	11126.750	*		
47	11202.483	*			11160.189		11160.248		11118.762	*		
48	11196.098	*			11152.920		11152.984	*	11110.674	*	11110.634	*
49	11189.529	*			11145.476		11145.556	*	11102.397	*	11102.357	*
50	11182.803	*			11137.884		11137.979		11093.923	*		
51					11130.134		11130.250		11085.313	*		
52	11168.838	*	11168.804	*	11122.221	*	11122.437	*	11076.568	*		
53					11114.155		11114.200				11067.705	*

Appendix III (cont.) -- $^5\Phi_3$ - $X^5\Delta_2$ (2,0)

J	R		Q		P	
2	11386.066		-		-	
3	11386.492				-	
4	11386.752		11382.347			
5	11386.865	*	11381.592			
6	11386.837	*	11380.644	*	11375.380	*
7	11386.647	*	11379.585	*	11373.366	*
8	11386.296		11378.367	*	11371.317	
9	11385.804		11376.999	*	11369.038	*
10	11385.157	*	11375.475		11366.640	
11	11384.356		11373.802	*	11364.090	
12	11383.383		11371.956		11361.381	
13	11382.297		11369.969		11358.523	
14	11381.034		11367.815		11355.502	
15	11379.626	*	11365.545		11352.336	*
16	11378.080		11363.096		11349.013	
17	11376.358		11360.509		11345.544	
18	11374.493		11357.764		11341.911	
19	11372.479		11354.878		11338.148	*
20	11370.313		11351.828			*
21	11368.009		11348.632		11330.156	
22	11365.545		11345.300		11325.921	
23	11362.972		11341.817		11321.557	
24	11360.265		11338.192		11317.080	*
25	11357.504		11334.467		11312.392	*
26	11354.878	*	11330.666		11307.629	
27			11327.045		11302.812	
28	11347.087				11298.185	*
29	11343.639		11317.182			
30	11339.976	*	11312.703		11286.242	
31	11336.180	*	11308.029	*	11280.743	
32	11332.231	*	11303.198	*	11275.012	*
33	11328.054		11298.185	*	11269.175	
34	11323.770		11293.015	*	11263.150	*
35	11319.361	*	11287.708		11256.953	
36	11314.725		11282.240		11250.639	
37	11309.960		11276.620		11244.117	*
38	11305.045	*	11270.811	*	11237.490	*
39	11299.997		11264.915		11230.689	
40	11294.781		11258.829		11223.716	*
41	11289.417	*	11252.584	*	11216.580	*
42	11283.857	*	11246.209		11209.393	
43	11278.212		11239.671		11201.983	
44	11272.385		11232.979		11194.428	
45	11266.447	*	11226.134		11186.722	
46	11260.270		11219.133		11178.861	

$^5\Phi_3$ - $X^5\Delta_2$ (2,0) (cont.)

J	R		Q		P	
47	11253.985		11211.986		11170.845	
48	11247.549		11204.663	*	11162.686	
49	11240.957		11197.235		11154.368	
50			11189.638		11145.904	
51			11181.894		11137.299	
52			11174.011		11128.554	*
53			11165.970			
54			11157.802			
55			11149.507			
56			11141.103			
57			11132.632			

$^5\Phi_4$ - $X^5\Delta_3$ (2,0)

J	R		Q		P	
3	11418.814	?	-		-	
4	11419.002	*	11414.698	*	-	
5	11419.002	*	11413.854	*	11409.563	*
6	11418.859		11412.847		11407.698	
7	11418.588		11411.681		11405.673	*
8	11418.157		11410.354		11403.471	
9	11417.583		11408.913		11401.114	*
10	11416.863		11407.304	*	11398.643	
11		*	11405.553		11395.992	
12	11414.994		11403.668		11393.236	
13	11413.854		11401.638		11390.296	
14	11412.579		11399.473		11387.253	
15	11411.165		11397.154	*	11384.097	*
16	11409.615		11394.737		11380.737	
17	11407.930		11392.163	*	11377.236	*
18	11406.110		11389.443		11373.670	
19	11404.150		11386.594	*	11369.969	*
20	11402.052		11383.617		11366.053	
21	11399.820		11380.491	*	11362.053	
22	11397.449		11377.236		11357.912	
23	11394.944		11373.845		11353.608	
24	11392.293		11370.313		11349.210	
25	11389.512		11366.640		11344.659	
26	11386.594	*	11362.833		11339.976	
27	11383.514	*	11358.884		11335.132	
28	11380.307		11354.800		11330.156	
29	11376.957		11350.564		11325.065	

Appendix III -- $^5\Phi_4 - X^5\Delta_3$ (2,0) (cont.)

J	R		Q		P	
30	11373.427	*	11346.178		11319.807	
31	11369.814		11341.681		11314.411	
32	11366.053		11337.027		11308.890	
33	11362.131		11332.231		11303.198	
34			11327.298		11297.393	
35	11353.775	*			11291.441	
36	11349.398		11316.873			
37	11344.899		11311.508		11279.018	*
38	11340.234		11305.993		11272.605	
39	11335.407	*	11300.308		11266.073	
40	11330.453		11294.485		11259.378	
41	11325.333		11288.500		11252.546	*
42	11320.063	*	11282.364		11245.540	*
43	11314.626		11276.076		11238.384	
44	11309.047	*	11269.630		11231.087	
45	11303.295		11263.029	*	11223.626	
46	11297.393	*	11256.289		11216.022	
47	11291.341		11249.386		11208.261	*
48	11285.151	*	11242.318		11200.348	
49	11278.750	*	11235.100		11192.274	
50	11272.232		11227.725		11184.049	
51	11265.556		11220.191		11175.670	
52	11258.710	*	11212.496	*	11167.129	
53	11251.729	*	11204.663	*	11158.431	*
54			11196.641		11149.583	
55			11188.464	?	11140.571	

$^5\Phi_5 - X^5\Delta_4$ (2,0)

J	R		Q		P	
4	11382.662		-		-	
5	11383.157				-	
6	11383.514	*	11376.999	*		
7	11383.809	*	11376.358		11369.882	*
8	11383.999	*	11375.645		11368.199	
9	11384.097	*	11374.817		11366.453	*
10	11384.097	*	11373.845	*	11364.577	*
11	11383.999	*	11372.858		11362.648	
12	11383.809	*	11371.740		11360.631	*
13	11383.514	*	11370.526		11358.472	
14	11383.084		11369.201	*	11356.233	*
15	11382.596		11367.786	*	11353.877	

$^5\Phi_5 - X^5\Delta_4$ (2,0) (cont.)

J	R		Q		P	
16	11381.989		11366.272		11351.431	
17	11381.279		11364.637		11348.919	
18	11380.491	*	11362.905		11346.252	
19	11379.533		11361.068		11343.501	
20	11378.495		11359.111		11340.640	
21	11377.335		11357.056		11337.692	
22	11376.066		11354.878	*	11334.610	
23	11374.681		11352.606		11331.428	
24	11373.182		11350.179		11328.119	
25	11371.549		11347.676		11324.698	
26	11369.814		11345.030		11321.157	
27	11367.921		11342.266		11317.498	
28	11365.922		11339.378		11313.717	
29	11363.779		11336.357		11309.809	
30	11361.510		11333.200		11305.805	*
31	11359.111		11329.917		11301.609	
32	11356.568		11326.497		11297.336	*
33	11353.877		11322.944		11292.875	
34	11351.043		11319.240		11288.335	*
35	11348.056		11315.404		11283.598	
36	11344.951		11311.417		11278.750	
37	11341.681		11307.259		11273.745	
38	11338.243	*	11303.002		11268.590	
39	11334.673		11298.554		11263.309	
40	11330.926		11293.955		11257.854	
41	11327.045		11289.213		11252.248	
42	11322.944		11284.306		11246.489	
43	11318.725		11279.229		11240.578	
44	11314.339		11274.003		11234.487	
45	11309.809	*	11268.590	*	11228.249	*
46	11305.045	*	11263.029	*	11221.845	
47	11300.123	*	11257.296		11215.273	
48	11295.044		11251.375		11208.531	
49	11289.791		11245.290		11201.615	
50	11284.343		11239.033		11194.532	
51	11278.750		11232.602	*	11187.266	
52	11272.957		11225.980		11179.835	
53	11266.982	*	11219.188		11172.219	
54	11260.810	*	11212.223		11164.433	
55	11254.499		11205.067		11156.458	
56	11247.968		11197.734		11148.309	
57	11241.269		11190.222		11139.982	
58	11234.376		11182.516		11131.473	
59	11227.289	*	11174.639		11122.764	
60	11220.081	*	11166.571		11113.905	

Appendix III -- $^5\Phi_5 - X^5\Delta_4$ (2,0) (cont.)

J	R	Q	P
61	11212.613	11158.317	11104.848 *
62	11205.003	11149.884	11095.571
63		11141.292	11086.171

$^5\Phi_7 - X^5\Delta_1$ (2,2)

J	R	Q	P
1		-	-
2			-
3		9598.371	
4		9597.827	
5		9597.137	
6	9602.535	9596.331	
7	9602.474	9595.356	
8	9602.273	9594.279 *	
9	9601.932	9593.027 *	9585.070
10	9601.458	9591.682	9582.825
11	9600.855	9590.205	9580.430
12	9600.131 *	9588.584	9577.914
13	9599.246	9586.811	9575.279
14	9598.241	9584.915	9572.484
15	9597.084	9582.886	9569.569
16	9595.836	9580.729	9566.518 *
17	9594.467	9578.446	9563.300 *
18		9576.052	9560.026
19			9556.566 *

$^5\Phi_3 - X^5\Delta_2$ (2,2)

J	R	Q	P
2		-	-
3	9653.548	9650.086 *	-
4	9653.857	9649.493	9646.015 *
5	9654.073 *	9648.783	9644.443 *
6	9654.155 *	9647.951	9642.671
7	9654.033 *	9646.985	*
8	9653.807 *	9645.881 *	9638.843
9	9653.472	9644.666	*
10	9652.977	9643.297	9634.469 *

$^5\Phi_3 - X^5\Delta_2$ (2,2) (cont.)

J	R	Q	P
11	9652.330	*	*
12	9651.584 *	9640.115	9629.550 *
13	9650.658 *	9638.323	9626.858 *
14	9649.602	9636.403	9624.041 *
15	9648.414	9634.344	9621.118
16	9647.110	9632.145	9618.072
17	9645.665	9629.844 *	9614.860
18	9644.076	9627.348	9611.499
19	9642.352	9624.741	9608.018
20	9640.500	9622.003	9604.391
21	9638.512	9619.137	9600.634
22	9636.403	9616.134	9596.763
23	9634.166	9613.011	9592.742 *
24	9631.826	9609.756	9588.584 *
25	9629.445	9606.407	9584.341
26	9627.246	9603.009	9579.985 *
27		9599.797	9575.576
28	9620.294		9571.357
29	9617.271	9590.838 *	
30	9614.084 *	9586.811 *	9560.334
31	9610.738	9582.599	9555.308 *
32	9607.256 *	9578.244	9550.099 *
33	9603.612	9573.752	9544.759 *
34	9599.845 *	9569.078	
35	9595.948	9564.317 *	
36	9591.891	9559.430 *	
37	9587.701	9554.353	
38	9583.383	9549.161	
39	9578.899	9543.831	
40	9574.308	9538.357	
41	9569.569 *	9532.754	
42		9527.027 *	
43		9521.127	

$^5\Phi_4 - X^5\Delta_3$ (2,2)

J	R	Q	P
3	9685.809 *	-	-
4	9686.014	9681.721 *	-
5	9686.112	9680.966	
6	9686.079 *	9680.047	
7	9685.896	9678.996 *	

Appendix III -- $^5\Phi_4$ - $X^5\Delta_3$ (2,2) (cont.)

J	R		Q		P	
8	9685.584		9677.795			
9	9685.136		9676.469			
10	9684.572		9675.016			
11	9683.876		9673.428			
12	9683.053		9671.730		9661.313	*
13	9682.110		9669.893		9658.563	
14	9681.032		9667.928		9655.720	
15	9679.861		9665.865		9652.764	
16	9678.556		9663.675	*	9649.671	
17	9677.123		9661.348		9646.458	
18	9675.581		9658.911		9643.146	*
19	9673.888		9656.353		9639.682	*
20	9672.109		9653.671		9636.118	
21	9670.196		9650.869		9632.432	
22	9668.164		9647.951		9628.618	
23	9665.998	*	9644.906		9624.693	*
24	9663.675	*	9641.736		9620.637	
25	9661.313	*	9638.425		9616.460	
26	9658.779		9635.026		9612.159	*
27	9656.120		9631.492		9607.740	
28	9653.339	*	9627.830	*	9603.195	*
29	9650.436		9624.041	*	9598.526	
30	9647.392	*	9620.124		9593.730	
31	9644.228		9616.066	*	9588.816	
32	9640.937		9611.906		9583.769	
33	9637.512	*	9607.646	*	9578.589	
34			9603.195	*	9573.269	
35	9630.183				9567.864	
36	9626.376		9593.852			
37	9622.442		9589.048			*
38	9618.353		9584.108		9550.720	
39	9614.120	*	9578.998		9544.759	*
40	9609.756	*	9573.791		9538.738	*
41	9605.255		9568.428		9532.463	
42	9600.634	*	9562.930		9526.124	*
43	9595.836	*	9557.291	*	9519.611	*
44	9590.932	*	9551.510	*	9512.976	
45	9585.876		9545.608		9506.184	*
46	9580.672		9539.561	*	9499.289	*
47	9575.338		9533.369		9492.247	
48	9569.873	*	9527.027	*		
49	9564.238	*	9520.531	*		
50	9558.458		9513.942			
51	9552.566		9507.188			
52	9546.493		9500.288			

$^5\Phi_4$ - $X^5\Delta_3$ (2,2) (cont.)

J	R		Q		P	
53			9493.258	*		
54			9486.050	*		

$^5\Phi_5$ - $X^5\Delta_4$ (2,2)

J	R		Q		P	
4	9649.602	*	-		-	
5	9650.149				-	
6	9650.620					
7	9651.006		9643.571			
8	9651.319	*	9642.953			
9		*	9642.260	*		
10	9651.695		9641.477			
11	9651.752	*	9640.617			
12	9651.752	*	9639.682	*		
13		*	9638.662			
14	9651.446		9637.542			
15	9651.167		9636.355	*		
16	9650.799		9635.076	*		
17	9650.342		9633.702	*		
18	9649.792		9632.233	*		
19	9649.153		9630.668			
20	9648.414	*	9629.049	*		
21	9647.570		9627.298			
22	9646.635		9625.450			
23	9645.592		9623.513			
24	9644.443		9621.465			
25	9643.194		9619.318			
26	9641.834		9617.063			
27	9640.344		9614.699			
28	9638.775		9612.232			
29	9637.074		9609.647		9583.081	
30	9635.253	*	9606.940		9579.514	
31	9633.311		9604.106		9575.805	
32	9631.251		9601.184		9571.976	
33	9629.049	*	9598.152	*	9568.075	*
34	9626.738		9594.938		9564.006	*
35		*	9591.620		9559.814	
36	9621.703		9588.173		9555.488	
37	9618.987		9584.594		9551.050	
38	9616.134	*	9580.884		9546.493	*
39	9613.114	*	9577.028			
40	9609.995		9573.030			

Appendix III -- $^5\Phi_5$ - $X^5\Delta_4$ (2,2) (cont.)

J	R	Q	P
41	9606.707	9568.908 *	
42	9603.273	9564.621	
43	9599.691	9560.193	
44	9595.948 *	9555.620	
45	9592.064	9550.887	
46	9588.022	9546.017	
47	9583.821	9540.982 *	
48	9579.466	9535.787	
49	9574.939	9530.439	
50	9570.261	9524.920	
51		9519.274 *	
52		9513.421 *	
53		9507.412 *	
54		9501.295 *	
55		9494.957	
56		9488.469	
57		9481.797 *	

$^5\Phi_2$ - $X^5\Delta_1$ (3,0)

J	R	Q	P
1	11928.725 *	-	-
2	11929.205 *	11926.573 *	-
3	11929.656 *	11926.132 *	11923.502 *
4	11929.925 *	11925.492 *	11921.952 *
5	11930.050 *	11924.736	11920.267 *
6	11930.050 *	11923.824	11918.494
7	11929.879 *	11922.770	11916.548 *
8	11929.543	11921.558	11914.462 *
9	11929.081	11920.203	11912.211 *
10	11928.468	11918.684 *	11909.819
11	11927.708 *	11917.034	11907.260 *
12	11926.788	11915.228 *	11904.566
13	11925.736	11913.281	11901.708 *
14	11924.544	11911.192	11898.745 *
15	11923.195 *	11908.959	11895.611 *
16	11921.689 *	11906.568 *	11892.350
17	11920.104	11904.050	11888.978 *
18	11918.367	11901.406	11885.360 *
19	11916.500 *	11898.633	11881.691 *
20	11914.509 *	11895.736 *	11877.859
21	11912.419 *	11892.719	

$^5\Phi_2$ - $X^5\Delta_1$ (3,0) (cont.)

J	R	Q	P
22	11910.228 *	11889.580	
23	11907.926 *	11886.326 *	
24		11883.016	

$^5\Phi_3$ - $X^5\Delta_2$ (3,0)

J	R	Q	P
2	11991.371	-	-
3	11991.807	11988.282	-
4	11992.101 *	11987.664 *	11984.184 *
5	11992.222 *	11986.935 *	11982.493 *
6	11992.222 *	11986.031 *	11980.687
7	11992.092 *	11984.946	11978.762
8	11991.755	11983.803	11976.637 *
9	11991.294	11982.448	11974.483
10	11990.694	11980.959	11972.130
11	11989.944 *	11979.328	11969.584
12	11989.058	11977.544	11966.931
13	*	11975.626	11964.122 *
14	11986.829	11973.565	11961.149
15	11985.535	11971.355	11958.058
16	11984.081	11968.999	11954.818
17	11982.493 *	11966.527	11951.449
18	11980.773	11963.898	11947.937
19	11978.909	11961.149	11944.290
20	11976.946	11958.241 *	11940.504
21	11974.836	11955.259	11936.589
22	11972.623	11952.128	11932.526 *
23	11970.295	11948.882	11928.381
24	11967.856	11945.525	11924.100 *
25	11965.314	11942.057	11919.721
26	11962.647	11938.489	11915.228
27		11934.783	11910.645
28			11905.920 *

Appendix III (cont.) -- $^5\Phi_4$ - $X^5\Delta_3$ (3,0)

J	R		Q		P	
3	12036.064		-		-	
4	12036.267	*	12031.953		-	
5	12036.333		12031.135		12026.866	*?
6	12036.267	*	12030.162	*	12024.975	
7	12036.000		12029.053		12023.045	*
8	12035.596		12027.773		12020.850	
9	12035.056		12026.336		12018.534	*
10	12034.366	*	12024.779		12016.104	*
11	12033.488	*	12023.045		12013.472	
12	12032.484		12021.161	*	12010.714	
13	12031.326		12019.132		12007.804	
14	12030.007		12016.941		12004.740	
15	12028.535		12014.603		12001.524	
16	12026.929		12012.113		11998.152	
17	12025.157		12009.459		11994.654	
18	12023.238		12006.667		11990.973	*
19	12021.161	*	12003.727		11987.161	
20	12018.940		12000.629		11983.188	
21	12016.572		11997.386		11979.051	
22	12014.045		11993.984		11974.804	
23	12011.372		11990.440		11970.376	
24	12008.545		11986.746		11965.807	
25	12005.559	*	11982.893		11961.096	
26	12002.455		11978.909		11956.224	
27	11999.186		11974.754		11951.203	
28	11995.768		11970.465		11946.036	
29	11992.222		11966.022		11940.733	
30	11988.478		11961.436		11935.268	
31	11984.614		11956.702		11929.656	
32	11980.605		11951.812		11923.904	
33			11946.790		11917.996	
34					11911.940	

$^5\Phi_5$ - $X^5\Delta_4$ (3,0)

J	R		Q		P	
4	12047.226		-		-	
5	12047.520		12042.116		-	
6	12047.676	*	12041.379		12036.000	*
7	12047.717		12040.529		12034.250	
8	12047.630		12039.548		12032.394	*
9	12047.427		12038.441		12030.353	*

$^5\Phi_5$ - $X^5\Delta_4$ (3,0) (cont.)

J	R		Q		P	
10	12047.098		12037.217		12028.227	
11	12046.634		12035.856		12025.959	
12	12046.045		12034.366		12023.613	
13	12045.329		12032.768		12021.106	
14	12044.485		12031.030		12018.443	*
15	12043.504		12029.161		12015.694	
16	12042.390		12027.160	*	12012.824	
17	12041.153		12025.039		12009.811	
18	12039.781		12022.783		12006.667	
19	12038.264		12020.384		12003.353	*
20	12036.626		12017.858		11999.972	
21	12034.846		12015.191		11996.425	
22	12032.929		12012.398		11992.728	*
23	12030.860		12009.459	*	11988.918	*
24	12028.672		12006.384		11984.946	*
25	12026.336	*	12003.164		11980.865	*
26	12023.822		11999.810		11976.637	*
27	12021.208	*	11996.311		11972.264	*
28	12018.443	*	11992.664		11967.735	*
29	12015.521		11988.876		11963.089	*
30	12012.460		11984.946	*	11958.241	*
31	12009.251		11980.865		11953.351	
32	12005.872		11976.637		11948.256	
33	12002.361	*	11972.264		11943.008	
34		*	11967.735		11937.623	
35	11994.896		11963.061	*	11932.089	
36	11990.934		11958.241		11926.404	
37	11986.829		11953.262		11920.550	
38	11982.551		11948.137		11914.579	
39	11978.134		11942.860		11908.438	*
40	11973.565		11937.444	*	11902.138	
41	11968.855		11931.862		11895.736	
42	11963.990		11926.132		11889.136	
43	11958.988		11920.267		11882.343	*?
44	11953.828		11914.247		11875.546	?
45	11948.552		11908.096			
46	11943.132		11901.801			
47	11937.623		11895.401			
48	11931.998		11888.856			
49	11926.312		11882.229	*		
50	11920.639	*	11875.546	*		
51	11915.039		11868.860			
52	11909.709	*?	11862.271			
53			11855.869	*?		

Appendix III (cont.) -- $^5\Phi_4$ - $X^5\Delta_3$ (3,3)

J	R		Q		P	
3	9450.388	*				
4	9450.693					
5	9450.870	*	9445.658	*		
6	9450.946		9444.850	*		
7	9450.822		9443.893			
8	9450.621		9442.827	*		
9	9450.263	*		*		
10	9449.787		9440.235	*		
11	9449.203	*	9438.738			
12	9448.468		9437.156			
13	9447.558	*	9435.391			
14	9446.587		9433.526	*		
15	9445.474			*		
16	9444.211		9429.403			
17	9442.827	*	9427.159	*		
18	9441.337		9424.714	*		
19	9439.680			*		
20	9437.918	*	9419.578			
21	9436.003		9416.812	*		
22	9433.992	*	9413.967	*		
23	9431.854			*		
24		*	9407.766	*		
25	9427.159	*	9404.474			
26	9424.642		9401.084	*		
27	9421.981		9397.554			
28	9419.210		9393.887			
29	9416.286		9390.090	*		
30	9413.257		9386.218			
31	9410.079		9382.176			
32	9406.805	*	9378.032			
33			9373.770	*		

$^5\Phi_5$ - $X^5\Delta_4$ (4,0)

J	R		Q		P	
4	12698.519	?	-		-	
5	12698.586	*?	12693.436	*?	-	
6	12698.586	*	12692.510	*	12687.267	?
7	12698.392		12691.406	*	12685.336	
8	12698.050		12690.244	*	12683.259	
9	12697.546		12688.844	*	12680.955	*
10	12696.900		12687.341		12678.673	*

$^5\Phi_5$ - $X^5\Delta_4$ (4,0) (cont.)

J	R		Q		P	
11	12696.113		12685.670	*	12676.107	
12	12695.155		12683.848		12673.426	
13	12694.057		12681.879		12670.522	*
14	12692.805		12679.749	*	12667.578	
15	12691.406	*	12677.495		12664.451	*
16	12689.853		12675.017	*	12661.179	
17	12688.150		12672.490		12657.707	
18	12686.299		12669.773	*	12654.090	*
19	12684.299		12666.906		12650.371	
20	12682.164		12663.885	*	12646.498	
21	12679.860		12660.724		12642.447	*
22	12677.427		12657.411		12638.283	*
23	12674.856		12653.965		12633.942	
24	12672.129		12650.371	*	12629.478	
25	12669.275		12646.632		12624.871	
26	12666.297		12642.764		12620.119	
27	12663.168	*	12638.759		12615.229	*
28	12659.951		12634.630		12610.177	*
29	12656.600		12630.383	*	12605.072	
30	12653.149		12626.003	*	12599.787	
31	12649.619		12621.560	*	12594.426	
32	12646.016		12617.009			
33	12642.396	*	12612.399			
34	12638.759	*	12607.757			
35	12635.175	*	12603.111			
36	12631.673	*	12598.504			
37			12593.981	*		
38			12589.648	*		

$^5\Phi_5$ - $X^5\Delta_4$ (5,1)

J	R		Q		P	
4	12432.106	*	-		-	
5	12432.146	*	12427.046		-	
6	12432.020		12426.064	*		
7	12431.739		12424.934	*		
8	12431.310	*	12423.621			
9	12430.706		12422.172			
10	12429.942		12420.562			
11	12429.036	*	12418.789			
12	12427.984	*	12416.865			
13	12426.737		12414.779			

Appendix III -- $^5\Phi_5$ - $X^5\Delta_4$ (5,1) (cont.)

J	R	Q	P
14	12425.355	12412.536 *	
15	12423.828	12410.153	
16	12422.132	12407.604	12393.935
17	12420.287	12404.903	12390.377
18	12418.289	12402.046	12386.655
19	12416.138	12399.038	12382.790
20	12413.818	12395.874	12378.791 *
21	12411.386 *	12392.566	12374.598
22	12408.772	12389.095	12370.284 *
23	12406.018	12385.481	12365.743 *
24	12403.103	12381.715	12361.154 *
25	12400.040	12377.788	12356.402
26	12396.828	12373.723	12351.469
27	12393.447	12369.486	12346.373
28	12389.911	12365.105	12341.190 *
29	12386.199	12360.564	12335.781
30	12382.277	12355.820	12330.204 *
31	12378.091	12350.928	12324.486 *
32	12373.370	12345.715	12318.549
33		12339.995	12312.328 *
34			12305.591 *

APPENDIX IV

Term Values for the $X^5\Delta$ State (cm^{-1})

The values for v = 0–3 were calculated from the least-squares-determined constants of Table XI. They have been printed uniformly to six decimal places and, in the vicinity of the microwave data of Table I (J = 5–6 for Ω = 2–4 of the v = 0 level), should be good to this accuracy; far from the region of the microwave data, the accuracy will be lower. Within any given substate, the rotational term values are well-determined relative to each other; between substates, the Ω = 2–3 interval is the most accurately determined. For v = 4, the term values were calculated from the upper state term values (Appendix VIII) and line frequencies (Appendix III) of the $^5\Phi_5 - X^5\Delta_4$ (1,4) band.

Appendix IV -- $X^5\Delta$ term values: v = 0

J	Ω: 0a	0b	1a	1b	2	3	4
0	384.313800	384.632063					
1	385.359033	385.677258	191.267017	191.267065			
2	387.449481	387.767630	193.346037	193.346180	0.373695		
3	390.585105	390.903140	196.464521	196.464807	3.474949	-187.820912	
4	394.765847	395.083730	200.622414	200.622890	7.609873	-183.709710	-372.929785
5	399.991632	400.309325	205.819644	205.820358	12.778398	-178.570831	-367.821744
6	406.262363	406.579830	212.056119	212.057118	18.980436	-172.404357	-361.692265
7	413.577927	413.895129	219.331730	219.333061	26.215884	-165.210388	-354.541440
8	421.938190	422.255090	227.646349	227.648058	34.484619	-156.989038	-346.369376
9	431.342998	431.659560	236.999831	237.001964	43.786503	-147.740440	-337.176198
10	441.792181	442.108367	247.392011	247.394615	54.121379	-137.464741	-326.962045
11	453.285547	453.601320	258.822707	258.825827	65.489073	-126.162106	-315.727070
12	465.822886	466.138211	271.291719	271.295400	77.889394	-113.832716	-303.471444
13	479.403970	479.718810	284.798828	284.803114	91.322134	-100.476770	-290.195351
14	494.028551	494.342870	299.343796	299.348733	105.787065	-86.094481	-275.898993
15	509.696361	510.010124	314.926369	314.931999	121.283945	-70.686080	-260.582587
16	526.407115	526.720286	331.546274	331.552640	137.812513	-54.251815	-244.246363
17	544.160507	544.473052	349.203219	349.210364	155.372491	-36.791948	-226.890569
18	562.956213	563.268098	367.896893	367.904859	173.963583	-18.306761	-208.515468
19	582.793891	583.105081	387.626970	387.635798	193.585476	1.203450	-189.121339
20	603.673179	603.983641	408.393104	408.402834	214.237840	21.738372	-168.708475
21	625.593695	625.903396	430.194929	430.205601	235.920327	43.297675	-147.277187
22	648.555040	648.863947	453.032065	453.043717	258.632573	65.881012	-124.827799
23	672.556795	672.864876	476.904109	476.916781	282.374194	89.488021	-101.360653
24	697.598523	697.905746	501.810645	501.824372	307.144790	114.118322	-76.876104
25	723.679766	723.986101	527.751234	527.766054	332.943946	139.771519	-51.374526
26	750.800050	751.105466	554.725422	554.741371	359.771225	166.447200	-24.856305
27	778.958880	779.263347	582.732736	582.749848	387.626176	194.144935	2.678153
28	808.155744	808.459232	611.772686	611.790994	416.508330	222.864278	31.228431
29	838.390109	838.692589	641.844761	641.864299	446.417200	252.604768	60.794093
30	869.661424	869.962868	672.948434	672.969235	477.352282	283.365924	91.374687
31	901.969121	902.269501	705.083161	705.105254	509.313054	315.147252	122.969748
32	935.312611	935.611900	738.248378	738.271794	542.298978	347.948240	155.578793
33	969.691287	969.989459	772.443503	772.468271	576.309498	381.768357	189.201323
34	1005.104523	1005.401552	807.667938	807.694085	611.344039	416.607060	223.836825
35	1041.551676	1041.847537	843.921064	843.948618	647.402012	452.463785	259.484768
36	1079.032082	1079.326750	881.202245	881.231232	684.482807	489.337955	296.144605
37	1117.545059	1117.838510	919.510830	919.541275	722.585800	527.228972	333.815776
38	1157.089908	1157.382119	958.846146	958.878072	761.710347	566.136226	372.497702
39	1197.665909	1197.956859	999.207503	999.240933	801.855788	606.059087	412.189789
40	1239.272326	1239.561991	1040.594195	1040.629150	843.021445	646.996910	452.891428
41	1281.908401	1282.196762	1083.005495	1083.041997	885.206624	688.949032	494.601991
42	1325.573362	1325.860397	1126.440661	1126.478729	928.410612	731.914775	537.320837

Appendix IV -- $X^5\Delta$ term values: v = 0 (cont.)

J	Ω: 0a	0b	1a	1b	2	3	4
43	1370.266414	1370.552104	1170.898931	1170.938584	972.632678	775.893442	581.047308
44	1415.986747	1416.271073	1216.379527	1216.420781	1017.872077	820.884321	625.780729
45	1462.733530	1463.016473	1262.881651	1262.924522	1064.128044	866.886682	671.520410
46	1510.505916	1510.787459	1310.404488	1310.448992	1111.399796	913.899780	718.265644
47	1559.303037	1559.583163	1358.947205	1358.993356	1159.686536	961.922852	766.015707
48	1609.124008	1609.402702	1408.508952	1408.556763	1208.987446	1010.955118	814.769861
49	1659.967927	1660.245172	1459.088860	1459.138343	1259.301692	1060.995781	864.527351
50	1711.833871	1712.109653	1510.686044	1510.737208	1310.628424	1112.044028	915.287403
51	1764.720900	1764.995206	1563.299598	1563.352454	1362.966773	1164.099029	967.049231
52	1818.628056	1818.900872	1616.928600	1616.983156	1416.315853	1217.159937	1019.812029
53	1873.554362	1873.825676	1671.572112	1671.628376	1470.674762	1271.225888	1073.574977
54	1929.498824	1929.768624	1727.229174	1727.287153	1526.042578	1326.296001	1128.337238
55	1986.460428	1986.728703	1783.898813	1783.958511	1582.418364	1382.369379	1184.097956
56	2044.438144	2044.704884	1841.580035	1841.641457	1639.801165	1439.445106	1240.856263
57	2103.430923	2103.696117	1900.271829	1900.334978	1698.190007	1497.522253	1298.611272
58	2163.437696	2163.701336	1959.973166	1960.038045	1757.583903	1556.599870	1357.362078
59	2224.457378	2224.719456	2020.683001	2020.749610	1817.981844	1616.676991	1417.107763
60	2286.488866	2286.749375	2082.400269	2082.468608	1879.382806	1677.752636	1477.847389
61	2349.531038	2349.789970	2145.123888	2145.193958	1941.785747	1739.825804	1539.580003
62	2413.582754	2413.840104	2208.852760	2208.924558	2005.189608	1802.895479	1602.304637
63	2478.642857	2478.898620	2273.585767	2273.659290	2069.593313	1866.960629	1666.020303
64	2544.710172	2544.964342	2339.321774	2339.397019	2134.995768	1932.020202	1730.725998
65	2611.783504	2612.036078	2406.059630	2406.136592	2201.395862	1998.073132	1796.420702
66	2679.861642	2680.112616	2473.798164	2473.876838	2268.792467	2065.118335	1863.103380
67	2748.943357	2749.192729	2542.536189	2542.616568	2337.184436	2133.154710	1930.772976
68	2819.027402	2819.275169	2612.272499	2612.354577	2406.570608	2202.181137	1999.428422
69	2890.112511	2890.358672	2683.005872	2683.089640	2476.949801	2272.196483	2069.068630
70	2962.197402	2962.441956	2754.735068	2754.820516	2548.320819	2343.199594	2139.692497
71	3035.280773	3035.523721	2827.458828	2827.545948	2620.682445	2415.189301	2211.298900
72	3109.361307	3109.602648	2901.175878	2901.264658	2694.033448	2488.164417	2283.886704
73	3184.437667	3184.677403	2975.884924	2975.975353	2768.372579	2562.123740	2357.454753
74	3260.508499	3260.746631	3051.584655	3051.676721	2843.698570	2637.066048	2432.001876
75	3337.572432	3337.808962	3128.273744	3128.367434	2920.010138	2712.990103	2507.526884
76	3415.628075	3415.863007	3205.950846	3206.046146	2997.305980	2789.894651	2584.028572
77	3494.674023	3494.907359	3284.614596	3284.711493	3075.584778	2867.778418	2661.505716
78	3574.708849	3574.940594	3364.263616	3364.362093	3154.845196	2946.640117	2739.957079
79	3655.731112	3655.961270	3444.896505	3444.996548	3235.085881	3026.478440	2819.381402
80	3737.739352	3737.967928	3526.511850	3526.613442	3316.305462	3107.292064	2899.777412
81	3820.732092	3820.959092	3609.108218	3609.211341	3398.502550	3189.079649	2981.143819
82	3904.707836	3904.933265	3692.684157	3692.788795	3481.675741	3271.839835	3063.479314
83	3989.665071	3989.888937	3777.238201	3777.344334	3565.823612	3355.571248	3146.782572
84	4075.602267	4075.824577	3862.768863	3862.876474	3650.944723	3440.272496	3231.052251

Appendix IV (cont.) -- $X^5\Delta$ term values: v = 1

J	Ω: 0a	0b	1a	1b	2	3	4
0	1255.404356	1255.744175					
1	1256.441783	1256.781556	1062.375876	1062.375927			
2	1258.516618	1258.856299	1064.439426	1064.439579	871.499493		
3	1261.628823	1261.968366	1067.534704	1067.535009	874.577780	683.325807	
4	1265.778341	1266.117700	1071.661657	1071.662165	878.682083	687.406712	498.236393
5	1270.965094	1271.304225	1076.820210	1076.820973	883.812331	692.507720	503.306994
6	1277.188988	1277.527844	1083.010274	1083.011341	889.968436	698.628748	509.391545
7	1284.449909	1284.788444	1090.231739	1090.233160	897.150295	705.769697	516.489954
8	1292.747722	1293.085892	1098.484476	1098.486302	905.357785	713.930452	524.602111
9	1302.082274	1302.420034	1107.768340	1107.770620	914.590768	723.110879	533.727892
10	1312.453395	1312.790699	1118.083166	1118.085949	924.849086	733.310831	543.867158
11	1323.860893	1324.197697	1129.428773	1129.432108	936.132565	744.530142	555.019755
12	1336.304558	1336.640818	1141.804959	1141.808895	948.441014	756.768631	567.185511
13	1349.784161	1350.119833	1155.211506	1155.216090	961.774223	770.026099	580.364240
14	1364.299455	1364.634494	1169.648177	1169.653457	976.131967	784.302331	594.555742
15	1379.850172	1380.184536	1185.114715	1185.120739	991.514001	799.597097	609.759797
16	1396.436027	1396.769672	1201.610848	1201.617661	1007.920064	815.910149	625.976175
17	1414.056714	1414.389598	1219.136284	1219.143933	1025.349878	833.241221	643.204626
18	1432.711909	1433.043989	1237.690713	1237.699243	1043.803146	851.590033	661.444886
19	1452.401270	1452.732505	1257.273807	1257.283263	1063.279555	870.956288	680.696676
20	1473.124434	1473.454782	1277.885220	1277.895645	1083.778774	891.339671	700.959700
21	1494.881021	1495.210440	1299.524586	1299.536024	1105.300455	912.739852	722.233648
22	1517.670631	1517.999081	1322.191524	1322.204017	1127.844233	935.156482	744.518193
23	1541.492844	1541.820286	1345.885633	1345.899223	1151.409723	958.589200	767.812992
24	1566.347224	1566.673618	1370.606493	1370.621222	1175.996526	983.037623	792.117688
25	1592.233313	1592.558620	1396.353667	1396.369575	1201.604223	1008.501355	817.431907
26	1619.150637	1619.474818	1423.126701	1423.143828	1228.232380	1034.979982	843.755260
27	1647.098701	1647.421719	1450.925121	1450.943504	1255.880543	1062.473074	871.087341
28	1676.076992	1676.398809	1479.748435	1479.768113	1284.548243	1090.980183	899.427729
29	1706.084978	1706.405557	1509.596134	1509.617144	1314.234992	1120.500847	928.775987
30	1737.122108	1737.441413	1540.467691	1540.490068	1344.940285	1151.034585	959.131663
31	1769.187813	1769.505809	1572.362559	1572.386338	1376.663599	1182.580900	990.494288
32	1802.281504	1802.598156	1605.280174	1605.305390	1409.404396	1215.139279	1022.863378
33	1836.402575	1836.717849	1639.219955	1639.246641	1443.162118	1248.709191	1056.238432
34	1871.550400	1871.864262	1674.181302	1674.209490	1477.936191	1283.290089	1090.618935
35	1907.724335	1908.036751	1710.163596	1710.193317	1513.726022	1318.881410	1126.004354
36	1944.923716	1945.234654	1747.166202	1747.197487	1550.531002	1355.482573	1162.394140
37	1983.147861	1983.457291	1785.188466	1785.221343	1588.350506	1393.092982	1199.787730
38	2022.396071	2022.703960	1824.229715	1824.264213	1627.183888	1431.712022	1238.184544
39	2062.667626	2062.973945	1864.289260	1864.325406	1667.030488	1471.339064	1277.583985
40	2103.961789	2104.266508	1905.366392	1905.404212	1707.889626	1511.973459	1317.985441
41	2146.277803	2146.580894	1947.460385	1947.499905	1749.760606	1553.614544	1359.388284
42	2189.614895	2189.916329	1990.570496	1990.611739	1792.642716	1596.261637	1401.791869

Appendix IV -- $X^5\Delta$ term values: v = 1 (cont.)

J	Ω: 0a	0b	1a	1b	2	3	4
43	2233.972270	2234.272021	2034.695963	2034.738951	1836.535223	1639.914043	1445.195535
44	2279.349118	2279.647158	2079.836005	2079.880761	1881.437380	1684.571045	1489.598605
45	2325.744607	2326.040911	2125.989825	2126.036370	1927.348421	1730.231913	1535.000387
46	2373.157891	2373.452433	2173.156607	2173.204961	1974.267563	1776.895899	1581.400171
47	2421.588101	2421.880857	2221.335518	2221.385699	2022.194005	1824.562238	1628.797231
48	2471.034352	2471.325298	2270.525706	2270.577732	2071.126930	1873.230149	1677.190826
49	2521.495740	2521.784854	2320.726302	2320.780189	2121.065502	1922.898833	1726.580197
50	2572.971344	2573.258604	2371.936418	2371.992182	2172.008869	1973.567474	1776.964570
51	2625.460224	2625.745607	2424.155149	2424.212805	2223.956162	2025.235241	1828.343153
52	2678.961419	2679.244905	2477.381573	2477.441134	2276.906492	2077.901283	1880.715140
53	2733.473954	2733.755524	2531.614750	2531.676228	2330.858955	2131.564737	1934.079706
54	2788.996833	2789.276467	2586.853719	2586.917126	2385.812630	2186.224717	1988.436012
55	2845.529043	2845.806723	2643.097505	2643.162851	2441.766576	2241.880325	2043.783200
56	2903.069553	2903.345260	2700.345115	2700.412409	2498.719837	2298.530644	2100.120398
57	2961.617311	2961.891030	2758.595535	2758.664786	2556.671439	2356.174740	2157.446715
58	3021.171252	3021.442965	2817.847737	2817.918952	2615.620391	2414.811662	2215.761245
59	3081.730287	3081.999980	2878.100673	2878.173858	2675.565683	2474.440443	2275.063066
60	3143.293315	3143.560972	2939.353278	2939.428438	2736.506291	2535.060098	2335.351237
61	3205.859211	3206.124819	3001.604469	3001.681609	2798.441169	2596.669626	2396.624803
62	3269.426836	3269.690381	3064.853146	3064.932268	2861.369258	2659.268007	2458.882790
63	3333.995032	3334.256502	3129.098190	3129.179298	2925.289478	2722.854207	2522.124209
64	3399.562623	3399.822005	3194.338465	3194.421561	2990.200736	2787.427172	2586.348053
65	3466.128414	3466.385698	3260.572819	3260.657902	3056.101917	2852.985834	2651.553300
66	3533.691192	3533.946367	3327.800079	3327.887149	3122.991891	2919.529104	2717.738909
67	3602.249729	3602.502785	3396.019058	3396.108114	3190.869511	2987.055881	2784.903825
68	3671.802775	3672.053704	3465.228547	3465.319587	3259.733612	3055.565041	2853.046972
69	3742.349066	3742.597858	3535.427324	3535.520345	3329.583012	3125.055449	2922.167261
70	3813.887316	3814.133965	3606.614147	3606.709145	3400.416510	3195.525948	2992.263585
71	3886.416225	3886.660724	3678.787756	3678.884726	3472.232891	3266.975366	3063.334819
72	3959.934474	3960.176815	3751.946874	3752.045811	3545.030919	3339.402515	3135.379823
73	4034.440724	4034.680902	3826.090207	3826.191105	3618.809344	3412.806187	3208.397438
74	4109.933622	4110.171631	3901.216443	3901.319295	3693.566895	3487.185160	3282.386489
75	4186.411794	4186.647630	3977.324253	3977.429050	3769.302287	3562.538192	3357.345784
76	4263.873850	4264.107509	4054.412288	4054.519023	3846.014216	3638.864026	3433.274114
77	4342.318381	4342.549861	4132.479185	4132.587848	3923.701362	3716.161387	3510.170253
78	4421.743963	4421.973260	4211.523562	4211.634143	4002.362385	3794.428983	3588.032958
79	4502.149151	4502.376263	4291.544018	4291.656506	4081.995930	3873.665503	3666.860968
80	4583.532484	4583.757410	4372.539137	4372.653521	4162.600624	3953.869622	3746.653006
81	4665.892484	4666.115223	4454.507483	4454.623752	4244.175077	4035.039997	3827.407778
82	4749.227655	4749.448205	4537.447606	4537.565747	4326.717880	4117.175265	3909.123972
83	4833.536481	4833.754846	4621.358035	4621.478034	4410.227610	4200.274048	3991.800258
84	4918.817433	4919.033609	4706.237283	4706.359127	4494.702823	4284.334952	4075.435292

Appendix IV (cont.) -- $X^5\Delta$ term values: v = 2

J	Ω: 0a	0b	1a	1b	2	3	4
0	2117.240416	2117.596192					
1	2118.270032	2118.625767	1924.223381	1924.223437			
2	2120.329246	2120.684897	1926.271456	1926.271624	1733.362441		
3	2123.418017	2123.773544	1929.343524	1929.343858	1736.417756	1545.211720	
4	2127.536291	2127.891652	1933.439528	1933.440086	1740.491428	1549.262320	1360.148322
5	2132.683989	2133.039143	1938.559396	1938.560232	1745.583387	1554.325446	1365.181476
6	2138.861017	2139.215923	1944.703038	1944.704207	1751.693547	1560.401015	1371.221090
7	2146.067260	2146.421876	1951.870342	1951.871899	1758.821801	1567.488927	1378.267071
8	2154.302584	2154.656870	1960.061181	1960.063182	1766.968029	1575.589067	1386.319308
9	2163.566836	2163.920752	1969.275410	1969.277907	1776.132089	1584.701302	1395.377678
10	2173.859845	2174.213350	1979.512864	1979.515911	1786.313827	1594.825483	1405.442041
11	2185.181419	2185.534473	1990.773359	1990.777011	1797.513066	1605.961444	1416.512240
12	2197.531349	2197.883913	2003.056696	2003.061004	1809.729614	1618.109002	1428.588105
13	2210.909405	2211.261439	2016.362656	2016.367672	1822.963264	1631.267960	1441.669448
14	2225.315339	2225.666804	2030.690999	2030.696776	1837.213787	1645.438101	1455.756067
15	2240.748884	2241.099742	2046.041473	2046.048060	1852.480939	1660.619193	1470.847744
16	2257.209754	2257.559966	2062.413801	2062.421250	1868.764458	1676.810988	1486.944244
17	2274.697644	2275.047173	2079.807693	2079.816052	1886.064066	1694.013220	1504.045318
18	2293.212229	2293.561037	2098.222838	2098.232157	1904.379466	1712.225608	1522.150701
19	2312.753166	2313.101217	2117.658907	2117.669233	1923.710343	1731.447853	1541.260111
20	2333.320094	2333.667350	2138.115555	2138.126935	1944.056366	1751.679639	1561.373253
21	2354.912629	2355.259056	2159.592415	2159.604896	1965.417186	1772.920636	1582.489813
22	2377.530374	2377.875935	2182.089106	2182.102733	1987.792436	1795.170494	1604.609464
23	2401.172908	2401.517569	2205.605225	2205.620042	2011.181734	1818.428848	1627.731861
24	2425.839794	2426.183521	2230.140354	2230.156404	2035.584677	1842.695317	1651.856646
25	2451.530574	2451.873334	2255.694054	2255.711381	2061.000846	1867.969503	1676.983442
26	2478.244773	2478.586532	2282.265870	2282.284514	2087.429806	1894.250990	1703.111858
27	2505.981897	2506.322623	2309.855328	2309.875330	2114.871102	1921.539346	1730.241487
28	2534.741431	2535.081093	2338.461937	2338.483335	2143.324265	1949.834124	1758.371906
29	2564.522843	2564.861410	2368.085185	2368.108018	2172.788805	1979.134858	1787.502677
30	2595.325583	2595.663024	2398.724545	2398.748849	2203.264215	2009.441067	1817.633344
31	2627.149080	2627.485366	2430.379470	2430.405281	2234.749974	2040.752251	1848.763436
32	2659.992745	2660.327847	2463.049395	2463.076748	2267.245540	2073.067896	1880.892468
33	2693.855972	2694.189862	2496.733739	2496.762667	2300.750355	2106.387469	1914.019937
34	2728.738133	2729.070784	2531.431900	2531.462435	2335.263844	2140.710423	1948.145323
35	2764.638584	2764.969969	2567.143259	2567.175433	2370.785412	2176.036191	1983.268093
36	2801.556661	2801.886754	2603.867180	2603.901022	2407.314450	2212.364192	2019.387695
37	2839.491683	2839.820459	2641.603009	2641.638547	2444.850330	2249.693826	2056.503564
38	2878.442947	2878.770382	2680.350071	2680.387332	2483.392406	2288.024478	2094.615116
39	2918.409734	2918.735804	2720.107676	2720.146686	2522.940015	2327.355516	2133.721753
40	2959.391306	2959.715990	2760.875116	2760.915899	2563.492478	2367.686289	2173.822859
41	3001.386907	3001.710181	2802.651662	2802.694243	2605.049096	2409.016132	2214.917803
42	3044.395760	3044.717605	2845.436571	2845.480970	2647.609155	2451.344362	2257.005938

Appendix IV -- $X^5\Delta$ term values: v = 2 (cont.)

J	Ω: 0a	0b	1a	1b	2	3	4
43	3088.417073	3088.737467	2889.229080	2889.275317	2691.171922	2494.670280	2300.086600
44	3133.450032	3133.768957	2934.028406	2934.076502	2735.736648	2538.993168	2344.159110
45	3179.493806	3179.811243	2979.833752	2979.883724	2781.302564	2584.312293	2389.222772
46	3226.547547	3226.863479	3026.644302	3026.696166	2827.868887	2630.626906	2435.276872
47	3274.610387	3274.924796	3074.459219	3074.512991	2875.434813	2677.936238	2482.320683
48	3323.681438	3323.994309	3123.277651	3123.333345	2923.999524	2726.239505	2530.353460
49	3373.759798	3374.071115	3173.098728	3173.156356	2973.562183	2775.535908	2579.374440
50	3424.844542	3425.154291	3223.921562	3223.981136	3024.121934	2825.824627	2629.382846
51	3476.934729	3477.242897	3275.745246	3275.806775	3075.677907	2877.104829	2680.377884
52	3530.029399	3530.335974	3328.568856	3328.632349	3128.229212	2929.375661	2732.358744
53	3584.127575	3584.432545	3382.391449	3382.456913	3181.774943	2982.636255	2785.324597
54	3639.228261	3639.531614	3437.212066	3437.279508	3236.314176	3036.885725	2839.274601
55	3695.330441	3695.632168	3493.029730	3493.099154	3291.845968	3092.123168	2894.207894
56	3752.433084	3752.733175	3549.843444	3549.914853	3348.369362	3148.347666	2950.123601
57	3810.535137	3810.833585	3607.652195	3607.725592	3405.883381	3205.558282	3007.020829
58	3869.635532	3869.932329	3666.454952	3666.530339	3464.387032	3263.754061	3064.898666
59	3929.733183	3930.028321	3726.250667	3726.328041	3523.879303	3322.934034	3123.756186
60	3990.826982	3991.120457	3787.038271	3787.117633	3584.359166	3383.097214	3183.592446
61	4052.915807	4053.207613	3848.816682	3848.898028	3645.825576	3444.242594	3244.406487
62	4115.998517	4116.288650	3911.584796	3911.668123	3708.277469	3506.369155	3306.197330
63	4180.073951	4180.362408	3975.341494	3975.426797	3771.713764	3569.475856	3368.963984
64	4245.140932	4245.427709	4040.085637	4040.172910	3836.133364	3633.561643	3432.705437
65	4311.198265	4311.483361	4105.816072	4105.905307	3901.535153	3698.625443	3497.420663
66	4378.244735	4378.528148	4172.531623	4172.622812	3967.917999	3764.666165	3563.108618
67	4446.279111	4446.560842	4240.231102	4240.324235	4035.280750	3831.682702	3629.768241
68	4515.300143	4515.580192	4308.913299	4309.008366	4103.622241	3899.673932	3697.398454
69	4585.306564	4585.584932	4378.576988	4378.673977	4172.941285	3968.638711	3765.998164
70	4656.297088	4656.573778	4449.220925	4449.319824	4243.236681	4038.575883	3835.566258
71	4728.270413	4728.545426	4520.843849	4520.944645	4314.507209	4109.484271	3906.101608
72	4801.225216	4801.498557	4593.444481	4593.547158	4386.751631	4181.362682	3977.603069
73	4875.160160	4875.431832	4667.021525	4667.126068	4459.968694	4254.209907	4050.069479
74	4950.073887	4950.343894	4741.573665	4741.680058	4534.157125	4328.024719	4123.499659
75	5025.965022	5026.233372	4817.099571	4817.207796	4609.315635	4402.805874	4197.892412
76	5102.832174	5103.098871	4893.597892	4893.707931	4685.442917	4478.552109	4273.246524
77	5180.673932	5180.938984	4971.067262	4971.179096	4762.537648	4555.262147	4349.560766
78	5259.488869	5259.752283	5049.506296	5049.619905	4840.598486	4632.934692	4426.833889
79	5339.275539	5339.537323	5128.913593	5129.028955	4919.624072	4711.568430	4505.064629
80	5420.032478	5420.292641	5209.287731	5209.404826	4999.613030	4791.162032	4584.251704
81	5501.758207	5502.016758	5290.627275	5290.746079	5080.563967	4871.714149	4664.393815
82	5584.451226	5584.708176	5372.930769	5373.051260	5162.475472	4953.223417	4745.489646
83	5668.110019	5668.365378	5456.196741	5456.318896	5245.346116	5035.688454	4827.537863
84	5752.733052	5752.986831	5540.423702	5540.547495	5329.174454	5119.107861	4910.537116

Appendix IV (cont.) -- $X^5\Delta$ term values: v = 3

J	Ω: 0a	0b	1a	1b	2	3	4
0	2969.821336	2970.191969					
1	2970.843143	2971.213729	2776.811461	2776.811522			
2	2972.886736	2973.257232	2778.844058	2778.844241	2585.965974		
3	2975.952079	2976.322437	2781.892907	2781.893274	2588.998310	2397.841665	
4	2980.039114	2980.409289	2785.957953	2785.958565	2593.041344	2401.861949	2212.810867
5	2985.147764	2985.517711	2791.039125	2791.040041	2598.095005	2406.887180	2217.806554
6	2991.277934	2991.647608	2797.136329	2797.137611	2604.159206	2412.917274	2223.801207
7	2998.429509	2998.798864	2804.249457	2804.251164	2611.233842	2419.952131	2230.794732
8	3006.602356	3006.971346	2812.378380	2812.380573	2619.318790	2427.991636	2238.787019
9	3015.796320	3016.164903	2821.522952	2821.525690	2628.413911	2437.035655	2247.777943
10	3026.011232	3026.379361	2831.683009	2831.686350	2638.519047	2447.084039	2257.767364
11	3037.246898	3037.614531	2842.858367	2842.862371	2649.634024	2458.136622	2268.755124
12	3049.503110	3049.870202	2855.048827	2855.053550	2661.758649	2470.193220	2280.741052
13	3062.779638	3063.146146	2868.254167	2868.259668	2674.892712	2483.253634	2293.724960
14	3077.076234	3077.442115	2882.474152	2882.480486	2689.035986	2497.317648	2307.706644
15	3092.392630	3092.757841	2897.708524	2897.715748	2704.188227	2512.385029	2322.685885
16	3108.728541	3109.093040	2913.957010	2913.965179	2720.349171	2528.455528	2338.662448
17	3126.083660	3126.447405	2931.219318	2931.228486	2737.518540	2545.528879	2355.636082
18	3144.457664	3144.820614	2949.495136	2949.505357	2755.696035	2563.604798	2373.606521
19	3163.850209	3164.212323	2968.784137	2968.795463	2774.881343	2582.682987	2392.573483
20	3184.260932	3184.622171	2989.085973	2989.098455	2795.074131	2602.763129	2412.536670
21	3205.689453	3206.049776	3010.400278	3010.413968	2816.274049	2623.844892	2433.495767
22	3228.135371	3228.494733	3032.726670	3032.741618	2838.480731	2645.927926	2455.450446
23	3251.598266	3251.956642	3056.064746	3056.081000	2861.693791	2669.011864	2478.400360
24	3276.077701	3276.435046	3080.414087	3080.431695	2885.912828	2693.096325	2502.345149
25	3301.573218	3301.929496	3105.774255	3105.793264	2911.137421	2718.180908	2527.284435
26	3328.084342	3328.439515	3132.144794	3132.165248	2937.367135	2744.265197	2553.217826
27	3355.610577	3355.964610	3159.525228	3159.547173	2964.601515	2771.348760	2580.144913
28	3384.151409	3384.504267	3187.915066	3187.938545	2992.840087	2799.431145	2608.065270
29	3413.706307	3414.057955	3217.313796	3217.338851	3022.082364	2828.511888	2636.978457
30	3444.274718	3444.625123	3247.720891	3247.747562	3052.327838	2858.590505	2666.884017
31	3475.856072	3476.205201	3279.135802	3279.164129	3083.575985	2889.666495	2697.781478
32	3508.449780	3508.797601	3311.557965	3311.587986	3115.826262	2921.739342	2729.670351
33	3542.055234	3542.401716	3344.986797	3345.018548	3149.078111	2954.808512	2762.550130
34	3576.671808	3577.016921	3379.421696	3379.455213	3183.330955	2988.873456	2796.420296
35	3612.298856	3612.642570	3414.862042	3414.897360	3218.584199	3023.933606	2831.280312
36	3648.935714	3649.278000	3451.307198	3451.344350	3254.837232	3059.988378	2867.129624
37	3686.581700	3686.922530	3488.756509	3488.795526	3292.089425	3097.037171	2903.967664
38	3725.236112	3725.575459	3527.209301	3527.250212	3330.340130	3135.079369	2941.793846
39	3764.898229	3765.236068	3566.664882	3566.707716	3369.588685	3174.114336	2980.607569
40	3805.567314	3805.903619	3607.122542	3607.167327	3409.834406	3214.141421	3020.408215
41	3847.242609	3847.577355	3648.581553	3648.628315	3451.076596	3255.159957	3061.195151
42	3889.923338	3890.256501	3691.041170	3691.089933	3493.314538	3297.169259	3102.967727

Appendix IV -- $X^3\Delta$ term values: v = 3 (cont.)

J	Ω: 0a	0b	1a	1b	2	3	4
43	3933.608706	3933.940264	3734.500629	3734.551416	3536.547498	3340.168624	3145.725276
44	3978.297900	3978.627832	3778.959148	3779.011980	3580.774724	3384.157334	3189.467116
45	4023.990090	4024.318375	3824.415927	3824.470824	3625.995447	3429.134654	3234.192547
46	4070.684425	4071.011042	3870.870148	3870.927129	3672.208882	3475.099830	3279.900856
47	4118.380036	4118.704967	3918.320976	3918.380058	3719.414225	3522.052095	3326.591310
48	4167.076037	4167.399263	3966.767556	3966.828755	3767.610654	3569.990660	3374.263160
49	4216.771522	4217.093027	4016.209017	4016.272348	3816.797331	3618.914724	3422.915644
50	4267.465567	4267.785334	4066.644470	4066.709945	3866.973399	3668.823466	3472.547980
51	4319.157231	4319.475245	4118.073007	4118.140638	3918.137986	3719.716049	3523.159370
52	4371.845552	4372.161799	4170.493703	4170.563499	3970.290200	3771.591619	3574.749001
53	4425.529553	4425.844019	4223.905614	4223.977584	4023.429133	3824.449304	3627.316042
54	4480.208236	4480.520908	4278.307779	4278.381930	4077.553859	3878.288217	3680.859647
55	4535.880585	4536.191453	4333.699219	4333.775557	4132.663434	3933.107452	3735.378952
56	4592.545567	4592.854619	4390.078938	4390.157467	4188.756898	3988.906088	3790.873077
57	4650.202130	4650.509357	4447.445920	4447.526644	4245.833273	4045.683185	3847.341125
58	4708.849205	4709.154597	4505.799133	4505.882053	4303.891563	4103.437787	3904.782184
59	4768.485701	4768.789251	4565.137526	4565.222643	4362.930755	4162.168921	3963.195322
60	4829.110515	4829.412215	4625.460031	4625.547344	4422.949819	4221.875596	4022.579593
61	4890.722520	4891.022364	4686.765563	4686.855069	4483.947706	4282.556806	4082.934033
62	4953.320574	4953.618557	4749.053018	4749.144713	4545.923352	4344.211525	4144.257663
63	5016.903516	5017.199634	4812.321273	4812.415153	4608.875673	4406.838713	4206.549486
64	5081.470168	5081.764417	4876.569190	4876.665249	4672.803570	4470.437311	4269.808487
65	5147.019332	5147.311710	4941.795612	4941.893842	4737.705924	4535.006242	4334.033635
66	5213.549794	5213.840298	5007.999364	5008.099757	4803.581601	4600.544414	4399.223884
67	5281.060320	5281.348950	5075.179253	5075.281799	4870.429448	4667.050718	4465.378168
68	5349.549660	5349.836415	5143.334069	5143.438758	4938.248295	4734.524025	4532.495407
69	5419.016546	5419.301426	5212.462585	5212.569403	5007.036954	4802.963192	4600.574503
70	5489.459689	5489.742697	5282.563554	5282.672489	5076.794222	4872.367057	4669.614339
71	5560.877786	5561.158924	5353.635713	5353.746751	5147.518876	4942.734441	4739.613784
72	5633.269514	5633.548784	5425.677782	5425.790907	5219.209676	5014.064148	4810.571688
73	5706.633533	5706.910939	5498.688462	5498.803658	5291.865364	5086.354966	4882.486886
74	5780.968483	5781.244030	5572.666436	5572.783685	5365.484668	5159.605664	4955.358194
75	5856.272990	5856.546683	5647.610371	5647.729655	5440.066294	5233.814995	5029.184412
76	5932.545659	5932.817504	5723.518915	5723.640215	5515.608934	5308.981694	5103.964322
77	6009.785078	6010.055082	5800.390699	5800.513994	5592.111260	5385.104478	5179.696689
78	6087.989818	6088.257989	5878.224336	5878.349605	5669.571929	5462.182049	5256.380263
79	6167.158432	6167.424777	5957.018422	5957.145643	5747.989579	5540.213090	5334.013774
80	6247.289454	6247.553983	6036.771535	6036.900685	5827.362831	5619.196268	5412.595936
81	6328.381403	6328.644125	6117.482236	6117.613291	5907.690288	5699.130231	5492.125446
82	6410.432777	6410.693703	6199.149067	6199.282002	5988.970538	5780.013610	5572.600983
83	6493.442059	6493.701199	6281.770555	6281.905344	6071.202147	5861.845021	5654.021211
84	6577.407713	6577.665078	6365.345206	6365.481824	6154.383669	5944.623061	5736.384773

Appendix IV (cont.) -- $X^5\Delta$ term values: v = 4, Ω = 5

J		J	
4	3056.241	47	4161.614
5	3061.180	48	4208.921
6	3067.135	49	4257.207
7	3074.076	50	4306.458
8	3082.003	51	4356.681
9	3090.931	52	4407.883
10	3100.848	53	4460.056
11	3111.756	54	4513.189
12	3123.644	55	4567.304
13	3136.543	56	4622.369
14	3150.408	57	4678.402
15	3165.274	58	4735.424
16	3181.138	59	4793.380
17	3197.979	60	4852.311
18	3215.811	61	4912.200
19	3234.637	62	4973.075
20	3254.450	63	5034.884
21	3275.270	64	5097.647
22	3297.055	65	5161.400
23	3319.822	66	5226.080
24	3343.582	67	5291.736
25	3368.332		
26	3394.075		
27	3420.800		
28	3448.515		
29	3477.202		
30	3506.881		
31	3537.554		
32	3569.205		
33	3601.829		
34	3635.443		
35	3670.034		
36	3705.625		
37	3742.190		
38	3779.723		
39	3818.247		
40	3857.748		
41	3898.213		
42	3939.679		
43	3982.112		
44	4025.522		
45	4069.906		
46	4115.274		

APPENDIX V

How the Weighting Was Done for the Ground State Fit

The weighting procedure was started by assigning the following weights to the spectral lines:

	Weight w_i
Good lines	1
Blended lines (*)	$\frac{1}{10}$
Uncertain lines (?)	$\frac{1}{100}$

If the i^{th} data point has standard deviation σ_i, this can be written as $\sigma_i = \sigma\sigma_i'$ where σ is a common factor for all the data points and σ_i' is the relative standard deviation. Similarly $w_i = ww_i'$, where $w = \frac{1}{\sigma^2}$ is a common factor. Since initially the common factor was unknown, it was necessary, as is common practice (1), to omit it. That is, really the weights w_i given above are w_i'.

Each combination difference is the difference between two lines — e.g.

$$R(J) \pm \sigma_R(J) - Q(J+1) \pm \sigma_Q(J+1) = \Delta_1F''(J) \pm \sigma_{1F''}(J)$$

$$\sigma_{1F''}(J) = \{[\sigma_R(J)]^2 + [\sigma_Q(J+1)]^2\}^{1/2}$$

$$[\sigma_{1F''}(J)]^2 = \frac{1}{w_R(J)} + \frac{1}{w_Q(J+1)}$$

Then

$$w_{1F''}(J) = \frac{1}{[\sigma_{1F''}(J)]^2}$$

The combination differences used for the least-squares fit were weighted averages involving all data — i.e. all transitions of all upper-state vibrational levels of both the $^5\Pi - X^5\Delta$ and $^5\Phi - X^5\Delta$ systems that yielded a given lower-state combination difference were used. The weighting was done in the usual manner (2):

$$\Delta_1 F''(J)_{avg} = \frac{\sum_i \Delta_1 F''(J)_i \cdot w_{1F''(J)_i}}{\sum_i w_{1F''(J)_i}}$$

$$\frac{1}{w_{1F''(J)_{avg}}} = \sum_i \frac{1}{w_{1F''(J)_i}}$$

The same procedure was used to determine the weights for the vibrational differences.

The laser measurements ($\Delta_1 F''$s, $\Delta_2 F''$s, and spin-orbit intervals) were weighted somewhat more arbitrarily than the FT measurements (these numbers having been obtained mostly by other workers in this laboratory). The laser measurements were also average values, in this case with the averaging being over the various subbands of the orange system. Though there tended to be fewer measurements contributing to each average value compared with the FT values, the laser measurements (for non-blended lines) were approximately three times more accurate. Since many of the best FT data points (after averaging) had weights of ~8, the best (average) laser values were weighted at 8, with appropriate lesser weights given to values of poorer quality.

After preliminary least-squares fitting, all data points which had residuals (i.e. observed - calculated values) ≥ 0.01 cm^{-1} were weighted down (if not already this low) to $w_i = 0.1$ and those with residuals ≥ 0.02 cm^{-1} were removed completely.

To weight the microwave values of Table I relative to the FT and laser measurements, the following procedure was used. A least-squares fit using all remaining data (FT and laser) *except* the microwave data was performed for the $v = 0$ level of the $X^5\Delta$ state. The least-squares program determined the common factor σ that, as described above, had been taken out of the variance-covariance matrix. The standard deviations quoted by Endo, Saito, and Hirota (3) were used for the microwave data. These were converted to the same relative basis as the FT and laser data by taking out the same common factor. The microwave data points were thus given relative weights of the order of $10^7 - 10^8$.

APPENDIX VI

The Data Used for the Ground State Least-squares Fit and the Residuals (cm^{-1})

Brief explanation of some of the labels:

Source: FT -- Fourier transform measurements of the infrared system.

L -- Laser-induced fluorescence measurements of the orange system.

M -- Microwave measurements (Table I).

Type: $\Delta_1 F$ -- Ground state rotational combination difference.

$\Delta_2 F$ -- Ground state rotational combination difference.

$\Delta_1 F_+ = F_b(J+1) - F_a(J)$

$\Delta_1 F_- = F_a(J+1) - F_b(J)$

s-o -- Spin-orbit interval. (The value given for Ω is the upper of the two values.)

Δv -- Vibrational interval. (The parity, a or b, is given when necessary. The value given for v is that for the upper level (v = 0 for the lower level).)

ΔJ -- Rotational line. (The J value given is that for the lower level.)

Residuals: Observed - Calculated values.

Appendix VI -- $X^5\Delta$ Least-Squares Fit: data and residuals

Source	Type	v	Ω	J	Data	Weight	Residuals
FT	Δ_1F_+	0	0	2	3.4488	0.55	-0.005
FT	Δ_1F_+	0	0	4	5.5449	1.05	0.001
FT	Δ_1F_+	0	0	5	6.5875	1.00	-0.001
FT	Δ_1F_+	0	0	6	7.6403	0.86	0.007
FT	Δ_1F_+	0	0	7	8.6746	1.27	-0.003
FT	Δ_1F_+	0	0	8	9.7185	1.05	-0.003
FT	Δ_1F_+	0	0	9	10.7627	2.33	-0.003
FT	Δ_1F_+	0	0	10	11.8086	2.46	-0.001
FT	Δ_1F_+	0	0	11	12.8548	1.83	0.002
FT	Δ_1F_+	0	0	12	13.9007	3.82	0.005
FT	Δ_1F_+	0	0	13	14.9449	1.25	0.006
FT	Δ_1F_+	0	0	14	15.9822	3.32	0.001
FT	Δ_1F_+	0	0	15	17.0221	3.32	-0.002
FT	Δ_1F_+	0	0	16	18.0652	2.91	-0.001
FT	Δ_1F_+	0	0	17	19.1068	2.91	-0.001
FT	Δ_1F_+	0	0	18	20.1529	2.51	0.004
FT	Δ_1F_+	0	0	19	21.1900	2.15	0.000
FT	Δ_1F_+	0	0	20	22.2308	3.45	0.001
FT	Δ_1F_+	0	0	21	23.2742	3.05	0.004
FT	Δ_1F_+	0	0	22	24.3095	3.91	-0.000
FT	Δ_1F_+	0	0	23	25.3475	3.55	-0.001
FT	Δ_1F_+	0	0	24	26.3871	4.36	-0.001
FT	Δ_1F_+	0	0	25	27.4261	3.91	0.000
FT	Δ_1F_+	0	0	26	28.4627	4.23	-0.001
FT	Δ_1F_+	0	0	27	29.4952	2.60	-0.005
FT	Δ_1F_+	0	0	28	30.5377	3.82	0.001
FT	Δ_1F_+	0	0	29	31.5731	3.05	0.000
FT	Δ_1F_+	0	0	30	32.6046	3.78	-0.004
FT	Δ_1F_+	0	0	31	33.6434	2.96	0.001
FT	Δ_1F_+	0	0	32	34.6764	3.05	-0.000
FT	Δ_1F_+	0	0	33	35.7150	2.42	0.005
FT	Δ_1F_+	0	0	34	36.7455	4.14	0.002
FT	Δ_1F_+	0	0	35	37.7737	3.64	-0.001
FT	Δ_1F_+	0	0	36	38.8136	2.27	0.007
FT	Δ_1F_+	0	0	37	39.8381	3.15	0.001
FT	Δ_1F_+	0	0	38	40.8610	2.37	-0.006
FT	Δ_1F_+	0	0	39	41.8955	2.73	-0.001
FT	Δ_1F_+	0	0	40	42.9240	2.64	-0.000
FT	Δ_1F_+	0	0	41	43.9566	3.09	0.005
FT	Δ_1F_+	0	0	42	44.9847	2.36	0.006
FT	Δ_1F_+	0	0	43	46.0074	2.68	0.003
FT	Δ_1F_+	0	0	44	47.0264	2.27	-0.003
FT	Δ_1F_+	0	0	45	48.0520	2.27	-0.002
FT	Δ_1F_+	0	0	46	49.0775	2.59	0.000
FT	Δ_1F_+	0	0	47	50.0916	0.87	-0.008
FT	Δ_1F_+	0	0	49	52.1435	1.09	0.002
FT	Δ_1F_+	0	0	50	53.1608	0.64	-0.001
FT	Δ_1F_+	0	0	51	54.1846	0.59	0.005
FT	Δ_1F_+	0	0	52	55.1929	0.59	-0.005
FT	Δ_1F_+	0	0	55	58.2543	0.10	0.010
FT	Δ_1F_+	0	0	56	59.2557	0.23	-0.002
FT	Δ_1F_+	0	0	57	60.2701	0.64	-0.000
FT	Δ_1F_-	0	0	2	2.8180	0.50	0.001
FT	Δ_1F_-	0	0	3	3.8646	0.59	0.002
FT	Δ_1F_-	0	0	5	5.9537	0.68	0.001
FT	Δ_1F_-	0	0	6	7.0002	1.68	0.002
FT	Δ_1F_-	0	0	7	8.0499	1.86	0.007
FT	Δ_1F_-	0	0	8	9.0917	1.37	0.004
FT	Δ_1F_-	0	0	9	10.1320	2.37	-0.001
FT	Δ_1F_-	0	0	10	11.1758	2.32	-0.001
FT	Δ_1F_-	0	0	11	12.2217	3.37	0.000
FT	Δ_1F_-	0	0	12	13.2623	2.92	-0.004
FT	Δ_1F_-	0	0	13	14.3100	2.10	0.000
FT	Δ_1F_-	0	0	14	15.3534	3.32	-0.000
FT	Δ_1F_-	0	0	15	16.3964	2.55	-0.001
FT	Δ_1F_-	0	0	16	17.4399	2.55	-0.000
FT	Δ_1F_-	0	0	17	18.4873	3.78	0.004
FT	Δ_1F_-	0	0	18	19.5296	3.45	0.004
FT	Δ_1F_-	0	0	19	20.5680	2.50	-0.000
FT	Δ_1F_-	0	0	20	21.6034	1.37	-0.007
FT	Δ_1F_-	0	0	21	22.6493	3.55	-0.002
FT	Δ_1F_-	0	0	22	23.6943	3.46	0.001
FT	Δ_1F_-	0	0	23	24.7351	4.28	0.001
FT	Δ_1F_-	0	0	24	25.7721	3.55	-0.002
FT	Δ_1F_-	0	0	25	26.8133	3.91	-0.001
FT	Δ_1F_-	0	0	26	27.8563	4.73	0.003
FT	Δ_1F_-	0	0	27	28.8842	2.69	-0.008
FT	Δ_1F_-	0	0	28	29.9288	2.10	-0.002
FT	Δ_1F_-	0	0	29	30.9735	3.24	0.005
FT	Δ_1F_-	0	0	30	32.0082	3.00	0.002
FT	Δ_1F_-	0	0	31	33.0427	2.95	-0.000
FT	Δ_1F_-	0	0	32	34.0822	2.60	0.003
FT	Δ_1F_-	0	0	33	35.1174	3.45	0.002
FT	Δ_1F_-	0	0	34	36.1432	4.18	-0.007
FT	Δ_1F_-	0	0	35	37.1866	4.19	0.002
FT	Δ_1F_-	0	0	36	38.2157	3.36	-0.003
FT	Δ_1F_-	0	0	37	39.2555	3.28	0.004
FT	Δ_1F_-	0	0	38	40.2858	2.05	0.002

Appendix VI -- $X^5\Delta$ Least-Squares Fit: data and residuals (cont.)

Source	Type	v	Ω	J	Data	Weight	Residuals
FT	Δ_1F-	0	0	39	41.3165	2.41	0.001
FT	Δ_1F-	0	0	40	42.3461	3.27	-0.000
FT	Δ_1F-	0	0	41	43.3721	2.32	-0.004
FT	Δ_1F-	0	0	42	44.4070	3.09	0.001
FT	Δ_1F-	0	0	43	45.4357	2.27	0.001
FT	Δ_1F-	0	0	44	46.4667	1.27	0.004
FT	Δ_1F-	0	0	45	47.4900	2.59	0.001
FT	Δ_1F-	0	0	46	48.5156	2.18	0.000
FT	Δ_1F-	0	0	47	49.5397	1.59	-0.001
FT	Δ_1F-	0	0	48	50.5655	0.55	0.000
FT	Δ_1F-	0	0	51	53.6422	0.59	0.009
FT	Δ_1F-	0	0	52	54.6510	0.09	-0.002
FT	Δ_1F	0	1	2	3.1138	0.71	-0.005
FT	Δ_1F	0	1	3	4.1613	0.93	0.003
FT	Δ_1F	0	1	4	5.1936	1.38	-0.004
FT	Δ_1F	0	1	5	6.2373	2.28	0.001
FT	Δ_1F	0	1	6	7.2764	1.46	0.001
FT	Δ_1F	0	1	7	8.3194	1.10	0.005
FT	Δ_1F	0	1	8	9.3454	1.50	-0.008
FT	Δ_1F	0	1	9	10.3887	1.00	-0.004
FT	Δ_1F	0	1	10	11.4323	2.32	0.001
FT	Δ_1F	0	1	11	12.4707	2.73	0.001
FT	Δ_1F	0	1	12	13.5120	2.32	0.005
FT	Δ_1F	0	1	13	14.5430	2.77	-0.002
FT	Δ_1F	0	1	14	15.5826	1.86	-0.000
FT	Δ_1F	0	1	15	16.6186	1.78	-0.002
FT	Δ_1F	0	1	16	17.6546	1.91	-0.003
FT	Δ_1F	0	1	17	18.6968	2.32	0.003
FT	Δ_1F	0	1	18	19.7284	1.95	-0.002
FT	Δ_1F	0	1	19	20.7629	1.33	-0.004
FT	Δ_1F	0	1	20	21.8011	1.86	-0.001
FT	Δ_1F	0	1	21	22.8379	1.45	0.000
FT	Δ_1F	0	1	22	23.8717	0.96	-0.001
FT	Δ_1F	0	1	23	24.9078	1.00	0.001
FT	Δ_1F	0	1	24	25.9420	1.28	0.001
FT	Δ_1F	0	1	25	26.9742	1.32	-0.001
FT	Δ_1F	0	1	26	28.0053	0.87	-0.003
FT	Δ_1F	0	1	27	29.0391	1.28	-0.001
FT	Δ_1F	0	1	28	30.0726	0.91	-0.000
FT	Δ_1F	0	1	29	31.1025	0.95	-0.002
FT	Δ_1F	0	1	30	32.1307	0.83	-0.005
FT	Δ_1F	0	1	31	33.1672	0.38	0.001
FT	Δ_1F	0	1	32	34.1944	0.38	-0.001
FT	Δ_1F	0	1	33	35.2242	0.75	-0.001
FT	Δ_1F	0	1	34	36.2543	0.78	0.001
FT	Δ_1F	0	1	36	38.3010	0.20	-0.008
FT	Δ_1F	0	1	37	39.3360	0.05	-0.000
FT	Δ_1F_+	0	1	5	6.2420	0.50	0.004
FT	Δ_1F_+	0	1	6	7.2750	0.19	-0.002
FT	Δ_1F_+	0	1	7	8.3198	0.77	0.004
FT	Δ_1F_+	0	1	8	9.3625	0.37	0.007
FT	Δ_1F_+	0	1	9	10.3945	1.15	-0.000
FT	Δ_1F_+	0	1	10	11.4334	0.74	-0.000
FT	Δ_1F_+	0	1	11	12.4748	0.78	0.002
FT	Δ_1F_+	0	1	12	13.5108	0.83	-0.001
FT	Δ_1F_+	0	1	13	14.5450	0.87	-0.005
FT	Δ_1F_+	0	1	14	15.5875	1.28	-0.001
FT	Δ_1F_+	0	1	15	16.6299	0.87	0.004
FT	Δ_1F_+	0	1	17	18.7050	0.87	0.003
FT	Δ_1F_+	0	1	18	19.7356	0.37	-0.003
FT	Δ_1F_+	0	1	19	20.7744	1.32	-0.001
FT	Δ_1F_+	0	1	20	21.8148	1.41	0.002
FT	Δ_1F_+	0	1	21	22.8497	0.96	0.001
FT	Δ_1F_+	0	1	22	23.8772	0.51	-0.007
FT	Δ_1F_+	0	1	23	24.9202	0.55	-0.000
FT	Δ_1F_+	0	1	24	25.9529	1.74	-0.002
FT	Δ_1F_+	0	1	25	26.9911	0.46	0.001
FT	Δ_1F_+	0	1	26	28.0174	0.87	-0.007
FT	Δ_1F_+	0	1	27	29.0576	0.33	-0.001
FT	Δ_1F_+	0	1	28	30.0912	0.79	-0.000
FT	Δ_1F_+	0	1	29	31.1203	0.29	-0.004
FT	Δ_1F_+	0	1	31	33.1863	0.95	-0.002
FT	Δ_1F_+	0	1	32	34.2175	0.38	-0.002
FT	Δ_1F_+	0	1	33	35.2519	0.95	0.001
FT	Δ_1F_+	0	1	35	37.3122	1.23	0.002
FT	Δ_1F_+	0	1	36	38.3426	0.74	0.004
FT	Δ_1F_+	0	1	37	39.3718	0.33	0.005
FT	Δ_1F_+	0	1	38	40.3983	0.19	0.004
FT	Δ_1F_+	0	1	39	41.4167	0.33	-0.005
FT	Δ_1F_+	0	1	40	42.4449	0.38	-0.003
FT	Δ_1F_+	0	1	41	43.4741	0.28	0.001
FT	Δ_1F_+	0	1	42	44.4998	0.28	0.002
FT	Δ_1F_+	0	1	43	45.5195	0.20	-0.002
FT	Δ_1F_+	0	1	44	46.5439	0.38	-0.001
FT	Δ_1F_+	0	1	45	47.5692	0.23	0.002
FT	Δ_1F_+	0	1	46	48.5831	0.19	-0.006
FT	Δ_1F_+	0	1	47	49.6115	0.32	0.002
FT	Δ_1F_+	0	1	48	50.6209	0.24	-0.008

Appendix VI -- $X^5\Delta$ Least-Squares Fit: data and residuals (cont.)

Source	Type	v	Ω	J	Data	Weight	Residuals
FT	Δ_1F_+	0	1	52	54.7004	0.14	0.001
FT	Δ_1F_-	0	1	6	7.2763	0.14	0.002
FT	Δ_1F_-	0	1	7	8.3093	0.32	-0.004
FT	Δ_1F_-	0	1	8	9.3506	0.45	-0.001
FT	Δ_1F_-	0	1	9	10.3928	0.33	0.003
FT	Δ_1F_-	0	1	10	11.4310	0.74	0.003
FT	Δ_1F_-	0	1	11	12.4693	0.29	0.003
FT	Δ_1F_-	0	1	12	13.5015	0.78	-0.002
FT	Δ_1F_-	0	1	13	14.5375	0.74	-0.003
FT	Δ_1F_-	0	1	14	15.5722	0.78	-0.005
FT	Δ_1F_-	0	1	15	16.6198	0.50	0.005
FT	Δ_1F_-	0	1	16	17.6561	1.32	0.005
FT	Δ_1F_-	0	1	17	18.6876	0.39	0.001
FT	Δ_1F_-	0	1	18	19.7215	0.51	-0.001
FT	Δ_1F_-	0	1	19	20.7554	0.96	-0.002
FT	Δ_1F_-	0	1	20	21.7899	0.60	-0.002
FT	Δ_1F_-	0	1	21	22.8187	1.28	-0.008
FT	Δ_1F_-	0	1	22	23.8563	0.96	-0.004
FT	Δ_1F_-	0	1	24	25.9323	0.50	0.005
FT	Δ_1F_-	0	1	25	26.9536	0.87	-0.006
FT	Δ_1F_-	0	1	26	27.9897	0.65	-0.002
FT	Δ_1F_-	0	1	27	29.0286	0.42	0.006
FT	Δ_1F_-	0	1	28	30.0469	0.38	-0.007
FT	Δ_1F_-	0	1	30	32.1170	1.28	0.003
FT	Δ_1F_-	0	1	31	33.1419	1.24	-0.001
FT	Δ_1F_-	0	1	32	34.1681	0.41	-0.004
FT	Δ_1F_-	0	1	34	36.2305	0.37	0.004
FT	Δ_1F_-	0	1	35	37.2542	1.23	0.001
FT	Δ_1F_-	0	1	36	38.2794	0.69	-0.000
FT	Δ_1F_-	0	1	38	40.3312	0.28	0.002
FT	Δ_1F_-	0	1	39	41.3599	0.42	0.007
FT	Δ_1F_-	0	1	40	42.3764	0.84	0.000
FT	Δ_1F_-	0	1	41	43.4032	0.41	0.004
FT	Δ_1F_-	0	1	42	44.4179	0.29	-0.002
FT	Δ_1F_-	0	1	44	46.4606	0.29	-0.000
FT	Δ_1F_-	0	1	45	47.4764	0.19	-0.004
FT	Δ_1F_-	0	1	46	48.4966	0.64	-0.002
FT	Δ_1F_-	0	1	47	49.5194	0.28	0.004
FT	Δ_1F_-	0	1	48	50.5347	0.28	0.003
FT	Δ_1F_-	0	1	49	51.5538	0.23	0.006
FT	Δ_1F	0	2	2	3.0992	2.00	-0.002
FT	Δ_1F	0	2	3	4.1367	1.05	0.002
FT	Δ_1F	0	2	4	5.1761	2.19	0.008
FT	Δ_1F	0	2	5	6.2011	2.28	-0.001
FT	Δ_1F	0	2	6	7.2404	2.55	0.005
FT	Δ_1F	0	2	7	8.2720	3.69	0.003
FT	Δ_1F	0	2	8	9.3037	3.65	0.002
FT	Δ_1F	0	2	9	10.3330	4.10	-0.002
FT	Δ_1F	0	2	10	11.3681	4.87	0.000
FT	Δ_1F	0	2	11	12.4027	5.91	0.002
FT	Δ_1F	0	2	12	13.4280	4.92	-0.005
FT	Δ_1F	0	2	13	14.4667	4.60	0.002
FT	Δ_1F	0	2	14	15.4932	5.42	-0.004
FT	Δ_1F	0	2	15	16.5326	6.24	0.004
FT	Δ_1F	0	2	16	17.5577	5.37	-0.002
FT	Δ_1F	0	2	17	18.5895	5.10	-0.002
FT	Δ_1F	0	2	18	19.6221	4.83	0.000
FT	Δ_1F	0	2	19	20.6537	5.14	0.001
FT	Δ_1F	0	2	20	21.6826	5.10	0.000
FT	Δ_1F	0	2	21	22.7120	4.24	-0.000
FT	Δ_1F	0	2	22	23.7412	4.60	-0.000
FT	Δ_1F	0	2	23	24.7706	5.10	0.000
FT	Δ_1F	0	2	24	25.7974	5.50	-0.002
FT	Δ_1F	0	2	25	26.8312	5.50	0.004
FT	Δ_1F	0	2	26	27.8564	5.10	0.001
FT	Δ_1F	0	2	27	28.8818	3.28	-0.000
FT	Δ_1F	0	2	28	29.9065	2.25	-0.002
FT	Δ_1F	0	2	29	30.9378	3.92	0.003
FT	Δ_1F	0	2	30	31.9603	3.65	-0.000
FT	Δ_1F	0	2	31	32.9874	2.79	0.001
FT	Δ_1F	0	2	32	34.0098	3.20	-0.001
FT	Δ_1F	0	2	33	35.0419	3.24	0.007
FT	Δ_1F	0	2	34	36.0602	3.69	0.002
FT	Δ_1F	0	2	35	37.0802	3.19	-0.001
FT	Δ_1F	0	2	36	38.1039	3.60	0.001
FT	Δ_1F	0	2	37	39.1254	3.55	0.001
FT	Δ_1F	0	2	38	40.1462	1.79	0.001
FT	Δ_1F	0	2	39	41.1687	3.14	0.003
FT	Δ_1F	0	2	40	42.1900	2.87	0.005
FT	Δ_1F	0	2	41	43.2045	2.87	0.001
FT	Δ_1F	0	2	42	44.2181	4.00	-0.004
FT	Δ_1F	0	2	43	45.2422	4.36	0.003
FT	Δ_1F	0	2	44	46.2500	4.50	-0.006
FT	Δ_1F	0	2	45	47.2736	2.21	0.002
FT	Δ_1F	0	2	46	48.2892	2.25	0.003
FT	Δ_1F	0	2	47	49.2998	3.01	-0.001
FT	Δ_1F	0	2	48	50.3125	2.42	-0.002
FT	Δ_1F	0	2	49	51.3267	2.55	0.000

Appendix VI -- $X^5\Delta$ Least-Squares Fit: data and residuals (cont.)

Source	Type	v	Ω	J	Data	Weight	Residuals
FT	Δ_1F	0	2	50	52.3392	3.27	0.001
FT	Δ_1F	0	2	51	53.3456	2.86	-0.003
FT	Δ_1F	0	2	52	54.3592	1.60	0.000
FT	Δ_1F	0	2	53	55.3718	2.23	0.004
FT	Δ_1F	0	2	54	56.3797	1.36	0.004
FT	Δ_1F	0	2	55	57.3880	0.37	0.005
FT	Δ_1F	0	2	56	58.3863	1.19	-0.002
FT	Δ_1F	0	2	57	59.3981	1.64	0.004
FT	Δ_1F	0	2	58	60.4012	1.10	0.004
FT	Δ_1F	0	2	59	61.3948	1.10	-0.006
FT	Δ_1F	0	2	60	62.4062	0.65	0.004
FT	Δ_1F	0	3	3	4.1031	2.78	-0.008
FT	Δ_1F	0	3	4	5.1327	2.71	-0.006
FT	Δ_1F	0	3	5	6.1615	4.45	-0.005
FT	Δ_1F	0	3	6	7.1880	3.65	-0.006
FT	Δ_1F	0	3	7	8.2194	4.37	-0.002
FT	Δ_1F	0	3	8	9.2485	5.60	-0.000
FT	Δ_1F	0	3	9	10.2747	4.00	-0.001
FT	Δ_1F	0	3	10	11.3035	5.41	0.001
FT	Δ_1F	0	3	11	12.3279	4.60	-0.001
FT	Δ_1F	0	3	12	13.3567	5.64	0.001
FT	Δ_1F	0	3	13	14.3874	5.82	0.005
FT	Δ_1F	0	3	14	15.4113	4.20	0.003
FT	Δ_1F	0	3	15	16.4348	5.36	0.001
FT	Δ_1F	0	3	16	17.4634	5.05	0.004
FT	Δ_1F	0	3	17	18.4877	5.05	0.002
FT	Δ_1F	0	3	18	19.5080	5.05	-0.002
FT	Δ_1F	0	3	19	20.5342	4.79	-0.001
FT	Δ_1F	0	3	20	21.5646	4.51	0.005
FT	Δ_1F	0	3	21	22.5845	5.24	0.001
FT	Δ_1F	0	3	22	23.6051	7.36	-0.002
FT	Δ_1F	0	3	23	24.6306	7.05	0.000
FT	Δ_1F	0	3	24	25.6548	7.05	0.002
FT	Δ_1F	0	3	25	26.6744	7.55	-0.001
FT	Δ_1F	0	3	26	27.7033	8.32	0.006
FT	Δ_1F	0	3	27	28.7188	7.00	-0.001
FT	Δ_1F	0	3	28	29.7429	7.05	0.002
FT	Δ_1F	0	3	29	30.7632	8.10	0.002
FT	Δ_1F	0	3	30	31.7799	5.86	-0.001
FT	Δ_1F	0	3	31	32.8016	5.95	0.001
FT	Δ_1F	0	3	32	33.8203	6.27	0.000
FT	Δ_1F	0	3	33	34.8372	4.12	-0.001
FT	Δ_1F	0	3	34	35.8558	1.30	-0.001
FT	Δ_1F	0	3	35	36.8761	3.05	0.002
FT	Δ_1F	0	3	36	37.8886	3.66	-0.002
FT	Δ_1F	0	3	37	38.9048	3.66	-0.002
FT	Δ_1F	0	3	38	39.9237	4.47	0.001
FT	Δ_1F	0	3	39	40.9376	3.66	-0.000
FT	Δ_1F	0	3	40	41.9540	3.74	0.002
FT	Δ_1F	0	3	41	42.9675	2.29	0.002
FT	Δ_1F	0	3	42	43.9815	2.11	0.003
FT	Δ_1F	0	3	43	44.9953	2.12	0.004
FT	Δ_1F	0	3	44	46.0070	2.80	0.005
FT	Δ_1F	0	3	45	47.0143	3.01	0.001
FT	Δ_1F	0	3	46	48.0262	1.51	0.003
FT	Δ_1F	0	3	47	49.0263	2.01	-0.006
FT	Δ_1F	0	3	49	51.0446	2.60	-0.004
FT	Δ_1F	0	3	50	52.0517	2.00	-0.003
FT	Δ_1F	0	3	51	53.0665	2.37	0.006
FT	Δ_1F	0	3	52	54.0604	1.88	-0.005
FT	Δ_1F	0	3	53	55.0737	1.02	0.004
FT	Δ_1F	0	3	54	56.0728	0.89	-0.001
FT	Δ_1F	0	3	55	57.0793	1.23	0.004
FT	Δ_1F	0	3	56	58.0801	1.18	0.003
FT	Δ_1F	0	3	57	59.0777	0.77	0.000
FT	Δ_1F	0	3	58	60.0745	2.00	-0.003
FT	Δ_1F	0	3	59	61.0690	0.32	-0.007
FT	Δ_1F	0	3	61	63.0618	0.28	-0.008
FT	Δ_1F	0	3	62	64.0681	0.23	0.003
FT	Δ_1F	0	4	4	5.1071	1.33	-0.001
FT	Δ_1F	0	4	5	6.1321	2.52	0.003
FT	Δ_1F	0	4	6	7.1459	2.65	-0.005
FT	Δ_1F	0	4	7	8.1706	3.23	-0.001
FT	Δ_1F	0	4	8	9.1940	3.42	0.001
FT	Δ_1F	0	4	9	10.2129	5.33	-0.001
FT	Δ_1F	0	4	10	11.2398	5.05	0.005
FT	Δ_1F	0	4	11	12.2583	4.65	0.003
FT	Δ_1F	0	4	12	13.2739	5.01	-0.002
FT	Δ_1F	0	4	13	14.2977	4.47	0.001
FT	Δ_1F	0	4	14	15.3175	5.55	0.001
FT	Δ_1F	0	4	15	16.3326	6.15	-0.004
FT	Δ_1F	0	4	16	17.3550	7.05	-0.001
FT	Δ_1F	0	4	17	18.3766	6.33	0.001
FT	Δ_1F	0	4	18	19.3947	7.73	0.001
FT	Δ_1F	0	4	19	20.4126	8.36	-0.000
FT	Δ_1F	0	4	20	21.4329	6.79	0.002
FT	Δ_1F	0	4	21	22.4460	7.28	-0.003
FT	Δ_1F	0	4	22	23.4696	6.87	0.002

Appendix VI -- $X^5\Delta$ Least-Squares Fit: data and residuals (cont.)

Source	Type	v	Ω	J	Data	Weight	Residuals
FT	Δ_1F	0	4	23	24.4856	7.15	0.001
FT	Δ_1F	0	4	24	25.5025	8.14	0.001
FT	Δ_1F	0	4	25	26.5189	7.24	0.001
FT	Δ_1F	0	4	26	27.5308	6.15	-0.004
FT	Δ_1F	0	4	27	28.5518	6.87	0.001
FT	Δ_1F	0	4	28	29.5632	6.93	-0.002
FT	Δ_1F	0	4	29	30.5799	5.38	-0.001
FT	Δ_1F	0	4	30	31.5951	6.01	0.000
FT	Δ_1F	0	4	31	32.6090	6.29	-0.000
FT	Δ_1F	0	4	32	33.6250	6.87	0.002
FT	Δ_1F	0	4	33	34.6351	4.47	-0.000
FT	Δ_1F	0	4	34	35.6478	5.69	-0.000
FT	Δ_1F	0	4	35	36.6578	6.42	-0.002
FT	Δ_1F	0	4	36	37.6724	6.93	0.001
FT	Δ_1F	0	4	37	38.6818	5.91	-0.000
FT	Δ_1F	0	4	38	39.6905	4.73	-0.002
FT	Δ_1F	0	4	39	40.7049	5.95	0.003
FT	Δ_1F	0	4	40	41.7074	5.55	-0.003
FT	Δ_1F	0	4	41	42.7221	7.14	0.003
FT	Δ_1F	0	4	42	43.7276	6.24	0.001
FT	Δ_1F	0	4	43	44.7337	6.28	0.000
FT	Δ_1F	0	4	44	45.7402	5.05	0.001
FT	Δ_1F	0	4	45	46.7490	5.78	0.004
FT	Δ_1F	0	4	46	47.7452	4.86	-0.005
FT	Δ_1F	0	4	47	48.7566	5.27	0.002
FT	Δ_1F	0	4	48	49.7584	5.18	0.001
FT	Δ_1F	0	4	49	50.7597	3.50	-0.000
FT	Δ_1F	0	4	50	51.7597	2.55	-0.002
FT	Δ_1F	0	4	51	52.7658	4.18	0.003
FT	Δ_1F	0	4	52	53.7669	3.65	0.004
FT	Δ_1F	0	4	53	54.7603	2.86	-0.002
FT	Δ_1F	0	4	54	55.7600	2.86	-0.001
FT	Δ_1F	0	4	55	56.7598	4.00	0.001
FT	Δ_1F	0	4	56	57.7556	4.09	0.001
FT	Δ_1F	0	4	57	58.7501	3.18	-0.001
FT	Δ_1F	0	4	58	59.7449	3.05	-0.001
FT	Δ_1F	0	4	59	60.7384	2.32	-0.001
FT	Δ_1F	0	4	60	61.7330	1.86	0.000
FT	Δ_1F	0	4	61	62.7312	2.50	0.007
FT	Δ_1F	0	4	62	63.7135	2.59	-0.002
FT	Δ_1F	0	4	63	64.7115	2.00	0.006
FT	Δ_1F	0	4	64	65.6979	1.18	0.003
FT	Δ_1F	0	4	65	66.6794	0.77	-0.003
FT	Δ_1F	0	4	66	67.6696	1.59	0.000
FT	Δ_1F	0	4	67	68.6628	0.73	0.007
FT	Δ_1F	0	4	68	69.6350	1.18	-0.005
FT	Δ_1F	0	4	69	70.6294	0.73	0.005
FT	Δ_1F	0	4	70	71.6090	1.14	0.003
FT	Δ_1F	0	4	71	72.5855	0.73	-0.002
FT	Δ_1F	0	4	72	73.5605	1.18	-0.007
FT	Δ_1F	0	4	73	74.5455	1.59	-0.002
FT	Δ_1F	0	4	75	76.4951	0.51	-0.007
FT	Δ_1F	0	4	76	77.4780	0.50	0.001
FT	Δ_1F	0	4	77	78.4460	0.09	-0.005
FT	Δ_1F	0	4	78	79.4190	0.01	-0.005
L	Δ_2F	0	0	2	5.2330	1.00	0.007
L	Δ_2F	0	0	3	7.3230	5.00	0.007
L	Δ_2F	0	0	4	9.4040	5.00	-0.002
L	Δ_2F	0	0	5	11.4960	5.00	-0.000
L	Δ_2F	0	0	6	13.5830	5.00	-0.003
L	Δ_2F	0	0	7	15.6730	5.00	-0.002
L	Δ_2F	0	0	8	17.7620	1.00	-0.003
L	Δ_2F	0	0	9	19.8510	1.00	-0.003
L	Δ_2F	0	0	10	21.9380	1.00	-0.004
L	Δ_2F	0	0	11	24.0240	5.00	-0.006
L	Δ_2F	0	0	12	26.1230	5.00	0.005
L	Δ_2F	0	0	13	28.2070	5.00	0.002
L	Δ_2F	0	0	14	30.2880	1.00	-0.004
L	Δ_2F	0	0	15	32.3780	5.00	0.000
L	Δ_2F	0	0	16	34.4670	5.00	0.004
L	Δ_2F	0	0	17	36.5510	5.00	0.002
L	Δ_2F	0	0	18	38.6280	5.00	-0.005
L	Δ_2F	0	0	19	40.7180	5.00	0.002
L	Δ_2F	0	0	20	42.7970	5.00	-0.002
L	Δ_2F	0	0	21	44.8880	1.00	0.007
L	Δ_2F	0	0	26	55.2790	5.00	0.001
L	Δ_2F	0	0	28	59.4380	1.00	0.008
L	Δ_2F	0	0	29	61.5030	5.00	-0.002
L	Δ_2F	0	0	30	63.5730	5.00	-0.005
L	Δ_2F	0	0	34	71.8680	5.00	0.009
L	Δ_2F	0	0	37	78.0570	5.00	0.000
L	Δ_2F	0	1	2	5.1940	5.00	-0.004
L	Δ_2F	0	1	3	7.2770	5.00	0.001
L	Δ_2F	0	1	4	9.3540	5.00	-0.001
L	Δ_2F	0	1	5	11.4370	5.00	0.003
L	Δ_2F	0	1	6	13.5130	5.00	0.001
L	Δ_2F	0	1	7	15.5900	5.00	-0.001
L	Δ_2F	0	1	8	17.6720	5.00	0.004

Appendix VI -- $X^5\Delta$ Least-Squares Fit: data and residuals (cont.)

Source	Type	v	Ω	J	Data	Weight	Residuals
L	Δ_2F	0	1	9	19.7420	5.00	-0.004
L	Δ_2F	0	1	10	21.8250	5.00	0.002
L	Δ_2F	0	1	11	23.8990	5.00	-0.001
L	Δ_2F	0	1	12	25.9730	8.00	-0.004
L	Δ_2F	0	1	13	28.0510	8.00	-0.002
L	Δ_2F	0	1	14	30.1270	8.00	-0.001
L	Δ_2F	0	1	15	32.2000	8.00	-0.003
L	Δ_2F	0	1	16	34.2780	8.00	0.000
L	Δ_2F	0	1	17	36.3520	8.00	0.001
L	Δ_2F	0	1	18	38.4240	8.00	-0.001
L	Δ_2F	0	1	19	40.4980	8.00	0.001
L	Δ_2F	0	1	20	42.5670	8.00	-0.002
L	Δ_2F	0	1	21	44.6400	8.00	0.000
L	Δ_2F	0	1	22	46.7090	5.00	-0.001
L	Δ_2F	0	1	23	48.7730	5.00	-0.007
L	Δ_2F	0	1	24	50.8460	5.00	-0.002
L	Δ_2F	0	1	25	52.9150	5.00	-0.001
L	Δ_2F	0	1	26	54.9830	5.00	0.000
L	Δ_2F	0	1	27	57.0480	5.00	-0.000
L	Δ_2F	0	1	28	59.1140	5.00	0.001
L	Δ_2F	0	1	29	61.1730	5.00	-0.004
L	Δ_2F	0	1	30	63.2420	5.00	0.002
L	Δ_2F	0	1	31	65.2990	5.00	-0.002
L	Δ_2F	0	2	3	7.2350	5.00	-0.001
L	Δ_2F	0	2	4	9.3030	5.00	-0.000
L	Δ_2F	0	2	5	11.3670	5.00	-0.004
L	Δ_2F	0	2	6	13.4370	5.00	-0.001
L	Δ_2F	0	2	7	15.5050	5.00	0.001
L	Δ_2F	0	2	8	17.5690	5.00	-0.002
L	Δ_2F	0	2	9	19.6340	5.00	-0.003
L	Δ_2F	0	2	10	21.6990	5.00	-0.004
L	Δ_2F	0	2	11	23.7690	5.00	0.001
L	Δ_2F	0	2	12	25.8340	5.00	0.001
L	Δ_2F	0	2	13	27.9010	5.00	0.003
L	Δ_2F	0	2	14	29.9570	1.00	-0.005
L	Δ_2F	0	2	15	32.0250	5.00	-0.000
L	Δ_2F	0	2	16	34.0970	1.00	0.008
L	Δ_2F	0	2	17	36.1490	5.00	-0.002
L	Δ_2F	0	2	18	38.2120	5.00	-0.001
L	Δ_2F	0	2	19	40.2730	5.00	-0.001
L	Δ_2F	0	2	20	42.3330	5.00	-0.002
L	Δ_2F	0	2	21	44.3960	5.00	0.001
L	Δ_2F	0	2	22	46.4550	5.00	0.001
L	Δ_2F	0	2	23	48.5110	5.00	-0.001
L	Δ_2F	0	2	30	62.8970	5.00	0.001
L	Δ_2F	0	2	32	66.9930	5.00	-0.003
L	Δ_2F	0	2	33	69.0480	5.00	0.003
L	Δ_2F	0	2	35	73.1360	5.00	-0.003
L	Δ_2F	0	2	36	75.1840	5.00	0.000
L	Δ_2F	0	2	38	79.2720	5.00	0.002
L	Δ_1F	0	2	3	4.1320	5.00	-0.003
L	Δ_1F	0	2	8	9.3000	5.00	-0.002
L	Δ_1F	0	2	9	10.3350	5.00	0.000
L	Δ_2F	0	3	4	9.2470	5.00	-0.003
L	Δ_2F	0	3	5	11.3070	5.00	0.002
L	Δ_2F	0	3	6	13.3610	5.00	0.001
L	Δ_2F	0	3	7	15.4170	5.00	0.002
L	Δ_2F	0	3	8	17.4700	5.00	0.000
L	Δ_2F	0	3	9	19.5260	5.00	0.002
L	Δ_2F	0	3	10	21.5760	5.00	-0.002
L	Δ_2F	0	3	11	23.6290	5.00	-0.003
L	Δ_2F	0	3	12	25.6840	1.00	-0.001
L	Δ_2F	0	3	13	27.7380	5.00	-0.000
L	Δ_2F	0	3	14	29.7900	5.00	-0.001
L	Δ_2F	0	3	15	31.8400	5.00	-0.003
L	Δ_2F	0	3	16	33.8940	5.00	-0.000
L	Δ_2F	0	3	17	35.9450	5.00	-0.000
L	Δ_2F	0	3	18	37.9950	5.00	-0.000
L	Δ_2F	0	3	19	40.0450	5.00	-0.000
L	Δ_2F	0	3	20	42.0960	5.00	0.002
L	Δ_2F	0	3	21	44.1400	5.00	-0.003
L	Δ_2F	0	3	22	46.1920	1.00	0.002
L	Δ_2F	0	3	23	48.2360	5.00	-0.001
L	Δ_2F	0	3	24	50.2820	5.00	-0.001
L	Δ_2F	0	3	25	52.3300	5.00	0.001
L	Δ_2F	0	3	26	54.3720	5.00	-0.001
L	Δ_2F	0	3	27	56.4130	5.00	-0.004
L	Δ_2F	0	3	28	58.4610	5.00	0.001
L	Δ_2F	0	3	29	60.4980	5.00	-0.004
L	Δ_2F	0	3	30	62.5420	5.00	-0.001
L	Δ_2F	0	3	31	64.5800	5.00	-0.002
L	Δ_2F	0	3	32	66.6210	5.00	-0.000
L	Δ_2F	0	3	35	72.7310	5.00	0.000
L	Δ_2F	0	3	36	74.7630	5.00	-0.002
L	Δ_2F	0	3	37	76.7980	5.00	-0.000
L	Δ_1F	0	3	3	4.1100	5.00	-0.001
L	Δ_1F	0	3	4	5.1410	5.00	0.002
L	Δ_1F	0	3	5	6.1670	5.00	0.001

Appendix VI -- $X^5\Delta$ Least-Squares Fit: data and residuals (cont.)

Source	Type	v	Ω	J	Data	Weight	Residuals
L	Δ_1F	0	3	6	7.1890	5.00	-0.005
L	Δ_1F	0	3	7	8.2260	5.00	0.005
L	Δ_1F	0	3	8	9.2480	5.00	-0.001
L	Δ_1F	0	3	9	10.2770	5.00	0.001
L	Δ_1F	0	3	10	11.2990	5.00	-0.004
L	Δ_1F	0	3	11	12.3290	5.00	-0.000
L	Δ_1F	0	3	14	15.4040	5.00	-0.004
L	Δ_2F	0	4	5	11.2390	8.00	0.001
L	Δ_2F	0	4	6	13.2850	8.00	0.005
L	Δ_2F	0	4	7	15.3210	8.00	-0.002
L	Δ_2F	0	4	8	17.3640	8.00	-0.001
L	Δ_2F	0	4	9	19.4100	8.00	0.003
L	Δ_2F	0	4	10	21.4480	8.00	-0.001
L	Δ_2F	0	4	11	23.4900	8.00	-0.001
L	Δ_2F	0	4	12	25.5330	8.00	0.001
L	Δ_2F	0	4	13	27.5740	8.00	0.001
L	Δ_2F	0	4	14	29.6190	8.00	0.006
L	Δ_2F	0	4	15	31.6510	8.00	-0.002
L	Δ_2F	0	4	16	33.6900	8.00	-0.002
L	Δ_2F	0	4	17	35.7320	8.00	0.001
L	Δ_2F	0	4	18	37.7690	8.00	-0.000
L	Δ_2F	0	4	19	39.8090	8.00	0.002
L	Δ_2F	0	4	20	41.8410	8.00	-0.003
L	Δ_2F	0	4	21	43.8780	8.00	-0.003
L	Δ_2F	0	4	22	45.9190	8.00	0.002
L	Δ_2F	0	4	23	47.9490	8.00	-0.003
L	Δ_2F	0	4	24	49.9910	8.00	0.005
L	Δ_2F	0	4	25	52.0220	8.00	0.002
L	Δ_2F	0	4	26	54.0490	8.00	-0.004
L	Δ_2F	0	4	27	56.0840	8.00	-0.001
L	Δ_2F	0	4	28	58.1150	8.00	-0.001
L	Δ_2F	0	4	29	60.1440	8.00	-0.002
L	Δ_2F	0	4	30	62.1740	8.00	-0.002
L	Δ_2F	0	4	31	64.2030	8.00	-0.001
L	Δ_2F	0	4	32	66.2320	8.00	0.000
L	Δ_2F	0	4	33	68.2610	8.00	0.003
L	Δ_2F	0	4	34	70.2840	8.00	0.001
L	Δ_2F	0	4	35	72.3090	8.00	0.001
L	Δ_2F	0	4	36	74.3360	8.00	0.005
L	Δ_2F	0	4	37	76.3560	8.00	0.003
L	Δ_2F	0	4	38	78.3760	8.00	0.002
L	Δ_2F	0	4	39	80.3950	8.00	0.001
L	Δ_2F	0	4	40	82.4100	8.00	-0.002
L	Δ_2F	0	4	41	84.4270	8.00	-0.002
L	Δ_2F	0	4	42	86.4450	8.00	-0.000
L	Δ_2F	0	4	43	88.4610	8.00	0.001
L	Δ_2F	0	4	44	90.4740	8.00	0.001
L	Δ_2F	0	4	45	92.4860	8.00	0.001
L	Δ_2F	0	4	46	94.4940	8.00	-0.001
L	Δ_2F	0	4	47	96.5060	8.00	0.002
L	Δ_2F	0	4	48	98.5100	8.00	-0.002
L	Δ_2F	0	4	49	100.5180	8.00	0.001
L	Δ_2F	0	4	51	104.5230	8.00	-0.002
L	Δ_2F	0	4	52	106.5230	8.00	-0.003
L	Δ_2F	0	4	53	108.5220	8.00	-0.003
L	Δ_1F	0	4	4	5.1100	5.00	0.002
L	Δ_1F	0	4	5	6.1260	5.00	-0.004
L	Δ_1F	0	4	6	7.1490	1.00	-0.002
L	Δ_1F	0	4	7	8.1750	5.00	0.003
L	Δ_1F	0	4	8	9.1960	5.00	0.003
L	Δ_1F	0	4	9	10.2170	5.00	0.003
L	Δ_1F	0	4	10	11.2340	5.00	-0.001
L	Δ_1F	0	4	11	12.2610	5.00	0.005
L	Δ_1F	0	4	12	13.2730	5.00	-0.003
L	Δ_1F	0	4	13	14.2970	5.00	0.001
L	Δ_1F	0	4	14	15.3190	5.00	0.003
L	Δ_1F	0	4	15	16.3350	5.00	-0.001
L	Δ_1F	0	4	16	17.3640	1.00	0.008
L	Δ_1F	0	4	17	18.3740	1.00	-0.001
L	Δ_1F	0	4	18	19.3950	5.00	0.001
L	Δ_1F	0	4	19	20.4130	5.00	0.000
L	Δ_1F	0	4	20	21.4370	5.00	0.006
L	s-o	0	3	11	191.6430	5.00	-0.008
L	s-o	0	3	16	192.0640	5.00	-0.000
L	s-o	0	3	18	192.2700	5.00	-0.000
L	s-o	0	3	19	192.3860	8.00	0.004
L	s-o	0	3	20	192.4980	8.00	-0.001
L	s-o	0	3	21	192.6220	8.00	-0.001
L	s-o	0	3	22	192.7520	8.00	0.001
L	s-o	0	3	23	192.8870	8.00	0.001
L	s-o	0	3	24	193.0290	8.00	0.003
L	s-o	0	3	25	193.1670	8.00	-0.005
L	s-o	0	3	26	193.3210	8.00	-0.003
L	s-o	0	3	27	193.4770	8.00	-0.004
L	s-o	0	3	28	193.6430	8.00	-0.001
L	s-o	0	3	29	193.8130	8.00	0.001
L	s-o	0	3	30	193.9910	8.00	0.005
L	s-o	0	3	31	194.1700	5.00	0.004

Appendix VI -- $X^5\Delta$ Least-Squares Fit: data and residuals (cont.)

Source	Type	v	Ω	J	Data	Weight	Residuals
L	s-o	0	3	32	194.3560	5.00	0.006
L	s-o	0	3	33	194.5430	5.00	0.002
L	s-o	0	3	34	194.7350	5.00	-0.002
L	s-o	0	2	21	194.2800	2.50	-0.000
M	ΔJ	0	4	4	5.10804241	0.8E+07	1.52E-06
M	ΔJ	0	4	5	6.12947918	0.5E+08	-2.35E-07
M	ΔJ	0	3	4	5.13887931	0.3E+08	4.25E-07
M	ΔJ	0	3	5	6.16647344	0.1E+09	-7.18E-08
M	ΔJ	0	2	4	5.16852405	0.7E+08	-6.05E-07
M	ΔJ	0	2	5	6.20203875	0.6E+08	5.32E-07
FT	Δ_1F_+	1	0	4	5.5280	0.64	0.002
FT	Δ_1F_+	1	0	7	8.6390	1.23	0.003
FT	Δ_1F_+	1	0	8	9.6733	2.59	0.001
FT	Δ_1F_+	1	0	9	10.7011	1.14	-0.007
FT	Δ_1F_+	1	0	10	11.7407	1.69	-0.004
FT	Δ_1F_+	1	0	11	12.7782	2.55	-0.002
FT	Δ_1F_+	1	0	12	13.8149	2.18	-0.000
FT	Δ_1F_+	1	0	13	14.8441	1.77	-0.006
FT	Δ_1F_+	1	0	14	15.8865	1.14	0.001
FT	Δ_1F_+	1	0	15	16.9186	1.77	-0.001
FT	Δ_1F_+	1	0	17	18.9909	1.77	0.004
FT	Δ_1F_+	1	0	18	20.0140	1.73	-0.007
FT	Δ_1F_+	1	0	19	21.0599	1.77	0.006
FT	Δ_1F_+	1	0	20	22.0876	1.73	0.002
FT	Δ_1F_+	1	0	21	23.1119	1.77	-0.006
FT	Δ_1F_+	1	0	22	24.1536	2.18	0.004
FT	Δ_1F_+	1	0	23	25.1791	1.73	-0.002
FT	Δ_1F_+	1	0	24	26.2042	2.59	-0.007
FT	Δ_1F_+	1	0	25	27.2443	2.18	0.003
FT	Δ_1F_+	1	0	26	28.2721	2.05	0.001
FT	Δ_1F_+	1	0	27	29.3043	1.77	0.004
FT	Δ_1F_+	1	0	28	30.3313	2.59	0.003
FT	Δ_1F_+	1	0	29	31.3505	1.36	-0.006
FT	Δ_1F_+	1	0	30	32.3873	1.77	0.004
FT	Δ_1F_+	1	0	31	33.4098	2.50	-0.001
FT	Δ_1F_+	1	0	32	34.4423	1.68	0.006
FT	Δ_1F_+	1	0	33	35.4607	2.59	-0.001
FT	Δ_1F_+	1	0	34	36.4883	1.77	0.002
FT	Δ_1F_+	1	0	35	37.5100	2.50	-0.000
FT	Δ_1F_+	1	0	36	38.5363	3.00	0.003
FT	Δ_1F_+	1	0	37	39.5481	2.18	-0.008
FT	Δ_1F_+	1	0	38	40.5801	1.68	0.002
FT	Δ_1F_+	1	0	39	41.6004	2.18	0.001
FT	Δ_1F_+	1	0	40	42.6128	2.50	-0.006
FT	Δ_1F_+	1	0	41	43.6350	2.00	-0.004
FT	Δ_1F_+	1	0	42	44.6547	2.00	-0.002
FT	Δ_1F_+	1	0	43	45.6733	1.59	-0.002
FT	Δ_1F_+	1	0	44	46.6907	1.59	-0.001
FT	Δ_1F_+	1	0	45	47.7055	1.09	-0.002
FT	Δ_1F_+	1	0	46	48.7223	1.50	-0.001
FT	Δ_1F_+	1	0	47	49.7416	1.09	0.004
FT	Δ_1F_+	1	0	49	51.7660	1.00	0.003
FT	Δ_1F_+	1	0	50	52.7715	0.18	-0.003
FT	Δ_1F_-	1	0	1	1.7420	0.09	0.007
FT	Δ_1F_-	1	0	3	3.8080	0.05	-0.002
FT	Δ_1F_-	1	0	4	4.8500	0.05	0.003
FT	Δ_1F_-	1	0	6	6.9281	1.18	0.006
FT	Δ_1F_-	1	0	7	7.9609	0.68	0.002
FT	Δ_1F_-	1	0	8	8.9980	1.18	0.002
FT	Δ_1F_-	1	0	9	10.0378	0.45	0.004
FT	Δ_1F_-	1	0	10	11.0740	1.23	0.004
FT	Δ_1F_-	1	0	11	12.1064	1.27	-0.001
FT	Δ_1F_-	1	0	12	13.1377	1.77	-0.006
FT	Δ_1F_-	1	0	13	14.1808	1.73	0.001
FT	Δ_1F_-	1	0	14	15.2085	2.09	-0.007
FT	Δ_1F_-	1	0	15	16.2522	0.91	0.001
FT	Δ_1F_-	1	0	16	17.2783	1.32	-0.009
FT	Δ_1F_-	1	0	17	18.3230	1.73	0.001
FT	Δ_1F_-	1	0	18	19.3532	2.14	-0.004
FT	Δ_1F_-	1	0	19	20.3859	1.73	-0.006
FT	Δ_1F_-	1	0	20	21.4249	2.59	-0.001
FT	Δ_1F_-	1	0	21	22.4633	2.18	0.003
FT	Δ_1F_-	1	0	22	23.4984	1.36	0.005
FT	Δ_1F_-	1	0	23	24.5337	1.77	0.007
FT	Δ_1F_-	1	0	24	25.5524	1.73	-0.007
FT	Δ_1F_-	1	0	25	26.5894	2.14	-0.003
FT	Δ_1F_-	1	0	26	27.6224	2.18	-0.001
FT	Δ_1F_-	1	0	27	28.6539	1.59	-0.001
FT	Δ_1F_-	1	0	28	29.6936	2.59	0.007
FT	Δ_1F_-	1	0	29	30.7162	2.59	-0.000
FT	Δ_1F_-	1	0	30	31.7529	2.09	0.006
FT	Δ_1F_-	1	0	31	32.7762	1.68	0.001
FT	Δ_1F_-	1	0	32	33.7998	2.59	-0.005
FT	Δ_1F_-	1	0	33	34.8322	2.05	-0.000
FT	Δ_1F_-	1	0	34	35.8632	2.59	0.003
FT	Δ_1F_-	1	0	36	37.9125	2.18	-0.001
FT	Δ_1F_-	1	0	37	38.9402	2.18	0.001
FT	Δ_1F_-	1	0	38	39.9652	2.14	0.001

Appendix VI -- $X^5\Delta$ Least-Squares Fit: data and residuals (cont.)

Source	Type	v	Ω	J	Data	Weight	Residuals
FT	$\Delta_i F_-$	1	0	39	40.9844	1.68	-0.003
FT	$\Delta_i F_-$	1	0	40	42.0088	2.50	-0.002
FT	$\Delta_i F_-$	1	0	41	43.0314	2.50	-0.003
FT	$\Delta_i F_-$	1	0	42	44.0602	1.59	0.004
FT	$\Delta_i F_-$	1	0	43	45.0718	1.59	-0.005
FT	$\Delta_i F_-$	1	0	44	46.0992	1.59	0.002
FT	$\Delta_i F_-$	1	0	45	47.1099	1.18	-0.007
FT	$\Delta_i F_-$	1	0	46	48.1320	1.00	-0.004
FT	$\Delta_i F_-$	1	0	47	49.1557	1.50	0.002
FT	$\Delta_i F_-$	1	0	48	50.1707	0.59	0.000
FT	$\Delta_i F_-$	1	0	49	51.1845	1.00	-0.002
FT	$\Delta_i F$	1	1	2	3.1038	0.65	0.008
FT	$\Delta_i F$	1	1	3	4.1212	0.73	-0.006
FT	$\Delta_i F$	1	1	4	5.1668	1.18	0.008
FT	$\Delta_i F$	1	1	5	6.1823	1.50	-0.008
FT	$\Delta_i F$	1	1	6	7.2235	1.59	0.002
FT	$\Delta_i F$	1	1	7	8.2516	1.18	-0.001
FT	$\Delta_i F$	1	1	8	9.2868	1.09	0.003
FT	$\Delta_i F$	1	1	9	10.3129	1.59	-0.002
FT	$\Delta_i F$	1	1	12	13.4128	1.59	0.006
FT	$\Delta_i F$	1	1	13	14.4341	1.55	-0.003
FT	$\Delta_i F$	1	1	14	15.4632	1.68	-0.004
FT	$\Delta_i F$	1	1	15	16.4905	1.69	-0.006
FT	$\Delta_i F$	1	1	16	17.5288	1.77	0.003
FT	$\Delta_i F$	1	1	17	18.5533	1.69	-0.002
FT	$\Delta_i F$	1	1	18	19.5868	1.64	0.003
FT	$\Delta_i F$	1	1	19	20.6088	2.09	-0.003
FT	$\Delta_i F$	1	1	20	21.6380	1.77	-0.002
FT	$\Delta_i F$	1	1	21	22.6661	2.18	-0.001
FT	$\Delta_i F$	1	1	22	23.6917	1.77	-0.003
FT	$\Delta_i F$	1	1	23	24.7158	2.14	-0.006
FT	$\Delta_i F$	1	1	24	25.7492	1.73	0.001
FT	$\Delta_i F$	1	1	25	26.7777	1.27	0.004
FT	$\Delta_i F$	1	1	26	27.8007	1.68	0.002
FT	$\Delta_i F$	1	1	27	28.8242	2.18	0.000
FT	$\Delta_i F$	1	1	28	29.8547	1.32	0.006
FT	$\Delta_i F$	1	1	29	30.8655	1.24	-0.007
FT	$\Delta_i F$	1	1	30	31.8969	1.20	0.001
FT	$\Delta_i F$	1	1	31	32.9125	1.20	-0.006
FT	$\Delta_i F$	1	1	33	34.9690	0.78	0.007
FT	$\Delta_i F_+$	1	1	4	5.1690	0.05	0.010
FT	$\Delta_i F_+$	1	1	5	6.1860	0.50	-0.005
FT	$\Delta_i F_+$	1	1	6	7.2220	0.50	-0.001
FT	$\Delta_i F_+$	1	1	9	10.3212	0.59	0.004
FT	$\Delta_i F_+$	1	1	10	11.3505	0.18	0.002
FT	$\Delta_i F_+$	1	1	11	12.3785	0.18	-0.002
FT	$\Delta_i F_+$	1	1	12	13.4120	1.00	0.001
FT	$\Delta_i F_+$	1	1	14	15.4720	1.00	-0.001
FT	$\Delta_i F_+$	1	1	15	16.5055	0.59	0.003
FT	$\Delta_i F_+$	1	1	17	18.5610	0.59	-0.002
FT	$\Delta_i F_+$	1	1	18	19.5880	1.00	-0.004
FT	$\Delta_i F_+$	1	1	19	20.6260	0.18	0.004
FT	$\Delta_i F_+$	1	1	20	21.6470	1.00	-0.004
FT	$\Delta_i F_+$	1	1	21	22.6845	0.18	0.005
FT	$\Delta_i F_+$	1	1	22	23.7081	0.59	0.000
FT	$\Delta_i F_+$	1	1	23	24.7343	0.55	-0.001
FT	$\Delta_i F_+$	1	1	24	25.7654	0.55	0.002
FT	$\Delta_i F_+$	1	1	25	26.7970	0.50	0.007
FT	$\Delta_i F_+$	1	1	27	28.8415	0.18	-0.001
FT	$\Delta_i F_+$	1	1	28	29.8681	0.14	-0.001
FT	$\Delta_i F_+$	1	1	29	30.8980	0.59	0.004
FT	$\Delta_i F_+$	1	1	30	31.9160	1.00	-0.003
FT	$\Delta_i F_+$	1	1	31	32.9368	0.59	-0.006
FT	$\Delta_i F_+$	1	1	32	33.9630	1.00	-0.004
FT	$\Delta_i F_+$	1	1	33	34.9860	1.00	-0.004
FT	$\Delta_i F_+$	1	1	34	36.0200	0.18	0.008
FT	$\Delta_i F_+$	1	1	35	37.0315	0.10	-0.002
FT	$\Delta_i F_+$	1	1	36	38.0540	0.09	-0.001
FT	$\Delta_i F_+$	1	1	38	40.0951	0.28	-0.001
FT	$\Delta_i F_+$	1	1	39	41.1135	0.10	-0.001
FT	$\Delta_i F_+$	1	1	40	42.1300	0.32	-0.004
FT	$\Delta_i F_+$	1	1	43	45.1816	0.60	-0.003
FT	$\Delta_i F_+$	1	1	44	46.2021	0.73	0.002
FT	$\Delta_i F_+$	1	1	45	47.2085	0.68	-0.007
FT	$\Delta_i F_+$	1	1	46	48.2215	0.10	-0.008
FT	$\Delta_i F_+$	1	1	47	49.2443	0.68	0.002
FT	$\Delta_i F_+$	1	1	48	50.2535	0.18	-0.001
FT	$\Delta_i F_+$	1	1	49	51.2650	1.00	-0.001
FT	$\Delta_i F_+$	1	1	51	53.2880	1.00	0.002
FT	$\Delta_i F_+$	1	1	52	54.3001	0.59	0.005
FT	$\Delta_i F_+$	1	1	53	55.3015	0.18	-0.001
FT	$\Delta_i F_+$	1	1	54	56.3110	1.00	0.002
FT	$\Delta_i F_+$	1	1	55	57.3122	0.59	-0.003
FT	$\Delta_i F_+$	1	1	56	58.3222	0.59	0.002
FT	$\Delta_i F_+$	1	1	58	60.3242	0.14	-0.002
FT	$\Delta_i F_+$	1	1	59	61.3335	1.00	0.006
FT	$\Delta_i F_+$	1	1	61	63.3289	0.55	0.001
FT	$\Delta_i F_+$	1	1	62	64.3282	0.14	0.002

Appendix VI -- $X^5\Delta$ Least-Squares Fit: data and residuals (cont.)

Source	Type	v	Ω	J	Data	Weight	Residuals
FT	$\Delta_i F_+$	1	1	65	67.3090	0.18	-0.005
FT	$\Delta_i F_+$	1	1	66	68.3120	0.09	0.004
FT	$\Delta_i F_-$	1	1	1	2.0570	0.09	-0.006
FT	$\Delta_i F_-$	1	1	3	4.1220	0.09	-0.005
FT	$\Delta_i F_-$	1	1	4	5.1670	0.50	0.009
FT	$\Delta_i F_-$	1	1	5	6.1940	0.09	0.005
FT	$\Delta_i F_-$	1	1	6	7.2200	0.09	-0.000
FT	$\Delta_i F_-$	1	1	8	9.2835	0.59	0.001
FT	$\Delta_i F_-$	1	1	10	11.3472	0.59	0.004
FT	$\Delta_i F_-$	1	1	12	13.3966	0.55	-0.006
FT	$\Delta_i F_-$	1	1	13	14.4278	0.59	-0.004
FT	$\Delta_i F_-$	1	1	14	15.4594	0.59	-0.002
FT	$\Delta_i F_-$	1	1	15	16.4910	0.59	0.001
FT	$\Delta_i F_-$	1	1	16	17.5203	0.59	0.002
FT	$\Delta_i F_-$	1	1	17	18.5425	0.18	-0.004
FT	$\Delta_i F_-$	1	1	18	19.5745	1.00	-0.000
FT	$\Delta_i F_-$	1	1	19	20.6005	1.00	-0.001
FT	$\Delta_i F_-$	1	1	20	21.6306	0.59	0.002
FT	$\Delta_i F_-$	1	1	21	22.6605	1.00	0.005
FT	$\Delta_i F_-$	1	1	22	23.6781	0.59	-0.004
FT	$\Delta_i F_-$	1	1	23	24.7015	1.00	-0.006
FT	$\Delta_i F_-$	1	1	24	25.7370	0.09	0.005
FT	$\Delta_i F_-$	1	1	26	27.7865	1.00	0.005
FT	$\Delta_i F_-$	1	1	28	29.8229	0.59	-0.005
FT	$\Delta_i F_-$	1	1	29	30.8568	0.59	0.006
FT	$\Delta_i F_-$	1	1	30	31.8750	0.55	0.002
FT	$\Delta_i F_-$	1	1	33	34.9380	0.09	0.003
FT	$\Delta_i F_-$	1	1	34	35.9503	0.59	-0.004
FT	$\Delta_i F_-$	1	1	35	36.9708	0.60	-0.002
FT	$\Delta_i F_-$	1	1	37	39.0088	0.65	0.000
FT	$\Delta_i F_-$	1	1	38	40.0216	0.24	-0.003
FT	$\Delta_i F_-$	1	1	40	42.0488	0.41	-0.007
FT	$\Delta_i F_-$	1	1	42	44.0812	0.33	-0.003
FT	$\Delta_i F_-$	1	1	43	45.0930	0.77	-0.004
FT	$\Delta_i F_-$	1	1	47	49.1454	0.55	0.005
FT	$\Delta_i F_-$	1	1	48	50.1500	0.18	0.001
FT	$\Delta_i F_-$	1	1	50	52.1698	0.59	0.007
FT	$\Delta_i F_-$	1	1	51	53.1715	0.18	0.003
FT	$\Delta_i F_-$	1	1	53	55.1800	0.18	0.002
FT	$\Delta_i F_-$	1	1	54	56.1829	0.59	0.002
FT	$\Delta_i F_-$	1	1	55	57.1787	0.55	-0.004
FT	$\Delta_i F_-$	1	1	56	58.1890	0.18	0.006
FT	$\Delta_i F_-$	1	1	57	59.1811	0.59	-0.002
FT	$\Delta_i F_-$	1	1	61	63.1648	0.55	-0.007

Source	Type	v	Ω	J	Data	Weight	Residuals
FT	$\Delta_i F_-$	1	1	64	66.1600	0.10	0.009
FT	$\Delta_i F_-$	1	1	66	68.1290	0.09	-0.003
FT	$\Delta_i F_-$	1	1	67	69.1220	0.09	0.002
FT	$\Delta_i F_-$	1	1	69	71.0910	0.05	-0.003
FT	$\Delta_i F$	1	2	3	4.0969	0.24	-0.007
FT	$\Delta_i F$	1	2	4	5.1387	0.36	0.008
FT	$\Delta_i F$	1	2	5	6.1541	1.37	-0.002
FT	$\Delta_i F$	1	2	6	7.1784	1.55	-0.004
FT	$\Delta_i F$	1	2	7	8.2043	1.45	-0.003
FT	$\Delta_i F$	1	2	8	9.2421	1.41	0.009
FT	$\Delta_i F$	1	2	9	10.2524	2.00	-0.006
FT	$\Delta_i F$	1	2	10	11.2787	2.37	-0.005
FT	$\Delta_i F$	1	2	11	12.3034	2.28	-0.005
FT	$\Delta_i F$	1	2	12	13.3328	2.27	-0.000
FT	$\Delta_i F$	1	2	13	14.3613	2.82	0.004
FT	$\Delta_i F$	1	2	14	15.3785	2.41	-0.004
FT	$\Delta_i F$	1	2	15	16.4057	3.27	-0.000
FT	$\Delta_i F$	1	2	16	17.4295	3.27	-0.000
FT	$\Delta_i F$	1	2	17	18.4518	3.23	-0.001
FT	$\Delta_i F$	1	2	18	19.4728	3.82	-0.004
FT	$\Delta_i F$	1	2	19	20.5038	3.36	0.005
FT	$\Delta_i F$	1	2	20	21.5261	2.00	0.004
FT	$\Delta_i F$	1	2	21	22.5470	2.65	0.003
FT	$\Delta_i F$	1	2	22	23.5627	2.77	-0.003
FT	$\Delta_i F$	1	2	23	24.5854	4.05	-0.001
FT	$\Delta_i F$	1	2	24	25.6113	2.82	0.004
FT	$\Delta_i F$	1	2	25	26.6288	3.27	0.001
FT	$\Delta_i F$	1	2	26	27.6498	3.18	0.002
FT	$\Delta_i F$	1	2	27	28.6697	2.77	0.002
FT	$\Delta_i F$	1	2	28	29.6884	2.77	0.002
FT	$\Delta_i F$	1	2	29	30.7024	2.77	-0.003
FT	$\Delta_i F$	1	2	30	31.7281	2.73	0.005
FT	$\Delta_i F$	1	2	31	32.7400	3.18	-0.001
FT	$\Delta_i F$	1	2	32	33.7612	3.09	0.004
FT	$\Delta_i F$	1	2	33	34.7747	2.77	0.001
FT	$\Delta_i F$	1	2	34	35.7902	2.77	0.000
FT	$\Delta_i F$	1	2	35	36.8094	3.59	0.004
FT	$\Delta_i F$	1	2	36	37.8262	3.18	0.007
FT	$\Delta_i F$	1	2	37	38.8372	3.18	0.004
FT	$\Delta_i F$	1	2	38	39.8412	2.73	-0.005
FT	$\Delta_i F$	1	2	39	40.8544	2.36	-0.005
FT	$\Delta_i F$	1	2	40	41.8705	2.32	-0.000
FT	$\Delta_i F$	1	2	41	42.8809	3.59	-0.001
FT	$\Delta_i F$	1	2	42	43.8986	2.77	0.006

Appendix VI -- $X^5\Delta$ Least-Squares Fit: data and residuals (cont.)

Source	Type	v	Ω	J	Data	Weight	Residuals
FT	Δ_1F	1	2	43	44.8953	1.82	-0.007
FT	Δ_1F	1	2	44	45.9092	2.32	-0.002
FT	Δ_1F	1	2	45	46.9160	2.36	-0.003
FT	Δ_1F	1	2	46	47.9266	1.73	0.000
FT	Δ_1F	1	2	47	48.9270	1.23	-0.006
FT	Δ_1F	1	2	48	49.9356	1.23	-0.003
FT	Δ_1F	1	2	49	50.9344	0.69	-0.009
FT	Δ_1F	1	2	51	52.9531	0.32	0.003
FT	Δ_1F	1	2	52	53.9506	1.18	-0.002
FT	Δ_1F	1	2	54	55.9511	1.14	-0.003
FT	Δ_1F	1	2	55	56.9486	1.14	-0.004
FT	Δ_1F	1	2	57	58.9463	0.73	-0.002
FT	Δ_1F	1	2	58	59.9434	1.59	-0.002
FT	Δ_1F	1	2	60	61.9434	0.15	0.009
FT	Δ_1F	1	3	3	4.0849	0.61	0.004
FT	Δ_1F	1	3	4	5.0933	0.95	-0.008
FT	Δ_1F	1	3	5	6.1209	2.33	-0.000
FT	Δ_1F	1	3	6	7.1451	3.27	0.004
FT	Δ_1F	1	3	7	8.1668	2.10	0.006
FT	Δ_1F	1	3	9	10.1908	1.55	-0.009
FT	Δ_1F	1	3	10	11.2103	2.10	-0.009
FT	Δ_1F	1	3	11	12.2481	2.00	0.010
FT	Δ_1F	1	3	12	13.2546	3.77	-0.003
FT	Δ_1F	1	3	13	14.2769	3.77	0.001
FT	Δ_1F	1	3	14	15.2900	4.59	-0.005
FT	Δ_1F	1	3	15	16.3155	5.00	0.002
FT	Δ_1F	1	3	16	17.3274	4.50	-0.004
FT	Δ_1F	1	3	17	18.3477	3.68	-0.001
FT	Δ_1F	1	3	18	19.3622	3.36	-0.004
FT	Δ_1F	1	3	19	20.3903	3.73	0.007
FT	Δ_1F	1	3	20	21.4069	1.50	0.007
FT	Δ_1F	1	3	21	22.4221	3.32	0.005
FT	Δ_1F	1	3	22	23.4318	3.77	-0.001
FT	Δ_1F	1	3	23	24.4509	3.36	0.002
FT	Δ_1F	1	3	24	25.4660	2.83	0.002
FT	Δ_1F	1	3	25	26.4737	4.18	-0.005
FT	Δ_1F	1	3	26	27.4943	4.14	0.001
FT	Δ_1F	1	3	27	28.5033	3.73	-0.004
FT	Δ_1F	1	3	28	29.5290	3.27	0.008
FT	Δ_1F	1	3	29	30.5323	5.00	-0.001
FT	Δ_1F	1	3	30	31.5460	4.18	-0.000
FT	Δ_1F	1	3	31	32.5612	3.59	0.003
FT	Δ_1F	1	3	32	33.5732	3.74	0.003
FT	Δ_1F	1	3	33	34.5730	2.92	-0.008
FT	Δ_1F	1	3	34	35.5990	3.29	0.008
FT	Δ_1F	1	3	35	36.6020	3.42	0.001
FT	Δ_1F	1	3	37	38.6191	3.10	0.000
FT	Δ_1F	1	3	38	39.6303	5.77	0.003
FT	Δ_1F	1	3	39	40.6320	1.95	-0.002
FT	Δ_1F	1	3	40	41.6435	1.92	0.002
FT	Δ_1F	1	3	41	42.6492	1.73	0.002
FT	Δ_1F	1	3	42	43.6511	2.55	-0.001
FT	Δ_1F	1	3	43	44.6553	2.68	-0.002
FT	Δ_1F	1	3	44	45.6621	1.86	0.001
FT	Δ_1F	1	3	45	46.6611	0.68	-0.003
FT	Δ_1F	1	3	46	47.6636	1.64	-0.003
FT	Δ_1F	1	3	48	49.6761	1.09	0.007
FT	Δ_1F	1	3	49	50.6701	1.59	0.001
FT	Δ_1F	1	3	50	51.6702	1.36	0.002
FT	Δ_1F	1	3	51	52.6643	2.14	-0.002
FT	Δ_1F	1	3	52	53.6683	1.73	0.005
FT	Δ_1F	1	3	54	55.6576	0.73	0.002
FT	Δ_1F	1	3	55	56.6497	1.27	-0.001
FT	Δ_1F	1	3	56	57.6379	2.77	-0.006
FT	Δ_1F	1	3	57	58.6393	2.64	0.002
FT	Δ_1F	1	3	58	59.6249	1.00	-0.004
FT	Δ_1F	1	3	60	61.6050	0.18	-0.004
FT	Δ_1F	1	3	61	62.6026	0.59	0.004
FT	Δ_1F	1	3	62	63.5895	0.59	0.003
FT	Δ_1F	1	3	63	64.5750	1.00	0.002
FT	Δ_1F	1	3	64	65.5523	0.14	-0.006
FT	Δ_1F	1	3	65	66.5425	0.59	-0.001
FT	Δ_1F	1	3	66	67.5255	0.59	-0.001
FT	Δ_1F	1	3	67	68.5009	0.55	-0.008
FT	Δ_1F	1	3	68	69.4925	0.18	0.002
FT	Δ_1F	1	3	71	72.4295	1.00	0.002
FT	Δ_1F	1	3	72	73.4015	1.00	-0.002
FT	Δ_1F	1	3	73	74.3825	1.00	0.004
FT	Δ_1F	1	3	74	75.3580	0.59	0.005
FT	Δ_1F	1	3	75	76.3248	0.59	-0.001
FT	Δ_1F	1	3	78	79.2360	0.50	-0.001
FT	Δ_1F	1	3	79	80.1980	0.50	-0.006
FT	Δ_1F	1	3	81	82.1440	0.05	0.009
FT	Δ_1F	1	4	4	5.0685	0.18	-0.002
FT	Δ_1F	1	4	5	6.0828	0.23	-0.002
FT	Δ_1F	1	4	6	7.0946	0.37	-0.004
FT	Δ_1F	1	4	7	8.1148	0.65	0.003
FT	Δ_1F	1	4	9	10.1454	1.32	0.006

Appendix VI -- $X^5\Delta$ Least-Squares Fit: data and residuals (cont.)

Source	Type	v	Ω	J	Data	Weight	Residuals
FT	Δ_1F	1	4	10	11.1506	1.69	-0.002
FT	Δ_1F	1	4	11	12.1679	2.14	0.002
FT	Δ_1F	1	4	12	13.1844	2.68	0.006
FT	Δ_1F	1	4	13	14.1929	2.27	0.001
FT	Δ_1F	1	4	14	15.2003	2.19	-0.004
FT	Δ_1F	1	4	15	16.2150	3.05	-0.001
FT	Δ_1F	1	4	16	17.2287	3.59	0.000
FT	Δ_1F	1	4	17	18.2425	4.00	0.002
FT	Δ_1F	1	4	18	19.2511	3.68	-0.001
FT	Δ_1F	1	4	19	20.2605	3.36	-0.002
FT	Δ_1F	1	4	20	21.2701	4.14	-0.004
FT	Δ_1F	1	4	21	22.2843	1.65	-0.000
FT	Δ_1F	1	4	22	23.2938	2.55	-0.001
FT	Δ_1F	1	4	23	24.3092	3.32	0.004
FT	Δ_1F	1	4	24	25.3165	3.77	0.002
FT	Δ_1F	1	4	26	27.3337	3.77	0.002
FT	Δ_1F	1	4	27	28.3355	2.65	-0.005
FT	Δ_1F	1	4	28	29.3485	3.82	0.000
FT	Δ_1F	1	4	29	30.3601	2.91	0.004
FT	Δ_1F	1	4	30	31.3619	2.82	-0.001
FT	Δ_1F	1	4	31	32.3718	3.64	0.003
FT	Δ_1F	1	4	32	33.3800	2.86	0.005
FT	Δ_1F	1	4	33	34.3788	2.91	-0.002
FT	Δ_1F	1	4	34	35.3905	2.55	0.005
FT	Δ_1F	1	4	35	36.3922	2.91	0.002
FT	Δ_1F	1	4	36	37.3917	2.55	-0.002
FT	Δ_1F	1	4	37	38.3984	3.36	0.002
FT	Δ_1F	1	4	38	39.3959	4.09	-0.004
FT	Δ_1F	1	4	39	40.3958	4.14	-0.006
FT	Δ_1F	1	4	40	41.4018	2.91	-0.001
FT	Δ_1F	1	4	41	42.4065	3.18	0.003
FT	Δ_1F	1	4	42	43.4020	3.27	-0.002
FT	Δ_1F	1	4	43	44.4064	3.68	0.003
FT	Δ_1F	1	4	44	45.4044	3.23	0.003
FT	Δ_1F	1	4	45	46.4007	2.74	0.001
FT	Δ_1F	1	4	46	47.3971	2.33	0.000
FT	Δ_1F	1	4	47	48.3908	2.27	-0.003
FT	Δ_1F	1	4	48	49.3900	1.73	0.001
FT	Δ_1F	1	4	49	50.3808	1.86	-0.004
FT	Δ_1F	1	4	50	51.3826	1.36	0.004
FT	Δ_1F	1	4	51	52.3732	2.19	0.001
FT	Δ_1F	1	4	52	53.3677	2.09	0.003
FT	Δ_1F	1	4	54	55.3422	1.64	-0.005
FT	Δ_1F	1	4	55	56.3363	2.05	-0.001
FT	Δ_1F	1	4	56	57.3231	1.68	-0.003
FT	Δ_1F	1	4	57	58.3092	0.77	-0.005
FT	Δ_1F	1	4	58	59.3013	1.59	-0.001
FT	Δ_1F	1	4	60	61.2705	2.00	-0.003
FT	Δ_1F	1	4	61	62.2568	2.00	-0.001
FT	Δ_1F	1	4	62	63.2407	1.59	-0.001
FT	Δ_1F	1	4	63	64.2326	1.18	0.009
FT	Δ_1F	1	4	65	66.1867	1.09	0.001
FT	Δ_1F	1	4	67	68.1486	1.05	0.005
FT	Δ_1F	1	4	68	69.1219	0.68	0.002
FT	Δ_1F	1	4	69	70.0955	1.00	-0.001
FT	Δ_1F	1	4	71	72.0355	1.00	-0.009
FT	Δ_1F	1	4	72	73.0230	1.00	0.005
FT	Δ_1F	1	4	73	73.9898	0.59	0.001
FT	Δ_1F	1	4	74	74.9681	0.59	0.009
FT	Δ_1F	1	4	75	75.9262	0.59	-0.002
FT	Δ_1F	1	4	76	76.8935	1.00	-0.003
FT	Δ_1F	1	4	77	77.8555	0.18	-0.007
FT	Δ_1F	1	4	78	78.8318	0.59	0.004
FT	Δ_1F	1	4	79	79.7905	0.59	-0.001
FT	Δv-a	1	0	2	871.0610	0.05	-0.006
FT	Δv-a	1	0	3	871.0530	0.09	0.009
FT	Δv-a	1	0	4	871.0133	1.14	0.001
FT	Δv-a	1	0	5	870.9670	0.73	-0.006
FT	Δv-a	1	0	7	870.8726	1.87	0.001
FT	Δv-a	1	0	8	870.8119	1.91	0.002
FT	Δv-a	1	0	9	870.7478	1.45	0.008
FT	Δv-a	1	0	10	870.6676	1.00	0.006
FT	Δv-a	1	0	11	870.5781	1.82	0.003
FT	Δv-a	1	0	12	870.4788	2.32	-0.003
FT	Δv-a	1	0	13	870.3811	2.41	0.001
FT	Δv-a	1	0	14	870.2652	1.37	-0.006
FT	Δv-a	1	0	15	870.1514	2.77	-0.002
FT	Δv-a	1	0	16	870.0311	1.92	0.002
FT	Δv-a	1	0	17	869.8920	3.19	-0.004
FT	Δv-a	1	0	18	869.7553	2.37	-0.000
FT	Δv-a	1	0	19	869.6019	2.82	-0.005
FT	Δv-a	1	0	20	869.4472	2.00	-0.004
FT	Δv-a	1	0	21	869.2839	2.33	-0.003
FT	Δv-a	1	0	22	869.1182	2.41	0.003
FT	Δv-a	1	0	23	868.9404	2.37	0.004
FT	Δv-a	1	0	25	868.5500	2.86	-0.004
FT	Δv-a	1	0	26	868.3532	3.64	0.003
FT	Δv-a	1	0	27	868.1364	3.68	-0.003

Appendix VI -- $X^5\Delta$ Least-Squares Fit: data and residuals (cont.)

Source	Type	v	Ω	J	Data	Weight	Residuals
FT	Δv-a	1	0	28	867.9236	3.23	0.002
FT	Δv-a	1	0	29	867.6988	3.64	0.004
FT	Δv-a	1	0	30	867.4572	3.27	-0.004
FT	Δv-a	1	0	31	867.2242	3.18	0.005
FT	Δv-a	1	0	32	866.9635	2.27	-0.005
FT	Δv-a	1	0	33	866.7107	2.41	-0.001
FT	Δv-a	1	0	34	866.4466	2.73	0.001
FT	Δv-a	1	0	35	866.1775	3.18	0.005
FT	Δv-a	1	0	36	865.8855	2.86	-0.006
FT	Δv-a	1	0	37	865.6069	3.68	0.004
FT	Δv-a	1	0	38	865.3043	3.64	-0.002
FT	Δv-a	1	0	39	865.0018	3.14	0.000
FT	Δv-a	1	0	40	864.6887	2.14	-0.001
FT	Δv-a	1	0	41	864.3701	3.09	0.001
FT	Δv-a	1	0	42	864.0447	2.68	0.003
FT	Δv-a	1	0	43	863.7029	2.18	-0.003
FT	Δv-a	1	0	44	863.3584	2.09	-0.004
FT	Δv-a	1	0	45	863.0137	2.18	0.003
FT	Δv-a	1	0	46	862.6515	1.59	-0.001
FT	Δv-a	1	0	47	862.2838	1.19	-0.001
FT	Δv-a	1	0	48	861.9132	1.09	0.003
FT	Δv-a	1	0	50	861.1360	0.50	-0.001
FT	Δv-a	1	0	51	860.7400	0.09	0.001
FT	Δv-a	1	0	52	860.3320	0.09	-0.001
FT	Δv-b	1	0	5	871.0032	0.82	0.008
FT	Δv-b	1	0	6	870.9461	1.68	-0.002
FT	Δv-b	1	0	7	870.8844	0.86	-0.009
FT	Δv-b	1	0	8	870.8336	1.69	0.003
FT	Δv-b	1	0	9	870.7630	1.95	0.002
FT	Δv-b	1	0	10	870.6795	1.91	-0.003
FT	Δv-b	1	0	11	870.5953	1.96	-0.001
FT	Δv-b	1	0	12	870.5083	1.46	0.006
FT	Δv-b	1	0	13	870.3971	2.78	-0.004
FT	Δv-b	1	0	14	870.2897	1.96	-0.002
FT	Δv-b	1	0	15	870.1722	2.28	-0.002
FT	Δv-b	1	0	16	870.0459	1.96	-0.004
FT	Δv-b	1	0	17	869.9121	2.74	-0.004
FT	Δv-b	1	0	18	869.7782	3.59	0.002
FT	Δv-b	1	0	19	869.6284	2.41	0.001
FT	Δv-b	1	0	20	869.4723	2.05	0.001
FT	Δv-b	1	0	21	869.3081	3.19	0.001
FT	Δv-b	1	0	22	869.1312	2.86	-0.004
FT	Δv-b	1	0	23	868.9520	3.23	-0.003
FT	Δv-b	1	0	24	868.7698	2.82	0.002
FT	Δv-b	1	0	25	868.5749	3.60	0.002
FT	Δv-b	1	0	26	868.3720	3.23	0.003
FT	Δv-b	1	0	27	868.1586	2.64	0.000
FT	Δv-b	1	0	28	867.9413	2.78	0.002
FT	Δv-b	1	0	29	867.7130	3.23	0.000
FT	Δv-b	1	0	30	867.4833	2.37	0.005
FT	Δv-b	1	0	31	867.2413	2.82	0.005
FT	Δv-b	1	0	32	866.9906	3.23	0.004
FT	Δv-b	1	0	33	866.7306	2.69	0.002
FT	Δv-b	1	0	34	866.4586	3.59	-0.004
FT	Δv-b	1	0	35	866.1916	2.36	0.002
FT	Δv-b	1	0	36	865.9084	3.18	0.001
FT	Δv-b	1	0	37	865.6155	3.55	-0.003
FT	Δv-b	1	0	38	865.3219	2.32	0.000
FT	Δv-b	1	0	39	865.0132	1.45	-0.004
FT	Δv-b	1	0	40	864.7028	2.68	-0.002
FT	Δv-b	1	0	41	864.3823	3.50	-0.002
FT	Δv-b	1	0	42	864.0488	2.59	-0.007
FT	Δv-b	1	0	43	863.7228	2.59	0.003
FT	Δv-b	1	0	44	863.3709	1.68	-0.005
FT	Δv-b	1	0	45	863.0318	1.68	0.007
FT	Δv-b	1	0	46	862.6713	1.50	0.006
FT	Δv-b	1	0	47	862.2962	2.00	-0.001
FT	Δv-b	1	0	48	861.9280	1.09	0.005
FT	Δv	1	1	1	871.1075	1.00	-0.001
FT	Δv	1	1	2	871.0888	0.65	-0.005
FT	Δv	1	1	3	871.0653	0.75	-0.005
FT	Δv	1	1	5	871.0081	2.10	0.007
FT	Δv	1	1	6	870.9502	1.68	-0.004
FT	Δv	1	1	7	870.9071	1.32	0.007
FT	Δv	1	1	8	870.8358	1.69	-0.002
FT	Δv	1	1	9	870.7690	1.27	0.000
FT	Δv	1	1	10	870.6889	1.69	-0.002
FT	Δv	1	1	11	870.6157	3.00	0.009
FT	Δv	1	1	12	870.5114	2.14	-0.002
FT	Δv	1	1	13	870.4118	1.77	-0.001
FT	Δv	1	1	14	870.3024	1.73	-0.002
FT	Δv	1	1	15	870.1886	1.73	0.000
FT	Δv	1	1	16	870.0638	2.50	-0.001
FT	Δv	1	1	17	869.9367	1.77	0.003
FT	Δv	1	1	18	869.7849	1.36	-0.009
FT	Δv	1	1	19	869.6483	1.36	0.001
FT	Δv	1	1	20	869.4943	3.00	0.002
FT	Δv	1	1	21	869.3309	2.14	0.001

Appendix VI -- $X^3\Delta$ Least-Squares Fit: data and residuals (cont.)

Source	Type	v	Ω	J	Data	Weight	Residuals
FT	Δv	1	1	22	869.1595	2.18	-0.000
FT	Δv	1	1	23	868.9829	1.32	0.001
FT	Δv	1	1	24	868.7951	2.59	-0.001
FT	Δv	1	1	25	868.5989	1.77	-0.004
FT	Δv	1	1	26	868.3972	1.27	-0.005
FT	Δv	1	1	27	868.1919	1.73	-0.001
FT	Δv	1	1	28	867.9770	1.73	0.001
FT	Δv	1	1	29	867.7605	1.24	0.008
FT	Δv	1	1	30	867.5229	0.91	0.003
FT	Δv	1	1	31	867.2830	0.83	0.003
FT	Δv	1	1	33	866.7830	0.78	0.006
FT	Δv	1	1	35	866.2372	0.28	-0.006
FT	Δv	1	1	36	865.9611	0.19	-0.004
FT	Δv-a	1	1	5	871.0000	0.09	-0.001
FT	Δv-a	1	1	6	870.9460	0.09	-0.008
FT	Δv-a	1	1	7	870.8958	0.59	-0.004
FT	Δv-a	1	1	8	870.8456	0.64	0.007
FT	Δv-a	1	1	9	870.7666	0.64	-0.002
FT	Δv-a	1	1	10	870.6966	0.64	0.005
FT	Δv-a	1	1	11	870.6056	0.64	-0.001
FT	Δv-a	1	1	12	870.5131	0.68	-0.000
FT	Δv-a	1	1	13	870.4119	0.23	-0.001
FT	Δv-a	1	1	14	870.3011	0.23	-0.003
FT	Δv-a	1	1	15	870.1846	0.23	-0.004
FT	Δv-a	1	1	16	870.0626	0.23	-0.002
FT	Δv-a	1	1	17	869.9346	1.09	0.001
FT	Δv-a	1	1	19	869.6505	0.68	0.004
FT	Δv-a	1	1	20	869.4960	1.09	0.004
FT	Δv-a	1	1	21	869.3277	0.68	-0.002
FT	Δv-a	1	1	22	869.1620	0.64	0.002
FT	Δv-a	1	1	24	868.7977	0.64	0.002
FT	Δv-a	1	1	25	868.6100	0.18	0.008
FT	Δv-a	1	1	26	868.4091	0.14	0.008
FT	Δv-a	1	1	27	868.1847	0.27	-0.008
FT	Δv-a	1	1	28	867.9814	0.19	0.006
FT	Δv-a	1	1	29	867.7553	0.27	0.004
FT	Δv-a	1	1	30	867.5234	0.59	0.004
FT	Δv-a	1	1	31	867.2824	1.05	0.003
FT	Δv-a	1	1	32	867.0327	0.68	0.001
FT	Δv-a	1	1	33	866.7795	0.68	0.003
FT	Δv-a	1	1	34	866.5070	0.10	-0.006
FT	Δv-a	1	1	35	866.2477	0.27	0.005
FT	Δv-a	1	1	37	865.6769	0.59	-0.001
FT	Δv-a	1	1	38	865.3836	0.19	0.000
FT	Δv-a	1	1	39	865.0817	0.14	-0.000
FT	Δv-a	1	1	40	864.7747	0.65	0.002
FT	Δv-a	1	1	41	864.4512	0.32	-0.004
FT	Δv-a	1	1	42	864.1366	0.29	0.007
FT	Δv-a	1	1	43	863.7953	0.15	-0.002
FT	Δv-a	1	1	45	863.1077	0.27	-0.001
FT	Δv-a	1	1	46	862.7543	0.32	0.002
FT	Δv-a	1	1	47	862.3851	1.05	-0.003
FT	Δv-a	1	1	48	862.0115	0.18	-0.005
FT	Δv-a	1	1	49	861.6280	0.09	-0.009
FT	Δv-a	1	1	51	860.8600	0.09	0.004
FT	Δv-a	1	1	53	860.0370	0.09	-0.006
FT	Δv-a	1	1	54	859.6290	0.09	0.004
FT	Δv-a	1	1	57	858.3200	0.09	-0.004
FT	Δv-a	1	1	59	857.4150	0.09	-0.003
FT	Δv-a	1	1	63	855.5060	0.09	-0.006
FT	Δv-a	1	1	64	855.0140	0.09	-0.003
FT	Δv-a	1	1	66	854.0040	0.09	0.002
FT	Δv-a	1	1	67	853.4760	0.09	-0.007
FT	Δv-b	1	1	5	871.0000	0.09	-0.001
FT	Δv-b	1	1	6	870.9500	0.50	-0.004
FT	Δv-b	1	1	7	870.8993	0.23	-0.001
FT	Δv-b	1	1	10	870.6923	0.27	0.001
FT	Δv-b	1	1	12	870.5072	0.23	-0.006
FT	Δv-b	1	1	13	870.4135	1.09	0.001
FT	Δv-b	1	1	14	870.3016	0.23	-0.003
FT	Δv-b	1	1	16	870.0625	0.23	-0.002
FT	Δv-b	1	1	18	869.7872	0.23	-0.007
FT	Δv-b	1	1	19	869.6450	0.59	-0.002
FT	Δv-b	1	1	20	869.4950	0.27	0.002
FT	Δv-b	1	1	21	869.3297	1.09	-0.001
FT	Δv-b	1	1	22	869.1680	0.27	0.008
FT	Δv-b	1	1	24	868.7957	0.27	-0.001
FT	Δv-b	1	1	25	868.6023	1.05	-0.001
FT	Δv-b	1	1	26	868.3940	0.18	-0.008
FT	Δv-b	1	1	28	867.9804	0.55	0.003
FT	Δv-b	1	1	30	867.5176	0.55	-0.003
FT	Δv-b	1	1	31	867.2820	0.27	0.001
FT	Δv-b	1	1	33	866.7748	0.59	-0.004
FT	Δv-b	1	1	34	866.5131	1.05	-0.002
FT	Δv-b	1	1	35	866.2402	0.60	-0.004
FT	Δv-b	1	1	37	865.6787	0.55	-0.001
FT	Δv-b	1	1	38	865.3882	0.33	0.002
FT	Δv-b	1	1	39	865.0877	0.24	0.003

Appendix VI -- $X^5\Delta$ Least-Squares Fit: data and residuals (cont.)

Source	Type	v	Ω	J	Data	Weight	Residuals
FT	Δv-b	1	1	40	864.7762	0.37	0.001
FT	Δv-b	1	1	41	864.4533	0.41	-0.005
FT	Δv-b	1	1	42	864.1286	0.83	-0.004
FT	Δv-b	1	1	43	863.7961	0.24	-0.004
FT	Δv-b	1	1	44	863.4510	0.10	-0.009
FT	Δv-b	1	1	46	862.7602	0.23	0.004
FT	Δv-b	1	1	47	862.3980	0.10	0.006
FT	Δv-b	1	1	50	861.2560	0.09	0.001
FT	Δv-b	1	1	51	860.8580	0.09	-0.002
FT	Δv-b	1	1	52	860.4600	0.09	0.002
FT	Δv-b	1	1	53	860.0550	0.09	0.007
FT	Δv-b	1	1	55	859.1970	0.09	-0.007
FT	Δv-b	1	1	59	857.4250	0.05	0.001
FT	Δv-b	1	1	60	856.9590	0.09	-0.001
FT	Δv-b	1	1	62	856.0010	0.05	-0.007
FT	Δv-b	1	1	63	855.5230	0.05	0.003
FT	Δv-b	1	1	64	855.0210	0.09	-0.004
FT	Δv-b	1	1	66	854.0050	0.09	-0.005
FT	Δv-b	1	1	68	852.9640	0.05	-0.001
FT	Δv	1	2	3	871.1008	0.82	-0.002
FT	Δv	1	2	4	871.0679	0.42	-0.004
FT	Δv	1	2	5	871.0323	1.60	-0.002
FT	Δv	1	2	6	870.9881	3.45	0.000
FT	Δv	1	2	7	870.9259	3.05	-0.008
FT	Δv	1	2	8	870.8680	2.70	-0.005
FT	Δv	1	2	9	870.8082	3.05	0.004
FT	Δv	1	2	10	870.7248	3.19	-0.003
FT	Δv	1	2	11	870.6454	3.78	0.002
FT	Δv	1	2	12	870.5488	4.46	-0.003
FT	Δv	1	2	13	870.4515	3.28	-0.001
FT	Δv	1	2	14	870.3462	5.05	0.001
FT	Δv	1	2	15	870.2323	4.47	0.002
FT	Δv	1	2	16	870.1056	4.23	-0.002
FT	Δv	1	2	17	869.9763	4.96	-0.001
FT	Δv	1	2	18	869.8421	3.84	0.002
FT	Δv	1	2	19	869.6939	5.96	-0.000
FT	Δv	1	2	20	869.5477	3.46	0.007
FT	Δv	1	2	21	869.3823	4.15	0.002
FT	Δv	1	2	22	869.2169	3.93	0.005
FT	Δv	1	2	23	869.0349	5.86	-0.001
FT	Δv	1	2	24	868.8505	5.78	-0.001
FT	Δv	1	2	25	868.6623	4.19	0.002
FT	Δv	1	2	26	868.4584	3.69	-0.003
FT	Δv	1	2	27	868.2565	4.14	0.002
FT	Δv	1	2	28	868.0353	2.79	-0.005
FT	Δv	1	2	29	867.8172	3.23	-0.001
FT	Δv	1	2	30	867.5862	4.01	-0.002
FT	Δv	1	2	31	867.3495	4.10	-0.001
FT	Δv	1	2	32	867.1068	3.69	0.001
FT	Δv	1	2	33	866.8557	4.37	0.003
FT	Δv	1	2	34	866.5875	4.50	-0.005
FT	Δv	1	2	35	866.3249	4.50	0.001
FT	Δv	1	2	36	866.0509	3.73	0.003
FT	Δv	1	2	37	865.7653	3.73	0.001
FT	Δv	1	2	38	865.4783	3.55	0.005
FT	Δv	1	2	39	865.1747	3.64	-0.000
FT	Δv	1	2	40	864.8669	3.05	-0.001
FT	Δv	1	2	41	864.5525	3.65	-0.002
FT	Δv	1	2	42	864.2276	3.64	-0.005
FT	Δv	1	2	43	863.9019	4.32	-0.001
FT	Δv	1	2	44	863.5619	3.55	-0.004
FT	Δv	1	2	45	863.2228	3.96	0.002
FT	Δv	1	2	46	862.8672	2.32	-0.001
FT	Δv	1	2	47	862.5038	2.42	-0.004
FT	Δv	1	2	48	862.1347	2.01	-0.005
FT	Δv	1	2	49	861.7625	1.92	-0.002
FT	Δv	1	2	50	861.3754	1.91	-0.005
FT	Δv	1	2	51	860.9963	1.86	0.007
FT	Δv	1	2	52	860.5969	0.96	0.006
FT	Δv	1	2	53	860.1835	0.91	-0.001
FT	Δv	1	2	54	859.7721	2.73	0.002
FT	Δv	1	2	56	858.9113	1.28	-0.008
FT	Δv	1	2	57	858.4892	1.69	0.007
FT	Δv	1	2	58	858.0423	1.32	0.005
FT	Δv	1	2	59	857.5777	1.69	-0.007
FT	Δv	1	2	60	857.1290	0.74	0.005
FT	Δv	1	2	63	855.7040	0.01	0.007
FT	Δv	1	3	4	871.1093	2.69	-0.007
FT	Δv	1	3	5	871.0780	1.46	-0.001
FT	Δv	1	3	6	871.0356	3.27	0.002
FT	Δv	1	3	7	870.9862	2.02	0.006
FT	Δv	1	3	8	870.9136	2.64	-0.006
FT	Δv	1	3	9	870.8539	2.10	0.003
FT	Δv	1	3	10	870.7699	3.01	-0.006
FT	Δv	1	3	11	870.6907	2.55	-0.001
FT	Δv	1	3	12	870.6075	3.05	0.006
FT	Δv	1	3	13	870.5056	4.28	0.003
FT	Δv	1	3	14	870.3993	3.37	0.002

Appendix VI -- $X^3\Delta$ Least-Squares Fit: data and residuals (cont.)

Source	Type	v	Ω	J	Data	Weight	Residuals
FT	Δv	1	3	15	870.2821	4.36	-0.001
FT	Δv	1	3	16	870.1629	3.77	0.001
FT	Δv	1	3	17	870.0294	5.18	-0.004
FT	Δv	1	3	18	869.8938	3.41	-0.003
FT	Δv	1	3	19	869.7516	3.91	-0.001
FT	Δv	1	3	20	869.6033	2.24	0.002
FT	Δv	1	3	21	869.4466	3.37	0.004
FT	Δv	1	3	22	869.2760	2.96	0.001
FT	Δv	1	3	23	869.1044	4.73	0.003
FT	Δv	1	3	24	868.9211	3.91	0.002
FT	Δv	1	3	25	868.7311	4.36	0.001
FT	Δv	1	3	26	868.5298	4.77	-0.003
FT	Δv	1	3	27	868.3213	4.36	-0.007
FT	Δv	1	3	28	868.1150	4.32	-0.001
FT	Δv	1	3	29	867.8979	5.09	0.002
FT	Δv	1	3	30	867.6705	5.59	0.002
FT	Δv	1	3	31	867.4331	3.86	-0.001
FT	Δv	1	3	32	867.1888	3.36	-0.002
FT	Δv	1	3	33	866.9429	3.42	0.002
FT	Δv	1	3	34	866.6778	1.40	-0.005
FT	Δv	1	3	35	866.4190	2.20	0.001
FT	Δv	1	3	36	866.1473	4.26	0.003
FT	Δv	1	3	37	865.8715	2.62	0.007
FT	Δv	1	3	38	865.5777	4.43	0.002
FT	Δv	1	3	39	865.2812	3.87	0.001
FT	Δv	1	3	40	864.9748	2.65	-0.002
FT	Δv	1	3	41	864.6670	2.64	0.001
FT	Δv	1	3	42	864.3453	2.86	-0.002
FT	Δv	1	3	43	864.0182	1.73	-0.002
FT	Δv	1	3	44	863.6778	2.10	-0.009
FT	Δv	1	3	45	863.3436	2.82	-0.002
FT	Δv	1	3	46	862.9949	1.77	-0.001
FT	Δv	1	3	47	862.6338	1.28	-0.006
FT	Δv	1	3	48	862.2828	1.82	0.008
FT	Δv	1	3	49	861.9017	0.82	-0.001
FT	Δv	1	3	50	861.5308	1.73	0.007
FT	Δv	1	3	51	861.1449	1.37	0.009
FT	Δv	1	3	52	860.7406	0.41	-0.001
FT	Δv	1	3	53	860.3313	0.43	-0.008
FT	Δv	1	3	54	859.9337	0.66	0.005
FT	Δv	1	4	4	871.1650	0.60	-0.001
FT	Δv	1	4	5	871.1276	0.96	-0.001
FT	Δv	1	4	6	871.0830	1.91	-0.001
FT	Δv	1	4	7	871.0330	0.60	0.002
FT	Δv	1	4	8	870.9678	1.15	-0.004
FT	Δv	1	4	9	870.9012	2.51	-0.003
FT	Δv	1	4	10	870.8323	2.11	0.003
FT	Δv	1	4	11	870.7488	3.38	0.002
FT	Δv	1	4	12	870.6552	3.79	-0.002
FT	Δv	1	4	13	870.5653	3.15	0.006
FT	Δv	1	4	14	870.4525	3.15	-0.002
FT	Δv	1	4	15	870.3419	3.64	-0.001
FT	Δv	1	4	16	870.2206	5.37	-0.002
FT	Δv	1	4	17	870.0984	5.32	0.003
FT	Δv	1	4	18	869.9571	4.74	-0.003
FT	Δv	1	4	19	869.8188	6.27	0.001
FT	Δv	1	4	20	869.6690	6.41	0.001
FT	Δv	1	4	21	869.5125	5.83	0.002
FT	Δv	1	4	22	869.3467	3.84	0.001
FT	Δv	1	4	23	869.1713	5.55	-0.002
FT	Δv	1	4	24	869.0012	4.33	0.007
FT	Δv	1	4	26	868.6093	4.19	-0.002
FT	Δv	1	4	27	868.4119	4.65	0.003
FT	Δv	1	4	28	868.1960	5.15	-0.003
FT	Δv	1	4	29	867.9836	5.19	0.002
FT	Δv	1	4	30	867.7528	4.56	-0.004
FT	Δv	1	4	31	867.5226	4.24	-0.002
FT	Δv	1	4	32	867.2847	4.24	0.000
FT	Δv	1	4	33	867.0362	4.05	-0.001
FT	Δv	1	4	34	866.7818	5.00	-0.000
FT	Δv	1	4	35	866.5187	4.14	-0.001
FT	Δv	1	4	36	866.2494	5.24	-0.000
FT	Δv	1	4	37	865.9700	4.70	-0.002
FT	Δv	1	4	38	865.6903	5.06	0.004
FT	Δv	1	4	39	865.3975	7.19	0.003
FT	Δv	1	4	40	865.0915	5.87	-0.002
FT	Δv	1	4	41	864.7862	4.96	-0.000
FT	Δv	1	4	42	864.4739	5.05	0.003
FT	Δv	1	4	43	864.1450	5.41	-0.003
FT	Δv	1	4	44	863.8180	5.45	0.000
FT	Δv	1	4	45	863.4804	4.92	0.000
FT	Δv	1	4	46	863.1327	4.74	-0.002
FT	Δv	1	4	47	862.7800	4.36	-0.001
FT	Δv	1	4	48	862.4183	3.83	-0.003
FT	Δv	1	4	49	862.0537	3.33	0.001
FT	Δv	1	4	50	861.6797	2.55	0.002
FT	Δv	1	4	51	861.2935	3.32	-0.000
FT	Δv	1	4	52	860.9055	2.95	0.002

Appendix VI -- $X^3\Delta$ Least-Squares Fit: data and residuals (cont.)

Source	Type	v	Ω	J	Data	Weight	Residuals
FT	Δv	1	4	53	860.5052	3.27	0.001
FT	Δv	1	4	54	860.1013	2.86	0.002
FT	Δv	1	4	55	859.6836	2.32	-0.002
FT	Δv	1	4	56	859.2639	3.68	-0.000
FT	Δv	1	4	57	858.8315	2.36	-0.004
FT	Δv	1	4	58	858.3984	2.27	-0.001
FT	Δv	1	4	59	857.9507	2.59	-0.005
FT	Δv	1	4	60	857.5111	2.55	0.007
FT	Δv	1	4	61	857.0412	2.59	-0.004
FT	Δv	1	4	62	856.5736	2.50	-0.005
FT	Δv	1	4	63	856.1048	2.18	0.001
FT	Δv	1	4	64	855.6276	1.77	0.005
FT	Δv	1	4	65	855.1326	1.68	0.000
FT	Δv	1	4	66	854.6326	1.23	-0.003
FT	Δv	1	4	67	854.1308	1.27	-0.000
FT	Δv	1	4	68	853.6164	0.82	-0.002
FT	Δv	1	4	69	853.1011	1.59	0.002
FT	Δv	1	4	70	852.5753	1.18	0.004
FT	Δv	1	4	71	852.0353	0.73	-0.001
FT	Δv	1	4	72	851.4884	0.77	-0.005
FT	Δv	1	4	73	850.9435	1.09	0.001
FT	Δv	1	4	74	850.3862	1.09	0.002
FT	Δv	1	4	75	849.8245	0.10	0.006
FT	Δv	1	4	77	848.6720	0.01	0.007
FT	$\Delta_1 F_+$	2	0	3	4.4648	0.19	-0.009
FT	$\Delta_1 F_+$	2	0	5	6.5336	0.60	0.002
FT	$\Delta_1 F_+$	2	0	6	7.5659	1.59	0.005
FT	$\Delta_1 F_+$	2	0	7	8.5973	0.68	0.008
FT	$\Delta_1 F_+$	2	0	9	10.6468	0.64	0.000
FT	$\Delta_1 F_+$	2	0	12	13.7322	1.55	0.002
FT	$\Delta_1 F_+$	2	0	13	14.7530	1.14	-0.004
FT	$\Delta_1 F_+$	2	0	14	15.7881	1.05	0.004
FT	$\Delta_1 F_+$	2	0	15	16.8126	1.55	0.001
FT	$\Delta_1 F_+$	2	0	16	17.8462	1.14	0.009
FT	$\Delta_1 F_+$	2	0	19	20.9120	1.59	-0.002
FT	$\Delta_1 F_+$	2	0	20	21.9355	1.18	-0.004
FT	$\Delta_1 F_+$	2	0	21	22.9581	1.14	-0.005
FT	$\Delta_1 F_+$	2	0	22	23.9899	1.14	0.003
FT	$\Delta_1 F_+$	2	0	23	25.0149	1.18	0.004
FT	$\Delta_1 F_+$	2	0	24	26.0297	1.18	-0.004
FT	$\Delta_1 F_+$	2	0	25	27.0543	1.18	-0.002
FT	$\Delta_1 F_+$	2	0	26	28.0869	1.55	0.009
FT	$\Delta_1 F_+$	2	0	27	29.0940	1.59	-0.005
FT	$\Delta_1 F_+$	2	0	28	30.1126	0.73	-0.007
FT	$\Delta_1 F_+$	2	0	29	31.1353	0.65	-0.005
FT	$\Delta_1 F_+$	2	0	31	33.1739	0.73	-0.005
FT	$\Delta_1 F_+$	2	0	32	34.2063	1.50	0.009
FT	$\Delta_1 F_+$	2	0	33	35.2160	0.69	0.001
FT	$\Delta_1 F_+$	2	0	34	36.2291	0.68	-0.003
FT	$\Delta_1 F_+$	2	0	35	37.2576	0.73	0.009
FT	$\Delta_1 F_+$	2	0	36	38.2731	1.55	0.009
FT	$\Delta_1 F_+$	2	0	37	39.2796	1.59	0.001
FT	$\Delta_1 F_+$	2	0	38	40.2975	1.59	0.005
FT	$\Delta_1 F_+$	2	0	39	41.3009	0.77	-0.005
FT	$\Delta_1 F_+$	2	0	40	42.3210	1.00	0.002
FT	$\Delta_1 F_+$	2	0	41	43.3266	0.59	-0.004
FT	$\Delta_1 F_+$	2	0	42	44.3405	0.59	-0.001
FT	$\Delta_1 F_+$	2	0	43	45.3435	0.59	-0.008
FT	$\Delta_1 F_+$	2	0	44	46.3700	0.18	0.009
FT	$\Delta_1 F_+$	2	0	45	47.3725	1.00	0.003
FT	$\Delta_1 F_+$	2	0	47	49.3795	0.18	-0.004
FT	$\Delta_1 F_-$	2	0	2	2.7380	0.05	0.005
FT	$\Delta_1 F_-$	2	0	4	4.8004	0.60	0.008
FT	$\Delta_1 F_-$	2	0	5	5.8303	0.23	0.008
FT	$\Delta_1 F_-$	2	0	6	6.8564	1.14	0.005
FT	$\Delta_1 F_-$	2	0	7	7.8744	0.73	-0.006
FT	$\Delta_1 F_-$	2	0	8	8.9058	0.69	-0.004
FT	$\Delta_1 F_-$	2	0	10	10.9762	1.18	0.008
FT	$\Delta_1 F_-$	2	0	11	11.9882	1.55	-0.009
FT	$\Delta_1 F_-$	2	0	12	13.0261	1.14	0.001
FT	$\Delta_1 F_-$	2	0	13	14.0490	1.14	-0.005
FT	$\Delta_1 F_-$	2	0	14	15.0874	1.10	0.005
FT	$\Delta_1 F_-$	2	0	15	16.1071	1.59	-0.003
FT	$\Delta_1 F_-$	2	0	16	17.1441	1.18	0.006
FT	$\Delta_1 F_-$	2	0	17	18.1660	1.14	0.001
FT	$\Delta_1 F_-$	2	0	18	19.1954	0.77	0.003
FT	$\Delta_1 F_-$	2	0	19	20.2207	2.00	0.002
FT	$\Delta_1 F_-$	2	0	21	22.2762	1.18	0.005
FT	$\Delta_1 F_-$	2	0	22	23.2938	1.59	-0.003
FT	$\Delta_1 F_-$	2	0	23	24.3222	1.14	-0.000
FT	$\Delta_1 F_-$	2	0	24	25.3460	1.14	-0.001
FT	$\Delta_1 F_-$	2	0	26	27.4000	1.18	0.005
FT	$\Delta_1 F_-$	2	0	28	29.4390	1.59	-0.003
FT	$\Delta_1 F_-$	2	0	29	30.4713	1.14	0.007
FT	$\Delta_1 F_-$	2	0	30	31.4846	0.77	-0.001
FT	$\Delta_1 F_-$	2	0	31	32.5050	1.05	-0.002
FT	$\Delta_1 F_-$	2	0	32	33.5191	1.14	-0.009
FT	$\Delta_1 F_-$	2	0	33	34.5534	1.09	0.005

Appendix VI -- $X^5\Delta$ Least-Squares Fit: data and residuals (cont.)

Source	Type	v	Ω	J	Data	Weight	Residuals
FT	Δ_1F_-	2	0	34	35.5628	0.69	-0.005
FT	Δ_1F_-	2	0	35	36.5920	1.05	0.005
FT	Δ_1F_-	2	0	36	37.6041	1.18	-0.001
FT	Δ_1F_-	2	0	37	38.6202	1.18	-0.002
FT	Δ_1F_-	2	0	38	39.6361	1.55	-0.003
FT	Δ_1F_-	2	0	39	40.6510	1.00	-0.004
FT	Δ_1F_-	2	0	40	41.6730	1.00	0.002
FT	Δ_1F_-	2	0	41	42.6872	1.09	0.002
FT	Δ_1F_-	2	0	42	43.7075	1.00	0.008
FT	Δ_1F_-	2	0	43	44.7154	0.55	0.003
FT	Δ_1F_-	2	0	45	46.7410	1.00	0.005
FT	Δ_1F_-	2	0	46	47.7533	0.59	0.006
FT	Δ_1F_-	2	0	48	49.7660	0.50	0.001
FT	Δ_1F	2	1	5	6.1490	0.50	0.005
FT	Δ_1F	2	1	6	7.1715	1.00	0.004
FT	Δ_1F	2	1	8	9.2140	0.27	-0.001
FT	Δ_1F	2	1	9	10.2383	0.68	0.001
FT	Δ_1F	2	1	10	11.2583	1.50	-0.002
FT	Δ_1F	2	1	11	12.2843	1.50	0.001
FT	Δ_1F	2	1	12	13.3051	1.18	-0.001
FT	Δ_1F	2	1	13	14.3271	1.59	-0.002
FT	Δ_1F	2	1	14	15.3480	2.00	-0.003
FT	Δ_1F	2	1	15	16.3649	1.59	-0.008
FT	Δ_1F	2	1	16	17.3968	1.18	0.002
FT	Δ_1F	2	1	17	18.4180	2.00	0.002
FT	Δ_1F	2	1	19	20.4545	1.00	-0.003
FT	Δ_1F	2	1	20	21.4820	1.00	0.005
FT	Δ_1F	2	1	21	22.4980	1.00	0.001
FT	Δ_1F_+	2	1	3	4.0905	0.14	-0.006
FT	Δ_1F_+	2	1	5	6.1494	0.55	0.005
FT	Δ_1F_+	2	1	6	7.1675	0.64	-0.001
FT	Δ_1F_+	2	1	8	9.2149	0.14	-0.002
FT	Δ_1F_+	2	1	9	10.2334	0.23	-0.007
FT	Δ_1F_+	2	1	10	11.2656	0.23	0.001
FT	Δ_1F_+	2	1	11	12.2807	0.23	-0.007
FT	Δ_1F_+	2	1	13	14.3356	0.64	0.001
FT	Δ_1F_+	2	1	14	15.3588	0.19	0.002
FT	Δ_1F_+	2	1	15	16.3721	0.28	-0.008
FT	Δ_1F_+	2	1	17	18.4240	0.73	-0.001
FT	Δ_1F_+	2	1	19	20.4682	0.28	0.000
FT	Δ_1F_+	2	1	22	23.5271	0.24	-0.004
FT	Δ_1F_+	2	1	23	24.5464	0.65	-0.005
FT	Δ_1F_+	2	1	24	25.5762	0.73	0.005
FT	Δ_1F_+	2	1	25	26.5941	0.69	0.004
FT	Δ_1F_+	2	1	27	28.6357	0.23	0.008
FT	Δ_1F_+	2	1	28	29.6417	0.68	-0.004
FT	Δ_1F_+	2	1	29	30.6632	0.23	-0.001
FT	Δ_1F_+	2	1	30	31.6827	0.68	0.002
FT	Δ_1F_+	2	1	31	32.6977	0.23	0.000
FT	Δ_1F_+	2	1	32	33.7077	0.60	-0.006
FT	Δ_1F_+	2	1	33	34.7326	0.68	0.004
FT	Δ_1F_+	2	1	35	36.7549	0.14	-0.003
FT	Δ_1F_+	2	1	37	38.7880	0.18	0.004
FT	Δ_1F_+	2	1	39	40.8170	0.18	0.009
FT	Δ_1F_+	2	1	41	42.8324	0.55	0.003
FT	Δ_1F_+	2	1	42	43.8433	0.14	0.005
FT	Δ_1F_+	2	1	44	45.8527	0.59	-0.003
FT	Δ_1F_+	2	1	48	49.8730	0.09	-0.006
FT	Δ_1F_+	2	1	49	50.8880	0.05	0.006
FT	Δ_1F_+	2	1	50	51.8920	0.05	0.007
FT	Δ_1F_+	2	1	51	52.8780	0.05	-0.009
FT	Δ_1F_+	2	1	53	54.8870	0.09	-0.001
FT	Δ_1F_-	2	1	4	5.1249	0.55	0.006
FT	Δ_1F_-	2	1	5	6.1395	0.14	-0.003
FT	Δ_1F_-	2	1	6	7.1665	0.10	0.000
FT	Δ_1F_-	2	1	8	9.2074	0.59	-0.005
FT	Δ_1F_-	2	1	9	10.2309	0.23	-0.004
FT	Δ_1F_-	2	1	10	11.2491	0.19	-0.008
FT	Δ_1F_-	2	1	11	12.2838	0.64	0.004
FT	Δ_1F_-	2	1	12	13.3018	0.23	0.000
FT	Δ_1F_-	2	1	13	14.3254	0.64	0.002
FT	Δ_1F_-	2	1	14	15.3394	1.09	-0.005
FT	Δ_1F_-	2	1	15	16.3732	0.55	0.007
FT	Δ_1F_-	2	1	16	17.3832	0.23	-0.003
FT	Δ_1F_-	2	1	17	18.4079	0.23	0.001
FT	Δ_1F_-	2	1	18	19.4274	0.64	0.001
FT	Δ_1F_-	2	1	20	21.4722	0.69	0.007
FT	Δ_1F_-	2	1	21	22.4865	0.69	0.002
FT	Δ_1F_-	2	1	22	23.5061	0.24	0.004
FT	Δ_1F_-	2	1	25	26.5526	0.77	-0.002
FT	Δ_1F_-	2	1	26	27.5614	0.69	-0.009
FT	Δ_1F_-	2	1	27	28.5811	0.23	-0.005
FT	Δ_1F_-	2	1	28	29.5950	1.05	-0.007
FT	Δ_1F_-	2	1	30	31.6288	0.59	-0.002
FT	Δ_1F_-	2	1	31	32.6350	0.10	-0.009
FT	Δ_1F_-	2	1	33	34.6680	0.59	-0.001
FT	Δ_1F_-	2	1	34	35.6763	0.59	-0.004
FT	Δ_1F_-	2	1	35	36.6925	0.10	0.001

Appendix VI -- $X^3\Delta$ Least-Squares Fit: data and residuals (cont.)

Source	Type	v	Ω	J	Data	Weight	Residuals
FT	Δ_1F_-	2	1	36	37.6960	0.10	-0.006
FT	Δ_1F_-	2	1	38	39.7226	0.14	0.002
FT	Δ_1F_-	2	1	39	40.7321	0.59	0.004
FT	Δ_1F_-	2	1	40	41.7318	0.14	-0.004
FT	Δ_1F_-	2	1	42	43.7437	0.55	-0.004
FT	Δ_1F_-	2	1	44	45.7570	0.05	-0.000
FT	Δ_1F_-	2	1	46	47.7610	0.05	-0.002
FT	Δ_1F_-	2	1	48	49.7670	0.05	0.002
FT	Δ_1F_-	2	1	50	51.7680	0.05	0.004
FT	Δ_1F_-	2	1	51	52.7650	0.05	0.003
FT	Δ_1F_-	2	1	53	54.7620	0.50	0.007
FT	Δ_1F_-	2	1	56	57.7400	0.50	0.003
FT	Δ_1F	2	2	2	3.0550	1.00	-0.000
FT	Δ_1F	2	2	3	4.0709	1.19	-0.003
FT	Δ_1F	2	2	5	6.1150	1.86	0.005
FT	Δ_1F	2	2	6	7.1283	0.96	0.000
FT	Δ_1F	2	2	7	8.1469	2.24	0.001
FT	Δ_1F	2	2	8	9.1593	1.37	-0.005
FT	Δ_1F	2	2	9	10.1776	1.87	-0.004
FT	Δ_1F	2	2	10	11.1938	2.14	-0.005
FT	Δ_1F	2	2	11	12.2217	1.45	0.005
FT	Δ_1F	2	2	12	13.2335	2.36	-0.000
FT	Δ_1F	2	2	17	18.3187	2.64	0.003
FT	Δ_1F	2	2	18	19.3285	3.14	-0.002
FT	Δ_1F	2	2	19	20.3500	2.77	0.004
FT	Δ_1F	2	2	20	21.3630	2.32	0.002
FT	Δ_1F	2	2	21	22.3745	1.87	-0.001
FT	Δ_1F	2	2	22	23.3914	1.87	0.002
FT	Δ_1F	2	2	23	24.4040	2.28	0.001
FT	Δ_1F	2	2	24	25.4112	2.32	-0.005
FT	Δ_1F	2	2	25	26.4254	1.91	-0.004
FT	Δ_1F	2	2	26	27.4431	2.69	0.002
FT	Δ_1F	2	2	28	29.4646	1.78	0.000
FT	Δ_1F	2	2	29	30.4784	1.55	0.003
FT	Δ_1F	2	2	30	31.4830	1.50	-0.003
FT	Δ_1F	2	2	31	32.4959	1.91	0.000
FT	Δ_1F	2	2	32	33.5035	1.42	-0.001
FT	Δ_1F	2	2	33	34.5206	1.78	0.007
FT	Δ_1F	2	2	34	35.5191	2.23	-0.002
FT	Δ_1F	2	2	35	36.5253	1.82	-0.004
FT	Δ_1F	2	2	36	37.5377	2.19	0.002
FT	Δ_1F	2	2	37	38.5418	1.36	-0.000
FT	Δ_1F	2	2	38	39.5456	2.19	-0.002
FT	Δ_1F	2	2	39	40.5485	1.32	-0.004
FT	Δ_1F	2	2	42	43.5640	0.32	0.001
FT	Δ_1F	2	2	43	44.5685	0.28	0.004
FT	Δ_1F	2	2	45	46.5715	0.10	0.005
FT	Δ_1F	2	2	46	47.5637	0.14	-0.002
FT	Δ_1F	2	3	3	4.0509	1.55	0.000
FT	Δ_1F	2	3	4	5.0583	1.77	-0.005
FT	Δ_1F	2	3	5	6.0744	1.41	-0.001
FT	Δ_1F	2	3	7	8.0970	2.68	-0.003
FT	Δ_1F	2	3	8	9.1075	1.82	-0.005
FT	Δ_1F	2	3	9	10.1273	2.68	0.003
FT	Δ_1F	2	3	10	11.1420	2.27	0.006
FT	Δ_1F	2	3	11	12.1480	3.18	0.000
FT	Δ_1F	2	3	12	13.1595	3.18	0.001
FT	Δ_1F	2	3	13	14.1728	3.59	0.003
FT	Δ_1F	2	3	14	15.1761	3.14	-0.005
FT	Δ_1F	2	3	15	16.1954	2.68	0.004
FT	Δ_1F	2	3	16	17.2016	2.59	-0.001
FT	Δ_1F	2	3	17	18.2116	2.18	-0.001
FT	Δ_1F	2	3	18	19.2167	2.18	-0.005
FT	Δ_1F	2	3	19	20.2286	3.50	-0.003
FT	Δ_1F	2	3	20	21.2409	3.18	-0.000
FT	Δ_1F	2	3	21	22.2480	3.14	-0.002
FT	Δ_1F	2	3	22	23.2581	2.77	-0.000
FT	Δ_1F	2	3	23	24.2692	2.77	0.003
FT	Δ_1F	2	3	24	25.2810	2.77	0.007
FT	Δ_1F	2	3	25	26.2858	2.36	0.004
FT	Δ_1F	2	3	26	27.2848	3.59	-0.004
FT	Δ_1F	2	3	27	28.2955	2.36	0.001
FT	Δ_1F	2	3	29	30.3080	2.18	0.002
FT	Δ_1F	2	3	30	31.3148	2.14	0.004
FT	Δ_1F	2	3	31	32.3190	2.59	0.003
FT	Δ_1F	2	3	32	33.3167	2.18	-0.003
FT	Δ_1F	2	3	33	34.3279	1.32	0.005
FT	Δ_1F	2	3	34	35.3300	0.82	0.004
FT	Δ_1F	2	3	35	36.3255	1.65	-0.002
FT	Δ_1F	2	3	36	37.3284	1.86	-0.001
FT	Δ_1F	2	3	37	38.3305	2.28	-0.000
FT	Δ_1F	2	3	38	39.3318	2.36	0.001
FT	Δ_1F	2	3	39	40.3342	2.77	0.003
FT	Δ_1F	2	3	40	41.3265	3.18	-0.003
FT	Δ_1F	2	3	41	42.3231	3.18	-0.005
FT	Δ_1F	2	3	42	43.3250	3.14	-0.001
FT	Δ_1F	2	3	43	44.3198	1.91	-0.003
FT	Δ_1F	2	3	44	45.3252	0.78	0.006

Appendix VI -- $X^3\Delta$ Least-Squares Fit: data and residuals (cont.)

Source	Type	v	Ω	J	Data	Weight	Residuals
FT	Δ_1F	2	3	45	46.3101	1.95	-0.004
FT	Δ_1F	2	3	46	47.3078	1.87	-0.001
FT	Δ_1F	2	3	47	48.3095	1.41	0.006
FT	Δ_1F	2	3	49	50.2923	1.05	0.004
FT	Δ_1F	2	3	51	52.2733	3.50	0.002
FT	Δ_1F	2	3	52	53.2570	1.86	-0.004
FT	Δ_1F	2	3	53	54.2512	2.18	0.002
FT	Δ_1F	2	3	54	55.2392	2.18	0.002
FT	Δ_1F	2	3	57	58.1902	0.36	-0.006
FT	Δ_1F	2	3	58	59.1841	0.19	0.004
FT	Δ_1F	2	3	59	60.1635	0.14	0.000
FT	Δ_1F	2	3	60	61.1505	0.55	0.005
FT	Δ_1F	2	3	61	62.1269	0.59	0.000
FT	Δ_1F	2	3	62	63.1022	0.59	-0.004
FT	Δ_1F	2	3	63	64.0765	0.18	-0.009
FT	Δ_1F	2	3	64	65.0645	0.18	0.001
FT	Δ_1F	2	3	65	66.0481	0.59	0.007
FT	Δ_1F	2	3	66	67.0205	0.59	0.004
FT	Δ_1F	2	3	67	67.9910	1.00	-0.000
FT	Δ_1F	2	3	68	68.9719	0.55	0.007
FT	Δ_1F	2	3	69	69.9310	0.10	-0.006
FT	Δ_1F	2	3	70	70.9080	0.10	-0.000
FT	Δ_1F	2	3	73	73.8085	0.55	-0.006
FT	Δ_1F	2	3	74	74.7800	0.18	-0.001
FT	Δ_1F	2	3	75	75.7382	0.14	-0.008
FT	Δ_1F	2	3	77	77.6795	0.10	0.007
FT	Δ_1F	2	4	4	5.0402	0.64	0.007
FT	Δ_1F	2	4	5	6.0337	0.19	-0.006
FT	Δ_1F	2	4	6	7.0468	1.18	0.001
FT	Δ_1F	2	4	7	8.0587	1.23	0.006
FT	Δ_1F	2	4	9	10.0716	1.23	0.007
FT	Δ_1F	2	4	10	11.0627	1.83	-0.007
FT	Δ_1F	2	4	12	13.0823	0.96	0.001
FT	Δ_1F	2	4	13	14.0856	2.19	-0.001
FT	Δ_1F	2	4	14	15.0976	1.55	0.006
FT	Δ_1F	2	4	15	16.0938	1.50	-0.003
FT	Δ_1F	2	4	16	17.0993	2.45	-0.002
FT	Δ_1F	2	4	17	18.1092	2.37	0.004
FT	Δ_1F	2	4	18	19.1146	2.41	0.005
FT	Δ_1F	2	4	19	20.1100	1.00	-0.003
FT	Δ_1F	2	4	20	21.1160	1.55	-0.001
FT	Δ_1F	2	4	21	22.1239	4.09	0.004
FT	Δ_1F	2	4	22	23.1256	3.27	0.003
FT	Δ_1F	2	4	23	24.1236	2.82	-0.001
FT	Δ_1F	2	4	24	25.1278	1.92	0.001
FT	Δ_1F	2	4	25	26.1309	1.60	0.002
FT	Δ_1F	2	4	26	27.1258	2.46	-0.004
FT	Δ_1F	2	4	27	28.1237	2.47	-0.007
FT	Δ_1F	2	4	28	29.1327	3.02	0.002
FT	Δ_1F	2	4	29	30.1389	2.61	0.008
FT	Δ_1F	2	4	30	31.1350	1.75	0.005
FT	Δ_1F	2	4	31	32.1321	2.60	0.003
FT	Δ_1F	2	4	32	33.1252	2.65	-0.002
FT	Δ_1F	2	4	33	34.1262	1.66	0.001
FT	Δ_1F	2	4	34	35.1197	3.06	-0.003
FT	Δ_1F	2	4	35	36.1231	2.97	0.004
FT	Δ_1F	2	4	36	37.1213	2.60	0.005
FT	Δ_1F	2	4	37	38.1110	1.95	-0.001
FT	Δ_1F	2	4	38	39.1089	2.27	0.002
FT	Δ_1F	2	4	39	40.0926	1.36	-0.008
FT	Δ_1F	2	4	40	41.0938	1.82	-0.001
FT	Δ_1F	2	4	41	42.0897	1.37	0.002
FT	Δ_1F	2	4	43	44.0716	1.00	-0.001
FT	Δ_1F	2	4	44	45.0665	1.32	0.003
FT	Δ_1F	2	4	45	46.0556	2.15	0.001
FT	Δ_1F	2	4	46	47.0401	1.45	-0.004
FT	Δ_1F	2	4	47	48.0354	1.33	0.003
FT	Δ_1F	2	4	48	49.0214	1.74	0.000
FT	Δ_1F	2	4	49	50.0144	2.64	0.006
FT	Δ_1F	2	4	50	50.9933	1.32	-0.002
FT	Δ_1F	2	4	51	51.9805	1.19	-0.000
FT	Δ_1F	2	4	52	52.9709	1.19	0.005
FT	Δ_1F	2	4	53	53.9505	1.27	0.001
FT	Δ_1F	2	4	54	54.9236	1.14	-0.010
FT	Δ_1F	2	4	55	55.9189	1.19	0.003
FT	Δ_1F	2	4	56	56.8943	0.82	-0.003
FT	Δ_1F	2	4	57	57.8760	1.00	-0.002
FT	Δ_1F	2	4	58	58.8530	1.00	-0.004
FT	Δ_1F	2	4	59	59.8291	0.59	-0.007
FT	Δ_1F	2	4	61	61.7820	1.00	-0.009
FT	Δ_1F	2	4	62	62.7645	1.00	-0.002
FT	Δ_1F	2	4	63	63.7480	0.50	0.006
FT	Δ_1F	2	4	65	65.6925	1.00	0.004
FT	Δ_1F	2	4	66	66.6632	0.59	0.004
FT	Δ_1F	2	4	68	68.6041	0.59	0.004
FT	Δ_1F	2	4	69	69.5660	1.00	-0.002
FT	Δ_1F	2	4	71	71.5010	0.50	-0.001
FT	Δ_1F	2	4	72	72.4710	0.09	0.005

Appendix VI -- $X^5\Delta$ Least-Squares Fit: data and residuals (cont.)

Source	Type	v	Ω	J	Data	Weight	Residuals
FT	Δ_1F	2	4	74	74.3880	0.50	-0.005
FT	Δ_1F	2	4	75	75.3540	0.09	-0.000
FT	Δ_1F	2	4	76	76.3130	0.50	-0.001
FT	Δ_1F	2	4	77	77.2720	0.50	-0.001
FT	Δv-a	2	0	2	1732.8760	0.05	-0.004
FT	Δv-a	2	0	4	1732.7778	0.59	0.007
FT	Δv-a	2	0	5	1732.6960	1.00	0.004
FT	Δv-a	2	0	6	1732.5948	0.64	-0.004
FT	Δv-a	2	0	7	1732.4850	1.14	-0.004
FT	Δv-a	2	0	8	1732.3607	0.28	-0.004
FT	Δv-a	2	0	9	1732.2241	0.70	0.000
FT	Δv-a	2	0	10	1732.0651	1.28	-0.003
FT	Δv-a	2	0	11	1731.9014	1.23	0.005
FT	Δv-a	2	0	12	1731.7078	1.36	-0.001
FT	Δv-a	2	0	13	1731.5049	1.33	-0.001
FT	Δv-a	2	0	14	1731.2793	1.73	-0.007
FT	Δv-a	2	0	15	1731.0539	1.37	0.001
FT	Δv-a	2	0	16	1730.7997	1.78	-0.003
FT	Δv-a	2	0	17	1730.5452	2.64	0.008
FT	Δv-a	2	0	18	1730.2615	0.96	0.005
FT	Δv-a	2	0	19	1729.9676	1.41	0.008
FT	Δv-a	2	0	20	1729.6484	2.64	0.001
FT	Δv-a	2	0	21	1729.3146	1.41	-0.004
FT	Δv-a	2	0	22	1728.9730	1.78	-0.002
FT	Δv-a	2	0	23	1728.6141	1.86	-0.002
FT	Δv-a	2	0	24	1728.2418	1.82	0.001
FT	Δv-a	2	0	25	1727.8528	1.78	0.002
FT	Δv-a	2	0	26	1727.4501	3.05	0.005
FT	Δv-a	2	0	27	1727.0229	2.14	-0.000
FT	Δv-a	2	0	29	1726.1343	1.32	0.002
FT	Δv-a	2	0	30	1725.6614	2.14	-0.003
FT	Δv-a	2	0	31	1725.1865	1.69	0.006
FT	Δv-a	2	0	32	1724.6768	1.27	-0.003
FT	Δv-a	2	0	33	1724.1590	1.69	-0.006
FT	Δv-a	2	0	34	1723.6357	1.64	0.002
FT	Δv-a	2	0	35	1723.0824	1.23	-0.004
FT	Δv-a	2	0	36	1722.5227	2.14	-0.002
FT	Δv-a	2	0	37	1721.9445	2.59	-0.002
FT	Δv-a	2	0	38	1721.3542	2.18	0.001
FT	Δv-a	2	0	39	1720.7438	1.23	-0.000
FT	Δv-a	2	0	40	1720.1217	1.50	0.003
FT	Δv-a	2	0	42	1718.8244	1.55	0.002
FT	Δv-a	2	0	43	1718.1523	1.50	0.002
FT	Δv-a	2	0	45	1716.7555	1.09	-0.005
FT	Δv-a	2	0	46	1716.0430	0.59	0.001
FT	Δv-a	2	0	47	1715.3112	0.56	0.004
FT	Δv-a	2	0	48	1714.5601	0.59	0.003
FT	Δv-a	2	0	50	1713.0080	0.50	-0.003
FT	Δv-b	2	0	4	1732.8080	0.18	0.000
FT	Δv-b	2	0	6	1732.6348	1.09	-0.001
FT	Δv-b	2	0	7	1732.5350	2.00	0.008
FT	Δv-b	2	0	8	1732.4078	0.69	0.006
FT	Δv-b	2	0	9	1732.2615	0.37	0.000
FT	Δv-b	2	0	10	1732.1026	1.64	-0.002
FT	Δv-b	2	0	11	1731.9343	1.28	0.001
FT	Δv-b	2	0	12	1731.7400	1.28	-0.006
FT	Δv-b	2	0	13	1731.5400	1.69	-0.003
FT	Δv-b	2	0	14	1731.3172	1.28	-0.007
FT	Δv-b	2	0	16	1730.8421	1.69	0.002
FT	Δv-b	2	0	17	1730.5756	1.69	0.001
FT	Δv-b	2	0	18	1730.2915	2.09	-0.001
FT	Δv-b	2	0	20	1729.6785	0.95	-0.005
FT	Δv-b	2	0	21	1729.3493	2.14	-0.006
FT	Δv-b	2	0	22	1729.0075	1.73	-0.004
FT	Δv-b	2	0	23	1728.6467	1.69	-0.006
FT	Δv-b	2	0	24	1728.2798	1.73	0.002
FT	Δv-b	2	0	25	1727.8838	1.77	-0.003
FT	Δv-b	2	0	26	1727.4815	1.36	0.000
FT	Δv-b	2	0	27	1727.0679	1.28	0.009
FT	Δv-b	2	0	28	1726.6232	1.77	0.001
FT	Δv-b	2	0	29	1726.1595	1.28	-0.009
FT	Δv-b	2	0	30	1725.7004	0.91	0.000
FT	Δv-b	2	0	31	1725.2222	1.65	0.006
FT	Δv-b	2	0	32	1724.7246	1.32	0.009
FT	Δv-b	2	0	33	1724.2044	2.14	0.004
FT	Δv-b	2	0	34	1723.6672	1.23	-0.002
FT	Δv-b	2	0	35	1723.1161	1.59	-0.006
FT	Δv-b	2	0	36	1722.5581	1.64	-0.002
FT	Δv-b	2	0	37	1721.9852	2.05	0.003
FT	Δv-b	2	0	38	1721.3899	1.27	0.002
FT	Δv-b	2	0	39	1720.7852	0.77	0.006
FT	Δv-b	2	0	40	1720.1588	1.18	0.005
FT	Δv-b	2	0	41	1719.5122	2.00	-0.001
FT	Δv-b	2	0	42	1718.8580	1.50	0.001
FT	Δv-b	2	0	43	1718.1762	0.64	-0.009
FT	Δv-b	2	0	44	1717.4930	0.27	-0.005
FT	Δv-b	2	0	45	1716.7933	1.50	-0.001
FT	Δv-b	2	0	46	1716.0725	1.00	-0.004

Appendix VI -- $X^5\Delta$ Least-Squares Fit: data and residuals (cont.)

Source	Type	v	Ω	J	Data	Weight	Residuals
FT	Δv-b	2	0	48	1714.5914	0.59	-0.000
FT	Δv	2	1	3	1732.8740	0.50	-0.005
FT	Δv	2	1	4	1732.8090	0.18	-0.008
FT	Δv	2	1	5	1732.7381	0.59	-0.002
FT	Δv	2	1	6	1732.6485	0.77	0.001
FT	Δv	2	1	7	1732.5413	1.59	0.003
FT	Δv	2	1	9	1732.2848	0.69	0.009
FT	Δv	2	1	10	1732.1281	1.68	0.007
FT	Δv	2	1	11	1731.9539	1.68	0.003
FT	Δv	2	1	12	1731.7610	1.77	-0.004
FT	Δv	2	1	13	1731.5585	2.18	-0.006
FT	Δv	2	1	14	1731.3486	1.64	0.001
FT	Δv	2	1	15	1731.1133	1.77	-0.002
FT	Δv	2	1	16	1730.8639	2.14	-0.004
FT	Δv	2	1	17	1730.6026	1.73	-0.002
FT	Δv	2	1	18	1730.3248	1.23	-0.002
FT	Δv	2	1	19	1730.0354	0.73	0.003
FT	Δv	2	1	20	1729.7267	1.50	0.003
FT	Δv	2	1	21	1729.4052	0.68	0.007
FT	Δv	2	1	22	1729.0600	1.09	0.002
FT	Δv	2	1	24	1728.3310	0.50	0.000
FT	Δv-a	2	1	5	1732.7420	0.09	0.002
FT	Δv-a	2	1	7	1732.5450	0.27	0.006
FT	Δv-a	2	1	8	1732.4061	0.28	-0.009
FT	Δv-a	2	1	9	1732.2741	0.73	-0.001
FT	Δv-a	2	1	10	1732.1259	0.28	0.005
FT	Δv-a	2	1	11	1731.9463	0.65	-0.004
FT	Δv-a	2	1	12	1731.7663	0.65	0.001
FT	Δv-a	2	1	13	1731.5600	0.65	-0.004
FT	Δv-a	2	1	14	1731.3506	0.32	0.003
FT	Δv-a	2	1	15	1731.1141	0.78	-0.001
FT	Δv-a	2	1	16	1730.8701	0.74	0.003
FT	Δv-a	2	1	17	1730.6014	1.23	-0.003
FT	Δv-a	2	1	18	1730.3296	0.28	0.004
FT	Δv-a	2	1	19	1730.0374	0.79	0.005
FT	Δv-a	2	1	20	1729.7218	0.46	-0.001
FT	Δv-a	2	1	21	1729.4059	0.79	0.008
FT	Δv-a	2	1	22	1729.0591	0.79	0.002
FT	Δv-a	2	1	23	1728.7068	0.42	0.006
FT	Δv-a	2	1	24	1728.3311	0.50	0.001
FT	Δv-a	2	1	25	1727.9458	0.42	0.003
FT	Δv-a	2	1	26	1727.5396	0.87	-0.001
FT	Δv-a	2	1	30	1725.7827	0.32	0.007
FT	Δv-a	2	1	31	1725.2952	1.18	-0.001
FT	Δv-a	2	1	32	1724.7984	0.28	-0.003
FT	Δv-a	2	1	33	1724.2872	0.69	-0.003
FT	Δv-a	2	1	34	1723.7574	0.23	-0.007
FT	Δv-a	2	1	35	1723.2143	0.27	-0.008
FT	Δv-a	2	1	36	1722.6650	0.23	0.000
FT	Δv-a	2	1	37	1722.0858	0.23	-0.006
FT	Δv-a	2	1	38	1721.5120	0.09	0.008
FT	Δv-a	2	1	39	1720.8910	0.05	-0.009
FT	Δv-a	2	1	41	1719.6490	0.05	0.003
FT	Δv-a	2	1	45	1716.9480	0.05	-0.004
FT	Δv-b	2	1	8	1732.4091	0.69	-0.006
FT	Δv-b	2	1	9	1732.2688	0.28	-0.007
FT	Δv-b	2	1	10	1732.1183	0.28	-0.003
FT	Δv-b	2	1	11	1731.9500	0.77	-0.001
FT	Δv-b	2	1	12	1731.7577	0.28	-0.008
FT	Δv-b	2	1	14	1731.3451	0.41	-0.003
FT	Δv-b	2	1	15	1731.1158	0.37	-0.000
FT	Δv-b	2	1	16	1730.8630	0.38	-0.006
FT	Δv-b	2	1	17	1730.6042	0.29	-0.001
FT	Δv-b	2	1	18	1730.3284	0.41	0.001
FT	Δv-b	2	1	19	1730.0280	0.37	-0.005
FT	Δv-b	2	1	20	1729.7152	0.83	-0.009
FT	Δv-b	2	1	21	1729.3960	0.83	-0.003
FT	Δv-b	2	1	22	1729.0547	0.83	-0.004
FT	Δv-b	2	1	24	1728.3332	0.79	0.001
FT	Δv-b	2	1	25	1727.9402	1.73	-0.005
FT	Δv-b	2	1	26	1727.5448	0.37	0.002
FT	Δv-b	2	1	27	1727.1247	0.37	-0.001
FT	Δv-b	2	1	28	1726.6926	0.64	0.000
FT	Δv-b	2	1	30	1725.7765	0.65	-0.003
FT	Δv-b	2	1	31	1725.3089	0.74	0.009
FT	Δv-b	2	1	33	1724.2895	0.74	-0.005
FT	Δv-b	2	1	34	1723.7690	1.64	0.001
FT	Δv-b	2	1	35	1723.2177	0.28	-0.009
FT	Δv-b	2	1	36	1722.6637	0.23	-0.006
FT	Δv-b	2	1	38	1721.5007	0.32	-0.009
FT	Δv-b	2	1	39	1720.9126	0.28	0.007
FT	Δv-b	2	1	40	1720.2935	0.69	0.007
FT	Δv-b	2	1	41	1719.6443	0.27	-0.008
FT	Δv-b	2	1	42	1718.9970	0.27	-0.005
FT	Δv-b	2	1	45	1716.9550	0.09	-0.004
FT	Δv	2	2	2	1732.9950	0.50	0.006
FT	Δv	2	2	3	1732.9487	1.50	0.006
FT	Δv	2	2	4	1732.8859	1.59	0.004

Appendix VI -- $X^5\Delta$ Least-Squares Fit: data and residuals (cont.)

Source	Type	v	Ω	J	Data	Weight	Residuals
FT	Δv	2	2	5	1732.8051	1.73	0.000
FT	Δv	2	2	6	1732.7127	1.41	-0.000
FT	Δv	2	2	7	1732.6010	1.74	-0.005
FT	Δv	2	2	8	1732.4808	2.50	-0.003
FT	Δv	2	2	10	1732.1830	2.10	-0.009
FT	Δv	2	2	11	1732.0254	2.50	0.001
FT	Δv	2	2	12	1731.8376	3.05	-0.003
FT	Δv	2	2	13	1731.6457	2.65	0.005
FT	Δv	2	2	17	1730.6913	3.46	-0.000
FT	Δv	2	2	18	1730.4193	2.92	0.003
FT	Δv	2	2	19	1730.1287	3.87	0.004
FT	Δv	2	2	20	1729.8238	3.78	0.005
FT	Δv	2	2	21	1729.4999	3.46	0.003
FT	Δv	2	2	22	1729.1582	2.93	-0.002
FT	Δv	2	2	23	1728.8094	3.46	0.002
FT	Δv	2	2	24	1728.4366	3.87	-0.003
FT	Δv	2	2	25	1728.0629	3.05	0.006
FT	Δv	2	2	26	1727.6561	2.15	-0.002
FT	Δv	2	2	27	1727.2498	3.74	0.005
FT	Δv	2	2	29	1726.3712	2.01	-0.000
FT	Δv	2	2	30	1725.9110	2.56	-0.001
FT	Δv	2	2	31	1725.4331	2.69	-0.004
FT	Δv	2	2	32	1724.9437	2.07	-0.003
FT	Δv	2	2	33	1724.4412	2.97	0.000
FT	Δv	2	2	34	1723.9208	2.64	0.001
FT	Δv	2	2	35	1723.3872	2.96	0.004
FT	Δv	2	2	36	1722.8297	2.88	-0.002
FT	Δv	2	2	37	1722.2634	3.00	-0.001
FT	Δv	2	2	38	1721.6838	1.51	0.002
FT	Δv	2	2	39	1721.0831	2.55	-0.001
FT	Δv	2	2	40	1720.4697	1.41	-0.001
FT	Δv	2	2	41	1719.8446	1.38	0.002
FT	Δv	2	2	42	1719.1941	0.50	-0.004
FT	Δv	2	2	43	1718.5388	1.37	-0.000
FT	Δv	2	2	44	1717.8592	0.41	-0.005
FT	Δv	2	2	46	1716.4602	0.06	-0.008
FT	Δv	2	3	3	1733.0282	1.60	-0.004
FT	Δv	2	3	4	1732.9716	2.41	-0.000
FT	Δv	2	3	5	1732.8938	1.50	-0.002
FT	Δv	2	3	6	1732.8075	2.32	0.002
FT	Δv	2	3	7	1732.7014	3.32	0.002
FT	Δv	2	3	8	1732.5689	3.05	-0.009
FT	Δv	2	3	9	1732.4382	3.37	-0.004
FT	Δv	2	3	10	1732.2886	3.86	-0.002
FT	Δv	2	3	11	1732.1230	3.77	-0.001
FT	Δv	2	3	12	1731.9455	3.95	0.004
FT	Δv	2	3	13	1731.7441	4.36	-0.001
FT	Δv	2	3	14	1731.5371	4.64	0.004
FT	Δv	2	3	15	1731.3016	3.37	-0.004
FT	Δv	2	3	16	1731.0649	3.36	0.002
FT	Δv	2	3	17	1730.8052	3.27	0.000
FT	Δv	2	3	18	1730.5313	3.19	-0.001
FT	Δv	2	3	19	1730.2469	3.73	0.002
FT	Δv	2	3	20	1729.9409	3.91	-0.000
FT	Δv	2	3	21	1729.6239	4.37	0.001
FT	Δv	2	3	22	1729.2894	4.82	-0.000
FT	Δv	2	3	23	1728.9399	3.96	-0.001
FT	Δv	2	3	24	1728.5778	4.73	0.001
FT	Δv	2	3	25	1728.2010	5.27	0.003
FT	Δv	2	3	26	1727.8085	4.41	0.005
FT	Δv	2	3	27	1727.3871	5.23	-0.007
FT	Δv	2	3	28	1726.9718	4.05	0.002
FT	Δv	2	3	29	1726.5268	4.73	-0.003
FT	Δv	2	3	30	1726.0707	3.64	-0.004
FT	Δv	2	3	31	1725.6018	3.23	-0.003
FT	Δv	2	3	32	1725.1203	3.68	0.001
FT	Δv	2	3	33	1724.6190	2.45	-0.000
FT	Δv	2	3	35	1723.5793	1.46	0.007
FT	Δv	2	3	36	1723.0219	2.79	-0.004
FT	Δv	2	3	37	1722.4607	2.92	-0.004
FT	Δv	2	3	38	1721.8900	2.56	0.002
FT	Δv	2	3	39	1721.2995	2.55	0.003
FT	Δv	2	3	40	1720.6914	2.73	0.002
FT	Δv	2	3	41	1720.0714	4.36	0.004
FT	Δv	2	3	42	1719.4309	3.42	0.001
FT	Δv	2	3	43	1718.7793	2.33	0.002
FT	Δv	2	3	44	1718.1066	3.01	-0.002
FT	Δv	2	3	45	1717.4202	2.74	-0.005
FT	Δv	2	3	46	1716.7225	2.55	-0.005
FT	Δv	2	3	47	1716.0103	3.37	-0.003
FT	Δv	2	3	48	1715.2895	1.60	0.005
FT	Δv	2	3	49	1714.5423	1.51	0.002
FT	Δv	2	3	50	1713.7865	2.28	0.006
FT	Δv	2	3	51	1713.0032	2.86	-0.003
FT	Δv	2	3	52	1712.2137	0.64	-0.002
FT	Δv	2	3	53	1711.4110	0.44	0.001
FT	Δv	2	3	54	1710.5969	0.75	0.007
FT	Δv	2	4	4	1733.0855	0.73	0.007

Appendix VI -- $X^5\Delta$ Least-Squares Fit: data and residuals (cont.)

Source	Type	v	Ω	J	Data	Weight	Residuals
FT	Δv	2	4	5	1733.0072	1.32	0.004
FT	Δv	2	4	6	1732.9071	1.68	-0.006
FT	Δv	2	4	7	1732.8037	2.23	-0.005
FT	Δv	2	4	8	1732.6977	1.87	0.009
FT	Δv	2	4	9	1732.5492	2.73	-0.005
FT	Δv	2	4	10	1732.4028	2.15	-0.001
FT	Δv	2	4	11	1732.2333	2.89	-0.006
FT	Δv	2	4	12	1732.0597	1.61	0.000
FT	Δv	2	4	13	1731.8636	2.16	-0.001
FT	Δv	2	4	14	1731.6532	3.46	-0.002
FT	Δv	2	4	15	1731.4319	3.51	0.002
FT	Δv	2	4	16	1731.1922	3.65	0.002
FT	Δv	2	4	17	1730.9352	5.32	-0.001
FT	Δv	2	4	18	1730.6682	3.24	0.002
FT	Δv	2	4	19	1730.3846	5.18	0.003
FT	Δv	2	4	20	1730.0795	1.83	-0.002
FT	Δv	2	4	21	1729.7661	5.36	-0.001
FT	Δv	2	4	22	1729.4390	4.91	0.002
FT	Δv	2	4	23	1729.0919	5.28	-0.001
FT	Δv	2	4	24	1728.7305	4.46	-0.002
FT	Δv	2	4	25	1728.3560	3.65	-0.002
FT	Δv	2	4	26	1727.9741	3.05	0.006
FT	Δv	2	4	27	1727.5656	4.50	0.002
FT	Δv	2	4	28	1727.1480	3.80	0.004
FT	Δv	2	4	29	1726.7101	4.39	0.001
FT	Δv	2	4	30	1726.2595	2.71	0.001
FT	Δv	2	4	31	1725.8003	3.40	0.007
FT	Δv	2	4	32	1725.3135	4.66	-0.000
FT	Δv	2	4	33	1724.8181	3.16	-0.001
FT	Δv	2	4	34	1724.3075	4.26	-0.001
FT	Δv	2	4	35	1723.7811	4.70	-0.002
FT	Δv	2	4	36	1723.2450	4.01	0.002
FT	Δv	2	4	37	1722.6858	4.69	-0.002
FT	Δv	2	4	38	1722.1173	2.61	-0.000
FT	Δv	2	4	39	1721.5318	3.45	-0.000
FT	Δv	2	4	40	1720.9291	3.36	-0.002
FT	Δv	2	4	41	1720.3143	3.37	-0.001
FT	Δv	2	4	42	1719.6868	2.51	0.002
FT	Δv	2	4	43	1719.0311	2.64	-0.008
FT	Δv	2	4	44	1718.3772	3.28	-0.001
FT	Δv	2	4	45	1717.7067	2.92	0.004
FT	Δv	2	4	46	1717.0121	2.41	0.001
FT	Δv	2	4	47	1716.3005	3.27	-0.004
FT	Δv	2	4	48	1715.5839	2.41	0.000
FT	Δv	2	4	49	1714.8458	3.27	-0.001
FT	Δv	2	4	50	1714.1007	3.64	0.005
FT	Δv	2	4	51	1713.3295	1.41	0.001
FT	Δv	2	4	52	1712.5479	1.82	0.001
FT	Δv	2	4	53	1711.7557	1.82	0.006
FT	Δv	2	4	54	1710.9374	2.23	0.000
FT	Δv	2	4	55	1710.1072	2.14	-0.003
FT	Δv	2	4	56	1709.2653	2.59	-0.002
FT	Δv	2	4	57	1708.4072	1.64	-0.002
FT	Δv	2	4	58	1707.5344	1.09	-0.002
FT	Δv	2	4	59	1706.6447	1.50	-0.004
FT	Δv	2	4	60	1705.7441	1.05	-0.001
FT	Δv	2	4	61	1704.8287	1.09	0.002
FT	Δv	2	4	62	1703.8845	1.00	-0.008
FT	Δv	2	4	63	1702.9415	1.09	-0.002
FT	Δv	2	4	64	1701.9860	1.00	0.007
FT	Δv	2	4	65	1700.9950	1.05	-0.005
FT	Δv	2	4	66	1700.0113	0.68	0.006
FT	Δv	2	4	67	1698.9957	0.68	0.000
FT	Δv	2	4	68	1697.9779	0.68	0.008
FT	Δv	2	4	72	1693.7167	0.59	0.000
FT	Δv	2	4	74	1691.4997	0.59	0.002
FT	Δv	2	4	75	1690.3687	0.10	0.003
FT	Δv	2	4	77	1688.0610	0.01	0.006
FT	$\Delta_1 F_+$	3	0	4	5.4695	0.18	-0.009
FT	$\Delta_1 F_+$	3	0	10	11.6088	0.23	0.005
FT	$\Delta_1 F_+$	3	0	12	13.6515	0.64	0.008
FT	$\Delta_1 F_+$	3	0	13	14.6588	0.14	-0.004
FT	$\Delta_1 F_+$	3	0	15	16.7028	0.60	0.002
FT	$\Delta_1 F_+$	3	0	16	17.7102	0.59	-0.009
FT	$\Delta_1 F_+$	3	0	17	18.7437	0.68	0.007
FT	$\Delta_1 F_+$	3	0	18	19.7515	1.05	-0.003
FT	$\Delta_1 F_+$	3	0	19	20.7711	1.05	-0.001
FT	$\Delta_1 F_+$	3	0	20	21.7866	0.64	-0.002
FT	$\Delta_1 F_+$	3	0	23	24.8378	0.59	0.001
FT	$\Delta_1 F_+$	3	0	24	25.8600	0.18	0.008
FT	$\Delta_1 F_+$	3	0	25	26.8695	0.68	0.003
FT	$\Delta_1 F_+$	3	0	26	27.8775	0.19	-0.003
FT	$\Delta_1 F_+$	3	0	27	28.8954	0.23	0.002
FT	$\Delta_1 F_+$	3	0	29	30.9217	0.59	0.003
FT	$\Delta_1 F_+$	3	0	30	31.9340	1.00	0.004
FT	$\Delta_1 F_+$	3	0	31	32.9509	0.59	0.009
FT	$\Delta_1 F_+$	3	0	33	34.9714	0.59	0.010
FT	$\Delta_1 F_+$	3	0	34	35.9790	1.00	0.008

Appendix VI -- $X^5\Delta$ Least-Squares Fit: data and residuals (cont.)

Source	Type	v	Ω	J	Data	Weight	Residuals
FT	Δ_1F_+	3	0	35	36.9810	0.09	0.002
FT	Δ_1F_+	3	0	36	37.9888	0.59	0.002
FT	Δ_1F_+	3	0	37	38.9900	0.59	-0.004
FT	Δ_1F_+	3	0	38	40.0015	0.59	0.001
FT	Δ_1F_+	3	0	39	41.0020	0.18	-0.003
FT	Δ_1F_+	3	0	42	44.0080	1.00	-0.009
FT	Δ_1F_+	3	0	43	45.0255	0.18	0.006
FT	Δ_1F_+	3	0	44	46.0275	0.51	0.007
FT	Δ_1F_+	3	0	47	49.0130	0.50	-0.006
FT	Δ_1F_-	3	0	3	3.7210	0.50	0.004
FT	Δ_1F_-	3	0	5	5.7640	0.18	0.004
FT	Δ_1F_-	3	0	6	6.7840	0.50	0.002
FT	Δ_1F_-	3	0	8	8.8280	0.18	0.003
FT	Δ_1F_-	3	0	10	10.8676	0.23	0.000
FT	Δ_1F_-	3	0	11	11.8821	0.64	-0.006
FT	Δ_1F_-	3	0	16	16.9909	1.05	0.000
FT	Δ_1F_-	3	0	18	19.0320	1.05	0.002
FT	Δ_1F_-	3	0	19	20.0497	1.05	0.001
FT	Δ_1F_-	3	0	20	21.0733	1.05	0.006
FT	Δ_1F_-	3	0	21	22.0856	1.05	0.000
FT	Δ_1F_-	3	0	22	23.0965	1.00	-0.007
FT	Δ_1F_-	3	0	24	25.1445	0.68	0.006
FT	Δ_1F_-	3	0	25	26.1539	0.64	-0.001
FT	Δ_1F_-	3	0	28	29.2057	0.59	0.004
FT	Δ_1F_-	3	0	29	30.2085	0.18	-0.008
FT	Δ_1F_-	3	0	31	32.2410	1.00	-0.004
FT	Δ_1F_-	3	0	32	33.2485	1.00	-0.009
FT	Δ_1F_-	3	0	33	34.2705	1.00	0.000
FT	Δ_1F_-	3	0	34	35.2855	0.59	0.004
FT	Δ_1F_-	3	0	35	36.2930	0.18	-0.000
FT	Δ_1F_-	3	0	36	37.3055	0.55	0.002
FT	Δ_1F_-	3	0	37	38.3070	0.50	-0.007
FT	Δ_1F_-	3	0	38	39.3250	1.00	0.002
FT	Δ_1F_-	3	0	39	40.3249	0.59	-0.006
FT	Δ_1F_-	3	0	41	42.3473	0.59	0.001
FT	Δ_1F_-	3	0	44	45.3580	0.09	-0.004
FT	Δ_1F_-	3	0	46	47.3700	0.50	0.001
FT	Δ_1F	3	1	5	6.0915	0.18	-0.006
FT	Δ_1F	3	1	6	7.1170	0.18	0.004
FT	Δ_1F	3	1	7	8.1220	0.18	-0.007
FT	Δ_1F	3	1	8	9.1460	0.18	0.001
FT	Δ_1F	3	1	10	11.1705	0.18	-0.005
FT	Δ_1F	3	1	11	12.1845	1.00	-0.006
FT	Δ_1F	3	1	12	13.2075	1.00	0.002
FT	Δ_1F	3	1	13	14.2247	0.59	0.004
FT	Δ_1F	3	1	14	15.2274	0.59	-0.007
FT	Δ_1F	3	1	15	16.2582	0.59	0.009
FT	Δ_1F	3	1	16	17.2578	0.59	-0.005
FT	Δ_1F	3	1	17	18.2760	0.09	-0.000
FT	Δ_1F	3	1	18	19.2930	1.00	0.003
FT	Δ_1F	3	1	19	20.3040	1.00	0.002
FT	Δ_1F	3	1	20	21.3194	0.59	0.004
FT	Δ_1F	3	1	21	22.3354	0.59	0.008
FT	Δ_1F	3	1	23	24.3460	1.00	-0.004
FT	Δ_1F	3	1	25	26.3765	0.18	0.005
FT	Δ_1F_+	3	1	21	22.3390	0.50	-0.002
FT	Δ_1F_+	3	1	22	23.3490	0.09	-0.005
FT	Δ_1F_+	3	1	26	27.3980	0.05	-0.004
FT	Δ_1F_+	3	1	28	29.4237	0.14	-0.000
FT	Δ_1F_+	3	1	29	30.4370	0.10	0.003
FT	Δ_1F_+	3	1	30	31.4345	0.10	-0.009
FT	Δ_1F_+	3	1	33	34.4586	0.14	-0.010
FT	Δ_1F_+	3	1	34	35.4810	0.05	0.005
FT	Δ_1F_+	3	1	36	37.4840	0.05	-0.004
FT	Δ_1F_+	3	1	40	41.5100	0.05	0.004
FT	Δ_1F_+	3	1	43	44.5070	0.05	-0.004
FT	Δ_1F_-	3	1	15	16.2360	0.05	-0.005
FT	Δ_1F_-	3	1	16	17.2500	0.05	-0.004
FT	Δ_1F_-	3	1	17	18.2620	0.05	-0.005
FT	Δ_1F_-	3	1	23	24.3270	0.05	-0.006
FT	Δ_1F_-	3	1	25	26.3500	0.05	-0.001
FT	Δ_1F_-	3	1	26	27.3650	0.05	0.005
FT	Δ_1F_-	3	1	29	30.3810	0.05	-0.001
FT	Δ_1F_-	3	1	30	31.3850	0.05	-0.003
FT	Δ_1F_-	3	1	33	34.4030	0.05	-0.000
FT	Δ_1F_-	3	1	34	35.4040	0.50	-0.003
FT	Δ_1F_-	3	1	37	38.4090	0.05	-0.005
FT	Δ_1F_-	3	1	40	41.4170	0.09	0.003
FT	Δ_1F_-	3	1	44	45.4120	0.05	0.008
FT	Δ_1F	3	2	5	6.0690	0.05	0.005
FT	Δ_1F	3	2	7	8.0920	0.09	0.007
FT	Δ_1F	3	2	8	9.1015	0.18	0.006
FT	Δ_1F	3	2	9	10.1030	0.09	-0.002
FT	Δ_1F	3	2	11	12.1316	0.59	0.007
FT	Δ_1F	3	2	13	14.1424	0.59	-0.001
FT	Δ_1F	3	2	14	15.1500	0.18	-0.002
FT	Δ_1F	3	2	15	16.1670	0.09	0.006
FT	Δ_1F	3	2	16	17.1760	0.05	0.007

Appendix VI -- $X^5\Delta$ Least-Squares Fit: data and residuals (cont.)

Source	Type	v	Ω	J	Data	Weight	Residuals
FT	Δ_1F	3	2	17	18.1790	0.18	0.001
FT	Δ_1F	3	2	18	19.1950	0.18	0.010
FT	Δ_1F	3	2	19	20.1905	1.00	-0.002
FT	Δ_1F	3	2	20	21.1975	1.00	-0.002
FT	Δ_1F	3	2	23	24.2171	0.59	-0.002
FT	Δ_1F	3	2	24	25.2160	0.50	-0.009
FT	Δ_1F	3	2	25	26.2221	0.59	-0.008
FT	Δ_1F	3	2	27	28.2425	0.18	0.004
FT	Δ_1F	3	2	28	29.2330	1.00	-0.009
FT	Δ_1F	3	2	29	30.2484	0.59	0.003
FT	Δ_1F	3	2	33	34.2540	0.50	0.001
FT	Δ_1F	3	2	35	36.2500	0.09	-0.003
FT	Δ_1F	3	3	3	4.0235	0.59	0.003
FT	Δ_1F	3	3	4	5.0323	0.27	0.007
FT	Δ_1F	3	3	6	7.0446	0.68	0.010
FT	Δ_1F	3	3	7	8.0355	1.18	-0.004
FT	Δ_1F	3	3	8	9.0401	0.73	-0.004
FT	Δ_1F	3	3	9	10.0408	0.78	-0.008
FT	Δ_1F	3	3	10	11.0510	1.23	-0.002
FT	Δ_1F	3	3	11	12.0568	0.77	0.000
FT	Δ_1F	3	3	12	13.0677	2.09	0.007
FT	Δ_1F	3	3	13	14.0576	1.60	-0.006
FT	Δ_1F	3	3	15	16.0730	2.05	0.002
FT	Δ_1F	3	3	16	17.0712	1.59	-0.002
FT	Δ_1F	3	3	17	18.0799	1.14	0.004
FT	Δ_1F	3	3	18	19.0793	1.50	0.001
FT	Δ_1F	3	3	19	20.0852	2.00	0.005
FT	Δ_1F	3	3	20	21.0893	1.05	0.007
FT	Δ_1F	3	3	21	22.0784	1.59	-0.005
FT	Δ_1F	3	3	22	23.0758	0.68	-0.008
FT	Δ_1F	3	3	23	24.0828	1.18	-0.002
FT	Δ_1F	3	3	24	25.0893	1.50	0.005
FT	Δ_1F	3	3	26	27.0767	1.50	-0.007
FT	Δ_1F	3	3	27	28.0840	2.00	0.002
FT	Δ_1F	3	3	28	29.0830	1.18	0.002
FT	Δ_1F	3	3	30	31.0813	1.50	0.005
FT	Δ_1F	3	3	31	32.0703	1.50	-0.002
FT	Δ_1F	3	3	32	33.0676	0.64	-0.002
FT	Δ_1F	3	3	33	34.0650	0.59	0.000
FT	Δ_1F	3	3	34	35.0652	0.59	0.005
FT	Δ_1F	3	3	35	36.0505	1.00	-0.004
FT	Δ_1F	3	3	36	37.0530	1.00	0.004
FT	Δ_1F	3	3	37	38.0495	1.00	0.007
FT	Δ_1F	3	3	38	39.0360	1.00	0.001
FT	Δ_1F	3	3	42	43.0054	0.55	0.006
FT	Δ_1F	3	3	43	43.9923	0.68	0.004
FT	Δ_1F	3	3	45	45.9614	0.14	-0.004
FT	Δ_1F	3	3	46	46.9555	0.10	0.003
FT	Δ_1F	3	3	47	47.9368	0.55	-0.002
FT	Δ_1F	3	3	48	48.9205	1.00	-0.004
FT	Δ_1F	3	3	49	49.9079	0.59	-0.001
FT	Δ_1F	3	3	50	50.8992	0.59	0.007
FT	Δ_1F	3	3	51	51.8769	0.59	0.001
FT	Δ_1F	3	3	52	52.8584	0.55	0.001
FT	Δ_1F	3	3	53	53.8386	0.59	-0.000
FT	Δ_1F	3	3	54	54.8131	0.59	-0.006
FT	Δ_1F	3	3	55	55.7914	0.23	-0.007
FT	Δ_1F	3	3	57	57.7617	0.60	0.007
FT	Δ_1F	3	3	58	58.7317	0.19	0.001
FT	Δ_1F	3	3	59	59.7125	0.18	0.006
FT	Δ_1F	3	3	62	62.6265	0.10	-0.001
FT	Δ_1F	3	3	63	63.6025	0.10	0.004
FT	Δ_1F	3	3	65	65.5480	0.09	0.010
FT	Δ_1F	3	3	73	73.2420	0.05	-0.009
FT	Δ_1F	3	4	4	4.9945	0.28	-0.001
FT	Δ_1F	3	4	6	6.9965	1.10	0.003
FT	Δ_1F	3	4	8	8.9982	1.29	0.007
FT	Δ_1F	3	4	9	9.9832	1.70	-0.006
FT	Δ_1F	3	4	10	10.9887	1.38	0.001
FT	Δ_1F	3	4	11	11.9861	2.20	0.000
FT	Δ_1F	3	4	12	12.9831	2.28	-0.001
FT	Δ_1F	3	4	13	13.9862	1.95	0.004
FT	Δ_1F	3	4	14	14.9793	2.28	0.000
FT	Δ_1F	3	4	15	15.9684	2.28	-0.008
FT	Δ_1F	3	4	16	16.9743	1.87	0.001
FT	Δ_1F	3	4	17	17.9730	2.10	0.003
FT	Δ_1F	3	4	18	18.9669	1.87	-0.000
FT	Δ_1F	3	4	19	19.9601	2.28	-0.003
FT	Δ_1F	3	4	20	20.9595	2.69	0.000
FT	Δ_1F	3	4	21	21.9496	2.20	-0.005
FT	Δ_1F	3	4	22	22.9470	1.79	-0.003
FT	Δ_1F	3	4	23	23.9534	2.20	0.009
FT	Δ_1F	3	4	24	24.9340	2.28	-0.005
FT	Δ_1F	3	4	25	25.9393	3.18	0.006
FT	Δ_1F	3	4	26	26.9220	2.28	-0.005
FT	Δ_1F	3	4	27	27.9178	1.87	-0.003
FT	Δ_1F	3	4	28	28.9225	2.18	0.009
FT	Δ_1F	3	4	29	29.9052	2.10	-0.000

Appendix VI -- $X^5\Delta$ Least-Squares Fit: data and residuals (cont.)

Source	Type	v	Ω	J	Data	Weight	Residuals
FT	Δ_1F	3	4	30	30.8947	1.73	-0.003
FT	Δ_1F	3	4	31	31.8887	2.00	-0.000
FT	Δ_1F	3	4	32	32.8790	2.00	-0.001
FT	Δ_1F	3	4	33	33.8752	2.00	0.005
FT	Δ_1F	3	4	35	35.8466	1.59	-0.003
FT	Δ_1F	3	4	36	36.8390	1.59	0.001
FT	Δ_1F	3	4	37	37.8307	2.00	0.004
FT	Δ_1F	3	4	38	38.8057	1.59	-0.008
FT	Δ_1F	3	4	39	39.8062	2.00	0.006
FT	Δ_1F	3	4	40	40.7817	1.18	-0.005
FT	Δ_1F	3	4	41	41.7722	2.00	-0.000
FT	Δ_1F	3	4	42	42.7641	1.18	0.007
FT	Δ_1F	3	4	43	43.7475	1.59	0.006
FT	Δ_1F	3	4	44	44.7270	2.00	0.002
FT	Δ_1F	3	4	45	45.7112	2.00	0.003
FT	Δ_1F	3	4	47	47.6745	1.59	0.003
FT	Δ_1F	3	4	49	49.6323	1.50	-0.000
FT	Δ_1F	3	4	50	50.6210	1.18	0.010
FT	Δ_1F	3	4	51	51.5872	2.00	-0.002
FT	Δ_1F	3	4	52	52.5645	2.00	-0.002
FT	Δ_1F	3	4	53	53.5461	0.68	0.002
FT	Δ_1F	3	4	54	54.5165	1.00	-0.003
FT	Δ_1F	3	4	55	55.4859	1.09	-0.008
FT	Δ_1F	3	4	56	56.4620	1.50	-0.006
FT	Δ_1F	3	4	58	58.4170	1.50	0.004
FT	Δ_1F	3	4	59	59.3910	1.00	0.007
FT	Δ_1F	3	4	60	60.3545	1.00	0.000
FT	Δ_1F	3	4	61	61.3260	0.50	0.002
FT	Δ_1F	3	4	62	62.2981	0.59	0.006
FT	Δv-a	3	0	4	2585.2691	0.68	-0.004
FT	Δv-a	3	0	6	2585.0185	0.64	0.003
FT	Δv-a	3	0	7	2584.8539	0.68	0.002
FT	Δv-a	3	0	9	2584.4600	0.68	0.007
FT	Δv-a	3	0	10	2584.2227	0.23	0.004
FT	Δv-a	3	0	11	2583.9670	0.18	0.006
FT	Δv-a	3	0	12	2583.6829	0.68	0.003
FT	Δv-a	3	0	13	2583.3749	1.05	-0.001
FT	Δv-a	3	0	15	2582.7027	0.27	0.006
FT	Δv-a	3	0	16	2582.3186	1.09	-0.003
FT	Δv-a	3	0	17	2581.9173	1.50	-0.006
FT	Δv-a	3	0	18	2581.5089	0.68	0.007
FT	Δv-a	3	0	19	2581.0623	1.50	0.006
FT	Δv-a	3	0	20	2580.5793	0.68	-0.008
FT	Δv-a	3	0	21	2580.1006	1.05	0.005
FT	Δv-a	3	0	22	2579.5846	1.05	0.004
FT	Δv-a	3	0	23	2579.0353	1.50	-0.006
FT	Δv-a	3	0	25	2577.8930	0.68	-0.001
FT	Δv-a	3	0	26	2577.2899	0.68	0.006
FT	Δv-a	3	0	27	2576.6541	0.68	0.002
FT	Δv-a	3	0	28	2576.0010	1.09	0.005
FT	Δv-a	3	0	29	2575.3152	1.09	-0.001
FT	Δv-a	3	0	30	2574.6110	1.50	-0.002
FT	Δv-a	3	0	31	2573.8892	1.09	0.002
FT	Δv-a	3	0	32	2573.1345	1.09	-0.003
FT	Δv-a	3	0	34	2571.5620	1.50	-0.005
FT	Δv-a	3	0	35	2570.7521	1.09	0.005
FT	Δv-a	3	0	36	2569.9024	1.09	-0.001
FT	Δv-a	3	0	37	2569.0422	1.09	0.006
FT	Δv-a	3	0	38	2568.1445	1.00	-0.002
FT	Δv-a	3	0	39	2567.2333	1.50	0.001
FT	Δv-a	3	0	40	2566.2972	1.09	0.002
FT	Δv-a	3	0	41	2565.3387	1.50	0.004
FT	Δv-a	3	0	42	2564.3527	1.50	0.003
FT	Δv-a	3	0	43	2563.3380	0.68	-0.004
FT	Δv-a	3	0	44	2562.3172	0.51	0.006
FT	Δv-a	3	0	45	2561.2610	0.50	0.004
FT	Δv-a	3	0	47	2559.0760	0.59	-0.001
FT	Δv-a	3	0	48	2557.9465	0.55	-0.005
FT	Δv-b	3	0	6	2585.0702	0.59	0.002
FT	Δv-b	3	0	10	2584.2693	0.27	-0.002
FT	Δv-b	3	0	11	2584.0184	1.09	0.005
FT	Δv-b	3	0	12	2583.7272	0.23	-0.005
FT	Δv-b	3	0	13	2583.4246	1.09	-0.003
FT	Δv-b	3	0	14	2583.0964	0.59	-0.003
FT	Δv-b	3	0	17	2581.9774	1.09	0.003
FT	Δv-b	3	0	18	2581.5546	1.09	0.002
FT	Δv-b	3	0	19	2581.1030	1.09	-0.004
FT	Δv-b	3	0	20	2580.6319	0.68	-0.007
FT	Δv-b	3	0	22	2579.6399	0.59	0.009
FT	Δv-b	3	0	23	2579.0854	1.09	-0.006
FT	Δv-b	3	0	24	2578.5307	1.09	0.001
FT	Δv-b	3	0	26	2577.3345	1.09	0.001
FT	Δv-b	3	0	28	2576.0356	1.09	-0.009
FT	Δv-b	3	0	29	2575.3630	0.68	-0.002
FT	Δv-b	3	0	30	2574.6594	1.05	-0.003
FT	Δv-b	3	0	31	2573.9337	1.50	-0.002
FT	Δv-b	3	0	32	2573.1907	1.50	0.005
FT	Δv-b	3	0	33	2572.4067	1.09	-0.006

Appendix VI -- $X^5\Delta$ Least-Squares Fit: data and residuals (cont.)

Source	Type	v	Ω	J	Data	Weight	Residuals
FT	Δv-b	3	0	35	2570.7869	1.09	-0.008
FT	Δv-b	3	0	36	2569.9518	0.59	0.001
FT	Δv-b	3	0	37	2569.0901	1.09	0.006
FT	Δv-b	3	0	38	2568.1940	1.09	0.001
FT	Δv-b	3	0	39	2567.2747	0.60	-0.004
FT	Δv-b	3	0	40	2566.3332	0.23	-0.008
FT	Δv-b	3	0	41	2565.3765	0.68	-0.004
FT	Δv-b	3	0	42	2564.4017	0.59	0.006
FT	Δv-b	3	0	43	2563.3831	0.68	-0.005
FT	Δv-b	3	0	46	2560.2165	0.59	-0.007
FT	Δv-b	3	0	47	2559.1257	0.59	0.004
FT	Δv-b	3	0	48	2558.0035	0.55	0.007
FT	Δv	3	1	5	2585.2269	0.64	0.007
FT	Δv	3	1	6	2585.0772	0.60	-0.003
FT	Δv	3	1	7	2584.9185	0.23	0.001
FT	Δv	3	1	9	2584.5177	0.60	-0.006
FT	Δv	3	1	10	2584.2961	0.64	0.005
FT	Δv	3	1	11	2584.0343	1.09	-0.002
FT	Δv	3	1	14	2583.1347	0.27	0.004
FT	Δv	3	1	16	2582.4143	1.50	0.003
FT	Δv	3	1	17	2582.0089	0.64	-0.008
FT	Δv	3	1	18	2581.6025	0.59	0.003
FT	Δv	3	1	19	2581.1615	1.09	0.003
FT	Δv	3	1	20	2580.6970	1.50	0.003
FT	Δv	3	1	21	2580.2052	0.64	-0.002
FT	Δv	3	1	22	2579.7007	1.50	0.004
FT	Δv	3	1	23	2579.1556	0.68	-0.007
FT	Δv	3	1	24	2578.5993	1.05	-0.006
FT	Δv	3	1	25	2578.0222	0.64	-0.003
FT	Δv	3	1	26	2577.4258	0.59	0.004
FT	Δv	3	1	27	2576.7900	0.09	-0.005
FT	Δv-a	3	1	9	2584.5300	0.05	0.007
FT	Δv-a	3	1	12	2583.7560	0.05	-0.001
FT	Δv-a	3	1	14	2583.1290	0.05	-0.001
FT	Δv-a	3	1	16	2582.4120	0.05	0.001
FT	Δv-a	3	1	17	2582.0080	0.05	-0.008
FT	Δv-a	3	1	22	2579.6974	0.14	0.003
FT	Δv-a	3	1	24	2578.6035	0.14	0.000
FT	Δv-a	3	1	27	2576.7849	0.23	-0.008
FT	Δv-a	3	1	30	2574.7703	0.15	-0.002
FT	Δv-a	3	1	31	2574.0486	0.23	-0.004
FT	Δv-a	3	1	32	2573.3053	0.60	-0.004
FT	Δv-a	3	1	33	2572.5345	0.19	-0.009
FT	Δv-a	3	1	36	2570.1085	0.18	0.004
FT	Δv-a	3	1	39	2567.4640	0.09	0.007
FT	Δv-a	3	1	43	2563.5940	0.05	-0.008
FT	Δv-b	3	1	15	2582.7897	0.14	0.006
FT	Δv-b	3	1	16	2582.4102	0.14	-0.002
FT	Δv-b	3	1	17	2582.0220	0.10	0.004
FT	Δv-b	3	1	18	2581.6030	0.09	0.002
FT	Δv-b	3	1	21	2580.1991	0.14	-0.009
FT	Δv-b	3	1	22	2579.6915	0.55	-0.006
FT	Δv-b	3	1	23	2579.1649	0.14	0.001
FT	Δv-b	3	1	24	2578.6138	0.55	0.006
FT	Δv-b	3	1	27	2576.7910	0.10	-0.006
FT	Δv-b	3	1	28	2576.1520	0.10	0.004
FT	Δv-b	3	1	29	2575.4653	0.14	-0.009
FT	Δv-b	3	1	30	2574.7780	0.10	-0.000
FT	Δv-b	3	1	31	2574.0570	0.14	-0.002
FT	Δv-b	3	1	33	2572.5545	0.10	0.004
FT	Δv-b	3	1	36	2570.1120	0.09	-0.001
FT	Δv	3	2	3	2585.5240	0.09	0.001
FT	Δv	3	2	5	2585.3140	0.09	-0.003
FT	Δv	3	2	6	2585.1785	0.18	-0.000
FT	Δv	3	2	8	2584.8281	0.55	-0.006
FT	Δv	3	2	9	2584.6207	0.23	-0.007
FT	Δv	3	2	11	2584.1392	0.64	-0.006
FT	Δv	3	2	13	2583.5713	1.50	0.001
FT	Δv	3	2	14	2583.2452	0.68	-0.004
FT	Δv	3	2	15	2582.9049	0.68	0.001
FT	Δv	3	2	16	2582.5320	0.18	-0.005
FT	Δv	3	2	17	2582.1430	1.09	-0.003
FT	Δv	3	2	18	2581.7338	0.64	0.001
FT	Δv	3	2	19	2581.2990	1.50	0.003
FT	Δv	3	2	20	2580.8403	1.50	0.004
FT	Δv	3	2	21	2580.3592	0.68	0.005
FT	Δv	3	2	22	2579.8496	0.68	0.001
FT	Δv	3	2	23	2579.3259	1.09	0.006
FT	Δv	3	2	24	2578.7673	1.50	-0.001
FT	Δv	3	2	25	2578.1930	1.00	-0.000
FT	Δv	3	2	26	2577.5992	0.59	0.003
FT	Δv	3	2	27	2576.9783	1.09	0.003
FT	Δv	3	2	28	2576.3306	0.23	-0.001
FT	Δv	3	2	29	2575.6665	1.09	0.001
FT	Δv	3	2	30	2574.9761	0.64	0.001
FT	Δv	3	2	31	2574.2537	1.50	-0.009
FT	Δv	3	2	32	2573.5244	1.09	-0.003
FT	Δv	3	2	33	2572.7740	1.50	0.005

Appendix VI -- $X^5\Delta$ Least-Squares Fit: data and residuals (cont.)

Source	Type	v	Ω	J	Data	Weight	Residuals
FT	Δv	3	2	34	2571.9815	1.00	-0.005
FT	Δv	3	2	36	2570.3491	0.59	-0.005
FT	Δv	3	2	37	2569.5095	1.00	0.006
FT	Δv	3	3	3	2585.6609	1.09	-0.002
FT	Δv	3	3	4	2585.5762	1.36	0.004
FT	Δv	3	3	5	2585.4645	0.91	0.006
FT	Δv	3	3	6	2585.3256	1.41	0.004
FT	Δv	3	3	7	2585.1617	1.78	-0.001
FT	Δv	3	3	8	2584.9769	2.82	-0.004
FT	Δv	3	3	9	2584.7691	1.50	-0.007
FT	Δv	3	3	10	2584.5441	1.64	-0.005
FT	Δv	3	3	11	2584.2944	2.32	-0.004
FT	Δv	3	3	12	2584.0226	3.23	-0.003
FT	Δv	3	3	13	2583.7367	2.86	0.006
FT	Δv	3	3	14	2583.4121	2.45	-0.000
FT	Δv	3	3	15	2583.0708	2.73	-0.000
FT	Δv	3	3	16	2582.7130	3.18	0.006
FT	Δv	3	3	17	2582.3189	2.23	-0.002
FT	Δv	3	3	18	2581.9063	2.73	-0.005
FT	Δv	3	3	19	2581.4775	2.68	-0.002
FT	Δv	3	3	20	2581.0302	2.73	0.005
FT	Δv	3	3	21	2580.5558	2.37	0.009
FT	Δv	3	3	22	2580.0495	1.95	0.003
FT	Δv	3	3	23	2579.5236	2.55	-0.000
FT	Δv	3	3	24	2578.9747	1.36	-0.003
FT	Δv	3	3	25	2578.4135	3.64	0.004
FT	Δv	3	3	26	2577.8164	3.09	-0.002
FT	Δv	3	3	27	2577.1983	3.00	-0.005
FT	Δv	3	3	28	2576.5667	2.68	-0.000
FT	Δv	3	3	30	2575.2200	3.50	-0.005
FT	Δv	3	3	31	2574.5237	3.00	0.004
FT	Δv	3	3	32	2573.7857	1.77	-0.005
FT	Δv	3	3	33	2573.0454	1.18	0.005
FT	Δv	3	3	34	2572.2628	0.73	-0.004
FT	Δv	3	3	35	2571.4707	1.09	0.001
FT	Δv	3	3	36	2570.6470	1.50	-0.003
FT	Δv	3	3	37	2569.8083	1.50	0.000
FT	Δv	3	3	38	2568.9452	0.68	0.002
FT	Δv	3	3	39	2568.0619	1.09	0.007
FT	Δv	3	3	40	2567.1525	0.68	0.008
FT	Δv	3	3	41	2566.2036	1.09	-0.007
FT	Δv	3	3	43	2564.2678	1.18	-0.007
FT	Δv	3	3	44	2563.2721	0.32	-0.001
FT	Δv	3	3	46	2561.1970	0.18	-0.003
FT	Δv	3	3	47	2560.1364	0.64	0.007
FT	Δv	3	3	48	2559.0393	0.64	0.004
FT	Δv	3	3	49	2557.9243	0.68	0.005
FT	Δv	3	3	50	2556.7798	0.68	0.000
FT	Δv	3	3	51	2555.6196	0.68	0.003
FT	Δv	3	3	52	2554.4308	0.23	-0.001
FT	Δv	3	3	53	2553.2178	0.19	-0.006
FT	Δv	3	3	54	2551.9829	0.14	-0.009
FT	Δv	3	3	55	2550.7335	0.18	-0.004
FT	Δv	3	3	56	2549.4700	0.05	0.009
FT	Δv	3	4	4	2585.7479	0.73	0.007
FT	Δv	3	4	5	2585.6347	0.50	0.006
FT	Δv	3	4	6	2585.4868	2.18	-0.007
FT	Δv	3	4	7	2585.3285	1.73	-0.008
FT	Δv	3	4	8	2585.1579	0.96	0.001
FT	Δv	3	4	9	2584.9588	2.77	0.005
FT	Δv	3	4	10	2584.7236	2.32	-0.006
FT	Δv	3	4	11	2584.4866	2.32	0.004
FT	Δv	3	4	12	2584.2160	2.36	0.004
FT	Δv	3	4	13	2583.9255	2.32	0.005
FT	Δv	3	4	14	2583.6076	2.45	0.002
FT	Δv	3	4	15	2583.2712	2.45	0.003
FT	Δv	3	4	16	2582.9061	2.82	-0.003
FT	Δv	3	4	17	2582.5282	3.68	0.001
FT	Δv	3	4	18	2582.1193	1.95	-0.003
FT	Δv	3	4	19	2581.6936	3.64	-0.001
FT	Δv	3	4	20	2581.2421	3.64	-0.003
FT	Δv	3	4	21	2580.7746	2.86	0.002
FT	Δv	3	4	22	2580.2784	3.27	0.000
FT	Δv	3	4	23	2579.7516	2.05	-0.009
FT	Δv	3	4	24	2579.2252	3.23	0.004
FT	Δv	3	4	25	2578.6581	3.68	-0.001
FT	Δv	3	4	26	2578.0794	3.64	0.005
FT	Δv	3	4	27	2577.4684	2.36	0.002
FT	Δv	3	4	28	2576.8324	3.18	-0.004
FT	Δv	3	4	29	2576.1866	3.19	0.002
FT	Δv	3	4	30	2575.5094	2.83	0.000
FT	Δv	3	4	31	2574.8060	2.46	-0.006
FT	Δv	3	4	32	2574.0868	3.14	-0.005
FT	Δv	3	4	33	2573.3442	1.91	-0.005
FT	Δv	3	4	34	2572.5845	3.14	0.001
FT	Δv	3	4	35	2571.7971	1.95	0.002
FT	Δv	3	4	37	2570.1498	2.14	-0.002
FT	Δv	3	4	38	2569.2993	3.00	0.003

Appendix VI -- $X^5\Delta$ Least-Squares Fit: data and residuals (cont.)

Source	Type	v	Ω	J	Data	Weight	Residuals
FT	Δv	3	4	39	2568.4186	2.18	0.001
FT	Δv	3	4	40	2567.5168	1.77	0.000
FT	Δv	3	4	41	2566.5930	3.00	-0.000
FT	Δv	3	4	42	2565.6494	2.55	0.002
FT	Δv	3	4	43	2564.6774	1.77	-0.001
FT	Δv	3	4	44	2563.6913	2.59	0.005
FT	Δv	3	4	45	2562.6783	3.00	0.006
FT	Δv	3	4	46	2561.6358	3.00	0.001
FT	Δv	3	4	47	2560.5726	2.59	-0.003
FT	Δv	3	4	48	2559.4967	2.18	0.003
FT	Δv	3	4	49	2558.3821	2.09	-0.006
FT	Δv	3	4	50	2557.2536	1.77	-0.007
FT	Δv	3	4	51	2556.1148	2.14	0.005
FT	Δv	3	4	52	2554.9388	3.00	0.002
FT	Δv	3	4	53	2553.7368	2.55	-0.004
FT	Δv	3	4	54	2552.5220	1.59	-0.000
FT	Δv	3	4	55	2551.2806	2.50	-0.000
FT	Δv	3	4	56	2550.0143	2.09	-0.002
FT	Δv	3	4	58	2547.4212	2.09	0.001
FT	Δv	3	4	59	2546.0892	2.50	0.002
FT	Δv	3	4	60	2544.7353	2.00	0.003
FT	Δv	3	4	61	2543.3530	1.50	-0.001
FT	Δv	3	4	62	2541.9470	2.00	-0.006
FT	Δv	3	4	63	2540.5301	1.18	0.001
FT	Δv	3	4	65	2537.6180	0.50	0.005

APPENDIX VII

Term Values for the $^5\Pi$ State (cm^{-1})

The number in parentheses following each term value gives the sum of the weights of the lines from which it was determined (e.g. a term value obtained from seven good lines, four blended lines, and one very bad line (or line of doubtful assignment) would have a total weight of 7.41).

Appendix VII -- $^5\Pi$ term values

v = 0

J	Ω = -1		Ω = 0		Ω = 1	
	a	b	a	b	a	b
1			0		1 10406.547 (1.10)	10406.452 (0.10)
2			1 10595.542 (1.20)		2 10408.354 (2.00)	10408.302 (1.00)
3	10813.935 (1.20)	10813.966 (0.40)	2 10597.355 (1.30)		3 10411.049 (0.40)	10411.053 (0.10)
4	10817.595 (0.40)	10817.613 (4.00)	3 10600.086 (1.40)	10637.982 (2.10)	4 10414.650 (1.30)	10414.640 (0.10)
5	10822.149 (1.30)	10822.202 (2.30)	4 10603.727 (2.40)	10641.575 (1.40)	5 10419.143 (1.40)	10419.203 (3.20)
6	10827.625 (3.40)	10827.693 (4.30)	5 10608.277 (1.50)	10646.101 (5.10)	6 10424.545 (2.40)	10424.621 (3.20)
7	10834.003 (5.20)	10834.098 (2.50)	6 10613.735 (2.40)	10651.512 (4.30)	7 10430.835 (4.30)	10430.966 (2.50)
8	10841.309 (3.40)	10841.427 (2.50)	7 10620.110 (2.50)	10657.822 (1.70)	8 10438.034 (1.50)	10438.189 (4.30)
9	10849.522 (2.50)	10849.664 (2.50)	8 10627.386 (6.30)	10665.042 (3.60)	9 10446.119 (2.50)	10446.324 (3.50)
10	10858.643 (3.40)	10858.818 (2.60)	9 10635.584 (2.70)	10673.163 (5.40)	10 10455.125 (4.40)	10455.366 (3.50)
11	10868.671 (5.30)	10868.885 (3.40)	10 10644.685 (3.60)	10682.177 (5.40)	11 10465.011 (3.60)	10465.307 (5.30)
12	10879.617 (3.50)	10879.857 (2.70)	11 10654.700 (3.60)	10692.103 (5.40)	12 10475.807 (2.60)	10476.150 (6.30)
13	10891.466 (4.50)	10891.754 (2.70)	12 10665.613 (3.60)	10702.919 (7.20)	13 10487.498 (4.50)	10487.898 (7.20)
14	10904.222 (1.70)	10904.556 (1.70)	13 10677.445 (4.50)	10714.645 (3.60)	14 10500.080 (3.50)	10500.543 (3.50)
15	10917.899 (1.70)	10918.278 (2.70)	14 10690.184 (3.60)	10727.268 (5.40)	15 10513.571 (7.10)	10514.091 (4.40)
16	10932.474 (5.40)	10932.908 (4.50)	15 10703.820 (4.50)	10740.789 (4.50)	16 10527.948 (2.60)	10528.544 (2.60)
17	10947.959 (0.90)	10948.439 (4.40)	16 10718.377 (5.40)	10755.212 (5.40)	17 10543.237 (5.30)	10543.896 (3.60)
18	10964.352 (6.30)	10964.892 (4.50)	17 10733.827 (4.50)	10770.535 (3.60)	18 10559.407 (5.40)	10560.146 (6.30)
19	10981.654 (2.70)	10982.254 (4.50)	18 10750.200 (5.40)	10786.751 (3.50)	19 10576.481 (5.40)	10577.301 (5.40)
20	10999.860 (5.40)	11000.523 (4.50)	19 10767.465 (4.50)	10803.852 (6.30)	20 10594.452 (6.30)	10595.355 (5.40)
21	11018.973 (4.50)	11019.692 (6.30)	20 10785.651 (5.40)	10821.827 (5.40)	21 10613.298 (3.60)	10614.308 (0.90)
22	11038.988 (2.70)	11039.776 (6.30)	21 10804.731 (8.10)	10840.658 (6.30)	22 10633.076 (4.40)	10634.160 (1.80)
23	11059.908 (3.60)	11060.766 (7.20)	22 10824.718 (4.50)	10860.383 (3.60)	23 10653.731 (7.20)	10654.909 (4.50)
24	11081.733 (3.60)	11082.661 (5.40)	23 10845.600 (5.40)	10881.069 (3.60)	24 10675.278 (6.30)	10676.554 (2.70)
25	11104.456 (6.30)	11105.459 (4.50)	24 10867.401 (4.50)	10902.731 (6.20)	25 10697.721 (6.30)	10699.099 (5.40)
26	11128.082 (6.30)	11129.138 (1.80)	25 10890.100 (3.50)	10925.304 (4.40)	26 10721.055 (5.40)	10722.539 (5.40)
27	11152.616 (3.50)	11153.788 (6.30)	26 10913.688 (5.40)	10948.753 (4.40)	27 10745.285 (6.30)	10746.883 (4.50)
28	11178.044 (6.30)	11179.301 (4.50)	27 10938.192 (4.40)	10973.080 (4.30)	28 10770.411 (6.30)	10772.106 (4.50)
29	11204.376 (3.60)	11205.706 (4.50)	28 10963.601 (4.50)	10998.287 (4.50)	29 10796.427 (4.50)	10798.238 (5.40)
30	11231.600 (4.50)	11233.029 (3.60)	29 10989.900 (4.50)	11024.386 (6.20)	30 10823.333 (4.40)	10825.253 (4.50)
31	11259.728 (4.40)	11261.259 (2.60)	30 11017.099 (3.60)	11051.361 (5.30)	31 10851.129 (4.50)	10853.171 (4.50)
32	11288.748 (5.40)	11290.333 (3.50)	31 11045.198 (5.40)	11079.225 (7.20)	32 10879.812 (3.50)	10881.982 (5.40)
33	11318.675 (4.20)	11320.381 (2.60)	32 11074.195 (4.50)	11107.959 (3.60)	33 10909.385 (5.40)	10911.687 (2.70)
34	11349.498 (3.50)	11351.299 (4.40)	33 11104.090 (6.30)	11137.572 (6.20)	34 10939.855 (4.50)	10942.278 (3.60)
35	11381.212 (2.60)	11383.120 (3.40)	34 11134.878 (6.30)	11168.120 (2.50)	35 10971.197 (5.40)	10973.764 (6.30)
36	11413.822 (4.50)	11415.843 (4.40)	35 11166.556 (4.50)	11199.483 (2.60)	36 11003.450 (8.10)	11006.130 (7.20)
37	11447.331 (7.20)	11449.472 (6.20)	36 11199.154 (4.50)	11231.750 (3.50)	37 11036.576 (3.50)	11039.398 (5.40)
38	11481.747 (4.50)	11484.005 (3.40)	37 11232.635 (0.70)	11264.916 (4.40)	38 11070.600 (4.50)	11073.551 (5.40)
39	11517.070 (3.50)	11519.468 (4.40)	38 11266.992 (1.60)	11298.973 (4.40)	39 11105.506 (2.60)	11108.592 (3.50)
40	11553.343 (4.30)		39 11302.242 (3.30)	11333.929 (4.40)	40 11141.294 (5.40)	11144.525 (3.60)
41	11590.741 (5.20)		40 11338.390 (3.30)	11369.781 (5.40)	41 11177.974 (7.20)	11181.342 (3.60)

v = 0 (cont.)

J	Ω = 0		Ω = 2		Ω = 3	
	a	b	a	b	a	b
41	11375.433 (2.20)	11406.533 (3.60)				
42	11413.359 (4.00)	11444.190 (2.50)				
43	11452.171 (0.40)	11482.748 (4.30)				
44	11491.875 (1.20)	11522.219 (4.40)				
45	11532.465 (2.10)	11562.617 (1.60)				
46	11573.929 (1.20)	11603.918 (3.20)				
47	11616.296 (2.10)	11646.181 (4.30)				
48	11659.546 (2.20)	11689.393 (2.00)				
49	11703.673 (2.10)	11733.636 (3.00)				
50	11748.681 (1.30)	11778.961 (2.10)				
51	11794.579 (0.40)					
52	11841.351 (0.40)					
53	11888.994 (2.10)					
54	11937.534 (2.20)					
55	11986.960 (1.20)					
56	12037.270 (3.00)					
2			10191.378 (2.10)			
3			10194.099 (5.00)		9982.973 (0.30)	
4			10197.725 (4.30)		9986.619 (1.40)	
5			10202.255 (6.30)		9991.179 (3.40)	
6			10207.691 (8.00)		9996.638 (1.40)	
7			10214.029 (6.10)		10003.020 (3.40)	
8			10221.278 (5.40)		10010.287 (0.70)	
9			10229.422 (7.20)		10018.490 (0.50)	10018.506 (1.40)
10			10238.467 (6.30)		10027.621 (0.70)	10027.658 (0.70)
11			10248.417 (7.20)		10037.673 (1.60)	10037.706 (0.70)
12			10259.268 (8.10)		10048.640 (0.70)	10048.672 (1.60)
13			10271.011 (8.10)		10060.512 (3.50)	10060.564 (3.40)
14			10283.661 (6.30)		10073.326 (7.10)	10073.385 (3.60)
15			10297.205 (8.10)		10087.067 (5.30)	10087.122 (2.60)
16			10311.643 (8.10)		10101.735 (3.40)	10101.795 (6.20)
17			10326.983 (5.40)		10117.333 (8.10)	10117.402 (5.40)
18			10343.213 (8.10)		10133.876 (7.20)	10133.950 (5.40)
19			10360.342 (6.30)		10151.355 (6.20)	10151.443 (7.10)
20			10378.364 (7.20)		10169.798 (4.40)	10169.889 (4.40)
21			10397.277 (7.20)		10189.206 (5.30)	10189.296 (7.20)
22			10417.080 (8.10)		10209.585 (7.20)	10209.668 (5.40)
23			10437.778 (8.10)		10230.947 (6.30)	10231.031 (4.50)
24			10459.366 (7.20)		10253.300 (5.40)	10253.385 (6.30)
25			10481.845 (9.00)		10276.668 (4.50)	10276.750 (4.50)
26			10505.209 (9.00)		10301.068 (3.60)	10301.140 (7.20)
27			10529.467 (8.10)		10326.524 (5.30)	10326.586 (5.30)
28			10554.614 (9.00)		10353.047 (2.60)	10353.093 (4.40)
29			10580.649 (8.10)		10380.661 (1.70)	10380.701 (1.80)
30			10607.570 (7.20)		10409.392 (1.80)	10409.413 (0.70)
31			10635.377 (8.10)		10439.256 (3.50)	
32			10664.073 (7.20)		10470.258 (2.70)	
33			10693.656 (6.30)		10502.415 (3.60)	
34			10724.113 (2.70)		10535.733 (2.70)	
35			10755.469 (0.90)	10755.478 (0.90)	10570.211 (3.60)	
36			10787.703 (1.80)	10787.733 (1.80)	10605.837 (2.60)	
37			10820.819 (2.70)	10820.869 (2.70)	10642.615 (3.30)	
38			10854.837 (3.60)	10854.878 (4.40)	10680.530 (0.06)	
39			10889.727 (5.40)	10889.776 (4.50)		
40			10925.509 (5.40)	10925.563 (6.30)		
41			10962.176 (4.40)	10962.233 (5.30)		
42			10999.728 (6.30)	10999.792 (7.20)		

J	Ω = 1	
	a	b
42	11215.547 (3.60)	11219.054 (7.20)
43	11254.015 (5.20)	11257.652 (4.50)
44	11293.386 (4.50)	11297.152 (3.40)
45	11333.702 (5.30)	11337.561 (2.60)
46	11375.010 (1.03)	11378.909 (3.30)
47		11421.226 (1.20)
48		11464.518 (1.10)
27	10278.604 (3.40)	
28	10305.852 (4.50)	
29	10333.943 (5.40)	

Appendix VII -- $^5\Pi$ term values (cont.)

v = 0 (cont.)

J	Ω = 2		Ω = 3	
	a	b	a	b
43	11038.161 (6.30)	11038.237 (6.20)		
44	11077.483 (5.40)	11077.561 (7.20)		
45	11117.689 (6.20)	11117.780 (6.20)		
46	11158.783 (7.10)	11158.880 (6.20)		
47	11200.759 (5.30)	11200.850 (4.40)		
48	11243.600 (6.10)	11243.709 (3.30)		
49	11287.330 (6.20)	11287.455 (6.10)		
50	11331.932 (6.30)	11332.063 (5.40)		
51	11377.398 (5.20)	11377.533 (4.40)		
52	11423.741 (5.30)	11423.881 (5.20)		
53	11470.937 (5.11)	11471.104 (4.31)		
54	11519.011 (4.21)	11519.178 (4.21)		
55	11567.952 (4.20)	11568.122 (4.10)		
56	11617.743 (3.20)	11617.939 (3.20)		
57	11668.393 (1.30)	11668.612 (3.10)		
58	11719.948 (2.10)	11720.184 (2.20)		
59	11772.380 (0.20)	11772.580 (2.10)		
60		11825.898 (1.00)		
30			10362.846 (3.50)	
31			10392.546 (4.50)	
32			10423.014 (5.40)	
33			10454.231 (5.40)	
34			10486.186 (3.60)	10488.370 (4.40)
35			10518.895 (6.30)	10520.446 (5.40)
36			10552.342 (4.50)	10553.522 (6.30)
37			10586.545 (5.40)	10587.500 (7.20)
38			10621.503 (6.30)	10622.318 (7.20)
39			10657.237 (5.30)	10657.948 (7.10)
40			10693.747 (6.30)	10694.399 (8.10)
41			10731.051 (2.70)	10731.649 (6.30)
42			10769.158 (5.40)	10769.716 (5.30)
43			10808.072 (6.30)	10808.596 (6.30)
44			10847.803 (5.40)	10848.308 (6.30)
45			10888.354 (4.50)	10888.845 (7.10)
46			10929.747 (3.60)	10930.215 (6.30)
47			10971.959 (3.50)	10972.413 (5.30)
48			11015.017 (3.30)	11015.465 (5.30)
49			11058.920 (7.00)	11059.360 (3.50)
50			11103.662 (4.10)	11104.094 (3.50)
51			11149.258 (3.21)	11149.680 (4.30)
52			11195.687 (2.30)	11196.116 (3.40)
53			11242.984 (3.20)	11243.399 (4.20)
54			11291.124 (4.10)	11291.532 (4.20)
55			11340.115 (1.40)	11340.525 (3.20)
56			11389.935 (3.20)	11390.398 (5.20)
57			11440.659 (1.20)	11441.111 (1.20)
58				11492.723 (0.20)
59				11545.138 (1.00)
60				11598.443 (0.01)

v = 1

J	Ω = -1		Ω = 0		Ω = 1	
	a	b	a	b	a	b
0						
1					11033.986 (1.10)	
2					11035.787 (3.10)	
3		11395.443 (0.10)			11038.456 (1.20)	
4		11399.154 (1.00)		11273.494 (0.10)	11042.035 (1.10)	11042.085 (2.10)
5	11403.666 (1.00)	11403.780 (0.10)	11213.498 (0.10)	11278.054 (2.00)	11046.503 (2.20)	11046.592 (3.10)
6	11409.195 (1.00)	11409.355 (1.00)		11283.511 (0.20)	11051.875 (2.20)	11052.009 (3.10)
7	11415.628 (1.00)	11415.813 (0.10)	11225.400 (0.10)	11289.877 (1.20)	11058.132 (3.10)	11058.307 (2.20)
8	11422.976 (0.10)	11423.234 (1.00)	11232.735 (1.10)	11297.146 (1.20)	11065.284 (2.30)	11065.509 (1.30)
9	11431.245 (0.10)	11431.554 (0.20)	11240.981 (2.10)	11305.365 (2.10)	11073.320 (2.30)	11073.605 (3.10)
10	11440.453 (0.10)	11440.818 (1.20)	11250.153 (0.30)	11314.474 (1.20)	11082.260 (5.00)	11082.613 (2.20)
11	11450.559 (3.00)	11450.989 (0.30)	11260.217 (0.30)	11324.516 (1.20)	11092.100 (2.30)	11092.510 (3.10)
12	11461.587 (2.00)	11462.083 (3.00)	11271.208 (2.10)	11335.481 (0.30)	11102.823 (4.10)	11103.321 (2.10)
13	11473.505 (2.10)	11474.102 (2.10)	11283.125 (0.30)	11347.362 (2.10)	11114.436 (3.20)	11115.016 (3.10)
14	11486.375 (2.10)	11487.042 (3.00)	11295.954 (3.00)	11360.182 (3.00)	11126.951 (4.10)	11127.616 (2.20)
15	11500.139 (2.10)	11500.913 (1.10)	11309.706 (0.30)	11373.932 (2.10)	11140.356 (3.20)	11141.110 (4.00)
16	11514.819 (1.10)	11515.675 (1.20)	11324.376 (1.20)	11388.628 (2.10)	11154.654 (5.00)	11155.506 (2.10)
17	11530.419 (1.10)	11531.365 (1.20)	11339.966 (1.20)	11404.265 (3.00)	11169.840 (3.20)	11170.802 (2.20)
18	11546.926 (1.20)	11547.971 (2.10)	11356.483 (0.30)	11420.856 (1.20)	11185.921 (4.10)	11186.987 (2.20)
19	11564.346 (1.10)	11565.498 (2.10)	11373.924 (1.20)	11438.408 (2.10)	11202.891 (4.10)	11204.074 (3.10)
20	11582.671 (1.20)	11583.941 (3.00)	11392.297 (1.10)	11456.921 (0.30)	11220.768 (4.10)	11222.060 (2.20)
21	11601.908 (2.10)	11603.279 (2.10)	11411.601 (3.00)	11476.406 (1.20)	11239.533 (4.10)	11240.950 (1.30)
22	11622.053 (2.10)	11623.552 (2.10)	11431.855 (1.20)	11496.881 (1.20)	11259.300 (4.10)	11260.737 (3.10)
23	11643.118 (3.00)	11644.731 (1.20)	11453.049 (1.20)	11518.335 (1.20)	11279.574 (4.10)	11281.481 (2.10)
24	11665.088 (1.20)	11666.818 (2.10)	11475.203 (1.20)	11540.783 (0.20)	11301.047 (3.20)	11302.785 (0.40)
25	11687.951 (3.00)	11689.813 (1.20)	11498.363 (1.20)	11564.214 (1.10)	11323.386 (2.30)	11325.316 (4.00)
26	11711.727 (0.30)	11713.718 (2.10)		11588.647 (2.00)	11346.586 (3.10)	11348.689 (2.10)
27	11736.409 (1.10)	11738.535 (3.00)			11370.678 (3.10)	11372.940 (4.00)
28	11761.997 (1.20)	11764.257 (2.10)			11395.657 (2.20)	11398.081 (2.20)
29	11788.481 (1.10)	11790.882 (1.10)			11421.531 (2.20)	11424.097 (2.20)
30	11815.879 (1.20)	11818.408 (2.10)		11395.361 (0.11)	11448.281 (4.00)	11451.029 (2.20)
31	11844.161 (2.10)	11846.840 (2.10)	18	11413.135 (0.30)	11475.918 (2.20)	11478.832 (3.10)
32	11873.354 (1.20)	11876.171 (3.00)	19	11431.763 (2.10)	11504.452 (4.00)	11507.526 (2.20)
33	11903.438 (1.20)	11906.410 (3.00)	20	11451.282 (1.20)	11533.871 (1.30)	11537.111 (2.20)
34	11934.422 (2.10)	11937.536 (3.00)	21	11471.698 (0.20)	11564.169 (3.10)	11567.587 (3.10)
35	11966.299 (3.00)	11969.566 (2.10)	22	11492.938 (2.10)	11595.351 (4.00)	11598.945 (2.20)
36	11999.071 (2.00)	12002.479 (1.20)	23	11515.048 (3.00)	11627.415 (3.00)	11631.195 (1.30)
37	12032.736 (3.00)	12036.314 (1.20)	24	11538.023 (2.10)	11660.373 (3.10)	11664.325 (2.20)
38	12067.290 (1.20)	12071.026 (1.20)	25	11561.827 (0.20)	11694.187 (2.10)	11698.344 (4.00)
39	12102.743 (2.10)	12106.623 (2.10)	26	11586.519 (0.30)	11728.922 (2.00)	11733.251 (3.10)
40	12139.076 (2.10)	12143.129 (2.10)	27 11534.609 (1.20)	11612.030 (0.30)	11764.519 (2.20)	11769.038 (2.20)
41	12176.304 (2.00)	12180.512 (3.00)	28 11561.011 (0.30)	11638.401 (0.30)	11801.002 (2.20)	11805.704 (3.10)
			29 11588.194 (2.10)			

v = 1 (cont.)

J	Ω = -1		Ω = 0		Ω = 1	
	a	b	a	b	a	b
42	12214.408 (2.00)	12218.795 (2.10)	11616.214 (1.20)	11665.598 (1.20)	11838.359 (3.10)	11843.258 (3.10)
43	12253.415 (2.10)	12257.948 (1.10)	11645.033 (2.10)	11693.641 (1.20)	11876.595 (2.10)	11881.693 (3.10)
44	12293.296 (2.00)	12297.989 (2.10)	11674.640 (1.20)	11722.561 (0.30)	11915.711 (3.10)	11921.000 (4.00)
45	12334.062 (2.10)	12338.929 (2.10)	11705.062 (1.20)	11752.292 (2.10)	11955.708 (3.00)	11961.183 (2.20)
46	12375.701 (2.10)	12380.739 (2.00)	11736.294 (1.20)	11782.895 (1.20)	11996.588 (2.20)	12002.261 (3.10)
47	12418.231 (2.00)	12423.432 (2.10)	11768.339 (0.30)	11814.330 (2.10)	12038.335 (3.10)	12044.211 (2.20)
48	12461.642 (1.20)	12467.008 (1.00)	11801.252 (1.20)	11846.633 (1.20)	12080.963 (1.20)	12087.031 (4.00)
49	12505.913 (1.20)	12511.460 (1.00)	11834.991 (0.30)	11879.794 (0.30)	12124.461 (2.20)	12130.738 (3.10)
50	12551.079 (3.00)	12556.782 (1.00)	11869.591 (2.10)	11913.839 (0.30)	12168.839 (3.10)	12175.310 (2.20)
51	12597.105 (0.20)	12602.978 (0.10)	11905.058 (1.20)	11948.708 (0.30)	12214.092 (2.10)	12220.733 (2.20)
52	12644.009 (0.10)	12650.036 (0.10)	11941.372 (1.20)	11984.436 (1.20)	12260.212 (2.10)	12267.078 (3.00)
53		12697.961 (1.00)	11978.576 (1.20)	12021.020 (1.20)	12307.209 (1.10)	12314.268 (3.00)
54	12740.433 (2.00)		12016.639 (0.30)	12058.432 (1.20)	12355.077 (1.20)	12362.329 (4.00)
55	12789.940 (2.00)		12055.571 (2.10)	12096.612 (0.30)	12403.816 (1.10)	12411.270 (1.20)
56	12840.328 (0.20)		12095.370 (1.20)	12135.572 (0.20)	12453.424 (0.10)	12461.069 (0.20)
57	12891.581 (1.20)		12136.040 (1.20)			12511.735 (2.00)
58	12943.688 (0.30)		12177.596 (2.10)			12563.275 (1.00)
59	12996.672 (1.20)		12220.021 (1.20)			
60	13050.512 (1.20)		12263.312 (2.10)			
61	13105.205 (1.10)		12307.470 (1.20)			
62	13160.748 (0.20)		12352.524 (0.20)			
63	13217.144 (0.10)		12398.415 (1.20)			
64	13274.450 (1.00)					
65	13332.572 (0.10)					
66	13391.558 (1.00)					
67	13451.388 (1.00)					

v = 1 (cont.)

J	Ω = 2	
	a	b
2	10830.972 (2.00)	
3	10833.640 (2.10)	
4	10837.213 (2.10)	
5	10841.695 (2.20)	
6	10847.069 (2.20)	
7	10853.326 (2.30)	
8	10860.489 (2.30)	
9	10868.549 (3.20)	
10	10877.494 (2.30)	
11	10887.341 (3.30)	
12	10898.073 (4.10)	
13	10909.703 (5.10)	
14	10922.228 (4.20)	
15	10935.649 (4.20)	
16	10949.966 (6.00)	
17	10965.169 (4.00)	
18	10981.266 (5.10)	
19	10998.257 (5.10)	
20	11016.136 (2.40)	
21	11034.911 (4.20)	
22	11054.571 (6.00)	
23	11075.134 (5.10)	
24	11096.585 (4.20)	
25	11118.920 (4.20)	
26	11142.147 (5.10)	
27	11166.270 (6.00)	
28	11191.281 (3.20)	
29	11217.186 (5.10)	
30	11243.990 (4.20)	
31	11271.736 (5.00)	
32	11299.740 (2.30)	
33	11329.484 (0.50)	11329.528 (0.50)
34	11359.873 (2.40)	11359.906 (2.30)
35	11391.100 (2.30)	11391.149 (2.40)
36	11423.225 (2.30)	11423.269 (5.10)
37	11456.228 (3.30)	11456.290 (3.30)
38	11490.127 (2.30)	11490.204 (5.10)
39	11524.924 (3.20)	11525.010 (3.20)
40	11560.639 (2.30)	11560.763 (5.10)
41	11597.308 (4.20)	11597.494 (2.30)

J	Ω = 3	
	a	b
3	10618.286 (1.00)	
4	10621.869 (1.30)	
5	10626.335 (4.00)	
6	10631.696 (1.30)	
7	10637.941 (3.10)	
8	10645.083 (3.10)	
9	10653.121 (3.30)	
10	10662.049 (4.20)	
11	10671.862 (4.20)	
12	10682.572 (4.20)	
13	10694.175 (4.20)	
14	10706.658 (4.20)	
15	10720.036 (3.30)	
16	10734.306 (4.20)	
17	10749.465 (4.20)	
18	10765.507 (1.50)	10765.545 (1.50)
19	10782.429 (4.20)	10782.536 (4.20)
20	10800.237 (5.10)	10800.422 (3.30)
21	10818.942 (2.30)	10819.166 (1.50)
22	10838.373 (2.30)	10838.796 (3.30)
23	10858.920 (3.20)	10859.302 (2.40)
24	10880.240 (3.10)	10880.686 (4.20)
25	10902.424 (4.10)	10902.951 (4.20)
26	10925.463 (4.10)	10926.099 (4.20)
27	10949.349 (3.10)	10950.128 (2.40)
28	10974.068 (3.20)	10975.050 (4.10)
29	10999.605 (2.30)	11000.843 (5.10)
30	11025.914 (3.20)	11027.521 (3.30)
31	11052.968 (3.20)	11055.086 (3.20)
32	11080.741 (4.10)	11083.519 (3.20)
33	11109.198 (3.10)	11112.841 (3.20)
34	11138.336 (2.20)	11143.032 (2.30)
35		11174.090 (2.30)
36		11206.023 (4.10)
37		11238.826 (4.10)
38		11272.490 (4.10)
39		11307.022 (3.20)
40		11342.400 (3.20)
41		11378.651 (3.20)
42		11415.749 (4.10)
43		11453.691 (5.00)

J	Ω = 3	
	a	b
44		11492.467 (2.30)
45		11532.083 (4.01)
46		11572.541 (4.01)
47		11613.803 (2.10)
48		11655.905 (3.01)
49		11698.812 (2.01)
50		11742.529 (1.10)
33	11117.809 (3.20)	
34	11147.446 (4.10)	
35	11178.102 (3.20)	
36	11209.752 (3.20)	
37	11242.377 (2.20)	
38	11275.960 (5.00)	
39	11310.460 (1.40)	
40	11345.879 (3.20)	
41	11382.213 (4.00)	
42	11419.445 (4.00)	
43	11457.573 (4.00)	
44	11496.588 (4.00)	
45	11536.491 (4.00)	
46	11577.277 (4.00)	
47	11618.933 (3.10)	
48	11661.486 (3.10)	
49	11704.923 (1.30)	
50	11749.211 (1.30)	
51	11794.385 (3.10)	
52	11840.431 (4.00)	
53	11887.348 (3.10)	
54	11935.136 (3.10)	
55	11983.792 (3.00)	
56	12033.318 (3.10)	
57	12083.711 (4.00)	
58	12134.964 (1.10)	
59	12187.082 (0.30)	
60	12240.062 (1.20)	

v = 2

J	Ω = -1		Ω = 0		Ω = -1	
	a	b	a	b	a	b
1			0		42	12873.515 (1.20)
2			1		43	12912.349 (3.00)
3			2		44	12952.060 (2.10)
4			3	11891.762 (0.10)		
5			4	11895.358 (0.20)		
6			5	11899.857 (1.10)		
7			6	11890.894 (0.20) 11905.242 (1.20)		
8		12086.572 (3.00)	7	11897.403 (1.30) 11911.522 (1.20)		
9	12094.702 (1.20)	12094.787 (2.20)	8	11904.836 (1.40) 11918.712 (1.10)		
10	12103.816 (2.10)	12103.898 (3.10)	9	11913.167 (0.50) 11926.786 (2.10)		
11	12113.833 (1.20)	12113.933 (4.00)	10	11922.463 (0.50) 11935.768 (1.30)		
12	12124.753 (3.00)	12124.872 (1.20)	11	11932.639 (1.40) 11945.641 (0.40)		
13	12136.592 (3.00)	12136.719 (1.30)	12	11943.779 (0.50) 11956.409 (0.50)		
14	12149.336 (2.10)	12149.526 (3.10)	13	11955.780 (1.40) 11968.069 (0.50)		
15	12162.991 (3.00)	12163.183 (3.10)	14	11968.711 (1.40) 11980.630 (1.50)		
16	12177.543 (3.00)	12177.763 (2.20)	15	11982.557 (2.40) 11994.085 (4.20)		
17	12193.011 (2.10)	12193.250 (3.10)	16	11997.305 (1.60) 12008.438 (1.40)		
18	12209.379 (3.00)	12209.652 (2.20)	17	12012.970 (0.70) 12023.676 (3.30)		
19	12226.665 (1.20)	12226.955 (1.30)	18	12029.534 (1.70) 12039.825 (1.60)		
20	12244.848 (1.20)	12245.157 (2.20)	19	12046.976 (0.70) 12056.851 (1.50)		
21	12263.943 (1.20)	12264.275 (1.30)	20	12065.342 (1.70) 12074.774 (2.50)		
22	12283.930 (2.10)	12284.296 (4.00)	21	12084.623 (3.50) 12093.595 (3.50)		
23	12304.815 (0.30)	12305.219 (2.20)	22	12104.781 (1.70) 12113.305 (1.70)		
24	12326.620 (2.10)	12327.050 (2.20)	23	12125.845 (2.60) 12133.902 (2.60)		
25	12349.316 (3.00)	12349.780 (3.10)	24	12147.805 (0.80) 12155.402 (3.50)		
26	12372.880 (2.10)	12373.414 (3.10)	25	12170.666 (3.50) 12177.788 (1.60)		
27	12397.324 (3.00)	12397.946 (3.00)	26	12194.420 (0.80) 12201.058 (2.60)		
28		12423.386 (1.20)	27	12219.091 (2.60) 12225.224 (2.50)		
29		12449.715 (2.10)	28	12244.631 (1.80) 12250.282 (3.50)		
30		12476.955 (0.30)	29	12271.085 (1.70) 12276.224 (1.60)		
31		12505.081 (2.10)	30	12298.418 (1.60) 12303.059 (2.50)		
32		12534.113 (2.10)	31	12326.677 (4.30) 12330.786 (3.40)		
33		12564.030 (3.00)	32	12355.828 (3.40) 12359.411 (0.70)		
34		12594.852 (3.00)	33	12385.866 (1.60) 12388.898 (2.50)		
35		12626.558 (2.10)	34	12416.797 (4.30) 12419.380 (1.40)	J	Ω = 0
36		12659.163 (2.00)	35	12448.632 (2.50)		a b
37		12692.661 (1.20)	36	12481.383 (2.50)	41	12658.602 (1.50)
38		12727.055 (0.30)	37	12515.030 (1.60)	42	12696.750 (2.40)
39		12762.331 (0.30)	38	12549.563 (1.60)	43	12735.803 (2.30)
40		12798.501 (1.20)	39	12585.007 (1.40)	44	12775.768 (1.40)
41		12835.571 (1.20)	40	12621.358 (3.30)	45	12816.624 (2.30)

v = 2 (cont.)

J	Ω = 2	
	a	b
2	11483.445 (2.00)	
3	11486.121 (4.10)	
4	11489.704 (3.10)	
5	11494.187 (3.20)	
6	11499.547 (2.40)	
7	11505.808 (3.30)	
8	11512.962 (4.40)	
9	11521.024 (5.30)	
10	11529.970 (4.40)	
11	11539.826 (5.30)	
12	11550.577 (5.30)	
13	11562.238 (6.20)	
14	11574.816 (5.30)	
15	11588.312 (2.50)	
16		
17		
18	11632.371 (1.20)	
19	11649.609 (3.20)	
20	11667.656 (2.40)	11667.735 (2.40)
21	11686.522 (5.10)	11686.581 (2.40)
22	11706.227 (3.30)	11706.293 (2.40)
23	11726.803 (4.10)	11726.877 (3.20)
24	11748.246 (4.10)	11748.344 (2.10)
25	11770.584 (3.30)	11770.707 (3.30)
26	11793.813 (4.10)	11793.968 (3.20)
27	11817.924 (3.20)	11818.149 (1.40)
28	11842.943 (3.10)	11843.282 (1.40)
29	11868.965 (4.00)	11869.345 (0.02)

J	Ω = 3	
	a	b
3	11282.269 (2.10)	
4	11285.836 (3.30)	
5	11290.298 (2.40)	
6	11295.644 (4.20)	
7	11301.891 (4.20)	
8	11309.021 (4.30)	
9	11317.049 (3.50)	
10	11325.968 (5.40)	
11	11335.772 (3.60)	
12	11346.467 (3.60)	
13	11358.061 (5.40)	
14	11370.541 (5.40)	
15	11383.908 (5.40)	
16	11398.167 (4.40)	
17	11413.314 (6.20)	
18	11429.357 (5.40)	
19	11446.276 (5.40)	
20	11464.090 (6.30)	
21	11482.783 (4.50)	
22	11502.369 (6.30)	
23	11522.843 (5.40)	
24	11544.204 (5.40)	
25	11566.440 (6.30)	
26	11589.572 (6.30)	
27	11613.576 (3.60)	
28	11638.469 (5.40)	
29	11664.216 (1.70)	11664.262 (0.80)
30	11690.862 (1.70)	11690.905 (4.40)
31	11718.377 (2.50)	11718.451 (4.30)
32	11746.744 (3.40)	11746.868 (2.50)
33	11775.965 (4.30)	11776.159 (4.30)
34	11806.007 (1.60)	11806.337 (2.50)
35	11836.807 (4.30)	11837.388 (3.40)
36	11868.301 (1.50)	11869.363 (4.30)

v = 3

J	Ω = 2	J	Ω = 3
2	12157.372 (1.00)	3	11960.634 (0.10)
3	12160.053 (1.10)	4	11964.203 (1.10)
4	12163.607 (1.10)	5	11968.644 (0.20)
5	12168.058 (2.00)	6	11973.985 (1.10)
6	12173.416 (2.00)	7	11980.203 (1.10)
7	12179.664 (2.00)	8	11987.310 (1.10)
8	12186.785 (2.00)	9	11995.316 (2.00)
9	12194.814 (2.00)	10	12004.203 (2.00)
10	12203.729 (2.00)	11	12013.984 (2.00)
11	12213.537 (2.00)	12	12024.650 (1.10)
12	12224.245 (2.00)	13	12036.207 (2.00)
13	12235.822 (2.00)	14	12048.656 (2.00)
14	12248.312 (1.10)	15	12061.985 (2.00)
15	12261.693 (2.00)	16	12076.208 (2.00)
16	12275.951 (2.00)	17	12091.315 (2.00)
17	12291.119 (2.00)	18	12107.310 (2.10)
18	12307.169 (1.10)	19	12124.193 (2.10)
19	12324.124 (2.00)	20	12141.968 (2.10)
20	12341.977 (1.10)	21	12160.633 (1.20)
21	12360.715 (2.00)	22	12180.179 (3.00)
22	12380.347 (3.00)	23	12200.620 (2.10)
23	12400.883 (3.00)	24	12221.944 (3.00)
24	12422.313 (3.00)	25	12244.161 (1.20)
25	12444.622 (3.00)	26	12267.264 (2.10)
26	12467.852 (2.10)	27	12291.259 (3.00)
27	12491.987 (3.00)	28	12316.145 (2.10)
28	12517.018 (1.20)	29	12341.925 (1.20)
29	12542.956 (3.00)	30	12368.579 (2.10)
30	12569.796 (2.00)		
31	12597.570 (1.20)		
32	12626.252 (2.10)		
33	12655.862 (1.20)		
34	12686.405 (2.10)		

APPENDIX VIII

Term Values for the $^5\Phi$ State (cm^{-1})

The number in parentheses following each term value gives the sum of the weights of the lines from which it was determined.

Appendix VIII -- $^5\Phi$ term values

v = 0

J	Ω = 1		Ω = 2	Ω = 3
	a	b		
1	10447.297 (0.20)	10447.305 (1.20)		
2	10449.149 (2.10)	10449.149 (3.10)	10334.175 (2.41)	
3	10451.921 (3.50)	10451.921 (1.40)	10336.934 (1.60)	10197.748 (4.20)
4	10455.622 (2.80)	10455.621 (4.50)	10340.606 (3.50)	10201.338 (3.50)
5	10460.240 (6.50)	10460.243 (4.70)	10345.206 (8.30)	10205.823 (6.20)
6	10465.783 (8.30)	10465.787 (5.50)	10350.723 (8.30)	10211.215 (6.50)
7	10472.256 (5.70)	10472.255 (8.10)	10357.155 (5.60)	10217.504 (8.30)
8	10479.652 (8.30)	10479.652 (6.50)	10364.508 (5.60)	10224.693 (9.30)
9	10487.956 (3.80)	10487.967 (4.80)	10372.782 (5.60)	10232.772 (7.40)
10	10497.202 (6.40)	10497.205 (6.60)	10381.975 (8.30)	10241.750 (7.50)
11	10507.359 (8.40)	10507.362 (7.50)	10392.084 (6.50)	10251.628 (9.20)
12	10518.443 (9.30)	10518.442 (11.10)	10403.116 (10.10)	10262.398 (10.20)
13	10530.433 (9.30)	10530.441 (8.30)	10415.068 (7.50)	10274.074 (9.30)
14	10543.359 (9.30)	10543.359 (8.40)	10427.942 (9.30)	10286.647 (10.10)
15	10557.183 (9.30)	10557.190 (9.30)	10441.738 (11.10)	10300.113 (9.20)
16	10571.936 (10.20)	10571.938 (9.30)	10456.458 (8.40)	10314.481 (9.10)
17	10587.603 (10.20)	10587.609 (9.30)	10472.103 (8.30)	10329.745 (10.20)
18	10604.184 (11.10)	10604.189 (8.40)	10488.681 (7.50)	10345.908 (11.10)
19	10621.676 (11.10)	10621.686 (12.00)	10506.185 (10.20)	10362.966 (10.20)
20	10640.083 (11.10)	10640.094 (11.10)	10524.618 (9.30)	10380.925 (10.20)
21	10659.410 (10.20)	10659.411 (10.10)	10543.994 (10.20)	10399.773 (9.30)
22	10679.638 (8.40)	10679.642 (9.30)	10564.312 (11.00)	10419.530 (11.10)
23	10700.774 (9.30)	10700.784 (10.20)	10585.578 (7.40)	10440.170 (9.30)
24	10722.825 (10.20)	10722.827 (10.20)	10607.794 (8.20)	10461.719 (9.20)
25	10745.777 (11.10)	10745.789 (9.30)	10630.971 (4.50)	10484.159 (11.10)
26	10769.640 (11.10)	10769.648 (10.20)	10655.124 (6.20)	10507.493 (12.00)
27	10794.404 (11.10)	10794.410 (8.40)	10680.255 (3.30)	10531.733 (7.40)
28	10820.076 (10.20)	10820.081 (10.20)	10706.388 (1.50)	10556.863 (8.40)
29	10846.651 (9.30)	10846.659 (11.10)	10733.530 (1.50)	10582.883 (10.20)
30	10874.123 (9.30)	10874.135 (11.10)	10761.699 (1.50)	10609.806 (11.10)
31	10902.500 (10.20)	10902.510 (9.30)	10790.928 (1.50)	10637.626 (10.20)
32	10931.773 (11.10)	10931.783 (10.20)	10821.216 (1.50)	10666.341 (11.10)
33	10961.949 (12.00)	10961.963 (11.10)	10852.612 (0.60)	10695.949 (11.00)
34	10993.019 (11.10)	10993.032 (11.10)	10885.128 (1.50)	10726.454 (11.10)
35	11024.992 (11.10)	11025.003 (9.20)		10757.861 (10.20)
36	11057.855 (11.10)	11057.870 (11.10)		10790.170 (9.10)
37	11091.616 (10.10)	11091.629 (10.20)		10823.381 (9.10)
38	11126.266 (12.00)	11126.277 (10.20)	10342.834 (0.20)	10857.500 (9.20)
39	11161.811 (12.00)	11161.821 (10.20)	10358.161 (1.30)	10892.538 (6.20)
40	11198.246 (10.20)	11198.263 (9.30)	10374.464 (1.30)	10928.498 (4.20)
41	11235.579 (10.20)	11235.590 (9.20)	10391.806 (1.30)	10965.410 (4.20)
			10410.148 (3.10)	11003.278 (6.00)
			10429.500 (2.10)	11042.161 (3.30)

v = 0 (cont.)

J	Ω = 1	
	a	b
42	11273.799 (9.30)	11273.812 (10.20)
43	11312.904 (9.20)	11312.921 (10.20)
44	11352.908 (9.30)	11352.923 (9.30)
45	11393.799 (9.11)	11393.815 (8.30)
46	11435.583 (10.10)	11435.600 (9.20)
47	11478.262 (9.20)	11478.280 (8.20)
48	11521.839 (4.51)	11521.856 (5.30)
49	11566.335 (4.20)	11566.352 (3.20)
50	11611.756 (3.10)	11611.774 (4.10)
51	11658.159 (1.30)	11658.179 (2.20)
52	11705.679 (3.10)	11705.695 (1.30)
53	11754.635 (0.03)	11754.654 (0.03)

J	Ω = 2
20	10449.841 (1.30)
21	10471.180 (1.30)
22	10493.516 (1.30)
23	10516.834 (2.20)
24	10541.132 (1.30)
25	10566.398 (1.30)
26	10592.617 (1.30)
27	10619.781 (2.20)
28	10647.880 (2.20)
29	10676.884 (1.30)
30	10706.790 (0.40)
31	10737.561 (0.40)
32	10769.190 (0.40)
33	10801.638 (1.30)
34	10834.880 (1.20)
35	10868.892 (0.40)
36	10903.646 (0.40)
37	10939.144 (0.40)
38	10975.326 (0.40)
39	11012.226 (0.40)
40	11049.838 (0.40)
41	11088.156 (1.30)
42	11127.202 (0.40)
43	11166.996 (1.30)
44	11207.533 (0.40)
45	11248.830 (1.30)
46	11290.912 (2.20)
47	11333.782 (0.40)
48	11377.443 (1.30)
49	11421.932 (1.30)
50	11467.226 (3.10)
51	11513.340 (1.30)
52	11560.286 (3.10)
53	11608.066 (1.30)
54	11656.681 (1.30)
55	11706.136 (3.10)
56	11756.426 (2.20)
57	11807.570 (3.10)
58	11859.554 (0.40)
59	11912.374 (1.30)
60	11966.056 (3.10)

J	Ω = 3
44	11082.106 (3.20)
45	11123.199 (5.10)
46	11165.537 (5.10)
47	11209.213 (2.40)
45	11107.011 (2.40)
46	11150.251 (2.40)
47	11193.974 (1.50)
48	11238.172 (1.50)
49	11282.859 (4.20)
50	11328.139 (4.20)
51	11374.085 (4.20)
52	11420.767 (3.30)
53	11468.231 (2.40)
54	11516.526 (3.30)
55	11565.664 (1.50)
56	11615.668 (2.40)
57	11666.559 (1.50)
58	11718.381 (4.20)
59	11771.178 (2.40)
60	11824.976 (0.60)
61	11879.846 (0.05)
62	11935.978 (0.05)
63	11993.743 (0.02)

J	Ω = 2
61	12020.573 (2.20)
62	12075.942 (0.40)
63	12132.162 (1.30)
64	12189.222 (1.30)
65	12247.125 (2.10)
66	12305.890 (1.20)
67	12365.483 (1.20)
68	12425.922 (0.30)
69	12487.226 (0.30)
70	12549.383 (0.20)
71	12612.389 (0.10)

Appendix VIII -- $^5\Phi$ term values (cont.)

v = 0 (cont.)

J	Ω = 4		J	Ω = 5	
4	10061.646	(7.30)	5	9916.917	(5.40)
5	10066.109	(5.50)	6	9922.254	(5.40)
6	10071.464	(5.50)	7	9928.472	(5.40)
7	10077.720	(8.40)	8	9935.582	(8.30)
8	10084.858	(6.60)	9	9943.581	(11.10)
9	10092.896	(7.50)	10	9952.465	(9.30)
10	10101.814	(9.30)	11	9962.241	(8.30)
11	10111.637	(8.40)	12	9972.910	(9.30)
12	10122.350	(7.50)	13	9984.459	(9.30)
13	10133.951	(8.40)	14	9996.897	(11.10)
14	10146.440	(12.00)	15	10010.222	(10.20)
15	10159.828	(12.00)	16	10024.433	(12.00)
16	10174.104	(12.00)	17	10039.535	(11.10)
17	10189.266	(11.10)	18	10055.515	(11.10)
18	10205.317	(10.20)	19	10072.385	(8.40)
19	10222.265	(12.00)	20	10090.144	(10.20)
20	10240.104	(9.30)	21	10108.777	(11.10)
21	10258.823	(8.40)	22	10128.297	(11.10)
22	10278.438	(8.40)	23	10148.706	(10.20)
23	10298.942	(10.20)	24	10169.992	(12.00)
24	10320.332	(10.20)	25	10192.163	(10.20)
25	10342.605	(11.10)	26	10215.214	(10.20)
26	10365.767	(10.10)	27	10239.147	(10.20)
27	10389.819	(9.30)	28	10263.959	(10.20)
28	10414.755	(9.30)	29	10289.652	(11.10)
29	10440.578	(10.20)	30	10316.227	(10.20)
30	10467.292	(12.00)	31	10343.677	(11.10)
31	10494.883	(10.20)	32	10372.002	(11.10)
32	10523.372	(11.10)	33	10401.214	(11.10)
33	10552.744	(9.30)	34	10431.290	(10.20)
34	10582.998	(8.40)	35	10462.252	(10.20)
35	10614.148	(11.10)	36	10494.080	(7.50)
36	10646.185	(9.30)	37	10526.788	(11.10)
37	10679.118	(9.30)	38	10560.363	(10.20)
38	10712.949	(11.10)	39	10594.812	(9.30)
39	10747.695	(9.30)	40	10630.134	(10.20)
40	10783.368	(11.10)	41	10666.324	(11.10)
41	10820.019	(9.30)	42	10703.386	(10.20)
42	10857.728	(8.40)	43	10741.315	(9.30)
43	10896.752	(11.10)	44	10780.108	(11.10)
44	10937.628	(6.60)	45	10819.771	(10.20)

Appendix VIII -- $^3\Phi$ term values (cont.)

v = 0 (cont.)

J	Ω = 4		Ω = 5	
44	10927.935	(6.60)		
45	10970.112	(7.50)		
46	11012.005	(6.60)	10860.299	(11.10)
47	11054.225	(1.10)	10901.687	(11.10)
48	11097.074	(8.40)	10943.939	(10.20)
49	11140.712	(9.30)	10987.056	(10.20)
50	11185.182	(9.30)	11031.031	(10.20)
51	11230.528	(8.40)	11075.866	(9.30)
52	11276.770	(5.70)	11121.561	(12.00)
53	11323.968	(9.20)	11168.115	(9.20)
54	11372.172	(5.70)	11215.525	(6.50)
55	11421.467	(5.70)	11263.785	(11.00)
56	11472.007	(5.30)	11312.898	(9.20)
57	11523.973	(6.20)	11362.865	(9.20)
58	11577.499	(4.50)	11413.683	(9.20)
59			11465.349	(8.30)
60			11517.867	(9.20)
61			11571.228	(10.00)
62			11625.432	(10.10)
63			11680.494	(9.10)
64			11736.382	(7.40)
65			11793.122	(8.20)
66			11850.690	(7.30)
67			11909.106	(5.50)
68			11968.361	(6.30)
69			12028.434	(7.20)
70			12089.358	(4.40)
71			12151.107	(5.30)
72			12213.689	(7.10)
73			12277.109	(6.20)
74			12341.330	(4.30)
75			12406.394	(6.10)
76			12472.277	(3.22)
77			12538.984	(4.11)
78			12606.515	(3.21)
79			12674.860	(3.11)
80			12744.024	(2.21)
81			12814.035	(1.11)
82			12884.776	(0.01)
56	11456.956	(3.60)		
57	11509.783	(5.40)		
58	11562.855	(5.40)		
59	11616.165	(2.70)		
60	11669.871	(5.40)		
61	11724.123	(5.40)		
62	11779.042	(4.50)		
63	11834.679	(4.50)		
64	11891.066	(3.50)		
65	11948.275	(3.50)		
66	12006.273	(5.30)		
67	12065.084	(5.20)		
68	12124.721	(6.10)		
69	12185.180	(1.70)		
70	12246.455	(2.60)		
71	12308.564	(3.40)		
72	12371.498	(4.40)		
73	12435.247	(7.00)		
74	12499.831	(4.40)		
75	12565.243	(3.40)		
76	12631.469	(3.30)		
77	12698.520	(2.40)		
78	12766.362	(1.30)		
79	12835.099	(3.10)		
80	12904.619	(2.20)		
81	12974.944	(2.20)		
82	13046.089	(1.30)		
83	13118.041	(0.10)		

Appendix VIII -- $^5\Phi$ term values (cont.)

v = 1

J	Ω = 1		Ω = 2		Ω = 3	
	a	b				
1	11063.062 (0.10)	11063.078 (1.10)				
2	11064.895 (2.00)	11064.890 (1.10)	2	10928.425 (2.31)		
3	11067.603 (3.00)	11067.608 (2.00)	3	10931.114 (5.10)	3	10791.201 (3.30)
4	11071.207 (1.10)	11071.226 (3.00)	4	10934.707 (1.50)	4	10794.790 (2.40)
5	11075.737 (4.00)	11075.733 (3.00)	5	10939.202 (5.00)	5	10799.282 (5.10)
6	11081.158 (4.00)	11081.161 (2.30)	6	10944.584 (6.00)	6	10804.664 (3.20)
7	11087.483 (3.10)	11087.499 (5.00)	7	10950.868 (5.10)	7	10810.963 (5.10)
8	11094.723 (3.30)	11094.731 (3.20)	8	10958.049 (5.00)	8	10818.132 (5.10)
9	11102.854 (4.20)	11102.867 (4.10)	9	10966.130 (4.20)	9	10826.210 (4.20)
10	11111.890 (5.00)	11111.913 (4.20)	10	10975.103 (5.10)	10	10835.200 (5.10)
11	11121.832 (5.00)	11121.855 (5.00)	11	10984.974 (5.10)	11	10845.078 (5.10)
12	11132.680 (4.20)	11132.701 (6.00)	12	10995.740 (5.10)	12	10855.854 (4.10)
13	11144.421 (4.10)	11144.447 (4.20)	13	11007.408 (6.00)	13	10867.538 (5.10)
14	11157.068 (6.00)	11157.106 (5.10)	14	11019.966 (6.00)	14	10880.138 (5.10)
15	11170.621 (4.10)	11170.657 (4.20)	15	11033.425 (4.10)	15	10893.659 (6.00)
16	11185.077 (6.00)	11185.113 (6.00)	16	11047.770 (5.10)	16	10908.143 (6.00)
17	11200.426 (5.10)	11200.467 (2.40)	17	11063.013 (6.00)	17	10923.654 (5.10)
18	11216.681 (6.00)	11216.732 (6.00)	18	11079.152 (4.20)	18	10940.374 (6.00)
19	11233.842 (4.20)	11233.894 (5.10)	19	11096.188 (6.00)	19	10958.559 (3.30)
20	11251.897 (3.30)	11251.954 (6.00)	20	11114.116 (5.10)		
21	11270.847 (4.20)	11270.916 (4.20)	21	11132.935 (5.10)	18	10935.917 (2.30)
22	11290.707 (5.10)	11290.777 (5.10)	22	11152.644 (4.20)	19	10953.933 (5.10)
23	11311.452 (4.20)	11311.532 (4.20)	23	11173.246 (5.10)	20	10972.427 (5.10)
24	11333.114 (6.00)	11333.190 (6.00)	24	11194.744 (5.10)	21	10991.493 (4.20)
25	11355.659 (6.00)	11355.746 (6.00)	25	11217.126 (5.10)	22	11011.298 (5.10)
26	11379.111 (6.00)	11379.192 (6.00)	26	11240.404 (5.10)	23	11031.915 (6.00)
27	11403.450 (6.00)	11403.534 (6.00)	27	11264.575 (6.00)	24	11053.380 (6.00)
28	11428.684 (4.20)	11428.785 (4.10)	28	11289.624 (4.20)	25	11075.704 (5.10)
29	11454.819 (6.00)	11454.923 (5.10)	29	11315.562 (5.10)	26	11098.890 (5.10)
30	11481.848 (6.00)	11481.958 (6.00)	30	11342.404 (4.20)	27	11122.965 (5.10)
31	11509.768 (5.00)	11509.882 (6.00)	31	11370.117 (2.40)	28	11147.896 (6.00)
32	11538.584 (5.10)	11538.696 (6.00)	32	11398.724 (3.20)	29	11173.719 (4.20)
33	11568.292 (6.00)	11568.412 (5.10)	33	11428.210 (1.50)	30	11200.408 (5.10)
34	11598.887 (5.10)	11599.015 (4.20)	34	11458.581 (3.30)	31	11227.968 (5.10)
35	11630.371 (4.20)	11630.506 (6.00)	35	11489.853 (3.30)	32	11256.413 (5.10)
36	11662.751 (5.10)	11662.889 (4.20)	36	11521.990 (1.50)	33	11285.727 (5.10)
37	11696.023 (5.10)	11696.156 (5.10)	37	11555.032 (3.90)	34	11315.919 (5.10)
38	11730.173 (6.00)	11730.314 (5.10)	38	11588.943 (2.00)	35	11346.975 (5.10)
39	11765.216 (5.10)	11765.361 (5.10)	39	11623.734 (2.10)	36	11378.928 (4.20)
40	11801.139 (6.00)	11801.298 (5.10)	40	11659.418 (3.00)	37	11411.734 (5.10)
41	11837.955 (5.00)	11838.115 (6.00)	41	11695.980 (3.00)	38	11445.418 (5.10)
			42	11733.405 (3.00)	39	11479.976 (4.20)

v = 1 (cont.)

J	Ω = 1				Ω = 2		Ω = 3	
	a		b					
42	11875.646	(6.00)	11875.808	(6.00)	11771.737	(2.80)	11515.400	(5.10)
43	11914.237	(4.20)	11914.399	(4.20)	11810.972	(3.60)	11551.698	(6.00)
44	11953.691	(3.20)	11953.868	(5.00)	11851.070	(6.30)	11588.870	(4.20)
45	11994.046	(5.10)	11994.210	(6.00)	11892.070	(4.60)	11626.907	(5.10)
46	12035.268	(4.10)	12035.441	(6.00)	11933.971	(2.80)	11665.814	(6.00)
47	12077.373	(5.00)	12077.553	(5.00)	11976.804	(2.60)	11705.582	(4.20)
48	12120.358	(1.10)	12120.534	(3.00)	12020.610	(2.40)	11746.227	(5.10)
49	12164.213	(3.00)	12164.393	(3.00)	12065.598	(0.40)	11787.736	(5.10)
50	12208.957	(1.20)	12209.163	(2.10)			11830.118	(6.00)
51	12254.584	(1.20)	12254.774	(2.10)			11873.389	(3.30)
52	12301.078	(1.20)	12301.269	(2.10)			11917.562	(3.30)
53	12348.443	(2.10)	12348.639	(1.10)			11962.437	(4.20)
54	12396.671	(1.20)	12396.868	(1.20)			12008.043	(4.10)
55	12445.794	(1.20)	12446.004	(0.30)			12054.722	(5.10)
56	12495.773	(1.20)	12495.986	(1.20)			12102.294	(4.20)
57	12546.636	(1.10)	12546.851	(1.20)			12150.715	(4.20)
58	12598.371	(2.00)	12598.584	(1.11)			12199.982	(5.10)
59	12650.977	(1.00)	12651.178	(1.10)			12250.110	(5.10)
60	12704.437	(1.00)	12704.662	(1.10)			12301.105	(5.10)
61	12758.762	(1.00)	12759.009	(0.10)			12352.959	(5.00)
							12405.698	(4.10)
							12459.349	(4.10)
							12513.850	(2.01)

Appendix VIII -- $^5\Phi$ term values (cont.)

v = 1 (cont.)

J	Ω = 4				Ω = 5	
	a		b			
4	10642.307	(5.11)			10498.300	(2.40)
5	10646.908	(5.30)			10503.631	(4.20)
6	10652.433	(6.20)			10509.831	(5.20)
7	10658.864	(6.20)			10516.924	(1.70)
8	10666.226	(5.30)			10524.901	(4.30)
9	10674.489	(4.40)			10533.768	(7.10)
10	10683.664	(4.30)			10543.518	(9.00)
11	10693.737	(3.50)			10554.146	(8.00)
12	10704.712	(5.20)			10565.667	(8.10)
13	10716.585	(7.00)			10578.067	(8.10)
14	10729.354	(7.10)			10591.356	(7.20)
15	10743.006	(5.20)			10605.523	(9.00)
16	10757.553	(7.10)			10620.578	(7.20)
17	10772.983	(7.10)			10636.506	(9.00)
18	10789.284	(7.10)			10653.325	(9.00)
19	10806.467	(6.20)			10671.025	(9.00)
20	10824.506	(7.00)			10689.600	(8.10)
21	10843.416	(0.70)			10709.055	(8.10)
22	10863.204	(6.10)			10729.394	(9.00)
23	10883.879	(7.10)			10750.607	(8.10)
24	10905.409	(5.30)			10772.698	(9.00)
25	10927.796	(7.10)			10795.666	(8.00)
26	10951.039	(8.00)			10819.516	(8.10)
27	10975.150	(8.00)			10844.236	(9.00)
28	11000.118	(7.10)			10869.834	(9.00)
29	11025.945	(8.00)			10896.302	(7.20)
30	11052.641	(7.10)			10923.651	(9.00)
31	11080.193	(7.00)			10951.864	(9.00)
32	11108.606	(7.00)			10980.953	(8.10)
33	11137.887	(7.00)			11010.905	(7.20)
34	11168.007	(3.30)			11041.731	(9.00)
35	11199.010	(6.10)			11073.431	(6.30)
36	11230.867	(5.10)			11105.994	(9.00)
37	11263.529	(2.40)	11263.584	(0.60)	11139.425	(9.00)
38	11297.154	(6.00)			11173.715	(9.00)
39	11331.593	(5.00)			11208.871	(8.10)
40	11366.896	(3.00)			11244.896	(8.10)
41	11403.050	(1.20)			11281.781	(9.00)
42	11440.068	(0.30)			11319.528	(6.30)
43	11477.939	(0.30)	11477.948	(0.30)	11358.138	(8.10)
44	11516.675	(0.30)	11516.689	(0.30)	11397.605	(9.00)

v = 1 (cont.)

J	Ω = 4		Ω = 5	
	a	b		
45	11556.253 (0.20)			
46	11596.708 (1.10)	11596.735 (0.30)	11437.924 (9.00)	
47	11638.022 (0.30)	11638.061 (0.30)	11479.107 (9.00)	
48	11680.186 (1.20)	11680.226 (1.20)	11521.140 (8.10)	
49	11723.200 (2.10)	11723.254 (2.10)	11564.034 (6.30)	
50	11767.081 (2.10)	11767.127 (3.00)	11607.776 (4.40)	
51	11811.819 (2.00)	11811.862 (1.20)	11652.375 (8.10)	
52	11857.399 (3.00)	11857.464 (2.10)	11697.816 (9.00)	
53	11903.829 (2.10)	11903.908 (2.10)	11744.114 (6.20)	
54	11951.126 (2.10)	11951.210 (2.10)	11791.257 (9.00)	
55	11999.267 (1.20)	11999.356 (2.10)	11839.250 (6.20)	
56	12048.269 (2.10)	12048.355 (2.10)	11888.080 (9.00)	
57	12098.106 (1.20)	12098.213 (2.10)	11937.757 (8.10)	
58	12148.801 (3.00)	12148.920 (2.10)	11988.286 (8.10)	
59	12200.345 (2.10)	12200.480 (2.10)	12039.646 (7.10)	
60	12252.738 (0.30)	12252.878 (2.10)	12091.853 (8.00)	
61	12305.981 (1.20)	12306.143 (1.20)	12144.892 (8.00)	
62	12360.060 (0.20)	12360.245 (0.30)	12198.774 (6.10)	
63	12415.059 (1.10)	12415.233 (1.10)	12253.491 (6.20)	
64	12470.885 (1.00)	12471.048 (1.00)	12309.037 (6.00)	
65	12527.538 (1.00)	12527.748 (0.10)	12365.413 (4.10)	
66	12585.092 (1.00)	12585.293 (1.00)	12422.635 (4.10)	
67			12480.678 (5.00)	
68			12539.545 (3.20)	
69			12599.250 (3.20)	
70			12659.769 (4.00)	
71			12721.120 (3.10)	
72			12783.292 (2.20)	
73			12846.282 (3.00)	
74			12910.094 (2.00)	
75			12974.730 (1.10)	
76			13040.163 (2.00)	
77			13106.424 (2.00)	
78			13173.484 (1.10)	
79			13241.368 (1.01)	
80			13310.062 (1.01)	
81			13379.571 (1.01)	
82			13449.932 (1.00)	

v = 2

J	Ω = 1		Ω = 2		Ω = 3
	a	b	a	b	
1					
2		11661.055 (0.10)	11525.051 (0.10)		11386.451 (1.20)
3		11663.727 (0.10)	11527.712 (2.01)		11389.970 (4.10)
4		11667.336 (0.10)	11531.266 (2.20)		11394.362 (5.10)
5		11671.815 (0.10)	11535.702 (1.30)		11399.639 (1.40)
6		11677.202 (1.10)	11541.036 (1.30)		11405.808 (3.30)
7		11683.512 (1.10)	11547.237 (3.20)		11412.849 (0.50)
8		11690.706 (1.20)	11554.348 (4.20)		11420.780 (3.30)
9		11698.795 (2.10)	11562.335 (2.40)		11429.596 (5.00)
10		11707.787 (1.20)	11571.206 (4.10)		11439.281 (2.30)
11		11717.673 (1.20)	11580.976 (5.10)		11449.844 (5.10)
12		11728.469 (2.10)	11591.637 (6.00)		11461.285 (4.20)
13		11740.152 (0.30)	11603.178 (4.20)		11473.613 (3.20)
14		11752.734 (1.10)	11615.610 (6.00)		11486.826 (5.00)
15		11766.219 (2.10)	11628.933 (2.30)		11500.915 (4.10)
16		11780.598 (1.20)	11643.140 (3.30)		11515.881 (5.10)
17		11795.885 (0.30)	11658.253 (4.20)		11531.729 (5.10)
18		11812.072 (3.00)	11674.276 (4.20)		11548.455 (5.00)
19		11829.162 (1.20)	11691.350 (1.20)		11566.063 (6.00)
20	11844.242 (1.00)	11847.141 (3.00)	11708.524 (1.20)		11584.554 (6.00)
21	11863.394 (2.00)	11866.022 (3.00)	11727.284 (3.00)		11603.930 (5.10)
22	11883.345 (2.10)	11885.815 (3.00)	11746.843 (1.20)		11624.190 (4.20)
23	11904.118 (3.00)	11906.510 (3.00)	11767.262 (2.10)		11645.343 (5.10)
24	11925.754 (3.00)	11928.102 (3.00)	11788.561 (0.30)		11667.408 (5.10)
25	11948.243 (2.10)	11950.602 (2.10)	11810.736 (2.10)		11690.443 (6.00)
26	11971.611 (3.00)	11974.007 (2.10)	11833.801 (1.20)		11714.674 (4.20)
27	11995.846 (2.10)	11998.324 (2.10)	11857.752 (1.20)		
28	12020.954 (0.30)	12023.551 (2.10)	11882.584 (2.10)		11763.602 (5.10)
29	12046.949 (3.00)	12049.687 (2.10)	11908.302 (1.20)		11790.057 (4.20)
30	12073.822 (2.10)	12076.739 (3.00)	11934.908 (2.10)		11817.344 (1.50)
31	12101.595 (2.10)	12104.709 (2.10)	11962.413 (0.30)		11845.488 (3.30)
32	12130.240 (1.20)	12133.586 (2.10)	11990.801 (0.30)		11874.503 (1.40)
33	12159.774 (2.10)	12163.373 (1.11)	12020.116 (1.20)		11904.356 (4.10)
34	12190.182 (2.10)	12194.120 (2.10)	12050.338 (0.30)		11935.115 (3.20)
35	12221.497 (3.00)	12225.767 (3.00)	12081.552 (1.20)		11966.729 (2.30)
36	12253.697 (3.00)	12258.332 (2.00)	12113.808 (0.30)		11999.205 (4.10)
37	12286.773 (1.10)	12291.814 (0.10)	12147.314 (0.30)		12032.548 (4.10)
38	12320.739 (2.10)	12326.210 (1.00)			12066.771 (3.20)
39	12355.601 (2.10)		12209.886 (0.30)	12209.911 (0.30)	12101.846 (4.10)
40	12391.344 (2.10)		12246.277 (0.30)	12246.294 (0.30)	12137.802 (4.10)
41	12427.981 (2.10)		12282.991 (0.30)	12283.021 (0.30)	12174.619 (2.30)
42			12320.349 (0.30)	12320.375 (0.30)	12212.300 (3.10)

Appendix VIII -- $^5\Phi$ term values (cont.)

v = 2 (cont.)

J	Ω = 1		Ω = 2		Ω = 3
	a	b	a	b	
42	12465.513 (3.00)				
43	12503.936 (3.00)		12358.472 (0.30)	12358.492 (1.20)	
44	12543.260 (3.00)		12397.386 (0.30)	12397.408 (1.20)	12250.849 (3.00)
45	12583.482 (1.20)		12437.156 (0.30)	12437.169 (0.30)	12290.260 (3.00)
46	12624.607 (1.20)		12477.742 (1.20)	12477.758 (0.30)	12330.534 (2.10)
47	12666.651 (2.10)		12519.180 (1.20)	12519.195 (1.20)	12371.672 (3.00)
48	12709.606 (0.01)		12561.474 (1.20)	12561.488 (0.30)	12413.670 (2.10)
49			12604.613 (1.20)	12604.653 (0.30)	12456.535 (3.00)
50			12648.620 (1.20)	12648.665 (1.20)	12500.264 (3.00)
51			12693.488 (1.20)	12693.549 (1.20)	12544.862 (1.10)
52			12739.204 (0.10)	12739.349 (0.20)	12590.327 (1.00)
53			12785.782 (1.10)	12785.773 (1.10)	12636.645 (1.00)
54					12683.845 (1.00)
55					12731.925 (1.00)
56					12780.904 (1.00)
57					12830.822 (1.00)

v = 2 (cont.)

J	Ω = 4		Ω = 5	
4	11230.996	(0.41)		
5	11235.287	(3.20)	11009.734	(1.10)
6	11240.443	(3.20)	11015.332	(2.20)
7	11246.470	(3.20)	11021.831	(4.10)
8	11253.378	(4.10)	11029.274	(3.20)
9	11261.172	(5.00)	11037.638	(1.40)
10	11269.838	(4.10)	11046.918	(2.20)
11	11279.396	(5.10)	11057.133	(3.20)
12	11289.832	(5.00)	11068.272	(2.30)
13	11301.160	(6.00)	11080.332	(2.30)
14	11313.377	(5.10)	11093.298	(2.20)
15	11326.481	(5.10)	11107.191	(3.20)
16	11340.478	(4.20)	11122.021	(4.10)
17	11355.364	(4.20)	11137.742	(4.10)
18	11371.137	(4.20)	11154.386	(4.10)
19	11387.800	(5.10)	11171.938	(4.10)
20	11405.350	(6.00)	11190.411	(4.10)
21	11423.790	(5.10)	11209.784	(4.10)
22	11443.114	(5.10)	11230.061	(4.10)
23	11463.332	(6.00)	11251.243	(5.00)
24	11484.431	(5.10)	11273.318	(5.00)
25	11506.409	(4.20)	11296.302	(5.00)
26	11529.279	(5.10)	11320.175	(5.00)
27	11553.028	(4.20)	11344.947	(5.00)
28	11577.663	(4.20)	11370.597	(6.00)
29	11603.171	(4.20)	11397.150	(5.10)
30	11629.561	(6.00)	11424.574	(6.00)
31	11656.833	(3.30)	11452.878	(4.20)
32	11684.972	(6.00)	11482.077	(5.10)
33	11713.998	(5.10)	11512.147	(3.30)
34	11743.902	(4.20)	11543.080	(5.10)
35			11574.885	(6.00)
36	11806.217	(3.20)	11607.555	(5.00)
37	11838.740	(6.00)	11641.090	(5.10)
38	11872.131	(5.10)	11675.497	(5.00)
39	11906.370	(5.10)	11710.746	(3.20)
40	11941.479	(3.30)	11746.853	(4.10)
41	11977.448	(3.30)	11783.815	(4.10)
42	12014.277	(5.10)	11821.630	(5.00)
43	12051.970	(3.30)	11860.273	(5.00)
44	12090.514	(3.30)	11899.778	(4.10)
			11940.113	(3.20)

Appendix VIII -- $^5\Phi$ term values (cont.)

v = 2 (cont.)

J	Ω = 4		J	Ω = 5	
45	12129.921	(2.40)	46	11981.291	(3.20)
46	12170.186	(4.20)	47	12023.304	(3.20)
47	12211.304	(4.10)	48	12066.142	(4.10)
48	12253.270	(4.10)	49	i2109.817	(5.00)
49	12296.095	(2.30)	50	12154.314	(5.00)
50	12339.768	(3.20)	51	12199.641	(3.20)
51	12384.286	(5.00)	52	12245.795	(3.10)
52	12429.663	(3.20)	53	12292.766	(3.10)
53	12475.875	(2.30)	54	12340.559	(2.20)
54	12522.939	(1.10)	55	12389.164	(3.10)
55	12570.833	(0.01)	56	12438.593	(4.00)
			57	12488.831	(3.10)
			58	12539.877	(3.00)
			59	12591.746	(3.00)
			60	12644.417	(1.20)
			61	12697.888	(2.10)
			62	12752.191	(3.00)
			63	12807.310	(2.00)

v = 3

J	Ω = 2	J	Ω = 3	J	Ω = 4	J	Ω = 5
2	12119.959 (0.30)	3	11991.753 (2.10)	4	11848.243 (2.11)	5	11674.296 (2.10)
3	12122.574 (0.30)	4	11995.280 (1.20)	5	11852.563 (3.20)	6	11679.698 (3.00)
4	12126.108 (0.30)	5	11999.675 (1.20)	6	11857.767 (1.40)	7	11685.990 (1.20)
5	12130.553 (2.10)	6	12004.983 (1.20)	7	11863.853 (4.10)	8	11693.177 (2.10)
6	12135.880 (1.20)	7	12011.162 (1.20)	8	11870.784 (3.20)	9	11701.263 (3.00)
7	12142.104 (1.20)	8	12018.280 (2.10)	9	11878.606 (3.10)	10	11710.246 (3.00)
8	12149.206 (1.20)	9	12026.242 (3.00)	10	11887.313 (3.20)	11	11720.135 (3.00)
9	12157.202 (3.00)	10	12035.078 (3.00)	11	11896.878 (4.10)	12	11730.904 (3.00)
10	12166.082 (1.20)	11	12044.818 (3.00)	12	11907.337 (2.30)	13	11742.572 (2.10)
11	12175.860 (3.00)	12	12055.434 (1.20)	13	11918.652 (5.00)	14	11755.125 (3.00)
12	12186.521 (0.30)	13	12066.944 (3.00)	14	11930.843 (3.20)	15	11768.581 (3.00)
13	12198.082 (2.10)	14	12079.347 (2.00)	15	11943.909 (4.00)	16	11782.921 (2.10)
14	12210.538 (2.10)	15	12092.629 (3.00)	16	11957.858 (5.00)	17	11798.148 (3.00)
15	12223.893 (3.00)	16	12106.817 (3.00)	17	11972.671 (3.20)	18	11814.263 (2.10)
16	12238.142 (0.30)	17	12121.898 (3.00)	18	11988.362 (3.20)	19	11831.264 (3.00)
17	12253.256 (1.20)	18	12137.868 (2.10)	19	12004.932 (4.00)	20	11849.147 (3.00)
18	12269.309 (2.10)	19	12154.738 (3.00)	20	12022.355 (4.10)	21	11867.915 (2.10)
19	12286.266 (2.00)	20	12172.501 (2.10)	21	12040.682 (3.20)	22	11887.569 (2.10)
20	12304.132 (0.20)	21	12191.180 (2.10)	22	12059.862 (4.10)	23	11908.098 (1.20)
21	12322.918 (1.10)	22	12210.757 (3.00)	23	12079.926 (3.10)	24	11929.503 (2.10)
22	12342.619 (1.10)	23	12231.255 (2.10)	24	12100.864 (4.10)	25	11951.792 (2.10)
23	12363.251 (0.20)	24	12252.668 (3.00)	25	12122.663 (4.00)	26	11974.953 (1.20)
24	12384.834 (1.10)	25	12275.000 (3.00)	26	12145.350 (2.30)	27	11998.977 (2.10)
		26	12298.263 (3.00)	27	12168.902 (5.00)	28	12023.891 (1.20)
		27	12322.414 (2.10)	28	12193.329 (5.00)	29	12049.666 (1.20)
				29	12218.633 (4.10)	30	12076.318 (2.10)
				30	12244.808 (5.00)	31	12103.835 (3.00)
				31	12271.847 (5.00)	32	12132.215 (3.00)
				32	12299.761 (5.00)	33	12161.459 (3.00)
				33	12328.553 (3.20)	34	12191.572 (2.10)
						35	12222.548 (1.10)
						36	12254.377 (3.00)
						37	12287.078 (3.00)
						38	12320.639 (2.10)
						39	12355.043 (3.00)
						40	12390.331 (2.10)
						41	12426.459 (3.00)
						42	12463.455 (2.01)
						43	12501.313 (2.01)
						44	12540.032 (2.00)
						45	12579.613 (2.00)

Appendix VIII -- $^5\Phi$ term values (cont.)

v = 3 (cont.)

J	Ω = 5
46	12620.070 (2.00)
47	12661.407 (2.00)
48	12703.632 (2.00)
49	12746.767 (1.10)
50	12790.839 (1.10)
51	12835.911 (1.10)
52	12882.086 (2.00)
53	12929.483 (0.02)

v = 4

J	Ω = 5
5	12325.593 (0.03)
6	12330.796 (1.11)
7	12336.888 (1.20)
8	12343.847 (1.20)
9	12351.682 (1.20)
10	12360.376 (3.00)
11	12369.946 (2.10)
12	12380.379 (2.10)
13	12391.682 (3.00)
14	12403.861 (1.20)
15	12416.917 (3.00)
16	12430.813 (1.20)
17	12445.602 (2.10)
18	12461.255 (2.10)
19	12477.786 (3.00)
20	12495.177 (1.20)
21	12513.451 (2.10)
22	12532.582 (3.00)
23	12552.602 (3.00)
24	12573.496 (2.10)
25	12595.258 (3.00)
26	12617.904 (2.10)
27	12641.437 (2.10)
28	12665.861 (2.10)
29	12691.171 (2.10)
30	12717.394 (2.10)
31	12744.524 (1.10)
32	12772.588 (2.00)
33	12801.598 (2.00)
34	12831.594 (1.10)
35	12862.596 (1.10)
36	12894.650 (1.10)
37	12927.807 (0.20)
38	12962.146 (0.10)

v = 5

J	Ω = 5
5	12930.352 (1.10)
6	12935.454 (0 20)
7	12941.413 (1.10)
8	12948.226 (2.00)
9	12955.901 (1.10)
10	12964.432 (2.00)
11	12973.809 (2.00)
12	12984.051 (1.10)
13	12995.146 (1.10)
14	13007.100 (1.10)
15	13019.912 (3.00)
16	13033.583 (3.00)
17	13048.105 (3.00)
18	13063.490 (3.00)
19	13079.735 (2.10)
20	13096.833 (3.00)
21	13114.789 (2.10)
22	13133.609 (1.20)
23	13153.291 (2.10)
24	13173.833 (3.00)
25	13195.222 (3.00)
26	13217.470 (3.00)
27	13240.580 (2.10)
28	13264.541 (3.00)
29	13289.339 (2.10)
30	13314.964 (2.10)
31	13341.414 (3.00)
32	13368.581 (2.10)
33	13396.232 (2.10)

PUBLICATIONS

A.W. Taylor and W.J. Balfour. "The $A^2\Pi-X^2\Sigma^+$ Emission Spectrum of Zinc Deuteride". J. Mol. Spectrosc. 1982, 91, 9-21.

A. S-C. Cheung, A.W. Taylor, and A.J. Merer. "Fourier Transform Spectroscopy of VO: Rotational Structure in the $A^4\Pi-X^4\Sigma^-$ System near 10 500 Å". J. Mol. Spectrosc. 1982, 92, 391-409.

A. S-C. Cheung, N. Lee, A.M. Lyyra, A.J. Merer, and A.W. Taylor. "Spectroscopic Properties of the $^5\Delta_i$ Ground State of FeO". J. Mol. Spectrosc. 1982, 95, 213-225.

A. S-C. Cheung, A.M. Lyyra, A.J. Merer. and A.W. Taylor. "Laser Spectroscopy of FeO: Rotational Analysis of Some Subbands of the Orange System". J. Mol. Spectrosc. 1983, 102, 224-257.

A.J. Merer, A. S-C. Cheung, and A.W. Taylor. "Two Singlet Electronic Transitions in the Near Infrared Attributed to VO^+". J. Mol. Spectrosc. 1984, 108, 343-351.

A.W. Taylor, A. S-C. Cheung, and A.J. Merer. "Fourier Transform Spectroscopy of the Low-Lying Excited Electronic States of FeO: A New Perturbing Σ State and Improved Ground State Constants". J. Mol. Spectrosc. 1985, 113, 487-494.